The Geochemistry of the Amphibolite-Granulite Facies Transition in Central South India

Philip Allen

Submitted in Partial Fulfillment of
the Requirements for the Degree of
Doctor of Philosophy

New Mexico Institute of Mining and Technology,
Socorro, New Mexico

1985

Acknowledgments

I would like to thank by advisor Dr. Kent C. Condie for suggesting the problem and for providing support for a Research Assistantship. He has been an important part of the study throughout the course of the research. I would also like to thank the members of my Committee, Drs. Philip R. Kyle, Antonius J. Budding, and Marshall Reiter for many helpful suggestions and comments.

I thank Drs. Hari Narain, S.M. Naqvi, and B.L. Narayana of the National Geophysical Research Institute, Hyderabad, for providing administrative, logistical, and technical support for that portion of the study carried out in south India. Dr. B.L. Narayana was a partner in the field aspects of this investigation for three field seasons in south India; he also provided assistance with sample analysis, and participated in many fruitful discussions on field relationships and the early analytical results. R. Nijaganuppa and D. Vaughn are thanked for help with modal analyses and sample preparation. Lisa Vance and the staff of the Geoscience Dept. Office are also thanked for their help.

Samples were irradiated at the Sandia National Laboratory (Albuquerque, N.M.) for neutron activation analyses, and at the Los Alamos National Laboratory (Los Alamos, N.M.) for delayed neutron activation analyses. The staffs of the nuclear reactors at these laboratories, and Dr. M.M. Minor of the Los Alamos Laboratory, are acknowledged. Kathleen Faris of the N.M. Tech X-ray Fluoresence Laboratory is thanked for the development of analytical procedures and

her help in supervising sample preparation and analyses. The staff of the N.M. Tech Computer Center provided assistance with the running of computer programs written in the course of this study. Finally, I would like to thank KBF for encouragement and confidence throughout the course of this research; it is deeply appreciated. The research was supported in large part by National Science Foundation Grants INT78-17128, EAR-05723, and EAR-8201227.

This is for LMBE.

> There is a solid bottom everywhere. We read that the traveller asked the boy if the swamp before him had a hard bottom. The boy replied that it had. But presently the traveller's horse sank in up to the girths, and he observed to the boy, "I thought you said that this bog had a hard bottom." "So it has," answered the latter, "but you have not got half way to it yet."
>
> Thoreau

Table of Contents

Appendixes

List of Figures

List of Tables

See also, Appendixes C.1 - C.10

Abstract

The prograde transition, from amphibolite to granulite-facies metamorphic grade, extends along an east-west arc across the Archaean terrane of south India. In the Transition Zone, the change in metamorphism is gradational, with consistent increases in temperature and pressure, and structures and rock types are preserved across the transition. The primary lithologies are gray tonalitic gneisses and charnockites, with subordinate granitic and granodioritic gneisses, that follow a calc-alkaline trend on an AFM diagram. The gneisses and charnockites are compositionally similar to equivalent Archaean Lewisian amphibolite and granulite-grade rocks from NW Scotland. Moving south (increasing metamorphic grade) across the Transition Zone, the gneisses develop dark, greasy patches that progressively grow into large masses of charnockite. Analyses of adjacent gneiss-charnockite pairs indicate that there is in general no consistent change in element abundances across the prograde reaction; though there is possible minor enrichment in Ta, Pb, and volatiles in the charnockite relative to the adjacent gneiss. In thin-section, orthopyroxene appears to develop in cleavages of lath-shaped biotite.

Average major and trace element concentrations grow more mafic with increasing metamorphic grade, which is the result of proportionally less granitic gneiss in the higher-grade terranes. Tonalitic charnockites from medium and high-pressure terranes are depleted in Rb, Cs, Th, and U, and to a lesser degree, K and Pb, relative to low-pressure Transition Zone tonalitic gneisses and charnockites. The depletion of these elements can be accounted for by the breakdown of hydrous biotite, in the presence of a CO_2-rich fluid phase, and the subsequent entry of these elements into, and their removal from the charnockite by the fluid phase. For other major and trace elements, tonalitic gneisses and charnockites from low and high-grade terranes are similar in composition; in particular, the REE do not show any significant change with increasing metamorphic grade.

The granitic gneisses of the low-grade Gneiss Terrane are enriched in Rb, Cs, Th, U, Pb, Sc, Y, Nb, and Ta relative to the granitic gneisses of the Transition Zone. The low-grade granitic gneisses of the Gneiss Terrane also have higher total REE with significant -Eu anomalies and are similar to other Archaean granites. The compositional change in granitic gneisses between the Gneiss Terrane and the Transition Zone may correlate with a Bouguer gravity low located in the area of the Transition Zone south of Bangalore. The source for the granitic gneisses of the Gneiss Terrane is uncertain, but field evidence suggests that they may not be genetically related to the tonalitic gneisses of the Transition Zone. The tonalitic gneisses, with fractionated REE patterns and depleted hREE, are probably derived from the partial melting of a mafic parent with variable hornblende, pyroxene, plagioclase, and garnet in the residue. Evidence from south India does not support the crustal model of a depleted, cumulus lower-middle crust with an enriched residual-liquid upper crust.

II Introduction

II.1 Overview of Archaean high-grade terrranes

Many recent studies conclude that the major portion of continental crust was created in the Archaean (> 2.5 Ga) (Armstrong and Hein, 1973; Windley, 1977; Tarney and Windley,1977; Condie, 1980; Taylor and McLennan, 1981); however, the processes of how this took place have been the subject of much debate. Two types of exposures comprise the remnants of this early crust, low-grade greenschist to amphibolite-facies granite-greenstone terranes and high-grade amphibolite to granulite-facies terranes. The high-grade terranes are found on all continents, and are generally characterized by a bimodal association of mafic inclusions and lenses (10-20% of exposed area) in tonalitic to granodioritic gneisses (Bridgewater et al., 1973; Kalsbeek, 1976). In many of the high-grade terranes, both amphibolite and granulite-facies rocks are exposed. The temperatures and pressures at which these rocks formed is in the range of 700-800 degrees C and 5-12 Kbar, which represents depths in the crust of about 20-40 km (Tarney and Windley, 1977; Newton, 1978; Janardhan et al., 1982). This association has led to the suggestion that petrogenetic and/or stratigraphic relationships exist between the amphibolite and granulite-grade terranes (Glikson and Lambert, 1973; Drury, 1974; Shackelton, 1976; Ermonovics and Davison, 1976).

In recent years, many detailed geochemical studies have focused on this relationship and in general have found that the high-pressure granulites are depleted in U, Th, Rb, and Cs, variably depleted in K, have higher K/Rb and Th/U, and undisturbed rare earth element (REE) distributions relative to the lower temperature and pressure amphibolite-grade gneisses (Heier, 1973; Tarney and Windley, 1977; Weaver and Tarney, 1981). This depletion of granulite-grade lower crust relative to intermediate crust has been attributed to two processes:

1) partial melting or fractional crystallization under conditions of moderate PH2O in which a) the lower crust represents the residuum and the intermediate crust the partial melt, or b) the lower and intermediate crust represent early and late stages, respectively, of a fractionally crystallizing liquid (Fyfe, 1973; Wyllie, 1977; Drury,1978; Field et al., 1980)

2) metamorphism-metasomatism of lower crust by CO2-rich fluids that raise solidus temperatures, inhibit partial melting, dehydrate hydrous mineral phases, and selectively remove trace elements (Heier, 1973; Tarney, 1976; Janardhan et al., 1979; Wells, 1979).

However, there are departures from this pattern of a depleted, granulite-grade lower crust; for example, in Brazil (Jequie Complex) (Sighinolfi et al., 1981); North Finland (Fennoscandia) (Barbey and Cuney, 1982); Australia (Musgrave and Arunta Blocks) (Gray, 1977; Allen, 1979). These observed differences in chemical abundances in amphibolite and granulite-grade rocks and the presence, or lack, of

depletion in the lower crust have been attributed to the following factors:

1) differences in the lithology and mineralogy, with corresponding differences in mineral-fluid or mineral-liquid partition coefficients, of the protolith (as for example, for metamorphosed supracrustal rocks) resulting in variable enrichment-depletion in granulite-grade gneisses (Gray, 1977; Barbey and Cuney, 1982)

2) a partial melting or fractional crystallization relationship between adjacent amphibolite and granulite-grade gneisses (Field et al., 1980; Drury, 1978)

3) variation of CO2/H2O in the fluid phase resulting in variable depletion in granulite-grade gneisses (Tarney and Windley, 1977; Condie and Allen, 1984)

4) retrograde metasomatism of granulite-grade gneiss to produce amphibolite-grade gneiss (Drury, 1978; Beach and Tarney, 1978, Lobato et al., 1983)

5) location of the rocks relative to the amphibolite-granulite transition; at the transition, low-pressure granulites do not show depletion relative to amphibolite-grade gneisses whereas the medium and high-pressure granulites do show depletion (Heier, 1973; Condie and Allen, 1984).

The processes that effect the relative elemental abundances in the lower and middle crust may operate together; for example, changes in CO2/H2O can result in changes in the fluid transport of selected elements and at the same time produce localized partial melting. Though variations in the depleted pattern for granulite-grade rocks

exist on local and regional scales, in general, granulite facies gneisses in Archaean high-grade terranes are depleted relative to amphibolite facies and are probably uplifted sections of the Archaean lower crust (20-40 km.).

The models that have been developed to describe the formation of a stratified crust and continental growth in the Archaean can be classified as one or a combination of three general types:

1) downwarping basin model: downsagging ultramafic to mafic volcanics, resulting from mantle diapirism, partially melt to produce tonalitic magmas that crystallize and undergo later metamorphism to amphibolite to granulite-grade (Glickson and Lambert, 1976)

2) andesite model: basaltic oceanic crust formed at spreading centers subducts to form andesitic island arcs which accrete at continental margins producing a partial melt; magma fractionally crystallizes progressively as residue to form a depleted lower crust and then, under lower T and P, as an intermediate and upper crust relatively enriched in light REE, large ion lithophile (LIL) elements, and SiO2 (Taylor, 1967; Nance and Taylor, 1976; Taylor and McLennon, 1981)

3) Cordilleran batholith model: basaltic oceanic crust with sediments subducts at continental margins with back arc basin, dehydrates and decarbonates producing partial melts in overlying mantle; this quartz-tholeiite magma differentiates in lower crust leaving an amphibolite-rich residue and tonalitic to granodioritic plutonism; release of CO2 from subducted oceanic crust and mantle produces a granulite-grade lower crust (Windley and Smith, 1976;

Tarney and Windley, 1977; Newton et al., 1980; Weaver and Tarney, 1983).

In south India, extensive areas of low-grade Archaean greenschist to amphibolite-facies (granite-greenstone) and high-grade granulite-facies terranes are exposed. The high-grade terrane encompasses both the low-pressure granulites along the amphibolite-granulite transition, and medium and high-pressure granulites that probably represent uplifted blocks of deeper crust. Exposures are common in most areas and as a result of ubiquitous quarrying, the outcrops typically provide broad, fresh surfaces for observation and sampling. As a result, south India provides an excellent area to study the relationship between Archaean low and high-grade terranes and compare these relationships with other Archaean terranes.

II.2 Purpose of study

The purpose of this study, within the broader context of earlier and continuing studies of Archaean high-grade terranes, is to examine the relationships between Archaean low and high-grade terranes in south India, specifically:

1) to examine the field, petrographic, and chemical characteristics of the tonalitic to granitic gneisses, mafic inclusions, and low-pressure granulites (charnockites) across a zone of increasing metamorphic grade (from the Bangalore-Kunigal and Bangalore-Kolar areas in the north to the Kollegal-Malavalli-Kabbaldurga and the Hosur-Krishnagiri-Dharmapuri areas across the prograde Transition Zone) (Fig. III-1),

2) to examine the field, petrographic, and chemical characteristics of the medium and high-pressure charnockites from the high-grade terrane (Shevaroy Hills and adjacent area, southern Biligirirangan Hills, and the Nilgiri Massif) and compare them with the amphibolite-grade gneisses and low-pressure charnockites from the prograde Transition Zone,

3) to examine retrograde gneisses and adjacent charnockites in the medium to high-pressure terrane (Salem, Bhavanisagur, and southern Biligirirangan Hills) and compare them with gneiss and adjacent low-pressure charnockite from the prograde Transition Zone (Kabbaldurga, Krishnagiri-Dharmapuri, Tiruvannamalai),

4) compare the characteristics of the Archaean high-grade terrane in India with high-grade terranes in other areas and examine possible sources for the gneiss, granitic gneiss, charnockite, and amphibolite inclusions.

II.3 Overview of the geology of south India

The geology of south India and Sri Lanka is dominated by the South India Craton of Archaean to Proterozoic age. The craton is delimited on the east and west by Mesozoic and younger sediments, and to the north by late Mesozoic-early Tertiary Deccan basalts and the Paleozoic-Mesozoic Narmada-Godavari rift and its associated sediments (Naqvi et al., 1974; Drury and Holt, 1980) (Fig. II-1). In a reconstructed Gondwanaland, the Indian subcontinent lies wedged between the east coast of Antarctica, Madagascar-south Africa, and southwestern Australia (Crawford, 1974; Barron et al., 1978; Katz, 1979) (Fig. II-2). The high-grade terrane of south Africa and

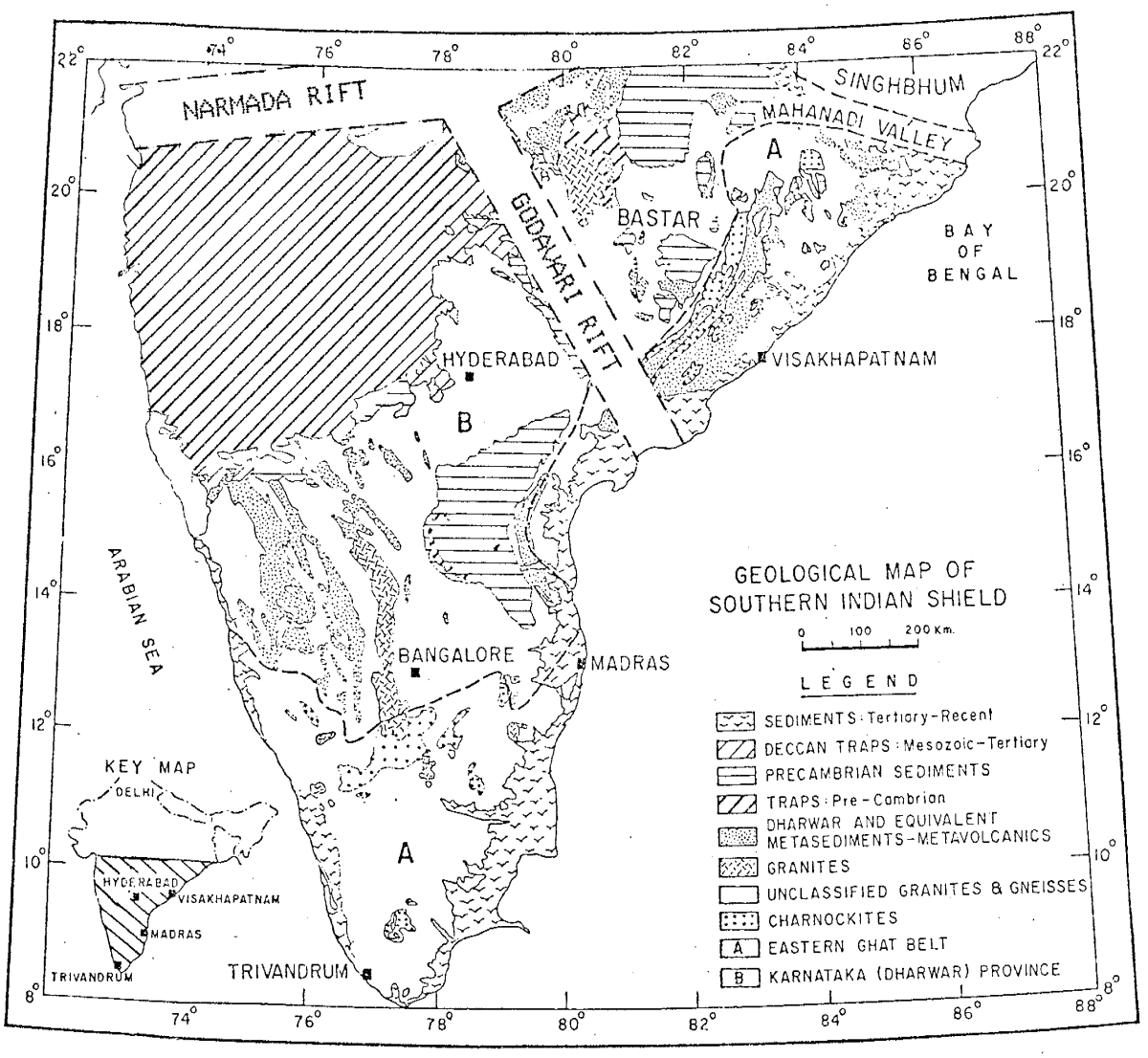

Fig. II-1. Generalized geological map of the south Indian shield. (Modified after original by NGRI, Hyderabad.) Dashed line indicates amphibolite-granulite transition, with low-grade to the north and high-grade to the south.

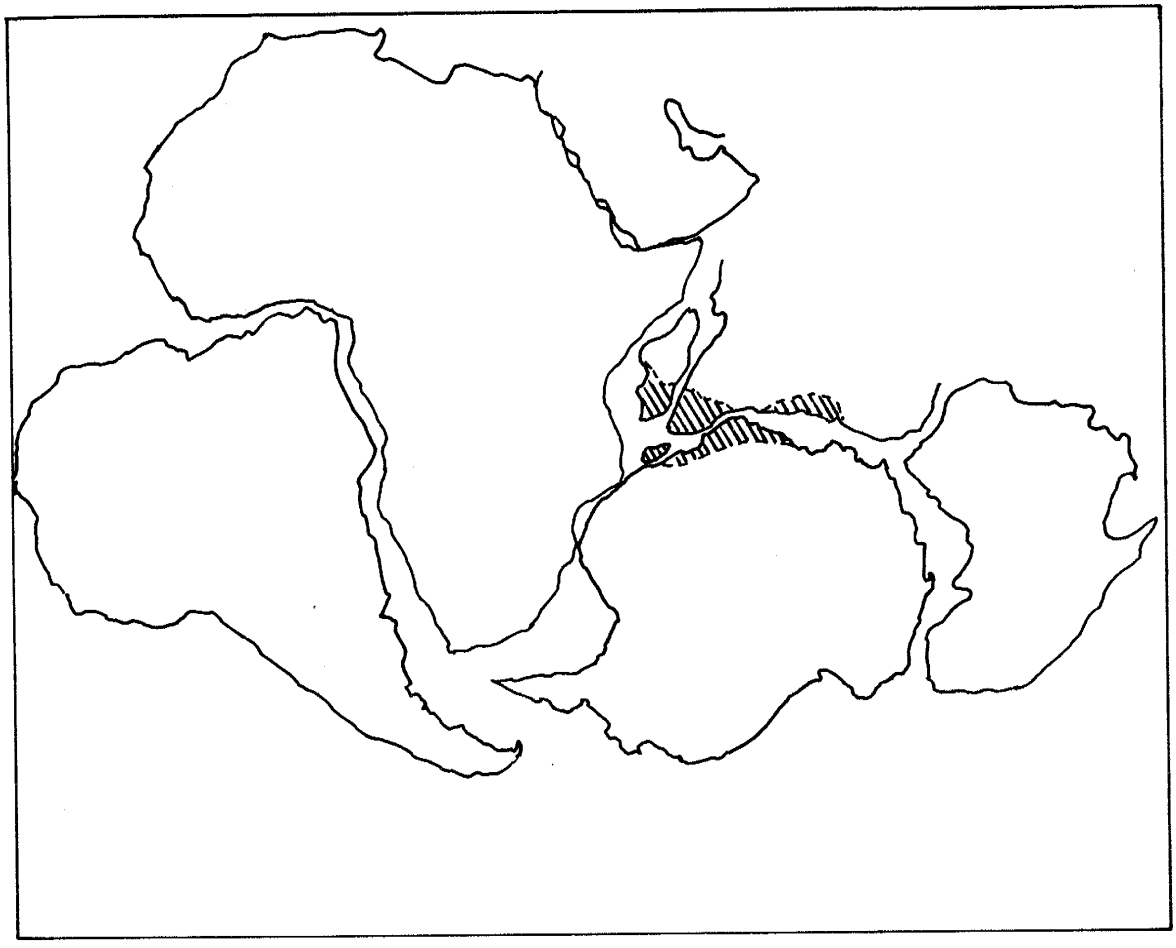

Fig. II-2. Reconstruction of Gondwanaland, after Smith and Hallam (1970), Katz and Premoli (1979), and Powell et al. (1980). Cross-hatched area indicates generalized high-grade terrane.

Madagascar (considered by Kroner, 1977, to have been part of the pre-Limpopo shield complex) is continuous with the high-grade terrane of south India (Crawford, 1974; 1978; Katz and Premoli, 1979). Recent studies in east Antarctica suggest that the high-grade terrane of the Napier Complex is also a continuation of the high-grade granulites in south India and Sri Lanka (Grew, 1978; Grew and Manton, 1979; Grew, 1981; DePaolo, 1982).

The South India Craton is transected by an irregular, crescent-shaped zone, stretching 600 km from Mangalore on the west coast to north of Madras on the east coast, that marks the transition from a low-grade greenschist to amphibolite-facies terrane in the north to a high-grade low to high-pressure granulite-facies terrrane in the south (Fig. II-3). North of the Transition Zone lies the low-grade, amphibolite-facies, polyphase "Peninsular Gneiss", which is characterized by gneisses and migmatites ranging in composition from tonalitic to granitic, with enclaves of amphibolite.

Recent determinations of ages of these gneisses show a range from 3.3 Ga to 2.5 Ga (for locations, see Fig. II-3):

Goru-Hassan area, Rb-Sr and Pb-Pb isochrons, 3.31-3.32 Ga and 3.08-3.12 Ga (Beckinsale et al., 1980, 1982);

Hiribelle, Rb-Sr isochron, 3.28 Ga (Drury et al., 1983);

Chicamagalur, Rb-Sr isochron, 3.03 Ga (Rajagopalan et al., 1980); Rb-Sr and Pb-Pb isochrons, 3.08 and 3.18 Ga, respectively (Ramakrishnan et al., 1984; Taylor et al., 1984);

Halekote, Rb-Sr isochron, 2.98 Ga (Stroh et al., 1983);

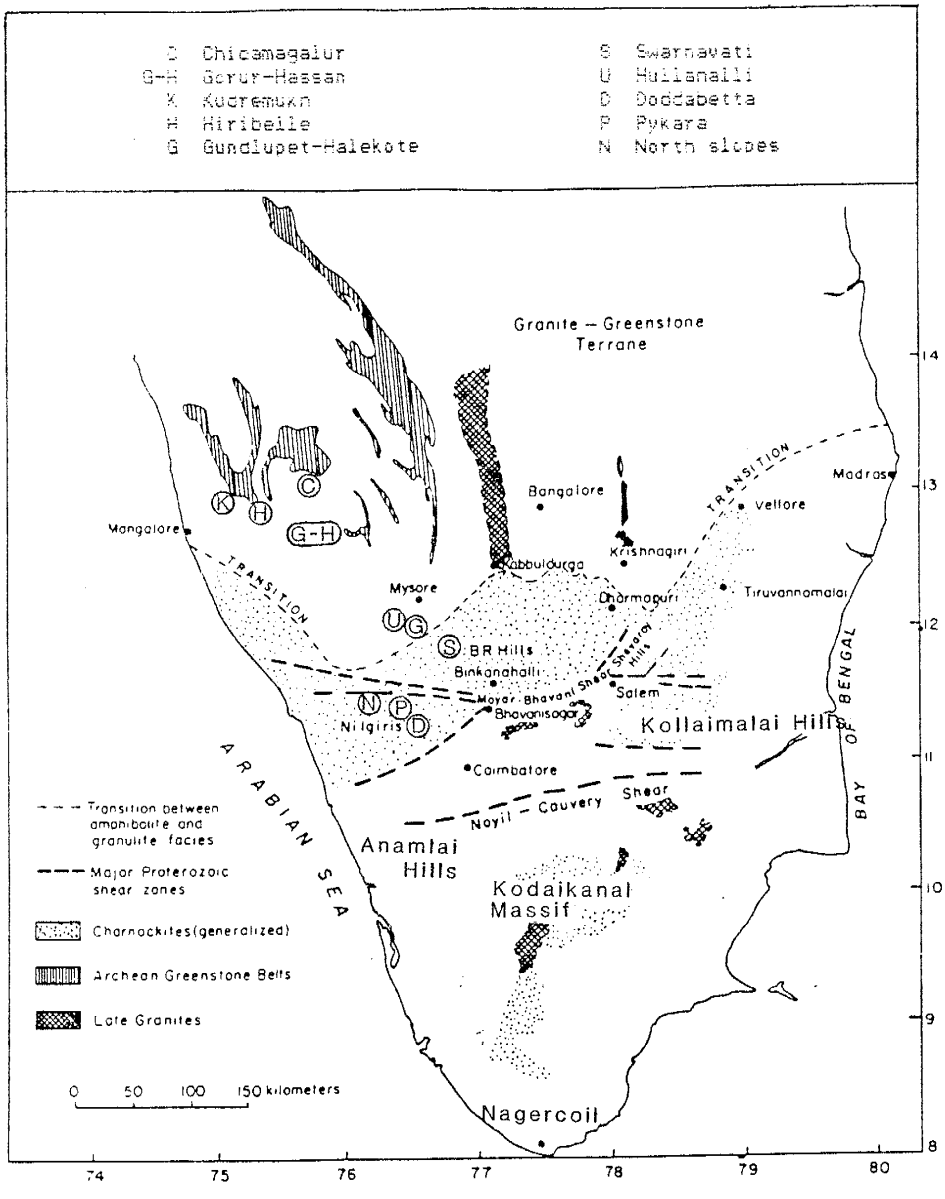

Fig. II-3. Generalized geologic map of southern India showing amphibolite-granulite facies transition and location of sites noted in the text.

Gundlupet, Rb-Sr isochron, 2.83 Ga (Janardhan and Vidal, 1982);

Bangalore area, Rb-Sr isochron, 3.01 Ga (Jayaram et al., 1976); Rb-Sr isochron, 2.52-2.56 Ga (Beckinsale et al., 1982);

Kabbaldurga, U-Pb from Allanite, 2.51 Ga (Grew and Manton, 1984); U-Pb from zircon, 2.5 Ga (Buhl et al., 1983).

Initial 87Sr/86Sr ratios for these gneisses range from low (0.7000 to 0.7009), indicating mantle derivation with short crustal residence times, to high ratios (0.7012 to 0.7034), suggesting some crustal contamination (Drury et al., 1984). The approximate 1.0 Ga range in age, and differences in degree of crustal contamination, indicate a long and complicated history in the development of the "Peninsular Gneiss."

The tonalitic to granitic gneisses appear to intrude or lie unconformably beneath arcuate to curvilinear, predominately north-trending greenstone successions (Ramakrishnan et al., 1976; Naqvi et al., 1978; Condie et al., 1982; Drury et al., 1984). These supracrustal rocks fall into two categories. The older Sargur Group (>3.0 Ga) is largely made up of mafic to ultramafic rocks, ironstones, aluminous sediments, and minor fuchsite quartzite; the younger Dharwar Supergroup (3.0 to 2.6 Ga) is comprised of a lower Bababuden Group (basal conglomerates, basalts, cross-bedded quartzite, and iron formations) and an upper Chitradurga Group (quartzites, limestones, iron formations, and greywackes) (Ramakrishnan et al., 1976; Viswanatha et al., 1982; Ramakrishnan and Viswanatha, 1983). Metavolcanics from the Kudremukh-West Coast greenstone belt, assigned to the lower Bababuden Group have

been dated by Sm-Nd whole rock isochron at 3.02 Ga (Drury et al., 1983).

The problem of assessing the proportions of paragneiss and orthogneiss in the Peninsular Gneiss Complex has been addressed by Rogers (1974); he concluded that the answer is difficult or impossible to accurately determine. The gneisses in south India cover an extensive area (>200,000 sq km) and are considered by most researchers to be intrusive into some or all of the Archaean to Proterozoic greenschist belts (Smeeth, 1916; Rogers, 1974; Pichamuthu, 1976; Naqvi, 1981; Pichamuthu, 1982). Chadwick (1981) describes examples of polyphase gneisses intruding, migmatizing, and picking up "rafts" of the older Sargur greenschists, and Ramakrishnan et al. (1976) considers the ubiquitous mafic inclusions and enclaves within the Peninsular Gneiss to be remnants of Sargur type schists intruded by the gneisses. Paragneisses are recognized within the younger Dharwar greenstone successions, such as the paragneisses with relict bedding that are observed in the basal unit of the Javanahalli schist belt where they are overlain by amphibolite and fuchsite quartzite (Naqvi et al., 1980; 1983). Localized occurences of metapelites are reported in Peninsular gneiss near the southern end of the Closepet batholith (Anantha Iyer and Narayanan Kutty, 1975; Jayaram et al., 1976; Harris and Jayaram, 1982) and elsewhere, but are seen as distinctive enclaves in the gneiss.

Initial Sr87/Sr86 ratios from 11 Rb-Sr isochrons (tonalitic gneisses) have a mean and standard deviation = 0.70144 +-0.00097, indicating a very short recycling time if the gneisses are paragneiss (for data sources, see above). Geochemical discrimination between paragneiss and orthogneiss is inconclusive: plots on an MgO-CaO-Al2O3

diagram (with fields after Leyreloup, 1977) of the mean values of tonalitic to granitic gneisses reported in this study fall along the igneous-metasedimentary boundary. Though the early work of Divakara Rao et al. (1974) suggested a sedimentary origin to the Peninsular Gneiss, field evidence of intrusive contacts with the Sargur Group greenschist belts and the presence of lenses and enclaves of amphibolite over a wide expanse of the gneiss, the great volume of the gneisses, and the low initial Sr87/Sr86 ratios all suggest that the Peninsular Gneiss Complex is predominantly orthogneiss.

Granitic bodies, both syn and post-tectonic, of varying size are found north and south of the Transition Zone but appear more prevalent in and near the zone. Geochemical and isotopic studies on the granites have been few. Crawford (1969) obtained an Rb-Sr isochron age of 2.38-2.56 Ga for the Closeplet granite; the best of the Rb-Sr isochron ages obtained by Venkatasubramanian and Narayanaswami (1974) for granites are in the range 2.5-3.0 Ga. Initial 87Sr/86Sr ratios are high for all the granites reported.

In contrast to the amphibolite-facies gneiss terrane, isotopic studies of the granulite facies in south India are relatively few: the Nilgiris, by Rb-Sr isochron, have been dated at 2.56 Ga (Crawford, 1969); the Coorg salient, by Rb-Sr isochron, at 2.56 Ga (Spooner and Fairbairn, 1970); and Kabbaldurga-Halagur, by Rb-Sr isochron, at 2.67 Ga (Venkatasubramanian and Narayanaswamy, 1974). The age for granulite facies rocks from the Fyfe Hills in East Antarctica (adjacent to the high-grade terrane of south India in a reconstructed Gondwanaland) is about 3.5 Ga (Sm-Nd isochron), similar to the oldest Rb-Sr date from the

Goru-Hassan area of south India (DePaulo et al., 1982) and represents the age of the protolith. A subsequent granulite-facies metamorphic event in the Napier Complex of East Antarctica, including the Fyfe Hills, took place at about 2.5 Ga (Zircon U-Pb data) (Grew and Manton, 1979; DePaolo et al., 1982). It is interesting to note that this date is similar to the 2.52 Ga date estimated for charnockite formation at Kabbaldurga (Grew and Manton, 1984).

Published results of geophysical research in the area of this study are few. Deep Seismic Soundings (DSS) traverses have been conducted across portions of central India. The first passes ~150 km north of Bangalore along a 600 km traverse roughly parallel to 14 N Latitude (Kaila et al., 1979). The results indicate 17 major crustal blocks separated by 15 deep, steep-angled faults and two major low-angle faults; depth to the Moho is between 35 and 41 km, with an average of ~36 km. The depth-velocity function shows an increase in velocity at 23 km, which is interpreted to represent a compositional change from granite to basalt (Kaila et al., 1979). Two additional E-W traverses were made further north near 17 and 18 N Latitude, about 475 km north of Bangalore (Kaila et al., 1981). The results are generally similar and show the Moho at a depth of ~30 km at the west coast and 36-40 km inland. A reflector at a depth of ~25 km, with a velocity increase from 6.6 km/sec to 6.76 km/sec, is again interpreted to represent a change in composition from granite to basalt (Kaila et al., 1981). These velocity increases observed by Kaila et al. (1979; 1981) may be the result of a change from granitic-tonalitic gneiss (s.g. ~=2.67 gm/cm3) to silicic-intermediate charnockite (s.g. ~=2.71-2.8 gm/cm3) (specific gravity data from Rama

Rao et al., 1979; Pichamuthu, 1953). However, the change in rock type appears more gradual than the observed relatively sharp increase in velocity. If the present depth to the Moho in the north is similar in the south, for example in the Krishnagiri-Dharmapuri area where Archaean crustal depths of ~15 km are exposed, an additional 15-25 km of crust has been added since the Archaean, assuming Archaean crustal thicknesses comparable to the present. This suggests that the southern side of the south India Archaean Craton has been underplated, possibly with basaltic rock.

Gravity studies have been made throughout India and are published at a scale of 1:5 000 000 (NGRI, 1978). The major feature in the region of this study is a marked Bouguer gravity low in an area south of Bangalore that extends westward towards Mysore and eastward towards Krishnagiri-Dharmapuri, thence southward towards Salem (NGRI, 1978; Kailasam, 1979). This Bouguer gravity low is possibly related to underlying, lower-density granitic plutons. Isostatic investigations over south India reveal a broad isostatic balance for the area (Subramanyam and Verma, 1980).

Heat flow data for the region of this study are very sparse (Gupta et al., 1979; Gupta, 1982). The two values reported by Gupta (1982) for Peninsular Gneiss southeast of Bangalore average 50.5 mW/m2, but it is not known if the measurements were made in amphibolite or granulite-facies terranes. The 50.5 mW/m2 heat flow value is low relative to the Proterozoic and younger terranes to the north, but slightly higher than heat flow values from other Archaean shields; for example, the Canadian Shield (~39 mW/m2), S.W. Australian Shield (~38

mW/m2), and Greenland (~40 mW/m2) (Rao and Jessop, 1975; Rao et al., 1982).

Pichamuthu (1953, 1965) observed a progressive increase in metamorphic grade from north to south across the central South India Craton and attributed this to exposures of gradually deeper levels of crust. Although uncertainties exist in the use of different geothermometers and geobarometers, and the effects of local metamorphic retrogression tend to lower estimates, recent studies indicate that there is a progressive increase in temperature and pressure from about 570 degrees C and 3.2 kb, in rocks 250 km north of Bangalore (Harris and Jayaram, 1982), to 720-900 degrees C and 8.3-9.5 kb, in rocks from the north slope of the Nilgir massif (Janardhan et al., 1982; Harris et al., 1982; Raith et al., 1983; Hansen et al., 1984) (Fig. II-4). The results from Molodezhnaya Station, west of the Fyfe Hills in East Antarctica, are 700 degress C and 5.5 kb (Grew, 1981) and indicate that these rocks are from an environment equivalent to the low-pressure granulites near the amphibolite-granulite transition in South India.

The South India Craton has been subdivided into north and south blocks along the east-west trending Noyil-Cauvery and Moyar-Bhavani Proterozoic shear zones (Drury and Holt, 1980; Drury et al., 1984)(Fig. II-3). The north block is characterized by predominant NNW to NNE structural trends as seen by the general orientation of the supracrustal belts, the Coorg salient of granulite, and the late intrusive Closepet granite. On a smaller scale, the overall foliation of the "Peninsular Gneiss" follows this trend. At the amphibolite-granulite facies transition, these trends pass without change into the

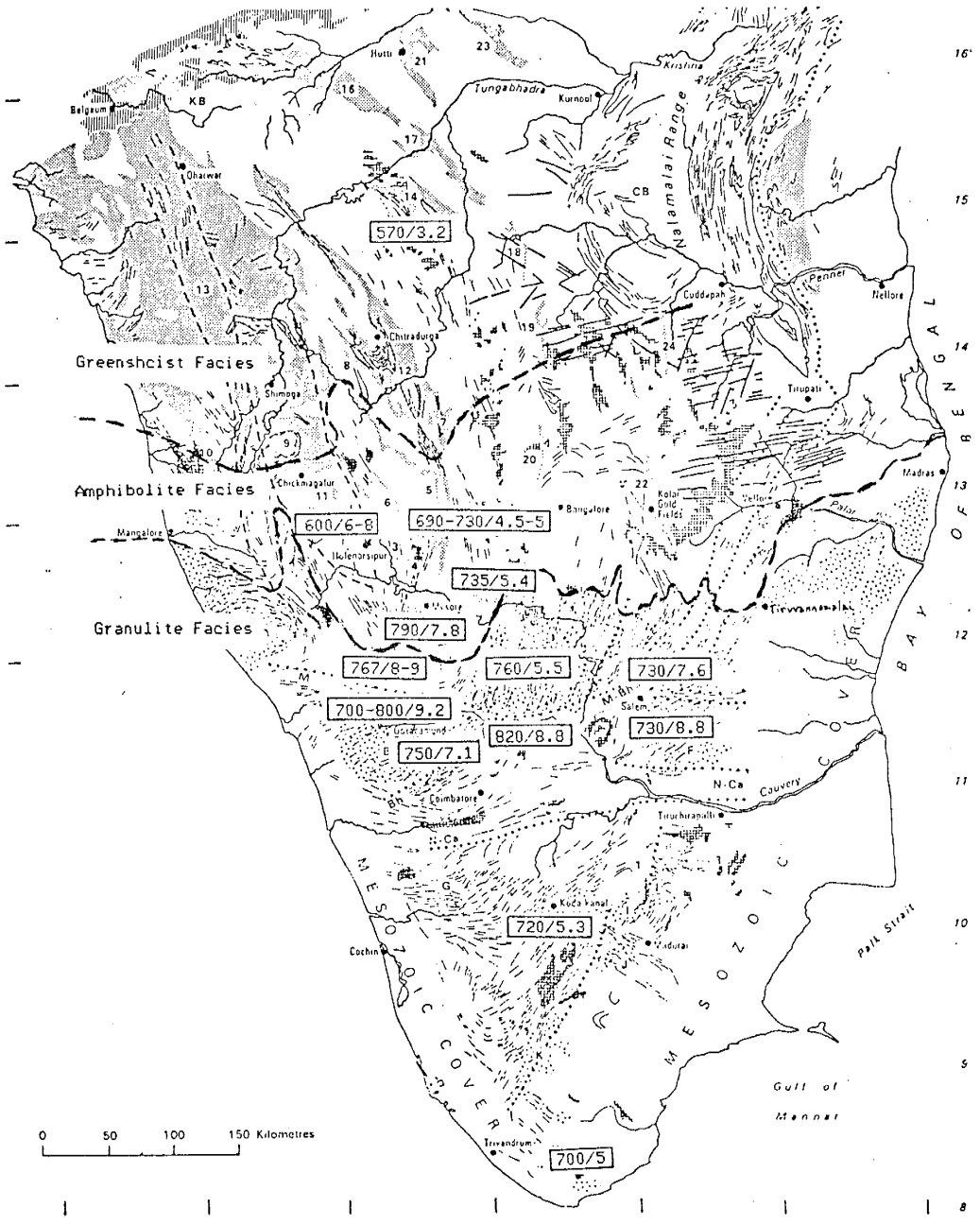

Fig. II-4. Selected temperature-pressure determinations for south India are shown in box as degrees C/kb. Sources for data cited in the text (Section II.3).

low-pressure region of the high-grade terrane (Drury and Holt, 1980).

In the northern block, the high-grade terrane south of the amphibolite-granulite transition extends to the Moyar-Bhavani shear zone, the northern limit of the Palghat-Cauvery shear zone (Drury and Holt, 1980; Drury et al., 1984)(Fig. II-3). It has been estimated that about 70 km of dextral displacement has occured along the Moyar-Bhavani shear zone and the Nilgiri massif is considered the pre-shear southern extension of the Biligirirangan Hills (Drury et al., 1984). Correlation within the high-grade terrane at the eastern end of the shear zone is less certain, but for this study, the Shevaroy Hills and the area adjacent to the north will be considered part of the northern block of the South India Craton.

The high-grade terrane of the southern block, south of the Palghat-Cauvery shear zone, includes both granulite and amphibolite-grade gneisses, migmatites, granites, and supracrustal rocks (Gopalakrishnan et al., 1975; Narayanaswami, 1975; Holt and Wightman, 1983; Ravindra Kumar et al., 1985), and extends to the southern tip of India and into Sri Lanka. The overall N-S structural trend that is predominant in the northern block is absent in the southern block, which has highly variable trends (Drury et al., 1984). The supracrustal sequences in the southern block contain less mafic and ultramafic volcanics and more clastic sediments (Gopalakrishnan et al., 1975; Narayanaswami, 1975), and layered gabbro-anorthosite-ultramafic complexes are also present (Windley and Selvan, 1975). The consistent, north to south temperature and pressure increase characteristic of the northern block is absent south of the Moyar-Bhavani shear zone. Vertical

displacement has exposed blocks of widely diverse environments; for example, temperature-pressure estimates for the north slope of the Nilgiri Massif are 720-900 degrees C and 8.3-9.5 kb (Harris et al., 1982; Janardhan et al., 1982; Raith et al., 1982), and that for the Kodaikanal Massif and Nagercoil, in the south central area of the southern block, are 700-720 degrees C and 5.0-5.3 kb (Harris et al., 1982). In the relatively low-pressure areas such as the Kodaikanal Massif, similar prograde gneiss-charnockite reactions are observed as occur in the prograde Transition Zone of the northern block (Holt and Wightman, 1983; Ravindra Kumar et al., 1985).

The study of the granulite facies and its relationship to amphibolite-grade rocks has had an interesting and long history in south India. Holland (1893, 1900) coined the term "charnockite" and "charnockite series" for granulite-facies rocks in the Madras area, after Job Charnock (died 1692) the founder of Calcutta, whose tombstone in Calcutta had been cut from rock in Madras (Pichamuthu, 1972). The term charnockite as used here refers to a quartzo-feldspathic, acid to intermediate, hypersthene-bearing rock.

The relationship between the high-grade (charnockite) and low-grade (Peninsular Gneiss) terranes in south India has been the subject of much discussion and debate. After examining field and petrographic relationships in a quarry near Salem, Holland (1900) with some reservations concluded that the gneisses had been intruded by a younger charnockite at depth. However, field and petrographic evidence from subsequent studies of other sites in which gneiss and charnockite are both present have led to differing interpretations. Pichamuthu (1953)

summarized the evidence for the predominant views (igneous and metamorphic origins); he concluded that although anatexis may be of local importance, prograde regional metamorphism was primarily responsible for the production of charnockite in southern India. More detailed observations at Kabbaldurga, southwest of Bangalore, by Pichamuthu (1960, 1961), Ramiengar et al. (1978), Janardhan et al. (1979, 1982), and Friend (1981, 1983, 1984) confirmed the role of prograde metamorphism in producing charnockite in that area. Ray (1972), however, using evidence from the same quarry concluded that earlier formed charnockite had undergone deformation to produce gneiss and migmatite. In the Sivasamudram-Malavalli area (20-25 km southwest of Kabbaldurga), conflicting conclusions were reported by Ziauddin and Yadav (1975), who described evidence for a metasomatic origin for the charnockite, and Mahabaleswar and Sodashivaiah (1976), who found the charnockites to be older than the gneisses.

Recent detailed studies examining mechanisms of charnockite formation at Kabbaldurga (Janardhan et al., 1979, 1982; Friend, 1981) suggest that metamorphism of the host tonalitic and granitic gneisses occurred in the presence of a fluid phase with a relatively high CO_2/H_2O ratio. Complicating the problem of charnockite formation in southern India are Proterozoic shear zones, for example the Palghat-Cauvery, which lie south of the gneiss-charnockite prograde Transition Zone and extend across India in a generally east-west trend. Field evidence of gneiss-charnockite relationships along these shear zones indicates that gneiss is retrogressive after charnockite (Janardhan et al., 1982; Drury and Holt, 1980; S.A. Drury, personal communication, 1982). As a result,

prograde relationships that exist in the Transition Zone may be reversed in the shear zones. Janardhan et al. (1982) and R.C. Newton (personal communication, 1982), however, note that the fluorine content of biotite and amphibole in the gneisses may be diagnostic of the direction of metamorphism: in prograde areas the fluorine content is high and in areas that are clearly retrograde, the fluorine is low.

II.4 Field Work

Field work was conducted by myself and Dr. B.L. Narayana of the National Geophysical Research Institute, Hyderabad, over three seasons, generally during the months of January and February for the years 1980, 1981, and 1982. Reconnaissance geology and sample collecting was initially concentrated on the amphibolite-granulite facies transition in the Krishnagiri-Dharmapuri area. This was followed in the second year by detailed mapping across the transition and the collection of additional samples from other relatively low-pressure amphibolite-granulite facies terranes and the medium and high-pressure granulite terranes to the south. During the final season, additional samples of charnockite from high-pressure terranes, and charnockite-gneiss sample pairs from both retrograde areas along the Moyar-Bhavani shear zone and the prograde Transiton Zone were collected.

III Field Geology

This section has been subdivided into sections covering the major terranes addressed in this study: Gneiss Terrane (Peninsular Gneiss Complex), Prograde Transition zone, medium and high-pressure charnockite terrane, and the retrograde gneiss terrane. Of the areas in which samples were collected, only the Krishnagiri-Dharmapuri area of the amphibolite-granulite facies prograde Transition Zone is mapped in detail; the observations recorded for other areas are of a reconnaisance nature associated with sample collection. Areas described in the text are shown on Fig. III-1.

III.1 Peninsular Gneiss complex

Peninsular Gneiss is a term that encompases a large and complex, heterogeneous suite of polyphase tonalitic-granodioritic gneisses. J.J.W. Rogers (1974) has pointed out the need for detailed investigations of the Peninsular Gneiss to determine the geochronology of formation, structural patterns, degree of metamorphism, and the delineation of possible gneiss "provinces" with similar characteristics. Pichamuthu (1970) subdivided the gneisses, in the area around Bangalore, into the following general succession: 1) an augen gneiss with associated "acid veins", 2) streaky or banded gneiss, 3) coarse-grained granodioritic gneiss, 4) medium and fine-grained granitic (sensu lato) gneisses, and 5) aplites and pegmatites. In this study, only a limited number of outcrops were examined in the Bangalore area, and the succession outlined by Pichamuthu could not be substantiated in detail, however, the younger

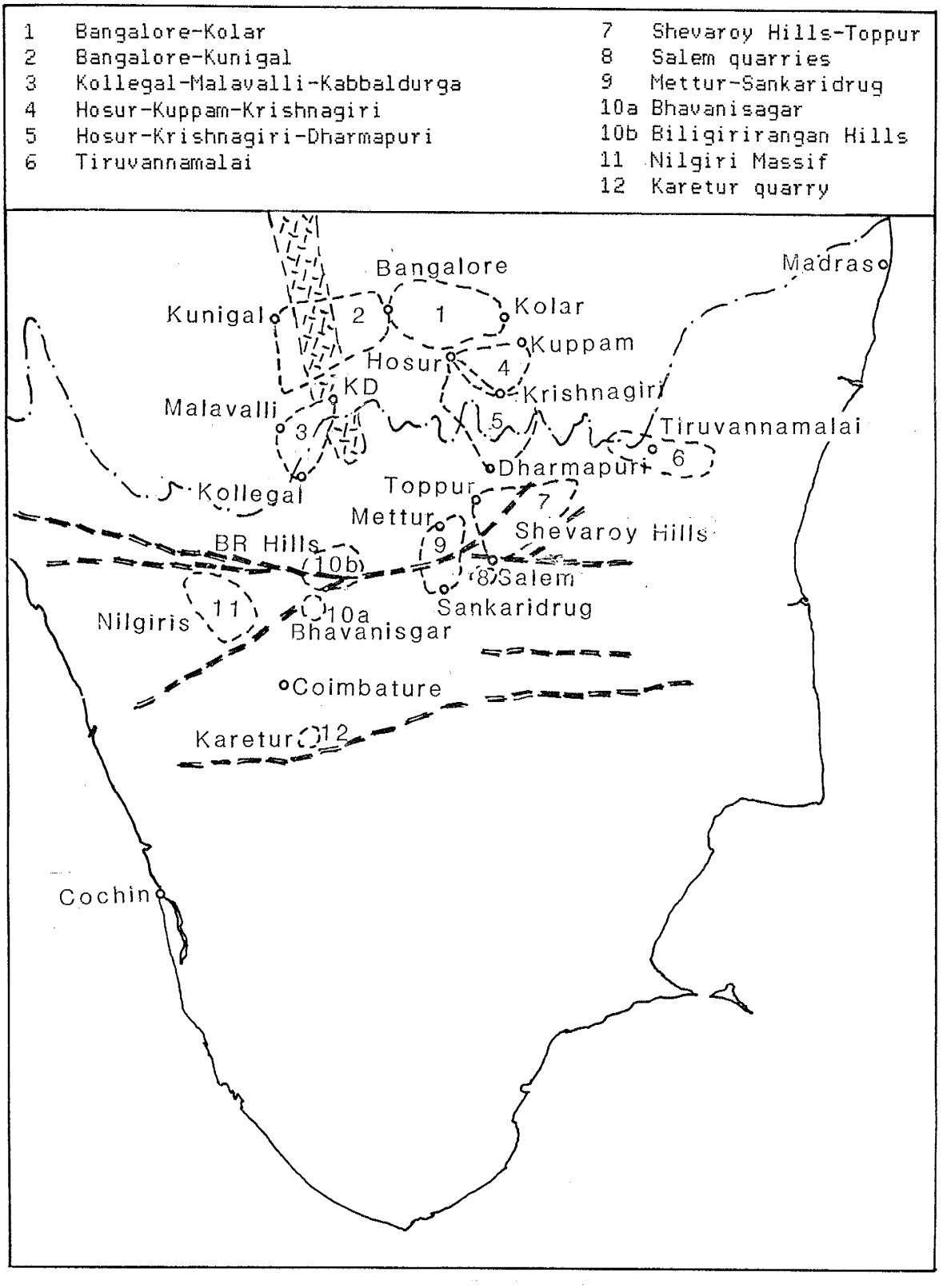

Fig. III-1. Sample and reconnaissance geology areas in south India mentioned in the text. Locations of individual samples are shown on the sample location maps in Appendix D. Broad dashed lines are Proterozoic shear zones. See Fig. II-3 for other identifications.

gneisses appear to be finer grained than the older phases.

III.1.1 Bangalore-Kunigal area

The gneisses vary from relatively homogeneous, medium-grained tonalitic to granodioritic rocks to banded gneisses comprised of three and more phases. In some outcrops these phases include gray, medium to coarse-grained gneisses intruded by a lighter gray, fine to medium-grained homogeneous gneiss. Leucocratic aplite pods and veins, and pegmatite veins, all of varied histories, are usually the youngest rocks. Inclusions of amphibolite of varying sizes are common in the gneisses. As the eastern edge of the Closepet granite is approached, zones of pinkish granitic gneiss and veins of granite are found within the gray gneiss, and blocks of gray gneiss lie within the granite. Friend (1983) has noted that the eastern contact of the Closepet with the Peninsular Gneiss is more diffuse than the sharper western contact. The trends of the gneisses range from N20E to N25W, with N10E predominant.

III.1.2 Bangalore-Kolar area

In the area north and northeast of Bangalore, the trends in the gneisses turn more easterly, N20E to N40E. Dark gray, medium to coarse-grained gneisses, sometimes containing amphibolite inclusions, are intruded by a medium gray homogeneous to foliated gneiss, which is in turn intruded by a light gray, fine to medium-grained homogeneous gneiss. All of the gneisses are cut by younger aplite and pegmatite veins. Towards Kolar, a typical assemblage is characterized by: medium to dark gray, medium to coarse-grained gneisses intruded by

light to medium gray porphyritic gneisses, and younger dark gray and medium gray, fine-grained gneisses; the more frequent occurence of amphibolite inclusions; and leucocratic bands and pegmatite veins of varying ages cross-cutting older phases. Trends are about N10E. Near Kolar, the gneissic terranes that were sampled are typically medium gray, medium-grained, homogeneous gneisses containing amphibolite inclusions and stringers and pods of aplite.

III.1.3 Hosur-Kuppam-Krishnagiri area

In a large quarry (exposed surface > 1 sq km) at Hosur the following phases, in order of decreasing age, were observed: 1) mafic enclaves, 2) a medium gray, coarse-grained gneiss, 3) medium gray, fine to medium-grained gneiss, 4) very light tan and very light gray, fine-grained gneiss, 5) cross-cutting migmatites, and 6) pegmatite veins. The trend of the gneisses is about N20E. The migmatites trend at about N10E and appear to have been formed as a result of a late stage shearing event.

Between Hosur and Krishnagiri, the trend of the gneisses varies between N-S and N20E. The gneisses are gray to light gray, sometimes pinkish gray, medium to coarse-grained, both homogeneous and banded; amphibolite inclusions are ubiquitous. In and north of Krishnagiri in the area covered by detailed mapping, the Gneiss Terrane is divided into six units: 1) hornblende schists of the southernmost extension of the Kolar greenstone belt, 2) contorted, migmatitic gneisses, 3) tectonized homogeneous gneiss, 4) homogeneous gneiss, 5) granitic gneiss, and 6) younger mafic dykes (Fig. III-2).

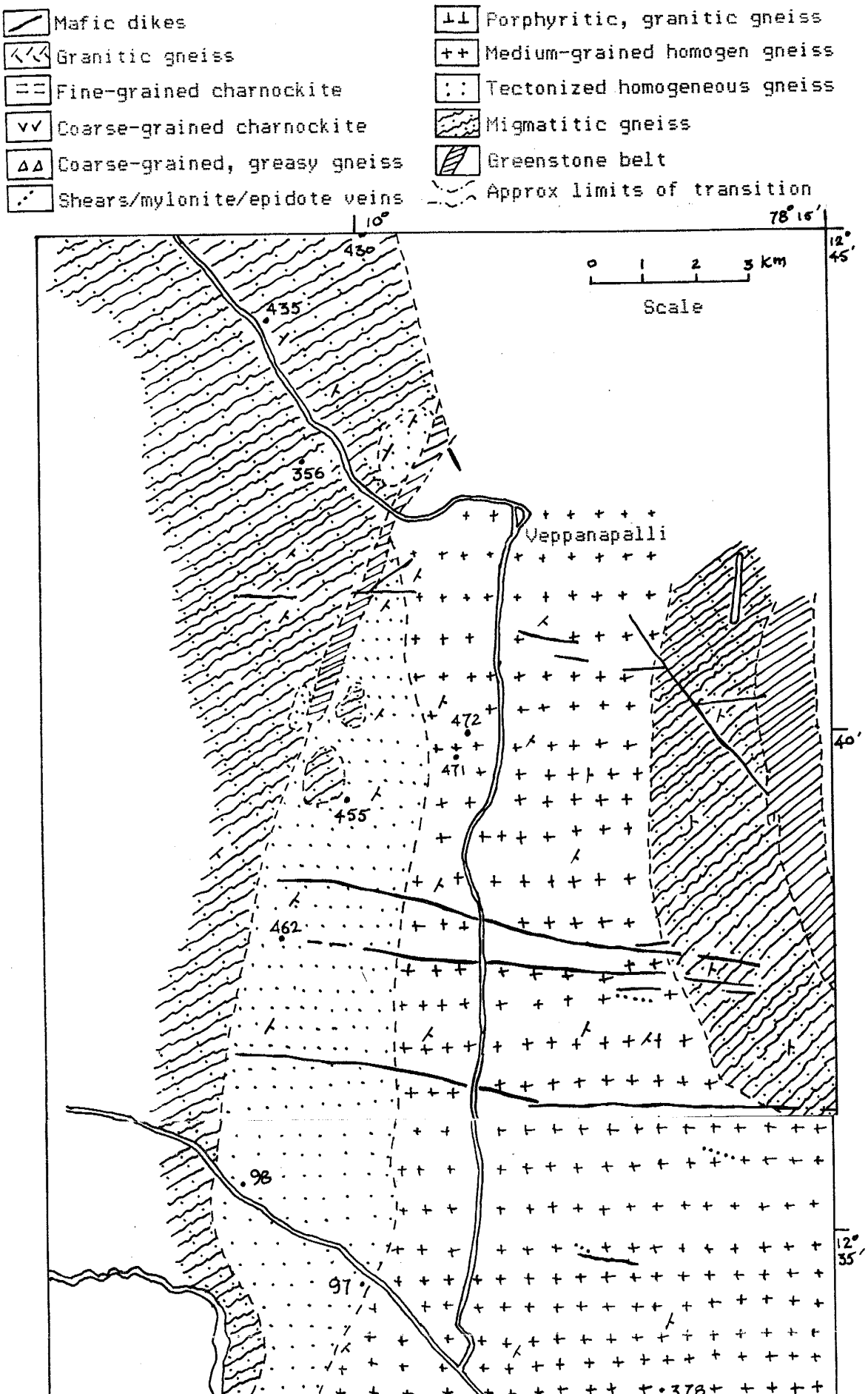
Mafic dikes
Granitic gneiss
Fine-grained charnockite
Coarse-grained charnockite
Coarse-grained, greasy gneiss
Shears/mylonite/epidote veins
Porphyritic, granitic gneiss
Medium-grained homogen gneiss
Tectonized homogeneous gneiss
Migmatitic gneiss
Greenstone belt
Approx limits of transition
78° 15'
10°
12° 45'
0 1 2 3 km
Scale
430
435
356
Veppanapalli
472
471
455
462
98
97
12° 40'
12° 35'

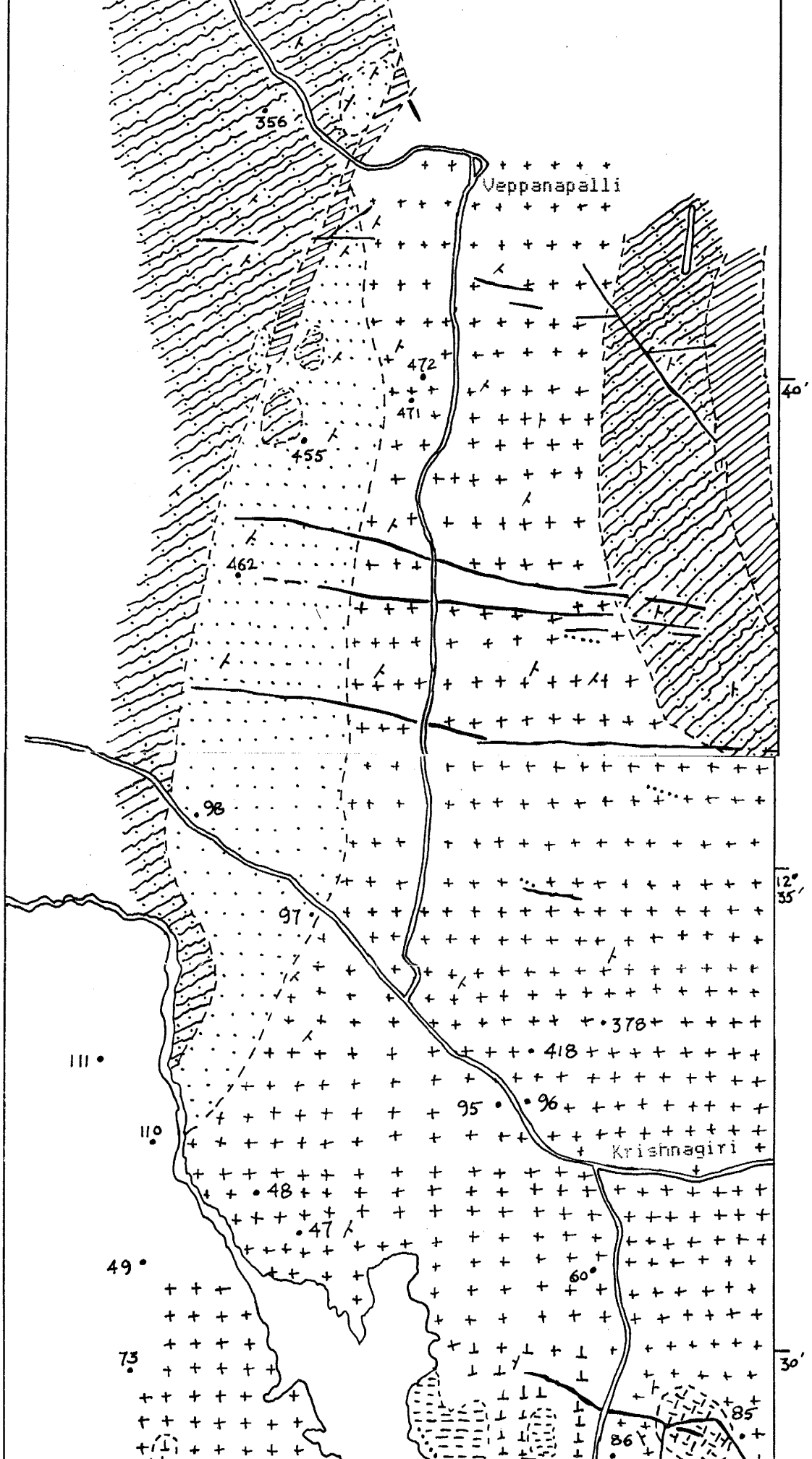
356
Veppanapalli
472
471
455
462
40'
98
97
12°
35'
378
418
111
110
95
96
Krishnagiri
48
47
49
60
73
30'
85
86

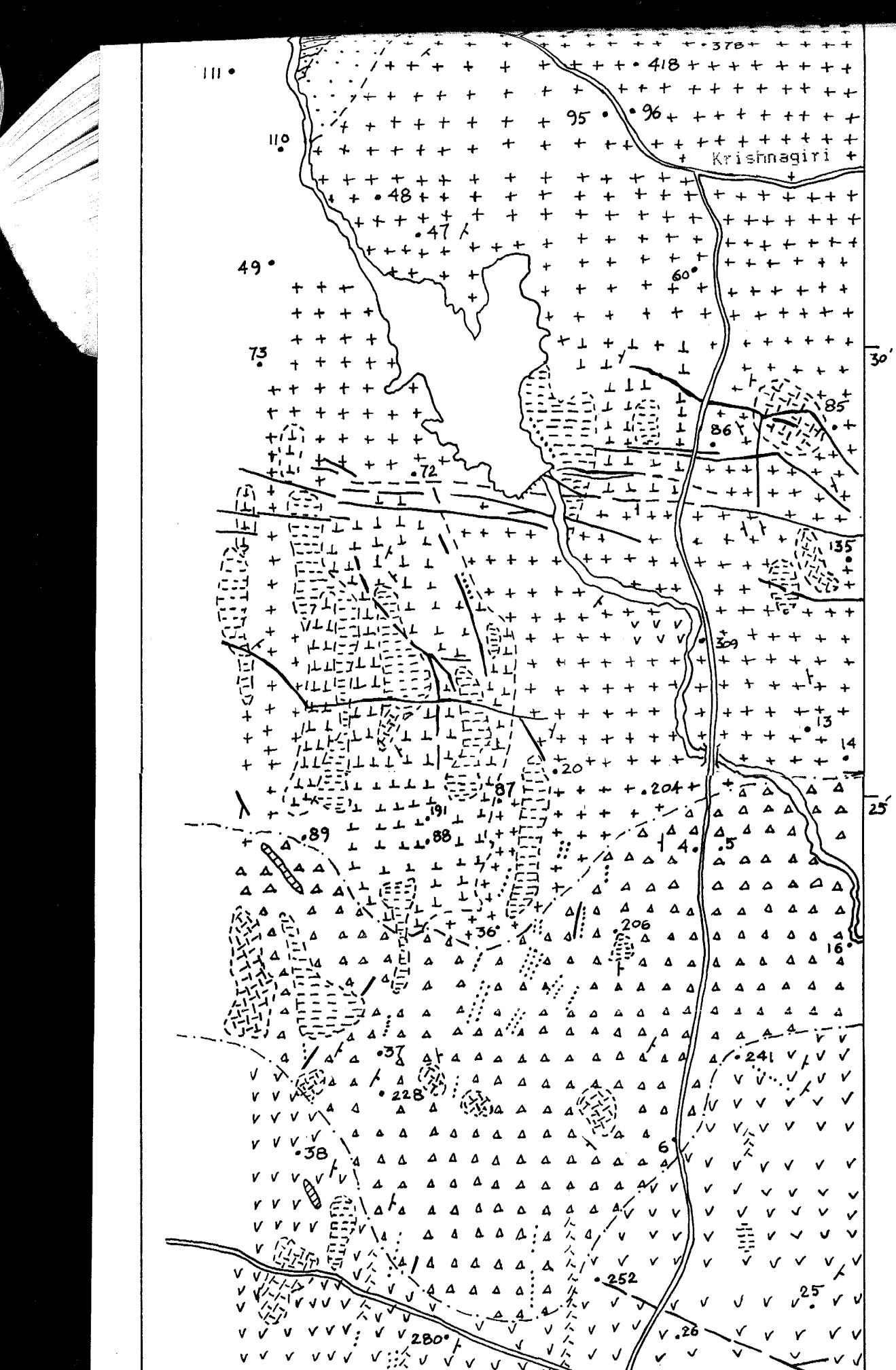
Krishnagiri
111
110
49
73
48
47
95
96
418
378
60
72
85
86
135
309
13
14
20
87
191
204
89
88
4
5
36
206
16
37
228
241
38
6
252
25
280
26
30'
25'

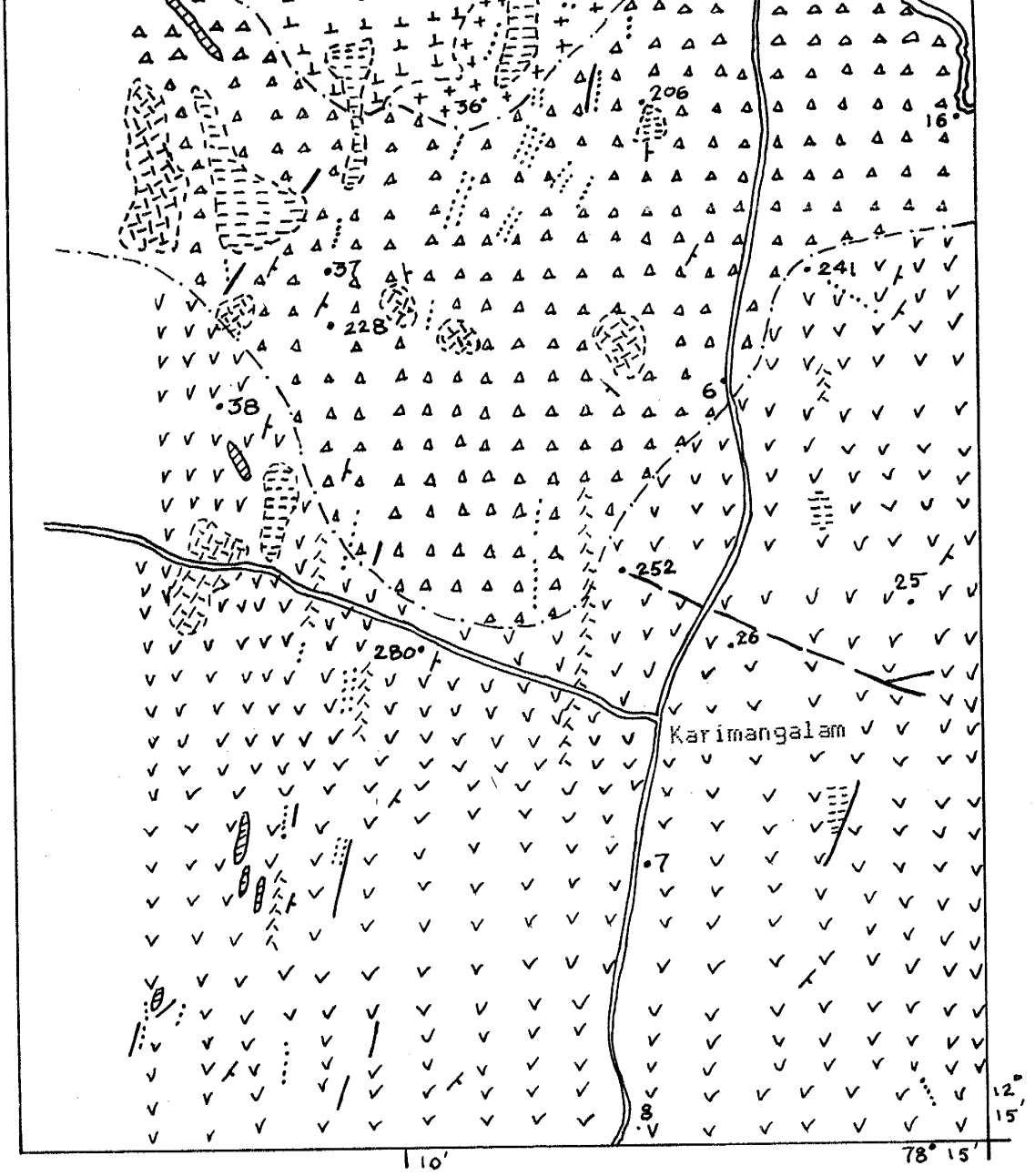

Fig. III-2 . Geologic map of Krishnagiri area, Tamil Nadu, south India, south section. (For the area covered by the composite map, sampling and reconnaissance geology by Narayana and Allen, 1980; the area north of Krishnagiri, mapped by Narayana and Allen, 1981; area south of Krishnagiri, mapped by Narayana, 1981, 1982.)

The contorted-migmatitic gneisses are exposed along both the northeast and northwest sides of the mapped area, adjacent to southern extensions of the Kolar schist belt. B.L. Narayana notes that Viswanatha and Ramakrishnan (1981) describe similar gneisses to the north, along the western margin of the main body of the Kolar schist belt. The oldest phases in the contorted gneiss are hornblende schist enclaves from the Kolar schist belt, and amphibolite inclusions that are also probably remnants of those schists. The amphibolites are sometimes rounded and broken but are more frequently stretched into long dyke-like bands within a migmatitic, medium to coarse-grained gray gneiss. Frequently a dark gray, medium-grained gneiss is concordant with or cross-cuts at shallow angles the earlier phases. Aplites and pegmatites of varying ages are found both as stringers or bands along foliation, and as cross-cutting veins. The gneiss trends N10E to N25E; pseudotachylite shears and flows, generally N20W to N50W with left-lateral displacement, cross-cut most units, though one outcrop showed right-lateral displacement. Some late pegmatites cross-cut the shears.

Along the northwest edge of the mapped area, the transition from the homogeneous gneiss (described below) to the contorted gneiss is gradational, and a transitional unit, the "tectonized" homogeneous gneiss, is delineated and mapped. In the northeast corner of the area, the contact beteen the contorted gneiss and the homogeneous gneiss is sharp. The tectonized gneiss is characterized by a medium gray, homogeneous gneiss that in general becomes progressively more

coarse-grained, foliated, and deformed from east to west across its mapped area. In the more deformed portions of the gneiss, long, stretched mafic inclusions and sinuous, leucocratic, quartzo-feldspathic bands with thin mafic selvedges are pulled out along the foliation. Trends of the gneiss are in the range N15E to N30E. Late stage, discordant pegmatite veins, N35W, are also present. In the more deformed areas, narrow pseudotachylite shear zones trending N10W to N20W cross-cut and offset the gneiss, leucocratic bands, and pegmatite veins. Offset is about 40-50 cm and the sense of movement is left lateral.

The homogeneous gneiss is gray, medium to coarse-grained and trends N5E to N20E. Foliation is weakly developed if at all. Mafic inclusions are present locally and though typically <30 cm in length, enclaves 7-8 m in length are found. Leucocratic, fine-grained gneisses or aplites are seen as pods and sickle-shaped masses (sometimes reaching 60 m in length) in the Krishnagiri area, and become lenticular shaped pods and bands, or are absent, to the north. The leucocratic bands are concordant with the foliation in some places and cross-cut at shallow angles in others, suggesting syn and/or post-tectonic injection. Late-stage pegmatite veins, more common in the Krishnagiri area than to the north of the mapped area, trend N35W to N50W, cross-cutting the gneisses and mafic inclusions.

In the area north of Krishnagiri, a single granite body was observed at the extreme north of the mapped area (sample site 430). Only the southern extremity of the pink, medium to coarse-grained granite was examined (total size of exposure not determined but in excess of 4 sq km). The granite is clearly intrusive into the contorted gneiss; in the area adjacent to the granite the gneiss is variably gray to pink in color.

Cross-cutting all of the gneisses are younger (Proterozoic) amphibolite dykes that trend N40W to N85W. These dykes are common in the area north, and immediately south, of Krishnagiri; they are not as distinctive in the low-pressure charnockite terrane between Krishnagiri and Dharmapuri, perhaps because their presence is masked by dark gray charnockite.

III.2 The prograde Transition Zone and Karetur quarry

III.2.1 Hosur-Krishnagiri-Dharmapuri area

Moving south from the Gneiss Terrane into the transition zone, the homogeneous gneisses become more migmatized; both porphyritic and fine-grained, banded gneisses are more prominant; pink gneisses and small granitic migmatites infolded in the gneisses become common; and concordant and cross-cutting pegmatite veins, frequently boudinaged, are increasingly more abundant. Granitic material is typically present in pink gneisses and cross-cutting veins. Infrequently, small granite domes (<1500 sq m) and dike-like intrusions are seen. In some areas, the gray, medium to coarse-grained gneiss appears to be intruded by a light gray and very light gray, fine-grained gneiss; in

other areas, the relationship between the coarse-grained and fine-grained gneisses is not clear. Generally there is a gradational relationship between the gneiss units mapped in the transition zone; for example, areas shown as fine-grained gneisses are predominantly fine-grained gneiss but will commonly contain all other types as well. The porphyritic gneisses are gray to pinkish gray, and have porphyroblasts of K-feldspar and frequently large biotite. The pink gneisses are medium to coarse-grained and are gradational with the gray gneisses; in some areas small, localized, migmatitic granites have developed. Pegmatite veins, frequently hornblende bearing, cross-cut the gneisses. Amphibolite inclusions are common in both the coarse-grained and fine-grained gneisses. As the Transition Zone is crossed, the gray and pink gneisses and the cross-cutting granitic and pegmatitic veins become glassy, then greasy in appearance as hypersthene increases in abundance.

In the Krishnagiri-Dharmapuri area, the actual transition from gneiss to charnockite is seen in only a few outcrops. Typically, migmatitic, gray and pink gneisses and their localized granites develop glassy or greasy blotches that appear, in the initial stages, to be controlled by the presence of mafic minerals; moving in the direction of the charnockite terrane, the blotches grow together into larger masses of charnockite. The charnockites are dark gray (sometimes greenish gray), greasy, fine to coarse-grained and porphyritic, and homogeneous to migmatitic; though textures are frequently obscured by the greasy appearance of the charnockite, the textures generally duplicate the range found in the amphibolite grade

gneisses north of the transition. The dark pinkish-gray, hypersthene-bearing granitic and pegmatitic veins within the charnockite indicate that these intrusions preceded charnockitization. Though the relationship between amphibolite-grade gneiss-granite-pegmatite and granulite-grade charnockite is predominantly a gradational one, infrequently, local occurences of remobilized gneiss intruding charnockite are found.

The trend of the foliation in the gneisses, charnockitic gneisses, and charnockites is N to N25E. Linear shear zones expressed by localized epidote veins and/or pseudotachylites have similar trends in both the Transition Zone and in the low-pressure charnockite terrane. No shearing or faulting is found parallel to the transition. Field evidence thus indicates a gradual transition from 1) the generally homogeneous to foliated gneisses north of Krishnagiri, to 2) migmatitic and granitic gneisses just south of Krishnagiri, to 3) charnockitic gneisses between Krishnagiri and Dharmapuri, to 4) charnockite near Dharmapuri.

III.2.2 Kollegal-Malavalli-Kabbaldurga area

In the Kollegal-Malavalli-Kabbaldurga area, the rocks and their relationships are similar to those in the Krishnagiri-Dharmapuri transition. Exposures at the Kabbaldurga quarry cover an extensive area (about 1 sq km) and are typically fresh as the result of continuous quarrying. Amphibolite inclusions or enclaves in the gneisses are found both as long, stretched bands and as rounded, fragmented masses. A medium gray, medium to coarse-grained, foliated

to banded gneiss, which may be the oldest gneiss unit, is intruded by a light gray, fine-grained, homogeneous gneiss. Pink gneisses, sometimes associated with veins of aplite or pegmatite, infiltrate or are infolded in the gray migmatitic gneisses. Pink, medium-grained granites also develop locally as large masses that intrude and cross-cut the foliation of the earlier gneisses. Late stage shears and pegmatites cross-cut all units.

In areas of incipient charnockitization, the charnockite appears as dark, greasy, discontinuous patches in the gneiss, with the gneiss-charnockite contact diffuse over 1-3 cm. These patches grow together into continuous branches or large masses as the degree of charnockitization increases. Structural inhomogeneities that cross-cut the gneisses, which might control the formation of the charnockites, are subtle and not generally observed. Although charnockite cross-cuts the fabric of the gneisses, charnockite in its initial stages appears to develop preferentially along foliation planes in the more mafic portions of the gneisses. The trend of the gneissic texture at Kabbaldurga is about N15E; in adjacent areas similar gneisses are found with trends of N to N15E.

III.2.3 Tirumannamalai area

At the few outcrops examined in the Tiruvannamalai area, the gneiss is more homogeneous than at Krishnagiri or Kabbaldurga. The gneiss is typically medium to dark gray, fine to medium-grained, with amphibolite inclusions and late-stage, cross-cutting pegmatites. Trends of the gneisses are N30E to N40E. The charnockite is medium to

coarse-grained and develops as dark gray, greasy patches and fingers in the gneiss. The charnockite pegmatite veins contain hypersthene and are medium gray and greasy. East of Tiruvannamalai, at the edge of a large granite intrusive, blocks of a gray, medium to fine-grained, homogeneous gneiss and a charnockitic, porphyritic granite with prominate hypersthene are caught up in a younger, pink, medium-grained granite. This suggests that in this area there was more than one intrusive event; an earlier, now granulite grade, granite, and a younger granite that intruded and picked up both amphibolite grade gneiss and granulite grade granite. The younger of the granites, which appears to outcrop over an area >150 sq km, is typically gray to pinkish gray, medium to coarse-grained, and locally porphyritic with large pinkish gray K-feldspars in a gray matrix. In the area east of Tiruvannamalai, with the exception of a few localities where hypersthene is seen, the granites are predominantly amphibolite grade.

III.2.4 Karetur quarry

In the Introduction it is noted that the South Indian Craton is divided into northern and southern crustal blocks by the Palghat-Cauvery shear zone. The southern block is characterized by uplifted blocks of differing vertical displacement that expose both high and low-pressure granulite and amphibolite-facies environments. The term "prograde transition zone" as used here delineates that area in the northern block that corresponds to a vertical section of the crust in which the transition from amphibolite to granulite-facies takes place. Exposures at the Karetur quarry, located in the southern

block, show similar relationships between gneiss and charnockite, and Karetur is regarded as a section of the vertical crust similar to that exposed in the prograde Transition Zone of the northern block.

Karetur is located south of Coimbatore at the foot of the Anaimalai Hills near the southern margin of the Palghat-Cauvery shear zone (Fig. II-3). The quarry lies around the circumference of a steep-sided, bald, rock dome that rises about 50 m above the surrounding flat terrain, and covers an area of <0.1 sq km. The northwest side of the dome shows the patchy development of dark gray, greasy charnockite in a gray, medium to coarse-grained gneiss that locally is granitic and contains stretched or folded mafic inclusions. Charnockitization progressively envelopes all phases of the gneiss and inclusions, though on a small scale it frequently appears controlled by the abundance of mafic minerals. Typically the structural controls guiding charnockitization are obscured; however, in some instances thin fractures or shears that cross-cut the gneiss and inclusions appear to direct the fluids responsible for charnockitization. On the east and southeast sides of the dome the relationship between gneiss and charnockite is reversed and the gneiss is retrograde after charnockite. These relationships are described in Section III.4.4, below.

III.3 Intermediate and high-pressure terrane

The areas in which these charnockites were observed and sampled lie near or south of the Moyar-Bhavani shear zone. Overall exposures are poorer than for the gneiss and low-pressure charnockite terrane described above. The Nilgiri Massif, the Biligirirangan

Hills, and the Shevaroy Hills rise abruptly from the relatively flat, sediment covered Coimbatore basin. These massifs are steep-sided and forested, and large expanses of fresh surfaces are generally confined to road cuts. In the low-lying areas, quarrying for road metal and building stone is present on a reduced scale relative to the low-pressure terranes and largely confined to outcrops at the foot of large hills or ranges of hills; for example, the Salem quarries lie at the base of the northwestern extremity of the Kollaimalai Hills. The dark color and greasy luster of the charnockites mask the texture and veining of the rock, and examination of these features was generally restricted to the bleached, retrograde gneisses described below. As a result of the masking, the degree of foliation and abundance of granitic and pegmatitic material in the charnockite is difficult to determine from a cursory examination of outcrops.

III.3.1 Toppur-Mettur area

The charnockite is dark gray, greasy, and both homogeneous and foliated to banded. The more mafic charnockite typically contains large porphyroblasts of garnet that are usually found in mafic bands that also contain horblende. Stretched mafic inclusions and greasy pegmatites are common. In some exposures, the pegmatitic veins are boudinaged. Trends are N to N45E. Metamorphosed mafic to ultramafic, and micaceous supracrustal rocks were observed at two localities and are probably extensive in the Toppur-Mettur area.

III.3.2 Shevaroy Hills and adjacent area

At lower elevations, the charnockite is dark gray to medium gray, medium to coarse-grained, glassy to greasy, and typically homogeneous; weakly foliated varieties are sometimes present. Mafic inclusions and greasy pegmatite veins are frequent but not ubiquitous. At higher elevations, garnet is sometimes seen as pods and veins in a relatively homogeneous to weakly foliated charnockite. Mafic inclusions, sometimes garnet-rich, are present but not common. Immediately south of Salem at the foot of the northernmost extension of the Kollaimalai Hills, the charnockites are medium gray to dark gray, medium to coarse-grained, weakly to moderately foliated, and greasy in appearance. Trend is about N20W to N30W. Thirty kilometers southwest of Salem, near Sankaridrug, a pink, medium to coarse-grained granite intrudes a strongly foliated to migmatitic, N30W-trending gneiss that may be a western extension of the retrograde gneisses found at Salem.

III.3.3 Nilgiri Massif

Outcrops with fresh surfaces were largely confined to roadcuts. The charnockite is medium gray to very dark gray and medium to coarse-grained. On the southeastern slope, the charnockite is foliated and sometimes contains stretched mafic bands and coarse-grained, quartzo-feldspathic veins concordant with the foliation. Garnet commonly develops in the more mafic bands and pods. Trend of foliation in the southern slopes is N40E to N60E. Charnockite in the central and northern areas is somewhat more homogeneous and the trends

are more northerly, N10E to N20W. Pegmatites concordant with the foliation are also found.

III.3.4 Biligirirangan Hills (south slope)

The outcrops examined were confined to roadcuts on the Sathyamangalam-Bangalore road and cover a vertical rise of about 600 m up the very steep southern margin of the Biligirirangan Hills. This margin marks the northern limit of the E-W trending Moyar-Bhavani shear zone. The charnockite is medium gray to very dark gray, medium to coarse-grained, homogeneous to weakly foliated, and greasy.

III.4 Retrograde gneiss areas

III.4.1 Salem

The relationships between charnockite and gneiss in the Salem area were examined in a group of quarries about 5.5 km south of Salem town that covers an area of about 2 sq km. The charnockites are typically medium to dark gray, and greasy and are cross-cut by subparallel, linear to curvilinear, bleached zones of retrograde gneiss with a diffuse, 1-3 cm boundary between gneiss and charnockite. As the retrogression increases, the narrow bleached zones grow into large islands of gneiss within the charnockite. Bleaching at the actual transition between charnockite and gneiss spreads locally along foliation, but the linear zones of bleached gneiss are controlled by thin fractures that typically cross-cut the gneissic foliation. The gneisses are light gray to medium gray, medium to coarse-grained, and in general are strongly foliated.

Migmatitic gneisses and narrow, pseudotachylitic (trap shotten) shear zones are present in some areas. However, the retrograde gneisses appear more homogeneous than those of the prograde Transition Zone, and migmatites and granitic material are not as common.

III.4.2 Bhavanisagar quarry

The charnockites and gneisses were observed in a large quarry about 6 km south of the town of Bhavanisagar. This area is considered to be a part of the eastern foothills of the Nilgiri Massif (Viswanathia and Tareen, 1970; Janardhan et al., 1982). The medium to dark gray charnockites, some with garnet, are cross-cut by linear to curvilinear bleached zones of light gray to medium gray, foliated gneiss, also with garnet. The bleached areas have diffuse borders and are controlled by thin fractures similar to the retrograde gneiss at Salem. Mafic to ultramafic inclusions and enclaves are present as are concordant and cross-cutting pegmatitic quartzo-feldspathic veins. Trend of the foliation is about N50E.

III.4.3 Biligirirangan Hills

Near the town of Binkanhalli (Fig. II-3) in the southern Biligirirangan Hills, charnockites are dark gray, greasy, medium-grained, and homogeneous to weakly foliated. Narrow, linear, bleached zones of retrograde gneiss controlled by thin fractures cross-cut the charnockites in a manner similar to the quarries at Salem and Bhavanisagar. The retrograde gneiss is gray and weakly foliated.

III.4.4 Karetur quarry

Karetur quarry is located south of Coimbatore (Fig. II-3). As noted in Section III.2.4, the quarry, which surrounds a bald, rock dome, shows evidence of prograde amphibolite to granulite facies metamorphism along its northwest quadrant; on the east and southeast sides of the dome the relationship between gneiss and charnockite is retrograde. Here the rock is dark gray, greasy charnockite cross-cut by narrow, diffuse, bleached zones of gneiss that are controlled by thin fractures. These bleached gneisses are similar in occurence and appearance to the retrograde gneisses described in Section III.4, though the large islands of retrograde gneiss seen at Salem have not developed here. The close proximity of prograde metamorphism (gneiss to charnockite) and retrogression (charnockite to gneiss) may be the result of the heterogeneous development of charnockite in which large masses of charnockite grow adjacent to unmetasomatized gneiss. As the adjacent gneiss is charnockitized, in its turn, water-rich fluids are released from its hydrous mineral phases and rise along fractures or zones of high permeability. The earlier-formed charnockite would be retrogressed (rehydrated) along the fractures or zones guiding the fluids released from the lower-lying, now charnockitizing gneiss. The retrograde east side of the dome at Karetur may have been situated above, and charnockitized before, the north side, which as it expelled water during charnockitization, selectively retrograded the overlying charnockite along fractures. Similar occurences of prograde and retrograde reactions are reported by Holt and Wightman (1983) from the Bodinayakkanur area of the Kodaikanal Massif, also of the southern

block (Fig. II-3). R.C. Newton (personal communication) reports the occurence of retrograde gneisses in a quarry at Channapatna, north of Kabbaldurga. Retrograde gneisses have not been observed in the Hosur-Krishnagiri-Dharmapuri area of the prograde transition zone. The samples collected at Karetur for this study were taken from the north, prograde side of the dome.

III.5 Summary and conclusions

III.5.1 Gneiss Terrane

The Gneiss Terrane (Peninsula Gneiss Complex) in the area immediately east and west of Bangalore is comprised of gray to dark gray, medium to coarse-grained, foliated gneisses, and gray and light gray, fine to medium-grained homogeneous gneisses. The coarser-grained gneisses appear to be the oldest phases of the gneisses, which is similar to the succession of augen and coarse-grained gneisses followed by medium and fine-grained gneisses observed by Pichamuthu (1970). Amphibolite inclusions are common. The youngest units are concordant and cross-cutting, fine-grained aplites, and pegmatites. The trends of the gneisses are predominantly N5E to N20E. The major granitic body in the Gneiss Terrane is the red to dark red, medium to very coarse-grained Closepet Granite; the contact of gneiss and Closepet granite is relatively sharp along its western edge, and gradational on the east, with blocks and islands of gray and pinkish gray gneiss lying in the granite.

North of Krishnagiri the terrane is comprised of gray, medium to coarse-grained, homogeneous gneiss with amphibolite inclusions and aplite pods and lenses; a tectonized, homogeneous gneiss that is transitional between the homogeneous and the contorted gneiss; and contorted-migmatitic gneisses with cross-cutting aplites and pegmatite veins. Trends of the gneisses are N5E to N25E. Pegmatite veins, found in all of the gneisses but more common towards the Transition Zone, trend N35W to N50W. Cross-cutting the tectonized gneiss, the contorted gneiss, and the younger pegmatite veins are narrow, N20W to N50W-trending pseudotachylitic shears, typically with left lateral movement. Adjacent to the contorted-migmatitic gneisses are southern outliers of the Kolar Schist Belt, amphibolite inclusions that may be remnants of the schists, and a granite intrusion.

III.5.2 Prograde Transition Zone

As the prograde Transition Zone is approached from the north, the gneiss, which include gray, coarse-grained, foliated gneisses and apparently younger, lighter-gray, finer-grained, more homogeneous gneisses, becomes more migmatitic. Granites, granitic migmatites, typically with porphyroblasts of K-feldspar, pegmatites, and aplites increase in frequency. Trends in the gneisses range from N to N15E southwest of Bangalore, to N to N25E near Krishnagiri, and N30E to N40E at Tiruvannamalai. Approaching the transition, the gneisses, migmatites, and localized granites develop greasy patches of charnockite that cross-cut foliation and grow into masses of dark gray, greasy, homogeneous charnockite. Greasy, hypersthene-bearing granitic and pegmatite veins indicate the intrusion of granite and

pegmatite prior to charnockitization. In rare instances, stretched lenses and bands of charnockite were observed in remobilized gneiss, and at Tiruvannamalai an amphibolite-grade granite intrudes older charnockitized gneiss and granite. In the Transition Zone, shears and faults generally trend N-S, similar to the foliation of the gneisses. Field evidence of consistent, gradational change suggests that the transition from amphibolite to granulite-grade gneisses is the result of exposure of increasingly deeper levels of crust and not the result of an uplifted fault block.

III.5.3 Medium to high-pressure terrane

Exposures of charnockite are restricted in size and frequency. The charnockites are typically gray to dark gray, greasy, medium-grained, and homogeneous to weakly foliated in appearance. Infrequently, mafic inclusions and greasy pegmatites were observed. In the more mafic charnockites or along mafic bands, garnet porphyroblasts are usually present; however, garnet was not observed on the south slopes of the Biligirirangan Hills. Trends of the charnockite are highly variable: N to N45E at Toppur; N20W to N30W at the Salem quarries; N50E at the Bhavanisagar quarry, at the foot of the Biligirirangan Hills; N40E to N60E along the south slope of the Nilgiri Massif; and N10E to N20W in the central areas and north slope of the Nilgiri Massif. At Sankaridrug, southwest of Salem, a large granite intrudes foliated gneiss, which may be an extension of the retrograde Salem gneiss, and as a result the granite may be retrograde after granulite-facies granite.

III.5.4 Retrograde gneiss areas

In the retrograde gneiss areas of the medium to high-pressure terrane, gray to dark gray, greasy charnockites are cross-cut by bleached zones of medium to coarse-grained retrograde gneiss. At Bhavanisagar, both the charnockite and retrograde gneiss contain garnet, and mafic to ultramafic inclusions and cross-cutting pegmatites are found. Retrograde gneisses were not observed in the Hosur-Krishnagiri-Dharmapuri area but have been reported at Chanapatna north of Kabbaldurga.

IV Petrography

This section has been subdivided, like that on Field Geology, by major terrane (Gneiss Terrane, Prograde Transition zone, medium and high-pressure charnockite, and retrograde gneiss) and specific geographical areas within each terrane (Fig. III-1). Samples have been broadly grouped by mineralogy and chemistry: tonalitic gneiss, granodioritic gneiss, granite and granitic gneiss, low-pressure charnockite, low-pressure granitic charnockite, medium and high-pressure charnockite, and mafic granulite. (For additional detail on this classification, see V.1, Chemical Results, Introduction.) Although the retrograde gneiss terrane lies within the high-pressure charnockite terrane, the retrograde gneisses and associated charnockites are treated as a special class. Sample numbers are given at the beginning of the area subdivisions. More detailed petrographic descriptions are located in Appendix B and sample locations are given in Appendix D.

IV.1 Gneiss Terrane

IV.1.1 Bangalore-Kolar (BK) area

(BK) Granitic gneiss (sample: BG1)

The gneisses in this area range from tonalitic to granitic. The one sample for which petrographic analysis was made is of a light gray, coarse-grained gneiss that is tonalitic in appearance. In thin-section, however, the rock is granitic with hypidiomorphic granular texture. Abundant microcline (40%) is present both as subhedral crystals and as late-stage, intergranular megacrysts and perthite is common. Plagioclase (An 30) comprises 25% of the sample , has sharp, generally straight twin lamellae, and shows some saussuritization; antiperthite is not seen. Quartz (29%) has undulose extinction. Biotite (3%) is greenish and lath-shaped with localized chlorite-epidote mineralization. Accessory minerals include opaques, sphene, zircon, apatite, and allanite. Epidote, sericite, chlorite, and carbonate are present in trace amounts. Myrmekite is infrequent.

IV.1.2 Hosur-Kuppam-Krishnagiri (HKK) area

(HKK) Tonalitic gneiss (samples: 103, 104)

The tonalitic gneisses are gray, medium-grained, and homogeneous to foliated. Texture is hypidiomorphic granular to granoblastic. Plagioclase (An 22-25) comprises 53-65% of the samples, has some antiperthite and varying degrees of saussuritization; twin lamellae are frequently absent. Quartz (20-26%) has undulose extinction and sometimes mortar texture along margins. Microcline (1-5%) is found both as subhedral crystals and intergranular megacrysts. Biotite (10%) is seen as pale yellow to dark brown laths, and as anhedral reddish brown stains. Hornblende (0.4-2%) is olive-brown to green. Accessory minerals include opaques, sphene, zircon, and apatite. Epidote (~1%) and trace amounts of sericite, chlorite, and carbonate are also found. Myrmekite is developed along plagioclase-microcline joins.

(HKK) Granodioritic gneiss (samples: 99-1, 99-2,101-1)

The gneiss is light gray and pink to dark gray, medium and coarse-grained. Texture is granoblastic to cataclastic. Plagioclase (An 24-27) comprises (43-53%) of the samples, has some antipertite and minor saussuritization; twin lamellae are usually absent. Microcline (17-26%) is present as both subhedral crystals and intergranular megacrysts. Quartz (16-20%) has undulose extinction in the larger grains; granulated, polygonal mortar texture is frequent along margins. Biotite (7-17%) is found as yellow to very dark olive-brown laths and as reddish brown to light brown, anhedral stains.

Accessories include opaques, zircon, apatite, and allanite. Trace amounts of chlorite and epidote are sometimes present. Mortar texture, myrmekite, and infrequent mylonite is also found.

(HKK) Granitic gneiss (sample: 99-3)

The gneiss is pink gray, medium to coarse-grained, and foliated. Texture is porphyroblastic to cataclastic. Plagioclase (An 28) comprises 38% of the sample, is usually devoid of twin lamellae, and shows saussuritization; antiperthite is rare. Quartz (17%) has undulose extinction. Microcline (41%) is present as subhedral crystals and intergranular megacrysts with some perthite. Biotite (3%) is present as yellow to brown laths that show a rough foliation. Accessory minerals are opaques (1%), rutile needles in quartz, zircon, and apatite. Epidote group minerals (0.1%) and traces of sericite, chlorite, and carbonate are also present. Mortar texture, myrmekite, and oriented biotite are found along shear lines.

IV.2 The Prograde Transition Zone

IV.2.1 Kollegal-Malavalli-Kabbaldurga (KMK) area

(KMK) Tonalitic gneiss (sample: 119-4)

The tonalitic gneiss is light gray, fine-grained, and homogeneous. Texture is granoblastic. Plagioclase (An 24) comprises 56% of the sample, has deformed twin lamellae, when present, and occasional antiperthite. Quartz (12%) usually has undulose extinction. Microcline (2%) is present predominantly as intergranular cyrstals. Olive-green hornblende (24%) is frequently associated with opaques and apatite. Biotite (0.4%) is present both as brown to yellow laths and as late stage reddish brown anhedral stains and margins on hornblende. Accessories include opaques (5%), zircon, and apatite. Some myrmekite is also present.

(KMK) Granodioritic gneiss (sample: 484-1b)

The gneiss is gray, medium-grained, and foliated. Texture is granoblastic. Plagioclase (An 29) comprises 50% of the sample, with twin lamellae usually absent or bent; antiperthite is not observed. Quartz (21%) commonly has undulose extinction. Microcline (19%) is predominantly seen as intergranular megacrysts. Biotite (6%) is present as brown to yellow laths; hornblende (3%) is olive-green. Accessories include opaques (1%), zircon, and apatite. Sericite, chlorite, and carbonate are not observed. Myrmekite is infrequent.

(KMK) Granitic gneiss (samples: 118-2, 119-2)

The granitic gneisses are pink, fine to medium-grained, and relatively homogeneous. Texture is granoblastic. Plagioclase (An 23-28) comprises 34-48% of the samples; twin lamellae are absent or deformed, and variable degrees of saussuritization are present. Antiperthite is rare or absent. Microcline (34%) is usually present both as subhedral crystals and as larger, intergranular cyrstals. Quartz (17-28%) commonly shows undulose extinction. Biotite (1-4%) is present as pale yellow to dark olive-brown, crinkle-textured laths and as anhedral stains. Hornblende is absent or present in trace amounts only. Accessory minerals include opaques, sphene, zircon, apatite, and allanite. Sericite, chlorite, and carbonate are also present. Myrmekite is found at plagioclase-microcline joins.

(KMK) Low-pressure charnockite (samples: KDA2, 119-5, 120-1
120-2, 120-4, 122-1, 122-2, 562-1)

The charnockites are predominantly gray to dark gray, medium-grained, and both homogeneous and foliated. Textures are hypidiomorphic granular to granoblastic, and for samples 122-1, 122-2, and 562-1, mylonite and microfractures are present and texture is granoblastic to cataclastic. Plagioclase (An 25-31) comprises 59-71% in the samples; twin lamellae are commonly absent or bent, and saussuritization and antiperthite are usually present. Quartz has a range of 6-18% in the intermediate charnockites and 23-37% in the silicious charnockites. The quartz usually has undulose extinction and variable amounts of mortar texture are seen in most samples.

Microcline is not generally observed except in sample KDA2 where it comprises 1.5%. Biotite (1-7%) is typically present both as yellow to brown laths and as anhedral, reddish brown stains along the margins and cleavages of some hypersthene grains. Hypersthene (1-8%) is usually pleochroic in shades of pale pink to pale green, and frequently has a lenticular or lath-shapped habit after biotite. Sample 119-5, which has a somewhat lower silica content (61%) than the other samples in this group, has a significant abundance of olive-green hornblende (38%) and 2% pale gray-green clinopyroxene. Accessories for all samples include opaques (0.2-2%), zircon, and apatite. Sericite, chlorite, and carbonate are also found in variable but trace amounts. Sample 120-4 shows a relatively high degree of alteration and plagioclase is partially saussuritized. Mortar texture is present in most samples. Evidence for prograde metamorphism is seen in the development of hypersthene from biotite and clinopyroxene from hornblende. Late-stage retrogession is evidenced by the development of reddish brown biotite patches along cleavages and margins of some pyroxenes. In the highly altered sample 120-4, hypersthene is largely replaced by reddish brown biotite.

(KMK) Low-pressure granitic charnockite (samples: 484-1a, 119-3)

The charnockites are gray and medium-grained. Texture is granoblastic. Plagioclase (An 20-25) comprises 28-48% of the samples; twin lamellae are either absent or faint. Antiperthite is not observed. Microcline (20-41%) is seen predominantly as intergranular megacrysts. Quartz (25-30%) usually has undulose extinction. Biotite

(0.3-4%) is present as pale brown to very dark brown laths, and as minor anhedral stains; hornblende (0.1-1%) is olive-green. Hypersthene (0.1-1%) is pleochroic in pale pink to pale green and shows late-stage regression to biotite along cleavage planes. Accessories include opaques (~1), zircon, apatite, and allanite. Sericite, chlorite, carbonate, and myrmekite are also usually present.

(KMK) Low-pressure mafic granulite (samples: KDA3, 120-3)

The granulites are dark gray, fine to medium-grained, and foliated. Texture is hypidiomorphic granular to granoblastic. Plagioclase (An 24-34) comprises 40-57% of the samples; twin lamellae are usually absent or deformed. Quartz (~2%) has undulose extinction. Microcline is absent or seen only in trace amounts. Mafic minerals (~57%) are principally hornblende and hypersthene. Accessory minerals include opaques (0.1-3%), zircon, and apatite. Sericite, chlorite, and carbonate are usually seen in trace amounts. The primary metamorphic reaction in these mafic granulites is prograde, hypersthene after hornblende.

IV.2.2 Hosur-Krishnagiri-Dharmapuri (HKD) area

(HKD) Tonalitic gneiss (samples: 77-1, 79, 108-1, 108-2)

The tonalitic gneisses are gray and pinkish gray, fine, medium, and coarse-grained, and usually foliated. Texture is hypidiomorphic granular to granolblastic; sample 108-1 is hypidiomorphic granular to cataclastic. Plagioclase (An 24-30) comprises 62-74% of the samples and usually contains some antiperthite; twin lamellae are typically absent or faint. Quartz (19-23%) commonly has undulose extinction. Microcline (0.4-11%) is intergranular. Biotite (5-11%) is usually present as yellow to dark olive-brown laths, and as anhedral stains. Hornblende is absent or seen in amounts of <1%. Accessory minerals include opaques (0.2-0.5%), zircon, and apatite. Sericite, chlorite, and carbonate are absent or found in trace amounts. Myrmekite and mortar texture are sometimes present.

(HKD) Granodioritic gneiss (samples: 64-1, 65)

The gneisses are light pinkish gray to gray, fine to medium-grained, and foliated. Texture is hypidiomorphic granular to porphyroblastic. Plagioclase (An 22-26) comprises 46-57% of the samples, usually has some antiperthite, and shows low degrees of saussuritization; twin lamellae are usually absent or faint. Quartz (18-30%) has undulose extinction. Microcline (8-20%) is present as both subhedral grains and intergranular megacrysts. Biotite (4-15%) is found both as yellow to dark brown laths and as reddish brown, anhedral stains or grains. Hornblende (~0.1%) is green to olive-

green. Accessories include opaques (~0.5%), zircon, apatite, and infrequent rutile needles in quartz. Allanite is also sometimes found. Sericite, chlorite, and carbonate are frequently seen as alteration products. Myrmekite is sometimes observed at plagioclase-microcline contacts. Mortar texture is relatively rare.

(HKD) Granite-granitic gneiss (samples: 3, 64-2, 67, 510-4)

The granitic gneisses are pink to gray, medium to coarse-grained, and both homogeneous and foliated. Texture is hypidiomorphic granular to porphyroblastic. Plagioclase (An 24-26) comprises 10-45% of the samples and usually shows the development of minor saussuritization; twin lamellae are usually absent or faint. Antiperthite is absent or rare. In sample 3, which appears to come from a distinct, granite stock, plagioclase is seen both as subhedral grains and as larger porphyroblasts. Quartz (21-32%) has undulose extinction, and the grains are sometimes elongate. Microcline (24-66%) is usually present as subhedral grains and intergranular megacrysts; seive texture is sometimes seen. Biotite (2-5%) is seen as yellow to brown or dark brown and yellow to greenish brown laths; reddish brown anhedral grains are less frequent. Accessories include opaques (0.1-0.8), zircon, and apatite; rutile needles are infrequently seen in quartz. Sericite, chlorite, and carbonate are usually present in trace amounts. Myrmekite, in varying amounts, is seen in all samples.

(HKD) Low-pressure charnockite (samples: 1, 2, 4-1, 66, 68, 69, 78, 107-1, 108-3, 488-4, 510-1)

The charnockites are gray to dark gray, sometimes greenish gray, greasy, medium to coarse-grained, and typically homogeneous but sometimes foliated. Texture is predominantly hypidiomorphic granular to granoblastic. Sample 107-1 is cataclastic. Plagioclase (An 24-30) comprises 46-73% of the samples with antiperthite usually present; twin lamellae are frequently absent, or faint and bent, and saussuritization is usually present in varying degrees. Quartz has a range of 13-32% in the silicious charnockites and 5-19% in intermediate charnockites; undulose extinction is common. Microcline (tr-2%) is intergranular and perthite is sometimes seen. Biotite (0.1-16%) is found both as pale yellow to brown and dark brown laths and as reddish brown, small prisms and anhedral and stains. In sample 108-3, horblende (20%) is present, some as late-stage alteration of pyroxene. Pyroxene (0.3-12%) is predominantly hypersthene. Accessories include opaques (0.5-3%), zircon, and apatite. Sericite, chlorite, and carbonate are also usually present in trace amounts. Myrmekite is infrequent; mortar texture is present in sample 107-1. Evidence for prograde and late-stage retrograde metamorphic reactions are both present. Hypersthene appears to have initially developed along cleavages in yellow to brown, lath-shaped biotite. Late-stage reddish brown biotite developes along margins and cleavages of pyroxene as strings and patches. In some cases, lath-shaped biotite

also acquires reddish brown margins or halos.

(HKD) Low-pressure mafic granulite (sample: 77-2)

The mafic granulite is dark gray to very dark gray, glassy to greasy, fine to medium-grained, and foliated. Texture is granoblastic. Plagioclase (An 39) comprises 34% of the sample and usually has generally well developed twin lamellae. Quartz (1%) has undulose extinction. Microcline and biotite are absent. Hornblende (55%) is green to olive-green; pyroxene (10%) is pale green to poorly pleochroic in pale pink to pale green. Accessories include opaques (0.2%), zircon, and apatite. Pyroxene appears to grow as a prograde reaction along cleavages in olive-green hornblende.

IV.2.3 Tiruvannamalai (T) area

(T) Tonalitic gneiss (sample: 514-2)

The gneiss is gray, medium-grained, and foliated. Texture is granoblastic to cataclastic. Plagioclase (An 25) comprises 64% of the sample and has some antiperthite; twin lamellae are absent, or weak and deformed. Quartz (32%) has undulose extinction; elongate grains are common. Microcline (1%) is seen as small intergranular crystals. Biotite (2%) is found as yellow to brown laths and as reddish brown stains. Accessories include opaques, zircon, and apatite. Sericite, chlorite, and carbonate are also found. Myrmekite and mortar texture are common.

(T) Low-pressure charnockite (sample: 514-3)

The charnockite is gray, greasy, medium-grained, and foliated. Texture is granoblastic. Plagioclase (An 23) comprises 82% of the sample, has some antiperthite and faint or absent twin lamellae. Quartz (14%) has undulose extinction. Microcline (2%) is found as small intergranular crystals. Biotite (2%) is present both as yellow to brown laths and as anhedral, reddish brown grains. Hornblende (tr) is green. Hypersthene (1%) is faintly pleochroic. Accessories are opaques (1%), zircon, and apatite. Sericite, chlorite, and carbonate are also found in trace amounts. Myrmekite is rare and mortar texture infrequent. Hypersthene is altered along cleavages and margins to reddish brown biotite.

IV.2.4 Karetur (K) area

(K) Granitic gneiss (sample: 565-5)

The gneiss is pinkish gray, medium to coarse-grained, and homogeneous. Texture is hypidiomorphic granular to granoblastic and cataclastic. Plagioclase (An27) comprises 41% of the sample and has minor dusty saussuritization; twin lamellae are usually present though sometimes deformed. Quartz (24%) is frequently seen as elongate grains; extinction is straight. Microcline (27%) typically lacks twinning; some perthite is found. Biotite (3%) is present as pale yellow to brown, crinkle-textured laths, and as anhedral stains along cleavages and margins of hornblende. Hornblende (2%) is green to olive-green. Accessories include opaques (2%), elongate grains of zircon, and apatite that is frequently clumped. Sericite, chlorite,

and carbonate are also present.

(K) Low-pressure granitic charnockite (samples: 565-1, 565-2)

The charnockites are dark gray, greasy, medium-grained, and homogeneous in appearance. Texture is hypidiomorphic granular to granoblastic and cataclastic. Plagioclase (An 31) comprises 52-56% of the samples; the presence of twin lamellae and antiperthite is not consistent. Quartz (12-15%) has straight extinction and is frequently found as large, sometimes elongate grains; mortar texture is present, locally intense. Microcline (27-29%), frequently as large crystals, lacks twinning; pertite is infrequent to rare. Biotite (0.3-1%) is found as pale yellow to brown, crinkle-textured laths and shreds, and as anhedral stains along cleavages and margins of pyroxene. Pyroxene (~1%) is either poorly pleochroic hypersthene or pale green clinopyroxene. Accessories include opaques (2%), zircon, and apatite. Sericite, chlorite, and carbonate are also present. Minor amounts of myrmekite are found at plagioclase-microcline joins. Mortar texture and shredded biotite are found along microshears.

IV.3 Intermediate and high-pressure charnockite terrane

IV.3.1 Shevaroy Hills - Toppur (ST) area

(ST) High-pressure charnockite (samples: 485-2, 486-1, 526-1, 528, 531-1, 531-2, 533, 535-2)

The charnockites are gray to dark gray, usually glassy to greasy, predominantly medium-grained, and homogeneous in appearance. Textures are granoblastic to porphyroblastic and cataclastic. Plagioclase (An 34-47) comprises 47-69% of the samples and has antiperthite and variable degress of saussuritization; twin lamellae are usually absent, deformed when present. Quartz, which is 4-24% in the intermediate charnockites and 26-34% in the silicious samples, generally has undulose extinction and frequent mortar texture; in sample 533, grains are large (~5mm) and elongate. Microcline (generally <2%) is largely coalesced antiperthite at the margins of plagioclase; twinning is rare. Biotite (tr-1%) is generally of two types: pale yellow to brown and reddish brown crinkle-textured laths that are found singley or in clumps, and brown to reddish brown small prisms and anhedral stains that form in cleavages or along margins of pyroxene. Hornblende (0-6%) is green to olive-green and is found predominantly along margins of pyroxene. Hypersthene (1-15%) is generally pleochroic in pale pink to pale green and schiller structure is sometimes seen. In sample 486-1, 12% pale green clinopyroxene is seen in addition to hypersthene. Garnet is found in samples (486-1, 528, 531-2, 535-2) where it is subhedral, porphyroblastic, and

contains inclusions of other mineral phases in the sample. Accessory minerals include opaques (1-3%), rutile needles in quartz, zircon, and apatite. Sericite, chlorite, and carbonate are absent or found in trace amounts. In some samples mylonite and calcite vein are present. Evidence for relatively minor late-stage regression is found in the growth of biotite and hornblende along margins of pyroxene.

(ST) High-pressure mafic granulite (sample: 485-1)

The mafic granulite is dark gray, coarse-grained, and foliated. Texture is porphyroblastic. Plagioclase (An 61) comprises 40% of the sample, is fresh looking, and has twin lamellae that are sharp but deformed. Quartz (tr) has undulose extinction. Microcline and biotite are absent. Hornblende (9%) is olive-green to olive-brown. Hypersthene (21%) is pleochroic and frequently has schiller structure; clinopyroxene (18%) is pale green. Garnet (11%) is porphyroblastic to glomeropophyroblastic and poikilitic. Accessories include opaques (2%), zircon, and apatite. Chlorite and carbonate are present in trace amounts. Pyroxene has formed in cleavages of hornblende.

IV.3.2 Biligirirangan Hills (BR) area

(BR) High-pressure charnockite (samples: 553, 554, 555, 556, 557, 558, 559)

The charnockites are gray to dark gray, greasy, generally medium-grained, and foliated. Texture is cataclastic. Plagioclase (An 27-33) comprises 61-83% of the samples and commonly has antiperthite and variable saussuritization; twin lamellae are usually absent, and deformed when present. Quartz (8-22%) frequently has elongate grains with undulose extinction; mortar texture is common. Microcline (tr-1%) is usually seen as coalesced antiperthite at the margins of plagioclase. Biotite (0.2-8%) is found as yellow to brown and very dark brown, crinkle-textured laths and shreds, frequently bent or oriented along microshears, and as anhedral brown and reddish brown stains in cleavages and along margins of pyroxene. Hornblende (0-2%) is pale green to green and also is found along cleavages and margins of pyroxene. Hypersthene (tr-13%) is poorly pleochroic and frequently has schiller structure. Though generally blocky in form, hypersthene sometimes has biotite-like habit and may have evolved from biotite. Hypersthene has experienced varying degrees of late-stage alteration, from the development of anhedral biotite and hornblende along cleavages and margins to the virtual replacement of hypersthene by micas, amphiboles, calcite, and quartz. Accessory minerals include opaques (0.3-2%), zircon, and apatite. Epidote, sericite, chlorite, and carbonate are present in trace amounts. Mortar texture, mylonite, and veinlets of carbonate are present in all samples.

IV.3.3 Nilgiri Massif (N) area

(N) High-pressure charnockite (samples: 477, 478, 480, 483, 567, 569)

The charnockites are dark gray, glassy to greasy, medium-grained, homogeneous and foliated. Texture is granoblastic to porphyroblastic and cataclastic. Plagioclase (An 36-49) comprises 30-66% of the samples and is frequently antiperthitic. Twin lamellae are frequently absent or deformed; saussuritization is present is some samples. Quartz, which is 21-35% in the silicious samples and 1-15% in the intermediate charnockites, has undulose extinction and grains are frequently elongate; mortar texture is also seen. Microcline (0-11%) generally lacks twinning and is commonly perthitic. Biotite (tr-15%) is of two types: yellow to reddish brown, crinkle-textured laths and shreds, frequently deformed, and yellow to reddish brown anhedral stains along cleavages and margins of pyroxene. Hornblende is present only in sample 483, where it has an abundance of 9% and is green to olive-green and subhedral. Hypersthene (1-8%) is poorly pleochroic to pleochroic in pale pink to pale green, and in many examples has a biotite-like habit; schiller structure is sometimes seen. Clinopyroxene, when present, is pale green. Garnet (0-26%) is subhedral, porphyroblastic, and usually contains inclusions of other mineral phases present in the rock. Accessory minerals include opaques (0.4-2%), zircon, and apatite. Sericite, chlorite, and carbonate are usually found in trace amounts. Mortar texture, myrmekite, and mylonite are variably developed; some samples show locally intense microshearing and alteration.

(N) High-pressure mafic granulite (sample: 481)

The mafic granulite is dark gray, greasy, medium to coarse-grained, and homogeneous. Texture is granoblastic to cataclastic. Plagioclase (An 50) comprises about 44% of the sample and is variably antiperthitic; twin lamellae are usually present but deformed. Quartz (0.3%) has undulose extinction. Microcline is absent. Biotite (0.5%) is seen as both yellow to reddish brown, crinkle-textured laths, and as reddish brown, anhedral stains along cleavages and margins of hypersthene and hornblende. Hornblende (29%) is frequently seen together with hypersthene and may replace hypersthene along cleavage planes. Hypersthene (24%) is poorly pleochroic to pleochroic. Garnet (1%) is subhedral, porphyroblastic, and contains inclusions of other mineral phases seen in the sample. Accessories include opaques (0.3%), zircon, and apatite. Carbonate is present in trace amounts. Hypersthene appears to have initially developed from olive-green hornblende; however, late-stage retrogression has produced patches and stains of chlorite, anhedral biotite, and pale green hornblende along cleavages and margins of hypersthene.

IV.4 The retrograde gneiss terrane

IV.4.1 Salem (S) area

(S) High-pressure charnockite (samples: 536-1, 536-3, 537-1, 541-3, 544-1)

The charnockites are gray, greasy, medium to coarse-grained, and homogeneous in appearance. Texture is granoblastic to pophyroblastic and locally cataclastic. Plagioclase (An 35-38) comprises 64-72% of the samples and has some antiperthite and variable saussuritization; twin lamellae are typically absent, or faint and deformed. Quartz (12-21%) has undulose extinction, is sometimes found as elongate grains or mortar texture. Microcline is not observed. Biotite (tr-2%) is found as yellow to brown, crinkle-textured laths, and as anhedral stains along cleavages and margins of hypersthene, hornblende, and lath-shaped biotite. Hornblende (0-13%) is pale green to olive-green and brownish green; sometimes a thin rim of micas, usually less pronounced than that for hypesthene, is observed on the margins of hornblende when it borders plagioclase. Hypersthene (3-15%) is poorly pleochroic and has a relatively thick, fibrous to prismatic reaction rim of sericite, chlorite, biotite, and cummingtonite; this rim is thin or absent where hypersthene borders quartz. In addition to hornblende and hypersthene, lath-shaped biotite and opaques frequently have thin reaction rims when bordering plagioclase. Accessories include opaques (1-3%), zircon, and apatite. Sericite, chlorite, cummingtonite, and carbonate are present, sometime locally intense.

(S) Retrograde gneiss (samples: 536-2, 537-2, 544-2)

The gneisses are gray, medium-grained, and foliated. Texture is granoblastic. Plagioclase (An 30-36) comprises 62-72% of the samples, is infrequently antiperthitic, and has variable saussuritization; twin lamellae are usually absent or deformed. Quartz (15-22%) has undulose extinction, some large, intergranular crystals, and minor mortar texture. Microcline is not observed. Biotite (1-11%) is found as yellow to olive-brown, crinkle-textured laths, and as brown to olive prismatic and anhedral stains along cleavages and margins of hornblende and lath-shaped biotite. Hornblende (0-20%) is pale green to olive-green and brown, with margins that are typically surrounded by a reaction rim of micas. Hypersthene is not observed; however, possible pseudomorphs after hypersthene, which have a thick corona of micas surrounding an interior of quartz, calicite, and opaques, are found in samples 537-2 and 544-2. Accessory minerals include opaques (0.6-1%), zircon, and apatite. Epidote group minerals, sericite, chlorite, and carbonate are present, sometimes in amounts of 1% or more. Alteration is locally intense in some samples.

IV.4.2 Bhavanisagar (B) area

(B) High-pressure chanockite (samples: 552-1a, 552-1e)

The charnockites are gray, greasy, fine to medium-grained, and homogeneous in appearance. Texture is granoblastic to cataclastic. Plagioclase (An 37-39) comprises 65-70% of the samples and has infrequent antiperthite; twin lamellae are usually absent or deformed. Quartz is 25% in the relatively silicious 552-1e and ~1% in 552-1a of intermediate composition. In both samples, quartz is present as a fine and medium-grained, intergranular mortar texture. Microcline comprises 0-1% of the samples. Biotite (0.3-3%) is found as pale yellow to dark brown, crinkle-textured laths, and as brown prisms and anhedral stains on margins of pyroxene. Hornblende (0.4-1%) is pale green to olive-green and found along cleavages and margins of pyroxene. Hypersthene (2-13%) is pleochroic in pale pink to pale green and frequently has schiller structure; clinopyroxene (0.5%) is pale green. Garnet is found in 552-1e (3%) where it is subhedral and has corroded margins; frequent vermicular inclusions of quartz are common. Accessories include opaques, zircon, and apatite. Epidote group minerals, sericite, chlorite, and carbonate are variably present, ususally as reaction coronas on mafic minerals; late-stage retrograde alteration is locally intense in sample 552-1e.

(B) Retrograde gneiss (sample: 552-2a)

The retrograde gneiss is gray, medium-grained, and foliated. Texture is cataclastic. Plagioclase (An 38) comprises 67% of the sample and has rare antiperthite and low but variable degrees of saussuritization; twin lamellae are usually absent. Quartz (19%) has ubiquitous, fine to medium-grained, intergranular mortar texture. Biotite (9%) is present as yellow to brown, crinkle-textured laths and shreds, which are strongly foliated along shear lines. Garnet (4%) is subhedral and found both as large porphyroblasts and as small grains. Accessories include opaques (tr), zircon, and apatite. Sericite, chlorite, and carbonate, which is frequently associated with biotite, are also found in trace amounts. Cataclastic deformation is relatively intense, producing biotite and elongate quartz foliation along shears, mortar texture, mylonite, and rotated plagioclase augen.

IV.4.3 Biligirirangan Hills (BR) area

(BR) High-pressure charnockite (sample:561-1)

The charnockite is gray, greasy, medium-grained, and foliated. Plagioclase (An 33) comprises 75% of the sample and has some antiperthite and variable saussuritization; twin lamellae are usually absent or deformed. Quartz (18%) has undulose extinction and some mortar texture. Microcline is not observed. Biotite (2%) is seen as pale brown to brown, crinkle-textured laths, and as small prisms and anhedral stains along cleavages and margins in hypersthene. Hornblende (tr) is olive-green and found along margins

of hypersthene. Hypersthene (3%) is poorly pleochroic. Accessories include opaques (1%), zircon, and apatite. Sericite, chlorite, and carbonate are also present. Texture is granoblastic to cataclastic.

(BR) Retrograde gneiss (sample: 561-2)

The gneiss is gray, medium-grained, and foliated. Texture is granoblastic to cataclastic. Plagioclase (An 33) comprises 68% of the sample and has variable amounts of antiperthite and saussuritization; twin lamellae are usually absent or deformed. Quartz (23%) has undulose extinction; some grains are elongate and mortar texture is present. Microcline is absent. Biotite (9%) is found as yellow to brown, crinkle-textured laths and shreds, which show a rough foliation. Green hornblende is present in trace amounts. Accessories include opaques (tr), zircon, and apatite. Sericite, chlorite, and carbonate are present in trace amounts. Some mylonite is observed along microshears.

IV.5 Conclusions

IV.5.1 Gneiss Terrane and Prograde Transition Zone

Tonalitic gneisses from these terranes are comprised predominantly of plagioclase (53-74%), quartz (12-32%), microcline (1-11%), biotite (0.4-10%), and hornblende (<5%). The gneisses and granitic gneisses have somewhat less plagioclase (10-63%), a greater abundance of microcline (17-66%), and similar abundances of other minerals compared to the tonalitic gneisses. Plagioclase for all classes of gneisses is An 22-30 with absent or weak twin lamellae that

are frequently deformed when present; antiperthite is found in the tonalitic gneisses but is less frequent or absent in the more granitic gneisses. Microcline is observed as both small, subhedral grains and as large, intergranular megacrysts. Though these megacrysts are absent or rare in the tonalitic gneiss, they form the predominant form of K feldspar in the granitic gneisses and probably represent a late-stage metasomatic event. Myrmekite is usually present at microcline-plagioclase joins. Quartz frequently has undulose extinction and is sometimes present as elongate grains. Mortar texture is frequently present but occurence is variable. Gneisses from the Bangalore-Kolar and Kollegal-Malavalli-Kabbuldurga areas appear to have a somewhat higher frequency of mortar texture than the gneisses from the Hosur-Krishnagiri-Dharmapuri area. Biotite is found both as crinkle-textured laths, sometimes bent, and as anhedral to prismatic secondary alteration stains. This dual occurence of biotite is seen in most samples containing biotite. In the gneisses, lath-shaped biotite is the predominant form and anhedral biotite develops as relatively minor patches along cleavages and margins on hornblende. Accessory minerals include opaques, (usually magnetite), zircon, apatite, allanite, and sphene; accessory minerals do not show significant variation between the tonalitic and granitic gneisses. Epidote (<1%), and trace amounts of sericite, chlorite, and carbonate are found, principally as saussuritization of plagioclase, or as thin veinlets. Cataclastic deformation and mylonite are uncommon, though more evident in samples from the Kollegal-Malavalli-Kabbaldurga area.

The low-pressure tonalitic charnockites have similar

abundances of the major minerals as the tonalitic gneisses and gneisses. The granitic charnockites are similar to granitic gneisses, with microcline, frequently as intergranular megacrysts, comprising 12-30% of the samples. Twinning in both K feldspar and plagioclase is frequently erased, or deformed when present. Antiperthite is common and sometimes coalesces at plagioclase margins to form discrete grains. Perthite in microcline is absent to infrequent. Pyroxene (0.1-8%) is present predominantly as hypersthene that frequently has a lath-shaped biotite habit, and the hypersthene may have developed from biotite, initially along cleavages. Most of the mafic minerals, including lath-shaped biotite, commonly have a late-stage overprint of reddish brown, anhedral biotite growing in patches along cleavages and margins.

Low-pressure mafic granulites from the prograde transiton zone have a more anorthitic plagioclase (An 24-39) than the tonalitic charnockites, but similar abundances of plagioclase and microcline. The abundance of quartz (1-6%) is less and the aggregate abundance of the mafic minerals, biotite (0-20%), hornblende (1-55%), and pyroxene (10-12%), is significantly greater in the mafic granulites. As in the tonalitic charnockites, pyroxene appears to develop along cleavages in hornblende and lath-shaped biotite. Minor to locally intense late-stage retrogression to anhedral, reddish brown biotite is also evident.

Accessory minerals for Transition Zone charnockites and mafic granulites include opaques, zircon, and apatite in amounts that are not significantly different from the tonalitic to granitic gneisses.

Sericite, chlorite, and carbonate are usually present in trace amounts, chiefly as weak saussuritization of plagioclase. Mortar texture and myrmekite are variable but are more prominant in samples from Kollegal-Malavalli-Kabbuldurga; mylonite and microfractures are also sometimes observed in samples from this area. Textures are predominantly hypidiomorphic granuluar to porphyoblastic and cataclastic.

IV.5.2 Medium and high-pressure terrane

The medium and high-pressure charnockites and mafic granulites from the Shevaroy Hills-Toppur, Biligirirangan Hills, and Nilgiri Massif areas are similar to low-pressure charnockites in plagioclase, quartz, and microcline. Plagioclase in the Biligirirangan Hills has a somewhat greater abundance than that from the Nilgiris and the Shevaroy Hills. In all high-P samples, twin lamellae in plagioclase are typically absent or deformed and antiperthite and saussuritization are variable but generally present. Anorthite content, however, is higher (An 27-61) for the high-pressure charnockites than for low-pressure charnockites. The overall abundance of biotite is similar to the low-pressure charnockites but shows great variation: the southern and central Nilgiris and the Biligirirangan Hills have higher values (tr-15%) than the Shevaroy Hills (<1%). Biotite, as in the prograde transition zone, occurs as both laths and as secondary, anhedral to prismatic stains along margins and cleavages of mafic minerals. Hornblende, and especially pyroxene (tr-24%), abundances are somewhat higher in the high-pressure charnockites relative to the low-pressure charnockites. Evidence for a prograde relationship between pyroxene

and hornblende or pyroxene and biotite is sometimes ambiguous: in some instances, hypersthene appears after hornblende, and in others, hornblende appears to grow along cleavages in hypersthene. However, the initial reaction appears to be prograde with pyroxene developing from lath-shaped biotite and hornblende; this was followed by a late-stage retrogression of pyroxene to anhedral biotite and pale green hornblende. Garnet is present in some samples from the Shevaroy Hills-Toppur and the Nilgiri Massif areas, typically as relict phenocrysts or porphyroblasts, but its distribution is very inhomogeneous and typically occurs in lenses and bands. Garnet is not observed in the Biligirirangan Hills. Opaques (0.3-4%), zircon, and apatite are also variably present in abundances similar to the low-pressure prograde Transition Zone rocks. Sericite, chlorite, cummingtonite, and carbonate are also variably present, usually as saussuritization granules in plagioclase, as thin veinlets and cavity fillings, and as reaction coronas around mafic minerals in some samples. Cataclastic deformation is more prevalent in the high-pressure charnockites, especially from the Nilgiris and the Biligirirangan Hills, and mortar texture, mylonite with shear-oriented biotite, microfractures, and cross-cutting veinlets of carbonate are more common than in charnockites from the prograde Transition Zone. Textures are predominantly porphyroblastic to cataclastic.

In general, the medium and high-pressure charnockites differ from the low-pressure charnockites of the prograde Transition Zone, by 1) the greater incidence of deformed twins in plagioclase and the

greater frequency of absent twin lamellae, 2) the higher degree of cataclastic deformation, 3) the greater frequency of late-stage, locally intense, secondary alteration of the mafic minerals, and 4) the presence of garnet.

IV.5.3 Retrograde gneiss terrane

The retrograde gneiss terrane lies within the medium to high-pressure charnockite terrane and, with the exception of the absence of pyroxene in the retrograde gneisses, the charnockites and retrograde gneisses are generally similar in essential and accessory minerals to the high-pressure charnockites. Plagioclase (An 33-39) is usually untwinned and antiperthitic and its abundance in the charnockite and adjacent retrograde gneiss is similar, while microcline is virtually absent in both rock types. Though the abundance of hornblende is similar, biotite and opaques, chiefly magnetite, appear to be consistently higher in the retrograde gneiss than in the charnockite. This increase in biotite and opaques probably mirrors the concurrent disappearence of hypersthene across the charnockite-retrograde gneiss reaction. The occurence of biotite as laths and anhedral alteration stains is similar to its presence in charnockites and gneisses from other terranes. Cataclastic deformation is present in samples from all retrograde areas but is particularly prominent at Bhavanisagar. Secondary alteration of samples from the retrograde areas are locally intense and reaction coronas of secondary hornblende, micas, cummingtonite, and carbonate develop along margins of mafic minerals, particularly at Salem and Bhavanisagar; these reaction coronas are absent from the sample pair from Binkanahalli (BR Hills). The degree

of both cataclastic deformation and late-stage alteration effects in the retrograde gneiss terrane samples are greater than in samples from both the high and low-pressure charnockite terranes. Textures are cataclastic to porphyroblastic.

V Chemical Results

V.1 Introduction

The chemical analyses for the south India samples are given in Appendix C. Means and standard deviations of elemental abundances of the major rock types are shown in Table V.1; other means with standard deviations can be found in Appendix C. Analytical methods are described in Appendix A. The following sections report the results of felsic rocks; mafic rocks are discussed separately in Section V.9.

Rocks have been classified, in general, using Ab-An-Or diagrams and fields delineated by O'Connor (1965) as modified by Barker (1979) (Figs. V-1, V-2). For the amphibolite-facies rocks (Fig. V-1), the few samples that fall into the quartz monzonite field are classified as granodiorites or granites. Trondhjemitic gneisses are classified with the tonalitic gneisses and the term "tonalitic" hereinafter will refer to "tonalitic-tondhjemitic." For the low and high-pressure charnockites (Fig. V-2), the few samples that lie in the granodiorite field are classified as either tonalitic charnockite or granitic charnockite. The south India samples are also grouped by silica content: SiO2 >= 65%, silicic; SiO2 >= 52% and <65%, intermediate; and <52%, mafic. Though the division of an heterogeneous population of rock samples into subgroups is artificial at the margins of the classification, where there may be considerable overlap of characteristics, such a division allows in general the comparison of major features of a subgroup with similar rocks from

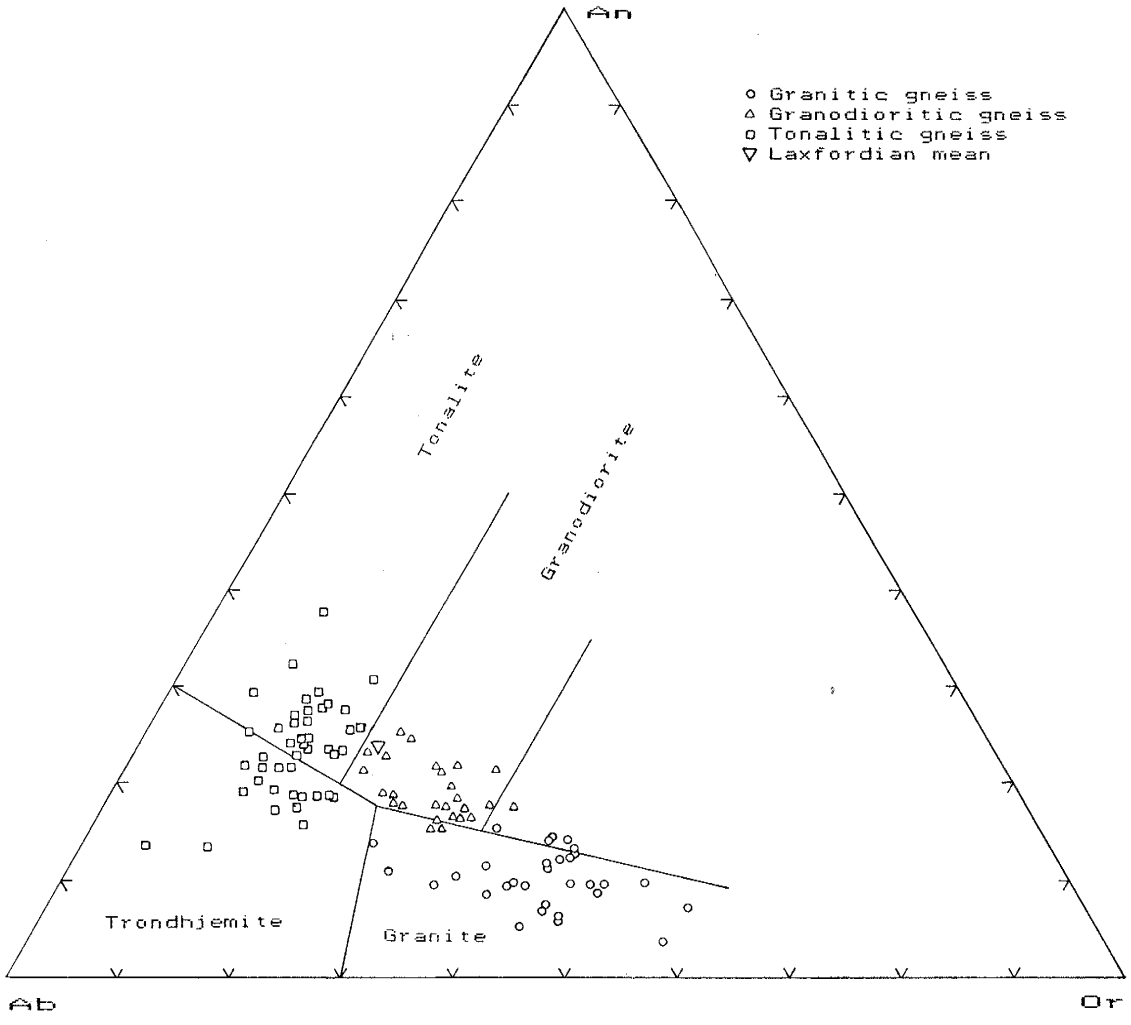

Fig. V-1. CIPW normative Ab-An-Or diagram for amphibolite-facies gneisses from south India; also shown is the mean for the Lewisian Laxford gneisses (Appendix C.11.3). Classification fields after O'Connor (1965) and Barker (1979).

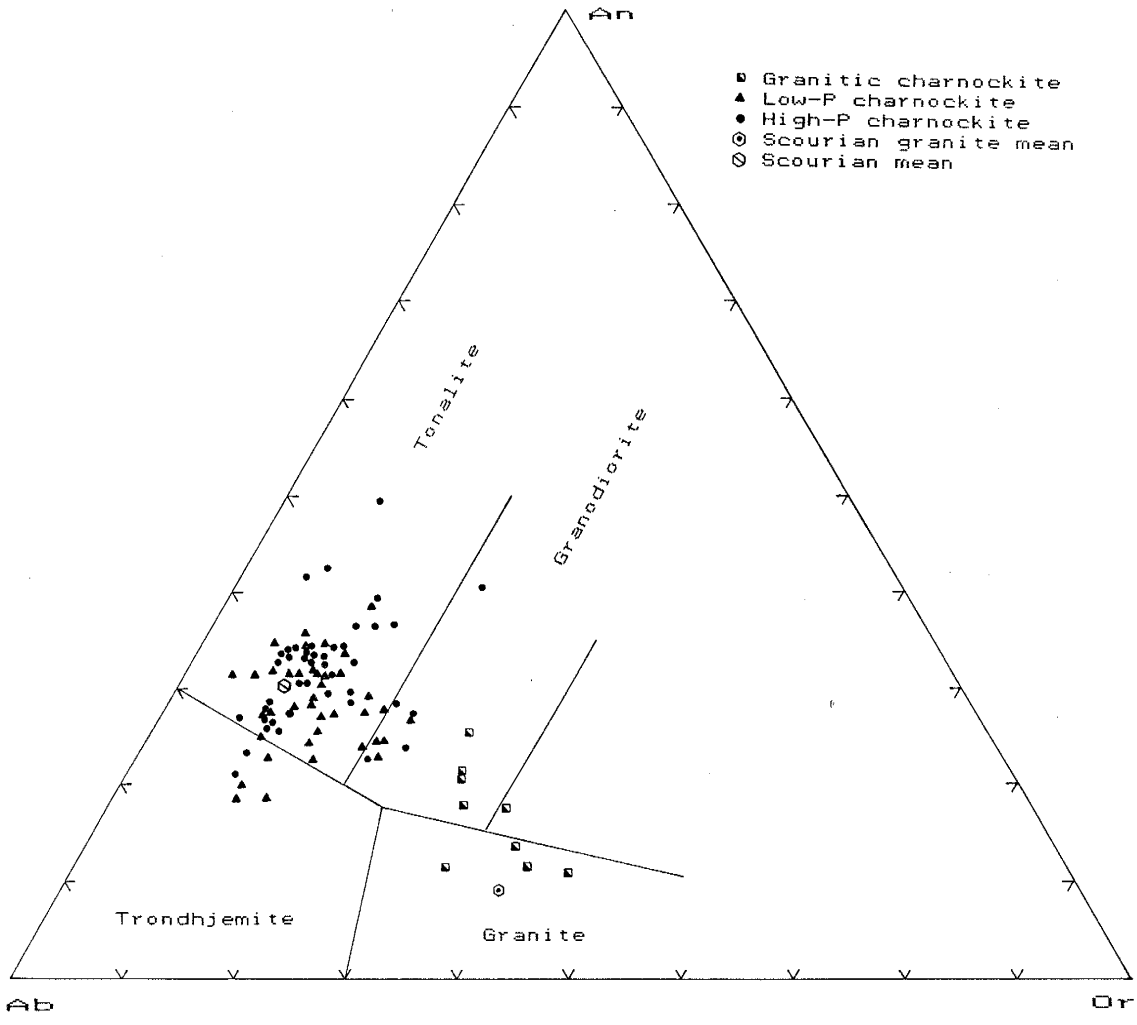

Fig. V-2. CIPW normative Ab-An-Or diagram for granulite-facies gneisses from south India; also shown are means for the Scourian granitic and tonalitic granulites (Appendixes C.11.4, C.11.9). Classification fields after O'Connor (1965) and Barker (1979).

other geographical areas. In particular, classification helps to isolate and identify chemical differences between rocks from comparative areas and between metamorphic terranes within a single area. The rock groups classified in this study are granitic gneiss, granodioritic gneiss (silicic and intermediate), tonalitic gneiss (silicic and intermediate), tonalitic low-P charnockite, low-P granitic (high-K) charnockite, and tonalitic high-P charnockite.

For discussion purposes, elements are grouped into the following categories: major elements, large-ion-lithophile (LIL) elements, high field strength (HFS) elements, transition metals, and rare earth elements (REE). LIL elements, with relatively large ionic radii and low charge/radius ratios, include K, Rb, Cs, Sr, Ba. Because of similar characteristics, Pb, U, and Th will be discussed with the LIL elements. HFS elements have small ionic radii, high charge/radius ratios, and less than five electrons in d orbitals; they include Sc, Y, Ti, Zr, Hf, Nb, and Ta. The remaining transition metals (Cr, Co, Ni, and Zn) are treated separately.

In examining the results, the rocks from south India are compared with rocks from other Archaean terranes. The criteria for selecting these areas were the amount and quality of analytical data available (particularly the trace elements), and the geographical relevance to south India in a reconstructed Gondwanaland. The areas chosen for comparison are the Scourian and Laxfordian terranes of the Lewisian in Scotland, the Amitsoq and Nuk terranes in West Greenland, the Uivak I terrane in the Nain province of Labrador, the gray gneiss terrane of the Ancient Gneiss Complex in Swaziland, the high-grade

terrane of the East Antarctic Shield, and the high-grade terrane at Madras, India. Of these terranes, the Lewisian of N.W. Scotland is the most important because of the long history of its study and the large quantity of analytical data. The Lewisian complex is comprised of a central core of granulite-facies, lower-crustal gneisses (the Scourian) that is juxtaposed north and south by what is considered equivalent upper-crustal amphibolite-facies gneisses (the Laxfordian) (Weaver and Tarney, 1980). In most cases, the elemental abundances of these gneisses and charnockites have been selected from published sources and combined and recalculated in order to conform to the classification used for gneisses from south India. The means and standard deviations calculated for these terranes, and the sources used, are shown in Appendixes C.10 and C.11.

V.2 Major geochemical characteristics

V.2.1 CIPW and mesonormative diagrams

On a CIPW normative Ab-An-Or diagram, gneisses from south India plot in a generally smooth pattern from granite to tonalite-trondhjemite (Fig. V-1). There is a hint that the gneisses may be of two separate populations, a granitic-granodioritic suite and a tonalitic-trondhjemitic suite. The distribution of low and high-pressure charnockites also suggests the possibility of a trondhjemite-tonalite suite and a subordinate group of low-P granitic charnockites (Fig. V-2). This distinction between tonalite and granite populations is more apparent in plots of samples from the Scourian (Rollinson and Windley, 1980b) and the the East Antarctic Shield

granulite-facies Vestfold Block Mossel gneisses and Napier Complex depleted gneisses (Sheraton and Black, 1983; Sheraton and Collerson, 1984). Amphibolite and granulite-facies gneisses from Southwest Greenland, however, do not have the compositional range of the Indian and Lewisian samples and plot in a tight population that is predominantly tonalitic-granodioritic (Wells, 1979). A similar grouping of granitic-granodioritic and tonalitic-trondhjmetic south India samples is observed on the normative Ab-Q-Or projection of the system Q-Ab-Or-An-H2O (Fig. V-3). Though there is scatter, the majority of the granitic gneisses lie near or on the Or side of the granite minimum at 1-10 Kb H2O. The mean of Scourian granitic rocks plots in the same area (Fig. V-3) (Rollinson and Windley, 1980b; Pride and Muecke, 1982).

For the system Q-Ab-Or-An-H2O, the Scourian gneisses exhibit a tonalite-trondhjemite trend along a line of decreasing Ab + An and increasing Qtz, with Or constant; and a tonalite-granite (calc-alkaline) trend along a line of decreasing Ab + An and increasing Or, with Qtz constant (Rollinson and Windley (1980b). These trends are characteristic of Archaean terranes (Barker and Arth, 1976; Condie,1981a). On the Ab-Q-Or ternary projection, plots of tonalitic gneisses and charnockites from West Greenland (Compton, 1978), Labrador (Bridgewater and Collerson, 1976); the Ancient Gneiss Complex (Hunter et al., 1978); and the East Antarctic Shield (Sheraton and Black, 1983; Sheraton and Collerson, 1984) also fall on a tonalite-trondhjemite trend, which suggests a cogenetic relationship between the constituent rock types: the tonalite may be parent to

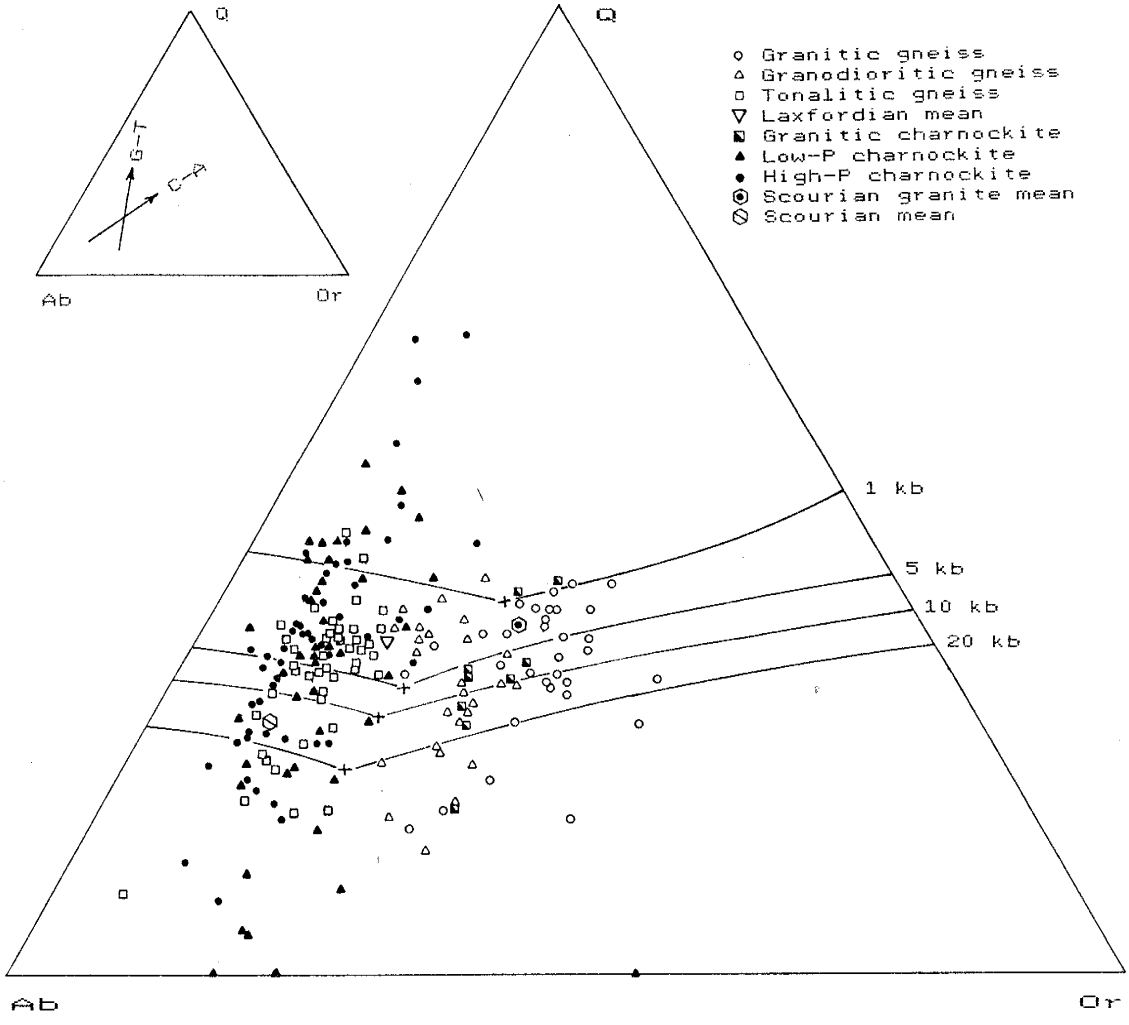

Fig. V-3. CIPW normative Ab-Q-Or diagram with quartz-feldspar field boundaries at 1, 5, 10, 20 kb PH20 after Huang and Wyllie (1975). Calc-alkaline (C-A) and gabbro-trondhjemite (G-T) trends from Barker and Arth (1976).

trondhjemite, and tonalite-trondhjemite parent to granite (Rollinson and Windley, 1980b). In the samples from south India these igneous trends are also present, though the granitic-granodioritic samples show more scatter and the tonalite-granite trend is less clearly defined than in the Scourian (Fig. V-4).

Mesonorm calculations (for metamorphic rocks of the mesozone, or amphibolite-facies) were made for the south India samples following the method of Barth (1959, 1962). In the mesonorm calculation, a portion of K2O is placed in biotite, which results in the reduction of normative orthoclase relative to the CIPW norm value. (A revised version of the mesonorm calculation, with a more accurate allocation of TiO2 that produces improved values for biotite and orthoclase, can be found in Mielke and Winkler, 1979, and Kosinowski, 1982; the revised mesonorm calculation is not used in this paper.) Results of the mesonorm calculations for the south India samples show a decrease in orthoclase in all samples, especially the charnockites, which in many examples lose all orthoclase. The mesonorm results more closely conform to the modal analyses of these rocks. Plots of mesorm values on the Ab-Q-An projection of the system Q-Ab-Or-An-H2O reveal the same trends observed for the CIPW norms; however, the mesonorm values for the granitic-granodioritic suite show a tighter population and a more defined trend (Fig. V-5).

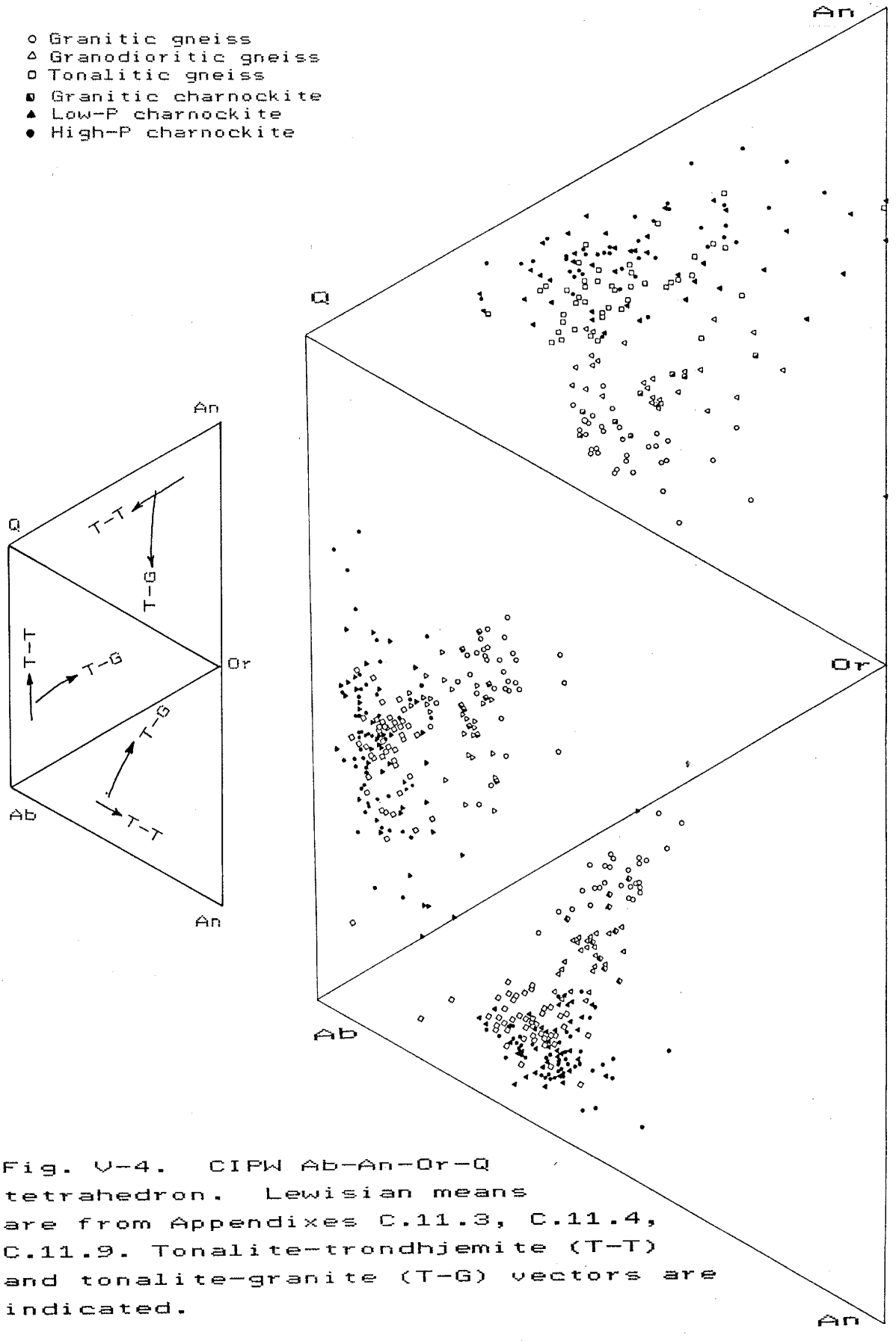

Fig. V-4. CIPW Ab-An-Or-Q tetrahedron. Lewisian means are from Appendixes C.11.3, C.11.4, C.11.9. Tonalite-trondhjemite (T-T) and tonalite-granite (T-G) vectors are indicated.

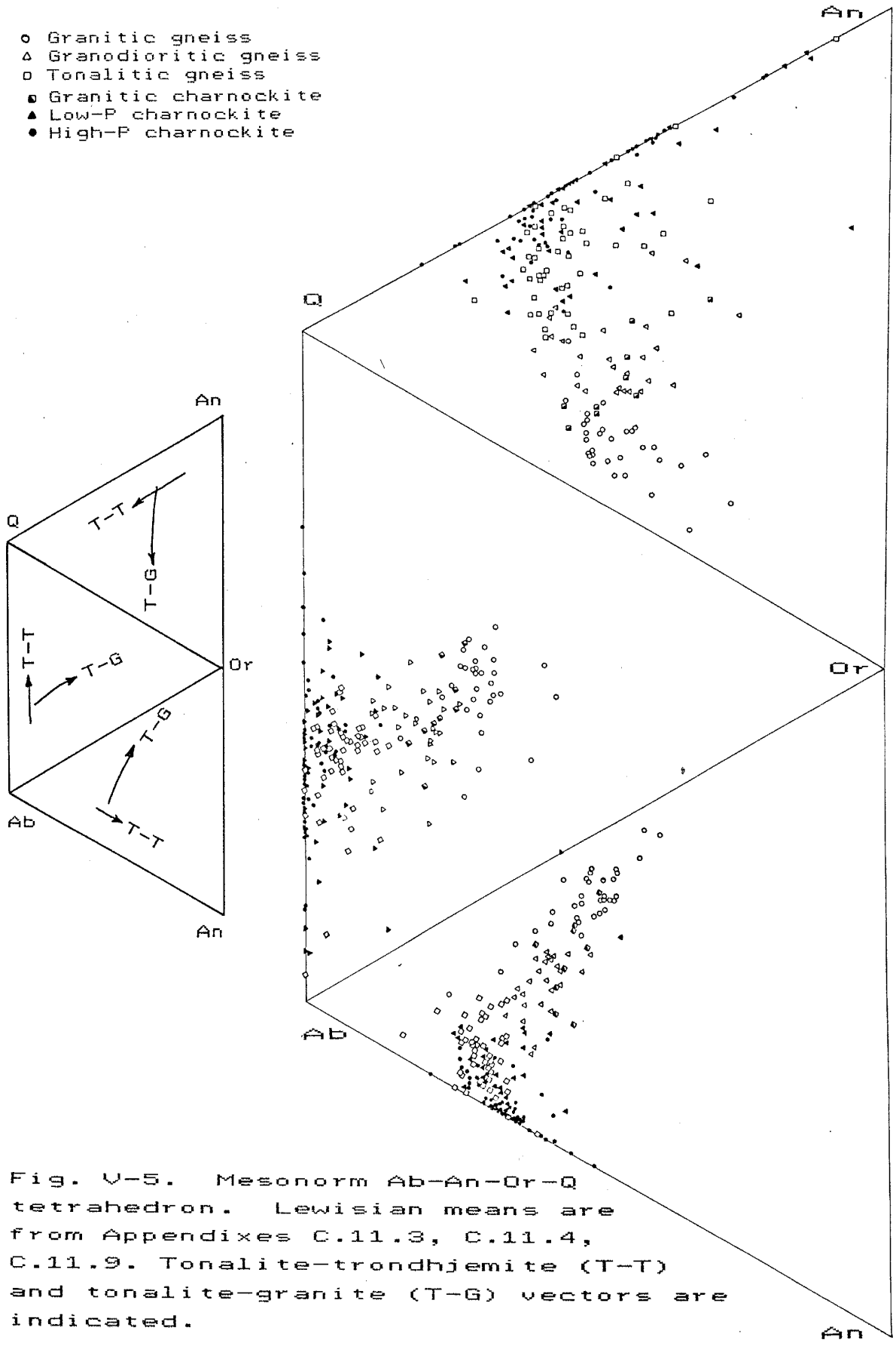

Fig. V-5. Mesonorm Ab-An-Or-Q tetrahedron. Lewisian means are from Appendixes C.11.3, C.11.4, C.11.9. Tonalite-trondhjemite (T-T) and tonalite-granite (T-G) vectors are indicated.

V.2.2 Na2O-CaO-K2O and AFM diagrams

The presence of two igneous trends is also suggested by the plot of Indian samples on a Na2O-CaO-K2O diagram: a granite-granodiorite, calc-alkaline trend for the K-rich gneisses (decreasing K2O with relatively constant CaO/Na2O), and a trondhjemite-tonalite-gabbro trend for the charnockites and tonalitic gneisses (relatively constant K2O with increasing CaO/Na2O) (Barker and Arth, 1976; Condie, 1981a) (Fig. V-6). As in the Ab-An-Or diagrams, the granitic-granodioritic gneisses and charnockites appear to comprise a suite distinct from that of the trondhjemitic-tonalitic gneisses and charnockites. The CaO-Na2O-K2O diagram also shows a relatively distinct population of mafic samples from south India that lies largely in the field of Archaean tholeiites (Fig. V-6). Samples of a composition intermediate between the mafic population and the predominant felsic rocks are relatively few, suggesting that the Archaean terrane in south India may have a bimodal character; evidence from the SiO2 variation diagrams supports this. However, this conclusion rest on the assumption that sampling is representative of the frequency of occurence of rock types. Mean values for Scourian charnockites and Laxfordian amphibolite-facies gneisses fall along a calc-alkaline trend (a tonalite-trondhjemite trend cannot be determined from the calculated means) (Fig. V-6). Published results of the Amitsoq gneisses also indicate the presence of a calc-alkaline trend, but a tonalite-trondhjemite trend is not observed (Lambert and Holland, 1976).

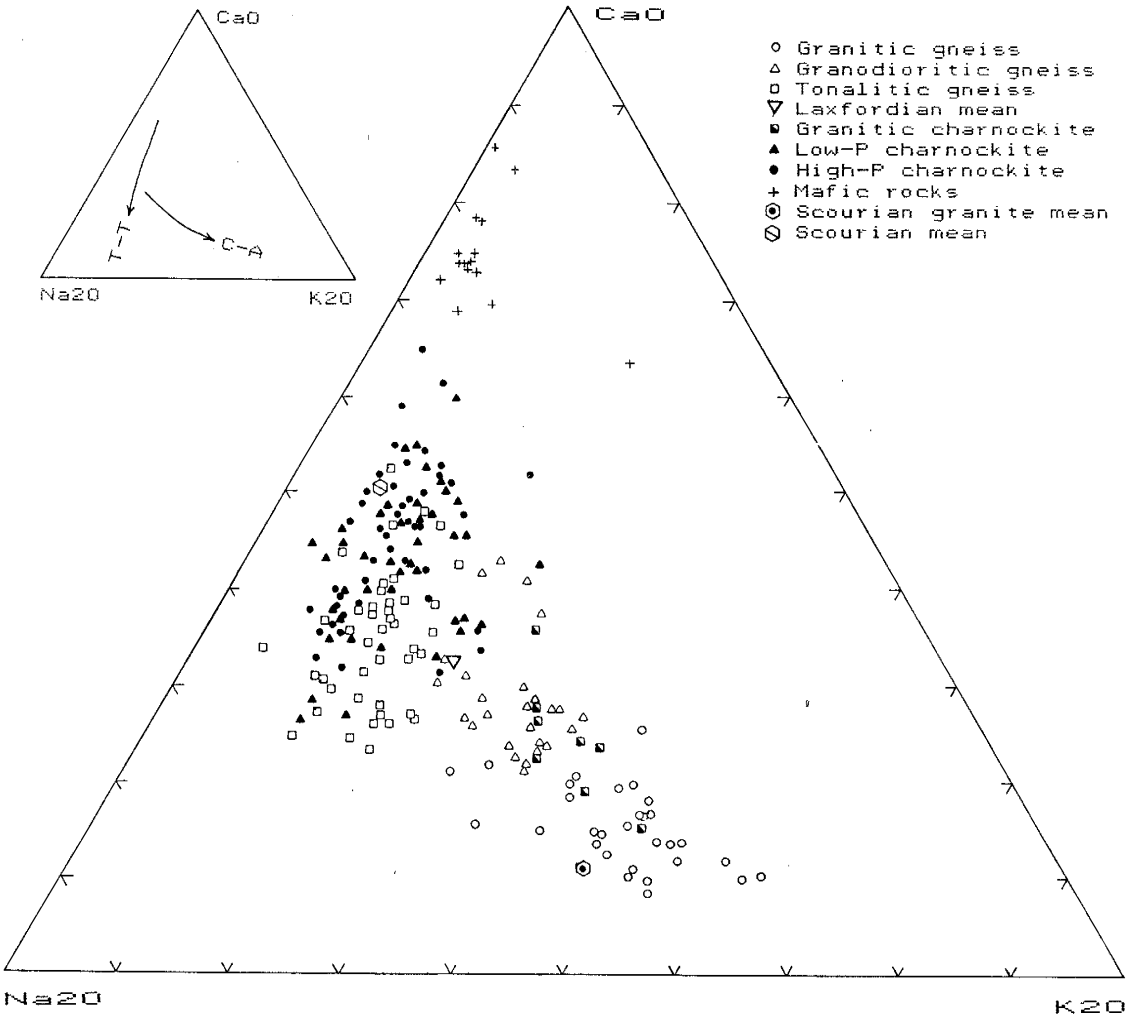

Fig. V-6. CaO-Na2O-K2O ternary diagram. Lewisian means are from Appendixes C.11.3, C.11.4, C.11.8, C.11.9. Tonalite-trondhjemite (T-T) and calk-alkaline (C-A) trends after Barker and Arth (1976).

On an AFM diagram, the samples from south India have a distinct calc-alkaline trend (Fig. V-7). A similar calc-alkaline trend is seen for the Scourian granitic-granodioric-tonalitic charnockites (Tarney, 1976; Rollinson and Windley, 1980b), the Uivak I gneisses from Labrador (Bridgewater and Collerson, 1976), the tonalitic gneisses from the Ancient Gneiss Complex (Hunter et al., 1978), and the depleted granulite-facies gneisses from East Antarctica (Sheraton and Black, 1983). The predominantly amphibolite-facies Nuk gneisses analysed by Compton (1978) and granulite-facies gneisses by Wells (1979), both from the Buksefjorden region, Southern West Greenland, also display a calc-alkaline trend. However, some Archaean gneisses have a distinct tholeiitic trend (O'Nions and Pankhurst, 1978): the Ilivertalik Granite suite of iron-rich granodioritic to tonalitic gneisses from Buksefjorden (Wells, 1979), the Amitsoq augen gneisses (Lambert and Holland, 1976), the Uivak II (post-Uivak I) porphyritic gneisses (Bridgewater and Collerson, 1976), the charnockites from Madras, India (Weaver, 1980), and the undepleted granulites from East Antarctica (Sheraton and Black, 1983).

Although there is considerable overlap, the south India amphibolite-facies gneisses are somewhat more alkalic on an AFM diagram than their equivalent charnockites, a relationship also seen in plots of the means of Lewisian Laxford (amphibolite-facies) gneisses and Scourian charnockites (Fig. V-7). Histograms of selected elements show a high frequencey of rocks with high SiO_2 and low Fe_2O_3, Sc, and Cr, accompanied by a dispersed pattern of lower frequency for rocks with low SiO_2 and high Fe_2O_3, Sc, and Cr (Fig. V-

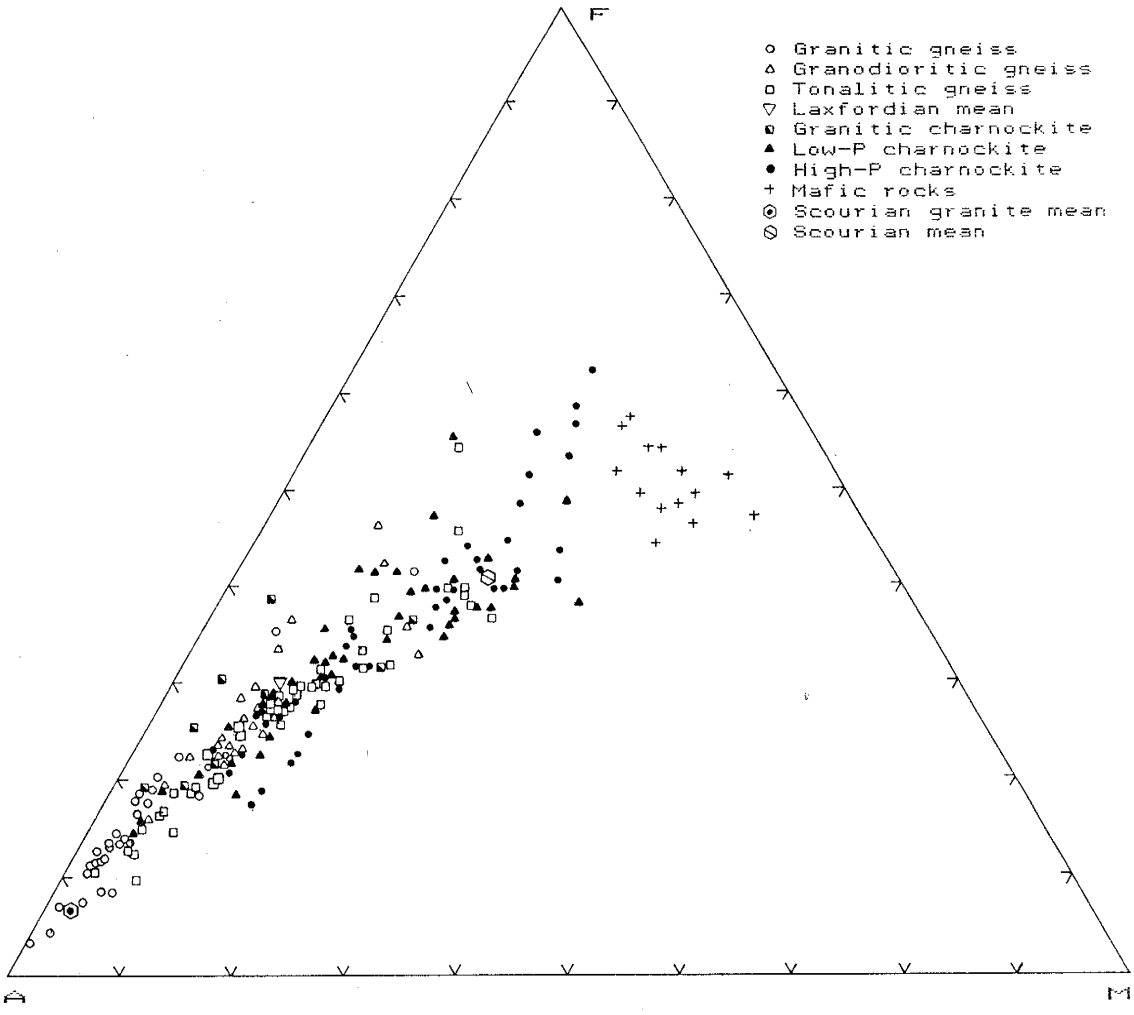

Fig. V-7. A-F-M ternary diagram. Lewisian means are from Appendixes C.11.3, C.11.4, C.11.8, C.11.9.

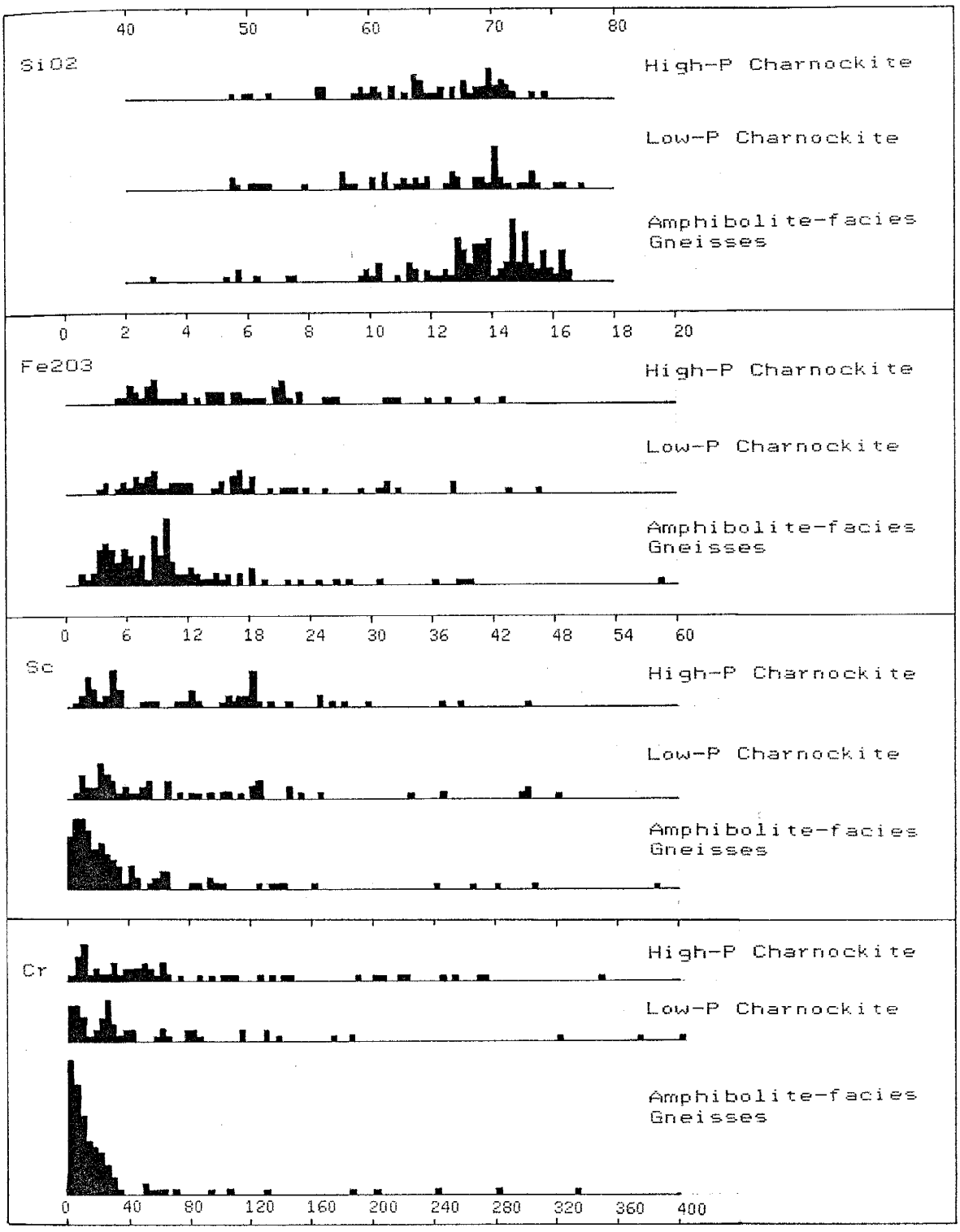

Fig. V-8. Histogram of selected elements for high-P charnockites, low-P charnockites, and amphibolite-facies gneisses from south India.

8). The histograms also show a shift between amphibolite-facies and low and high-P charnockites; the latter are somewhat lower in SiO2 with corresponding increases in Fe2O3, Sc, and Cr.

In general, there is similarity between samples from south India and the Lewisian (Laxford and Scourian) on the Ab-Q-An projection of the system Q-Ab-Or-An-H2O, and the CaO-Na2O-K2O and AFM ternary diagrams. Samples from both areas have a relatively broad compositional range (calc-alkaline AFM trend) that apparently falls into two general populations: a granitic-granodioritic group with a tonalite-granite (calc-alkaline) trend, and a trondhjemitic-tonalitic group with a gabbro-tonalite-trondhjemite trend.

V.3 Major Elements

The major element results are summarized in Table V-1. The results are graphically displayed on element-area diagrams that compare element abundances from different metamorphic terranes in south India with other Archaean terranes (Fig. V-9). The south India results are shown on the right half of the diagram with metamorphic grade increasing from left to right; estimated temperatures and pressures range from ~700 C and 5 Kb, for amphibolite-facies gneisses, to ~800 C and 9 Kb, for the medium to high-pressure charnockites (Fig. II-4) (Janardhan et al., 1982; Harris and Jayaram, 1982; Harris et al., 1982; Raith et al., 1983). The left to right orientation corresponds to the north-south progression in south India from the Gneiss Terrane gneisses, to the Transition Zone gneisses, to the Transition Zone low-P charnockites, and to the medium and high-P

	S O U T H I N D I A F E L S I C S A M P L E S																	
	TONALITIC GNEISS			GRANODIORITIC GNEISS			GRANITIC GNEISS			LOW-P CHARNOCKITE			LOW-P GRANITIC CHARNOCKITE			MEDIUM TO HIGH-P CHARNOCKITE		
	n	Mean	%SD	n	Mean	%SD	n	Mean	%SD	n	Mean	%SD	n	Mean	%SD	n	Mean	%SD
SiO2	45	67.91	6.5	26	68.11	5.6	32	72.41	4.8	43	65.55	10.0	9	68.92	6.5	45	65.55	7.7
TiO2	45	0.43	71.2	26	0.50	60.0	32	0.24	89.8	43	0.58	58.6	9	0.50	46.1	45	0.53	38.5
Al2O3	45	15.96	5.7	26	15.45	6.3	32	14.26	7.1	43	15.79	8.3	9	14.46	9.2	45	15.91	7.4
Fe2O3t	45	3.50	56.5	26	3.59	46.8	32	1.95	78.2	43	4.76	55.4	9	3.80	39.5	45	5.33	51.9
MnO	45	0.05	82.5	24	0.04	52.8	29	0.03	108	43	0.06	68.1	9	0.05	40.0	45	0.07	54.8
MgO	45	1.39	60.9	26	1.14	58.0	32	0.49	106	43	2.08	74.8	9	1.13	83.1	45	2.37	51.5
CaO	45	3.61	27.8	26	3.03	29.8	32	1.57	31.1	43	4.56	29.7	9	2.82	41.1	45	4.48	28.6
Na2O	45	5.02	13.0	26	4.20	6.3	32	3.78	16.1	43	4.49	11.5	9	3.82	9.7	45	4.22	21.4
K2O	45	1.61	23.5	26	3.29	17.0	32	4.80	17.8	43	1.51	43.9	9	3.80	10.8	45	1.21	34.8
P2O5	44	0.16	88.8	24	0.20	81.5	32	0.08	93.1	42	0.20	83.9	9	0.16	54.1	45	0.17	49.7
LOI	45	0.48	75.0	25	0.41	57.5	32	0.38	67.2	42	0.46	49.7	9	0.41	54.3	45	0.32	59.5
Rb	46	45	54.7	27	87	35.3	32	139	51.2	42	39	118	9	78	22.7	45	13	106
Cs	39	~1	141	22	~1	128	29	1.4	133	30	~0.7	187	7	0.36	47.7	26	<0.1	93.8
Sr	46	635	83.8	27	541	47.4	32	369	51.1	43	543	35.2	9	509	53.6	45	586	41.7
Ba	43	567	74.5	26	1063	45.5	32	1153	54.8	43	475	48.8	9	1104	54.9	45	499	53.8
Th	42	4.7	97.6	27	13	68.5	32	25	83.3	43	2.9	166	8	13	68.0	40	~1.4	182
U	35	<1	160	23	~1	108	31	3.8	137	37	~0.4	148	8	0.5	80.1	40	~0.2	95.3
Pb	26	<7	42.2	20	~13	45.6	31	23	46.1	11	<8	107	7	~18	52.3	13	<5	65.4
Sc	43	5.4	98.7	26	5.6	98.0	32	3.2	131	43	9.7	82.1	9	7.0	76.7	44	11	69.0
Y	44	12	121	27	18	104	32	25	105	42	13	75.0	9	15	50.7	42	13	67.9
Zr	46	153	70.6	27	215	67.5	32	174	53.4	43	158	55.9	9	224	54.1	45	134	34.7
Hf	43	4.2	66.3	26	5.7	51.2	32	5.5	58.3	43	4.2	47.6	9	6.5	67.7	45	3.5	36.8
Nb	45	7.5	81.6	27	9.8	88.7	31	11	83.2	43	8.1	61.8	9	8.3	35.4	44	5.3	46.7
Ta	26	<1	128	14	<1	101	25	<1	96.9	19	<1.5	90.4	5	~0.7	31.7	43	~0.17	99.6
Cr	41	28	130	24	17	131	28	7.9	91.2	42	49	124	9	20	123	45	79	98.1
Ni	36	17	84.5	18	20	111	24	6.7	63.6	31	49	118	8	14	74.1	45	41	99.4
Co	29	12	72.0	17	10	71.4	30	6.0	123	21	22	58.7	5	7.0	104	45	16	60.4
Zn	16	52	62.5	14	52	34.2	26	45	108	19	75	60.2	5	42	50.4	37	58	44.9
La	43	29	72.2	26	64	51.6	32	64	67.9	43	36	88.3	9	58	41.9	45	31	55.3
Ce	43	55	83.8	26	115	53.6	32	120	71.7	43	65	98.2	9	98	43.2	43	60	60.4
Nd	17	22	60.8	12	41	56.2	22	48	70.8	20	31	116	5	34	50.5	30	22	63.4
Sm	43	3.8	109	26	6.5	62.2	32	6.9	79.1	43	4.9	93.1	9	5.5	42.0	45	5.1	146
Eu	43	1.3	42.8	26	1.6	38.3	32	1.4	46.2	43	1.5	43.1	9	1.7	23.4	45	1.3	32.7
Tb	43	0.44	103	26	0.67	68.8	32	0.84	88.3	43	0.58	75.3	9	0.57	46.3	45	0.47	69.4
Yb	43	0.94	127	26	1.6	122	32	2.3	123	43	1.1	85.7	9	1.3	58.8	45	1.1	72.2
Lu	40	0.15	142	25	0.24	139	31	0.36	126	41	0.18	89.3	8	0.46	181	42	0.18	66.5
Eu/Eu*	43	2.1	102	26	1.2	63.5	32	1.8	129	43	1.8	72.3	9	1.3	34.8	45	1.6	81.9
?REE	43	90	80.8	26	190	51.5	32	197	69.9	43	108	93.0	9	165	41.6	43	100	58.3
K/Rb	45	631	197	26	345	27.9	32	344	39.1	41	695	92.4	9	421	20.7	45	1374	68.4
K/Ba	43	33	62.5	26	32	57.1	32	45	50.4	43	30	41.6	9	41	72.1	45	24	63.0
Rb/Sr	46	0.087	61.3	27	0.25	93.6	32	0.65	116	42	0.076	108	9	0.27	105	45	0.036	159
Ba/Sr	43	1.0	57.0	26	2.1	30.7	32	3.5	46.4	43	0.93	48.6	9	2.8	57.8	45	0.93	55.9

Table V-1. Means and standard deviations of the major felsic rock types from south India.

charnockites south of the Moyar-Bhavani shear zone (Fig. II-3). The left side of the element-area diagram displays results from other Archaean terranes. Although these areas are widely separated geographically and the temperature-pressure environments less certain, an attempt has been made to order these results with increasing metamorphic grade from left to right. Published estimates of temperature and pressure for the Archaean terranes used for comparison range from ~600 C and 7 Kb, for the amphibolite-facies gneisses from Southwest Greenland (Wells, 1979), to >900 C and 11 Kb for the Scourian (O'Hara and Yardwood, 1978; Pride and Muecke, 1980).

The results are displayed by rock classification, for example, tonalitic (intermediate) gneiss; vertical bars represent one standard deviation. Representative terrane-mean values are shown for both the Indian results and from other Archaean terranes; lines connecting these means indicate general trends in element abundances accompanying change in metamorphic grade. The analytical results for south Indian can be found in Appendixes C.1 - C.9, and for the other Archaean terranes, Appendix C.10. Sample population sizes for the different rock classifications and areas vary widely. Results from very small populations are shown if they appear representative. The large standard deviation shown for some calculated values is in part the result of small sample populations. A full description of the abbreviated names used in the element-area diagrams can be found in Table V-2.

Label	Rock Type and Locality
Swazi Tn S	Swaziland: Ancient Gneiss Complex Tonalitic gneiss (silicic)
Lax Tn S	Lewisian: Laxfordian tonalitic gneiss (silicic)
Lax Tn I	Lewisian: Laxfordian tonalitic gneiss (intermediate)
Lab Gr	Labrador: Granitic gneiss
Lab Gd I	Labrador: Granodioritic gneiss (intermediate)
Uivak Tn S	Labrador: Uivak tonalitic gneiss (silicic)
Nuk Lo-P $\overline{X}$	West Greenland: Mean of amphibolite-facies Nuk gneisses
Nuk Gd S	West Greenland: Nuk granodioritic (silicic) gneiss
Nuk Tn S	West Greenland: Nuk tonalitic (silicic) gneiss
Nuk Tn I	West Greenland: Nuk tonalitic (intermediate) gneiss
Amit Gr	West Greenland: Amitsoq granitic gneiss
Amit Gd S	West Greenlnad: Amitsoq granodioritic (silicic) gneiss
Amit Tn S	West Greenland: Amitsoq tonalitic (silicic) gneiss
Amit Tn I	West Greenland: Amitsoq tonalitic (intermediate) gneiss
Nuk Hi-P $\overline{X}$	West Greenland: Mean of granulite-facies Nuk gneisses
Ant-N Gr	East Antarctica: Napier Complex granitic gneiss
Ant-N Gd S	East Antarctica: Napier Complex granodiritic (silicic) gneiss
Ant-N Tn S	East Antarctica: Napier Complex tonalitic (silicic) gneiss
Ant-F Tn S	East Antarctica: Fyfe Hills tonalitic (silicic) gneiss
Ant-M Tn S	East Antarctica: Mossel tonalitic (silicic) gneiss
Madrs Gr	south India: Madras granitic gneiss
Madrs Tn I	south India: Madras tonalitic (intermediate) gneiss
Scour Gr	Lewisian: Scourian granitic granulite
Scour Gd S	Lewisian: Scourian granodioritic (silicic) granulite
Scour Tn S	Lewisian: Scourian tonalitic (silicic) granulite
Scour Tn I	Lewisian: Scourian tonalitic (intermediate) granulite
Scour $\overline{X}$	Lewisian: mean of Scourian granulite-facies gneisses
GT Gr	south India: Gneiss Terrane granitic gneiss
GT Gd S	south India: Gneiss Terrane granodioritic (silicic) gneiss
GT $\overline{X}$	south India: mean of Gneiss Terrane gneisses
GT Tn S	south India: Gneiss Terrane tonalitic (silicic) gneiss
GT Tn I	south India: Gneiss Terrane tonalitic (intermediate) gneiss
TZgn Gr	south India: Transition Zone granitic gneiss
TZgn Gd S	south India: Transition Zone granodioritic (silicic) gneiss
TZgn Gd I	south India: Transition Zone granodioritic (intermediate) gneiss
TZgn $\overline{X}$	south India: mean of Transition Zone gneisses
TZgn Tn S	south India: Transition Zone tonalitic (silicic) gneisses
TZgn Tn I	south India: Transition Zone tonalitic (intermediate) gneiss
TZch Gr	south India: Transition Zone granitic charnockite
TZch $\overline{X}$	south India: mean of Transition Zone charnockites
TZch Tn S	south India: Transition Zone tonalitic (silicic) charnockite
TZch Tn I	south India: Transition Zone tonalitic (intermediate) charnockite
Hi-P Ch $\overline{X}$	south India: mean of medium to high-pressure charnockites

Table V-2. Description of abbreviated names used in element-area diagrams.

For the south Indian samples, the general trends of the major-element terrane-mean values are decreasing SiO2 (Fig. V-9) and K2O (Fig. V19), and increasing Fe2O3, MgO, and CaO (Figs. V-10, V-11) with increasing metamorphic grade; there is an apparent but small increase in TiO2 (Fig. V-9). Na2O remains relatively constant in all terranes(Fig. V-11). Although there is a high degree of variability among different rock types, the trends of mean values, for increasing metamorphic grade, are similar to other Archaean terranes. However, both the Amitsoq and Madras tonalitic (intermediate) gneisses are very Fe and Ti rich on element-area diagrams (Figs. V-9, V-10); as noted above, these two groups also have a distinct Fe-rich tholeiitic trend on an AFM diagram.

It is interesting to note that for the south India results, changes in the mean abundances with metamorphic grade are not generally accompanied by changes in element abundances of the individual rock classifications. For example, the increase in the abundances of TiO2, Fe2O3, MgO, and CaO in the calculated means for each terrane from the amphibolite to granulite-facies, is not in general accompanied by an increase in the component rock types that comprise each terrane (for example, in the granitic, granodioritic, tonalitic gneisses and charnockites). This is also true for K2O, though not to the same degree (Fig. V-19). (A full discussion of K can be found in Section V.4.) This suggests that the increasing mean values of the mafic major-elements in the high-grade rocks (and corresponding decreasing means of SiO2) is largely the result of a relative decrease in the granitic component in the total mix that

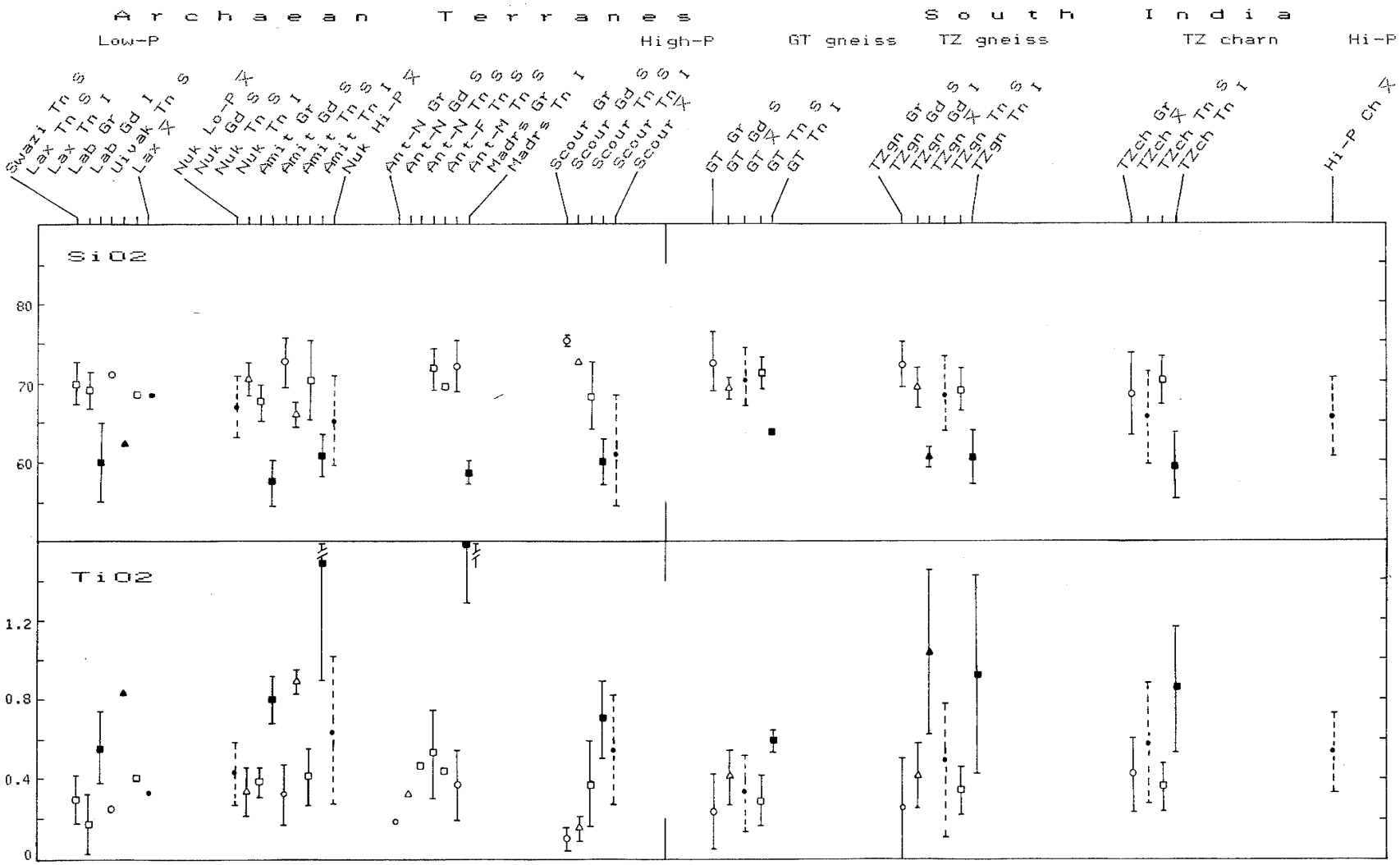

Fig. V-9. Element-area diagram for SiO2 and TiO2. (For description of localities and rock types see Table V-2, for data sources see Appendix C.)

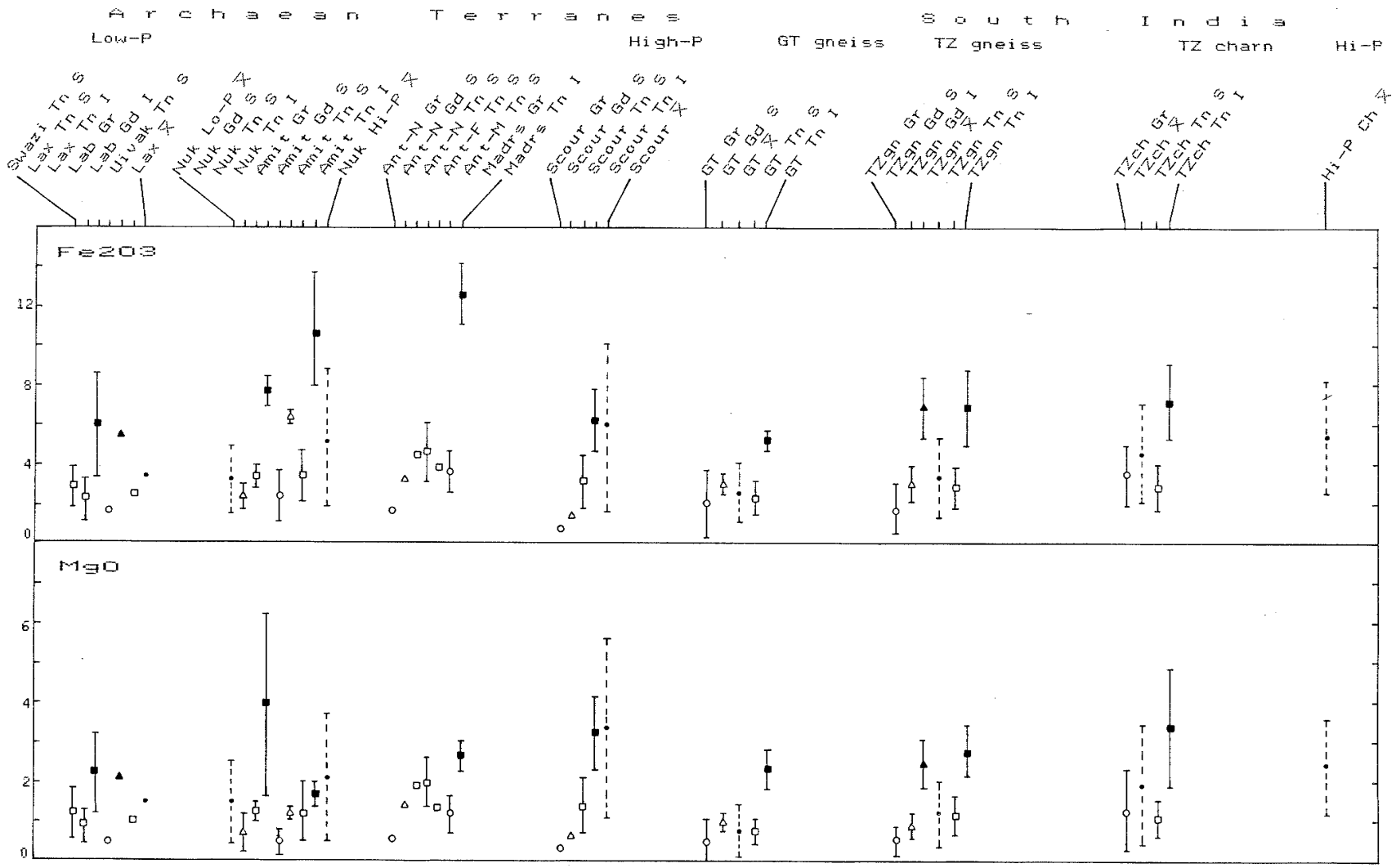

Fig. V-10. Element-area diagram for Fe2O3 and MgO. (For description of localities and rock types see Table V-2, for data sources see Appendix C.)

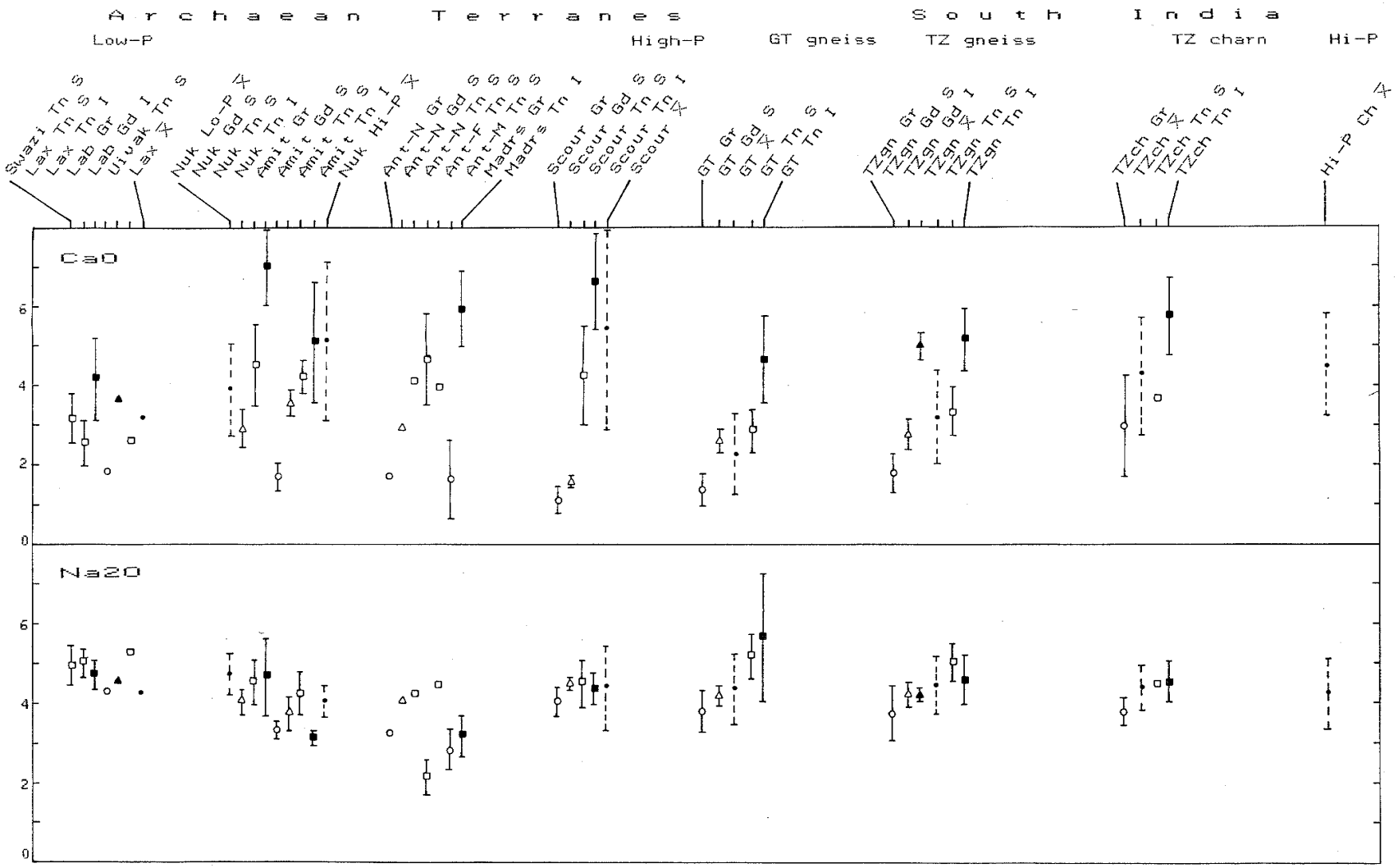

Fig. V-11. Element-area diagram for CaO and Na2O. (For description of localities and rock types see Table V-2, for data sources see Appendix C.)

comprises the mean of the higher grade terrane. Relative to the amphibolite-facies terrane-mean value, which compositionally is a mix of granitic and tonalitic gneisses, the higher-grade terranes increasingly become devoid of granitic gneisses (Figs. V-9 to V-11, V-19). This conclusion, of course, rests on the assumption that the sampling and analysis is not biased towards any specific rock type and that the mean value for each terrane is representative of the element abundances in that terrane. However, in other Archaean terranes, particularly the Lewisian Laxford-Scourian association, similar relationships between terrane-means and their component rock groups appear to exist for SiO2, TiO2, Fe2O3, and MgO, while the behavior of CaO is unclear.

SiO2 variation diagrams (Figs. V-12 to V-18, and V-25) show generally smooth trends with negative correlation for the granite-granodiorite-tonalite gneisses for TiO2, Fe2O3, MgO, CaO, and P2O5. The pattern of plots for Al2O3 is broad but generally retains a negative correlation with SiO2. Na2O and K2O have scattered patterns with no consistent trend (Figs. V-16, V-25) The patterns and trends in these variation diagrams are very similar to plots of Scourian granulites (Rollinson and Windley, 1980b), and other Archaean terranes (Tarney, 1976). The generally smooth trends of the intermediate and silicic south India samples on these variation diagrams suggests a cogenetic relationship between most of these rocks. The mafic samples generally plot as a population distinct from the other gneisses on variation diagrams, again suggesting a bimodal distribution to the south India rocks. Further discussion of the amphibolites and mafic

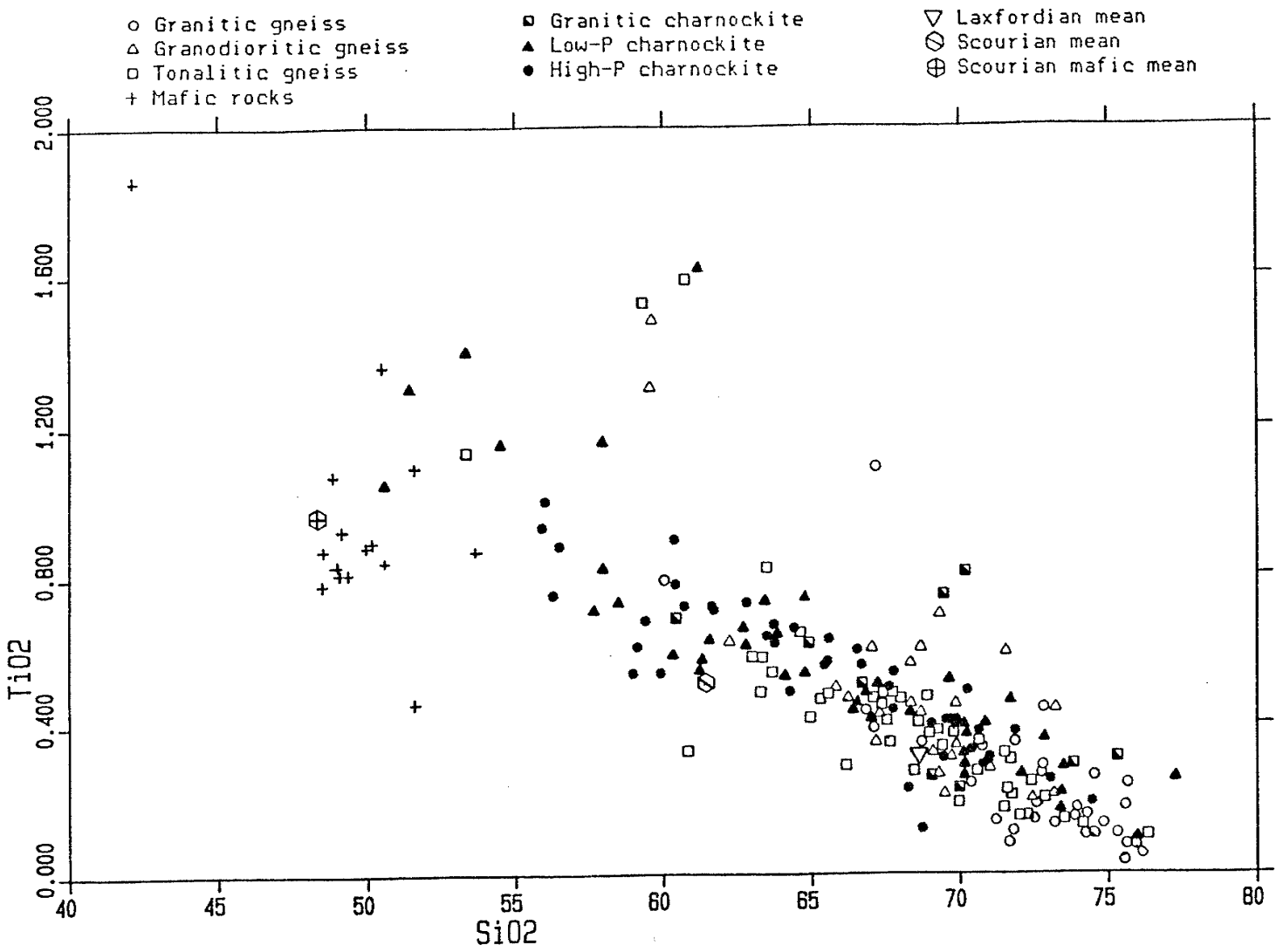

Fig. V-12. TiO2 vs SiO2 plot. Data from Appendix C.

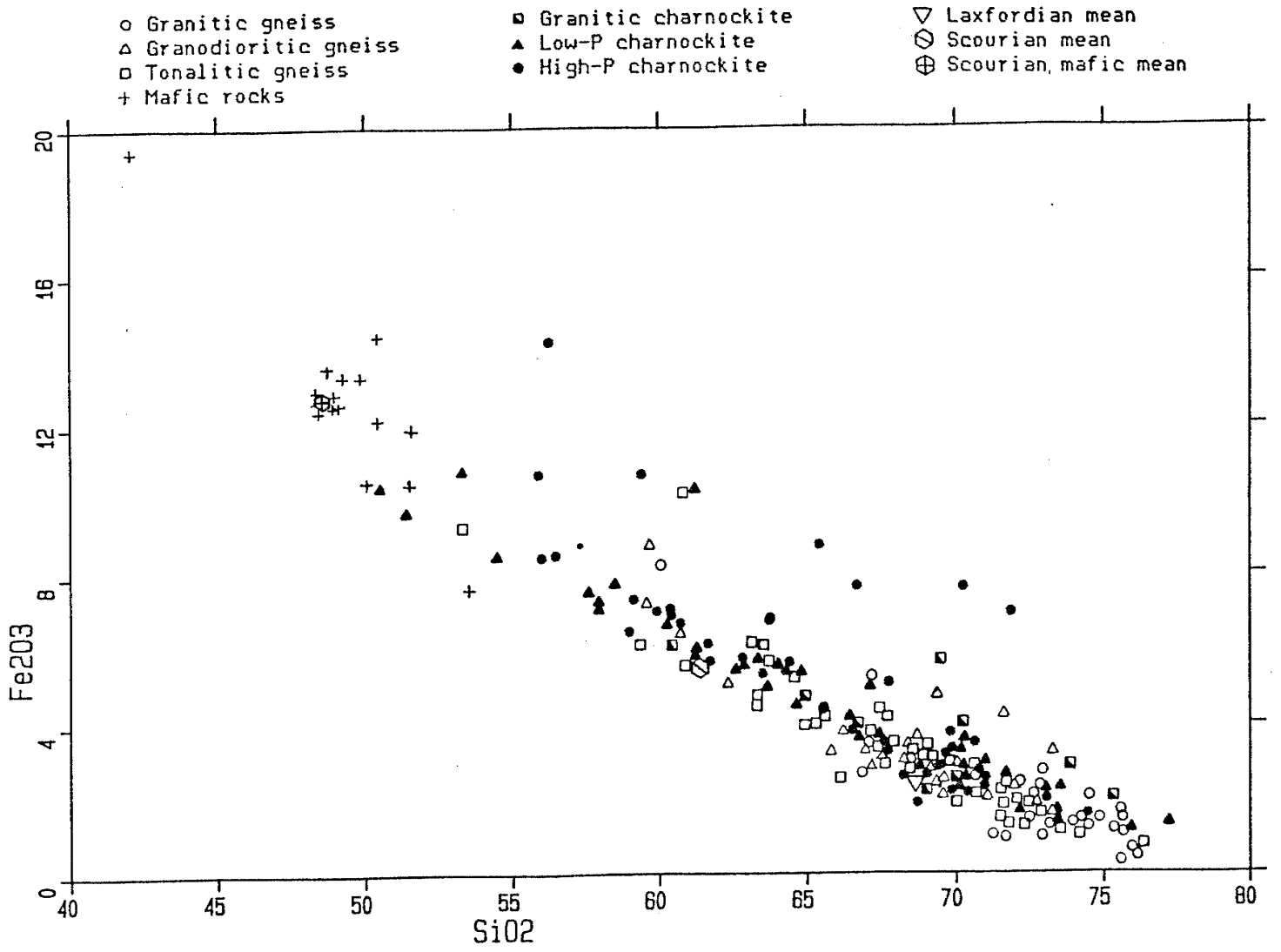

Fig. V-13. Fe203 vs SiO2 plot. Data from Appendix C.

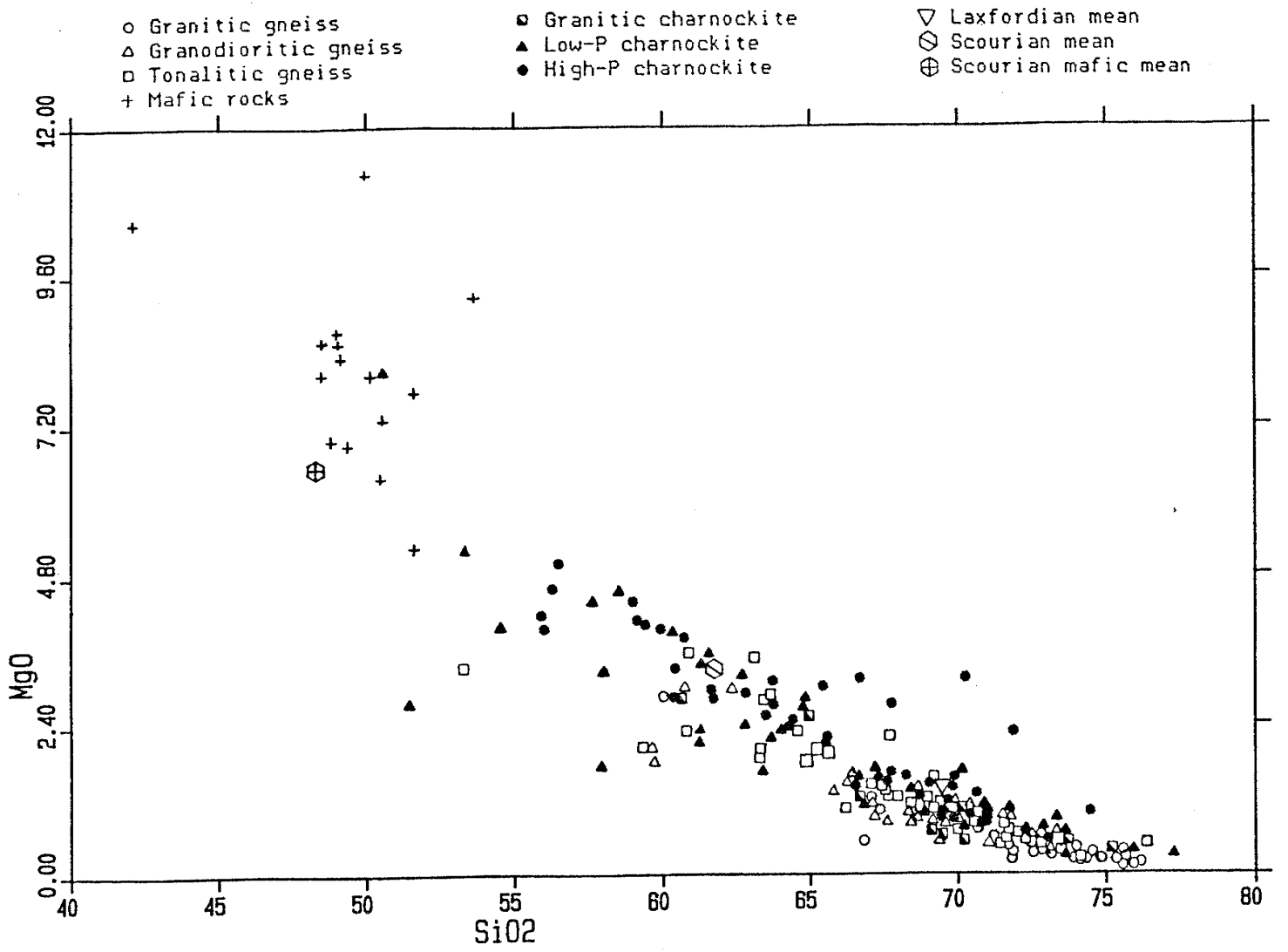

Fig. V-14. MgO vs SiO2 plot. Data from Appendix C.

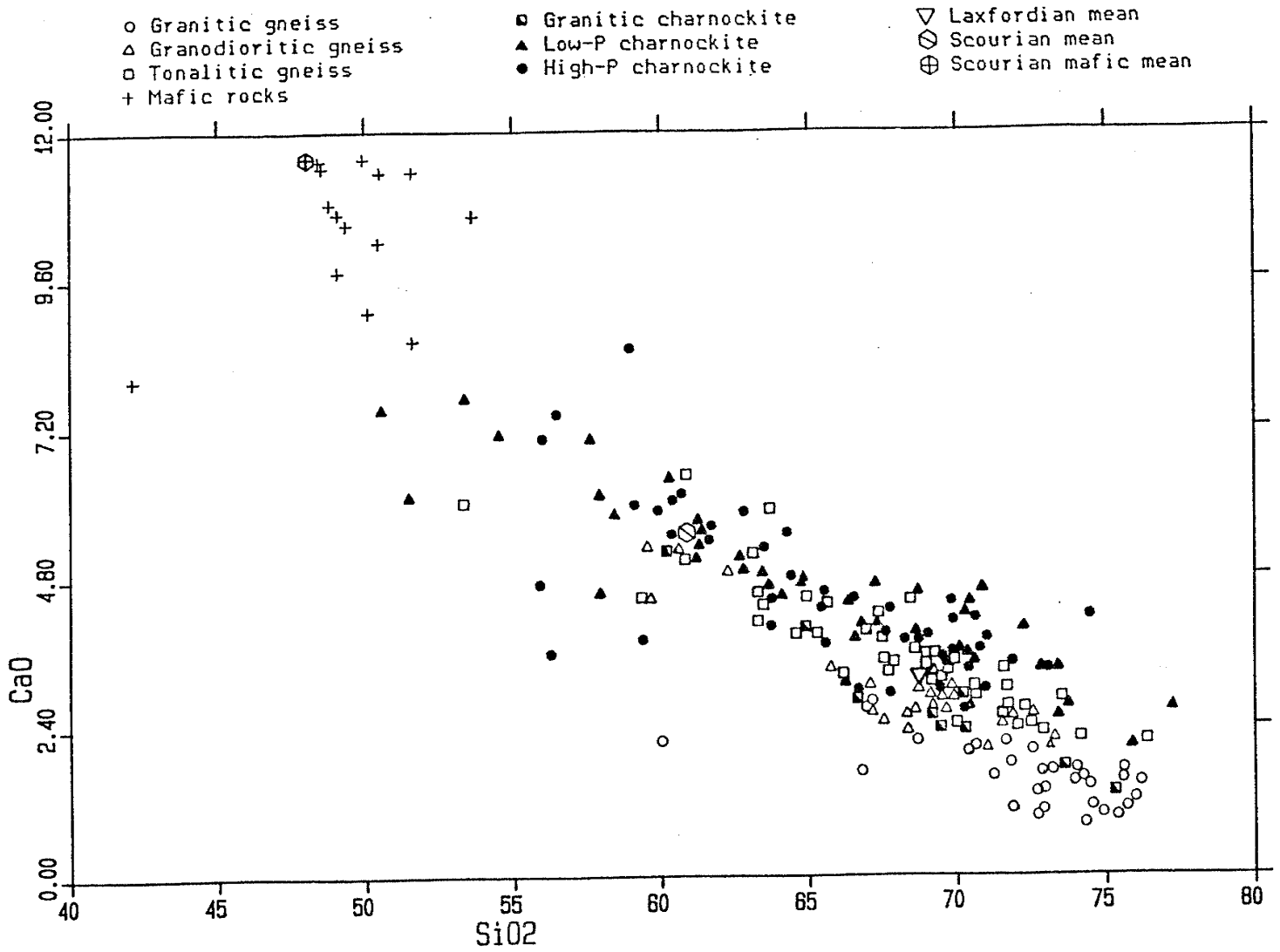

Fig. V-15. CaO vs SiO2 plot. Data from Appendix C.

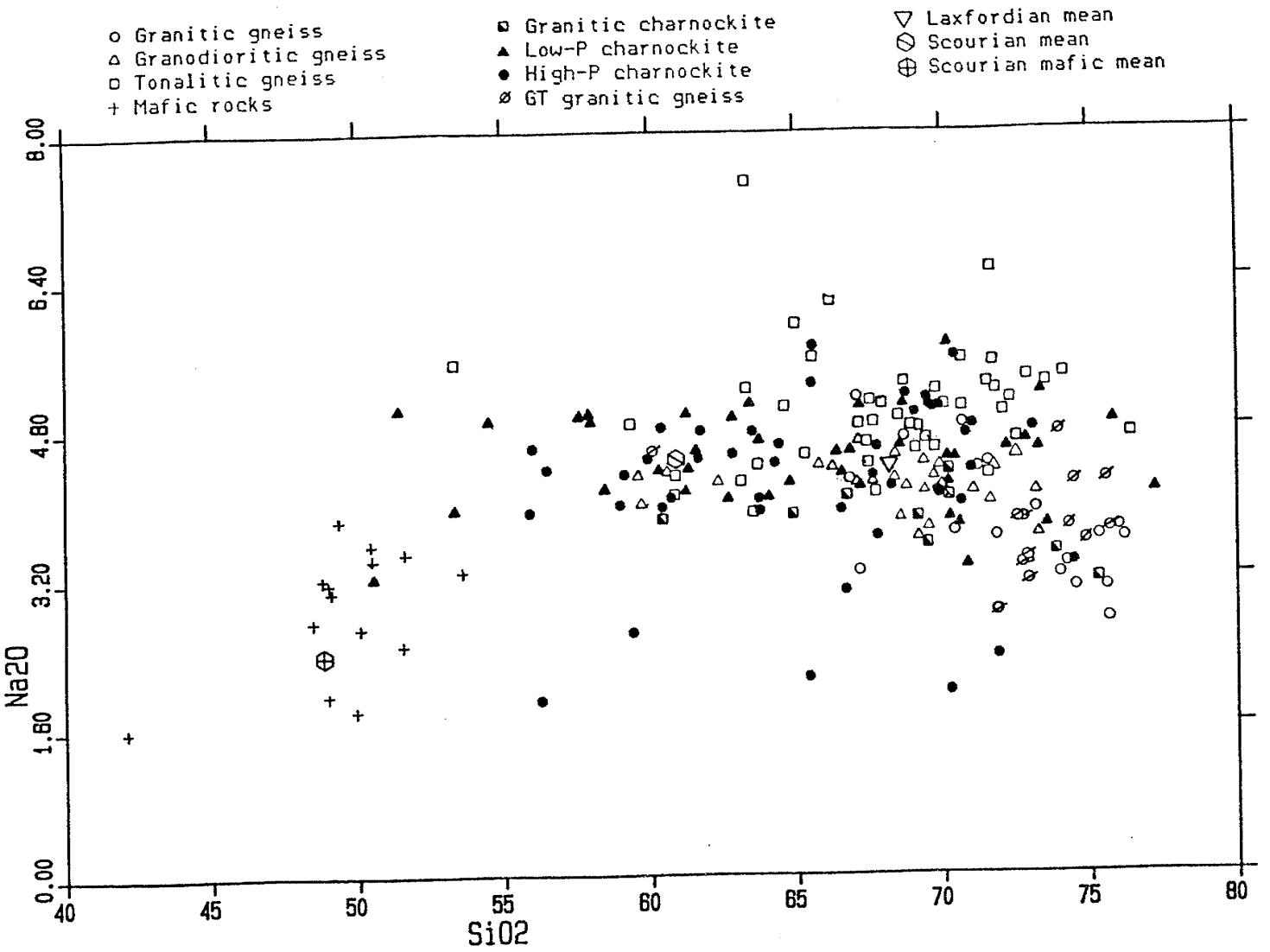

Fig. V-16. Na2O vs SiO2 plot. Data from Appendix C.

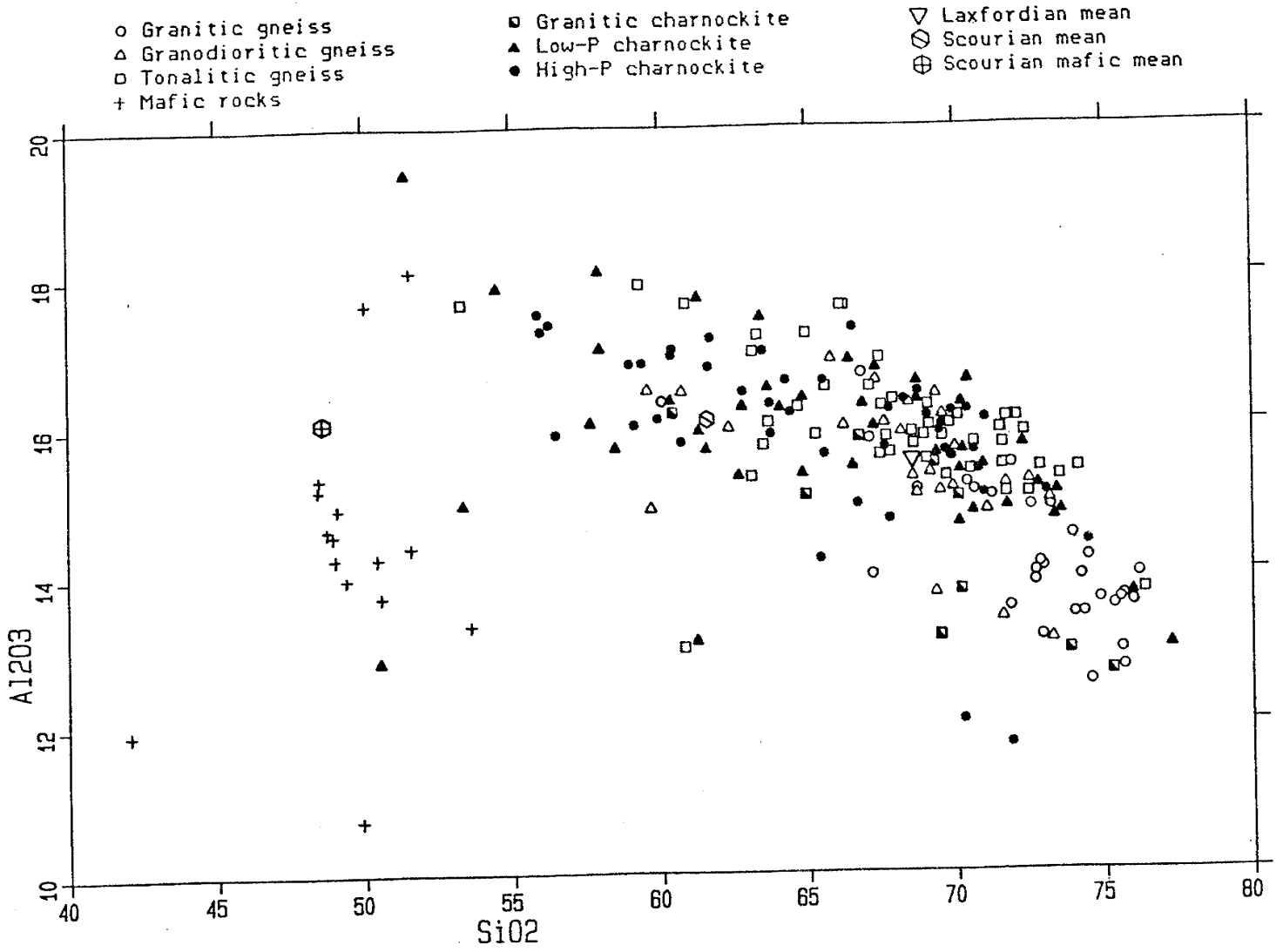

Fig. V-17. Al2O3 vs SiO2 plot. Data from Appendix C.

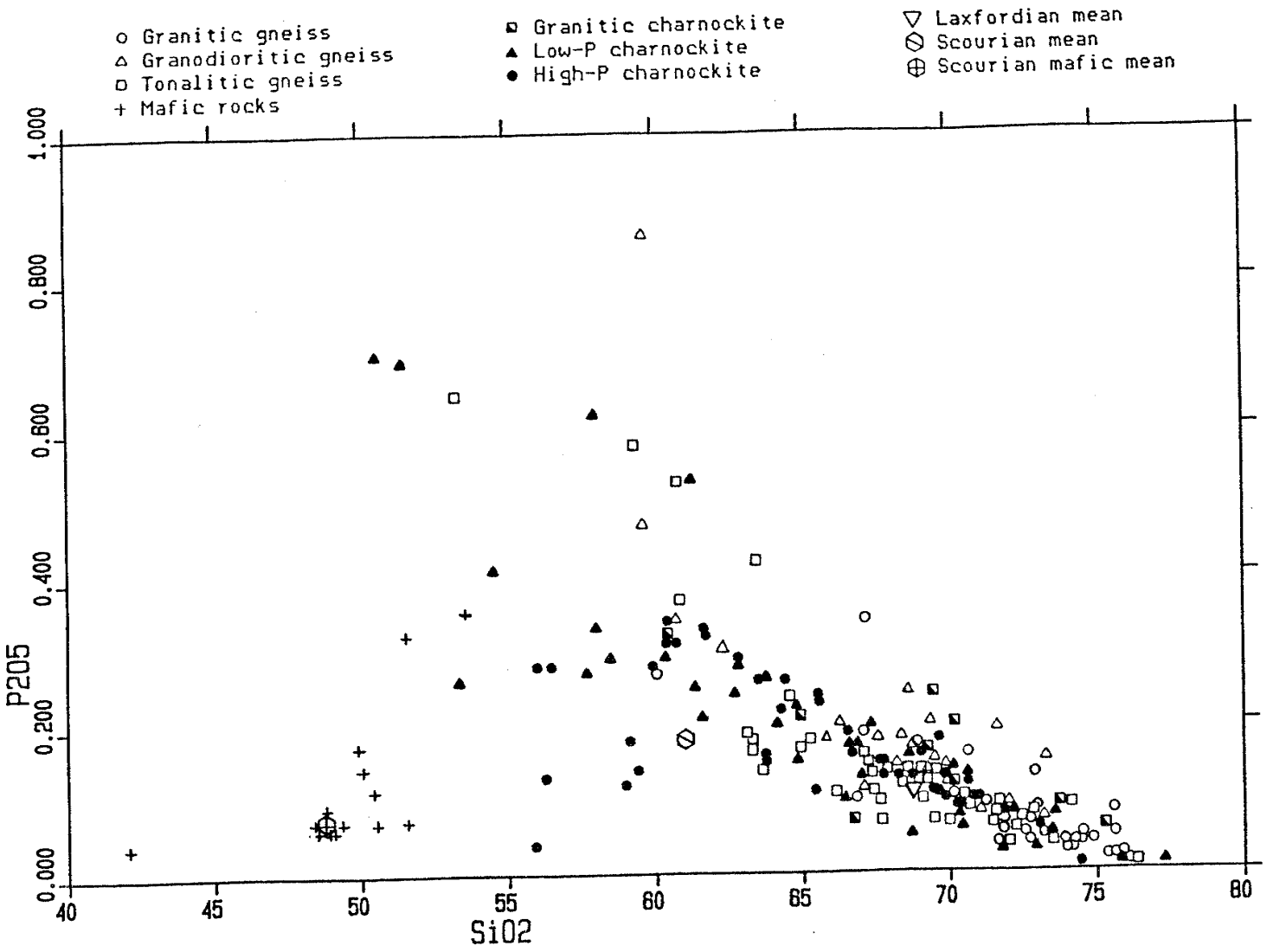

Fig. V-18. P205 vs SiO2 plot. Data from Appendix C.

granulites can be found in Section V.9.

V.4 Large-ion-lithophile and similar elements

V.4.1 Element-area diagrams

For the south India samples, K, Rb, Cs, U, Th, and Pb show a decrease in abundance with increases in metamorphic grade on element-area diagrams (Figs. V-19 to V-24). Data from other Archaean terranes indicates a similar trend. Of the other LIL elements, Ba has a high degree of variability in samples from both India and other Archaean terranes but does appear to be less abundant in the high-grade south India samples (~500 ppm), but relatively constant in other Archaean terranes (~750 ppm). K/Ba also has high variability with a similar weak trend to lower values in the higher-grade samples; a decrease of this ratio, with increase in metamorphic grade, is also evident in the Laxford and Scourian gneisses (Fig. V-23). Sr has rather constant values relative to changes in metamorphic grade for both south India and other Archaean terranes. The decrease of Ba/Sr in the terrane-mean values shows less variability than K/Ba, especially for the tonalitic (silicic and intermediate) gneisses. The decrease of Ba/Sr in the high-P terrane-mean values appears to result from the smaller contribution of granitic and granodioritic rocks which have higher Ba/Sr (Fig. V-22). Thus, neither Ba nor Sr appear to be significantly mobilized by increasing metamorphic grade.

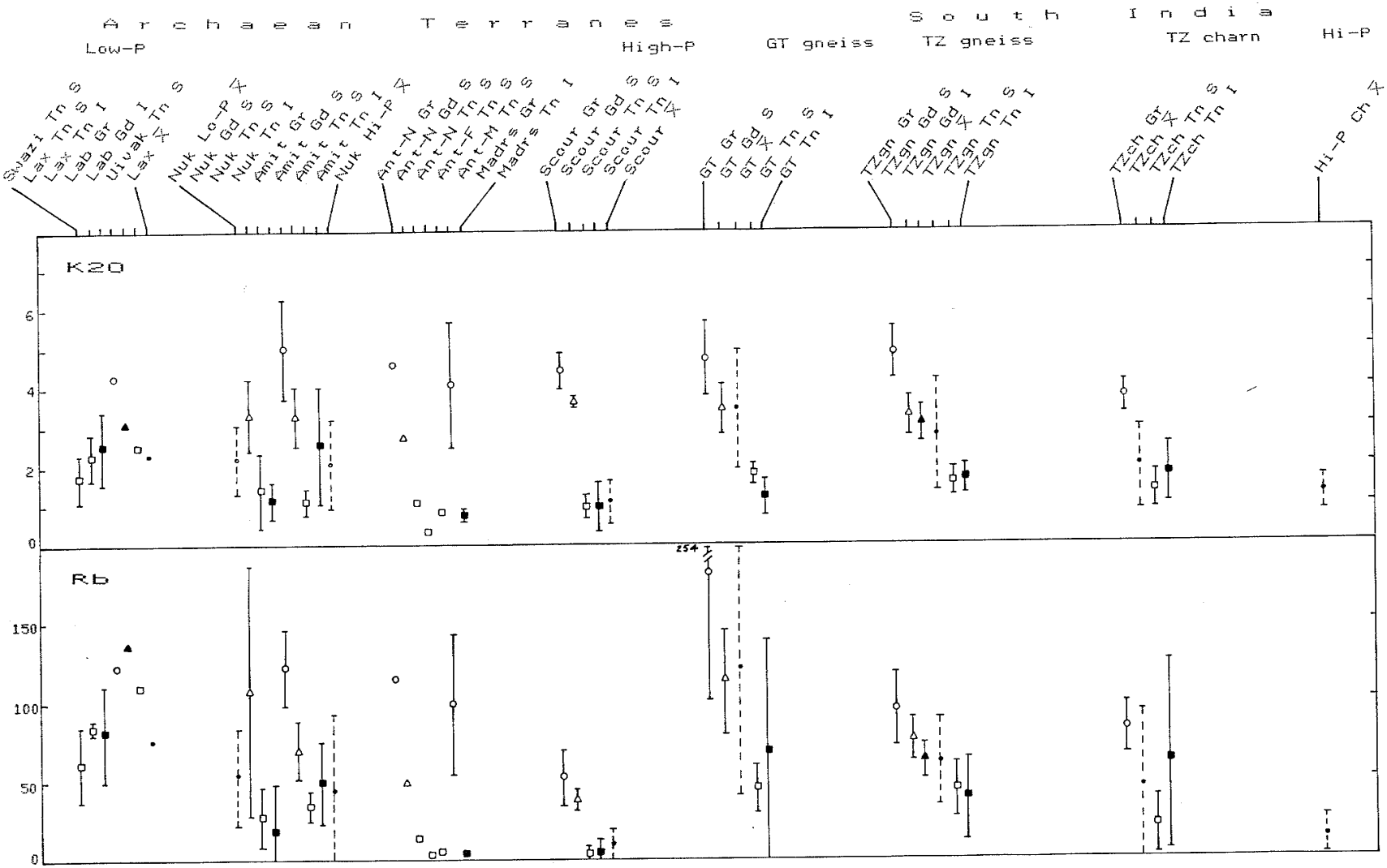

Fig. V-19. Element-area diagram for K20 and Rb. (For description of localities and rock types see Table V-2, for data sources see Appendix C.)

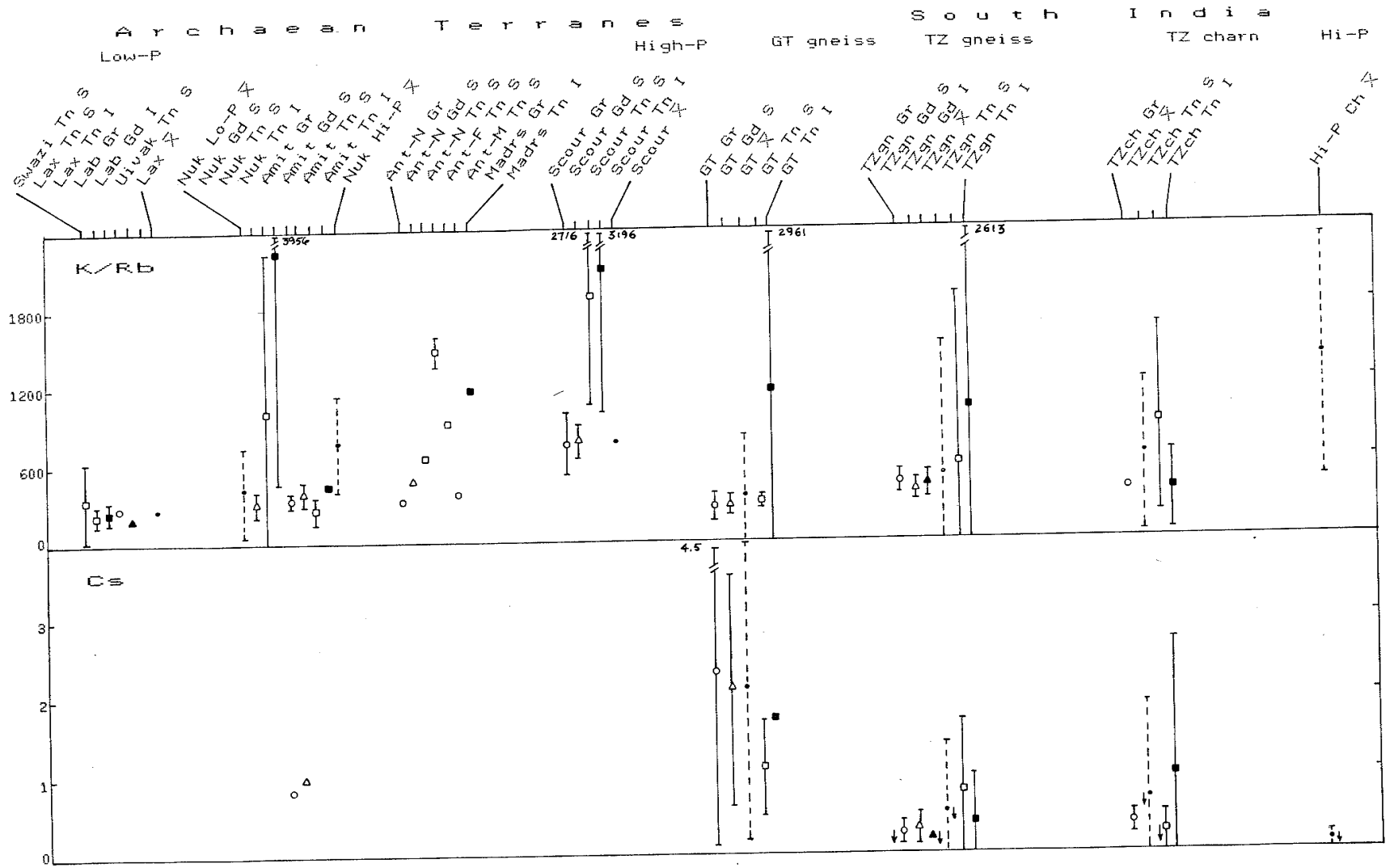

Fig. V-20. Element-area diagram for K/Rb and Cs. (For description of localities and rock types see Table V-2, for data sources see Appendix C.)

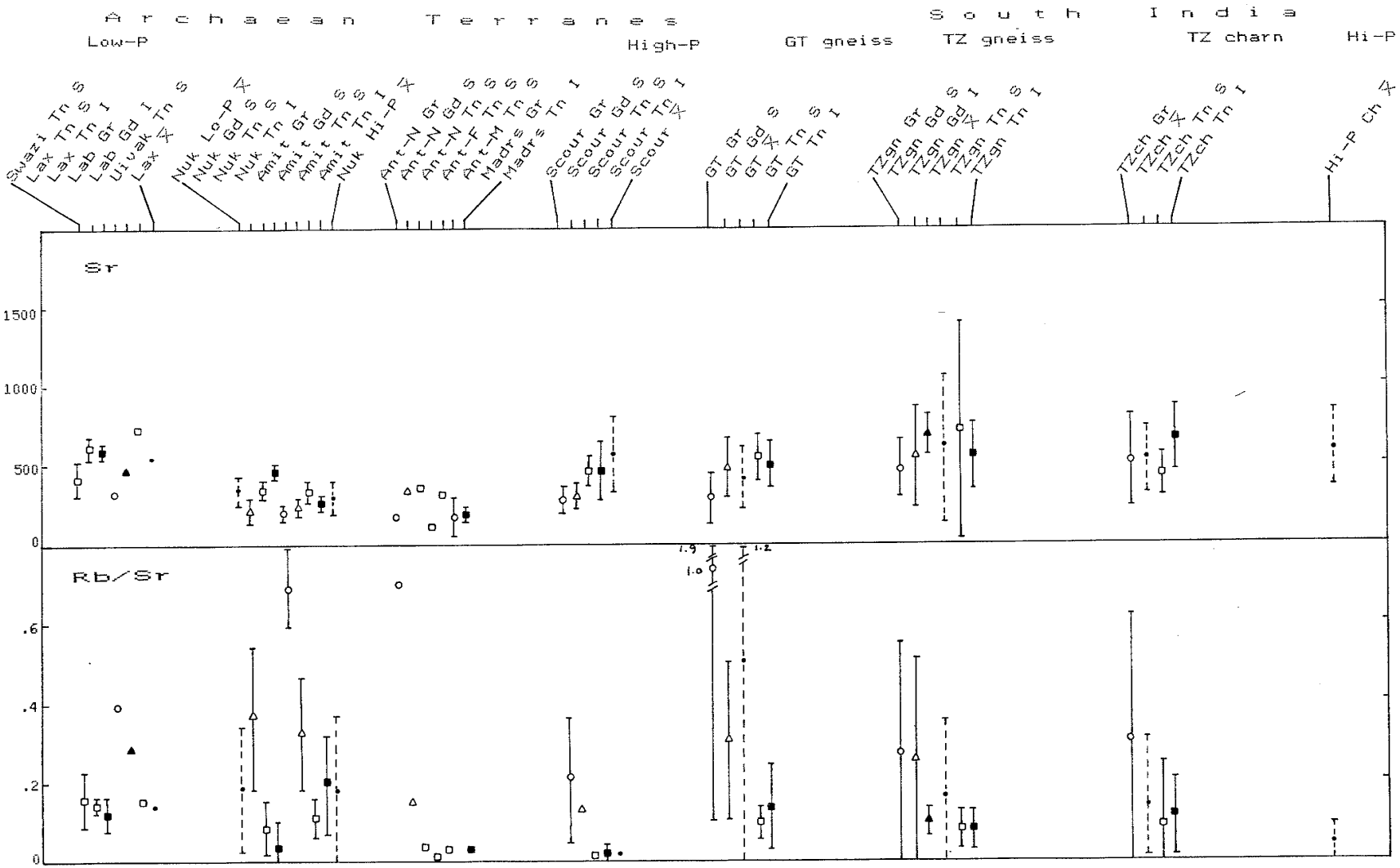

Fig. V-21. Element-area diagram for Sr and Rb/Sr. (For description of localities and rock types see Table V-2, for data sources see Appendix C.)

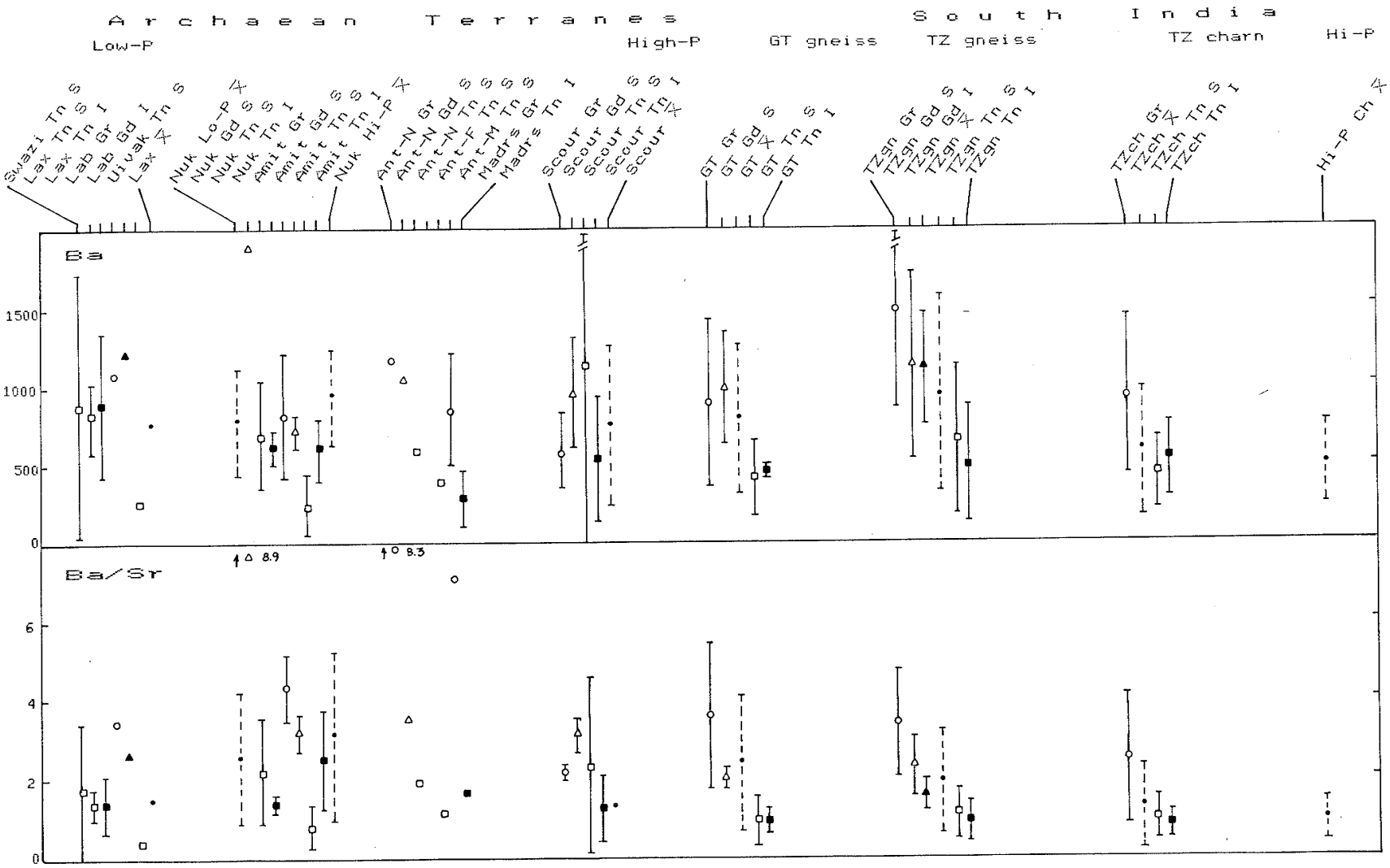

Fig. V-22. Element-area diagram for Ba and Ba/Sr. (For description of localities and rock types see Table V-2, for data sources see Appendix C.)

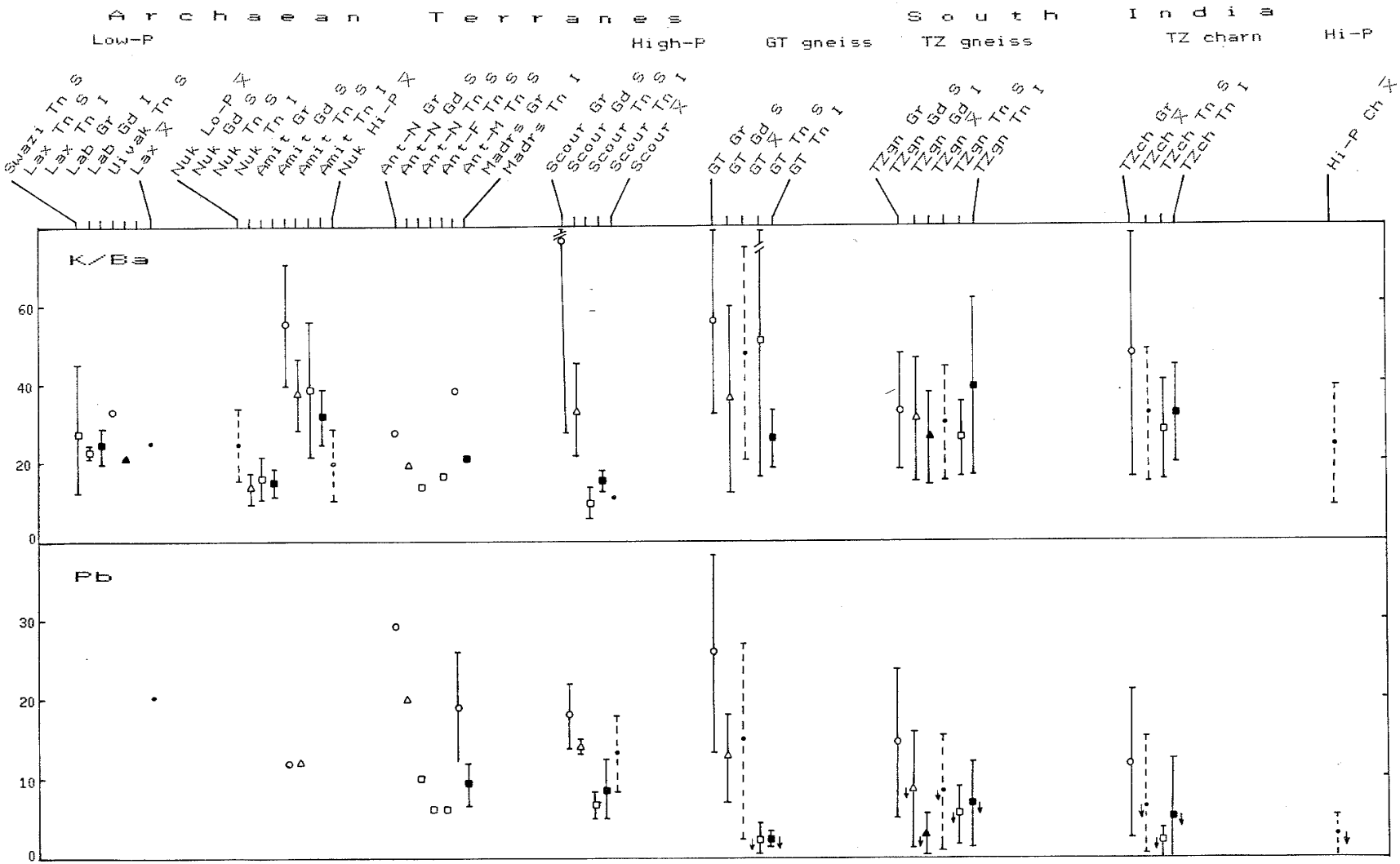

Fig. V-23. Element-area diagram for K/Ba and Pb. (For description of localities and rock types see Table V-2, for data sources see Appendix C.)

The Rb/Sr and K/Rb values in the south India samples have high variability, with K/Rb showing an increase, and Rb/Sr a decrease with metamorphic grade, indicating loss of Rb (Figs. V-20, V-21). Rb/Sr drops from 0.53 in the Gneiss Terrane, to 0.16 in the amphibolite-facies and 0.13 in the granulite-facies of the Transition Zone, and 0.036 in the high-P charnockites. The decrease in the terrane-mean values is accompanied by a decrease of Rb/Sr in the component granitic and granodioritic gneisses; however, the Rb/Sr value in the tonalitic gneisses remains relatively constant until the decrease in the high-P charnockites. The decrease in Rb/Sr from the Laxfordian (0.138) to Scourian (0.018) is less sharp and appears to occur both in the mean values for each terrane but also in the component granitic and tonalitic gneisses (Fig./ V-21).

It is interesting to note the differences between the decrease in abundances, with increases in metamorphic grade, of K, Rb, Cs, U, Th, and Pb. The K values within each component rock are relatively constant or exhibit a small decrease (Fig. V-19). As noted above, the major decrease in the overall mean value of K in the high-grade terranes appears to result from the relative decrease of the granitic and granodioritic component and the predominance of tonalitic gneiss in that terrane; and low K values are characteristic of tonalitic gneiss (Barker et al., 1976; Arth et al., 1978; Barker, 1979). Nevertheless, there is some K movement in gneisses of tonalitic-trondhjemitic composition; in the Lewisian there is a 30% depletion of K in the granulite facies Scourian (mean K2O=1.25%) relative to the amphibolite-facies gneisses from Gruinard Bay (mean K2O=1.75%)

(Rollinson and Windley, 1980a). This apparent decrease in both the terrane-means and component rocks between the Scourian and Laxforian gneisses is also seen on the K2O element-area diagram (Fig. V-19). A comparison of south India tonalitic gneiss and tonalitic charnockite plots on an Ab-An-Or ternary diagram (Figs. V-1, V-2), also indicates that the higher pressure charnockites have slightly lower K as evidenced by lower normative Or. Thus, K2O experiences a slight decrease in the component rock groups, but a more severe decrease in the all inclusive terrane-mean values.

In contrast to K, the decreases of Rb, Cs, U, and Th in the south India samples typically occur in all rock groups, for example, in the granites and tonalitic (silicious and intermediate) gneisses. This suggests that Rb, Cs, U, and Th are preferentialy mobilized relative to K in high-grade rocks. For other Archaean terranes there is insufficient data for Cs and U, but the behavior of Rb and Th in the component rock groups of other terranes parallels that seen in south India (Figs. V-20, V-24). The increase in K/Rb with metamorphic grade for the component rock groups, both in south India and other Archaean terranes, also indicates different rates of loss for Rb and K (Tarney and Windley, 1977; Rollinson and Windley, 1980a)(Fig. V-19). The K/Rb ratio is lower in biotite than in K-feldspar (Heier and Adams, 1964; Heier and Billings, 1970a) and the breakdown of biotite, with K-feldspar stable, during granulite-facies metamorphism increases the K/Rb ratio of the whole rock. In addition, the K/Rb ratio of K-feldspar also increases during metamorphism (Heier and Billings, 1970a). R.C. Newton and E.C. Hansen (personal

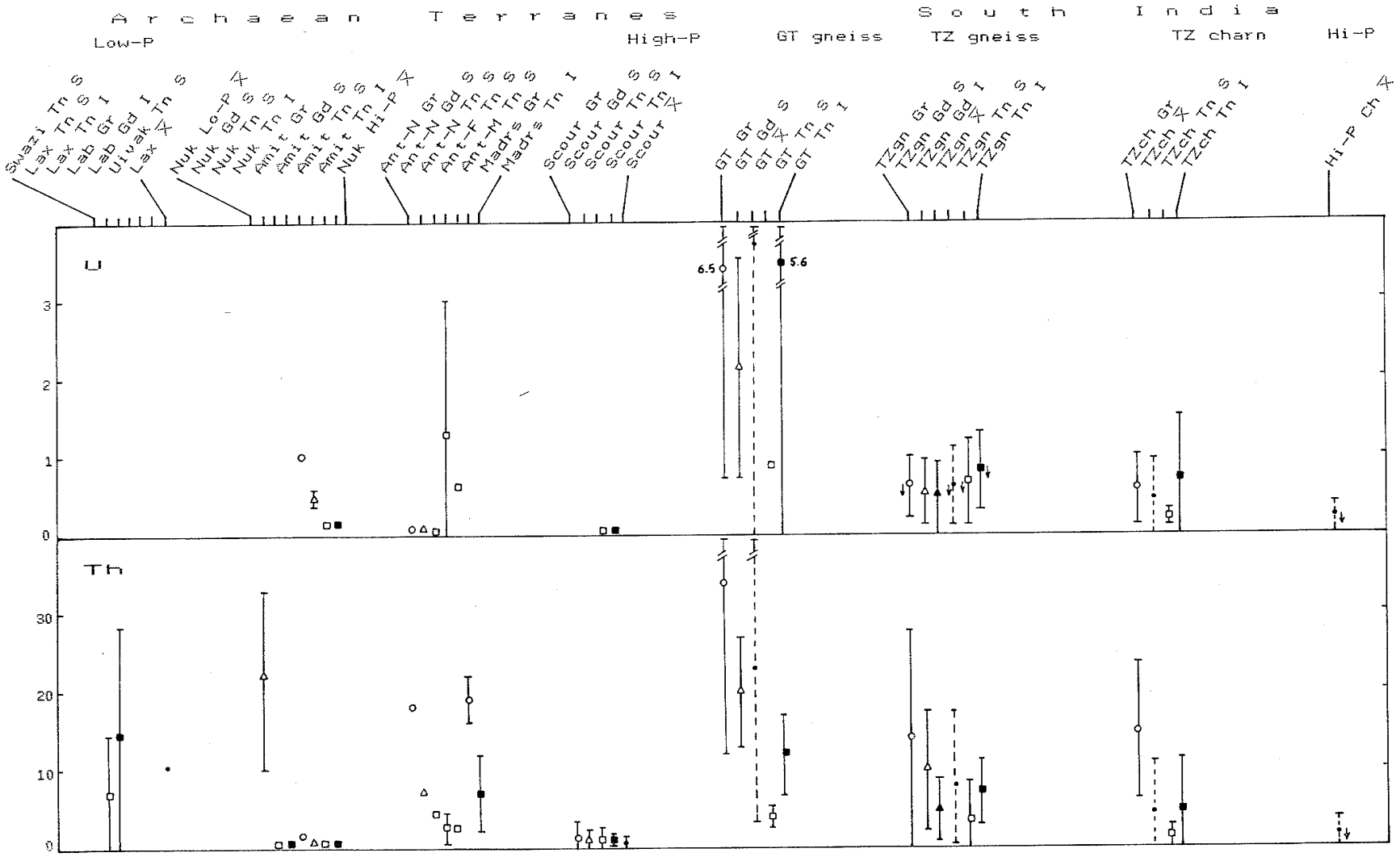

Fig. V-24. Element-area diagram for U and Th. (For description of localities and rock types see Table V-2, for data sources see Appendix C.)

communication, 1985) have observed a correlation between increasing K/Rb ratios in biotite accompanying decreasing modal biotite in samples of increasing metamorphic grade near Kabbaldurga. This suggests that even in the biotite not replaced by high-grade metamorphism, the K/Rb ratio increases. Though there is an apparent decrease in Pb abundances in granitic gneisses and high-K charnockite with increase in metamorphic grade, the change in abundance in the tonalitic gneisses is less certain; for many of the tonalitic samples the value is below the detection limit and accurate estimate of abundance difficult (Fig. V-23). Pb substitutes for K in biotite and K-feldspar, though predominantly in the latter (Wedepohl, 1974), and its change in concentration relative to metamorphic grade probably is similar to Ba, which is also more abundant in K-feldspar than in biotite.

V.4.2 K and K/Rb plots

On the K2O - SiO2 variation diagram (Fig. V-25) the tonalitic gneisses and charnockites show little change of K2O with SiO2 (K2O ~= 0.8-2.4%). However, the granitic gneisses plot as a relatively distinct population with high K2O, and the granodioritic gneisses fall in an intermediary position between granite and tonalite. Plots of Laxfordian, Scourian, and Scourian-mafic major-element mean values show the close similarity of the Lewisian with the results from south India (Figs. V-12 to V-18). There is also a good similarity between plots of representative Scourian granitic-tonalitic-gabbro samples on a K2O - SiO2 diagram (Rollinson and Windley, 1980b) and samples from south India; both show a flat pattern for rocks of tonalitic

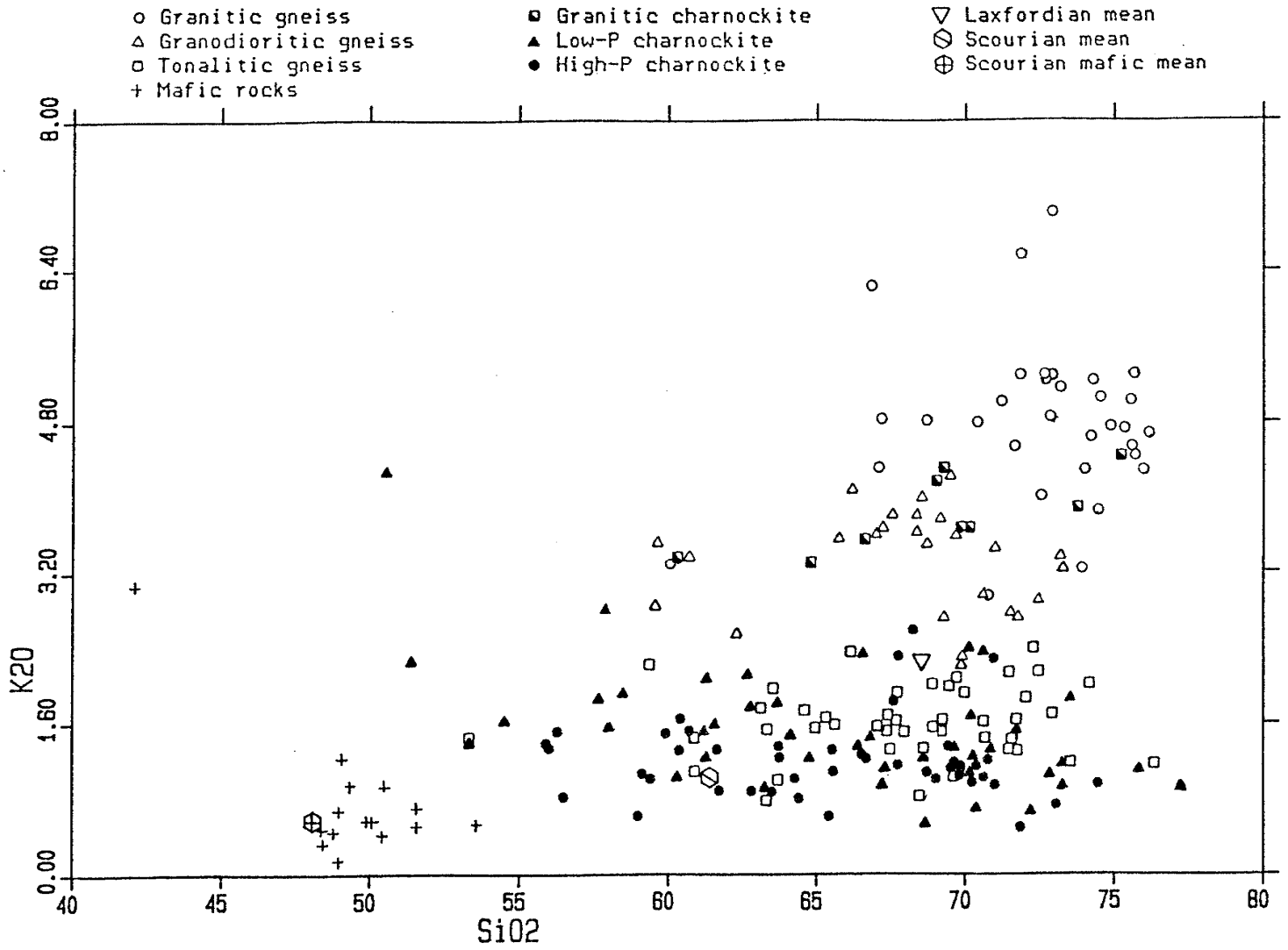

Fig. V-25. K2O vs SiO2 plot. Data from Appendix C.

composition and a sharply elevated pattern for the granitic-granodioritic rocks.

A comparison of the K2O - SiO2 and Rb - SiO2 diagrams (Figs. V-25 and V-26) also suggests the different behavior of K and Rb. In the K2O - SiO2 diagram, tonalitic gneisses and charnockite lie in a similar field, with granitic rocks defining a separate group. In the Rb - SiO2 diagram, the tonalitic and granodioritic gneisses and low-P charnockites generally comprise a grouping (with granitic gneisses somewhat enriched in Rb), with the high-P and some low-P charnockites, relatively low in Rb, making up a separate suite. This is comparable to plots of Scourian rocks (Rollinson and Windley, 1980b): granulite-facies trondhjemitic-tonalitic gneisses define a flat trend (with Rb <20 ppm), and granitic rocks have a pattern with sharply enriched Rb. For the south India rocks, the change in K abundance occurs primarily along compositional lines, between the granitic and tonalitic gneisses; the change in Rb, however, occurs largely along metamorphic lines, between amphibolite facies gneisses and high-P charnockite.

For upper crustal rocks, Shaw (1968) defined an igneous K-Rb fractionation "Main Trend" with a slope of K/Rb=433 at K=0.1% and K/Rb=195 at K=10%, where the average upper crust falls on the trend K/Rb=230. In high-grade rocks there is a sharp departure from this trend, and high K/Rb values (K/Rb>1000) are found at low levels of Rb and K (Green et al., 1972; Lewis and Spooner, 1973; Sheraton et al., 1973; Tarney and Windley, 1877). These trends are seen in the results from south India where charnockite and tonalitic gneisses define a

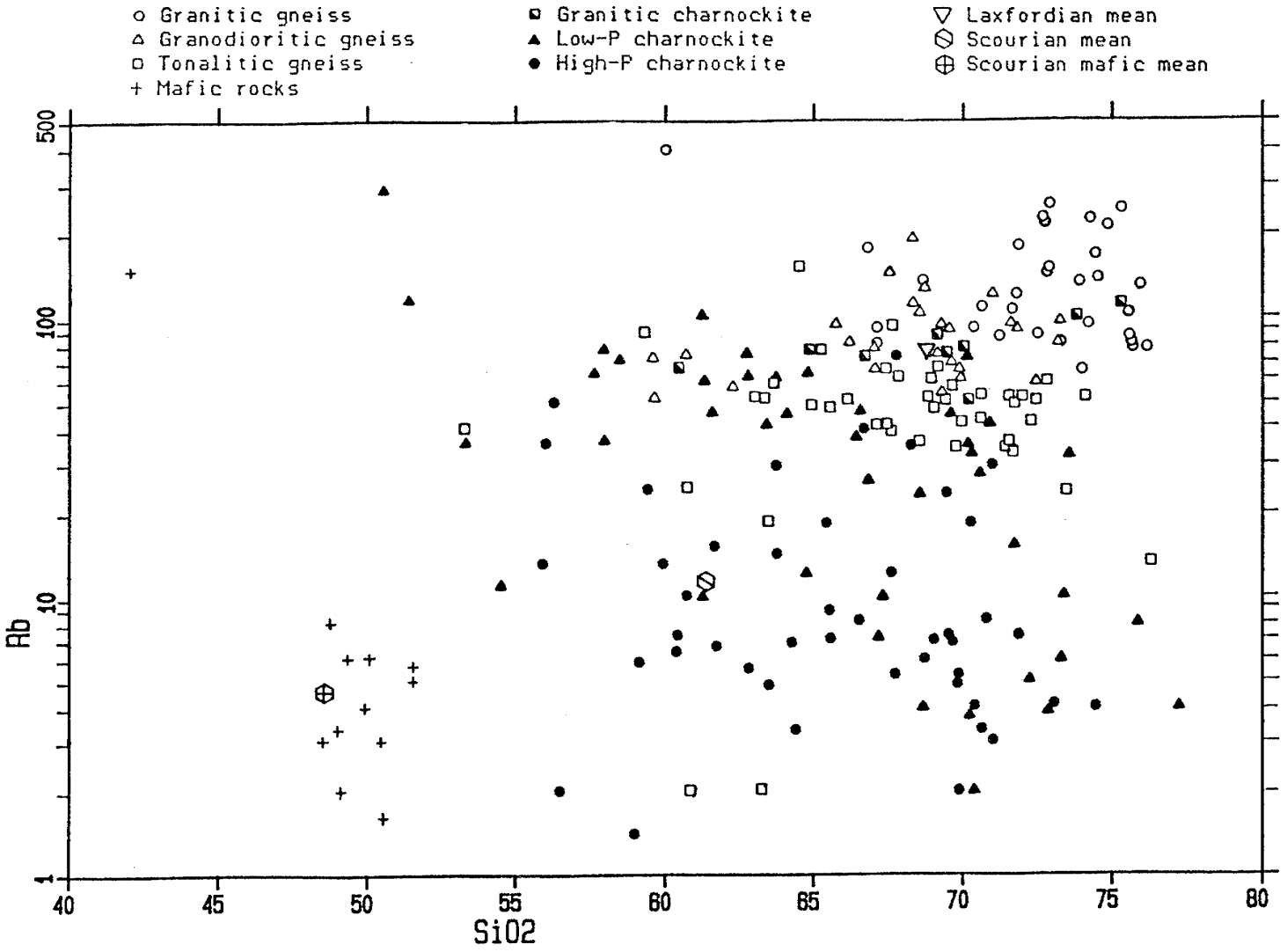

Fig. V-26. Rb vs SiO2 plot. Data from Appendix C.

trend of constant to gently rising K (%K~=0.6-2.0) and sharply changing K/Rb, and the amphibolite-facies granitic-granodioritic-tonalitic gneisses define a trend along increasing K and relatively constant K/Rb values (K/Rb~=200-500) (Fig. V-28).

The relatively high-P tonalitic charnockites from the Scourian (Sheraton, 1970; Rollinson and Windley, 1980a; Pride and Muecke, 1982) and the East Antarctic Shield (Sheraton and Black, 1983; Sheraton and Collerson, 1984) have a flat to gently rising trend with increasing Rb and plot in the same general field as the south India tonalites and charnockites. This same trend is seen in those granulite-facies Nuk gneisses from Buksefjorden, West Greenland, with Rb ~<20 ppm; however, the majority of the Nuk gneisses have higher Rb and fall along an upper-crust fractionation trend of K/Rb~=200-600 (Wells, 1979). This same trend, of a relatively constant K/Rb at Rb~> 20 ppm, is seen in the amphibolite-facies Uivak I gneisses, Labrador (K/Rb=100-300) (Bridgewater and Collerson, 1976) and Laxford gneisses from Rhiconich and Harris and Lewis, Scotland (K/Rb~=230)(Sheraton, 1970). Granulite-facies, granitic and granodioritic rocks (Rb~=20-80) from the Scourian (Rollinson and Windley, 1980a; Pride and Muecke, 1982) and the East Antarctic Shield (Sheraton and Black, 1983; Sheraton and Collerson, 1984), and (Rb~=40-200 from Madras (Weaver et al., 1978), are relatively enriched in K and fall above the gently rising trend of the high-grade tonalitic granulites. However, close examination of plots of Scourian granitic charnockites on a K- Rb diagram (Rollinson and Windley, 1980a) shows a pattern with a trend of similar orientation to that for the tonalitic rocks; this suggests that in

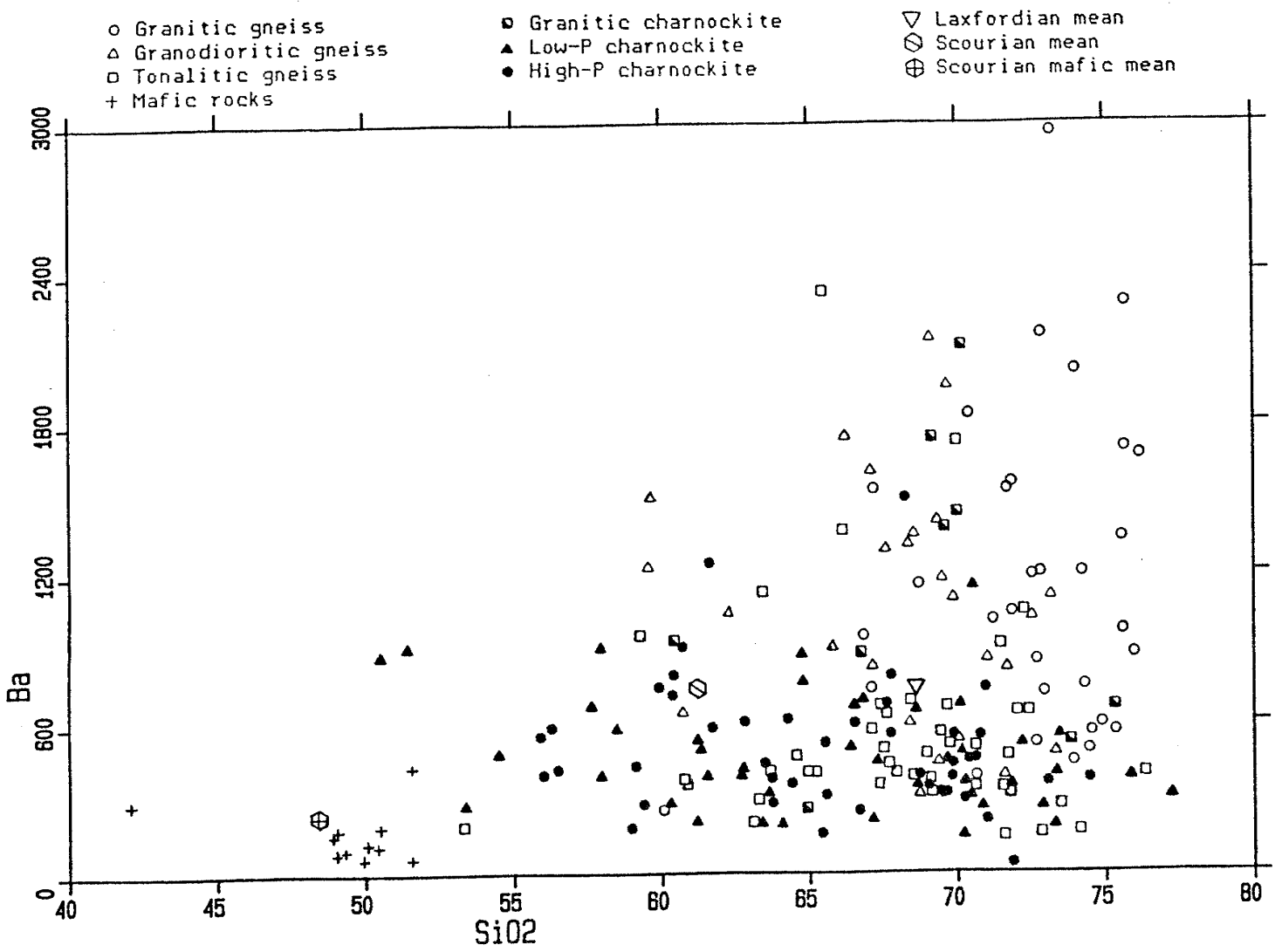

Fig. V-27. Ba vs SiO2 plot. Data from Appendix C.

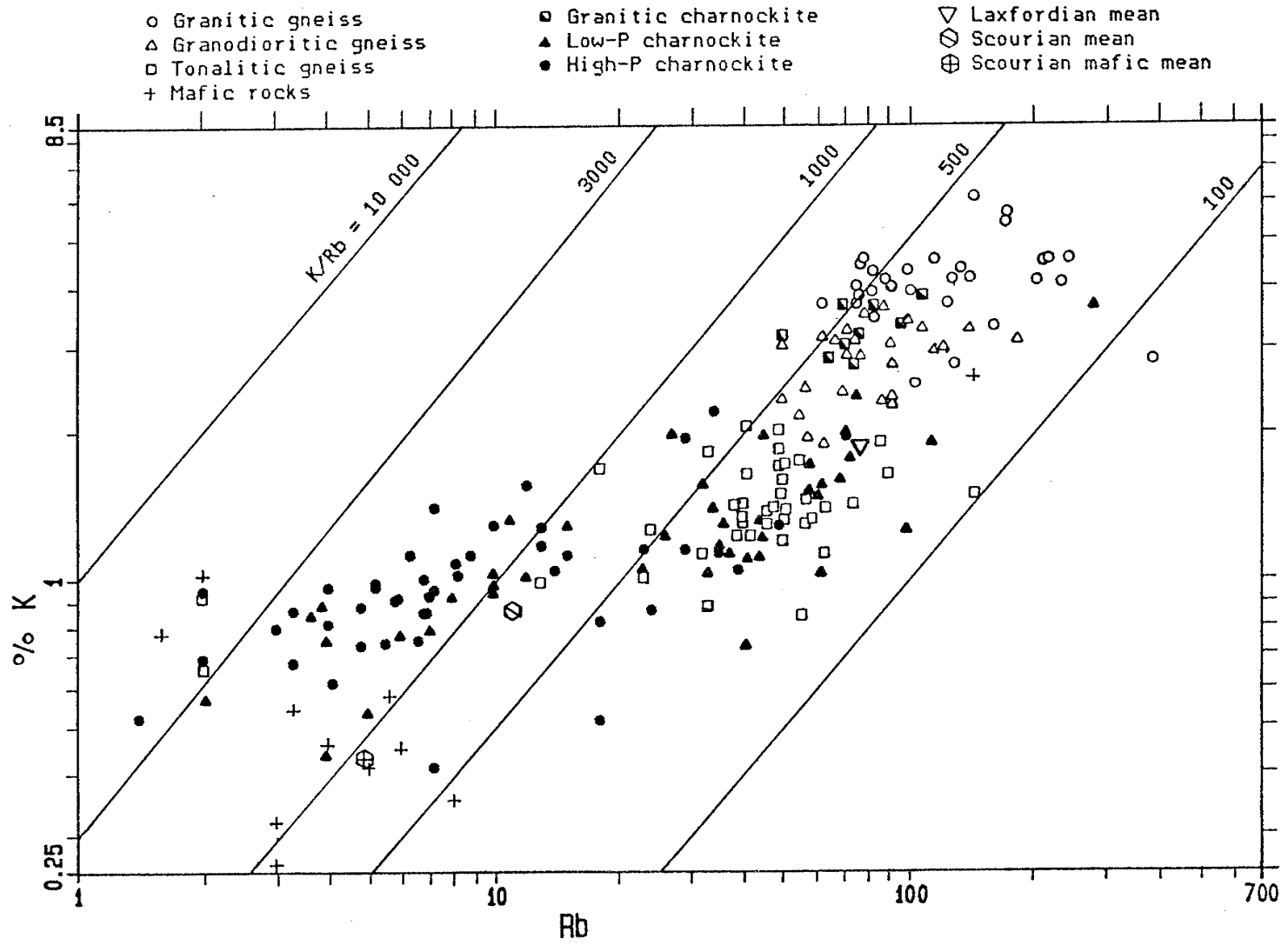

Fig. V-28. %K vs Rb plot. Data from Appendix C.

high-grade terranes the depletion of Rb in granites parallels that in the tonalite. When biotite is stable in medium-grade metamorphic terranes the K/Rb is controlled by biotite (McCarthy, 1976; Barbey and Cuney, 1982); in granulite-facies terranes where hydrous biotite breaks down, K feldspar or other mineral phases control the value of K/Rb (Whitney, 1969), which results in higher K/Rb values and the change in the slope of plots on a K - Rb diagram.

The K/Rb - K plot for the south India samples shows relatively flat K/Rb values for the granitic to tonalitic gneiss trend, but high K/Rb, with decreasing K, for the tonalitic gneiss to high-P charnockite trend (Fig. V-29). A very similar pattern is seen in the Lewisian with the Laxfordian gneisses lying along a flat trend, with constant K/Rb for increasing K; and the granulite-grade Scourian defining a distinctly separate population, with the majority of the samples having K/Rb~=500-1400 at %K~=0.4-1.2 (Sheraton, 1970). It is interesting to note the relatively distinct high-P charnockite populations in both the K - Rb and K/Rb - K plots.

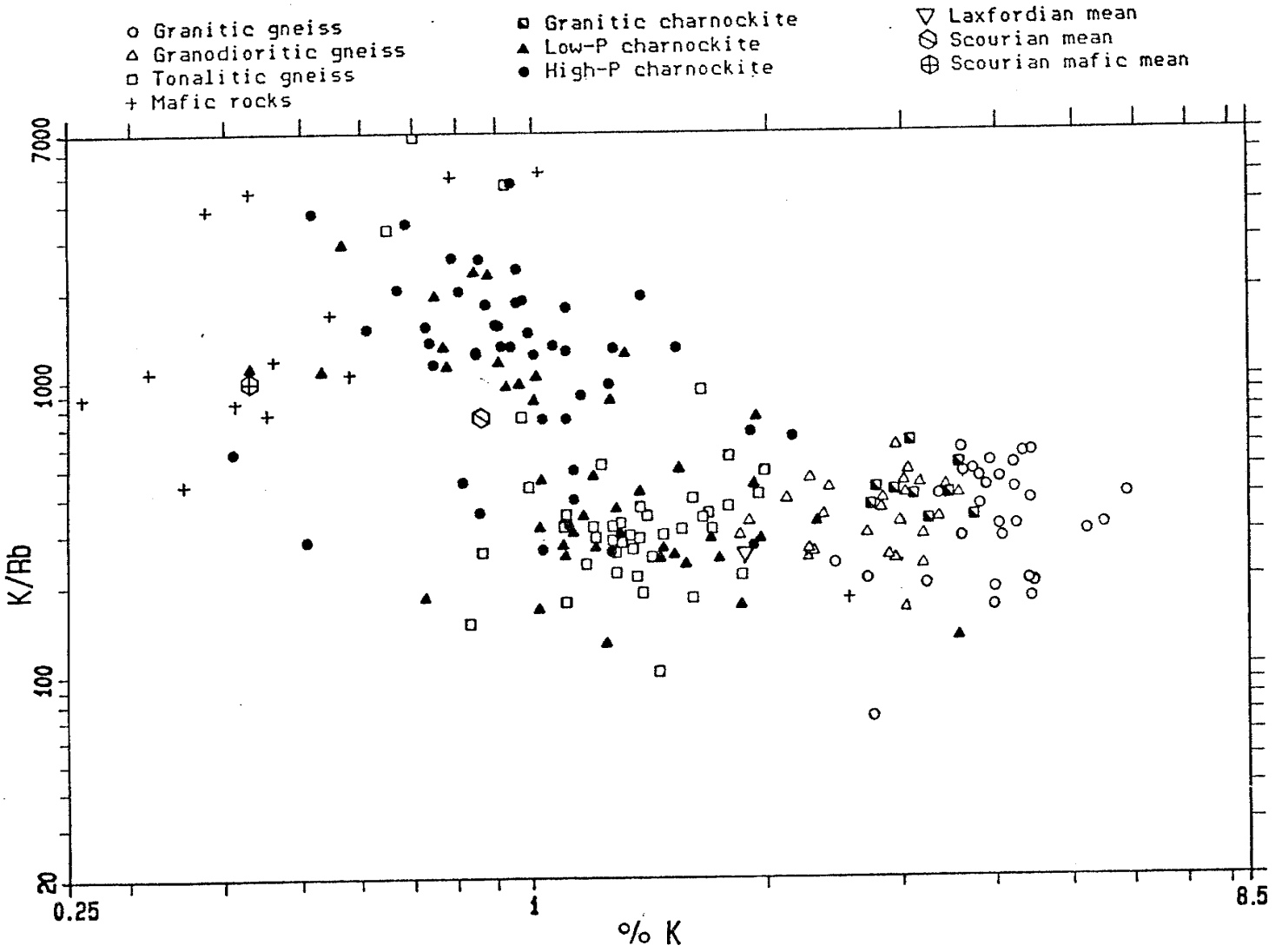

Fig. V-29. K/Rb vs %K plot. Data from Appendix C.

V.4.3 Ba, K/Ba, and Ba/Sr

Ba relative to SiO2 behaves similarly to that of K2O and SiO2: the tonalitic gneisses and charnockites generally define a flat or gently rising pattern (Ba~=300-900 ppm) with increasing SiO2, and the granitic gneisses and high-K charnockite have elevated Ba (Fig. V-27). In the Scourian, similar relationships are seen on K - SiO2, Rb - SiO2, Pb - SiO2, and Ba - SiO2 plots, where samples roughly define a tonalite-trondhjemite trend, with little change in element abundance for increasing SiO2, and a tonalite-granite trend, with sharply higher element abundance at higher SiO2 (Rollinson and Windley, 1980b). On a K2O - Ba diagram (Fig. V-30), the south India samples predominantly lie between K/Ba=15 to 45. Though there is scatter for samples with high Ba and K2O, the tonalitic gneisses and charnockites generally fall into two overlapping suites with parallel trends of gently increasing K2O with increasing Ba. The mean value of the Lewisian amphibolite-facies Laxford gneisses falls within the low-grade field of the south India tonalitic rocks (K/Ba~=25) as do plots of Amitsoq gneisses (Lambert et al., 1976). The Scourian mean value is lower (K/Ba~=10) and lies in the high-grade field. It is noteworthy that the trend of both the low and high-grade populations crosscut lines of constant K/Ba, resulting in a range of K/Ba values for each population; however, the high-grade suite tends to have lower K2O for a given level of Ba than the low grade group. The K/Ba element-area diagram shows a decrease of K/Ba both in the terrane-mean values and in the component rock types, though the granite component is highly variable (Fig. V-23). The decrease in K/Ba

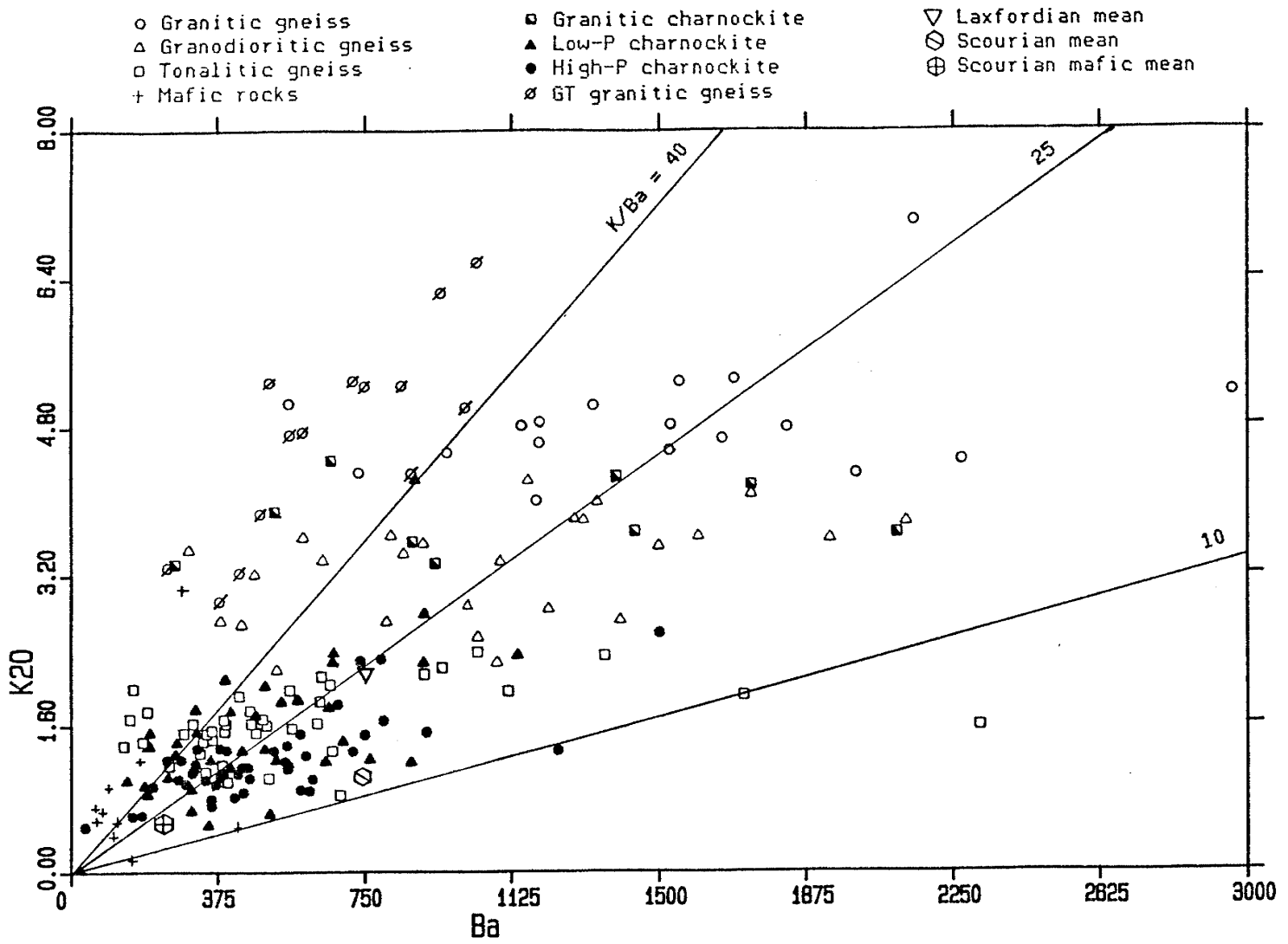

Fig. V-30. K2O vs Ba plot. Data from Appendix C.

indicates that with increasing metamorphic grade, K is lost somewhat faster than Ba; this suggests the breakdown of biotite, which has higher K/Ba than K feldspar (Puchelt, 1972).

O'Nions and Pankhurst (1978) distinguish two groups of Archaean gneisses on a Ba - Sr plot, a tonalitic group (Ba/Sr<2) and a granitic group (Ba/Sr>2). In the south India samples, the granitic and granodioritic gneisses are scattered but typically have Ba/Sr>1.5 (Fig. V-31). The tonalitic gneisses and charnockites, which have a slight positive correlation between Ba and Sr, generally have Ba/Sr =< 1.0,. The calculated means for Laxford and Scourian rocks plot together, with Ba/Sr slightly >1.0 (Fig. V-31). Plots of representative samples from the North Atlantic Craton (Tarney, 1976) generally have Ba/Sr>1.0; however, granitic gneisses (Amitsoq) and granitic charnockite from Madras (Weaver, 1980) are greatly enriched in Ba and have Ba/Sr>3.0. As in the Ba - SiO2 diagram, the Ba-Sr plot indicates that while the amphibolite-facies Laxford gneisses, and other North Atlantic Craton gneisses, fall within the field of Indian gneisses, the high-grade charnockites from south India are depleted in Ba relative to the Scourian. It was suggested above that the decline of the Ba/Sr terrane-mean values, with increasing metamorphic grade, on the Ba/Sr element-area diagram resulted from the progressive loss of the granitic component in the higher grade terranes (Fig. V-22). The broadly overlapping populations of amphibolite-facies tonalitic gneisses and granulite-facies tonalitic charnockite on the Ba - Sr plot support this observation.

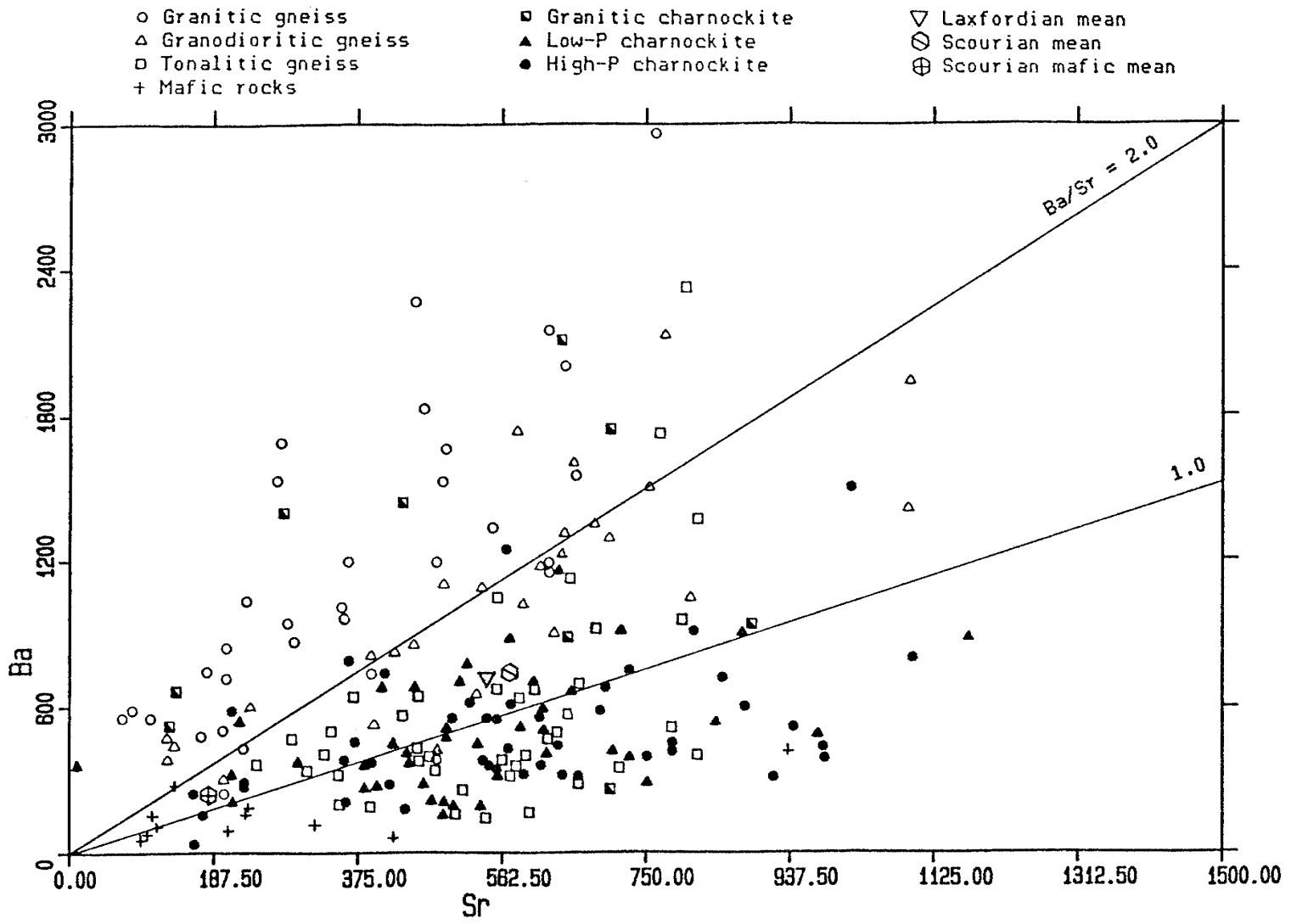

Fig. V-31. Ba vs Sr plot. Data from Appendix C.

V.4.4 Rb/Th, Cs/Th, and U/Th

Rb, Cs, and U generally show a positive correlation with Th (Fig. V-32 to V-34). Although there is scatter, particularly with Cs, the high and low-pressure charnockites have the greatest depletion in these elements, and the amphibolite-facies granitic and granodioritic gneisses the greatest abundance. The trends of Rb, Cs, and U relative to Th are roughly linear on log-log plots. On the Rb - Th plot the Laxford mean lies with the amphibolite-facies south India gneisses, and the granulite-facies Scourian rocks (Lambert et al., 1976) fall in the same depleted field as the Indian high-P charnockites. Rb/Th values for the amphibolite-facies and low-P charnockites lie along a trend of Rb/Th~=3; however, for the majority of the high-P charnockites the pattern of Rb/Th is flat and scattered. This suggests that at low levels of Rb, depletion of Rb is not correlated with Th, indicating that after initial depletion in the high-grade charnockites Th is resident in relatively resistant phases. The Th/U ratios are high for south India, with Th/U>5 for the majority of samples; similar U-Th patterns and ratios are seen in tonaltic gneisses from Fiskenaesset (Kalsbeek, 1976). The values for Th/U, however, appear to decrease in the higher-grade rocks, with ratios for some samples <1 (Fig. V-23). As with Rb, this suggests that at low concentrations (U<0.2 ppm) U in the presence of a fluid phase is resident in resistant crystal structures or phases relative to Th.

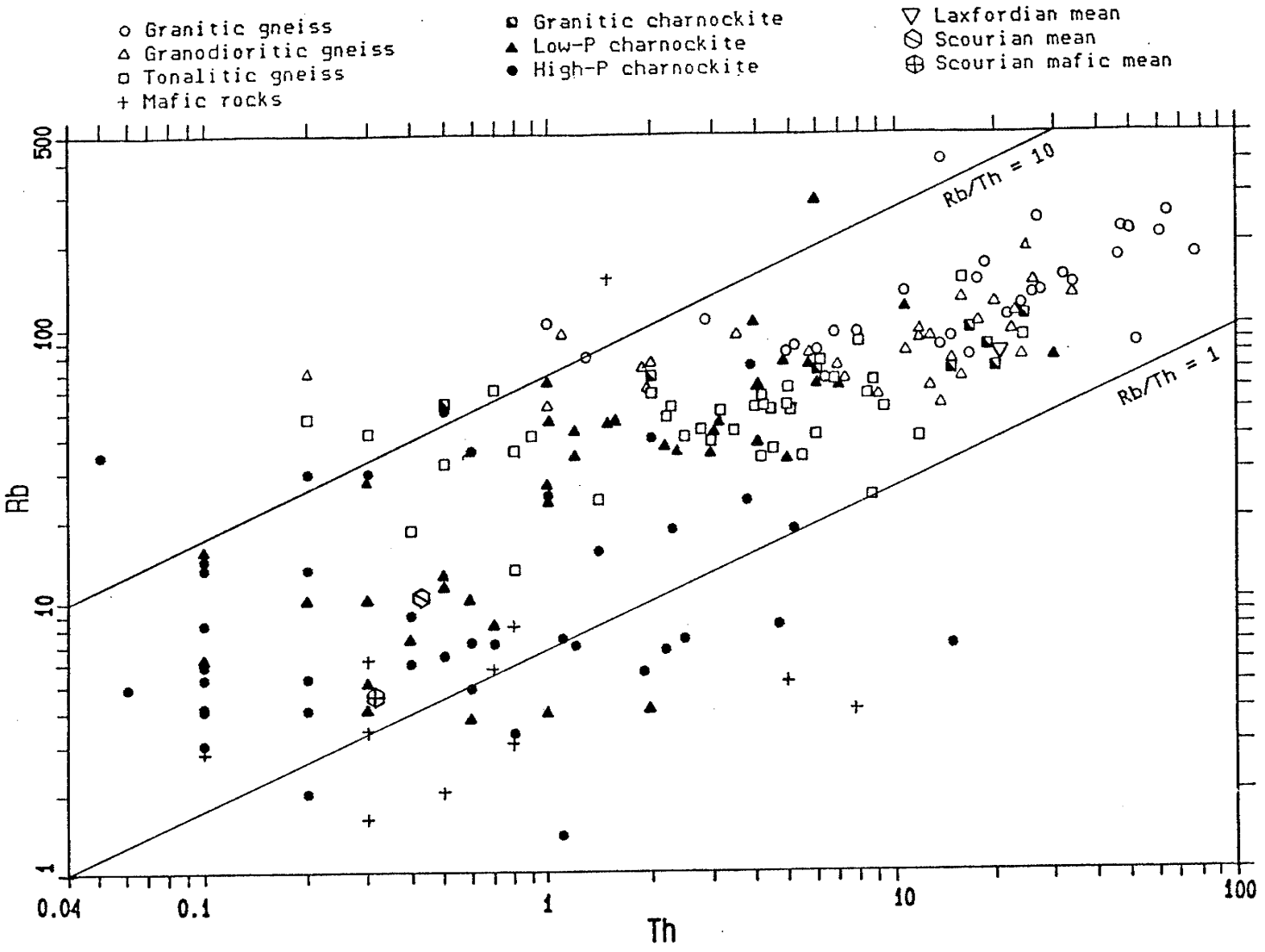

Fig. V-32. Rb vs Th plot. Data from Appendix C.

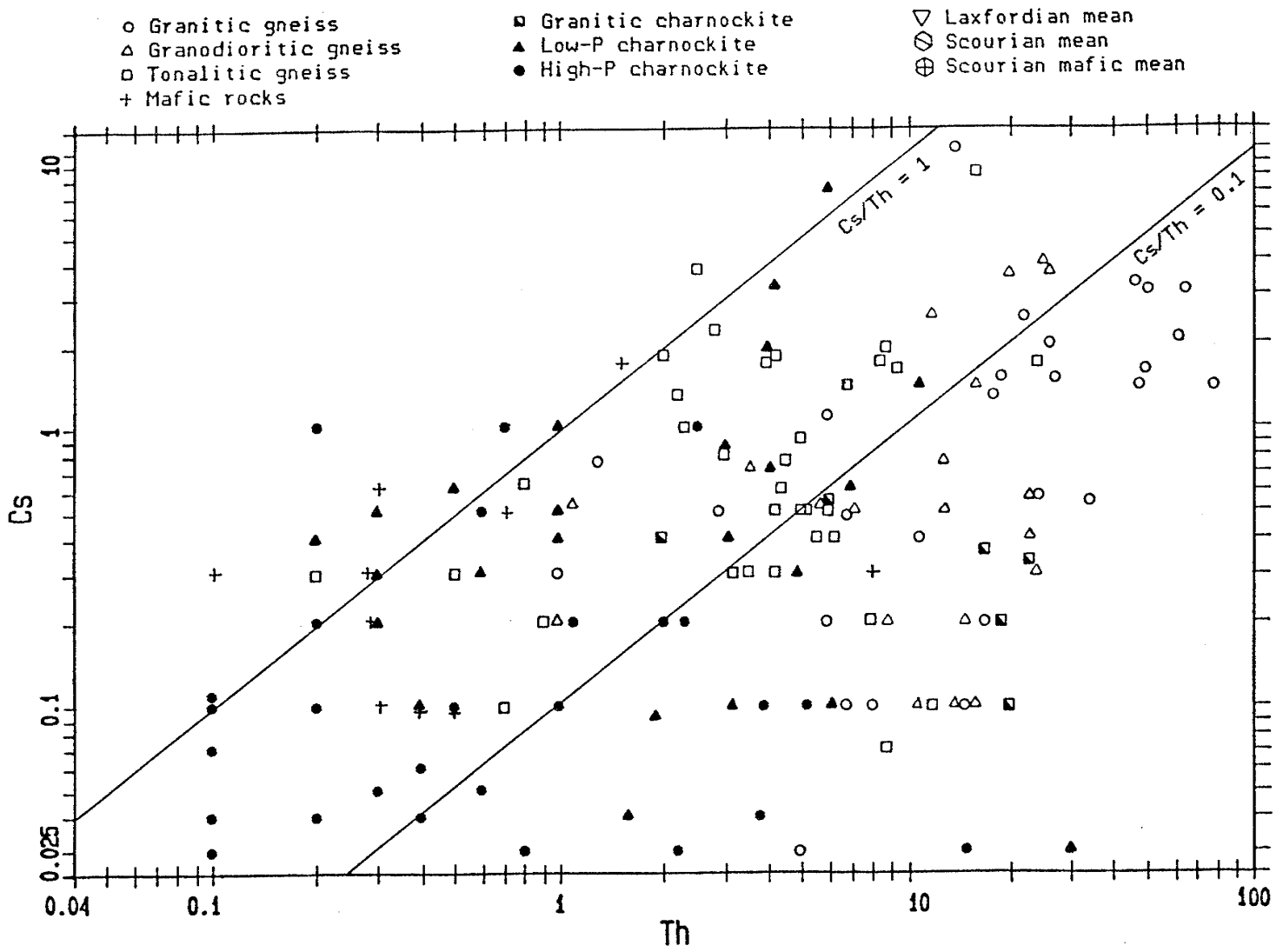

Fig. V-33. Cs vs Th plot. Data from Appendix C.

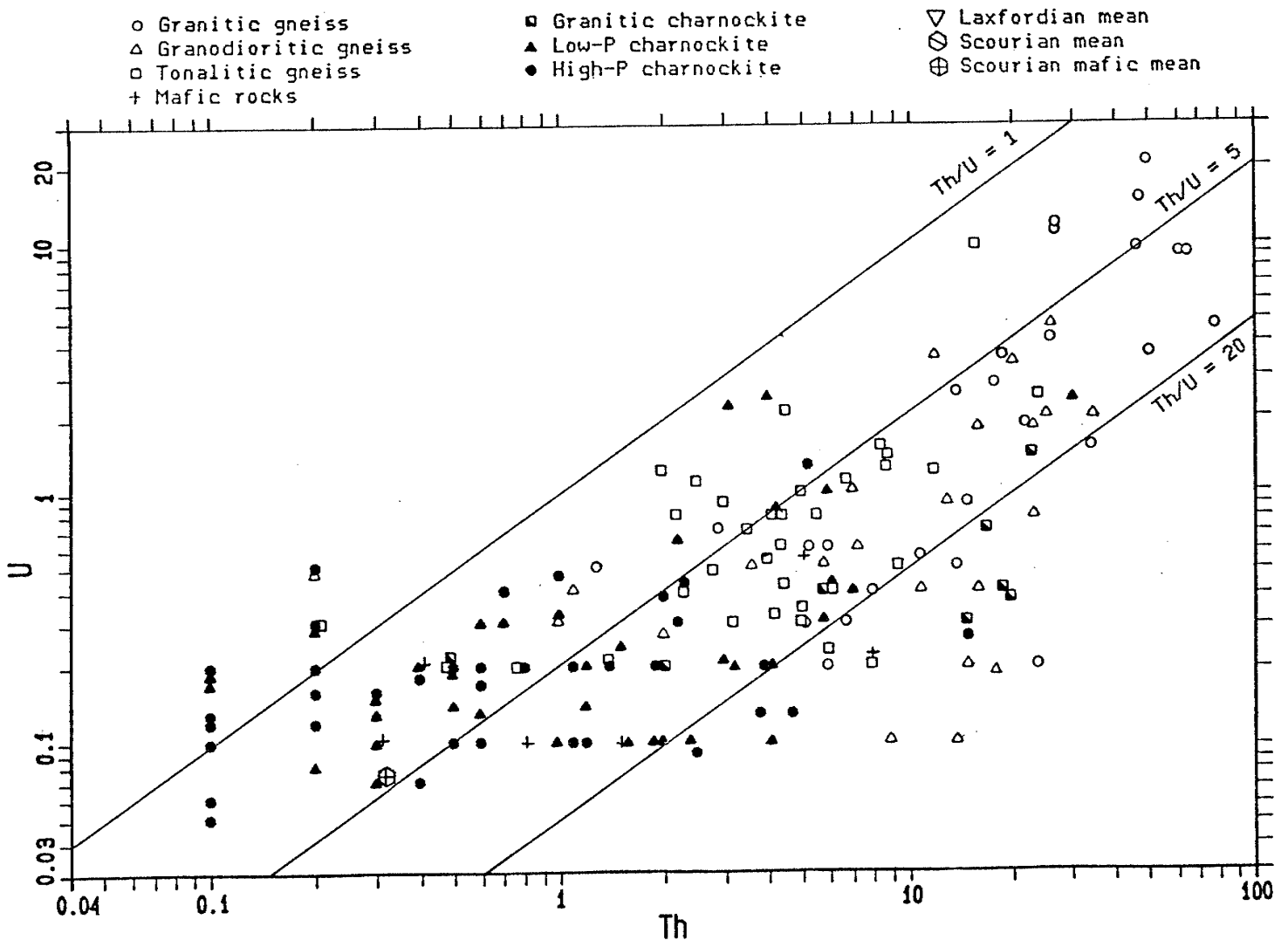

Fig. V-34. U vs Th plot. Data from Appendix C.

V.4.5 Inter-terrane and intra-terrane variation

The most significant inter-terrane change of LIL element concentrations within a single rock classification is that between the granitic gneisses of the Gneiss Terrane (Kunigal-Bangalore-Kolar) and the granitic gneisses of the eastern Transition Zone (Fig. III-1). Though both granitic gneisses are amphibolite-facies, the granitic gneisses from the Gneiss Terrane are enriched in Rb, Cs, Th, U, and Pb, and depleted in Sr and Ba relative to their counterpart granitic gneisses in the Transition Zone (see the granitic gneiss terrane-mean values, Appendixes C.9.1 and C.9.3.). For example the Gneiss Terrane - Transition Zone values are Rb: 177 vs 95 ppm, Cs: 2.3 vs 0.25 ppm, and Sr: 281 vs 467 ppm. Although the standard deviations are high for these elements, the t-test of the paired sample populations for each element indicates that the means show an increase or decrease between metamorphic terranes at a confidence level >99%. On element-area plots the change in LIL element values between the granitic gneisses of the Gneiss Terrane and the granitic gneisses of the Transition Zone is relatively sharp (Fig. V-15 to V-18), while the changes in LIL element abundances within the Transition Zone and at higher metamorphic grades is relatively gradual. This sharp change suggests that the variation in the LIL element values in the amphibolite-facies granitic gneisses, between the Gneiss Terrane and Transition Zone, is not the result of a gradual increase in metamorphic grade. In addition, the LIL element mean values in the Gneiss Terrane are relatively elevated as the result of the high values in the Gneiss Terrane granitic gneiss. Further discussion on

the differences in the granitic gneisses can be found in the HFS element and REE Sections (V.5, V.8.2).

Intra-terrane variation can be seen in the tonalitic and granodioritic terrane-mean values for the Malavalli-Kabbaldurg area (western Transition Zone) and the Krishnagiri-Dharmapuri area (eastern Transtion Zone)(Fig. III-1). The Malavali-Kabbaldurga area is enriched in Rb, Cs, Th, U, and Pb, and depleted in Sr and Ba relative to Krishnagiri-Dharmapuri. This enrichment-depletion is similar, but to a lesser degree, to that observed between the granitic gneisses from the Gneiss Terrane and Transition Zones. This suggests that some of the granitic gneisses in the Malavalli-Kabbaldurga area are similar to those from the Kunigal-Bangalore-Kolar area of the Gneiss Terrane to the north.

V.4.6 Summary of major and LIL element behavior

An overview of major element and LIL element behavior between amphibolite and granulite-facies terranes for south India and other Archaean terranes suggests the following. The changes in SiO_2, Fe_2O_3, MgO, CaO, K_2O, and possibly Pb, in the amphibolite to granulite terrane-mean values are not accompanied by changes of the same magnitude in the component rock groups that comprise the mean value of each terrane. In the Scourian, the abundance of K in the terrane-mean is somewhat less than that in the high-P charnockites from south India. There is also an apparent decrease in K in the tonalitic component, from the Laxford gneiss to the Scourian, indicating that there was greater loss of K by secondary processes in the Scourian

than in south India.

Though the results for Ba and Sr show little or no change on element-area diagrams, there is an apparent decrease in Ba/Sr and K/Ba with increased metamorphic grade in south India, which is predominantly but not entirely the result of the loss of the granitic component in the high-grade rocks. Changes in the terrane-mean values for Rb, Cs, U, Th, Rb/Sr, and K/Rb are generally accompanied by corresponding changes in the component rocks in each terrane indicating that depletion of these elements occurs in all rock types. On the other hand, changes in the terrane-mean values of other elements is not observed or not of the same magnitude in the component rock types. The higher Fe_2O_3, MgO, TiO_2, and lower SiO_2 seen in the high-P granulite terrane is the result of less granitic rock in the high-grade terrane. This suggests that the average granulite-grade gneiss (charnockite) in south India and in other Archaean terranes approximates the composition of amphibolite-facies tonalitic (silicic and intermediate) gneiss. The depletion of Rb, Cs, Th, and U in the granulite-grade rocks is the result of a later mobilization process. Though the low levels of K in the high-grade terranes are largely inherited from the amphibolite-facies tonalitic-trondhjemitic gneiss, some K, and probably Pb, was mobilized along with Rb, Cs, Th, and U.

The patterns on the element-area diagrams seem scattered, especially for the Archaean terranes from the Atlantic craton and elsewhere. On closer examination, however, there is a very strong internal coherence. For example, the tonalitic (silicic) gneisses from India and other terranes behave in a very similar manner. The

granitic and granodioritic gneisses, with generally large standard deviations, also have relatively consistent values between similar metamorphic terranes. The tonalitic (intermediate) gneisses from different terranes frequently have large standard deviations but with similar means. For the LIL and major elements, the Archaean terranes that appear to have the least correspondence with the south India samples analysed in this study are the Amitsoq and Madras, which also have tholeiitic trends on an AFM diagram. The similarity with the other Archaean terranes is striking.

V.5 High field-strength elements

The high field-strength elements Sc, Y, Zr, Hf, Nb, Ta, and Phosphorus exhibit a varied response to changes in metamorphic grade (Figs. V-35 to V-37). In the south India samples, phosphorus has a strong correlation with SiO2 irrespective of metamorphic grade (Fig. V-18). The Sc increase from a terrane value of ~5 ppm in the amphibolite-facies gneisses to 10-15 ppm in the high-pressure charnockites (Fig. V-35) is similiar to increases in TiO2, Fe2O3, and MgO, and decrease in SiO2, which is attributed to the loss of the granitic components and a high-pressure charnockite that approximates the composition of intermediate tonalitic gneisses. There are few Sc analyses for other Archaean terranes but the Scourian results suggest slightly higher values than for the high-grade Indian terrane (Sc~=15 ppm vs 11 ppm).

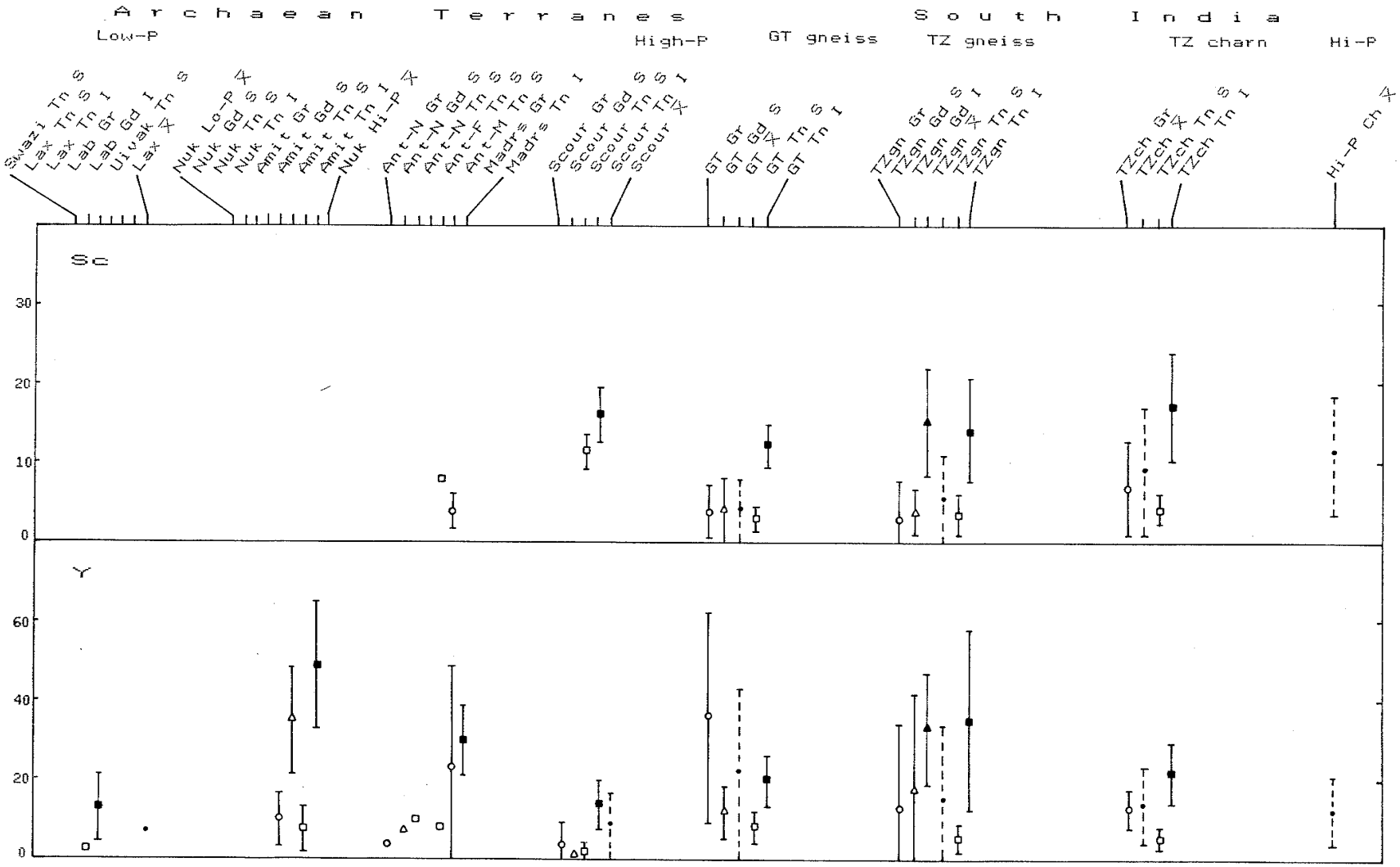

Fig. V-35. Element-area diagram for Sc and Y. (For description of localities and rock types see Table V-2, for data sources see Appendix C.)

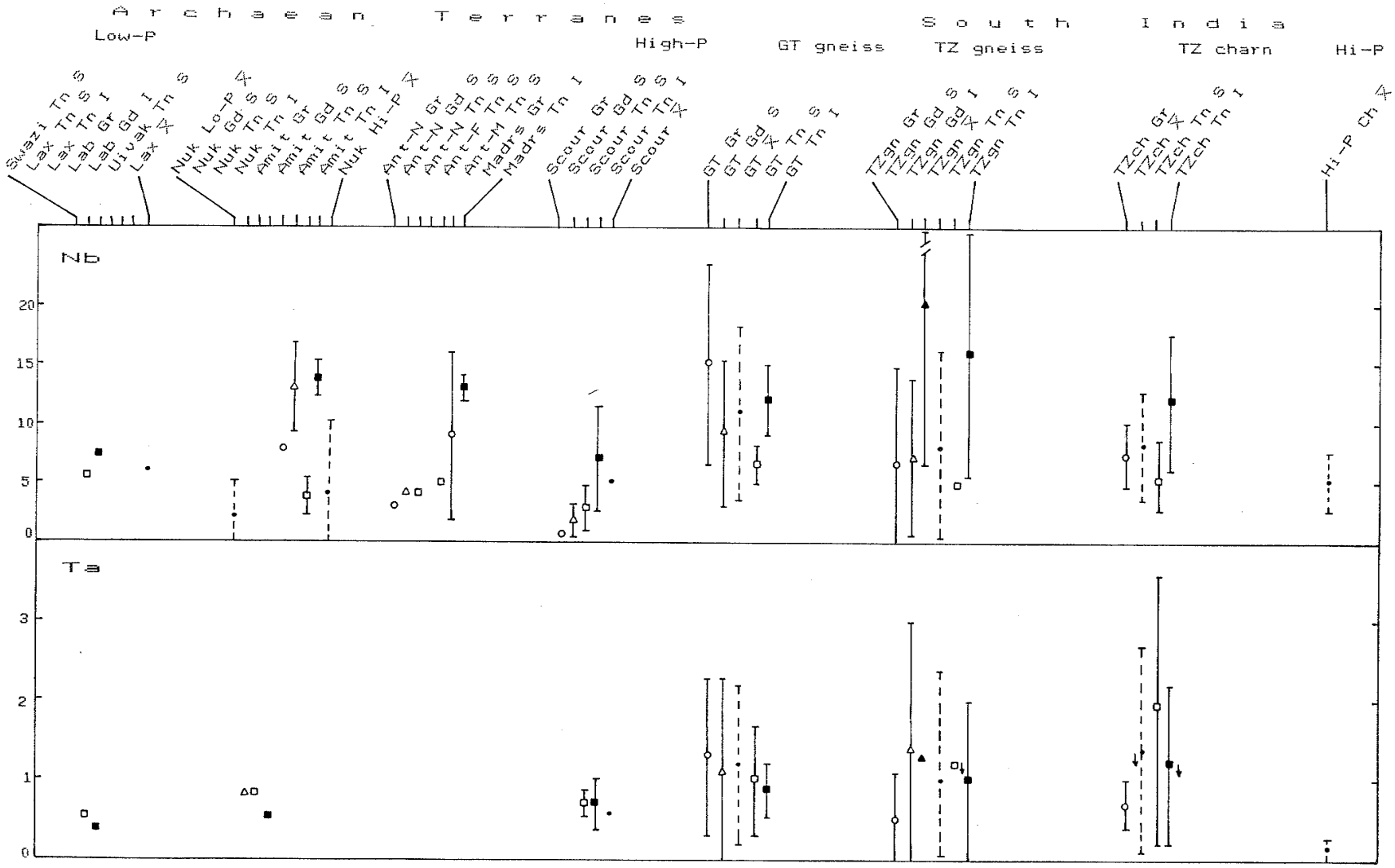

Fig. V-36. Element-area diagram for Nb and Ta. (For description of localities and rock types see Table V-2, for data sources see Appendix C.)

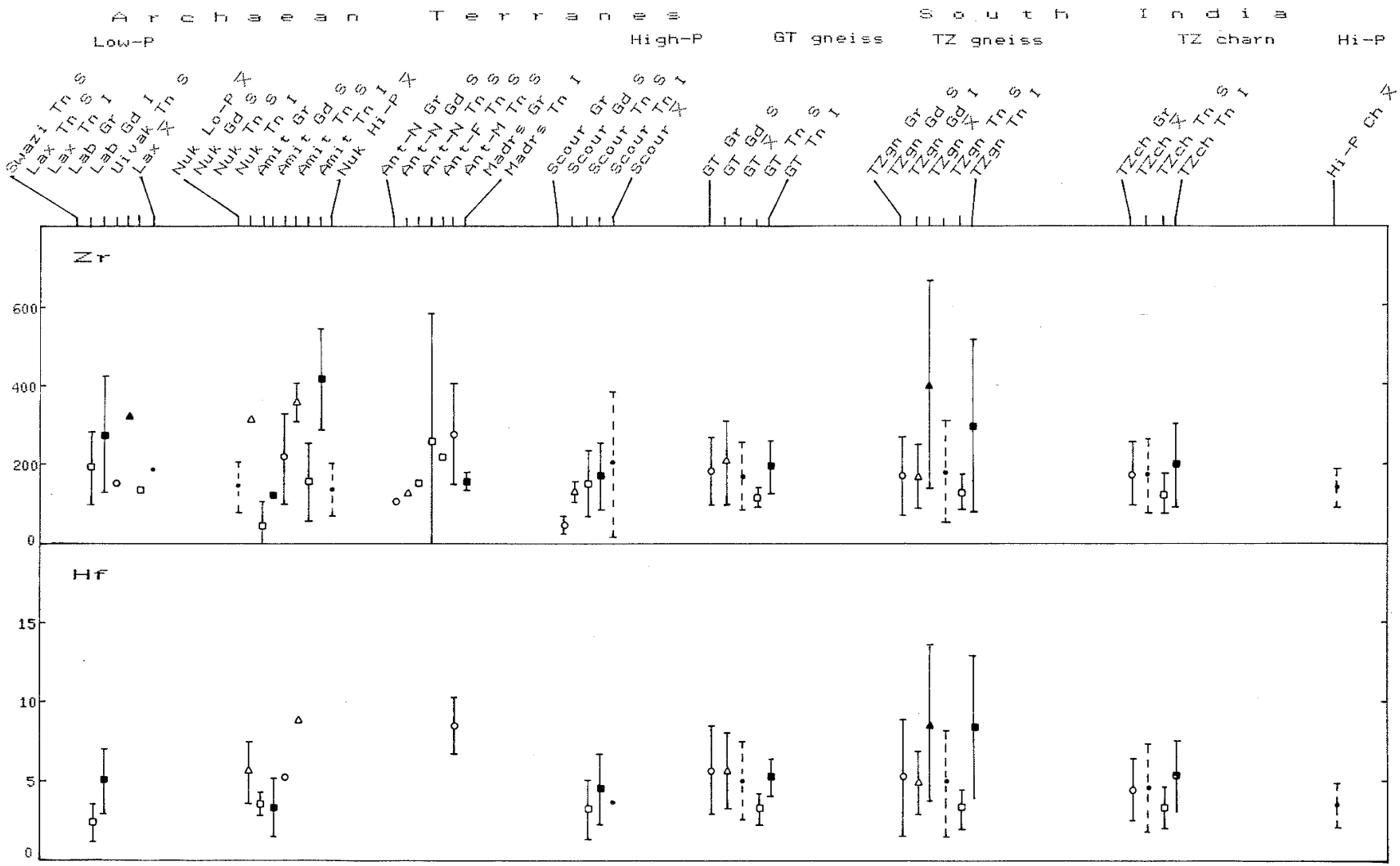

Fig. V-37. Element-area diagram for Zr and Hf. (For description of localities and rock types see Table V-2, for data sources see Appendix C.)

Nb and Ta show a slight decrease in the terrane-mean value with increase in metamorphic grade, but have high standard deviations and the significance of the decrease is uncertain. This decrease in the terrane-mean value for Nb is largely between the Gneiss Terrane and the Transition Zone. As discussed earlier, the granitic gneisses from the Gneiss Terrane are enriched in certain LIL elements relative to the granitic gneisses from the Transition Zone (Section V.4). The Gneiss Terrane granitic gneisses are also enriched in Y (36 vs 13 ppm), Nb (15 vs 6.6 ppm), and Ta (1.3 vs <0.5 ppm) relative to their counterpart in the Transition Zone and may represent a more evolved granite than the other granites. Y does not vary significantly in the other component rocks and if the high-Y granitic gneiss is not included in the Gneiss Terrane mean value, the south India Y terrane-mean value does not significantly vary with metamorphic grade.

Significant changes in the abundances of Y, Nb, and Ta with increasing metamorphic grade are not apparent in the other Archaean terranes (Figs. V-35, V-36). Y concentrations in both the Laxford and Scourian terranes (Y<10 ppm) are lower than the value in the Indian gneiss terrane (Y=22 ppm) and the high-P charnockite (Y=13 ppm). Nb concentration in the Scourian granites is about equal to that of the south India high-P charnockites. Significantly higher concentrations of Nb are found in the intermediate tonalitic and granodioritic gneisses from Amitsoq, Madras, and the south India Transition Zone (Fig. V-36); however, Nb substitutes for Ti (Taylor, 1965), and these groups all have high TiO2 and Fe2O3 (Fig. V-9, V-10). Ta is sharply lower (Ta=0.17 ppm) in the India high-P

charnockite relative to the Scourian (Ta~=0.6 ppm) and Laxfordian (Ta~=0.5 ppm), but higher in the India Transition Zone (Ta=1 to 1.5 ppm). In south India and other Archaean terranes, Zr and Hf do not show significant change. It is interesting to note that in the south India samples the greatest variability in values tends to occur in the Transition Zone. On Sc - Y and Nb - TiO2 plots there is a positive correlation for the tonalitic gneisses and charnockites, but scatter for the granitic gneisses from the Gneiss Terrane; for further discussion see Section VI.2 (Figs. VI-1, VI-2).

V.6 Transition Metals

The transition metals Cr, Ni, and Co terrane-mean values increase with metamorphic grade in south India and other Archaean terranes (Figs. V-38, V-39). Zn has high variability but exhibits no significant change. Though there is an apparent increase of Cr in the component rocks, the increase in the terrane-mean value from Cr~=10 ppm in the amphiblite-facies gneisses to Cr~=80 ppm in the high-P charnockites largely results from the increase of the intermediate tonalitic component in the high-grade terrane (Fig. V-39). The increase in the terrane-mean values of Ni and Co, from Ni~=10 ppm and Co~=7 to N~=40 ppm and Co~=16, follows the same pattern. Relative to the high-P charnockite, the Scourian is somewhat enriched in Cr (~=88 ppm) and Ni (~=58 ppm), but exhibits similar relationships to its lower grade companion, the Laxfordian gneisses as the high and low-grade India rocks (Figs. V-38, V-39).

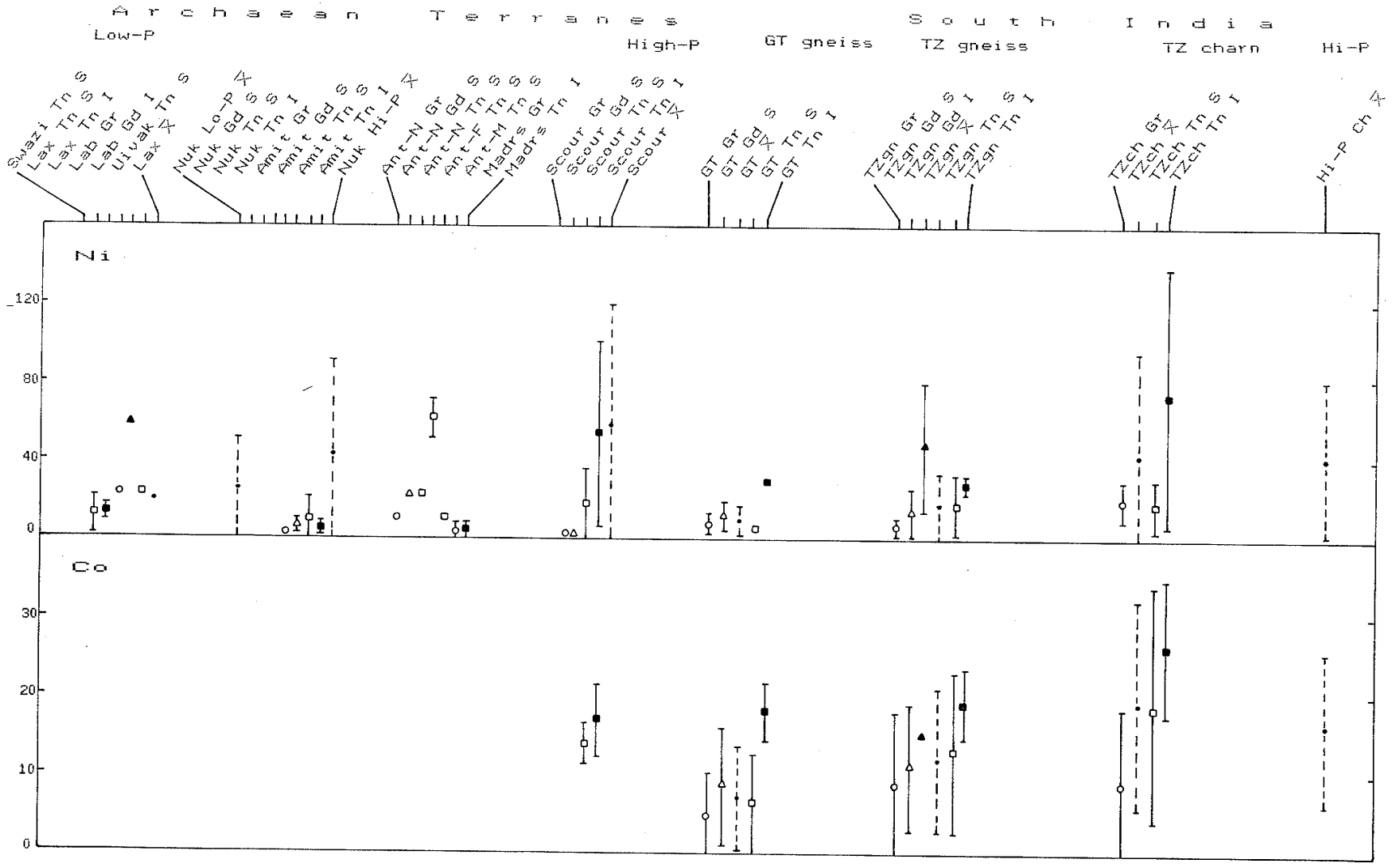

Fig. V-38. Element-area diagram for Ni and Co. (For description of localities and rock types see Table V-2, for data sources see Appendix C.)

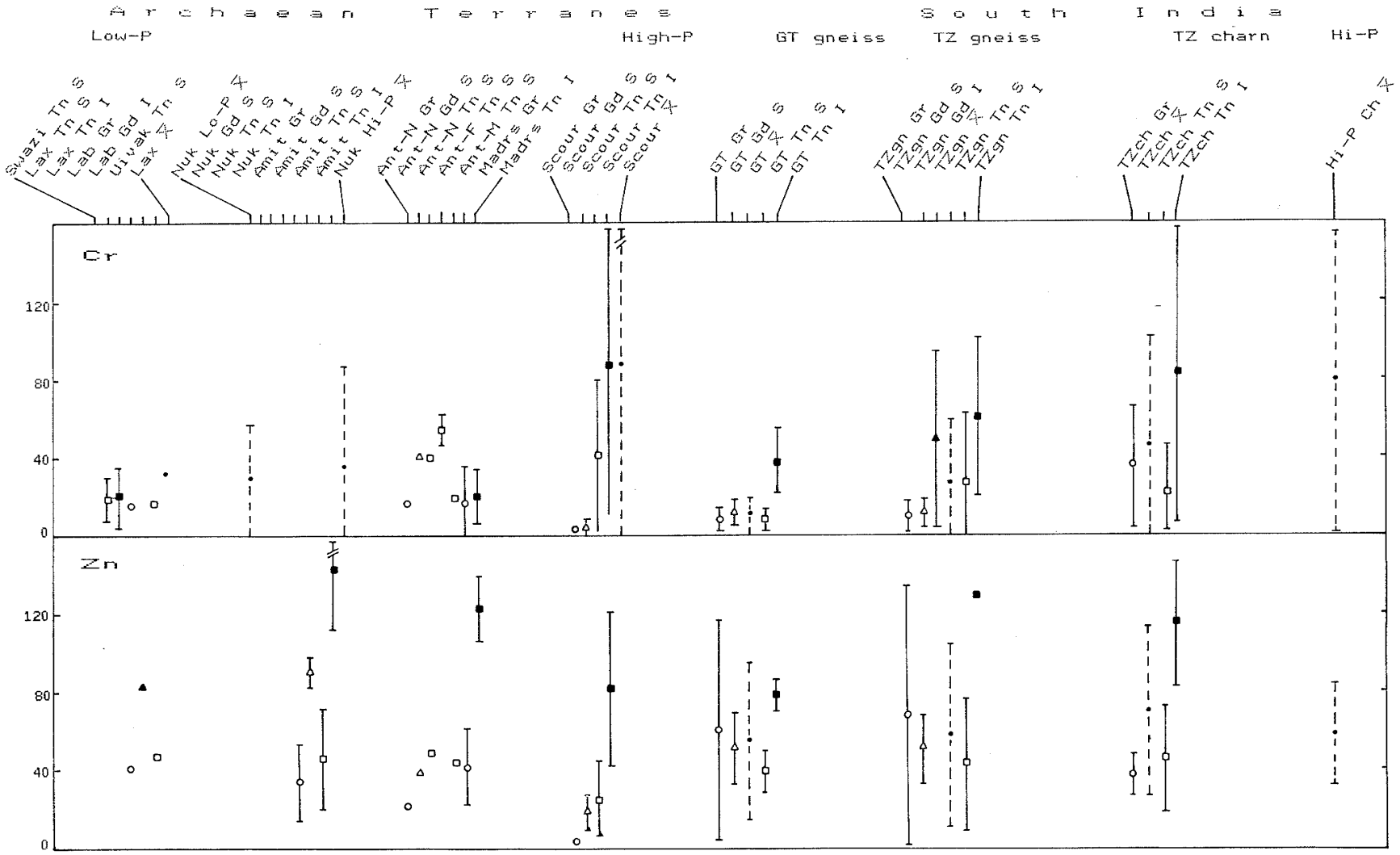

Fig. V-39. Element-area diagram for Cr and Zn. (For description of localities and rock types see Table V-2, for data sources see Appendix C.)

V.7 Major and Trace Element Variation in the High-P Terrane

The medium to high-pressure granulite terrane south of the Moyar-Bhavani shear zone (Fig. II-3) is exposed over a large area in discontinuous massifs and outcrops that are frequently separated by tectonic features. A comparison of the chemistry of the major medium and high-P groups shows a close similarity in abundance for some elements, and a wide variation for others (Appendix C.9.7 and Figs. V-40 to V-42). For most elements and ratios, the extremes of the range in values are represented by samples from the Nilgiris and the Biligirirangan Hills (BR Hills); this is also true of the REE patterns, discussed below. The difference in the composition of these two area is interesting because the Nilgiris may have been the southern extension of the BR Hills prior to the ~70 km left lateral displacement along the Moyar-Bhavani shear zone (Drury et al., 1984).

In general, the Nilgiris are enriched in Ti, Fe, Mg, Sc, Y, Cr, Ni, and Co relative to the other high-P areas, although the Shevaroy-Toppur area is roughly similar (Figs. V-40 to V-42). The BR Hills are slightly more siliceous, have low Ti, Fe, Mg, Sc, Cr, Ni, Co, and Y, and higher Na and Sr. K, Ba, Hf, and Zr are relatively invariant between the different high-P areas. Th (0.53-2.6 ppm) and U (<0.1-0.43 ppm) are both depleted relative to lower grade terranes but are relatively constant between the high-P areas; in the BR Hills, there is great variability in Th values but a narrow range of U. Rb (30 ppm), Cs (0.17 ppm), Ta (0.39 ppm), and Nb (7.5 ppm) have significantly higher values in the Nilgiris than in the other high-P areas, which is interesting because this group is high in Fe, Mg, Sc,

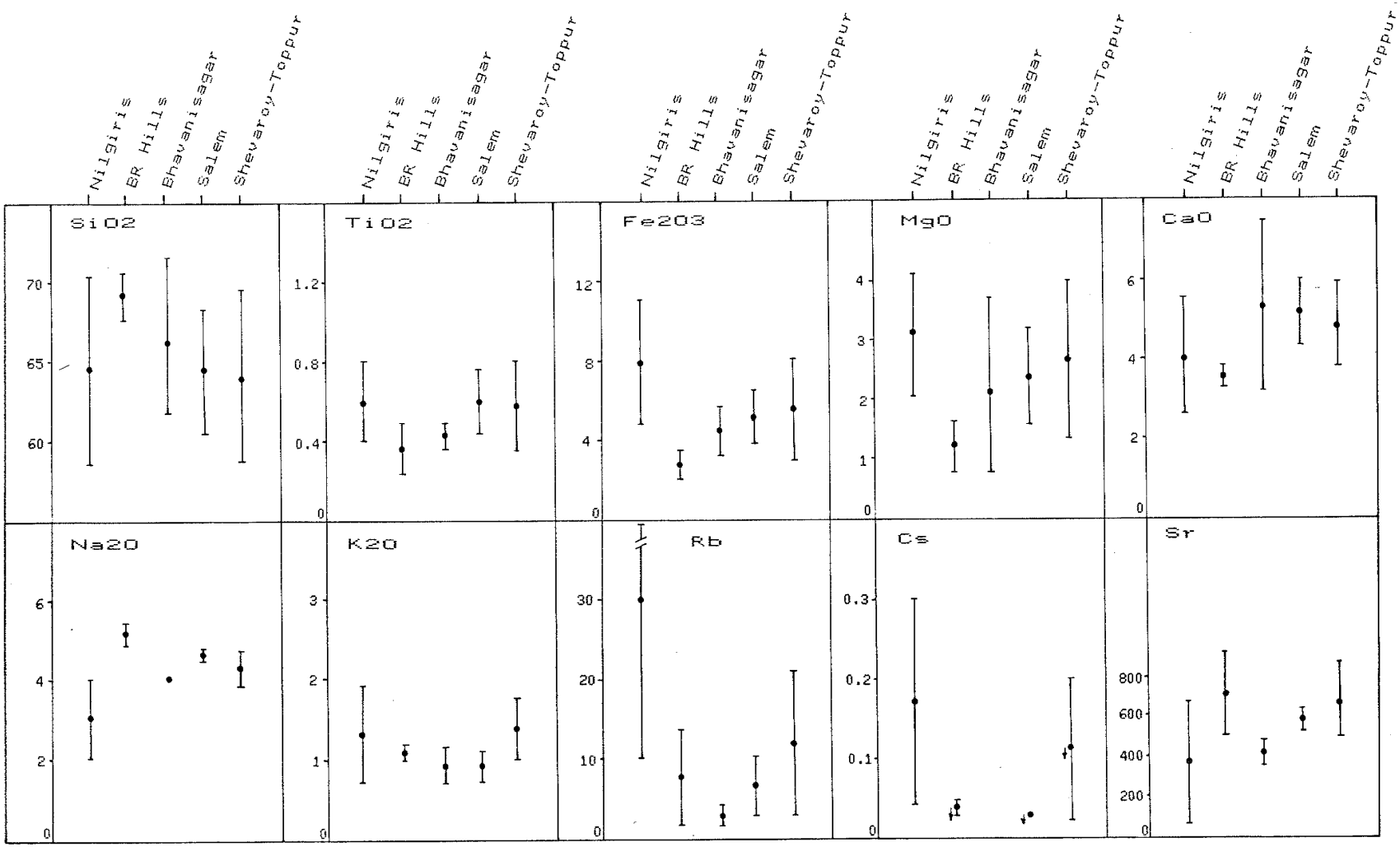

Fig. V-40. High-P terrane element-area diagrams for SiO2, TiO2, Fe2O3, MgO, CaO, Na2O, K2O, Rb, Cs, and Sr. (Data from Appendix C.)

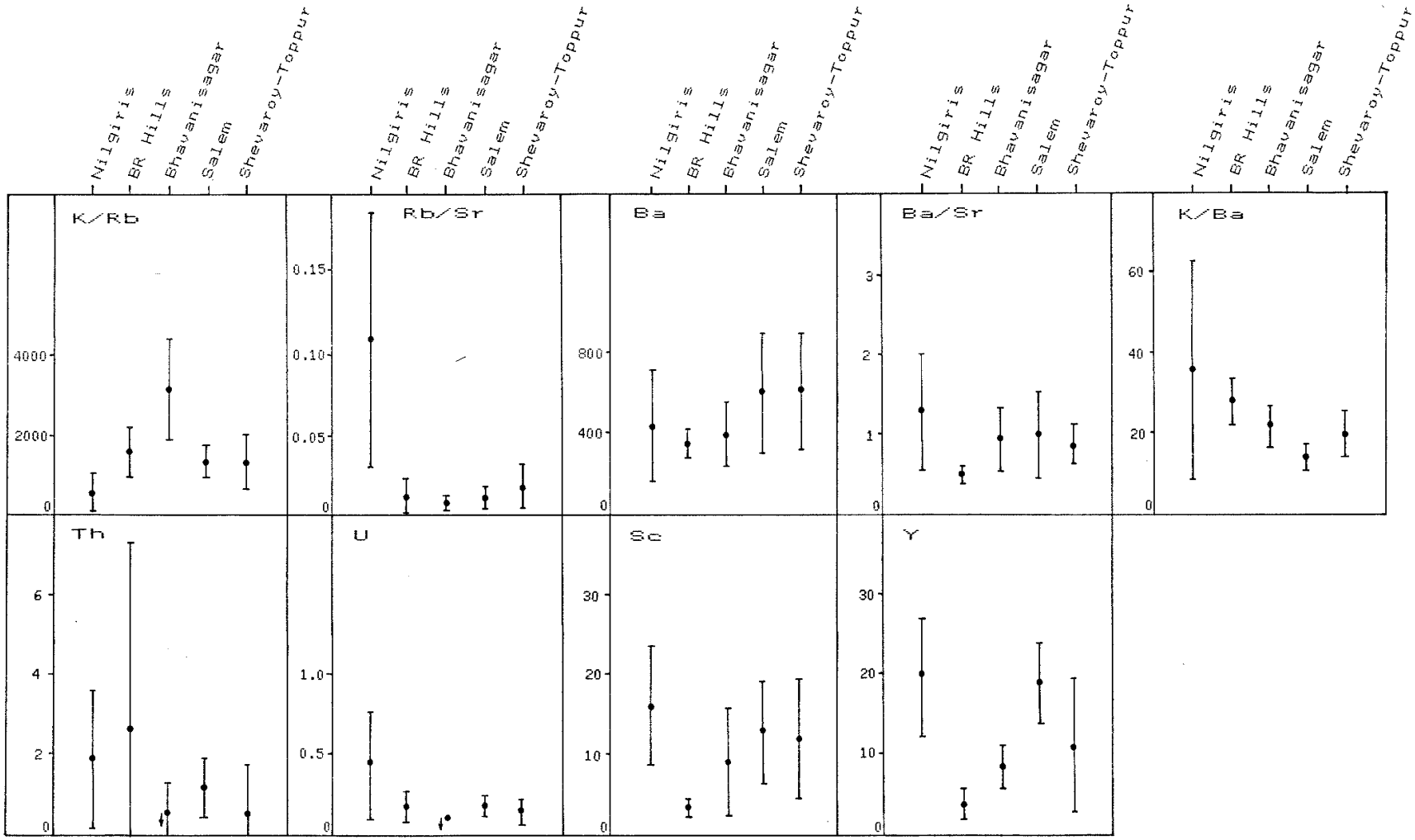

Fig. V-41. High-P terrane element-area diagrams for K/Rb, Rb/Sr, Ba, Ba/Sr, K/Ba, Th, U, Sc, and Y. (Data from Appendix C.)

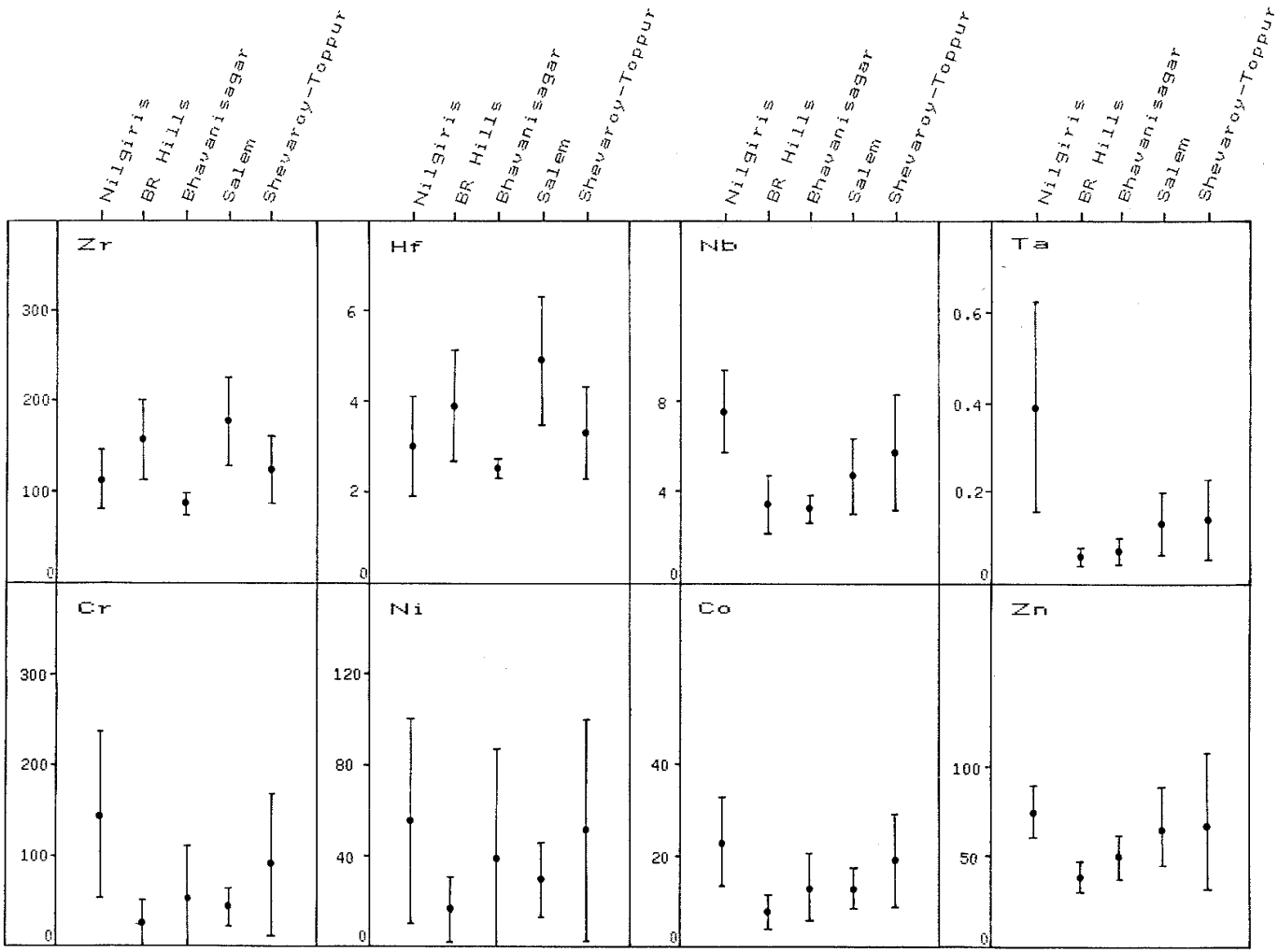

Fig. V-42. High-P terrane element-area diagrams for Zr, Hf, Nb, Ta, Cr, Ni, Co, and Zn. (Data from Appendix C.)

Cr, Ni, and Co; however, the standard deviations for the LIL elements and Ta are large indicating that the Nilgiri massif is relatively heterogeneous for these elements. It should be noted that the area from which samples were collected in the Nilgiris is far larger than the other high-P sample areas (Appendix D: D.0 and D.11). The high Rb/Sr (0.11) and low K/Rb (530) for the Nilgiris are primarily the result of the elevated Rb values; K/Ba is also higher but with a very large standard deviation. Thus, for the medium and high-P granulite terrane, there is a general similarity for most major and transition metals; LIL and HFS element abundances are also similar for the BR Hills, Bhavanisagar, Salem, and Shevaroy-Toppur (the central and eastern region). In the Nilgiris, some of the LIL and HFS elements are sharply higher; this suggests that the Nilgiri massif is a somewhat more heterogeneous terrane than the other high-P areas and was subject to localized enrichment processes (for example, partial melting or fluid transport) not evident in the other areas.

V.8 Rare Earth Elements

The rare earth element analyses are presented on chondrite normalized plots arranged in order, by geographical area and rock type, from amphibolite-facies to granulite-facies terranes. Areas mentioned in this section are delineated in Fig. III-1 and the Appendix D Index Map. Chondrite values are from Haskin et al. (1968). Where rare earth analyses are available from other Archaean terranes, they are presented for comparison; the data used to construct these REE plots can be found in Appendix C.10. Sources for the data are in Appendix C.11 and in general will not be repeated in the text. The approach in this presentation is to provide a graphical comparison of rare earth patterns from different Archaean terranes, different metamorphic terranes, and different rock type within a metamorphic terrane.

V.8.1 Amphibolite-facies tonalitic gneisses

The rare earth patterns of the felsic rocks from south India are variably light-rare-earth element (lREE) enriched, heavy-rare-earth element depleted (hREE), have total REE greater than chondrites, and are in general similar to the REE patterns of comparable rocks elsewhere. The few tonalitic (silicic) gneisses sampled in the northern part of the Gneiss Terrane (Kunigal-Bangalore-Kolar area) have a smooth pattern with lREE~=60XCh, CeN/YbN~=35, and no Eu anomaly (Fig. V-43d). The tonalitic (silicic) gneisses in the southern part of the Gneiss Terrane (Hosur-Kuppam-Krishnagiri) are not as depleted

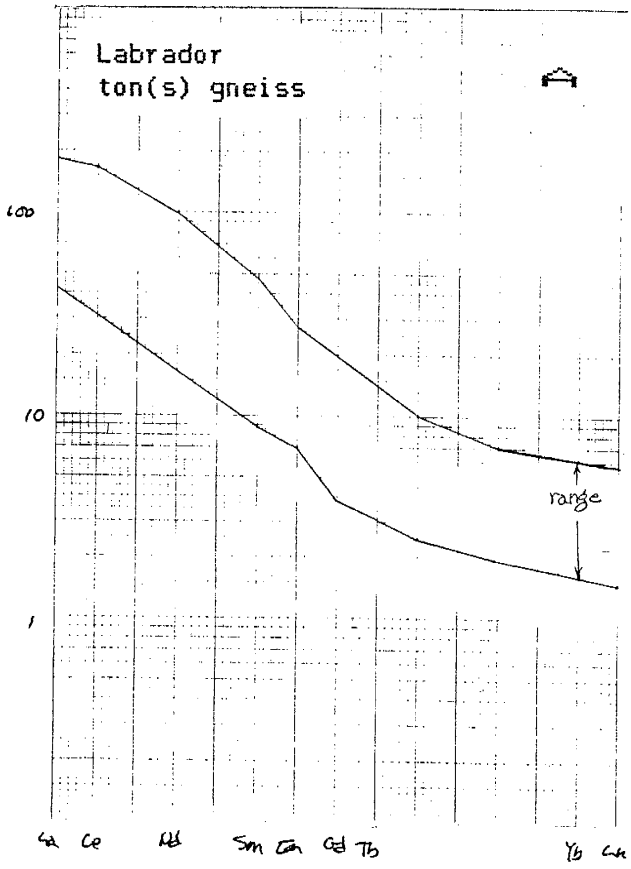
Labrador
ton(s) gneiss
100
10
1
range
La Ce Nd Sm Eu Gd Tb Yb Lu

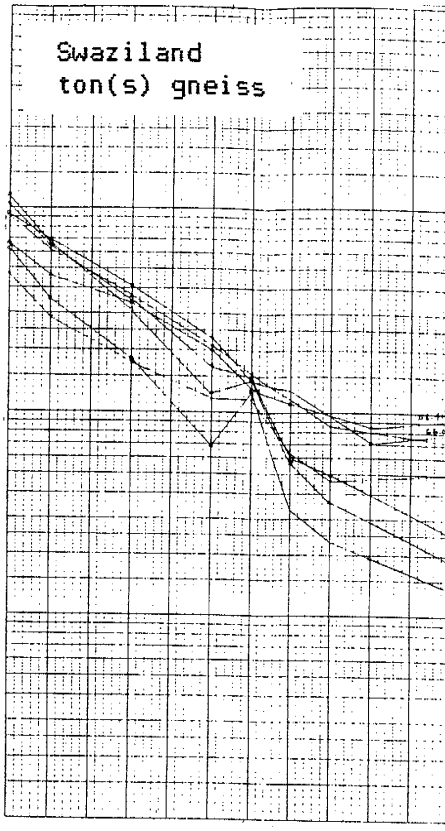
Swaziland
ton(s) gneiss

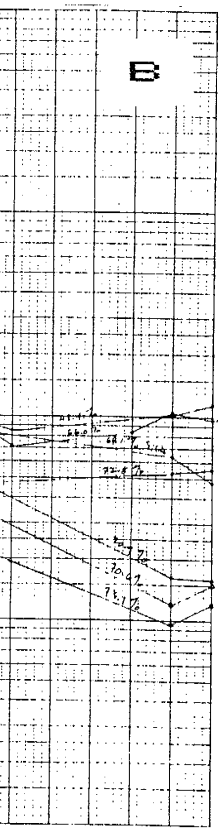
B

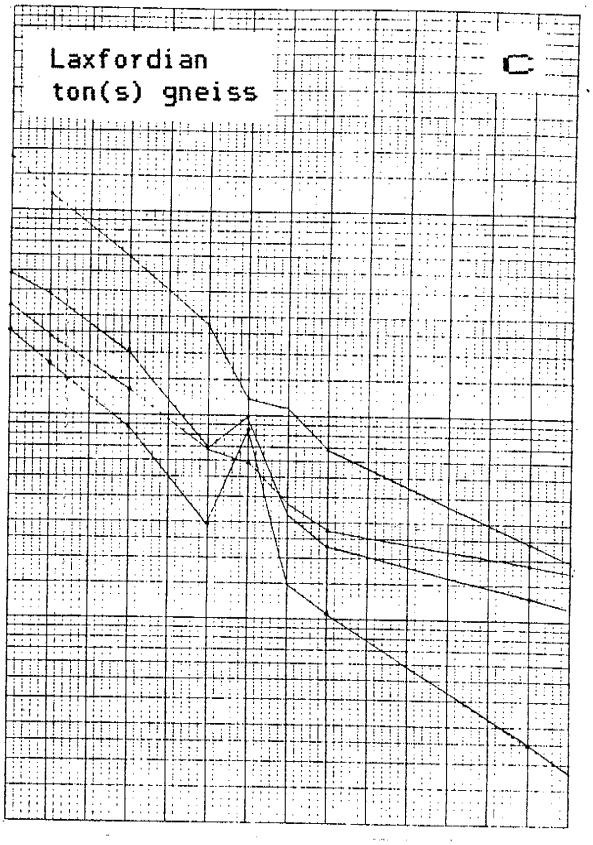
Laxfordian
ton(s) gneiss
C

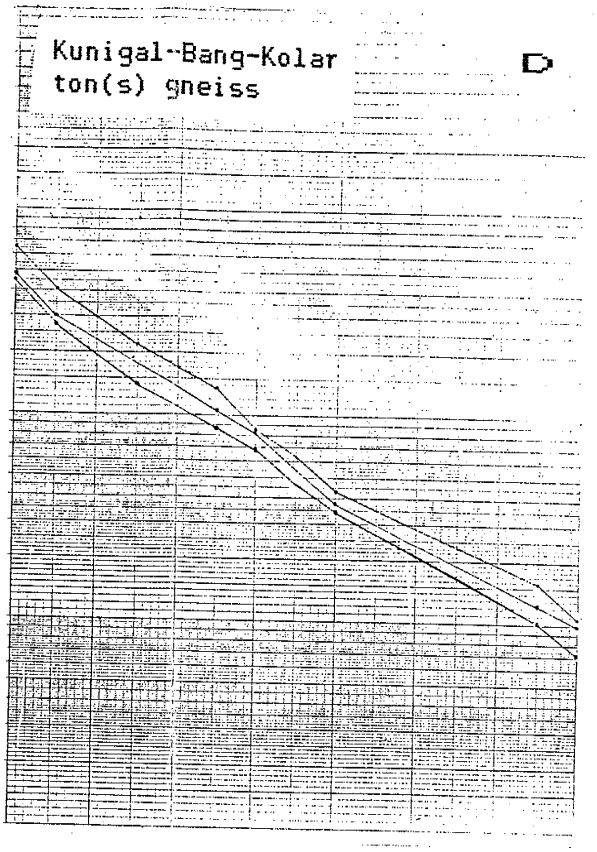
Kunigal-Bang-Kolar
ton(s) gneiss
D

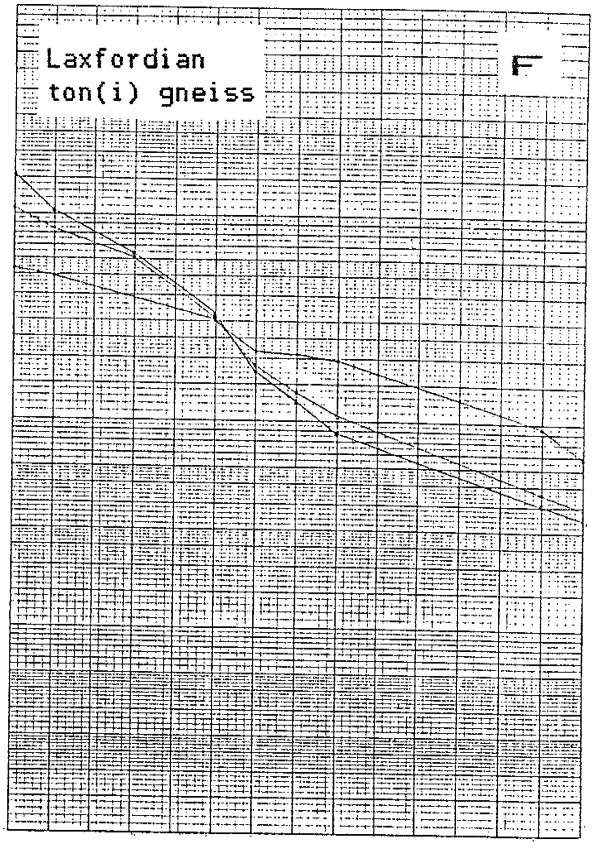
Laxfordian
ton(i) gneiss
F

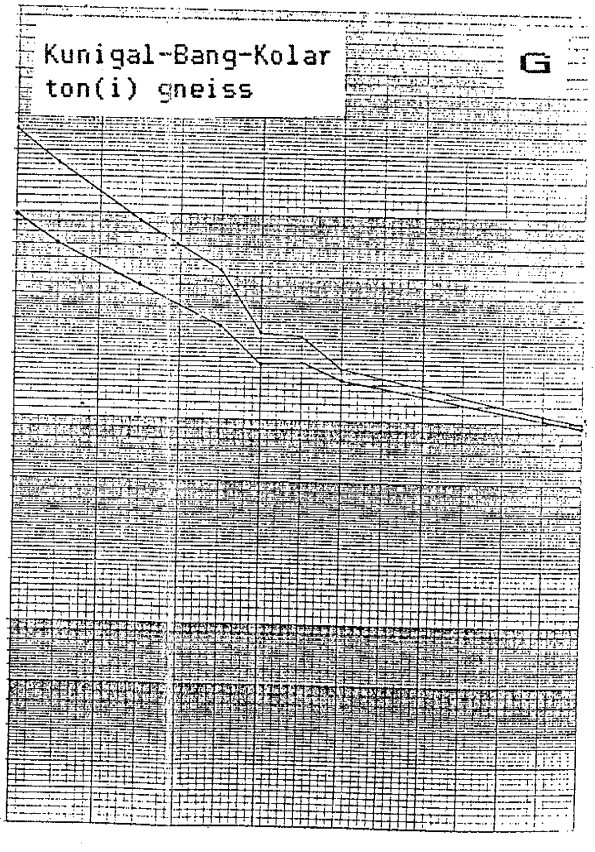
Kunigal-Bang-Kolar
ton(i) gneiss
G

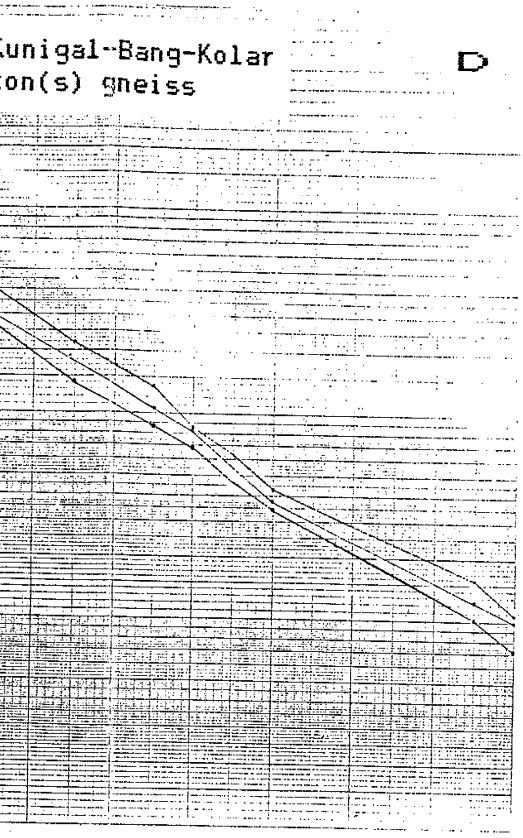

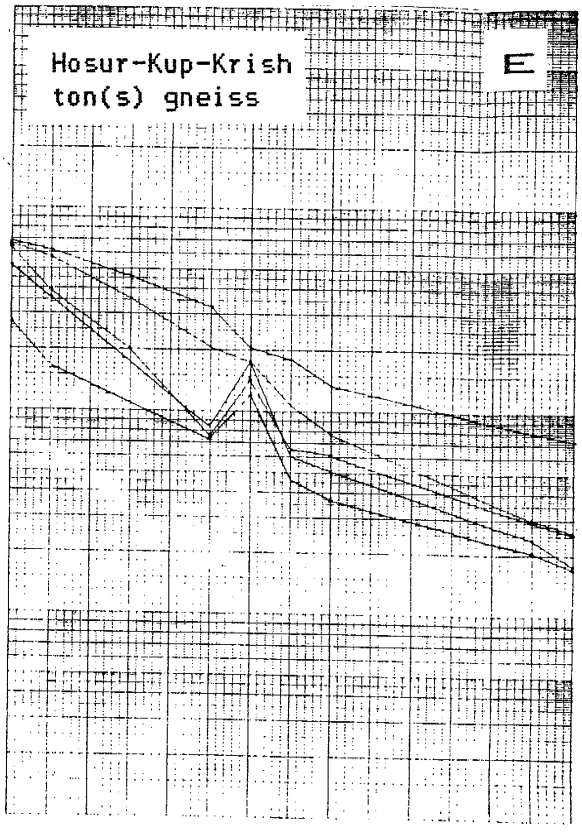

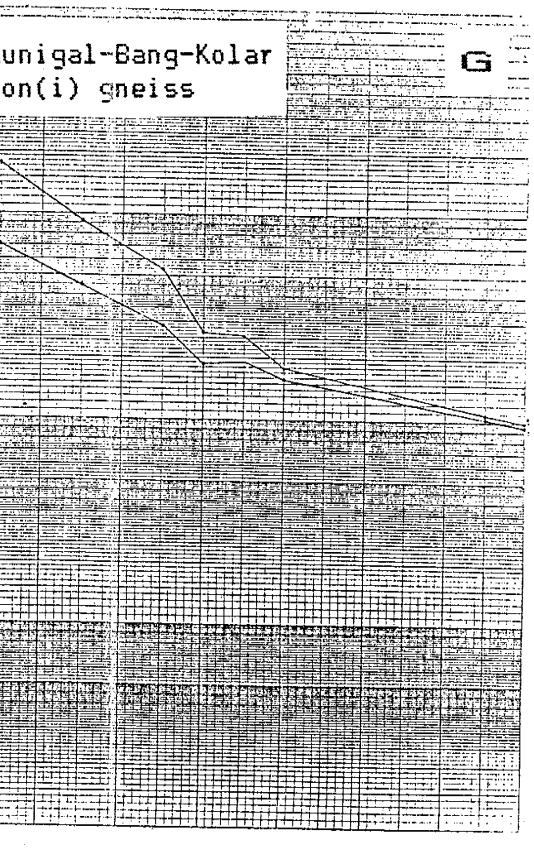

Fig. V-43. Gneiss Terrane: tonalitic gneiss. Data in Appendix C.

in the hREE (CeN/YbN=7.7-20) and have lower total REE and a +Eu anomaly (Fig. V-43e). It is interesting to note that the three samples from this area with relatively lower total REE and +Eu anomalies come from the southern edge of the Gneiss Terrane, and have a similar pattern to the tonalitic (silicic) gneisses in the Transition Zone to which they are adjacent (Figs. V-43e, V-44b,c). Another example of this change in pattern along the southern margin of the Gneiss Terrane can be seen in the granitic gneisses, discussed below. This suggests that though the actual delineation of the Gneiss Terrane and Transition Zone is somewhat arbitrary, there does appear to be a distinct change in the characteristics of the gneisses near the border of these two areas.

The tonalitic (intermediate) gneisses from the Gneiss Terrane are enriched in the lREE (~=150XCh), and have CeN/YbN~=15 with small -Eu anomalies. In general, the intermediate gneisses from all terranes in south India have somewhat higher total REE, slight to significant -Eu anomalies, and similar CeN/YbN ratios compared to the REE patterns of the silicic gneisses. REE patterns from comparable Archaean amphibolite-facies terranes are similar. Tonalitic (silicic) gneisses from Labrador (Uivak I) have a mean CeN/YbN of ~=23, but no significant overall Eu anomaly (Fig. V-43a); gneisses from the Ancient Gneiss Complex have CeN/YbN=7-45, and +Eu anomalies for gneisses with relatively lower total REE (Fig. V-43b); and the Laxfordian gneisses have CeN/YbN=13-65, and also +Eu anomalies for low total-REE samples (Fig. V-43c). The tonalitic (intermediate) gneisses from Laxford have CeN/Yb~=14 with no significant Eu anomaly

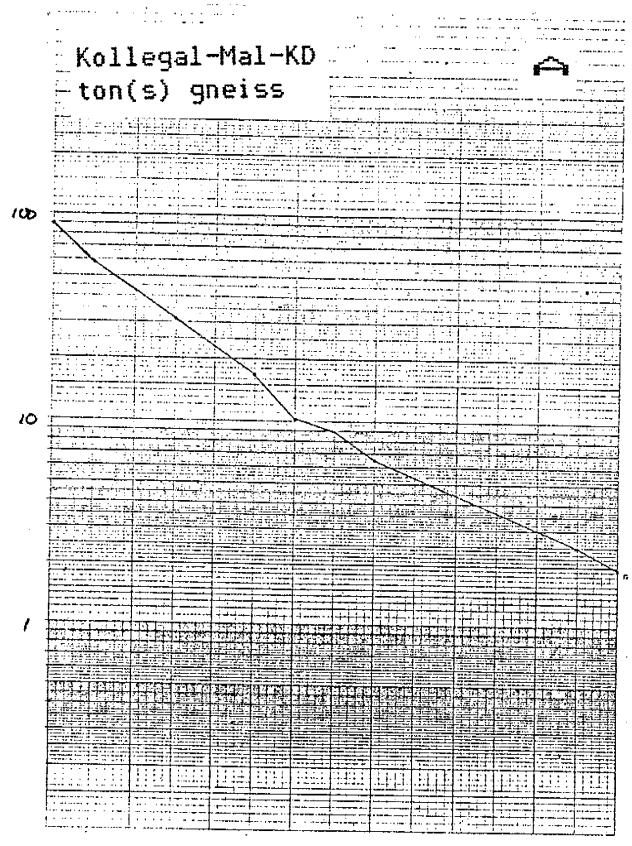
Kollegal-Mal-KD
ton(s) gneiss
A
100
10
1

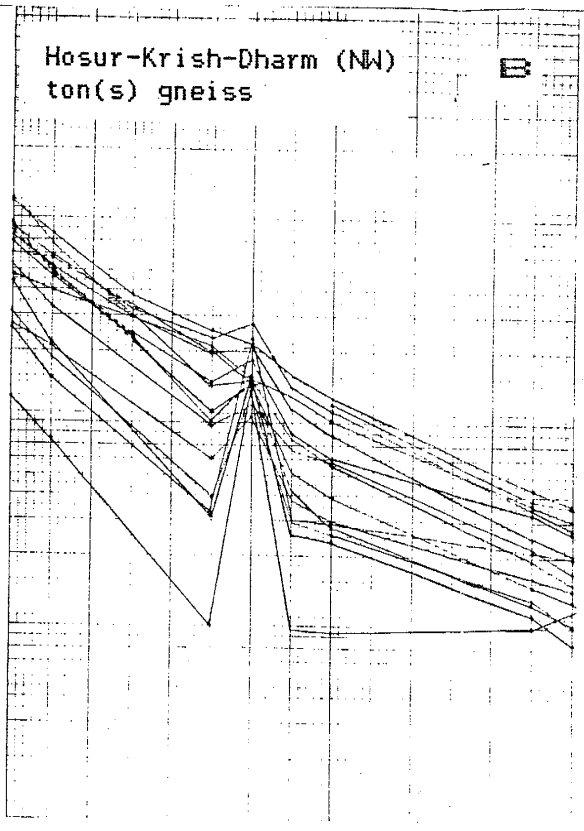
Hosur-Krish-Dharm (NW)
ton(s) gneiss
B

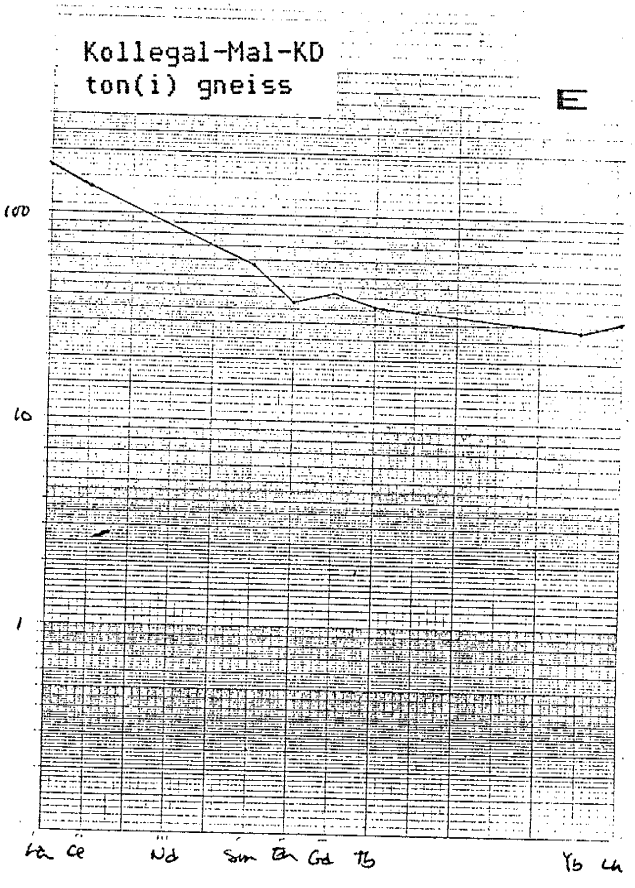
Kollegal-Mal-KD
ton(i) gneiss
E
100
10
1
La Ce Nd Sm Eu Gd Tb Yb Lu

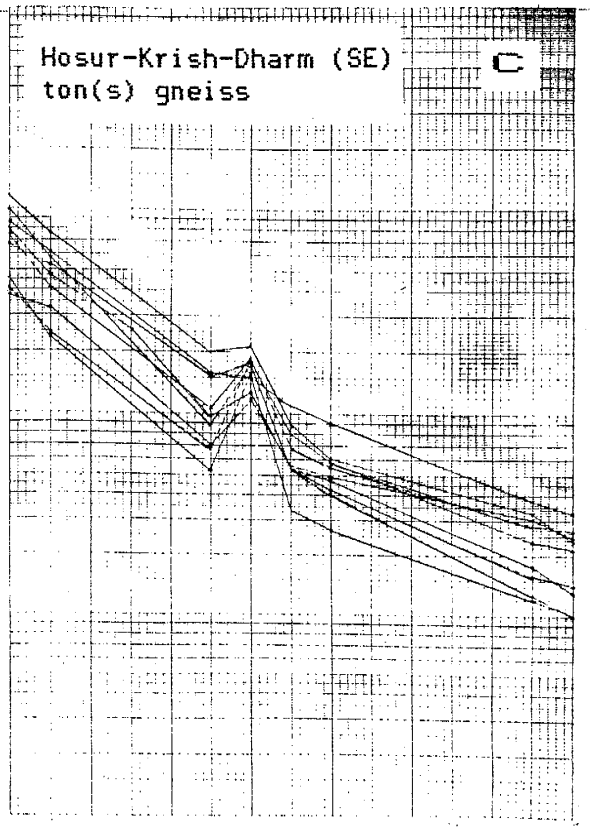

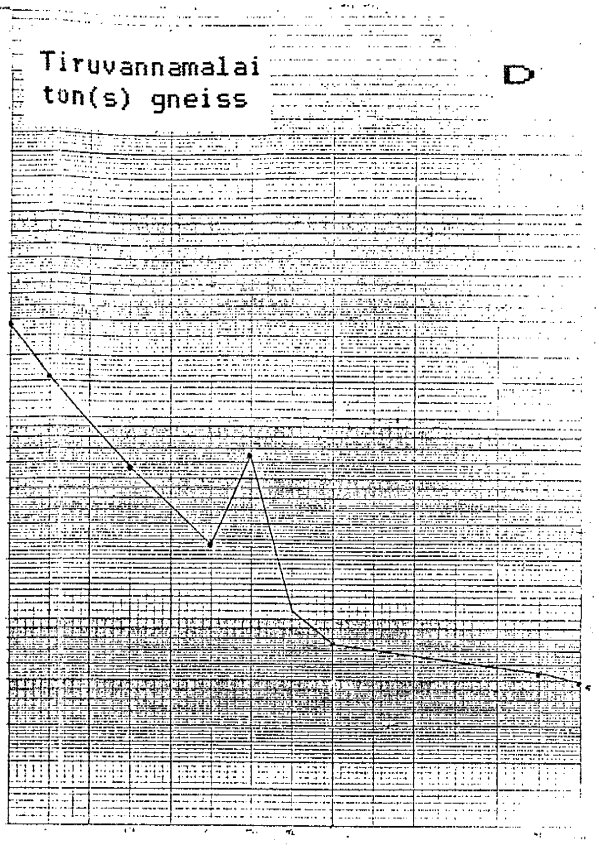

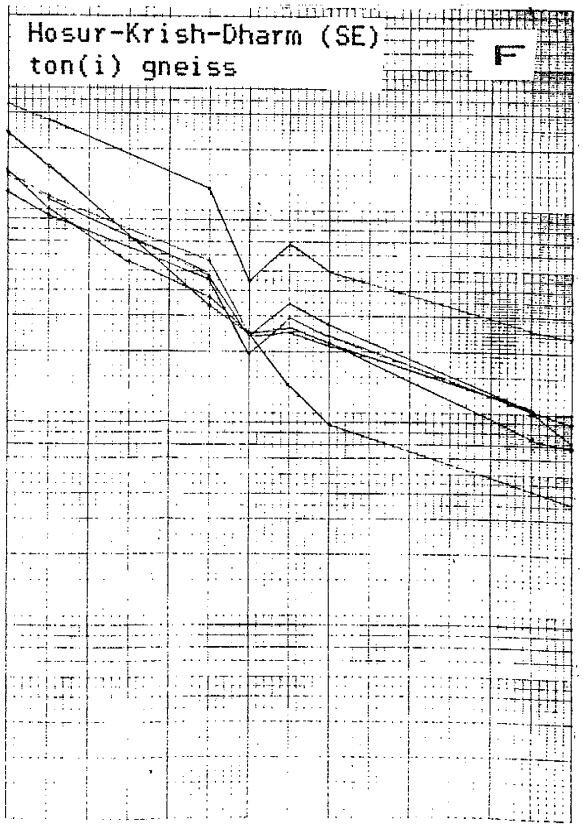

Fig. V-44. Transition Zone: tonalitic gneiss. Data in Appendix C.

(Fig. V-43f).

The REE patterns of tonalitic (silicic) gneisses from the eastern portion of the Transition Zone (Hosur-Krishnagiri-Dharmapuri) have similar slopes (CeN/TbN~=25) and generally significant +Eu anomalies (Fig. V-44b,c). A tonalitic (silicic) gneiss from the western part of the Transition Zone (Kollegal-Malavalli-Kabbaldurga) has a similar CeN/YbN ratio but with no significant Eu anomaly (Fig. V-44a); another gneiss from Tiruvannamalai has a low CeN/YbN (~=4) with lower total REE (Fig. V-44d). The tonalitic (intermediate) gneisses from Hosur-Krishnagiri-Dharmapuri have CeN/YbN~=15 and -Eu anomalies (Fig. V-44f); a sample from the western Transition Zone has a flatter pattern and a small -Eu anomaly (Fig. V-44e). A comparison of the Transition Zone REE plots indicates that though there is some east-west variation, the patterns for the tonalitic (silicic) gneisses have variable total REE, generally steep, fractionated patterns, and +Eu anomalies, while the intermediate gneisses have higher total REE, flatter patterns, and -Eu anomalies.

V.8.2 Amphibolite-facies granitic and granodioritic gneisses

A comparison of the granitic and granodioritic gneisses from the Gneiss Terrane and Transition Zone reveal significant differences between the two terranes (Fig. V-45). This difference is also evident in the relative abundances of the LIL and some HFS elements. The granitic gneisses from the northern part of the Gneiss Terrane (Kunigal-Bangalore-Kolar) have high total REE, a mean CeN/YbN~=16, and significant -Eu anomalies (Fig. V-45c), and are similar to

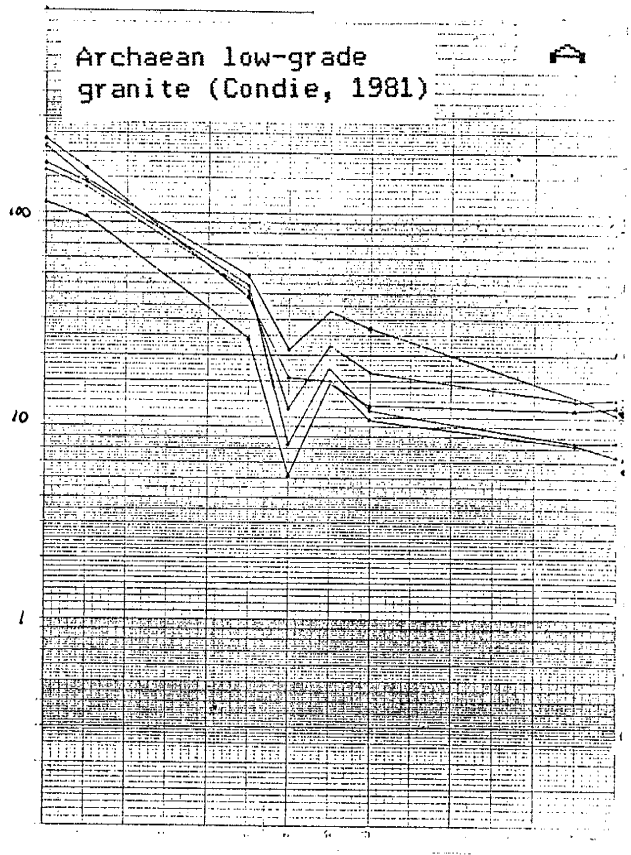

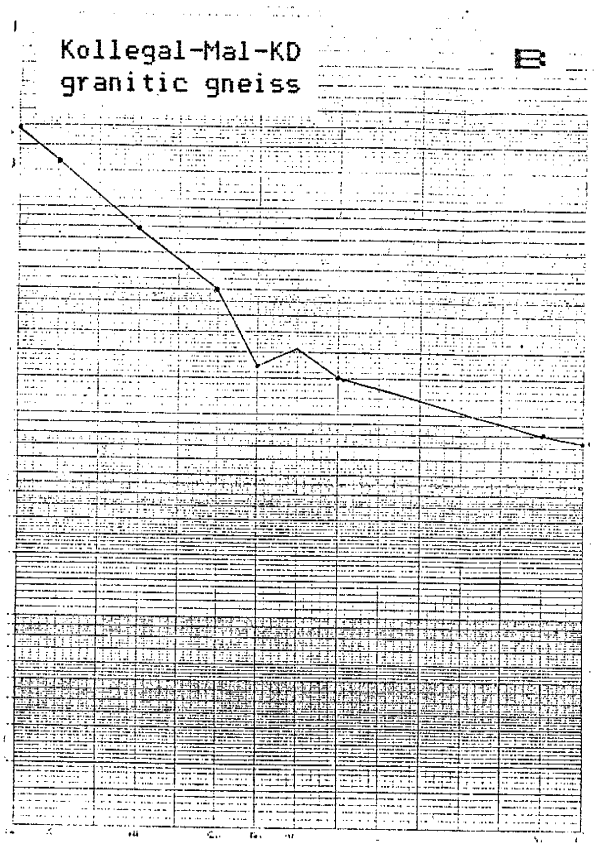

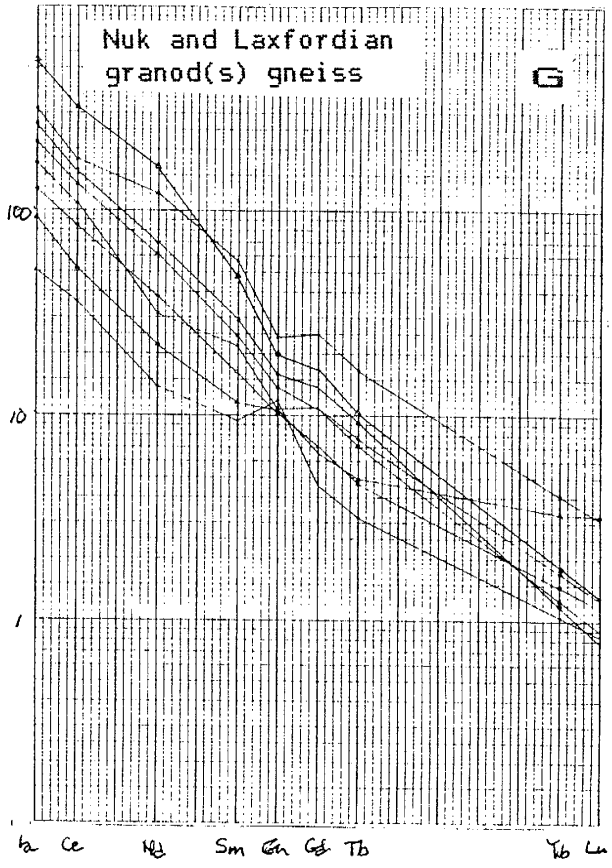

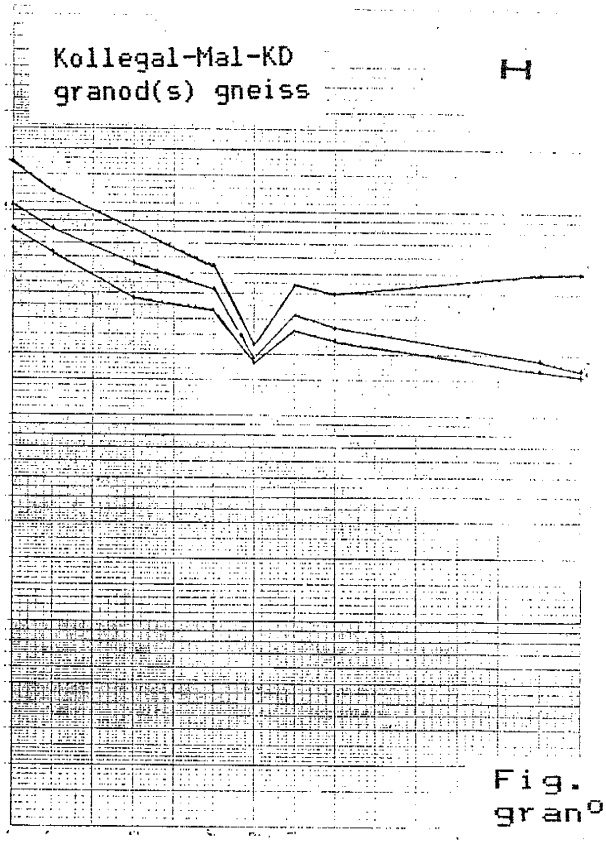

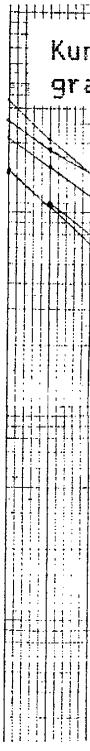

Fig. V-45
granodior

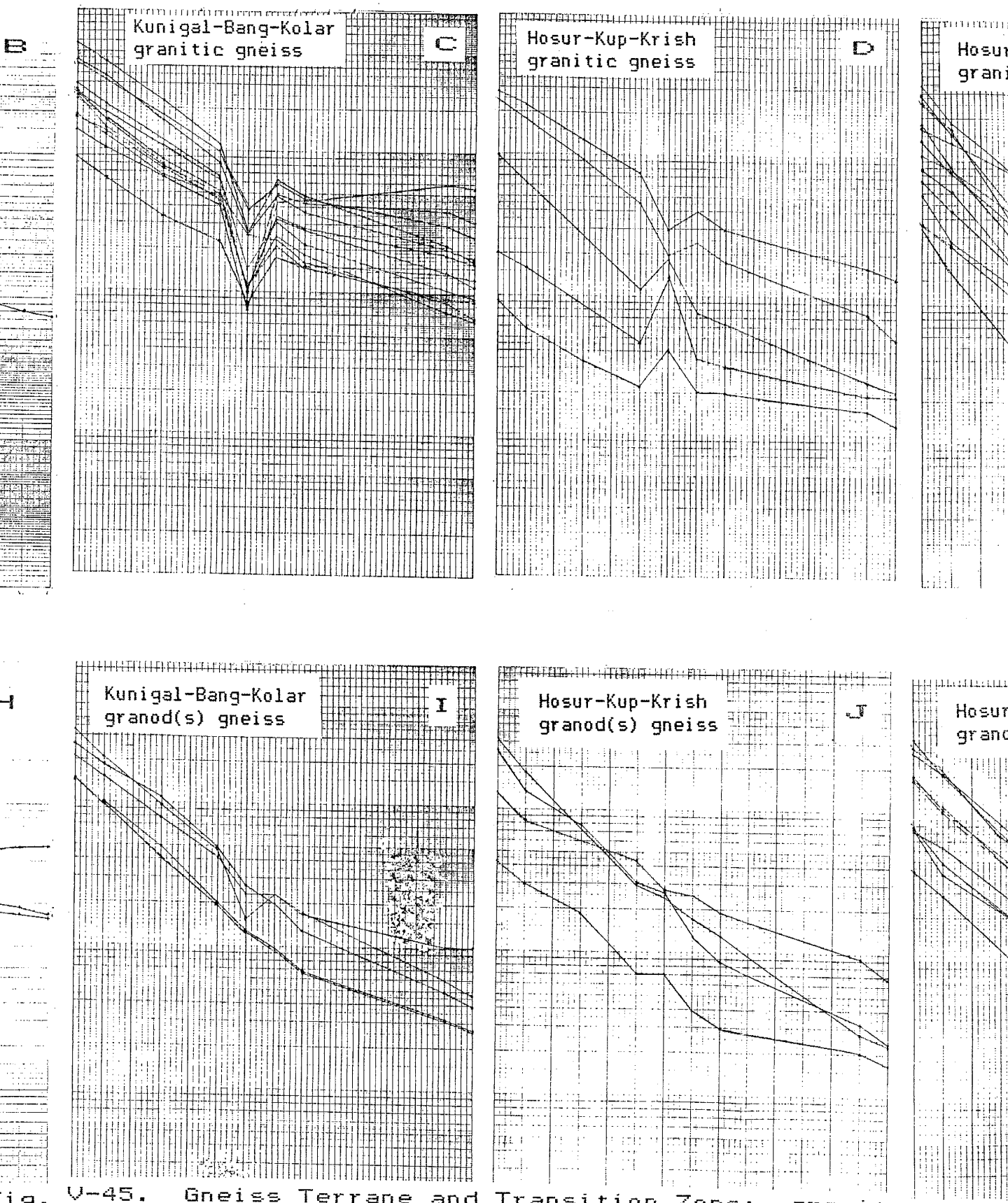

Fig. V-45. Gneiss Terrane and Transition Zone: granitic and granodioritic gneisses. Data in Appendix C.

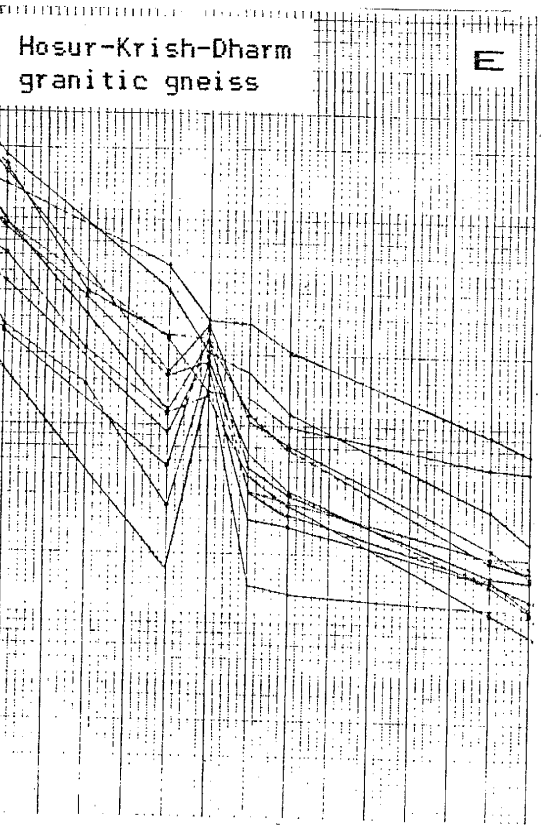
Hosur-Krish-Dharm
granitic gneiss
E

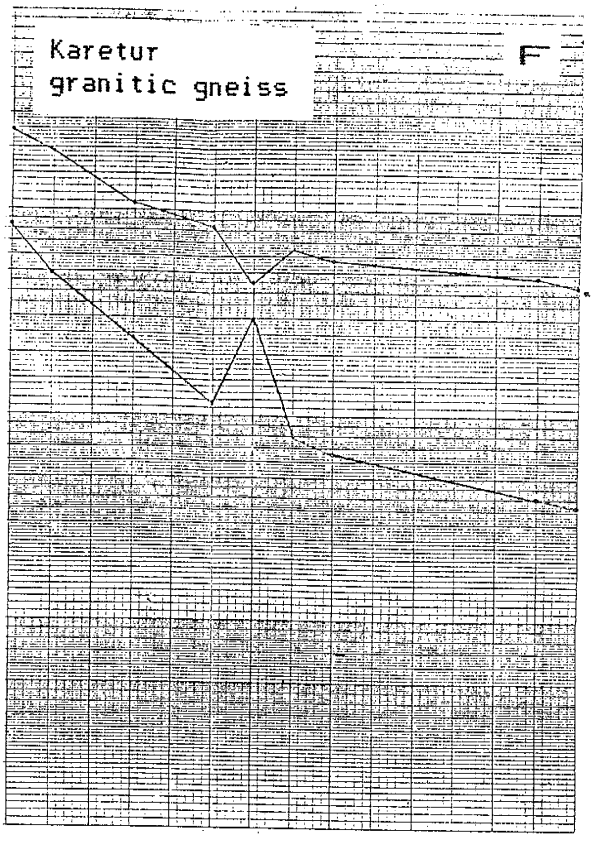
Karetur
granitic gneiss
F

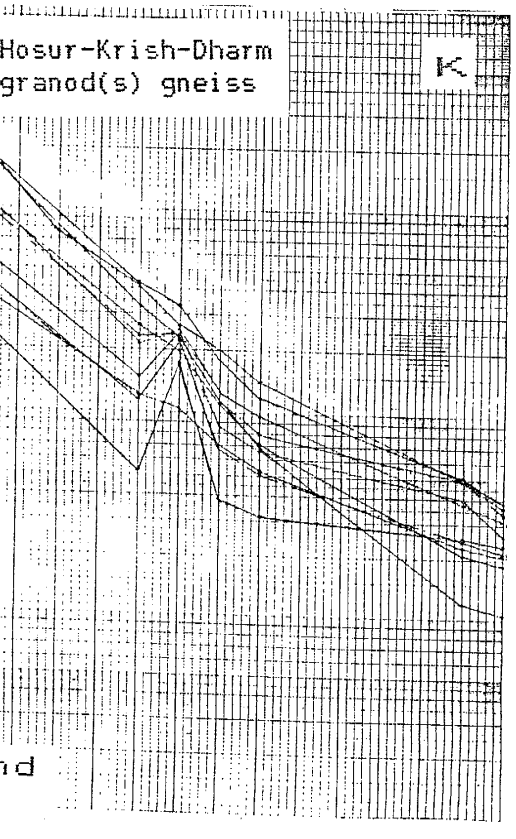
Hosur-Krish-Dharm
granod(s) gneiss
K

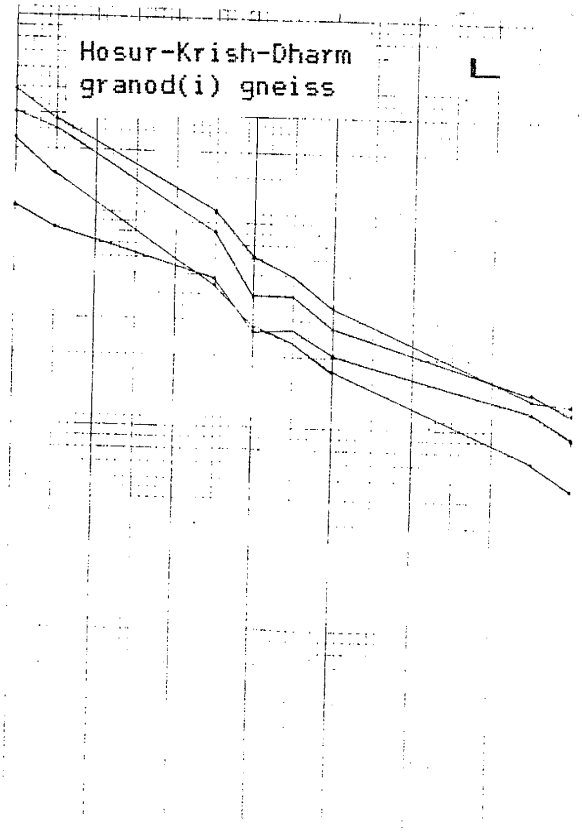
Hosur-Krish-Dharm
granod(i) gneiss
L

representative granitic gneisses from other Archaean low-grade terranes (Fig. V-45a). However, the granitic gneisses from the eastern Transition Zone have lower total REE, a mean of CeN/YbN~=20, and significant +Eu anomalies (Fig. V-45e). Granitic gneisses from the southern Gneiss Terrane (Hosur-Kuppam-Krishnagiri), adjacent to the Transition Zone, have divided patterns: two samples from the Hosur area have elevated patterns and -Eu anomalies, and three samples south and east of Hosur have lower total REE and +Eu anomalies, similar to the Transition Zone granitic gneisses (Fig. V-45d). As noted above, this same change in REE patterns is observed in the tonalitic gneisses from the southern Gneiss Terrane.

The relationship between the REE patterns of the two adjacent granitic gneisses is similar to patterns derived by simple partial melting (Field et al., 1980) or fractional crystallization models (Weaver, 1980). These models, with a mineralogy of about 30% quartz, 60% plagioclase, 5% orthopyroxene, and 5% other oxides in the solid residue, or cumulate for fractional crystallization, produce a liquid with REE patterns similar to the granitic gneisses of the Gneiss Terrane, and a residue or cumulate similar to the granitic gneisses of the Transition Zone.

The one granitic gneiss from the western Transition Zone (Kollegal-Malavalli-Kabbaldurga) has high total REE and a -Eu anomaly, and has greater similarity to the granitic gneisses of the Gneiss Terrane than to the eastern Transition Zone (Fig. V-45b). The same relationship appears to exist in less dramatic fashion for the granodioritic (silicic) gneisses: the gneisses from the Gneiss

Terrane and western Transition Zone have high total REE, with highly variable CeN/YbN, and -Eu anomalies (Fig. V-45h,i); the companion gneisses from the eastern Transition Zone have somewhat lower total REE and +Eu anomalies (Fig. V-45j,k). For comparison, the Nuk granodioritic (silicic) gneisses have somewhat greater total REE and highly fractionated patterns, with very depleted hREE and CeN/YbN~=80 (Fig. V-45g); however, the Nuk Eu anomalies are in general similar to the south India samples for a given level of total REE. The REE pattern of the granodioritic (intermediate) gneisses from the Transition Zone (Fig. V-451)is similar to the high total-REE granodioritic (silicic) pattern. The two granitic gneiss samples from the Karetur quarry have REE patterns (Fig. V-45f) that are similar to the patterns from the southern Gneiss Terrane (Hosur-Kuppam-Krishnagiri), which suggests that similar, but localized, partial melting - fractional crystallization processes may be present.

V.8.3 Transition Zone low-P charnockites

The REE patterns of the tonalitic (silicic) low-P charnockites from the Transition Zone are remarkably similar from west to east (Fig. V-46). The high total REE, mean CeN/YbN values ~=22, and the significant +Eu anomalies are relatively constant, except for the samples from Tiruvannamali, which have lower total REE and CeN/YbN~=15 (Fig. V-46f). Tonalitic (silicic) Amitsoq and Nuk gneisses-granulites have similar patterns to the south India low-P silicic charnockites, though the West Greenland samples have somewhat lower CeN/YbN values and +Eu anomalies (Fig. V-46a,b). The tonalitic (intermediate) low-P charnockites have slightly higher total REE and

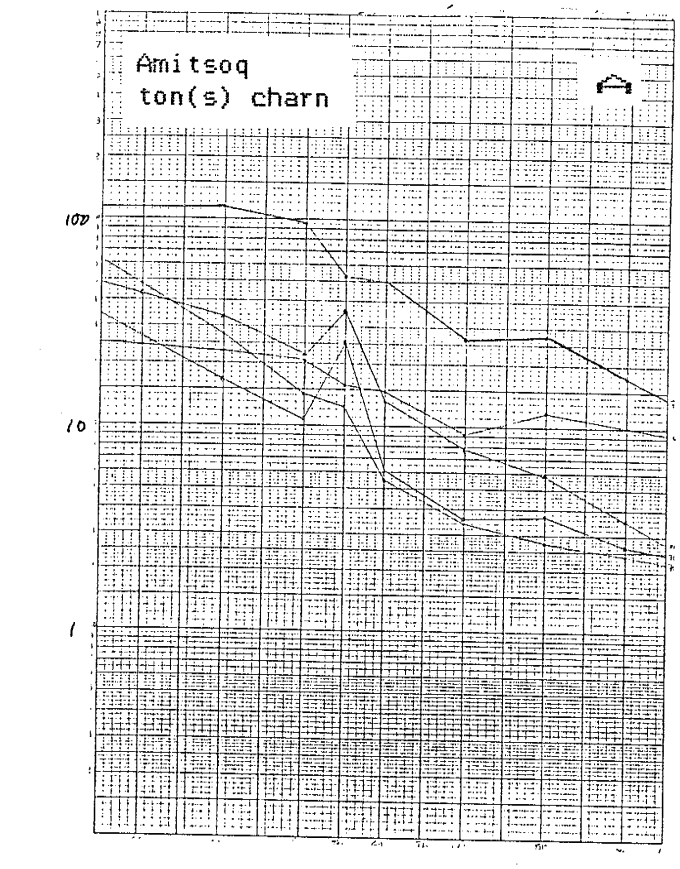
Amitsoq
ton(s) charn
A
100
10
1

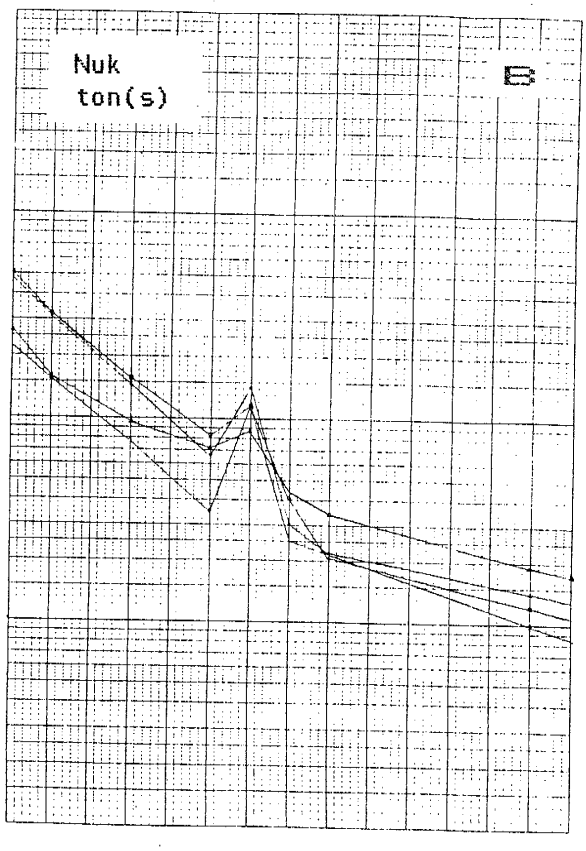
Nuk
ton(s)
B

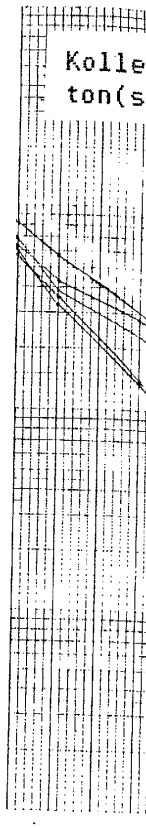
Kolle
ton(s

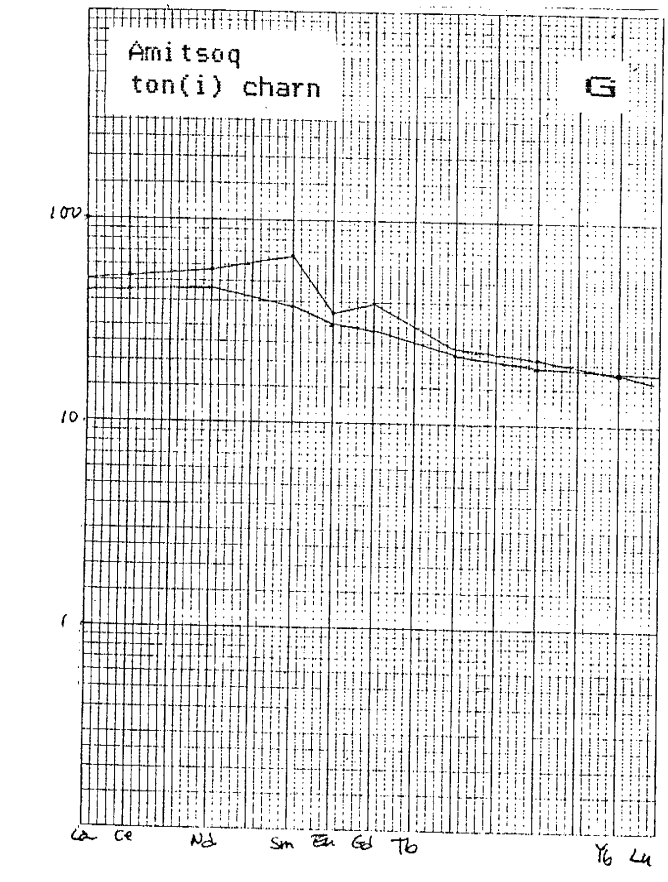
Amitsoq
ton(i) charn
G
100
10
1
La Ce Nd Sm Eu Gd Tb Yb Lu

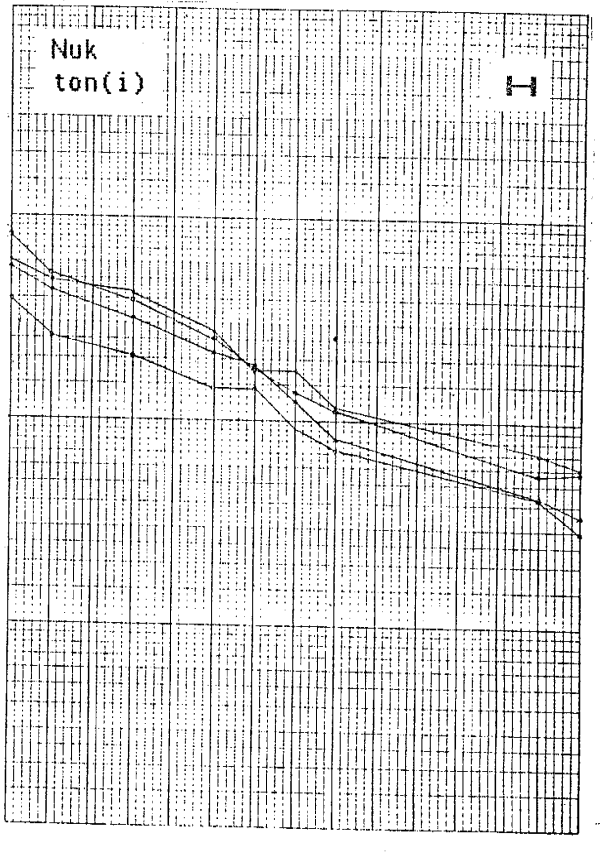
Nuk
ton(i)
H

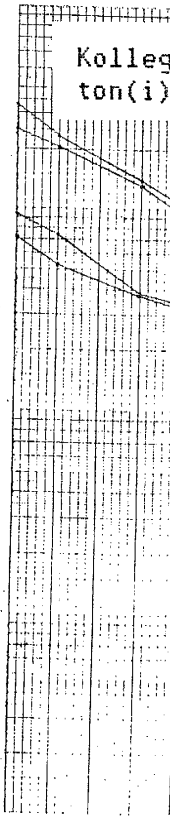
Kolleg
ton(i)

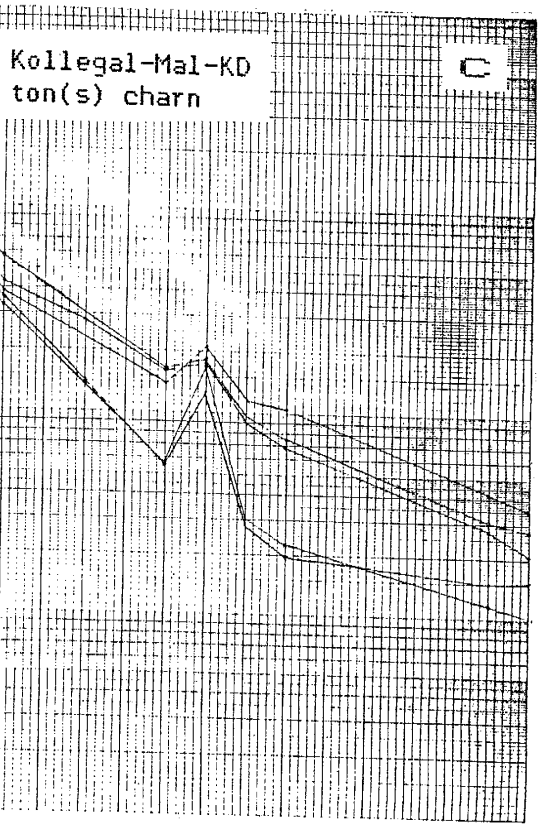
Kollegal-Mal-KD
ton(s) charn
C

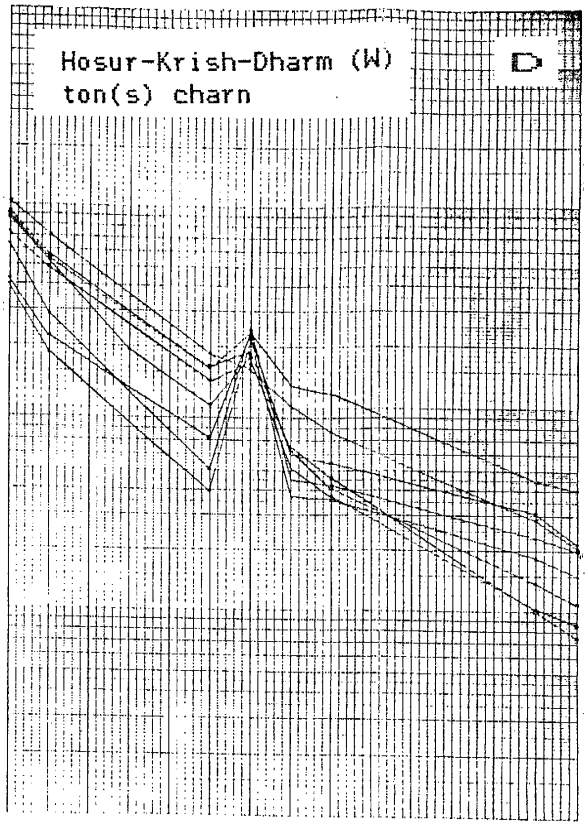
Hosur-Krish-Dharm (W)
ton(s) charn
D

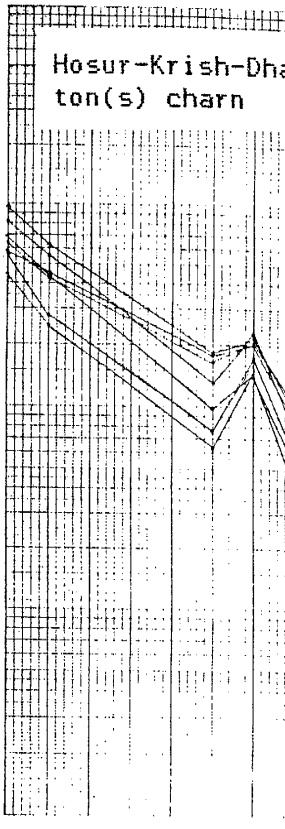
Hosur-Krish-Dha
ton(s) charn

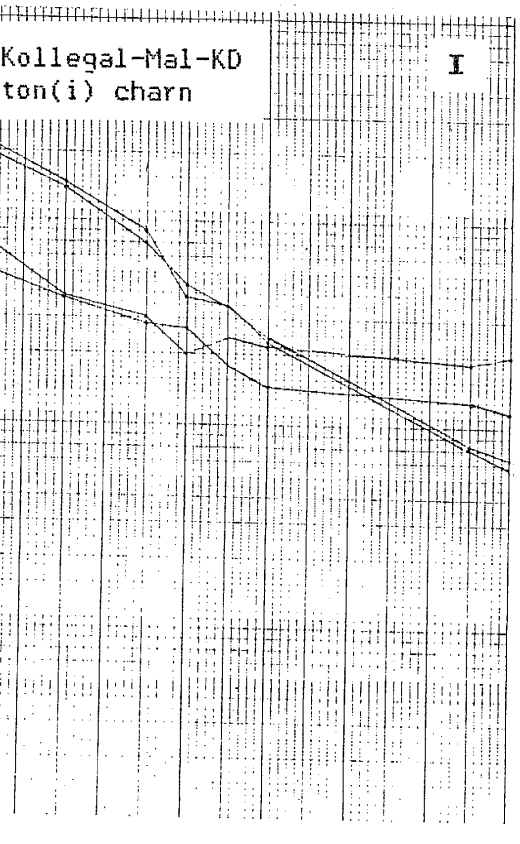
Kollegal-Mal-KD
ton(i) charn
I

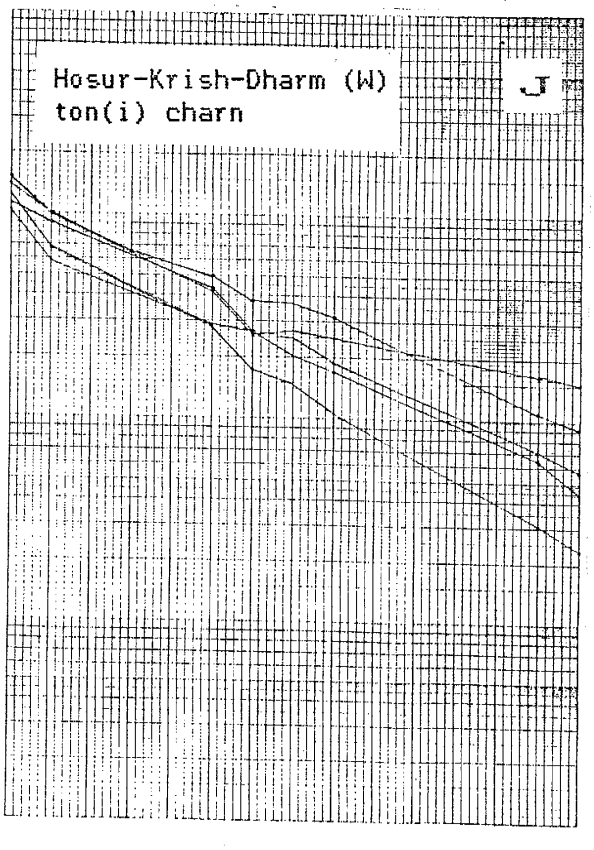
Hosur-Krish-Dharm (W)
ton(i) charn
J

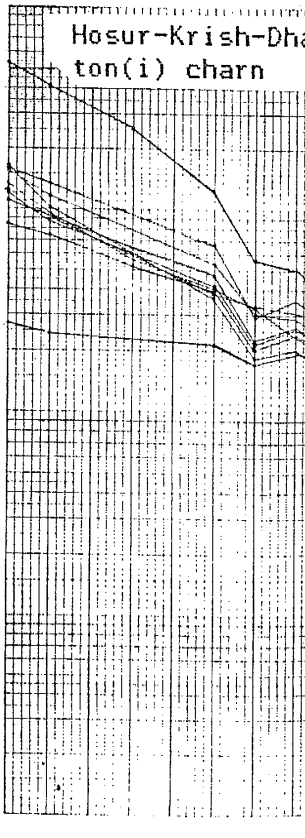
Hosur-Krish-Dha
ton(i) charn

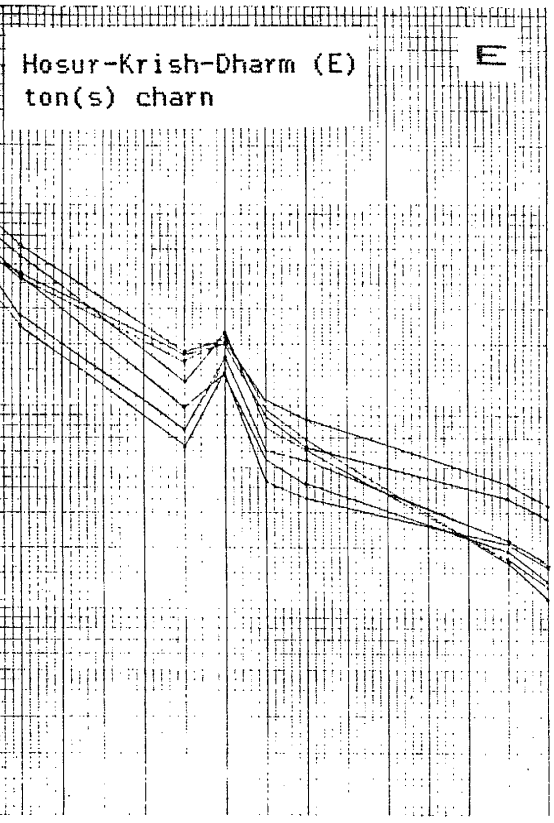

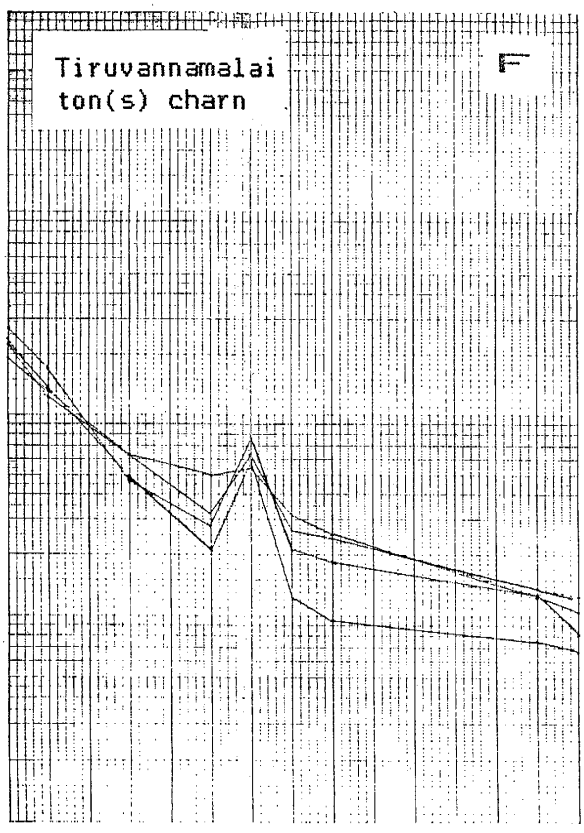

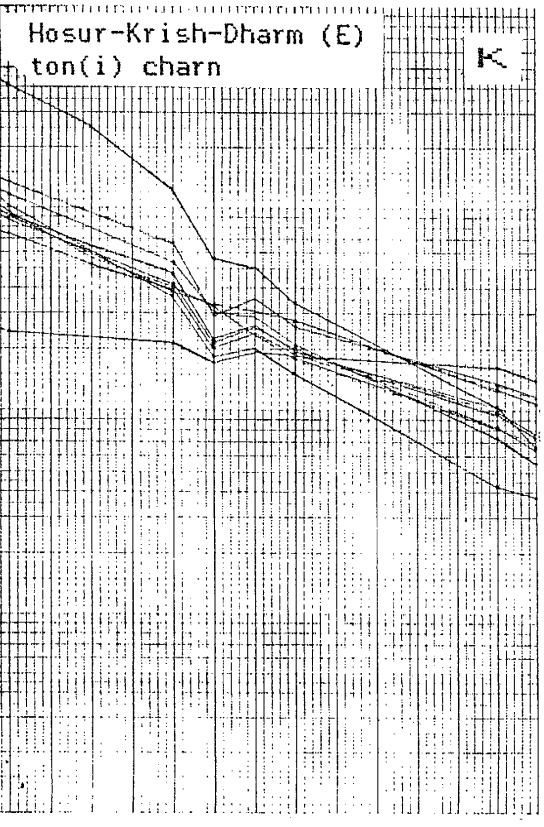

Fig. V-46.
Transition Zone:
charnockite. Data
in Appendix C.

more scatter in the slopes of CeN/YbN (2-40); however, most samples have a mean CeN/YbN~=11 andsmall -Eu anomalies (Fig. V-46i,j,k). The REE patterns of comparable tonalitic (intermediate) Amitsoq and Nuk gneisses are generally similar (Fig. V-46g,h).

The Transition Zone low-P granitic charnockites have patterns that are similar to the granitic gneisses and granodiorites in the area from which they were sampled. Thus, the granitic charnockites from the western Transition Zone (Fig. V-47b) have REE patterns with relatively low CeN/YbN ratios (~6-25) and variable Eu anomalies, and the eastern Transition Zone charnockites (Fig. V-47c) have a more fractionated REE pattern (CeN/YbN~=8.5-95) and variable, but usually positive, Eu anomalies. The Karetur granitic charnockites are also roughly similar to the granitic gneisses from Karetur (Fig. V-47d). The REE patterns of granitic granulites from other Archaean terranes have a wide range. Most of the Amitsoq samples have a less fractionated pattern (CeN/YbN~=9) (Fig. V-47a). The high-P granitic granulites from the Scourian have significantly lower total REE, strong +Eu anomalies, and relatively flat hREE (Fig. V-47e). This Scourian pattern is very different from the Transition Zone, low-P granitic charnockites (Fig. V-47b,c), but similar to those Transition Zone tonalitic and granitic gneisses with low total REE (Fig. V-46c,d,e). South India high-pressure granitic charnockites were not sampled. The granitic charnockites from Madras have variable total REE and CeN/YbN values (Fig. V-47f); however, the lower total-REE samples have patterns similar to the Scourian. The median total-REE samples from Madras are similar to the south India Transition Zone

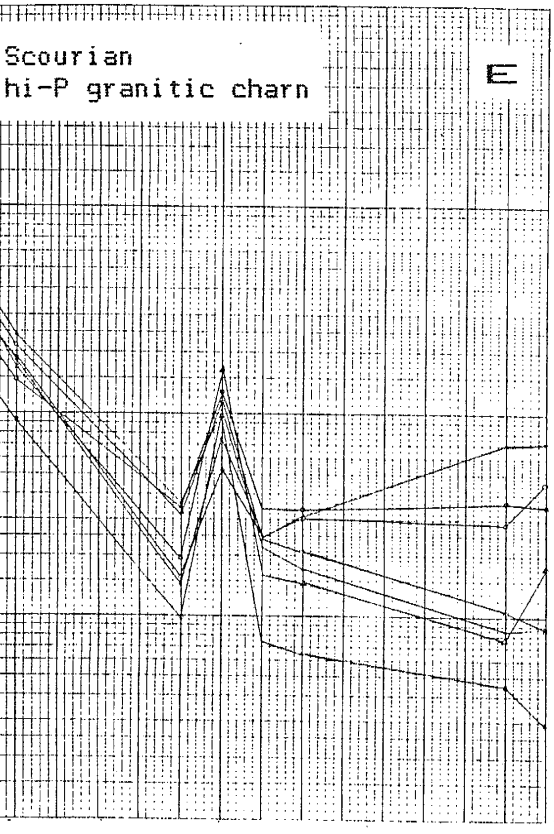
Scourian
hi-P granitic charn
E

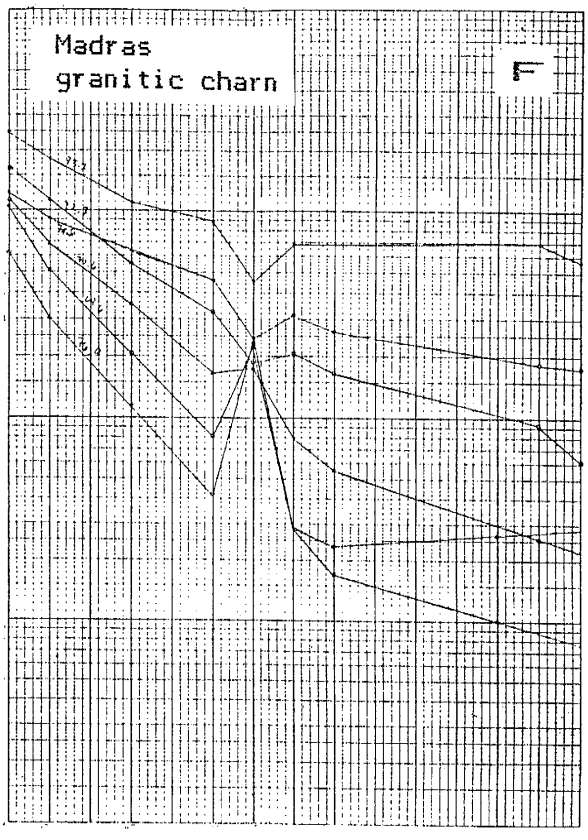
Madras
granitic charn
F

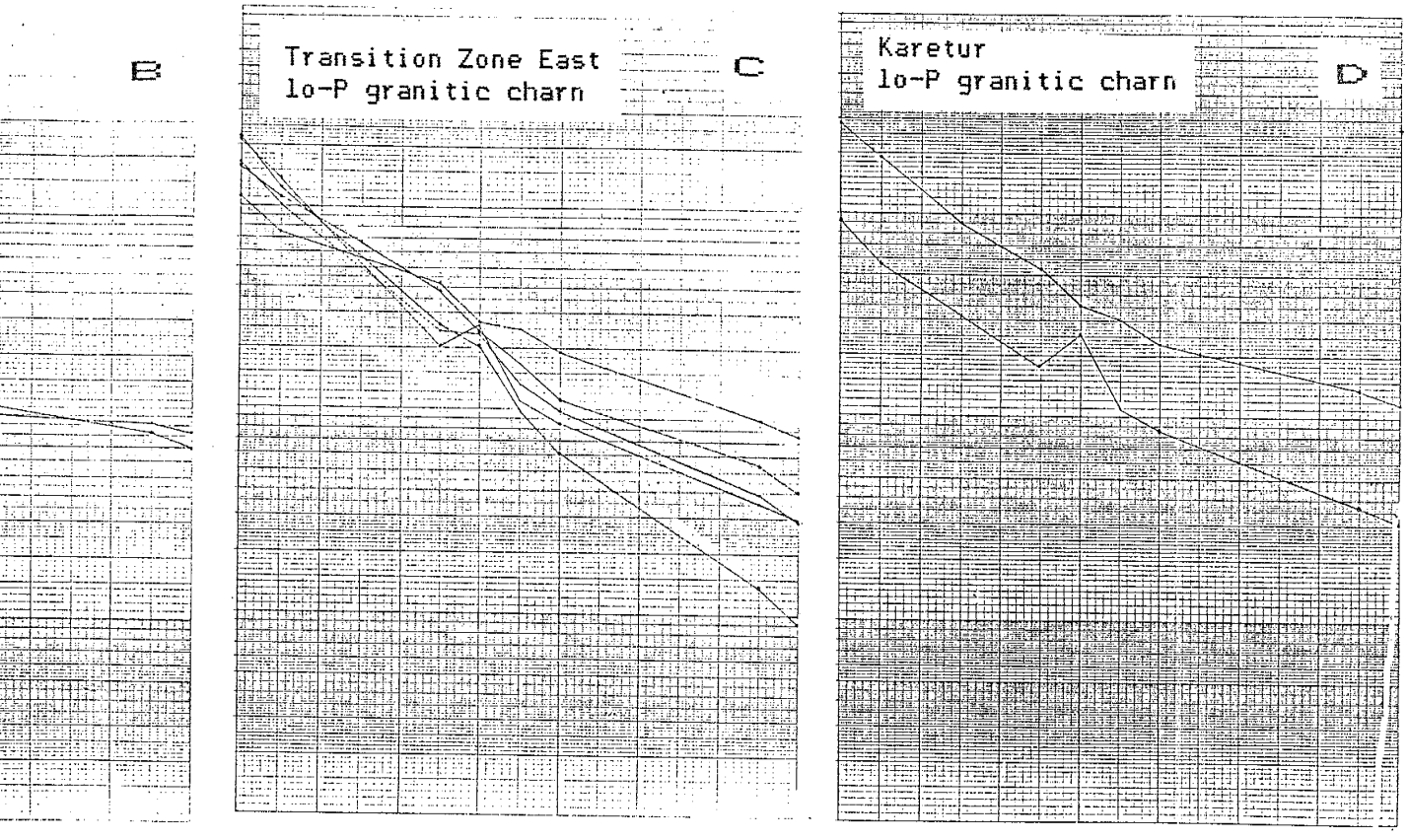

Fig. V-47. Transition Zone and high-pressure terrane: granitic charnockite. Data in Appendix C

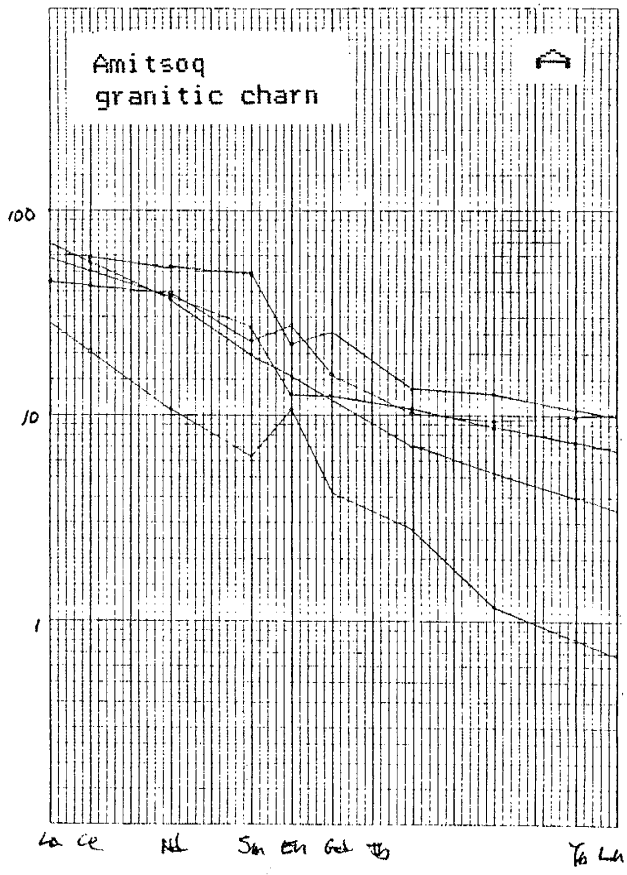
Amitsoq
granitic charn
A
100
10
1
La Ce Nd Sm Eu Gd Yb Lu

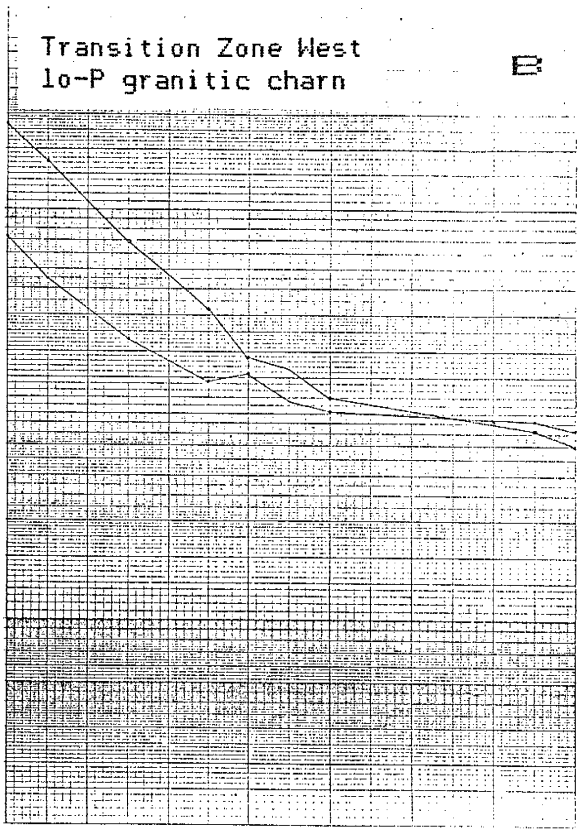
Transition Zone West
lo-P granitic charn
B

charnockites, and the high total-REE samples have relatively flat patterns with -Eu anomalies. The Transition Zone granitic charnockite samples (Fig. V-47b,c) thus fall midway in the continuum between low total-REE and +Eu anomalies, and high total REE and -Eu anomalies of the Madras samples (Fig. V-47f).

V.8.4 Medium and high-P charnockites

The tonalitic (silicic) medium to high-pressure charnockites from south India have REE patterns that are variable (Fig. V-48). During the discussion of major and trace element variation in the high-P terrane (Section V.7), it is noted that the Nilgiris and the BR Hills represented the extremes in the range of element abundances, with the Nilgiris enriched in mafic elements and Rb, Cs, Ta, and Nb relative to the other high-P areas in south India. In general, the range of REE patterns in the high-P terrane is also represented by the Nilgiris and the BR Hills. The tonalitic (silicic) charnockites from the Nilgiris, and Bhavanisagar (west and central regions) (Fig. III-1) have relatively flat patterns (CeN/YbN=5-17) and Eu anomalies that range from positive to negative depending on the level of total REE (Fig. V-48b,c). In contrast, the patterns from the BR Hills, and Salem and Shevaroy-Toppur (central and eastern regions) are relatively depleted in hREE, have CeN/YbN~=40, and have +Eu anomalies (Fig. V-47d,e,f). Silicic tonalitic granulites from the Scourian are similar to the BR Hills-Salem-Shevaroy samples but with slightly lower CeN/YbN (~=25) (Fig. V-47a).

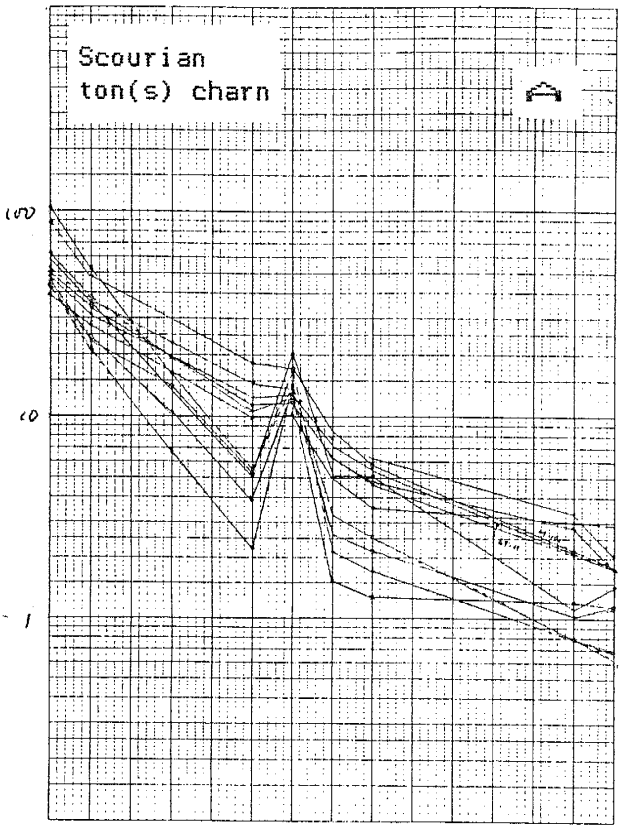
Scourian
ton(s) charn
A

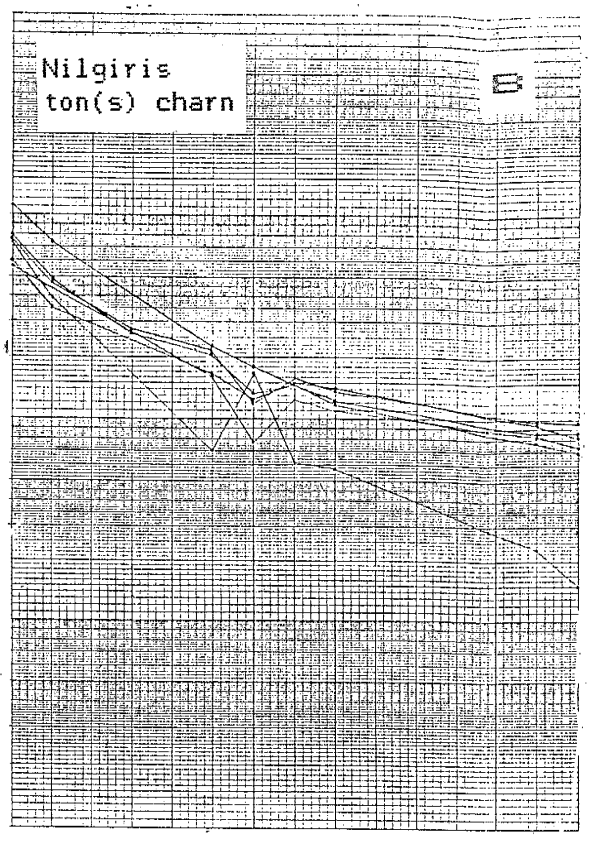
Nilgiris
ton(s) charn
B

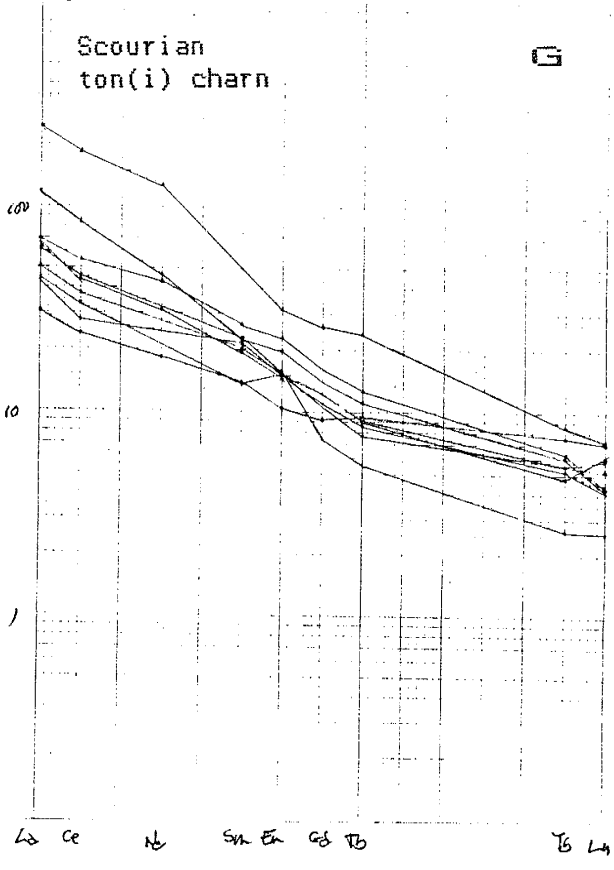
Scourian
ton(i) charn
G

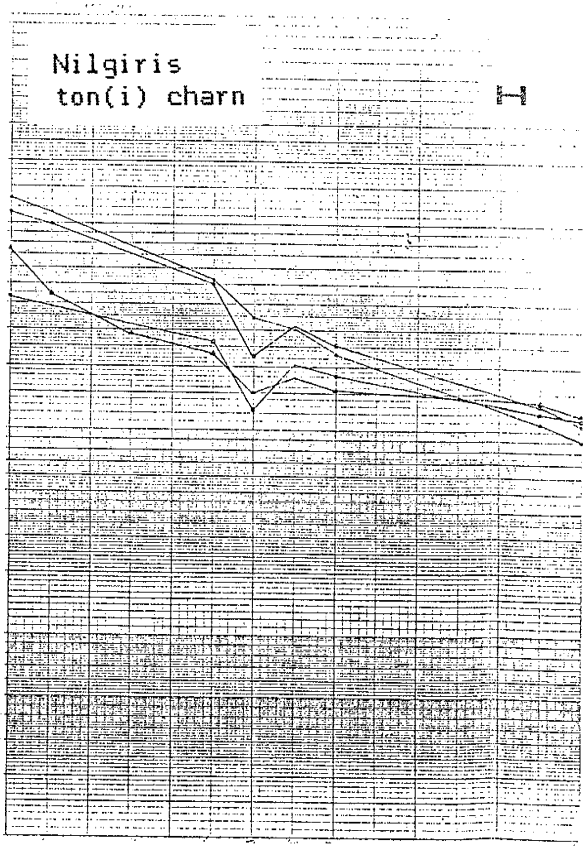
Nilgiris
ton(i) charn
H

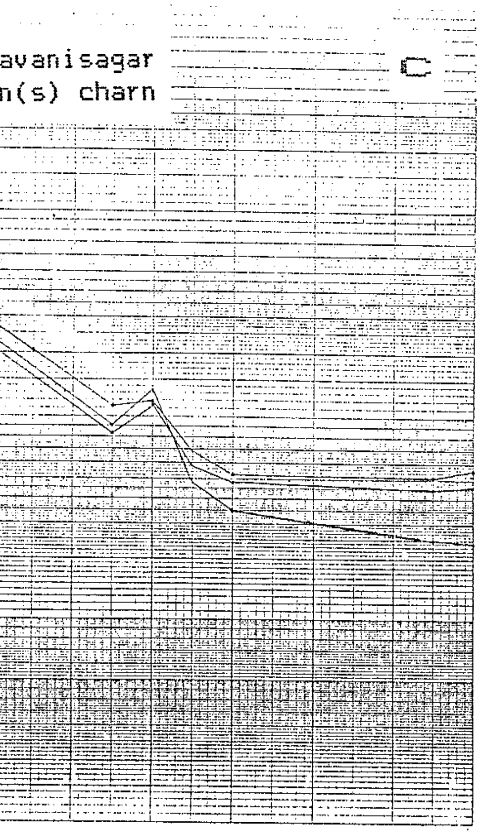

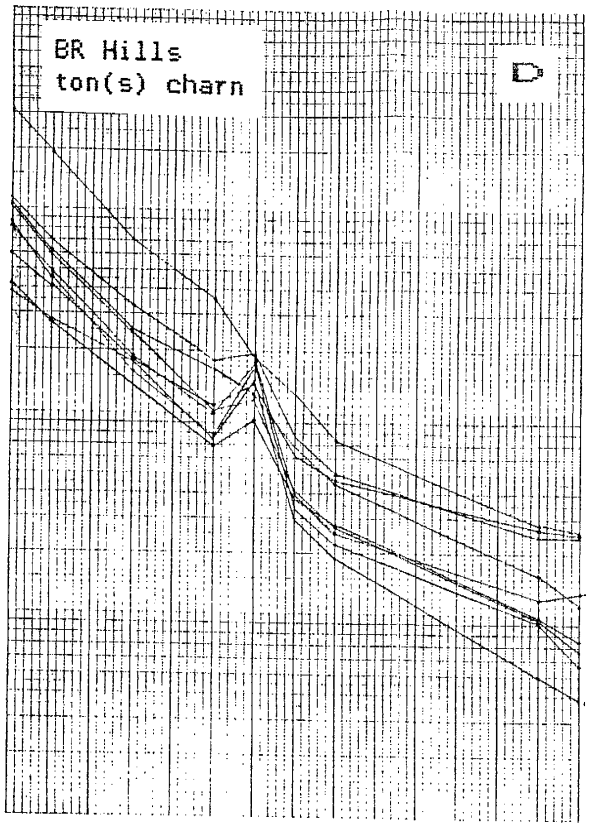

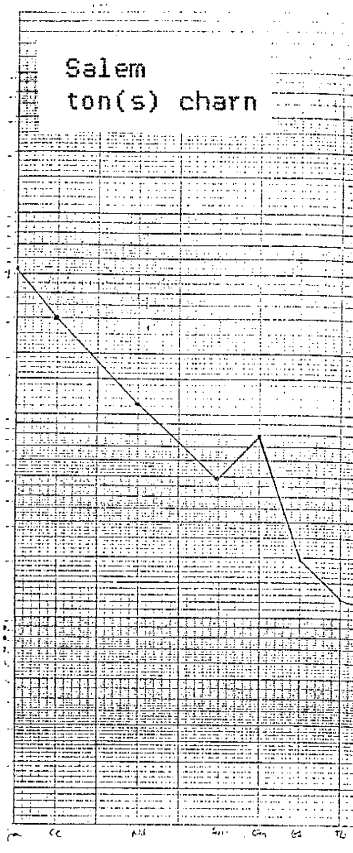

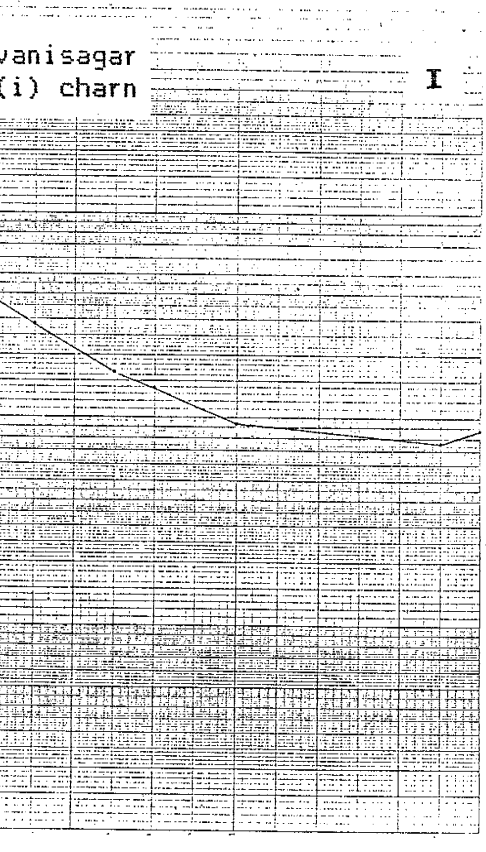

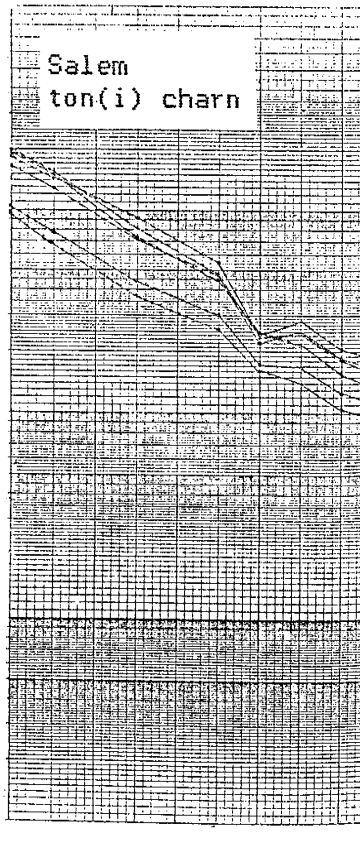

Fig. V-48. Medium to high-pressure charnockite. Data in Appendix C.

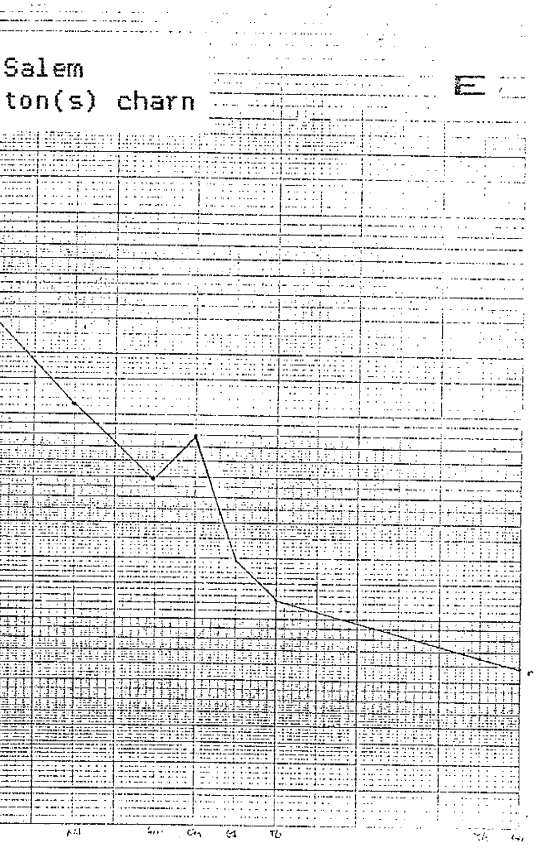
Salem
ton(s) charn
E

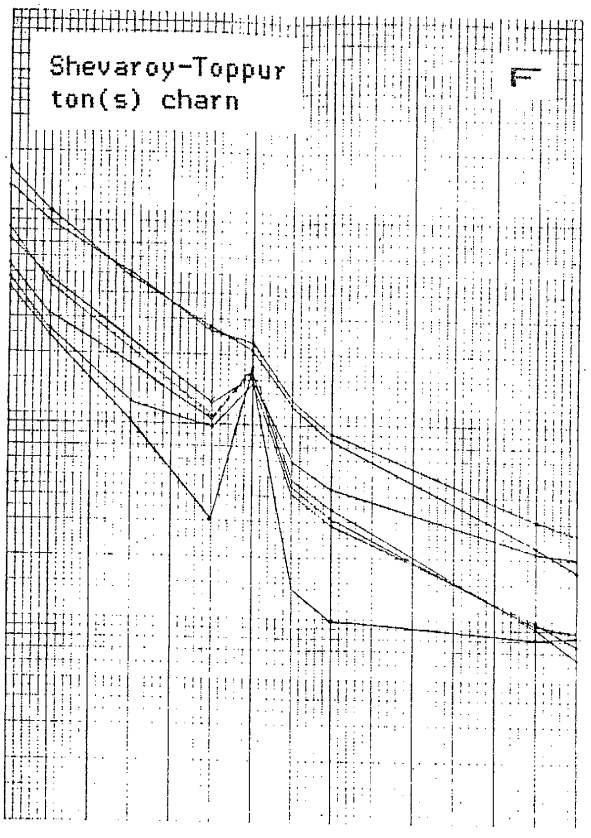
Shevaroy-Toppur
ton(s) charn
F

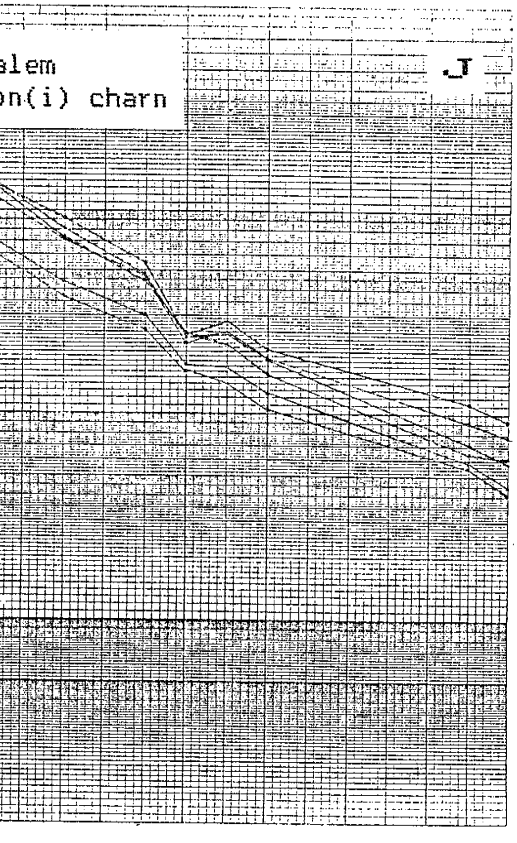
alem
on(i) charn
J

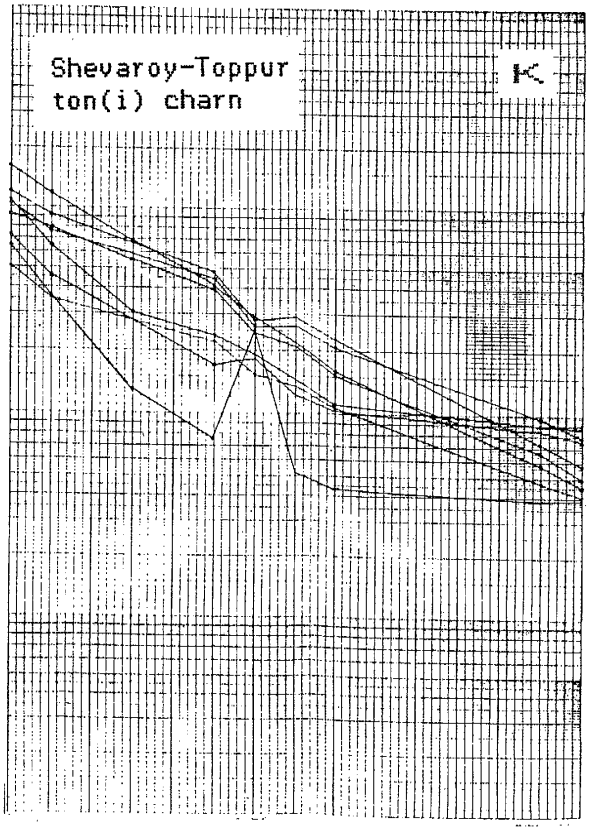
Shevaroy-Toppur
ton(i) charn
K

The more fractionated patterns of the eastern region are also observed in the REE plots of the tonalitic (intermediate) charnockites, which have higher CeN/YbN than seen in the samples from the Nilgiris and Bhavanisagar (Fig. V-48h,i,j,k). Negative Eu anomalies are observed in samples from the Nilgiris, Salem, and Shevaroy-Toppur. Tonalitic (intermediate) granulites from the Scourian have broadly similar patters as the south India high-P charnockites but without the -Eu anomalies (Fig. V-47g).

V.8.5 Comparison of low and high-grade results

The comparisons made above illustrate the variability of REE patterns within metamorphic terranes. In order to examine changes in REE patterns between metamorphic terranes, a north to south traverse of REE patterns from areas of increasing metamorphic grade are shown in Fig. V-49. Along the traverse, representative REE patterns are shown for the tonalitic gneisses from the northern and southern regions of the Gneiss Terrane (Kunigal-Bangalore-Kolar and Hosur-Kuppam-Krishnagiri, respectively), the tonalitic gneisses and low-P charnockites from the eastern Transition Zone (Hosur-Krishnagiri-Dharmapuri), and tonalitic medium and high-P charnockites from the eastern region of the high-grade terrane south of the Moyar-Bhavani shear zone (Shevaroy-Toppur)(Figs. III-1, V-49). As was noted above, there is a significant difference between the amphibolite-facies gneisses of the northern Gneiss Terrane (Fig. V-49c) and the Transition Zone (Fig. V-49e,f). However, the REE patterns of the tonalitic (silicic) gneisses from the southern Gneiss Terrane (Hosur-Kuppam-Krishnagiri) (Fig. V-49d) and the eastern Transition Zone are

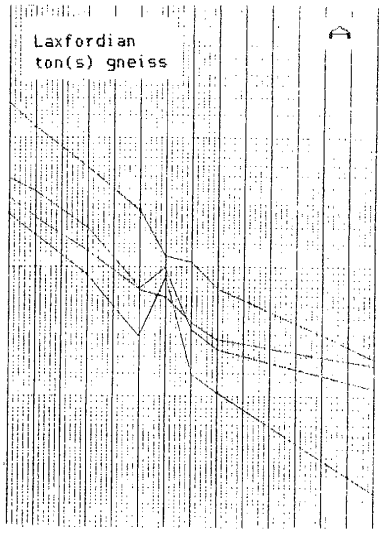

Fig. V-49. Representative REE plots
tonalitic (silicic and intermediate)
gneiss and charnockite. North to so
traverse (increase in metamorphic gr
is from left to right. Data in Appe

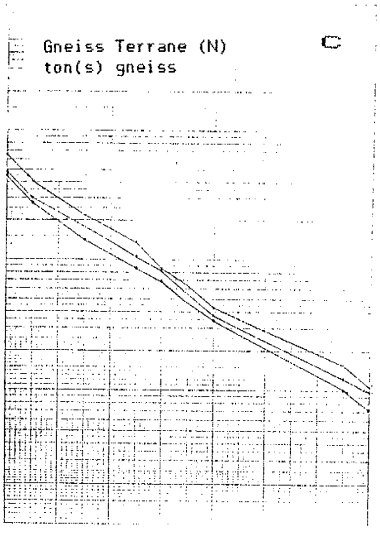

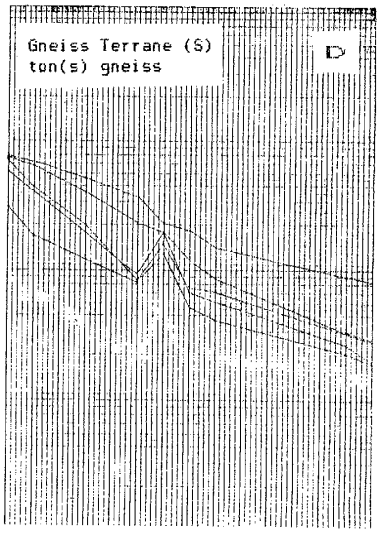

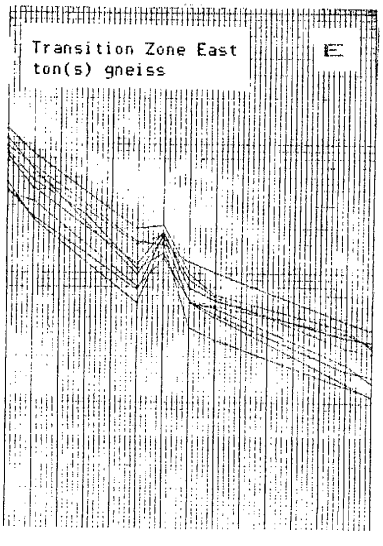

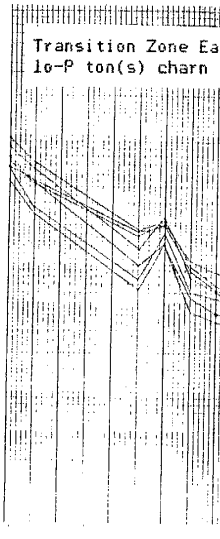

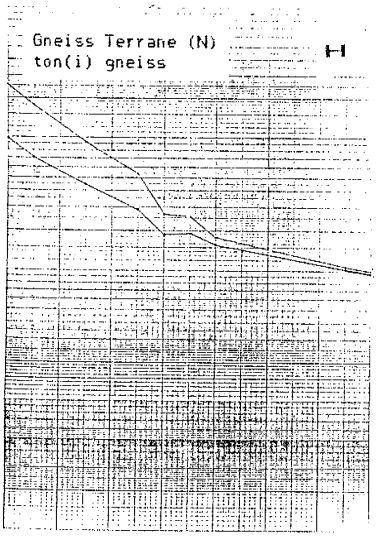

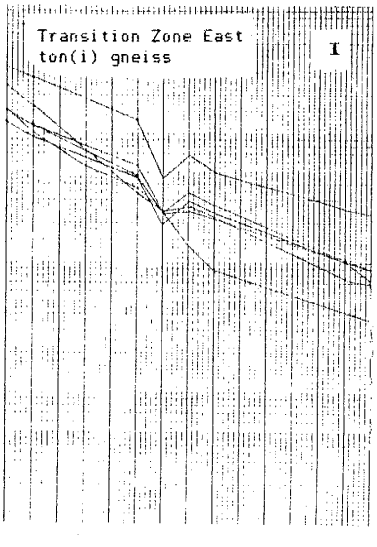

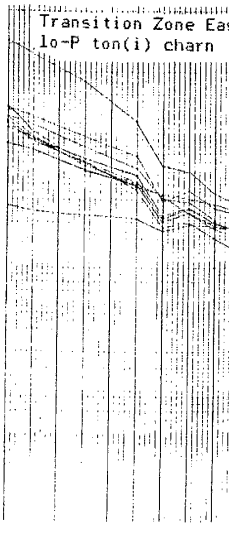

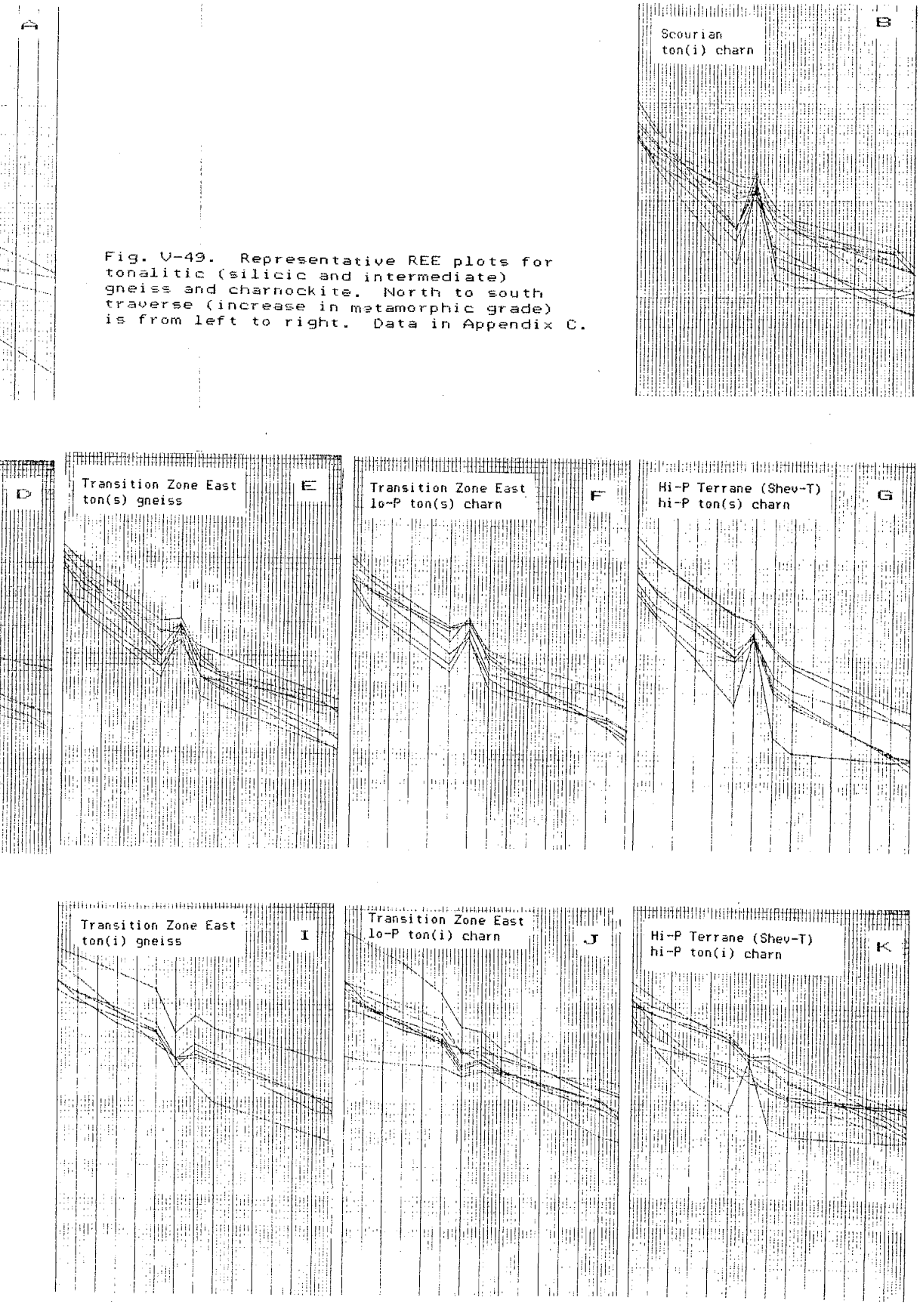

Fig. V-49. Representative REE plots for tonalitic (silicic and intermediate) gneiss and charnockite. North to south traverse (increase in metamorphic grade) is from left to right. Data in Appendix C.

remarkably similar to each other and to the low and high pressure charnockites from the eastern Transition Zone and the Shevaroy-Toppur area (Fig. V-49g). These patterns are characterized by high total REE, depleted hREE, +Eu anomalies, and CeN/YbN ranging from 8-20 (southern Gneiss Terrane) to 15-30 (Transition Zone) to 30-40 (high-P charnockite terrane). The REE patterns have internal variability and the slight increase of CeN/YbN, with metamorphic grade for the tonalitic (silicic) rocks between the Transition Zone and the high-P terrane is probably not significant. A comparison of the amphibolite-facies Laxford tonalitic (silicic) gneisses (Fig. V-49a) and Scourian granulites (Fig. V-49b) also suggests little change with increasing metamorphic grade.

The REE patterns for the tonalitic (intermediate) gneisses also display a very close similarity between the amphibolite-facies Gneiss Terrane and the high-P charnockite terrane (Fig. V-49h,i,j,k). The mean values for CeN/YbN are ~13-15 for all groups, though the plots for Transition Zone low-P charnockites are more variable than the other groups. Negative Eu anomalies are characteristic of the patterns in all groups. In general, for both silicic and intermediate tonalitic gneisses, there is great similarity in the REE patterns of samples from areas of increasing metamorphic grade. The variability observed in the patterns from different metamorphic terranes is less or of the same magnitude as the variability within any terrane. Thus, an examination of comparable REE patterns does not indicate any significant mobilization of REE with increases of metamorphic grade.

V.8.6 Eu/Eu*

The relationship between Eu anomalies, expressed as Eu/Eu*, and SiO2 and other elements is examined on a group of X - Y plots (Figs. V-50 to V-53). At first glance, the Eu/Eu* - SiO2 plot indicates only broad scatter (Fig. V-50). However, the granitic gneiss samples in the lower right hand corner of the plot, at low Eu/Eu* and high SiO2, are the unique group from the northern Gneiss Terrane; if these samples are not considered, the remaining gneiss and charnockite samples have a rough positive correlation of increasing Eu/Eu* with increasing levels of SiO2, or greater +Eu anomalies at higher SiO2. A similar trend is described for the Scourian (Pride and Muecke, 1980). Though there is considerable overlap, there is a suggestion that the charnockites have slightly higher Eu/Eu* values for a given level of SiO2; plots of the mean values of Laxford and Scourian gneisses have this same relationship (Fig. V-50). On an Eu/Eu* - Total-REE plot, there is again a rough linear trend for most of the gneisses and charnockites, with high scatter at low Eu/Eu* and high Total REE for the granitic gneisses from the northern Gneiss Terrane (Fig. V-51). This indicates that +Eu anomalies are occuring at low levels of Total REE and -Eu anomalies at high levels, which is also observed on the REE patterns. Similar relationships can be seen on the Eu/Eu* - SmN and Eu/Sm - Sm diagrams (Figs. VI-3, VI-4). For further discussion see Section VI.2.

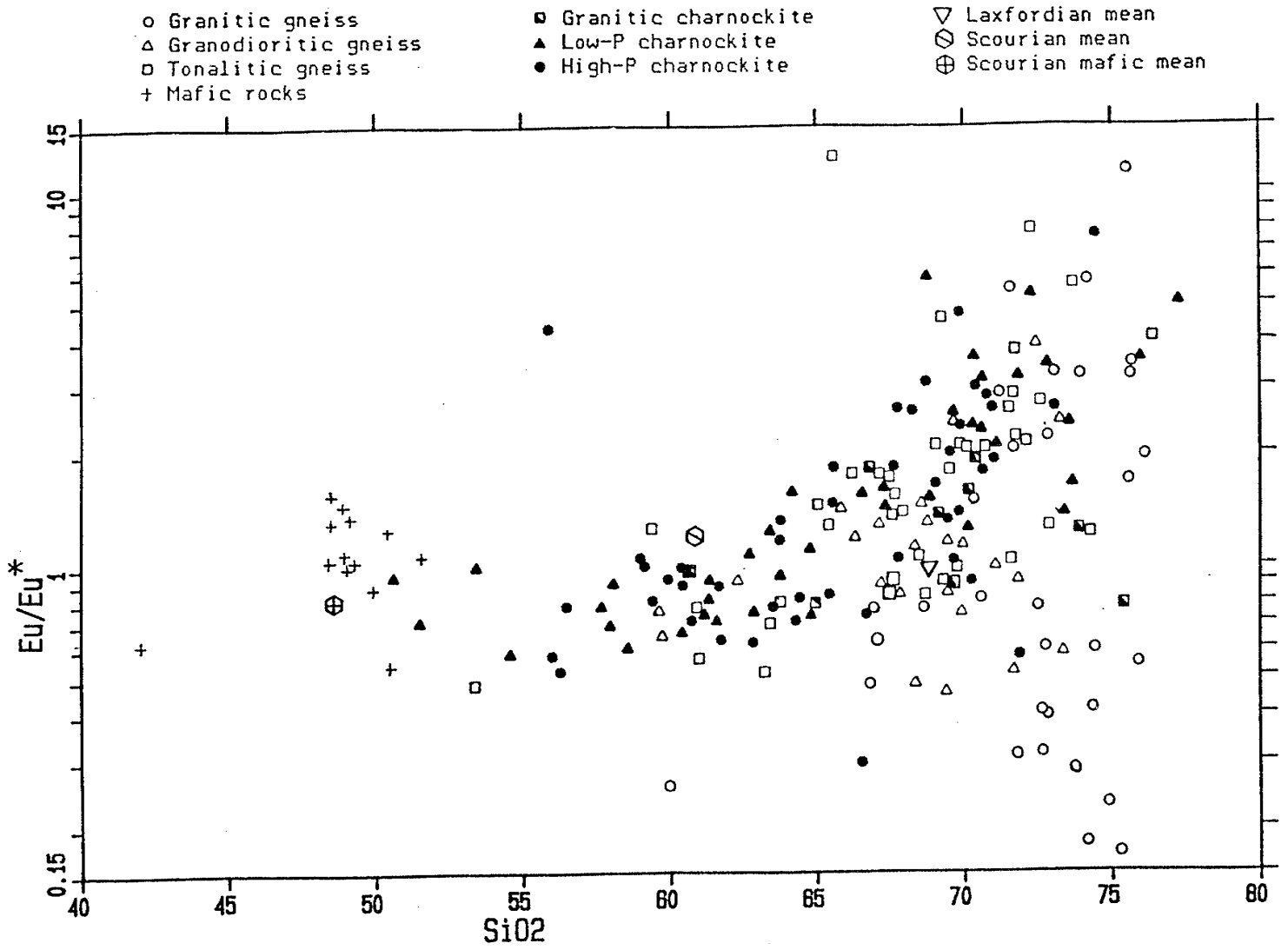

Fig. V-50. Eu/Eu* vs SiO2 plot. Data from Appendix C.

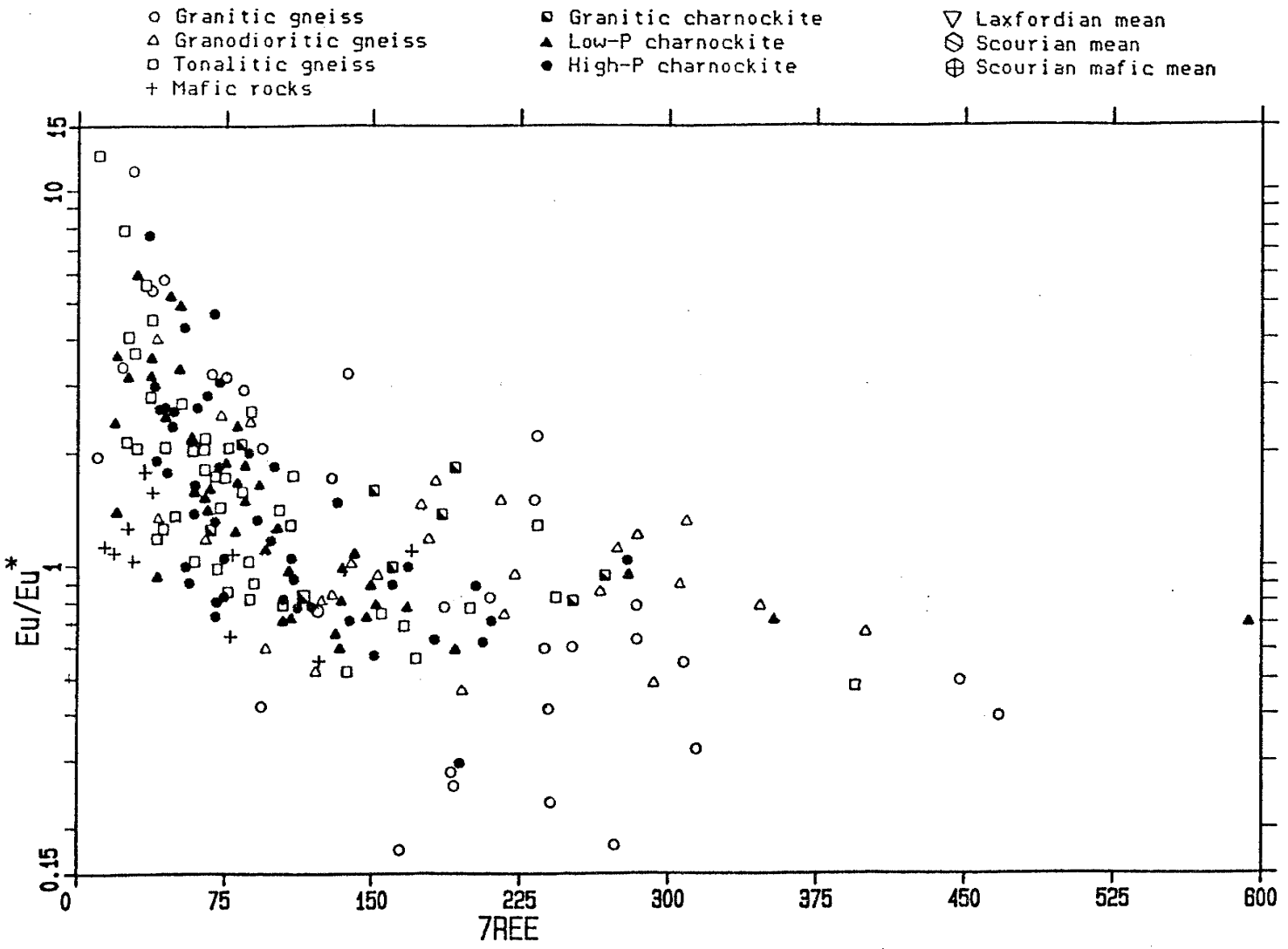

Fig. V-51. Eu/Eu* vs 7REE plot. Data from Appendix C.

A plot of Eu/Eu* against modal plagioclase (Fig. V-52) does not show any significant overall correlation for the samples for which there is modal data. However, the tonalitic high-P charnockites have a very rough correlation between Eu/Eu* and plagioclase, and higher modal plagioclase than the gneisses. A similar plot of Eu/Eu* and modal plagioclase for the Scourian granulites also exhibits a rough positive correlation (Pride and Muecke, 1980). A very broad positive correlation is also observed for the south India samples on a Eu - Sr plot (Fig. V-53). Sr and Eu+2 both have distribution coefficients >1 for K feldspar and plagioclase (Henderson, 1982; Condie, compiled data) and a Eu vs Sr plot might be expected to have a positive correlation, indicating a relationship between Eu and plagioclase fractionation. The low correlation in the Eu/Eu* - Plag and Eu - Sr plots suggests that other factors in addition to plagioclase fractionation controlled Eu abundance in the south India samples.

V.8.7 La/Yb, CeN/YbN

A La/Yb - SiO2 plot also shows wide scatter, though the tonalitic gneisses and charnockites fall on a very broad trend of increasing REE fractionation with increasing SiO2 (Fig. V-54). The terrane-mean values of Laxford and Scourian gneisses lie on the trend with the Scourian having lower La/Yb and SiO2 than the Laxford; however, the decrease of La/Yb and SiO2 with increasing metamorphic grade for the Scourian-Laxford pair is not as pronounced as the south India results. A plot of Scourian samples on a La/Yb - SiO2 diagram defines the REE fractionation trend more sharply than the south India samples (Pride and Muecke, 1980). A plot of total REE against SiO2

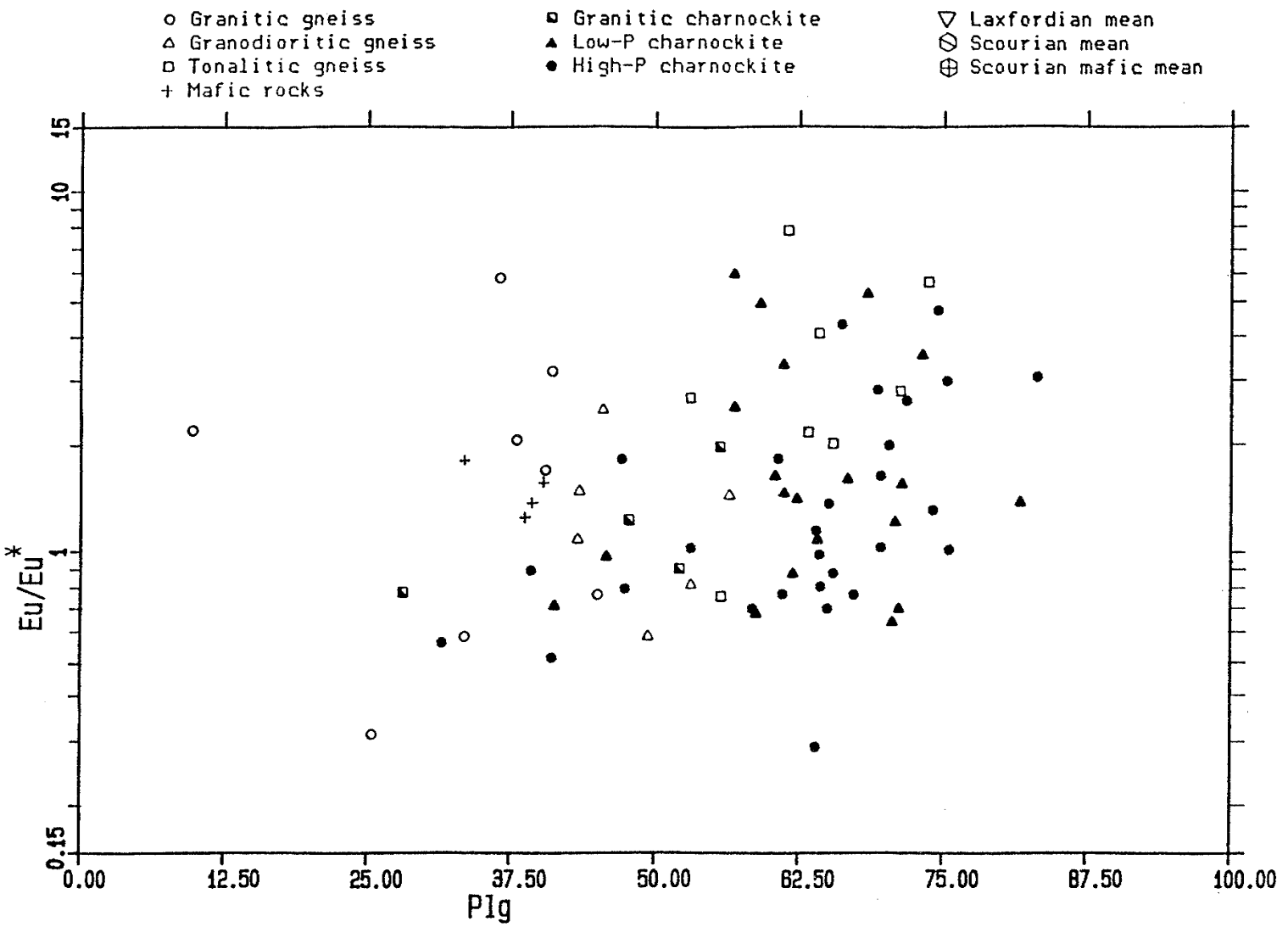

Fig. V-52. Eu/Eu* vs Plagioclase plot. Data from Appendix C.

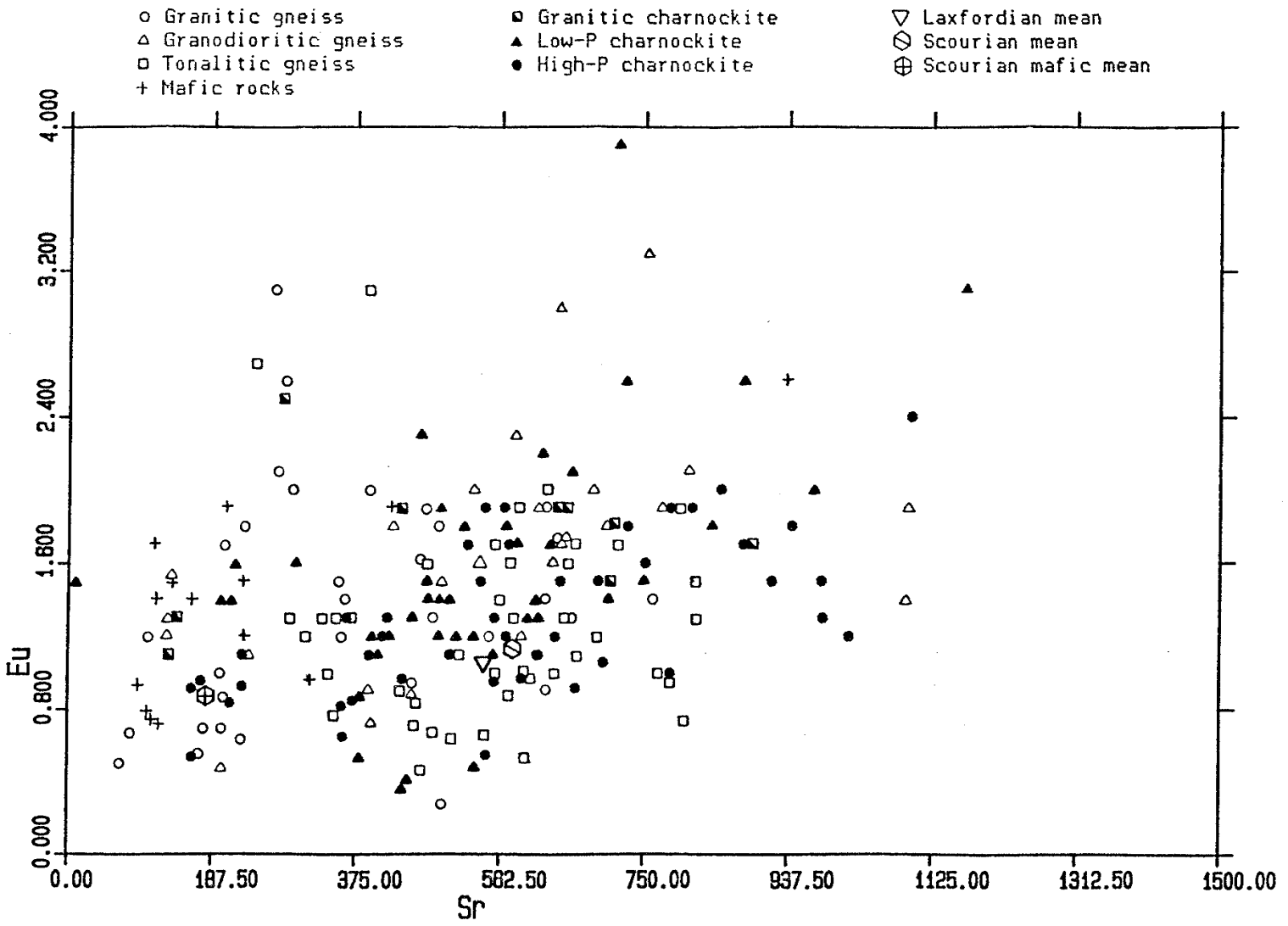

Fig. V-53. Eu vs Sr plot. Data from Appendix C.

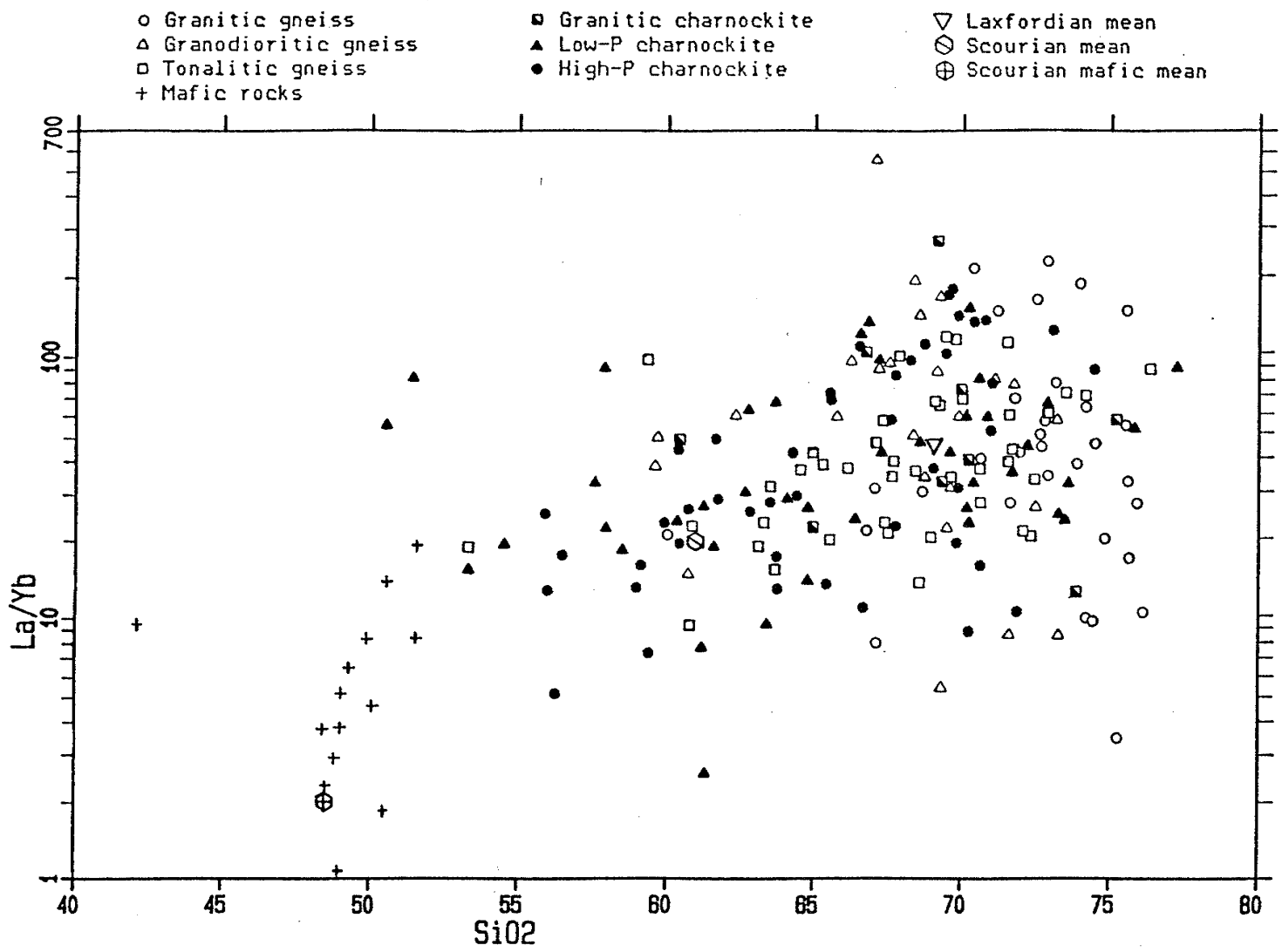

Fig. V-54. La/Yb vs SiO2 plot. Data from Appendix C.

reveals a dispersed pattern for many granitic gneisses but a rather consistent negative correlation for the tonalitic gneisses and charnockites (Fig. V-55). Many of the scattered granitic gneisses with high total REE and SiO2 are again from the northern area of the Gneiss Terrane. The relatively strong correlation between total REE and SiO2 for the tonalitic gneisses and low-P charnockites can be seen in Fig. V-56. The high-P charnockites have a similar but slightly more scattered trend. A rough negative correlation between the hREE and REE fractionation is evident in the south India tonalitic gneisses and charnockites (Fig. VI-5). For further discussion see Section VI.2.

V.8.8 Summary of REE results

The REE patterns of the south India gneisses and charnockites, with one major exception (the Gneiss Terrane and Transition Zone granitic gneisses), are in general consistent within each rock compositional classification and area. The silicic gneisses and charnockites from all terranes have somewhat lower total REE and and higher Eu/Eu* (+Eu anomalies) than their companion intermediate gneisses. Both silicic and intermediate gneisses have generally similar CeN/YbN ratios. This relationship between level of REE and magnitude and direction of the Eu anomaly is also observed in plots of tonalitic gneiss and charnockite samples, which exhibit a negative correlation between total REE and SiO2, and a positive correlation between Eu/Eu* and SiO2. Even though there is scatter, the pattern of tonalitic gneisses and charnockites on a La/Yb vs SiO2 plot suggests a rough positive correlation between REE fractionation and SiO2.

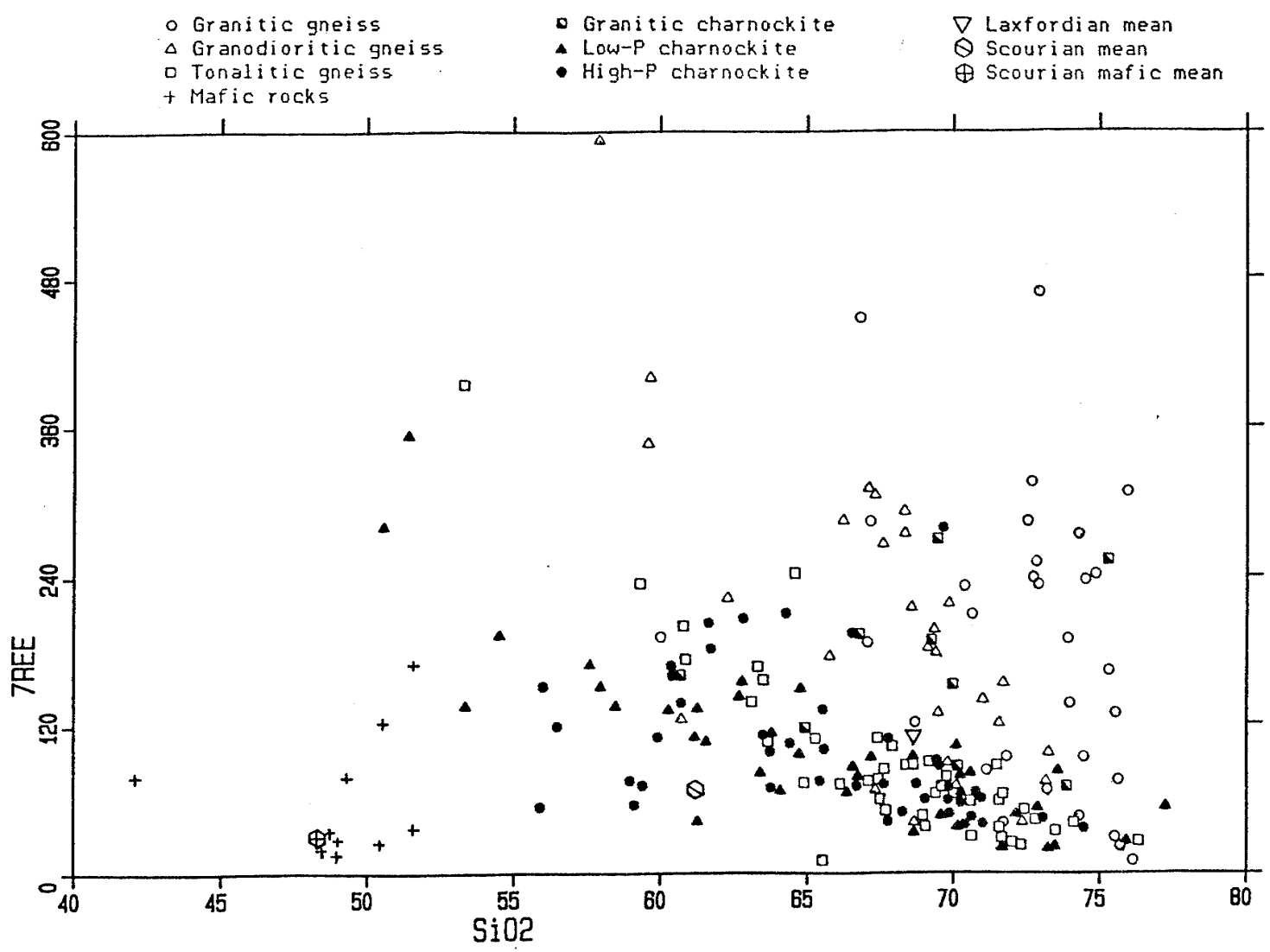

Fig. V-55. 7REE vs SiO2 plot; all samples. Data from Appendix C.

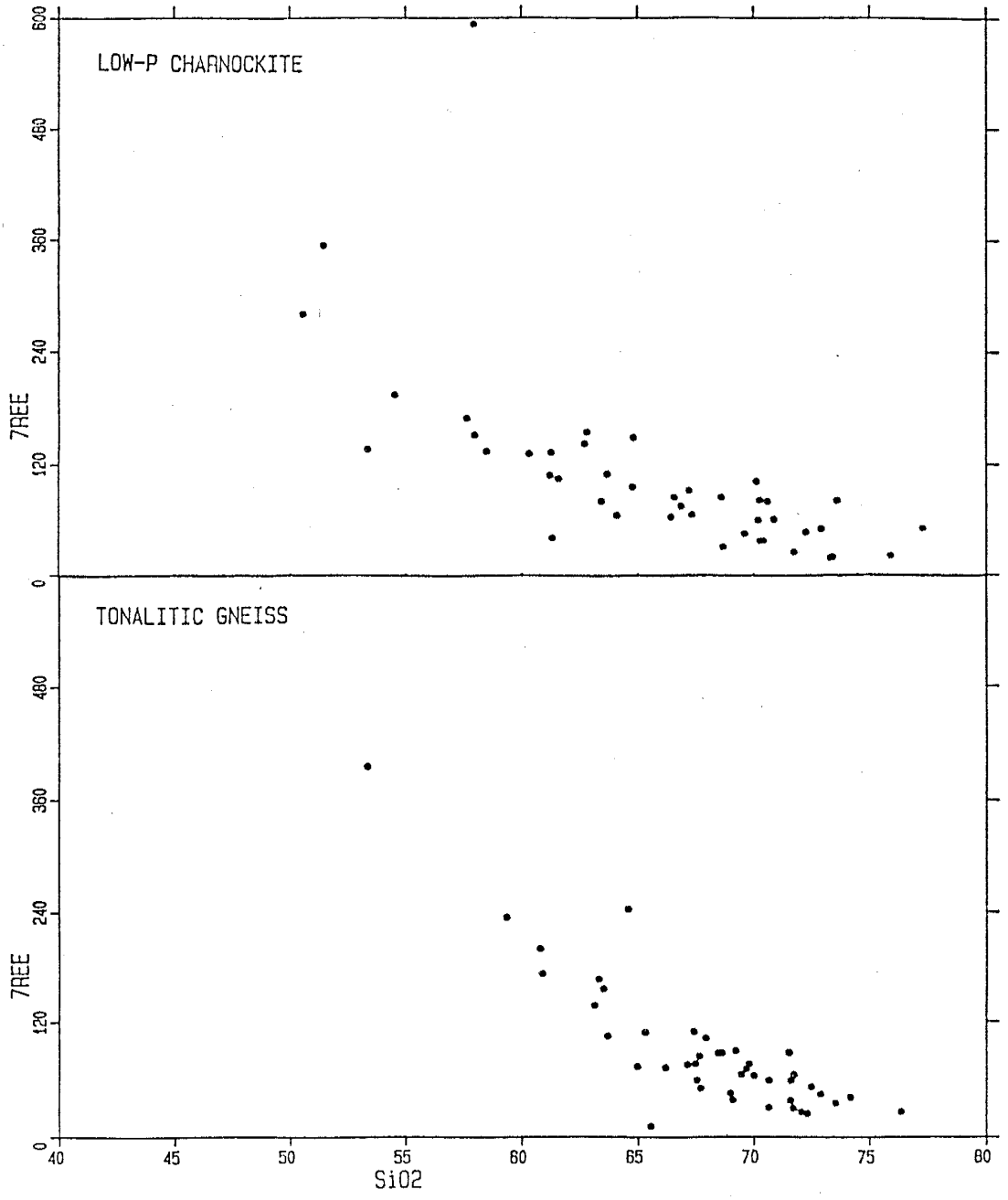

Fig. V-56. Total REE vs SiO2 plot; tonalitic gneiss and low-P charnockite. Data from Appendix C.

The major difference in the REE patterns of the south India gneisses is that between the high total-REE, -Eu anomaly, granitic gneisses of the Gneiss Terrane and the lower total-REE, +Eu anomaly, granitic gneisses of the Transition Zone. (A similar difference is apparent between the tonalitic gneisses of these two terranes, but there are insufficient samples to definitively characterize the tonalitic gneisses of the Gneiss Terrane.) The Gneiss Terrane granitic gneisses form scattered but generally distinct patterns on Eu/Eu*, Eu/Sm, SiO2, and Total REE plots, which illustrate their relatively high SiO2 and total REE, and low Eu/Eu*.

In the region southeast of Bangalore, the change in the granitic gneiss REE patterns is observed in samples from the Hosur-Kuppam-Krishnagiri area, near its boundary with the eastern Transition Zone area. The granitic gneisses of the eastern Transition Zone have relatively lower total REE and +Eu anomalies, similar to the patterns for the tonalitic gneisses from the same area. However, the few tonalitic, granodioritic, and granitic gneiss samples in the western Transition Zone (Kollegal-Malavalli-Kabbaldurga) have greater similarity to the Gneiss Terrane gneisses than to the eastern Transition Zone. This suggests that in the west, the Gneiss Terrane granites extend further south into the Transition Zone itself, and the distinction between low and high-grade granites in the western prograde amphibolite-facies granulite-facies transition becomes obscured. The low-P granitic charnockites roughly follow the same east-west variation of the granitic and granodioritic gneisses in the Transition Zone. There is also variation within the medium to high-

pressure granulite terrane. The Nilgiris represent one extreme of the range with less fractionated REE and generally -Eu anomalies, while the BR Hills and the eastern areas have higher depletion of the hREE and +Eu anomalies. There is relatively little change in the REE patterns with increasing metamorphic grade. However, there is a suggestion that the charnockites have a slightly higher Eu/Eu* ratio than the tonalitic gneiss.

In a comparison with other Archaean terranes, the tonalitic gneisses of the Transition Zone are similar to Ancient Gneiss Complex (Swaziland) and Laxfordian gneisses, which have depleted hREE and +Eu anomalies. The few samples of tonalitic gneiss from the Gneiss Terrane have steeper patterns than, but similar Eu anomalies to, the Uivak I gneisses. The high total REE, -Eu anomaly granites from the Gneiss Terrane are similar to other low-grade Archaean granites; however, the granitic gneisses from the eastern Transition Zone, with lower total REE and distinct +Eu anomalies, are similar to the high grade Scourian granites. Most low-P tonalitic charnockites from the Transition Zone are similar to Nuk gneisses. However, the low-P granitic charnockites, with high total REE, fractionated patterns, and undistinctive +Eu anomalies, are different from both the Transition Zone granitic gneisses and the high grade Scourian granitic charnockites, but similar to some of the granitic charnockites from Madras. Of the high-P tonalitic charnockites, the BR Hills, Salem, and the Shevaroy Hills have a close similarity to equivalent Scourian granulites. The Nilgiris and Bhavanisagar charnockites have less fractionated patterns and variable but typically -Eu anomalies.

V.9 Amphibolites and Mafic Granulites

The mafic samples from south India are divided into three subgroups: amphibolites from the Gneiss Terrane and Transition Zone, low-P mafic granulites from the Transition Zone, and high-P mafic granulites from the high-pressure granulite terrane. The south India results are compared with calculated mean values from representative Archaean terranes, which include mafic gneisses-gabbro from the Scourian (Pride and Muecke, 1980; Rollinson and Windley, 1980), basaltic amphibolites from Fiskenaesset (Weaver et al., 1982), Tryne mafic granulites from the East Antarctic Shield (Sheraton and Collerson, 1984), and basic granulites from Madras (Weaver et al., 1978; Weaver, 1980).

The mafic samples from south India are olivine normative (Appendix C), and fall within a relative tight grouping on an AFM diagram, with little or no Fe enrichment (Fig. V-57). On an Na2O-CaO-K2O diagram the mafic samples are also tightly grouped in the tholeiitic field (Fig. V-58). Representative mean values of mafic granulites from other Archaean terranes plot in the same field; an exception being the Group I basic granulites from Madras (Weaver et al., 1978), which show a strong Fe enrichment on the AFM diagram and low CaO/Na2O ratios on the Na2O-CaO-K2O diagram. The Al2O3-CaO-MgO diagram shows the south India samples forming a tight pattern in the tholeiite field (Bavington and Taylor, 1980).

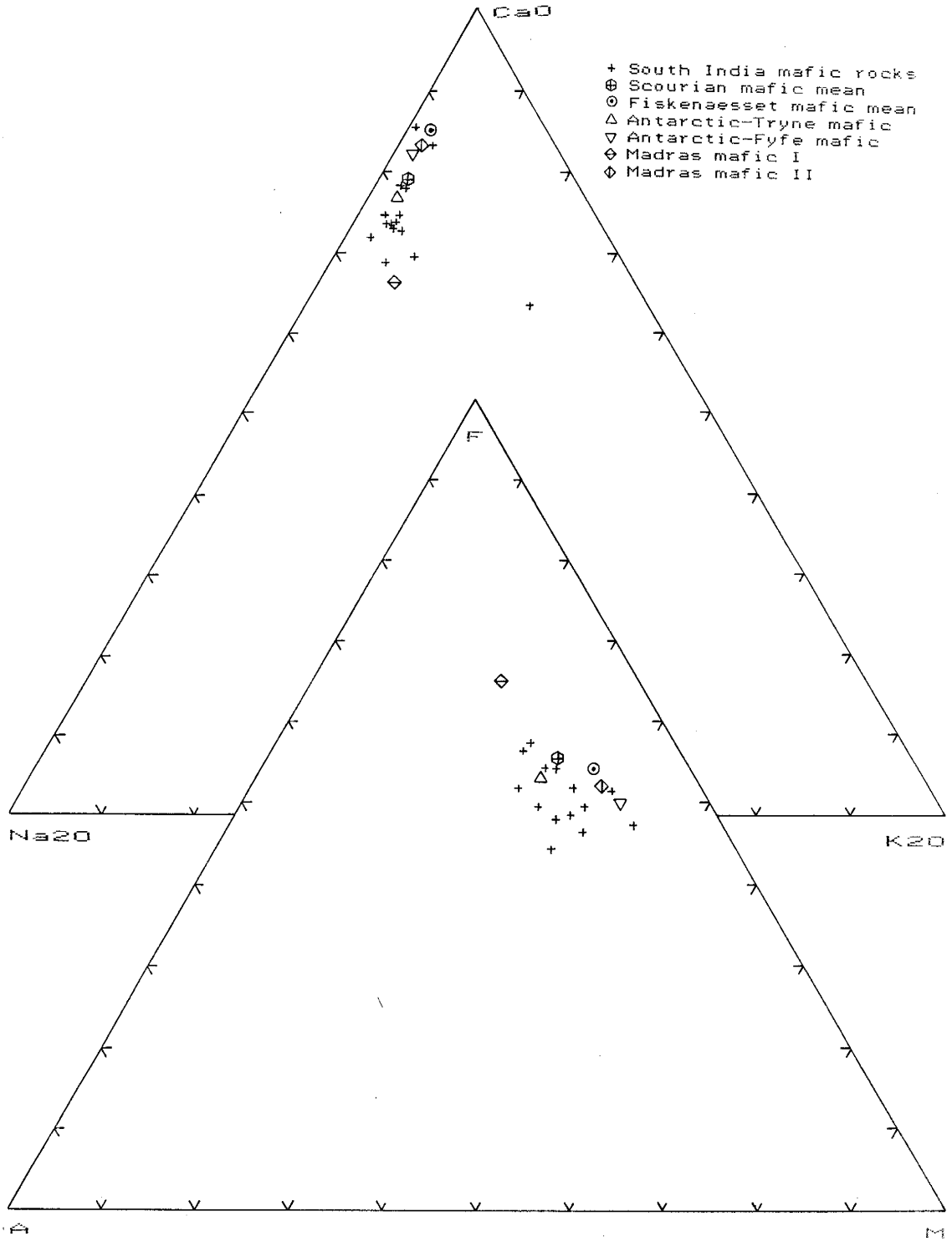

Fig. V-57. AFM and Na2O-CaO-K2O ternary diagrams for mafic rocks. Data from Appendix C.

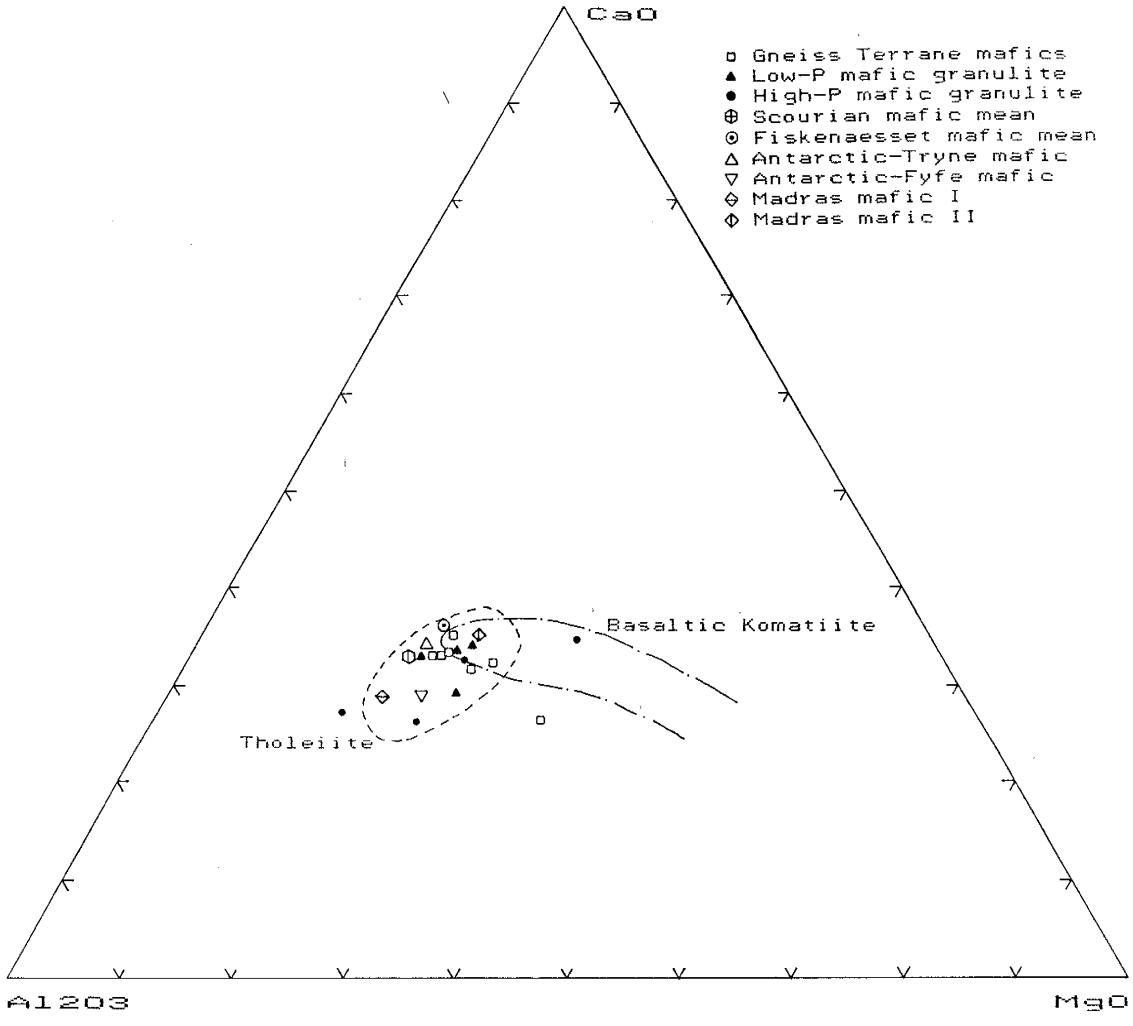

Fig. V-58. CaO-Al2O3-MgO ternary diagram. Data from Appendix C. Tholeiite and basaltic komatiite fields are from Bavington and Taylor (1980).

Element-area diagrams have been constructed to compare the results from south India with other Archaean terranes (Figs. V-60 to V-63). The south India samples are represented by two terrane-mean values: one for all mafic rocks (from both low and high-grade terranes), and another mean value for the high-grade terrane only. These results are compared to mean values from the Scourian, Fiskenaesset, the East Antarctic Shield, and Madras. The Madras samples were originally divided into two groups (I and II) by Weaver et al. (1978), because of their respective major and trace element characteristics, but later reclassified as a single group in a subsequent paper (Weaver, 1980). The original division is retained here because it is felt that these samples represent two distinct groups.

In general, there is a strong similarity between the south India high-P mafic granulites and mafic granulites from other Archaean terranes, with the exception, for some elements, of the Madras I samples (Fig. V-57). Of the south India samples, the high-P samples have a better correspondence to values from other Archaean terranes than the composite south India mean, which includes the lower grade amphibolite. For the major elements, the south India rocks have slightly less Al_2O_3 and CaO, somewhat more MgO and P_2O_5, and virtually similar abundances of the other major elements, than the overall values from the North Atlantic Craton, East Antarctic Shield, and Madras II. The Madras I mafics, however, have sharply higher TiO_2, Fe_2O_3, and P_2O_5, and lower MgO and CaO.

On SiO2 variation diagrams, the mafic rocks typically form a population distinct from the other gneisses; however, for Fe2O3, MgO, and CaO the mafic samples lie within the overall trend of the gneisses. For TiO2, Na2O, Al2O3, P2O5, and K2O relative to SiO2, the mafic samples define a different trend than the gneisses and the TiO2, Al2O3, and P2O5 values for the mafic rocks fall below the tonalite-granodiorite-granite fractionation line of decreasing abundance with decreasing SiO2 (Figs. V-12 to V-16, V-25). The mafic samples can thus not represent a TiO2-Al2O3 enriched cumulate (or residue) in equilibrium with the parent liquid that produced, by fractional crystallization or partial melting, the tonalite-granite samples. Decreasing P2O5 with increasing SiO2 suggests the removal of apatite in a fractionating cumulate; however as in the Scourian granulites, the P2O5 abundances in the mafic rocks are too low to represent this cumulate (Rollinson and Windley, 1980b).

The terrane-mean values for LIL elements and ratios of the mafic rocks have greater variability than the major elements (Figs V-60 to V-63). The south India mafic granulites have similar abundances of Rb, Sr, Ba, and Pb as the other Archaean terranes but higher Th; U appears high, though uncertain because of samples below the detection limit. The high-P mafics have a K/Rb value similar to that for Madras, but slightly less than the Scourian and slightly greater than the Fiskenaesset. The Rb/Sr ratio is appearantly lower in the south India samples; however, the values from other Archaean terranes generally have very high variability. It is interesting to note that the amphibolite-facies south India samples have higher K, Rb, and Sr

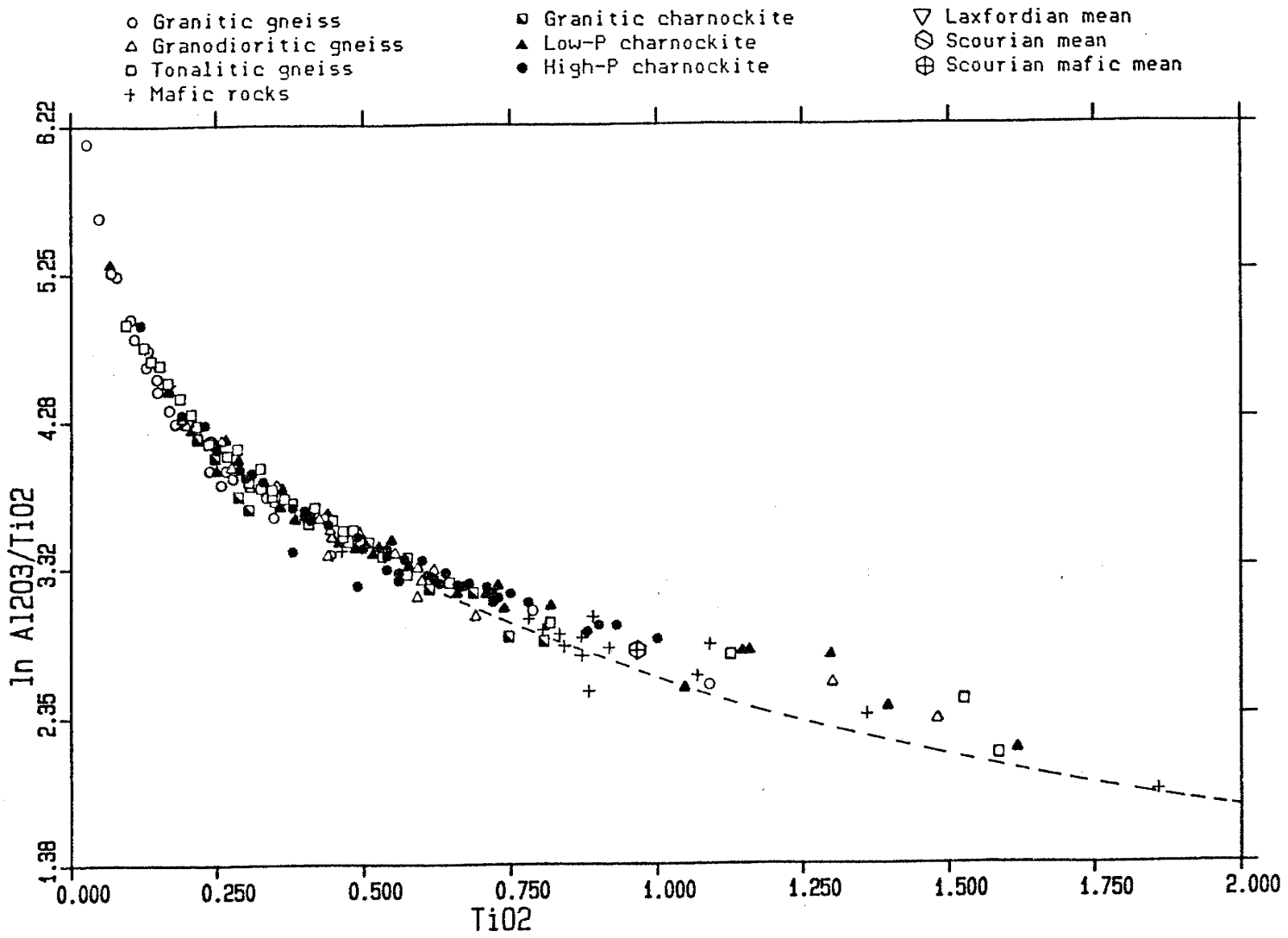

Fig. V-59. Al2O3/TiO2 vs TiO2 plot. Data from Appendix C. Fractional crystallization trend from Weaver et al., 1982.

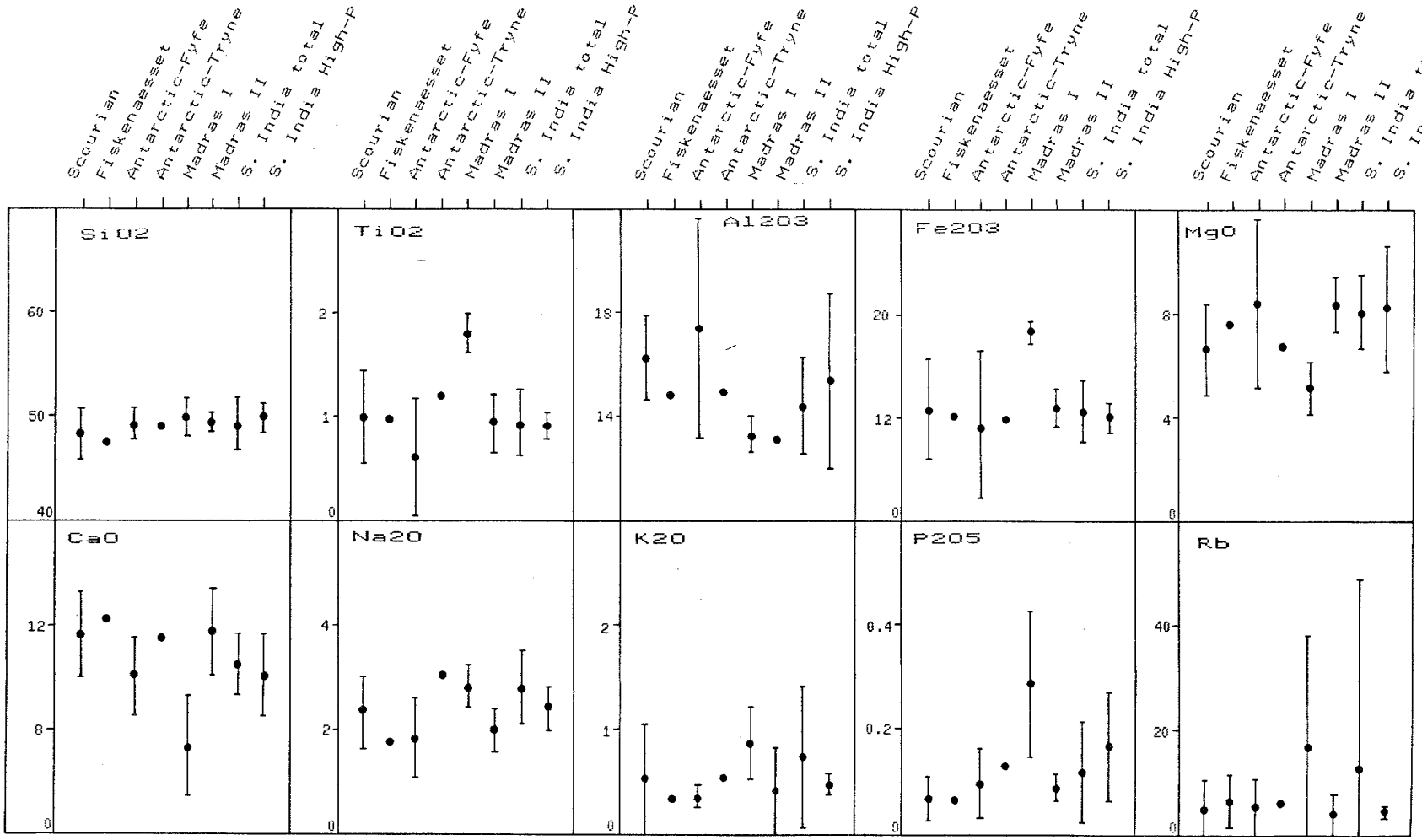

Fig. V-60. Mafic rocks element-area diagrams for SiO2, TiO2, Al2O3, Fe2O3, MgO, CaO, Na2O, K2O, P2O5, and Rb. (Data from Appendix C.)

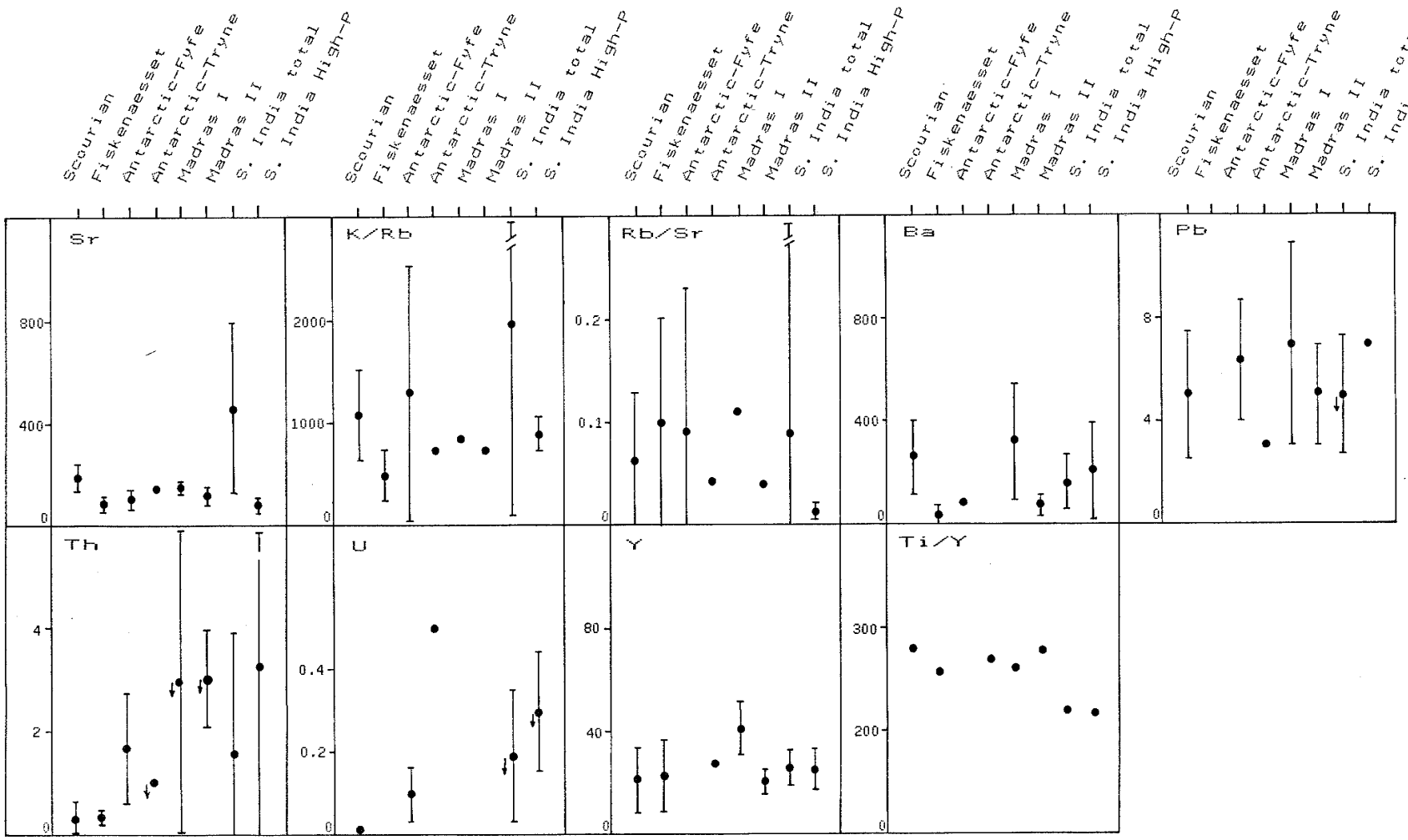

Fig. V-61. Mafic rocks element-area diagrams for Sr, K/Rb, Rb/Sr, Ba, Pb, Th, U, Y, and Ti/Y. (Data from Appendix C.)

concentrations, and apparently higher, but extrememly variable, K/Rb and Rb/Sr values than their companion higher pressure granulites. The mafic samples form distinct groups, or occupy the extremes of the range of the tonalitic-granodioritic-granitic gneisses, on %K - Rb, K/Rb -%K, K20 - Ba, and Ba - Sr diagrams (Figs. V-28 to V-31). In all of these diagrams, the mean value of the Scourian mafic granulites plots in the same field as the south India mafic samples. On the K/Rb - %K plot, the mafic rocks have broadly similar K/Rb values as the high-P charnockites but at lower K concentrations. This indicates that the same degree of Rb depletion relative to K appears to have occured in both groups.

For the HFS elements Y, Nb, Ta, Zr, and Hf there is again a strong correspondence between the high-P south India samples and the Scourian, Fiskenaesset, East Antarctica, and Madras II terranes (Fig. V-61, V-62). However, the Nb/Ta and Zr/Hf values are higher in south India (~=20, ~=40) than in the North Atlantic Craton (~=12, ~=32, respectively). The Madras I samples are again anomalous with high levels of Y, Nb, Zr, and Hf. In south India, Nb is higher in the lower pressure amphibolites than for the high-P granulites; however, the other incompatible elements Zr, Hf, and P are very similar as are Fe/Mg ratios suggesting that there cannot be significant fractionation between the lower and higher pressure mafic rocks. Though the south India Zr/Nb values are somewhat less than for the Scourian, the element-area plot has a lot of scatter (Fig. V-62). The Sc - Y diagram shows the south India mafic rocks have strongly elevated Sc relative to the trend of the other gneisses (Fig. VI-1). The partial

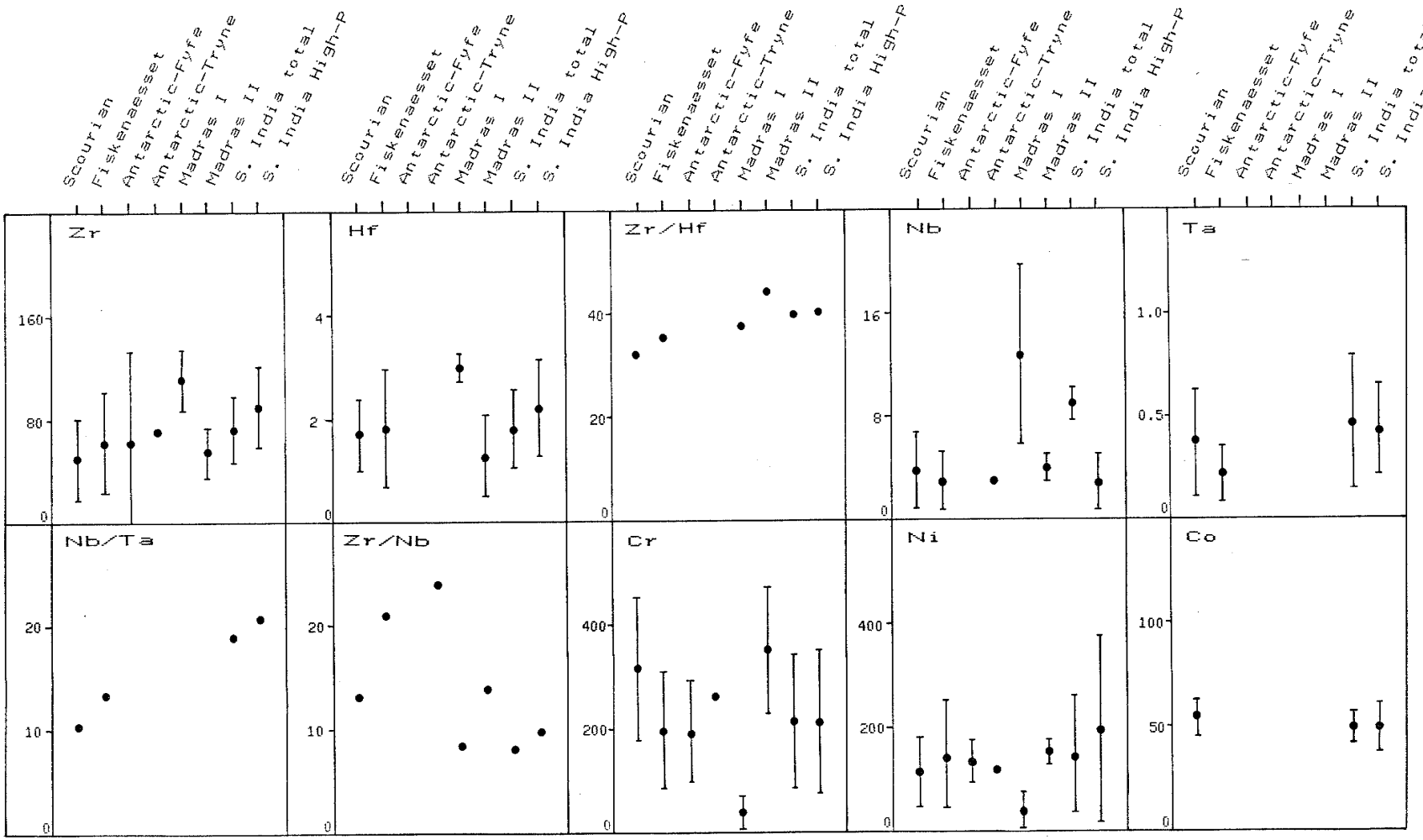

Fig. V-62. Mafic rocks element-area diagrams for Zr, Hf, Zr/Hf, Nb, Ta, Nb/Ta, Zr/Nb, Cr, Ni, and Co. (Data from Appendix C.)

melting trajectories for garnet, hornblende, and clinopyroxene indicate that the south India mafics are too enriched in Sc to produce the tonalitic gneisses and charnockite. However, on a Nb - TiO2 plot (Fig. VI-2), the mafic samples lie along the partial melting trajectory of hornblende relative to the tonalitic gneiss.

For the transition metals and ratios, Ni, Ni/Co, and Ni/Mg are higher in the high-P mafic granulites relative to the amphibolites and samples from other Archaean terranes (Fig. V-63). Cr/Mg and Fe/Mg are virtually identical for the south India terranes and similar to the Fiskenaesset and East Antarctica, but lower than the Scourian. Though the Fe/Mg and Ni/Cr values from Madras II are similar to south India and elsewhere, the Cr, Ni, and Cr/Mg values show a wide diversity (Fig. V-63). Zn has rather consistent concentrations (80-140 ppm) for all terranes; however, Zn/Co is slightly higher in south India relative to the Scourian.

Because of its relative immobility in metamorphic environments, Zr can be an effective monitor of fractionation in cogenetic rocks when plotted against elements that are also immobile during metamorphism (Pearce and Cann, 1973; Weaver et al., 1982). The incompatible HFS elements (Ti, P, Y) and LIL elements (K, Sr, Ba), and the compatible transition elements (Ni, Cr) are plotted against Zr and compared to similar plots of the Fiskenaesset basaltic amphibolites (Weaver et al., 1982) (Fig. V-64, V-65). Though there is some scatter (especially for samples 435a and 487-1), the south India results in general define linear fractionation patterns of increasing HFS element values vs increasing Zr, which parallel the fields

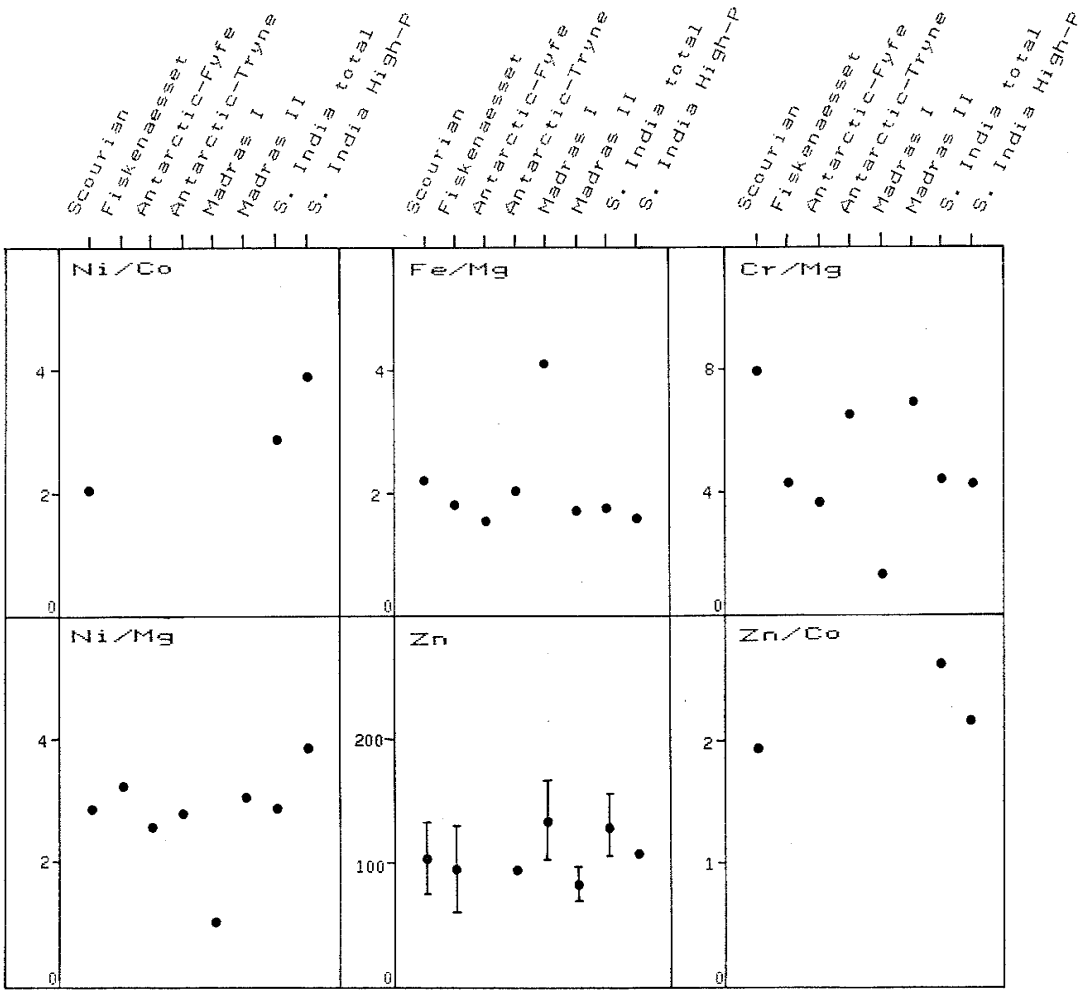

Fig. V-63. Mafic rocks element-area diagrams for Ni/Co, Fe/Mg, Cr/Mg, Ni/Mg, Zn, Zn/Co. (Data from Appendix C.)

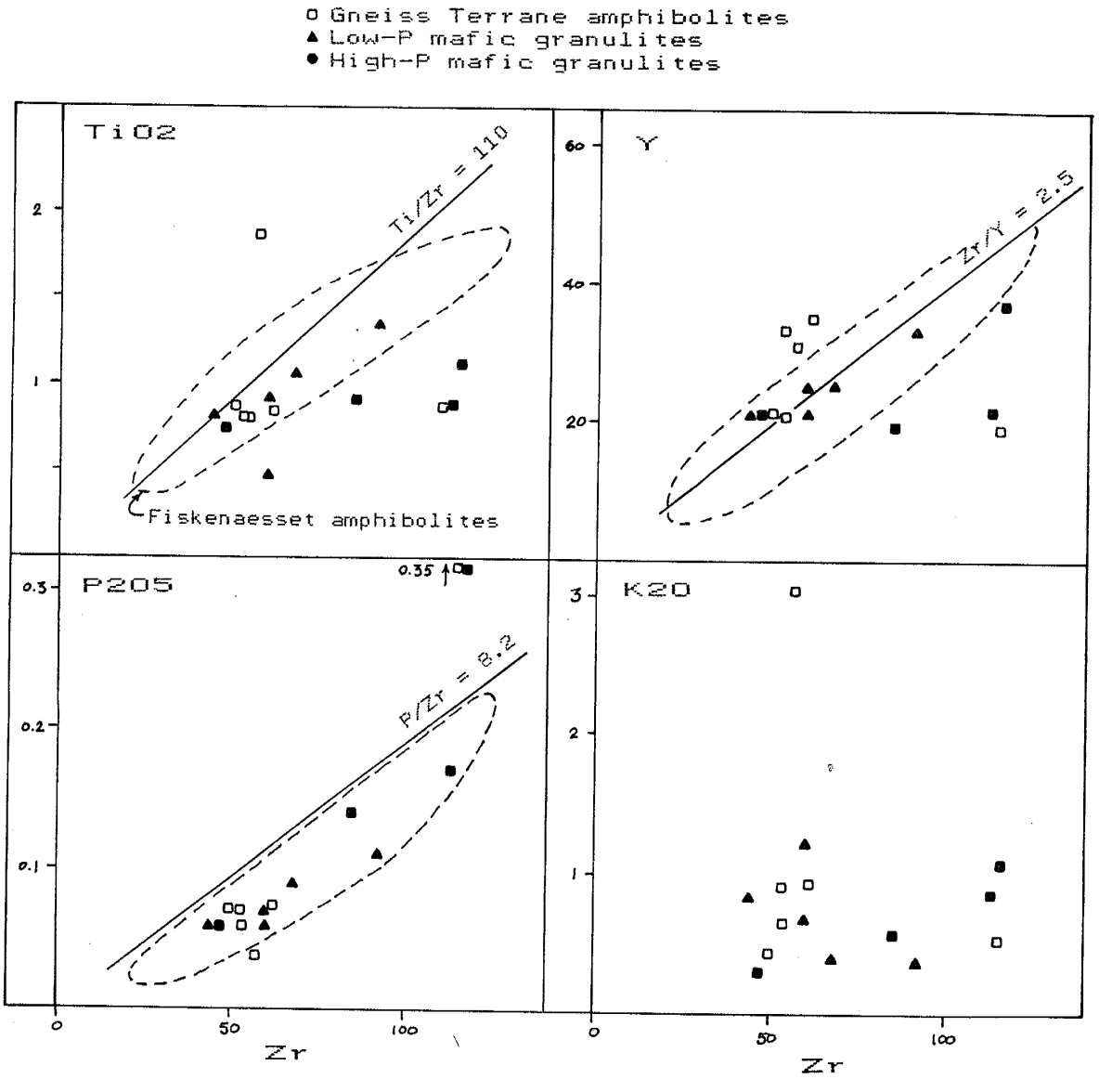

Fig. V-64. TiO2, P2O5, Y, and K2O vs Zr plots of south India mafic rocks. Fields of Fiskenaesset amphibolites from Weaver et al. (1982).

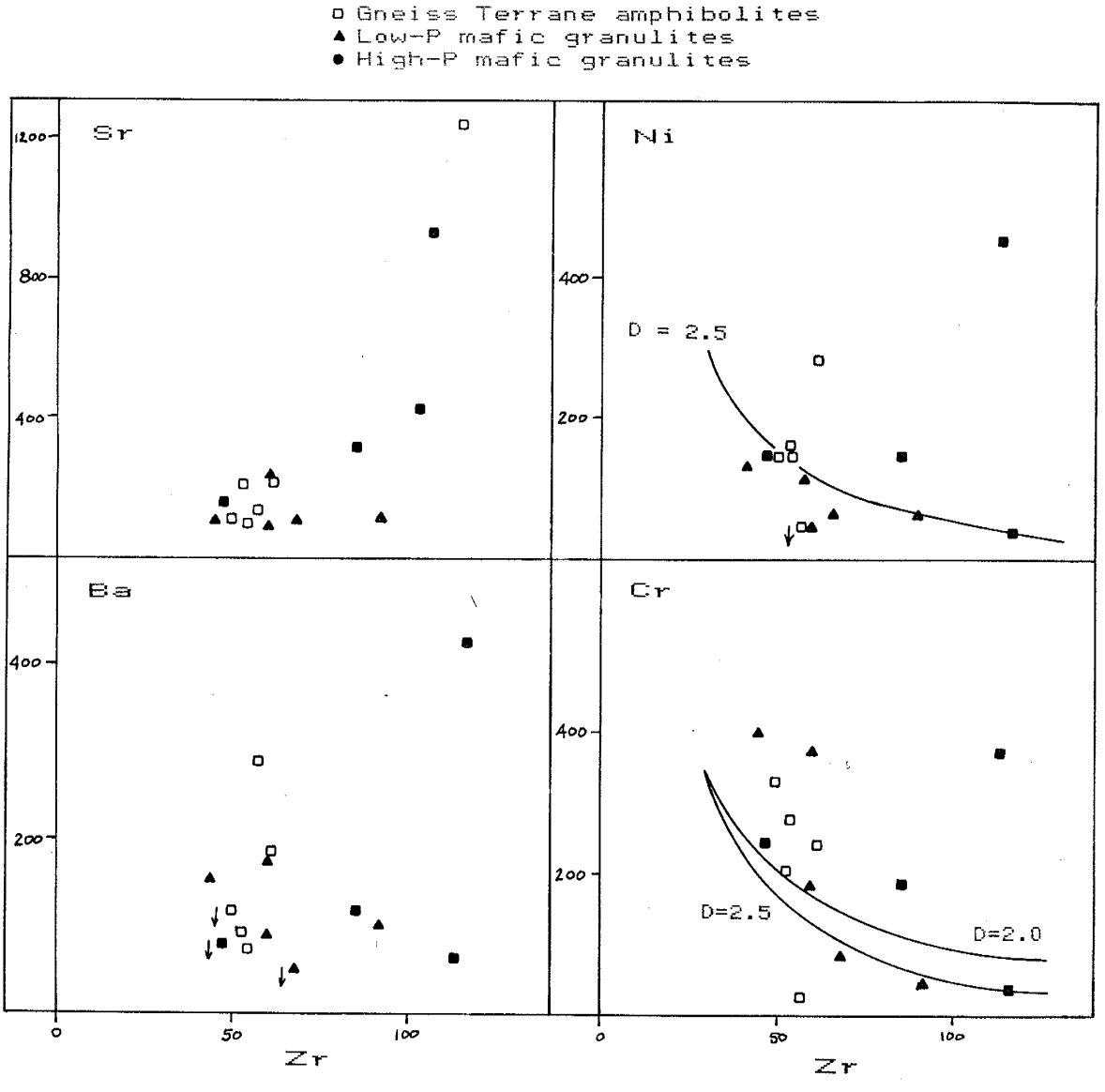

Fig. V-65. Sr, Ba, Ni, and Cr vs Zr plots of south India mafic rocks. Fractional crystallization trends for bulk D=2.5 and D=2.0 after Weaver et al. (1982).

representing the Fiskenaesset samples (Fig. V-64). However, the LIL elements - Zr plots (Figs. V-60, V-61) show broad scatter, also similar to the Fiskenaesset results (Weaver et al., 1982), which indicates that K, Sr, and Ba do not fall along a fractionation trend and may have been mobilized during later metamorphic events. The compatible-element vs Zr plots show generally decreasing Ni and Cr values with increasing Zr (Fig. V-65). Fraction trends for bulk distribution coefficients D=2.0 and D=2.5 (Weaver et al., 1982) are shown for comparison. As is noted above for the element-area plots, the HFS and transition element vs Zr plots do not show any consistent fractionation relationship between the lower and higher pressure mafic rocks.

However, on a comparison of REE plots the amphibolites have somewhat higher CeN/YbN (1.7-5.6) than the low-P mafic granulites (CeN/YbN=0.9-4) and most of the high-P mafic granulites (CeN/YbN~=2.2) (Fig. V-66). The Eu/Eu* values for the amphibolites and high-P granulites are variably 1, <1, and >1, while for the low-P granulites Eu/Eu* ~>1. The Scourian and Fiskenaesset have REE patterns that are relatively flat (CeN/Yb~=1.9,0.8, respectively), and the Scourian REE plots have small but consistent -Eu anomalies. The Madras samples have generally flat patterns but cover a large range of total REE. The high total REE samples (Madras I) have significant -Eu anomalies; the lower total REE samples (Madras II) have negative or no Eu anomalies and compare more favorably with the south Indian mafic granulites (Fig. V-66).

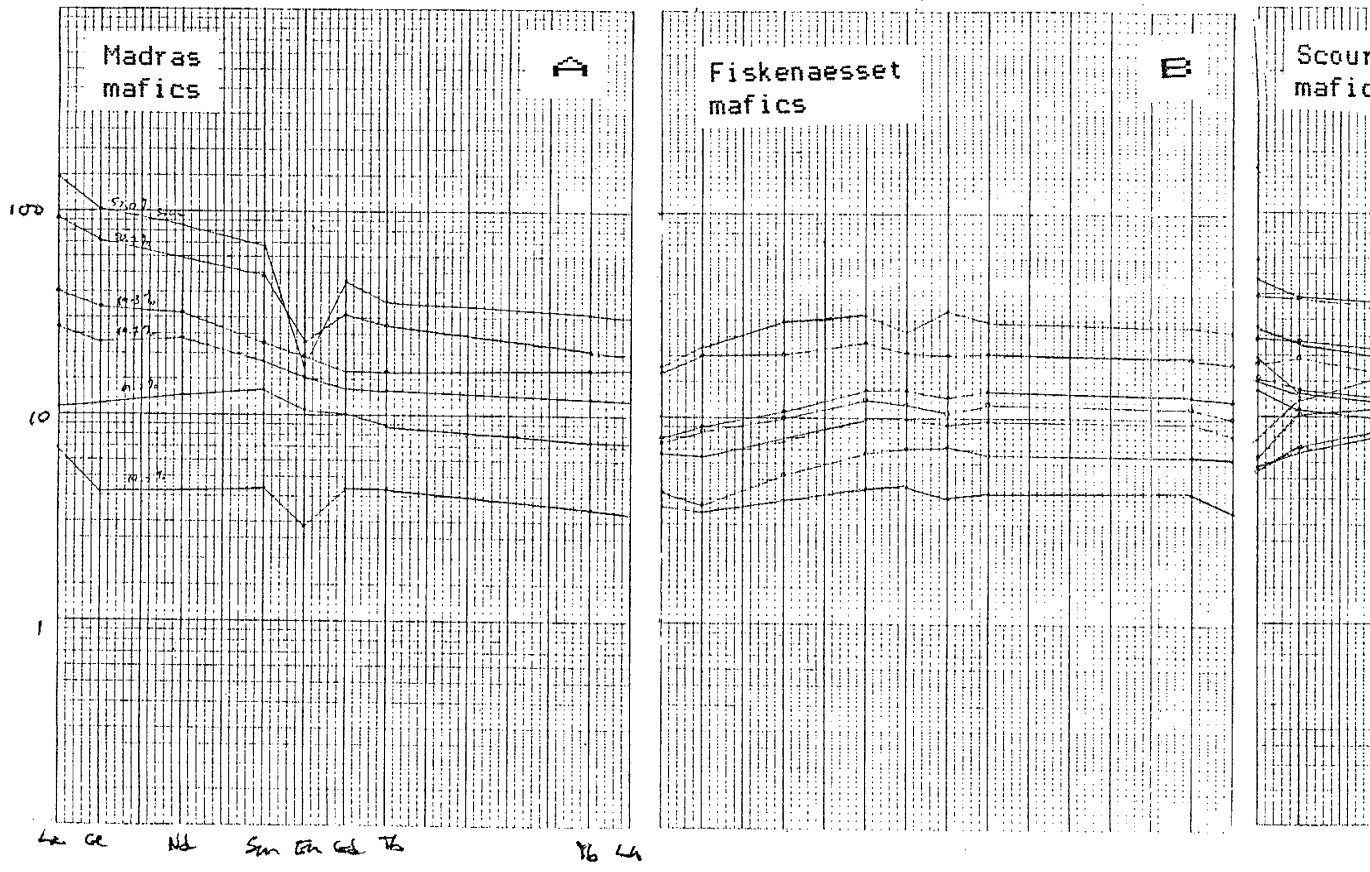

Fig. V-

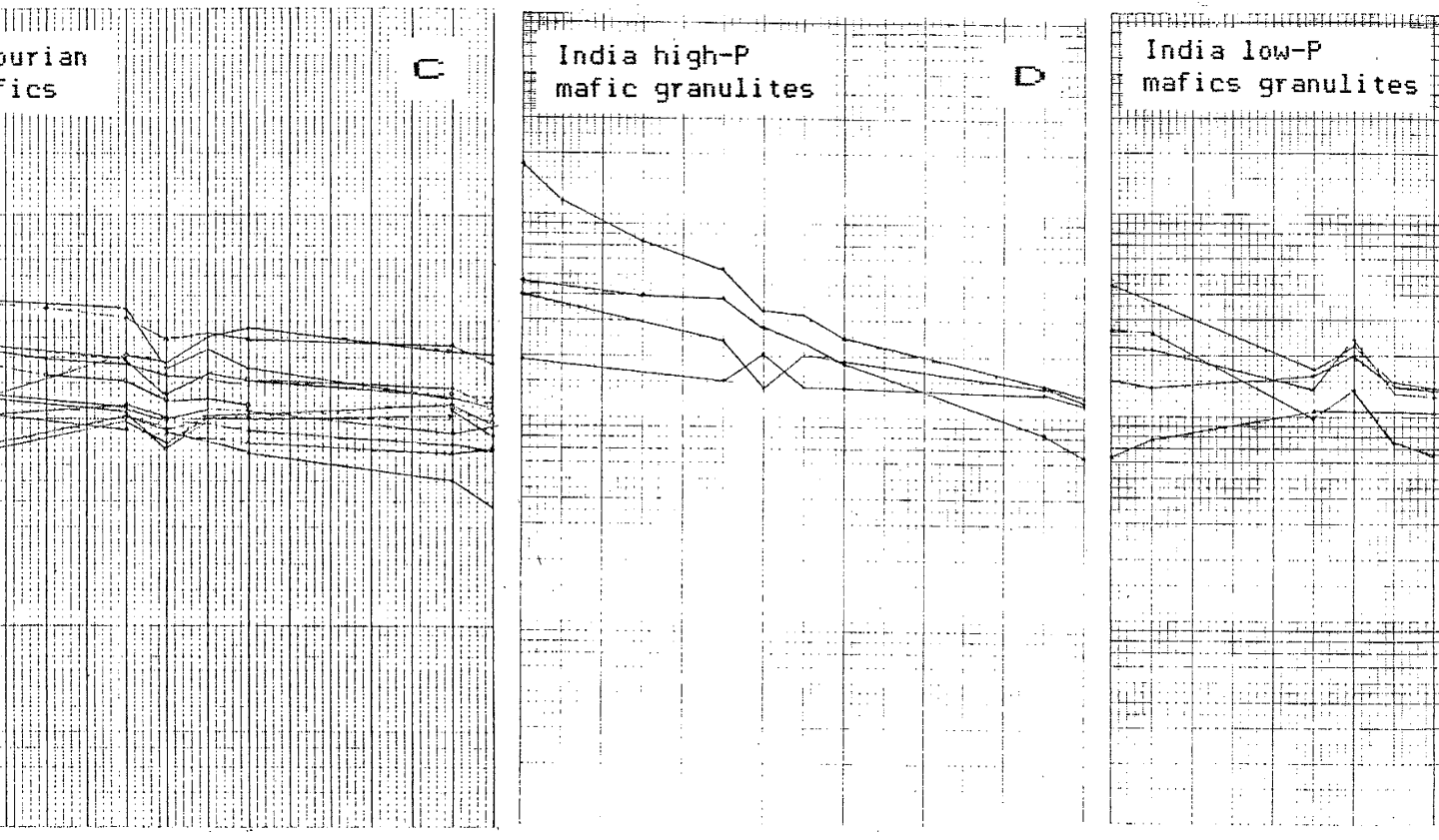

V-66. REE plots of mafic rocks. Data in Appendix C.

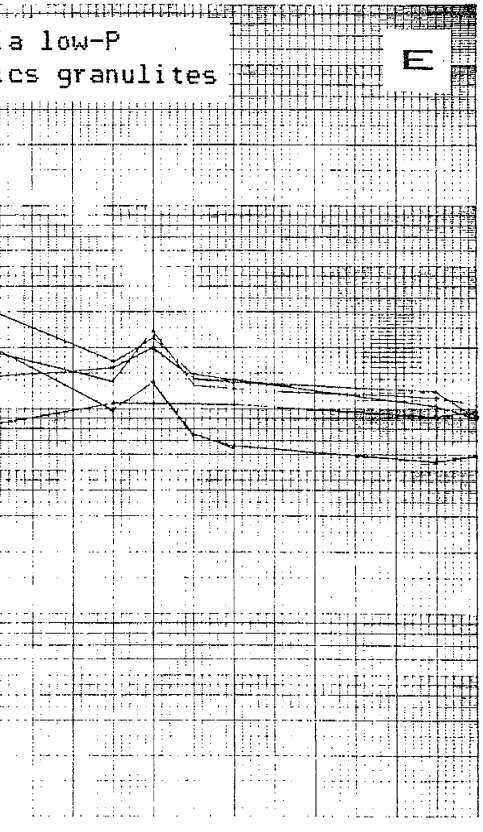

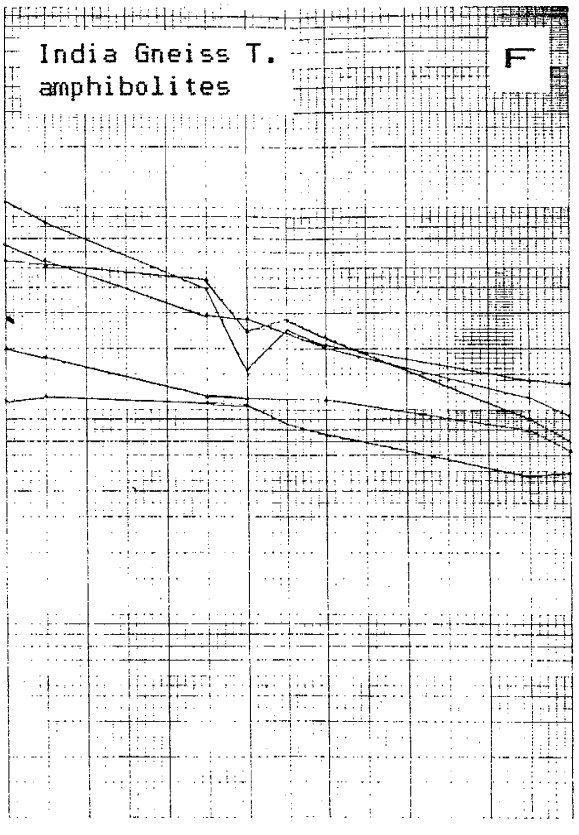

c.

On a YN - CeN/Yn plot, the mafic samples though somewhat scattered have high YN and low CeN/YN relative to the gneisses, and generally lie along the partial melting-fractional crystallization trend of garnet and hornblende relative to the other gneisses (Fig. VI-5). The Eu/Eu* values are similar to the tonalitic (intermediate) charnockites, but at lower SiO2 (Fig. V-50). On an Eu/Eu* - SmN diagram, the mafics are loosely grouped near the center of the other gneisses and could in a general way be related to these gneisses by partial melting or fractional crystallization; similar relationships can be seen on the Eu/Sm - Sm plot (Figs. VI-3, VI-4). The amphibolites and mafic granulites can also be the source of the tonalitic gneisses and charnockites through partial melting-fractional crystallization of hornblende, garnet, and pyroxene as shown on the CeN/TnN - TbN/YbN plot (Fig. VI-6).

In studying the Fiskenaesset basaltic amphibolites, Weaver et al. (1980) concluded that the fractional crystallization of a plagioclase-rich cumulate was the dominant process in the evolution of the amphibolites, and a model of a crystal fractionation trend of Al2O3/TiO2 vs TiO2 was calculated for the Fiskenaesset samples. This fractionation trend is superimposed on the south India samples and the closeness of fit suggests that fractional crystallization of a plagioclase-rich (~=50%) cumulate may also have produced the south India amphibolite-mafic granulite suite (Fig. V-59).

A partial melting-fractional crystallization relationship between the mafic rocks and the south India gneisses is allowed by the fractionation of 1) Fe_2O_3, MgO, and CaO relative to SiO_2, 2) Al_2O_3/TiO_2 and Nb relative to TiO_2, and 3) the REE. However, the depletion of TiO_2, Al_2O_3, and P_2O_5 relative to SiO_2 in the mafic rocks, and the high Sc abundances relative to Y indicate that partial melting-fractional crystallization relationships did not exist between the amphibolite-mafic granulite suite and the gneisses.

V.10 Prograde and Retrograde Reactions

The field geology, sampling, and analytical results discussed above have been for the most part concerned with terrane-wide similarities and differences. In order to better study small scale changes that occur during prograde amphibolite to granulite-grade metamorphism, paired samples taken from across the margins of a prograde transition (reaction) were analysed and compared to sample pairs from an analogous retrograde granulite to amphibolite transition (reaction). Samples representing the prograde transition from gneiss to charnockite were collected at Kabbaldurga, Dharmapuri, and Tiruvannamalli (Fig. II-3). Retrograde samples were collected at Bhavanisagar, Binakanahalli in the southern Biligirirangan Hills (BR Hills), and at Salem, south of the Shevaroy Hills, and lie on or near the Bhavani-Moyar shear zone as described by Drury and Holt (1980). All sample sites are situated in actively worked stone quarries, which permit examination of the gneiss-charnockite transition on fresh surfaces and over relatively large areas.

V.10.1 Field Relationships

In areas of incipient charnockitization in the prograde Transition Zone the charnockite appears as greasy, discontinuous patches in gneiss, with the gneiss-charnockite contact diffuse over 1-3 cm. The patches grow into continuous branches or masses as the degree of charnockitization increases. Although charnockite cross-cuts the fabric of the gneisses, in its initial stages of development it appears to grow preferentially along foliation in the more mafic portions of the gneisses. In retrograde areas, the gneiss initially develops as bleached areas in the charnockites with a diffuse 1-3 cm boundary; as retrogression procedes, the narrow zones grow into islands of gneiss within the charnockite. Bleaching spreads locally along foliation, but at a larger scale it is controlled by thin fractures. Similar retrograde bleaching controlled by thin fractures in greenish charnockite from southern Norway is reported by Field and Roheim (1980). The gneisses in the retrograde areas appear more homogeneous than those of the prograde Transition Zone, and migmatites and granitic material are not as common. (For a more detailed discription of field relationships see Sections III.2 and III.4.)

V.10.2 Sampling and Petrography

Gneiss and charnockite samples were collected from fresh exposures in which the gneiss-charnockite relationship is clear. Care was taken to sample only the homogeneous portions of the exposure. Gneiss-charnockite pairs were collected at distances of about 5-10 cm from each other across the boundary. Samples 484-1A,-1B,-1C were cut

from a single piece at intervals of about 1.5 cm. Samples were homogeneous and of medium-grain size. Except for 484-1A,-1B,-1C, sample size was 200-250 g of which 75-100 g was powdered and homogeneized. Powders of samples 484-1A,B,C were 50-60 g each.

Gneiss-charnockite pairs from prograde Transition Zone areas generally contain quartz, plagioclase (An 17-27), K-feldspar, and biotite. Hornblende is present in some gneisses and charnockites, and ortho and/or clinopyroxene are characteristic of the charnockites. Common accessory minerals are opaques (mostly magnetite), apatite, zircon, and minor carbonate and/or chlorite that occurs chiefly as tiny veinlets in plagioclase. Twinning in plagioclase is frequently absent and antiperthite is observed but uncommon. K-feldspar is often perthitic. Ortho and clinopyroxene in the charnockites appear to develop without a gradual transition as it is difficult in thin section to find unequivocal evidence of the transformation of hornblende and/or biotite into pyroxene. However, in some charnockite samples, pyroxene develops along cleavage planes in hornblende. A common feature is a late, minor retrogressive overprinting in which pale brown biotite forms small patches or stains along cleavage planes and margins of pyroxenes.

The retrograde areas are all located in the medium to high-pressure granulite-facies terrane. Charnockite-gneiss pairs from the retrograde areas are generally similar in mineral content to prograde pairs. However, K-feldspar is absent, except as antiperthite in plagioclase, garnet occurs as an accessory mineral, and the An content of plagioclase (An 27-38) is higher than that of samples from prograde

sites. Mylonitic, myrmekitic, and mortar textures, as well as rotated plagioclase augen are common in most samples and quartz grains typically exhibit undulose extinction. Carbonate is present as thin veinlets within plagioclase, as interstitial fillings along mylonitic zones, and as late-stage veins cross-cutting the foliation. Biotite develops as thin, bent and broken laths within and along mylonitic zones, as pale brown reaction rims on hornblende and pyroxene, and as patches along cleavage planes in pyroxenes. Reaction rims of pale green amphibole, cummingtonite, and symplectic quartz are ubiquitous on hornblende and pyroxene.

V.10.3 Geochemical Results

In order to portray chemical changes between charnockite-gneiss pairs, element abundances and selected element ratios are normalized to the assumed protolith of the pair, either to coexisting gneiss (for prograde pairs) or to coexisting charnockite (for retrograde pairs). At a few sites where more than one charnockite or gneiss sample was collected (KD III, S I, S III, and BS), sample pair ratios were calculated using both charnockite or gneiss samples relative to their coexisting sample, in order to estimate intra-site variability.

Normalizing element abundances and element ratios increases the calculated error of the resulting value approximately by the addition of the errors of its constituents. Thus, the error associated with the element abundance of Th is <+-8%; the error for the gneiss-charnockite ratio of Th is about +-16%, and the error for

the gneiss-charnockite ratio for Th/U is about +-32%. Sample pair ratios are plotted on a log scale (Figs. V-67 to V-70). A value of 1.0 indicates no chemical change within a sample pair; a value greater than 1.0 indicates a gain of that element or element ratio in the derivative rock relative to the protolith, a value of less than 1.0, a loss of that element. The distance that the sample pair ratio lies above or below 1.0 on the log scale is a measure of the relative enrichment or depletion in the derivative rock. Confidence intervals are constructed using a non-parametric statistical method, the Wilcoxon signed-rank test for paired comparisons (Bhattacharyya and Johnson, 1977).

Non-parametric statistics are useful when the sample size is small and a normal population distribution cannot be assumed. The confidence interval is based upon the ranking of sample pairs obtained by calculating the differences between paired samples, in this study the difference between the logarithm of the element abundance in the derivative rock and the logarithm of element abundance in the protolith for each sample pair: ln(D conc.) - ln(P conc.) = ln (D conc./P conc.), which is the normalized ratio of the sample pair plotted on the log scale. These differences are ranked by magnitude, from the most enriched to the most depleted, and the confidence interval is calculated based on the number of samples using the appropriate Wilcoxon signed-rank tables (Battacharyya and Johnson, 1977).

Granulite-facies/amphibolite-facies terrane-mean element ratios for south India are compared to representative terrane-mean ratios from Labrador (Bridgewater and Collerson, 1976), Nuk gneisses (Wells, 1979), and the Lewisian (Laxfordian: Tarney, 1976; Weaver and Tarney, 1981; Scourian: Sheraton, 1970) in Fig. V-67a, V-67b. The south India samples are presented as two ratios: low-P charnockite normalized to amphibolite-facies gneiss, and high-P charnockites also normalized to amphibolite-facies gneiss. The diagram shows that in general there are increases in TiO2, MnO, MgO, CaO, Cr, Ni, K/Rb, Cr/Mg, Ni/Mg, and K/Th, and decreases in SiO2, K2O, Rb, Cs, Th, U, Pb, K/Ba, Rb/Ce/, and Fe/Mg in the higher-grade terrane-mean values relative to the amphibolite-facies (Fig. V-67a, V-67b). However, as noted earlier (Sections V.3 to V.6), the major factor in these changes, with the exception of Rb, Cs, Th, U, and possibly K and Pb, is the predominance of the tonalitic component, and lower granitic component, in the high-grade terrane-mean value relative to the low-grade terrane-mean.

For the study of chemical changes at the reaction margins, prograde and retrograde pairs sampled across the margin were tested for major elements, 25 trace elements, and over 50 element ratios; the results for many elements and ratios are displayed in Figs. V-68a, V-68b. Significant differences in element abundances or element ratios are assumed to exist only when the ~> 90% confidence interval about the median value of charnockite/gneiss or gneiss/charnockite ratios is >1 or <1. Changes defined in this manner are illustrated in Figs. V-69, V-70.

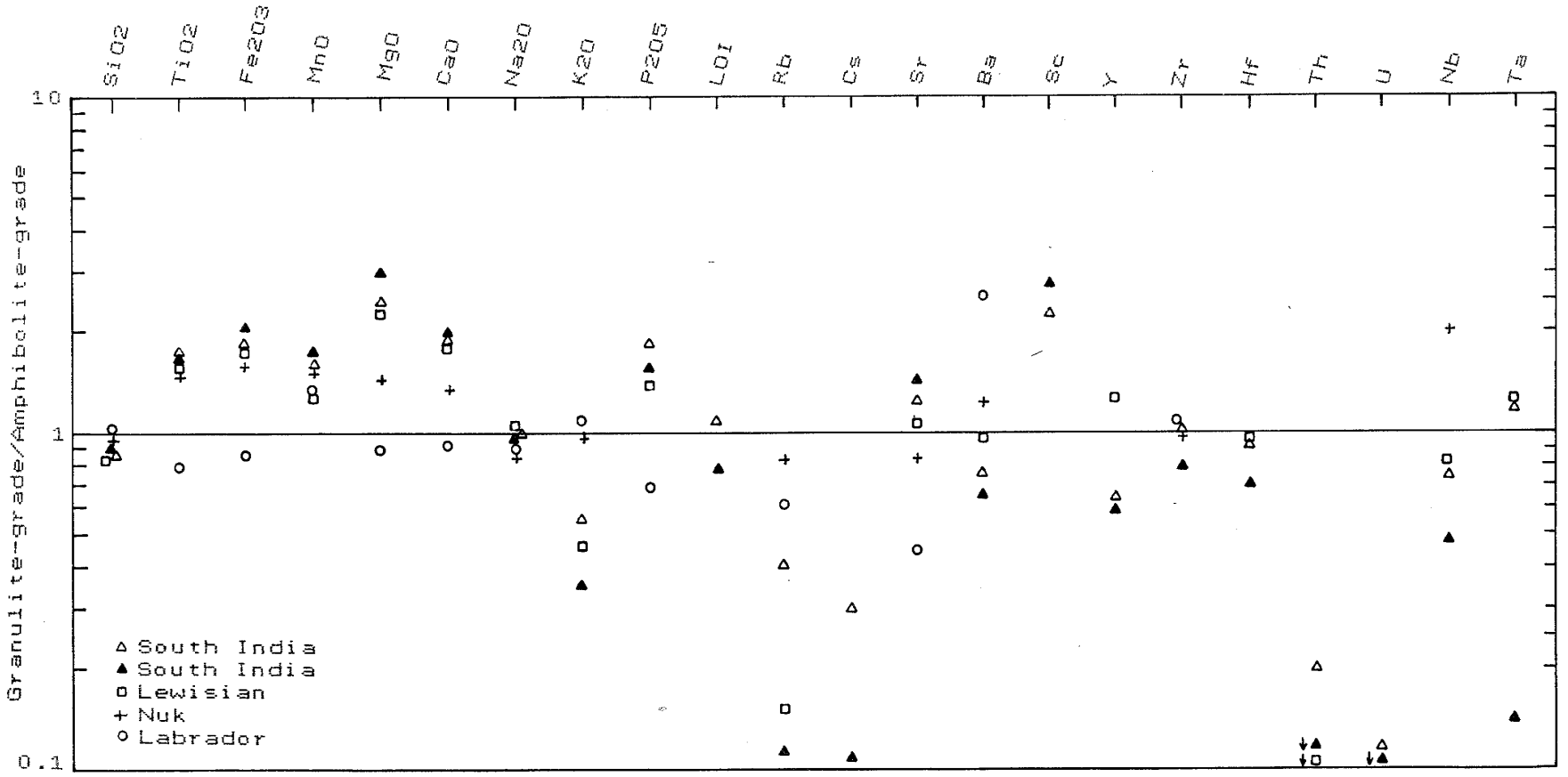

Fig. V-67a. Normalized element distributions for prograde amphibolite and granulite-grade rocks from south India and other Archaean terranes. A value of 1.0 indicates no change in abundance, while values greater or less that 1.0 indicate additions or losses, respectively. For south India, △ = low-P charnockite/gneiss; ▲ = high-P charnockite/gneiss.

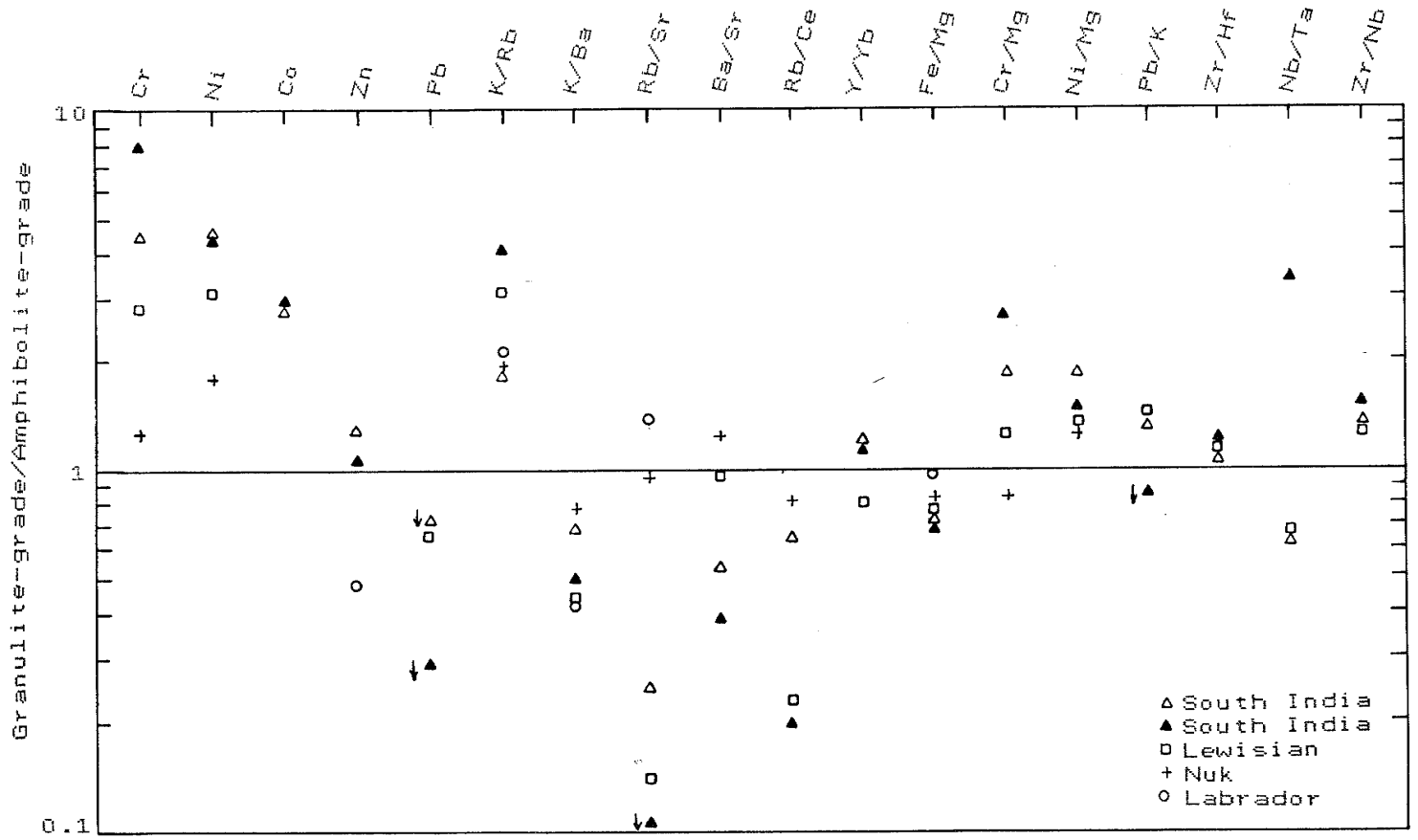

Fig. V-67b. Normalized element distributions for prograde amphibolite and granulite-grade rocks from south India and other Archaean terranes. A value of 1.0 indicates no change in abundance, while values greater or less that 1.0 indicate additions or losses, respectively. For south India, △ = low-P charnockite/gneiss; ▲ = high-P charnockite/gneiss.

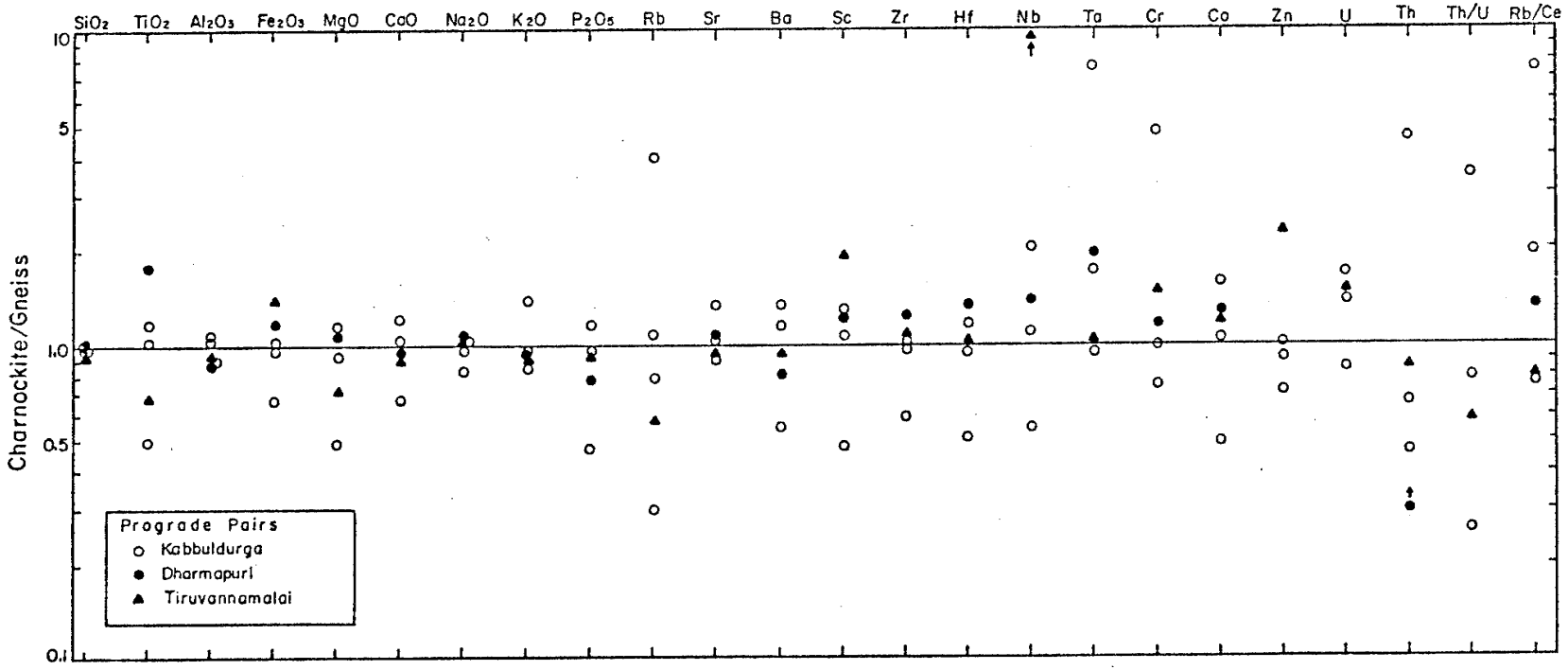

Fig. V-68a. Normalized element distributions in prograde charnockite-gneiss pairs from south India. A value of 1.0 indicates no change in element concentration, while values greater or less than 1.0 indicate additions or losses, respectively.

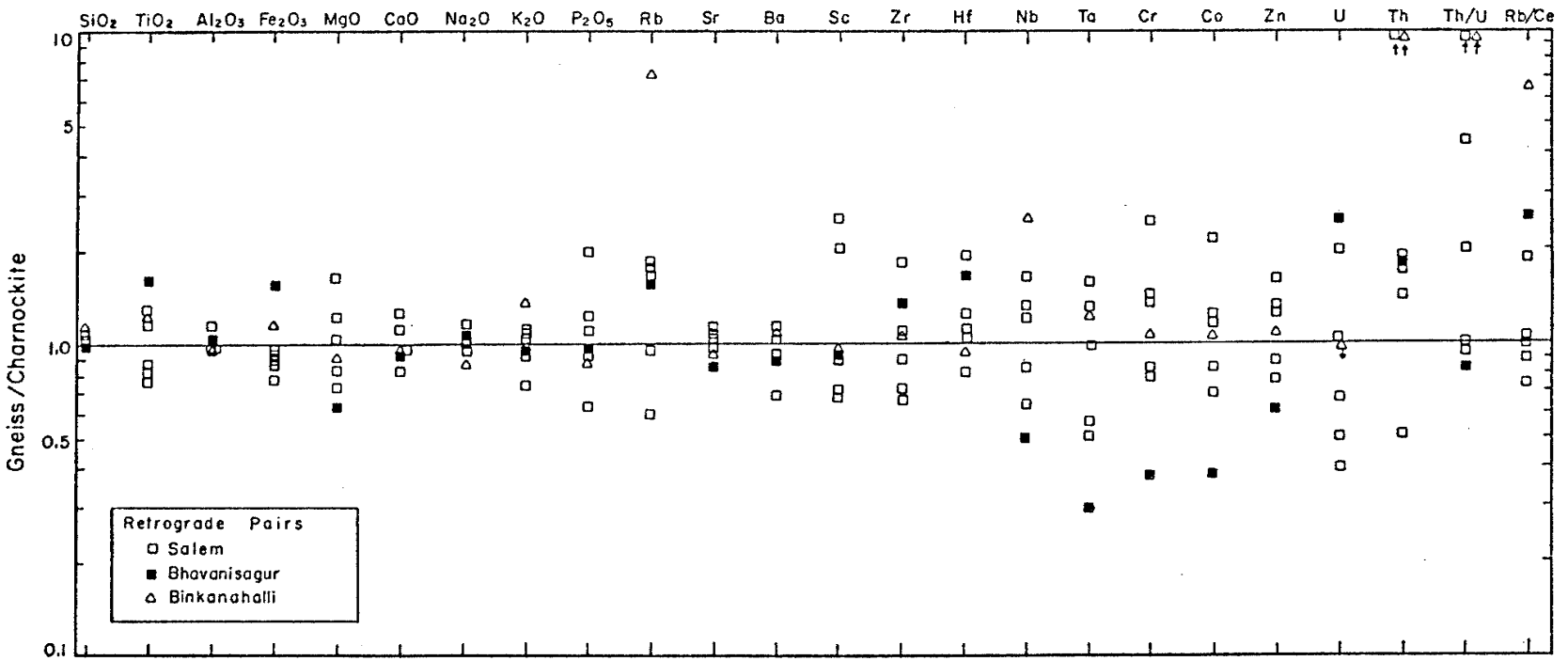

Fig. V-68b. Normalized element distributions in retrograde charnockite-gneiss pairs from south India. A value of 1.0 indicates no change in element concentration, while values greater or less than 1.0 indicate additions or losses, respectively.

The presence and nature of fluid phases and the mobility of elements during prograde and retrograde metamorphism has received considerable attention in recent years (Touret, 1971; Collerson and Fryer, 1978; Flynn and Burnham, 1978; Wells, 1979; Janardhan et al., 1979; Newton et al., 1980; Rollinson and Windley, 1980a; Alderton et al., 1980; Hynes, 1980; Taylor et al., 1981; Weaver and Tarney, 1981). Investigations have largely focused on the composition of metamorphic fluids (H2O, CO2, F, Cl, and other volatiles) and the effects of fluids on element mobility. Changes in element abundances in rocks into which a fluid phase has been introduced depend upon: 1) the stability of mineral phases in reaction with the incoming fluid and the concentrations of elements within these mineral phases, 2) the concentration of elements in the fluid, 3) the ability of the fluid to carry elements released from the breakdown of mineral phases and 4) the availibility of crystallographic sites in minerals forming in the fluid phase to accommodate these elements.

It has been suggested that in minerals forming from a fluid phase, ionic size is the most important factor in controlling subsitution of elements in crystal lattice sites (Morgan and Wandless, 1980; Eade and Fahrig, 1973). In the rocks here under study, the trace elements that show the greatest consistency in behavior across the prograde and retrograde transitions fall roughly into four overlapping groups: 1) elements of ionic size that substitute for Fe+3, Fe+2, and Mg, 2) elements that subsitute for K or Ca, 3) elements that substitute for Ti or Zr, and 4) the REE's which in addition to residing in high concentrations in apatite, are found in

Fe, Mg, and Zr minerals. The minerals showing the greatest change in abundance or degree of alteration during the prograde and retrograde gneiss-charnockite reactions are hornblende, ortho and clinopyroxene, biotite, and plagioclase. With the possible exception of Zr, all elements that show consistent movement and are discussed below can enter or exit the fluid phase from or to these minerals.

Sample pairs from prograde Transition Zone sites range in composition from tonalite to granite and are generally higher in SiO2 and K2O and lower in CaO than the more uniformally tonalitic sample pairs from the high-P terrane retrograde areas (Tables V-3, V-4). Rb, Cs, Th, and U are depleted in both the charnockite and gneiss samples of the retrograde pairs relative to the charnockite and gneiss samples of the prograde pairs, which are generally similar in abundances to tonalitic and granitic gneisses and charnockites from many sites along the prograde Transition Zone. The charnockite and gneiss samples from the retrograde pairs, however, have concentrations of these four elements that are similar to those of the high-pressure charnockites of the Nilgiri massif and the Shevaroy hills.

V.10.4 Major elements

The major elements generally show small to moderate degrees of scatter about 1.0 for both the prograde and retrograde pairs (Figs. V-68a, V-68b). In prograde areas, the Fe/Mg ratio increases in charnockites relative to gneisses (Fig. V-69). In the Fe/Mg ratio, Fe represents both Fe+2 and Fe+3 as total Fe. Though a fraction of Fe+2, in addition to Mg, may have been removed from the

	Kabbaldurga							Dharmapuri		Tiruvannamalai	
	KD I		KD II		KD III						
	119-2 gn	119-3 ch	119-4 gn	119-5 ch	484-1A ch	484-1B gn	484-1C gn	488-1 gn	488-4 ch	514-2 gn	514-4 ch
SiO2	74.6	75.3	60.8	61.2	73.9	73.3	71.6	60.9	60.3	76.4	75.9
TiO2	0.26	0.31	1.59	1.62	0.29	0.44	0.59	0.33	0.59	0.10	0.07
Al2O3	12.5	12.7	13.0	13.1	12.9	13.1	13.4	17.6	16.3	13.7	13.7
Fe2O3(T)	2.03	2.01	10.2	10.3	2.87	3.25	4.19	5.56	6.69	0.76	1.11
MnO	0.02	0.05	0.14	0.15	0.05	0.04	0.05	0.10	0.10	0.01	0.02
MgO	0.30	0.35	2.31	2.13	0.43	0.68	0.86	3.54	3.87	0.48	0.34
CaO	1.10	1.37	5.09	5.11	1.73	2.16	2.48	6.43	6.38	2.18	2.09
Na2O	3.07	3.16	4.09	4.15	3.46	3.64	3.99	4.30	4.36	4.72	4.86
K2O	5.05	4.44	1.47	1.49	3.89	3.22	2.73	1.11	1.01	1.16	1.09
P2O5	0.05	0.06	0.53	0.53	0.09	0.15	0.19	0.37	0.29	0.01	0.01
LOI	0.07	0.09	0.04	0.24	0.44	0.08	0.19	0.59	0.50	0.22	0.18
TOTAL	99.05	99.84	99.26	100.02	100.05	100.06	100.27	100.83	100.39	99.74	99.37
Rb	135	109	24	100	98	93	91	2	<2	13	8
Cs	0.54	0.33	0.07	1.9	0.36	0.53	0.71	0.20	0.4	0.03	<0.03
Sr	107	141	246	211	132	128	129	717	750	462	445
Ba	557	665	365	205	523	472	385	351	281	390	381
Sc	2.0	2.5	21	23	3.0	6.3	6.4	14	17	0.7	1.4
Y	20	16	61	35	18	40	47	26	22	2.0	2.0
Zr	197	194	360	217	150	116	149	80	100	63	68
Hf	6.6	7.9	11	5.8	4.9	4.5	5.0	2.6	3.5	2.1	2.2
Nb	4.8	11	19	21	8.2	10	15	4.6	7.1	< 2	3.5
Ta	0.1	1.1	1.2	2.1	0.6	0.5	0.6	0.1	0.2	<0.03	<0.03
Cr	2.6	2.6	28	138	4.9	6.2	6.6	68	80	0.7	1.0
Co	2.4	2.6	22	36	4.0	5.9	7.6	17	22	1.0	1.3
Ni	3	4	26	155	7	8	12	32	47	<3	3
Zn	30	30	129	116	44	49	60	-	-	9.5	22
Pb	26	22	14	18	22	17	18	<2	<2	<2	2
U	1.5	1.3	1.4	2.4	0.7	0.4	0.5	<0.2	<0.2	0.2	0.3
Th	34	23	8.8	4.0	17	1.1	3.6	<0.2	0.2	0.8	0.7
La	79	89	58	31	24	30	35	51	41	9.7	7.9
Ce	146	154	119	65	39	54	71	105	78	15	12
Nd	48	41	-	23	14	23	35	-	-	3.5	3.0
Sm	7.4	6.1	11	5.6	2.6	6.0	7.6	10	7.8	0.43	0.38
Eu	1.2	1.3	2.7	1.4	1.1	1.2	1.3	1.7	1.5	0.47	0.41
Tb	0.71	0.57	1.7	1.1	0.49	1.1	1.3	1.3	0.96	0.04	0.05
Yb	1.7	1.6	5.8	3.8	1.8	3.3	3.8	2.2	1.7	0.11	0.15
Lu	0.26	0.25	1.1	.71	0.29	0.53	0.58	0.31	0.22	0.016	0.023

Table V-3. Prograde reaction analyses.

	Salem I			Salem II		Salem III			Salem IV		Salem V		Bhavanisagar			Binkanahalli	
	536-1 ch	536-3 ch	536-2 gn	537-1 ch	537-2 gn	540-1 ch	540-3 ch	540-2 gn	542-1 ch	542-2 gn	544-1 ch	544-2 gn	552-1C ch	552-1H ch	552-2A gn	561-1 ch	561-2 gn
SiO2	64.4	63.5	60.6	73.1	69.5	61.7	62.8	64.3	61.6	64.7	64.3	63.8	70.6	69.9	70.4	70.4	71.0
TiO2	0.66	0.64	0.79	0.25	0.38	0.71	0.73	0.60	0.72	0.54	0.49	0.61	0.38	0.41	0.32	0.33	0.38
Al2O3	16.2	17.0	16.8	15.1	16.2	17.2	16.4	16.3	16.8	16.4	16.6	16.5	15.6	15.5	15.6	16.2	16.0
Fe2O3(T)	5.67	5.36	6.19	1.97	2.81	5.69	5.78	4.84	6.16	4.50	5.43	5.04	3.48	3.33	3.05	2.15	2.06
MnO	0.06	0.06	0.06	0.01	0.02	0.05	0.05	0.05	0.07	0.05	0.06	0.06	0.05	0.04	0.04	0.02	0.01
MgO	2.48	2.55	3.12	0.56	0.88	2.83	2.91	2.32	2.97	2.08	2.37	2.41	1.30	1.57	0.87	0.96	0.88
CaO	4.81	5.27	6.25	3.33	3.55	5.63	5.85	5.12	5.40	5.01	5.50	5.13	4.14	4.10	4.02	3.32	3.13
Na2O	4.63	4.77	4.41	4.80	5.53	4.78	4.53	4.54	4.49	4.75	4.43	4.57	4.00	4.09	4.43	5.58	4.87
K2O	0.80	0.87	0.91	0.73	0.75	0.89	0.88	0.81	1.32	1.00	1.01	1.03	1.02	1.12	1.04	1.14	1.54
P2O5	0.26	0.26	0.31	0.06	0.12	0.32	0.29	0.27	0.33	0.21	0.22	0.24	0.12	0.13	0.12	0.09	0.08
LOI	0.16	0.09	0.67	0.30	0.36	0.14	0.18	0.88	0.26	0.77	0.23	1.02	0.01	0.17	0.84	0.25	0.27
TOTAL	100.13	100.37	100.11	100.21	100.10	99.94	100.40	100.03	100.12	100.01	100.64	100.41	100.70	100.36	100.73	100.44	100.22
Rb	3.3	4.8	7.4	4.1	8.3	6.6	5.5	5.7	15	8.8	6.8	11	3.3	2.0	4.2	4.0	28
Cs	0.03	<0.03	<0.03	<0.03	<0.03	0.03	<0.03	<0.03	<0.04	0.08	<0.05	0.19	<0.03	<0.03	<0.03	<0.04	0.13
Sr	612	634	588	545	579	690	573	677	567	560	520	534	371	497	348	784	738
Ba	359	441	405	360	363	587	609	569	1243	855	617	653	457	554	435	453	499
Sc	11	11	26	1.1	2.1	17	18	12	13	8.8	18	16	5.2	4.0	4.6	2.4	2.2
Y	12	15	35	<2	2.0	21	27	16	20	13	20	12	7.6	5.1	3.8	<2	<2
Zr	189	172	189	71	127	205	178	179	231	147	195	139	73	100	121	133	137
Hf	5.0	4.6	6.0	1.9	3.7	5.8	5.2	6.1	6.3	5.0	5.6	5.8	2.3	2.7	4.1	3.8	3.6
Nb	5.9	5.2	7.3	<2	2.0	5.1	5.3	3.4	6.1	5.2	3.6	4.5	3.3	3.3	<2	<2	2.0
Ta	0.2	0.2	0.1	0.1	0.1	0.2	0.1	0.1	0.07	0.07	0.05	0.08	0.06	0.08	<0.03	0.04	0.05
Cr	48	44	62	3.3	7.8	48	52	42	74	55	41	57	21	36	11	6.3	6.9
Co	13	13	16	3.1	5.6	15	16	13	19	13	14	17	8.6	9.4	5.5	5.3	5.5
Ni	28	28	39	3	6	41	46	39	46	30	17	39	11	14	6	5	7
Zn	70	65	87	20	32	74	70	65	85	65	78	95	40	53	38	38	39
Pb	2.7	3.1	4.9	2.3	4.8	2.8	3.3	4.0	<2	<2	2.9	6.2	<2	<2	5.3	6.8	8.1
U	0.2	0.1	0.1	0.1	0.1	0.3	0.2	0.1	0.2	0.1	0.1	0.2	<0.1	<0.1	0.1	0.2	<0.2
Th	0.8	0.6	1.0	0.1	9.5	2.2	1.9	3.5	1.4	0.7	1.2	2.2	<0.1	<0.1	0.1	0.2	2.8
La	33	34	50	17	36	55	60	57	63	54	65	62	15	16	14	13	12
Ce	64	69	121	26	58	113	130	111	127	98	132	115	27	29	24	24	25
Nd	23	29	57	6.4	18	44	55	40	43	35	49	45	-	-	-	10	12
Sm	4.8	5.5	12	0.85	2.2	8.5	10	7.0	8.1	5.1	8.6	7.9	1.5	1.7	1.6	1.4	1.4
Eu	1.1	1.2	1.9	0.55	0.62	1.5	1.7	1.3	1.9	1.7	1.7	1.8	0.85	1.1	0.68	1.0	1.1
Tb	0.51	0.59	1.3	0.06	0.15	0.89	0.98	0.80	0.73	0.49	0.89	0.79	0.23	0.17	0.19	0.09	0.10
Yb	1.1	1.2	2.9	0.14	0.30	1.9	2.3	1.3	1.3	0.94	1.5	1.4	0.91	0.50	0.62	0.10	0.90
Lu	0.14	0.15	0.37	<0.03	0.04	0.26	0.31	0.21	0.21	0.14	0.20	0.18	0.16	0.08	0.09	<0.02	<0.02

Rb, Y, Nb, and Pb valuse <10 are reported to two significant figures for calculating element ratios.

Table V-4. Retrograde reaction analyses.

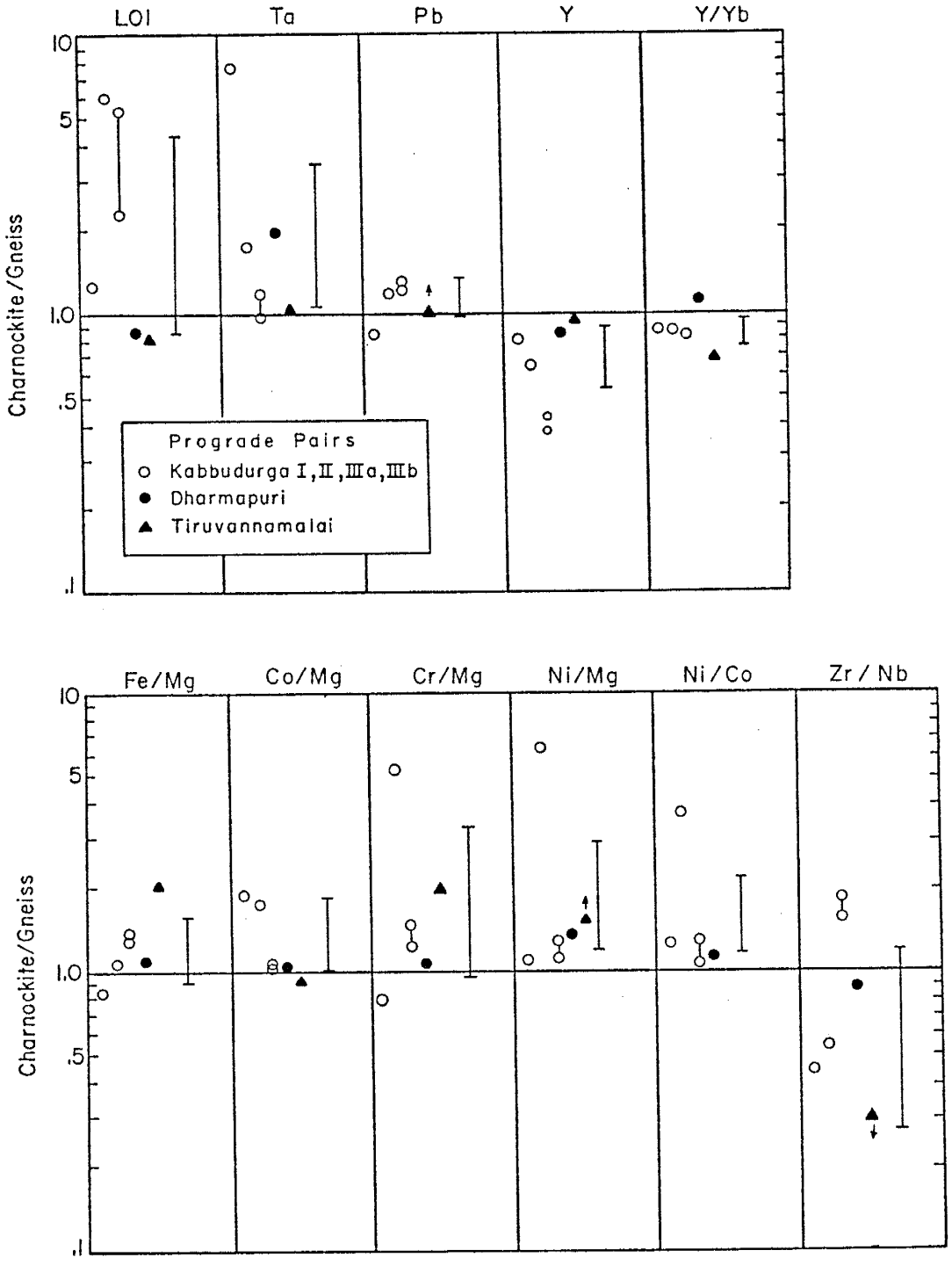

Fig. V-69. Selected elements and element ratios exhibiting consistent trends between prograde gneiss-charnockite pairs. Vertical bar represents the range of the median value for the population of charnockite/gneiss ratios at the ~> 90% confidence level. Intra-site variation of charnockite is shown by vertical tie lines between samples.

mineral phase, it may be largely masked by the presence of Fe+3 in the Fe/Mg ratio. Schulien (1980) reports that at <= 2 kb and 500-700°C, Mg is preferentially partitioned into biotite and Fe+2 into a supercritical aqueous chloride solution. If this is also true of pyroxene, there may have been a small net loss of Fe+2 from the charnockites even though the Fe/Mg ratio showed an increase. Though Kosterin (1959), Bandurkin (1961), and Mineyev (1963) report evidence for the formation of Mg and Fe halide and carbonate complexes, Korzhinsky (1981) cites recent work that concludes that chloride is the most important complexing agent for extraction and transport of Fe and Mg in fluids. The observed increase in Fe/Mg probably refects a loss of Mg relative to Fe in charnockite as is suggested by the behavior of Mg compared to the transition metals described below and by the variation of Mg shown in Fig. V-68a.

Loss on ignition (LOI) exhibits an increase in charnockite in the prograde pairs and an increase in gneiss in retrograde pairs (Figs. V-69, V-70). This indicates that an increase in volatile content accompanies both prograde and retrograde charnockite-gneiss reactions. Recent fluid inclusion studies in gneisses and charnockites near Kabbaldurga indicate a progressive increase in the CO2/H2O ratio with metamorphic grade (Hansen et al., 1984). Though chemical data are not currently available, the volume percent increase in hydrous mineral phases in the retrogressed gneiss suggests that the CO2/H2O ratio may have been lower in retrogressive fluids.

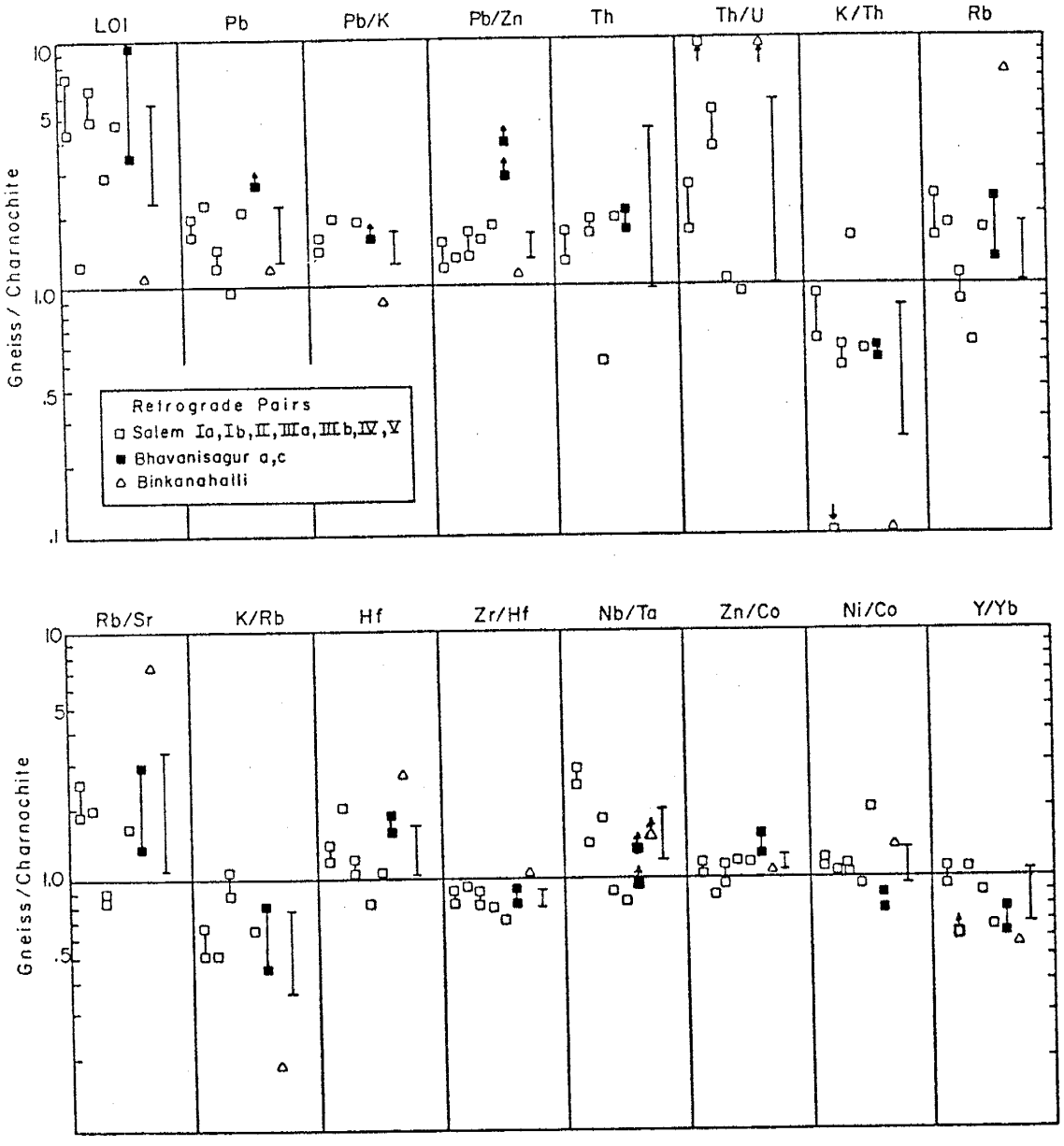

Fig. V-70. Selected elements and element ratios exhibiting consistent trends between retrograde charnockite-gneiss pairs. Vertical bar represents the range of the median value for the population of gneiss/charnockite ratios at the ~> 90% confidence level. Intra-site variation of charnockite is shown by vertical tie lines between samples.

V.10.5 Alkali and Related Elements

Pb increases in prograde charnockite relative to gneiss (Fig. V-69). This is puzzling because evidence from this and many other studies indicates that granulite-facies terranes are generally depleted in Pb relative to amphibolite-facies terranes (Moorbath et al., 1969; Eade and Fahrig, 1973; Drury, 1973) (Fig. V-23). However, the depletion of Pb in the south India terrane-mean values appears to occur largely as the result of a smaller or missing granitic component in the high-pressure granulites, which are compositionally equivalent to tonalite (Fig. V-23). Tonalite characteristically has low K (Barker and Arth, 1976) and probably low Pb. There is, however, an apparent but small depletion of K in the high-grade rocks that is probably the result of the same fluid depletion processes that are responsible for the low abundances of Rb, Cs, Th, and U. Thus, Pb may be low in tonalites but also experience some mobilization and depletion similar to K during high-grade metamorphism.

The ionic radius of Pb is similar to that of K and substitutes for K in K-feldspar and biotite (Heinrichs et al., 1980). Pb forms stable chloride complexes in hydrothermal fluids at a pH less than 5.5 and T <= 200°C (Nriagu, 1971) and in magmatic gases at 600°C (Krauskopf, 1957). Upward movement of a chloride bearing CO2-rich fluid through the lower crust during granulite-facies metamorphism may account in part for the strong depletion of Pb in high-pressure granulites in southern India and elsewhere. The apparent increase in Pb in the Transition Zone charnockites relative to their paired gneisses may represent a local condition at the wave front of the

fluid phase where slight differences in pH or fluid composition disassociate Pb chloride complexes and fix Pb in biotite or K feldspar. Though Pb can enter K sites in both K-feldspar and biotite, Pb has a greater preference for K-feldspar (Heinrichs et al., 1980), a phase which is more prevalent in the Transition Zone charnockites than high-pressure charnockites (see Section IV). The breakdown of some biotite at deeper crustal levels may be accompanied by the complexing of Pb back into the fluid phase and its transport out of the system, thus accounting for some of the depletion of Pb observed in the high-pressure charnockites. The minor Pb enrichment in charnockites at the prograde Transition Zone, therefore, may reflect fluid-phase transport from greater crustal depths.

In retrograde areas, Pb apparently increases in gneiss relative to charnockite (Fig. V-70). Although K does not show a significant trend, the Pb/K ratio also increases in the gneisses. The increase in Pb is also apparent in the Pb/Zn ratio which is greater in the gneisses. Zn substitutes for Fe+2 and Mg in biotite, amphibole, pyroxene, and garnet (Wedepohl, 1972), while Pb substitutes for K in biotite (Heinrichs et al., 1980). Zn (Wedepohl, 1972), K (Korzhinsky, 1981), and Pb (Nriagu, 1971) form stable chloride complexes, of which the Pb chloride complex has the highest vapor pressure and is the most stable (Wedepohl, 1972). Thus, the retrogressive fluid phase may have been an aqueous chloride solution enriched in Pb relative to K and Zn, where Pb is entering K lattice sites in newly forming biotite and amphibole, and if so, could explain the increase in Pb relative to these elements. It appears, therefore, that some Pb is removed from

gneiss during prograde metamorphism in a CO2-rich fluid, and returned during retrogression. Rb follows a similar pattern to Pb in retrograde areas and increases in gneiss relative to charnockite. The K/Rb ratio decreases, and Rb/Sr increases, in the retrograde gneiss reflecting Rb gain. Although U and K do not show consistent relationships in retrograde areas, Th and the Th/U ratio increase in the gneiss, while the K/Th ratio decreases.

U, Th, Rb, and Cs, which are depleted in south Indian high-pressure charnockites do not exhibit consistent relationships in the prograde Transition Zone. In retrograde areas Th, Rb, and Pb are higher in gneiss relative to paired charnockite; however, Th and Rb concentrations do not reach the levels found in the gneiss and charnockite samples from the lower pressure prograde Transition Zone. Meaningful relationships for Cs in the retrograde areas cannot be determined because concentrations in many cases are below the limits of detection.

V.10.6 Transition Metals

Transition metals do not exhibit consistent relationships between sample pairs during prograde metamorphism. However, ratios of transition metals relative to Mg all show an increase in charnockite (Fig. V-69). Although the increase in the metal/Mg ratios could represent an increase in Co, Ni, and Cr relative to Mg, it is probable that some Mg has been mobilized and removed from the system during charnockitization relative to these elements and to Fe (Fig. V-68a). As noted above, Mg can be mobilized as halide complexes.

The Ni/Co ratio shows an increase in prograde charnockite relative to gneiss. The reason for the apparent fractionation of these two similar elements, both occupying Mg and Fe+2 octahedral sites in amphibole, pyroxene, and biotite (Turekian, 1974a) is uncertain. Ni, however, has a higher crystal field stabilization energy (Mason and Moore, 1982) and may compete more successfully than Co for such sites during granulite-facies recrystallization. In retrograde areas, neither Zn or Co show consistent trends between charnockite and gneiss. However, Zn/Co and Ni/Co ratios are slightly higher in the retrograde gneisses, suggesting that relative to Ni and Zn, Co has been lost (Fig. V-70). Ni, Co, and Zn all compete for Mg and Fe+2 octahedral sites (Wedepohl, 1972; Turekian 1978a, 1978b).

V.10.7 High Field Strength Elements

Of the HFS elements (Zr, Hf, Ta, Nb), Ta increases and the Zr/Nb ratio decreases during charnockitization (Fig. V-69). In addition, the data suggest that Nb may increase (Fig. V-68a), a feature which may explain the observed decrease in the Zr/Nb ratio. The primary host minerals for Ta are biotite, pyroxene, hornblende, magnetite, and zircon (Wedepohl, 1978). Ta is probably soluble as fluoride complexes (Beus, 1958; Korzhinsky, 1958) and as carbonate complexes similar to Ti and Zr (Hynes, 1980). The reason for the observed increase of Ta in transition charnockite is uncertain. Nb, like Ta is probably mobilized by fluoride complexes (Beus, 1958; Korzhinsky, 1981) and as a high valence cation in carbonates (Hynes, 1980). The observed decrease in the Zr/Nb ratio in the charnockites

might be the result of the incorporation of Nb, carried into the system as fluoride or carbonate complexes, in newly formed pyroxene. The results reported here suggest that Ta and Nb were most soluble in deep-seated granulite-facies metamorphic fluids of southern India. As with Pb, changing conditions in the fluid phase at the wave front appear to have led to their deposition in the charnockites.

In the retrograde areas, Hf increases in gneiss and the lower Zr/Hf ratio may reflect this increase. The relationships between Zr and Hf and the mechanisms for their mobility in fluids have been studied by numerous investigators. Hf can substitute for Zr in accessory zircon (Erlank et al., 1978b) but it is also competes with Zr for Mg and Fe+2 sites in pyroxene, amphibole, and biotite (Vlasov, 1966), and the Zr/Hf ratio in zircons may not represent that for the whole rock. In autometasomatic rocks, zircons appear to have lower Zr/Hf ratios than unaltered rocks (Pavlenko et al., 1957). This decrease in the ratio is thought to be the result of a loss of Zr (Lyakhovich et al., 1962; Vlasov, 1966). Hynes (1980) reports that CO2-rich fluids may create high order carbonate complexes, and rocks with high CO2 have low Zr.

In hydrothermal deposits, however, the Zr/Hf ratio may be higher than in unaltered rocks (Pavlenko et al., 1957), resulting from the somewhat greater stability for Zr than Hf in fluoride complexes (Gerasimonskiy et al., 1972). Although Butler and Thompson (1965), using differing diffusion rates of Hf and Zr, conclude that Hf is enriched relative to Zr in an aqueous fluorine-bearing solution, Gerasimonskiy et al. (1972) report that Zr is more stable than Hf in

fluoride complexes. Beus (1958) states that Zr fluoride complexes become more stable than Hf complexes as the fluid phase becomes more alkaline. It is possible that the Hf and Zr/Hf relationships in the retrograde gneisses reflect the presence of a progressively more alkaline fluoride-bearing fluid phase in which Hf preferentially disassociates from fuoride complexes and enters retrogressive hornblende and biotite.

Although neither Nb or Ta show consistent relationships in retrograde sample pairs, the Nb/Ta ratio increases in the gneisses. Beus (1958) notes that both Nb and Ta form fluoride complexes in aqueous fluid phases, and that Nb behaves similarly to Hf, disassociating from its fluoride complexes before Ta in response to increasing alkalinity. Thus, in minerals formed from such a fluid in a relatively alkaline environment, the Nb/Ta ratio may increase. Wedepohl (1978) also reports that biotite, which in part is created during retrogression, concentrates Nb relative to Ta. Hynes (1980) states, however, that high valence cations, such as Ta and Nb, may form high-order carbonate complexes if high levels of CO2 are present in the fluid phase. Although fractionation of Nb relative to Ta in carbonate complexes is uncertain, the fluid phase responsible for retrogrssion probably has a lower CO2/H2O ratio than that responsible for the prograde reactions.

V.10.8 REE, Y

REE distributions in samples from prograde areas show a slight decrease in total REE in the charnockite of three sample pairs, and little change in two other pairs (Fig. V-71). A change from a negative to a positive Eu anomaly in going from gneiss to charnockite is recognized at only one sample site (484). Y, which behaves like the heavy REE, also shows a decrease going from gneiss to charnockite (Fig. V-69). The reason for the decrease in the Y/Yb ratio is uncertain, although it may reflect the increase in the Fe/Mg ratio. In pyroxene, Y and Yb substitute for Fe+2 and Mg. However,Yb, with a lower electronegativity and smaller ionic radius than Y, may be preferentially incorportated into structural sites in pyroxene accompanying the relative loss of Mg in the charnockite, resulting in a lower Y/Yb ratio.

In retrograde areas, REE patterns do not exhibit systematic relationships. At the Salem sample sites (Fig. V-72), two sample pairs show a significant increase in total REE in the retrograde gneiss, two show a small decrease, and one sample no significant change. The other two retrograde areas also exhibit ambiguous results (Fig. V-73). The Y/Yb ratio is lower in retrograde gneiss, which may be the result of a relative loss of Mg following the breakdown of pyroxene and the preferential entry of Yb into amphibole.

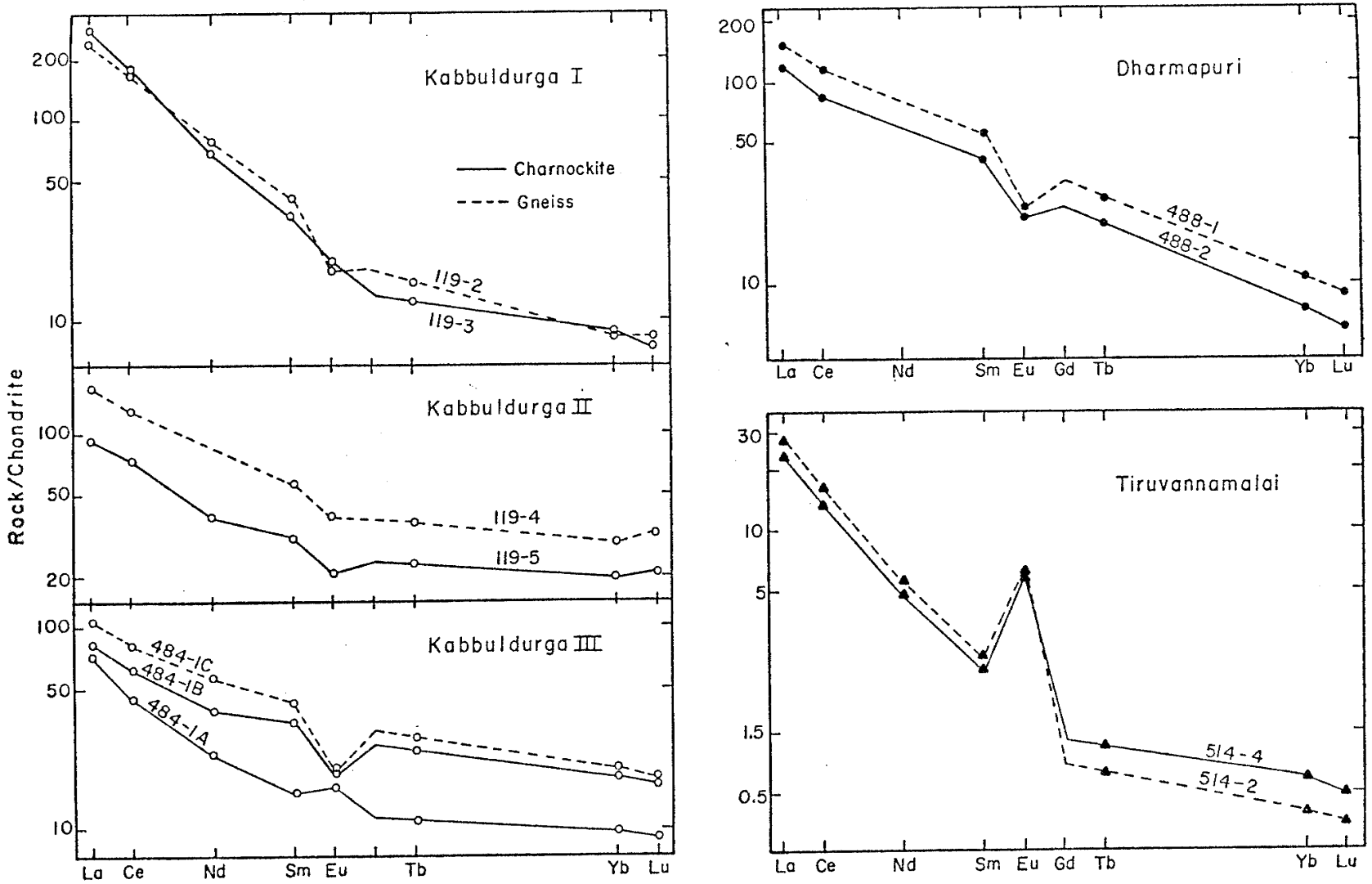

Fig. V-71. Chondrite-normalized REE distributions in prograde gneiss-charnockite pairs from Kabbaldurga, Dharmapuri, and Tiruvannamalai.

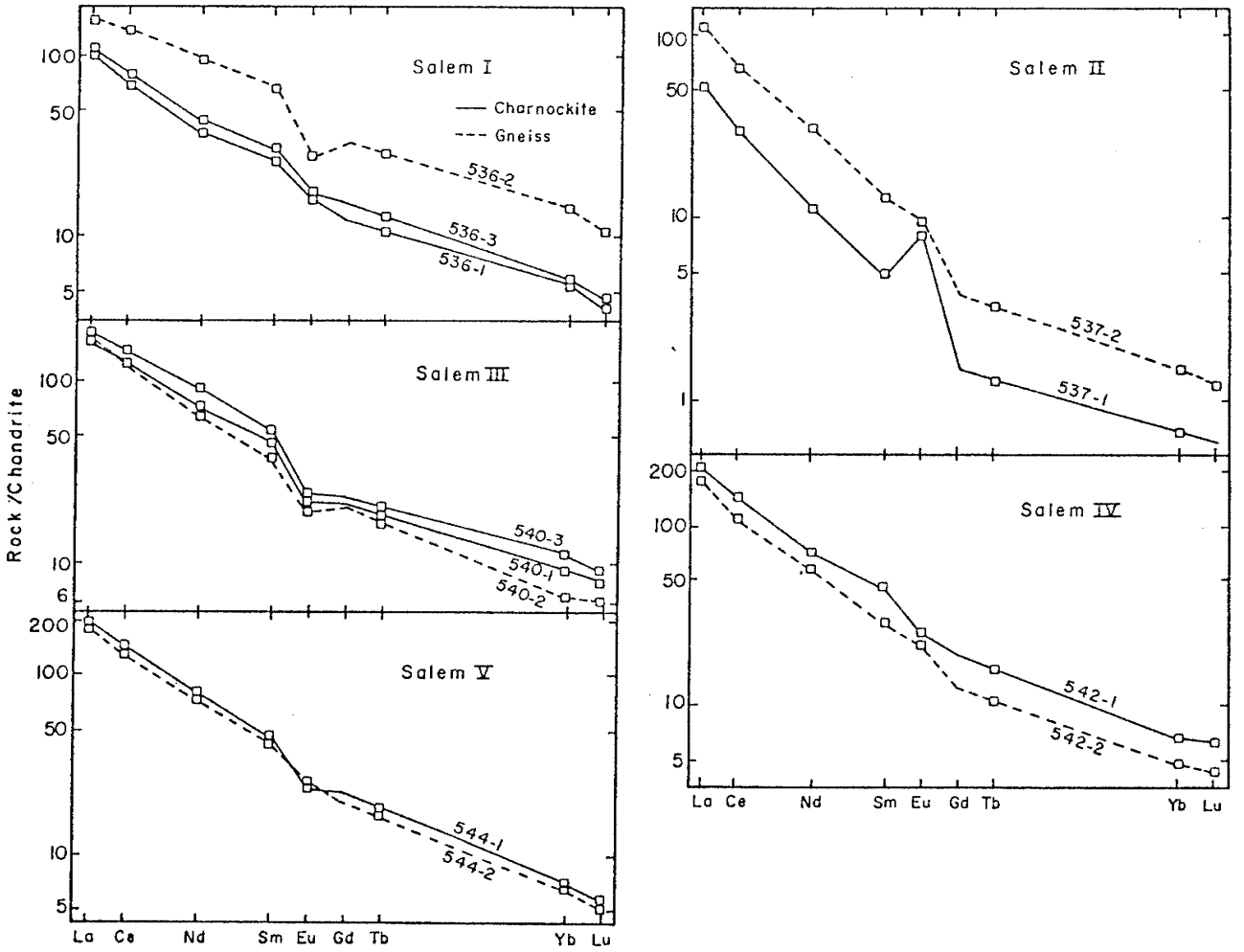

Fig. V-72. Chondrite-normalized REE distributions in retrograde charnockite-gneiss pairs from Salem.

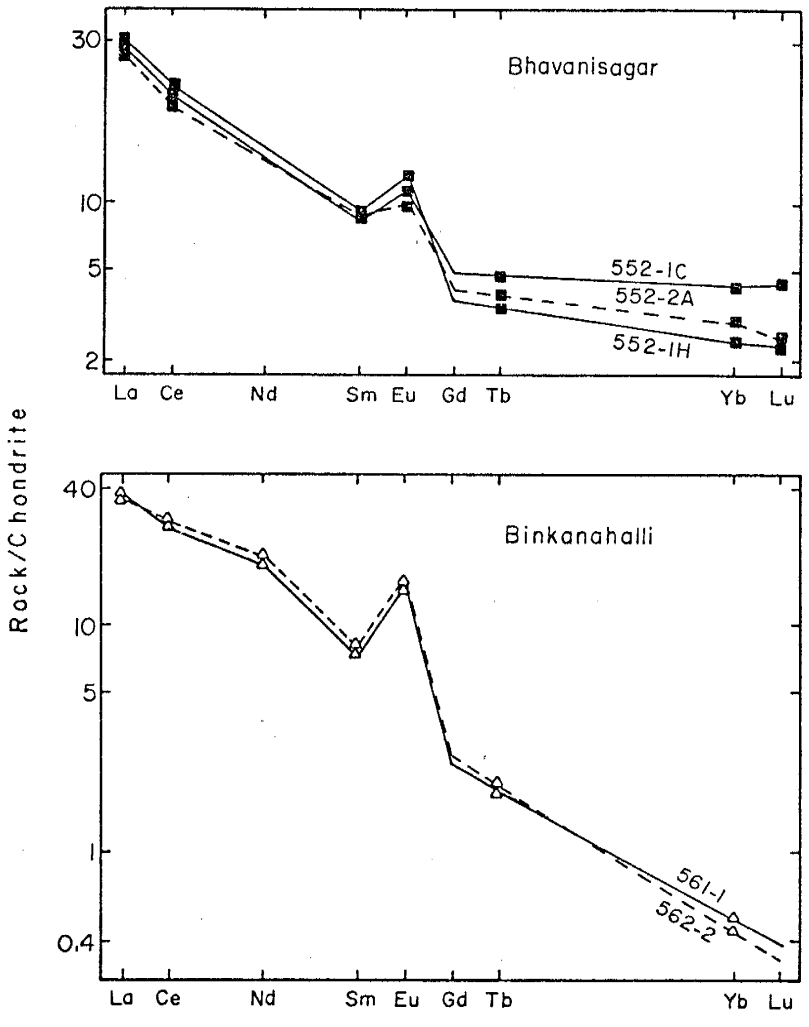

Fig. V-73. Chondrite-normalized REE distributions in retrograde charnockite-gneiss pairs from Bhavanisagar and Binkanahalli.

The terrane-wide results from south India discussed above (Section V.8), and other previous studies suggest that REE are not significantly disturbed in going from amphibolite to granulite-facies metamorphic terranes (Rollinson and Windley, 1980a; Weaver and Tarney, 1981). Numerous investigators, however, conclude that the means for REE transport may be present in high-grade metamorphic terranes. The work of Naumov (1959) and Kosterin (1959), and more recently of Collerson and Fryer (1978), concludes that CO2-rich fluids can mobilize REE. Beus (1958), Bandurkin (1961), Mineyev (1963), Flynn and Burnham (1978), Barsukova et al. (1979), Taylor and Fryer (1980), and Korzhinsky (1981) find evidence that the formation of halogen complexes can also significantly effect the mobility of many elements including the REE's. Taylor et al. (1981), summarizing the conclusions of many of these and other studies, state that the light and intermediate REE are dissolved primarily in chlorine-rich fluids while the heavy REE are mobilized in fluorine and CO2-rich fluids. The changes in REE observed during both prograde and retrograde reactions in southern India probably reflect local changes in the halogen content of the fluid phase at the wave front. However, representative charnockites from the prograde transition zone and high-pressure sites do not, in general, show any correlation with metamorphic grade.

V.10.9 Summary of prograde and retrograde reactions

Within the limits of sampling and analysis, retrogression produces a greater number of consistent relationships between gneiss and charnockite than does charnockitization. Factors responsible for this may include the depth at which metamorphism and metasomatism occurred and the nature of the fluid phase responsible. The difficulties in recognizing unequivocal petrographic evidence of charnockitization appear to result from minor retrogression of the prograde relationships following uplift. This same retrogression also overprints pre-existing geochemical relationships between charnockite and gneiss along the original relatively CO2-rich wave front and thus may contribute to the existence of few systematic geochemical changes across the front. Beach and Tarney (1978) in their study of retrogressed granulite-facies gneisses in Scotland note that, unlike the retrogressive phase, prograde metamorphism did not produce large-scale geochemical equilibrium.

The results of the study of prograde and retrograde reactions at the margin indicate that, in general, there is broad scatter of elemental abundances, though subtle systematic changes in element abundances, and especially element ratios, are apparent in both the prograde and retrograde reactions. However, some overall differences occur between the two types of reaction:

1. In prograde areas, charnockitization generally results in small losses of Y and REE, and in Mg relative to Fe and transition metals, and gains of Ta, Pb, and CO2.

2. Retrogressed gneisses are generally enriched in Pb, Th, Hf, and Rb. In addition, they are also enriched in Zn relative to Co, in Nb relative to Ta, and in Hf relative to Zr.

3. Both prograde and retrograde metamorphic fluid phases probably contained a mixture of CO2, H2O, and halogens. However, evidence suggests that the prograde fluids had a higher CO2/H2O ratio than the retrograde fluids. Although halides were present in both fluids, they may have been more important as complexing agents in retrograde fluids, especially in the transport and fractionation of Pb-Zn-K, Hf-Zr, and Nb-Ta.

The distribution of elements across both the prograde CO2-rich and the retrograde H2O-rich wave fronts may not be characteristic of regions fully saturated with the respective fluid phases. Localized effects at the wave fronts may be responsible for the overall non-systematic geochemical variations observed in this investigation of the reaction margins. Such effects include changes in pH, varying CO2/H2O/halide ratios in the fluid phases, original compositional variations in the rocks, and quantity of fluid that has passed through the rock.

In prograde areas at the margin there is a slight increase in Pb in the charnockite and no significant change in U, Th, Rb, and Cs. However, as discussed above (Section V.4), all five of these elements are depleted in the high-pressure charnockite terranes relative to tonalitic gneiss protoliths. This difference may reflect the fact that an insufficent quantity of fluid had passed through the charnockites at the wave front to cause such a depletion. Only at greater depths, where comparatively large volumes of fluid had passed through the crust, are significant amounts of these elements removed. During retrogression, H_2O-rich fluids, probably derived from H_2O descending along major shear zones, such as the Moyar-Bhavani Shear Zone, may rise as plumes controlled by small cracks and fissures. Retrogressed gneisses are enriched in Th, Rb, and Pb; however, these changes may not characterize retrogressed gneisses found at greater distances from the wave front. Also, although gneisses in retrograde areas are enriched in these three elements, only Pb approaches the concentrations present in tonalitic gneiss protoliths, assumed to be represented by gneisses from north of the prograde transition zone. Thus, of the U, Th, Rb, Cs, and Pb that are depleted in high-pressure charnockite terranes, as seen here by the charnockites of the retrograde areas, only Pb is significantly replenished by the retrogressive fluid phase.

VI Discussion

VI.1 Overview of south India gneisses

The gneisses and charnockites from south India are calc-alkaline on an AFM diagram, and range from mafic to trondhjemite (along a gabbro-tonalite-trondhjemite trend) and tonalite to granitic (along a calc-alkaline trend) on Ab-An-Or-Q and Na2O-CaO-K2O diagrams. Although trends are generally smooth and continuous, the granite-granodiorite samples may define a separate population from the tonalite-trondhjemite group. On some plots and diagrams, the mafic rocks define different populations or trends that suggest a bimodal distribution in the south India Archaean terrane, though this pattern is not observed on all diagrams.

The average composition of gneiss and charnockite becomes less silicic and more mafic moving from the low-grade Gneiss Terrane in the north to the higher metamorphic grade terranes in the south. However, the enriched character of the terrane-mean value of the low-grade terranes is not accompanied by comparable enrichment in the granitic, granodioritic, and granitic components that comprise these terrane-mean values. For example, the average composition of the high-pressure granulite terrane is similar for most elements to the tonalitic gneisses from the southern amphibolite-facies Gneiss Terrane, indicating that the more mafic higher grade terrane-mean values largely reflect the decline of the granitic component in the high grade terrane. A similar observation is made by Weaver and

Tarney (1983). The significant differences observed between granulite and amphibolite-grade terranes are the depletion in the high-pressure terrane charnockites of Rb, Cs, Th, and U, and to a lesser degree, K and Pb. Discussion of the depletion of these elements can be found below (Section V.3).

The major unexpected petrogenetic relationship found in the south India samples is between amphibolite-facies enriched "low-grade" and "high-grade" granitic gneisses near the somewhat arbitrary boundary of the Gneiss Terrane and the Transition Zone. These enriched granitic gneisses, with distinctive high total REE and -Eu anomalies, are also found in the western region of the Transition Zone where they encroach into areas that are now charnockite. As a result, a simple temperature-pressure distinction between low and high-grade granites is obscured. The enriched granitic gneisses are not observed in the eastern Transition Zone (Hosur-Krishnagiri-Dharmapuri). This compositional change between the Gneiss Terrane and the Transition Zone may be correlated with a Bouguer gravity low that lies south of Bangalore that extends in a broad arc to the west towards Mysore, east to Krishnagiri-Dharmapuri, and south towards Salem (NGRI, 1978; Kailasam, 1979). The difference between the specific gravities of the exposed gneisses should be minimal, which suggests the possibility of an underlying, lower-density pluton beneath the eastern Transition Zone that may have contributed to the observed compositional differences in the overlying gneisses. Thus both lateral and vertical composition heterogeneities unrelated to the regional progressive metamorphism may be present.

Differences between the western and eastern Transition Zone are also evident in the somewhat greater frequency of myrmekite, mortar texture, and mylonite in the west. The high-pressure charnockites along and south of the Moyar-Bhavani shear zone also have a much higher incidence of cataclastic textures and deformed, commonly twinless plagioclase; late stage secondary alteration is locally severe.

Though the amphibolites have higher K, Rb, and Sr than the mafic granulites, there is no apparent petrogenetic relationship between low and high-grade mafic rocks. There also does not appear to be a simple genetic relationship between the mafic samples and the tonalitic gneiss.

Representative samples from the Transition Zone in the Krishnagiri-Dharmapuri area (6 granitic gneisses, 6 tonalitic gneisses, and 7 charnockites) were dated by Rb/Sr isochron by Ph. Vidal and J.J. Peucat of the Universite de Clermont and Universite de Rennes, respectively. Their results (personal communications, 1983) give a date of 2508 my and an initial Sr^{87}/Sr^{86} ratio I=0.70192 for the granitic gneisses, 2463 my and I=0.70209 for the tonalitic gneisses, and 2492 my and I=0.70244 for the charnockites. The tightness of these values (within the limits of error) suggests that the granulite facies metamorphism responsible for the charnockite occured contemporaneously with the formation of granites. Similar dates are reported from the Bangalore and Kabbaldurga areas of the Transition Zone (Beckinsale et al., 1983; Grew and Manton, 1984), and

Friend (1981; 1984) also concludes that the production of anatectic granites in the Kabbaldurga area occured at the same time as the formation of the charnockite. The low initial Sr87/Sr86 ratios suggest that there has been no crustal contamination and a low crustal residence time (<=350 my).

VI.2 Origin of gneisses: Partial melting - crystallization models

Approaches to the chemistry of the south India gneisses and charnockites fall into two general categories: 1) the petrogenetic origin of the gneisses, and 2) the relationship (igneous and/or metamorphic) between amphibolite-facies gneisses and granulite-facies charnockites. The emphasis of this study is on the lithologic, petrographic, and chemical characteristics and changes relative to increasing metamorphic grade; however, in the next two sections brief attention will be given to the petrogenesis of the gneisses.

Two models have been suggested for the origin of Archaean tonalite, including the south India tonalitic gneiss: 1) fractional crystallization of a basaltic magma (Barker and Arth, 1976; Arth et al., 1978; Rollinson and Windley, 1980b); and 2) partial melting of a mafic parent having variable amounts of hornblende and garnet in the residue (Arth and Hanson, 1972; Arth and Barker, 1976; Weaver and Tarney, 1980; Condie et al., 1982). Although Rollinson and Windley (1980b) support a fractional crystallization model for the Scourian, other researchers consider partial melting as the major petrogenetic process to produce tonalite in Archaean terranes; for example, the

Lewisian (Weaver and Tarney, 1980; 1981), the East Antarctic Shield (Sheraton and Black, 1983; Sheraton and Collerson, 1984), south India (Condie et al., 1982; and this study), and east-central India (Sengupta et al., 1983). Partial melting to produce tonalite has been favored for one or more of the following reasons: 1) the terranes are variably bimodal and SiO2 variation diagrams reveal relatively few samples of intermediate composition between the mafic and felsic populations, contrary to what would be expected in a continuously fractionating liquid; 2) the cumulate expected from this fractionating liquid, which would be growing at mid to lower crustal depths, is missing or present in only minor amounts; 3) the mafic rocks that might represent such a cumulate typically have trends or patterns on variation diagrams and other plots that differ from the felsic gneisses; and 4) compatible elements such as Ni, Co, and Cr are present in the tonalites at levels that are unrealistic for a liquid in equilibrium with a mafic cumulate.

In order to examine the role of high-pressure mineral phases in batch (equilibrium) melting, X - Y plots of elements and element ratios sensitive to mineral-melt equilibria are shown for the south India samples along with partial melt trajectories of important mineral phases. Fractional crystallization trajectories are not shown; however, their orientation is in general similar to the partial melt vectors. On a Sc - Y plot (Fig. VI-1), there is a positive correlation between these two elements for the tonalitic gneisses and charnockites, though the tonalitic gneisses are somewhat more scattered, with some samples having elevated Y concentrations

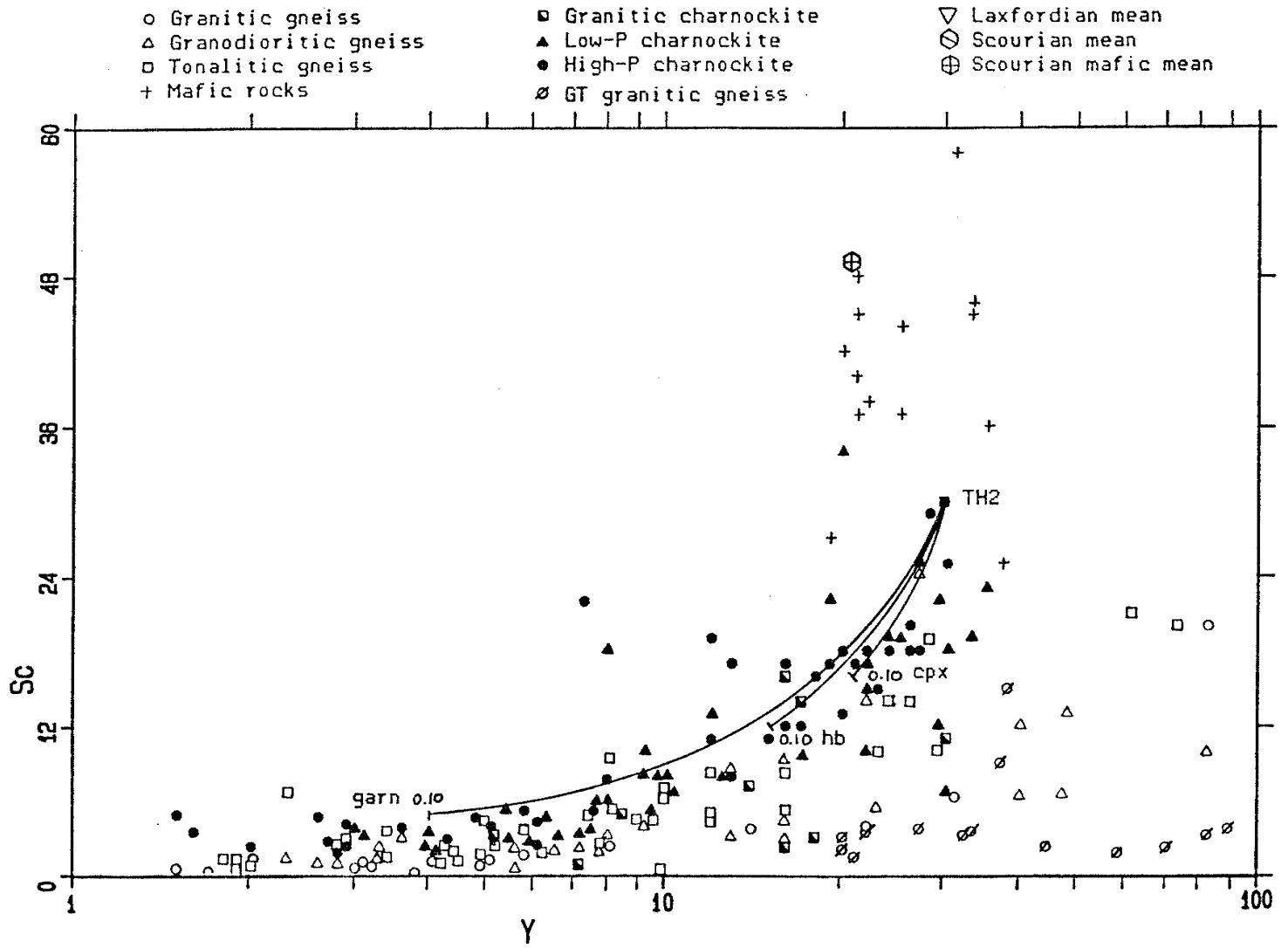

Fig. VI-1. Sc vs Y plot. Data from Appendix C. Partial melting vectors to F=0.10 for garnet, hornblende, and clinopyroxene are shown. TH2 is enriched Archaean tholeiite from Condie (1981a).

(Fig. VI-1). The granitic gneisses have low levels of Sc (Sc~<6 ppm) throughout the range of Y, with samples having elevated Y concentrations coming from the Gneiss Terrane. The granodioritic gneisses are scattered. The slight increase of Sc with metamorphic grade that is apparent on the element-area diagram (Fig. V-35) is also evident here; though both the tonalitic gneisses and charnockite follow the same trend, the charnockites consistently have elevated Sc values. The distribution of the tonalitic gneisses and charnockites generally follows the partial melting trajectories of garnet, hornblende, and clinopyroxene. As a point of reference, the composition of TH2, an average enriched Archaean tholeiite (Condie, 1981a) is shown as a source composition at the origin of the equilibrium (batch) melt trajectory (Fig. VI-2).

Though the pattern is less clear on a Nb - TiO2 plot, a similar relationship exists between Nb and TiO2 (Fig. VI-2). The granitic and granodioritic samples have broad scatter, largely the result of higher Nb at lower TiO2 for the Gneiss-Terrane granitic gneisses. Though the tonalitic gneisses and charnockites roughly follow the partial melting trajectory of hornblende, the charnockites have somewhat lower levels of Nb for a given value of TiO2. This variable decrease of Nb with increasing TiO2 in the tonalitic gneisses and charnockite is also observed on Nb and TiO2 element-area diagrams (Figs. V-9, V-36). The Scourian-mean value is also depleted in Nb relative TiO2 when compared to the amphibolite-facies Laxfordian gneisses (Fig. VI-2).

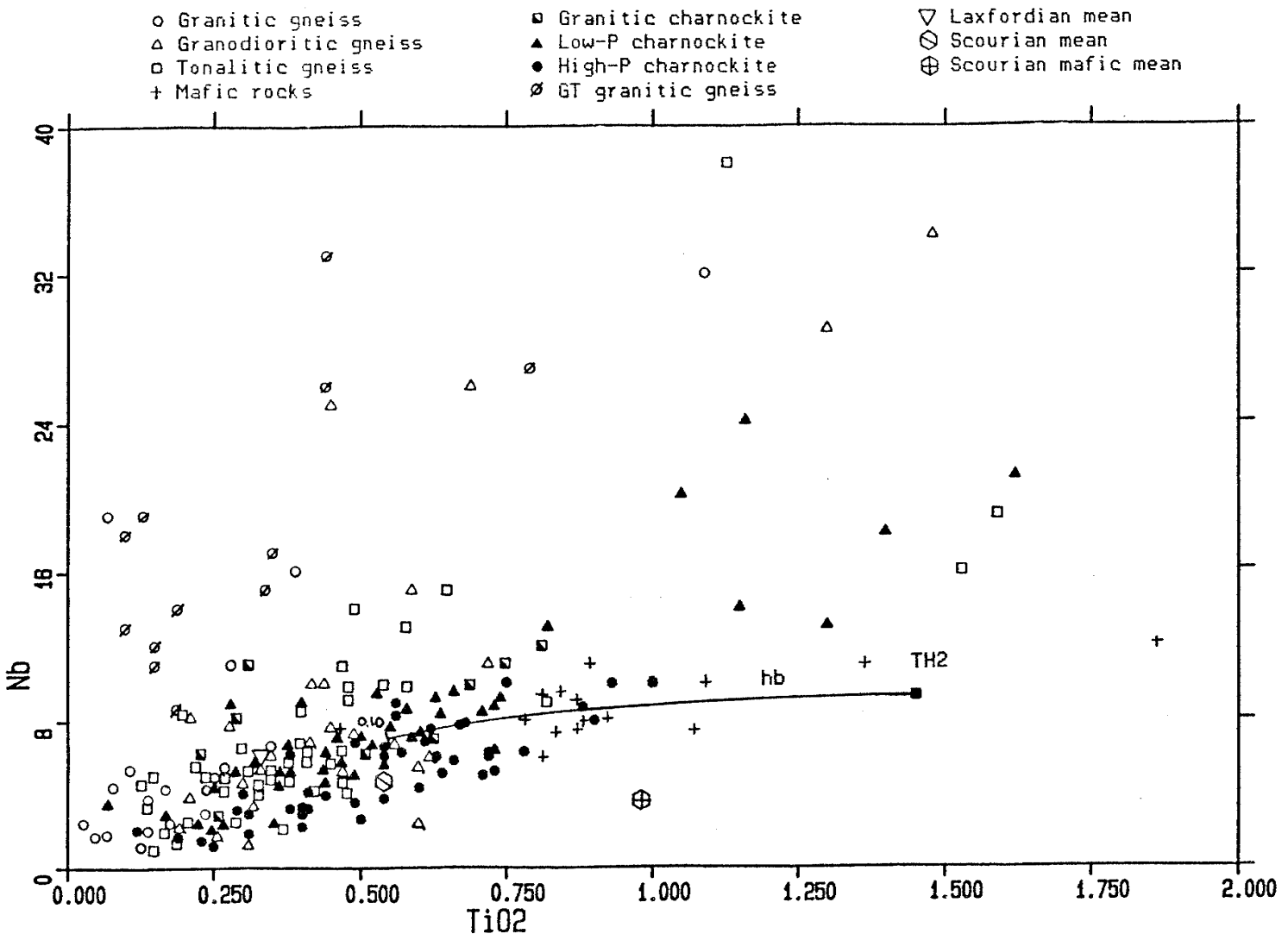

Fig. VI-2. Nb vs TiO2 plot. Data from Appendix C. Partial melting vector to f=0.10 for hornblende is shown. TH2 is enriched Archaean tholeiite from Condie (1981a).

On Eu/Eu* - SmN and the Eu/Sm - Sm diagrams, where Sm and SmN monitor the level of total REE, the sign and magnitude of the Eu anomaly (measured either as Eu/Eu* or Eu/Sm) shows a strong negative correlation with total REE (Figs. VI-3, VI-4). The somewhat scattered granitic gneisses from the Gneiss Terrane have low Eu/Eu* or Eu/Sm values. Partial-melt mineral trajectories indicate that a combination of hornblende, garnet, clinopyroxene, and plagioclase in the residue can produce the trend of high +Eu anomalies at low Sm levels observed for the south India samples. For the Lewisian a similar mineral assemblage in the residue to produce tonalitic gneiss is suggested by Weaver and Tarney (1980).

A negative correlation between the hREE (represented by YN or YbN) and REE fractionation (represented by CeN/YN or CeN/YbN) is observed in Archaean terranes, for example in the granitic and tonalitic-trondhjemitic Scourian granulites (Tarney and Windley, 1977; Rollinson and Windley, 1980; Weaver and Tarney, 1980) and in charnockites from Madras (Weaver et al., 1978). In south India, the tonalitic gneisses and charnockites roughly follow this trend of decreasing YN with increasing CeN/YN, however, the granitic and granodioritic gneisses with low YN and high CeN/YN are scattered (Fig. VI-5). The combination of high REE fractionation with strong hREE depletion, requires that liquids parental to the tonalites evolve with hornblende and garnet in the residue, as indicated by hornblende and garnet partial melting trajectories. A similar pattern is observed in the Scourian (Weaver and Tarney, 1980).

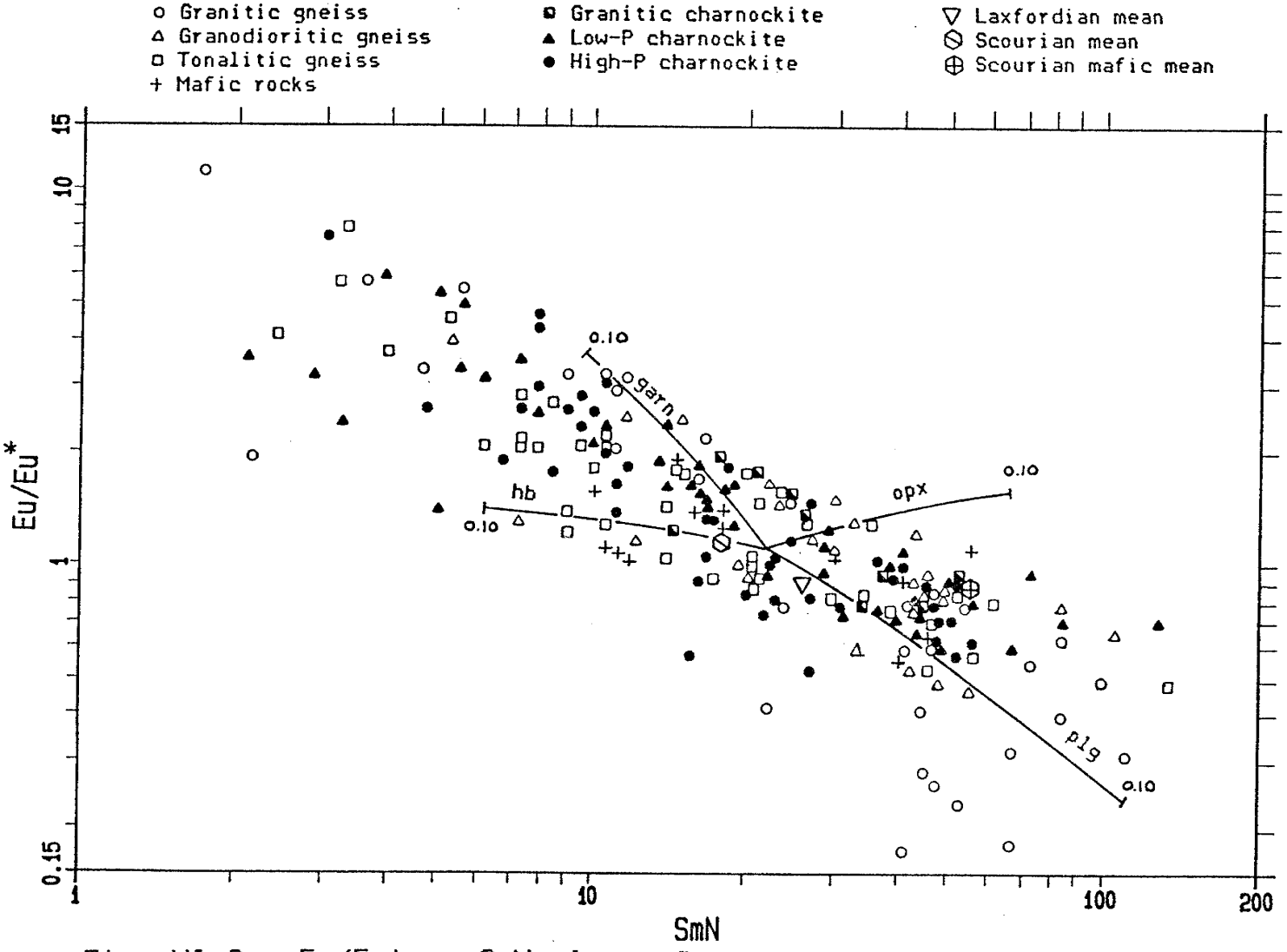

Fig. VI-3. Eu/Eu* vs SmN plot. Data from Appendix C. Partial melting vectors to F=0.10 for garnet, hornblende, orthopyroxene, and plagioclase are shown.

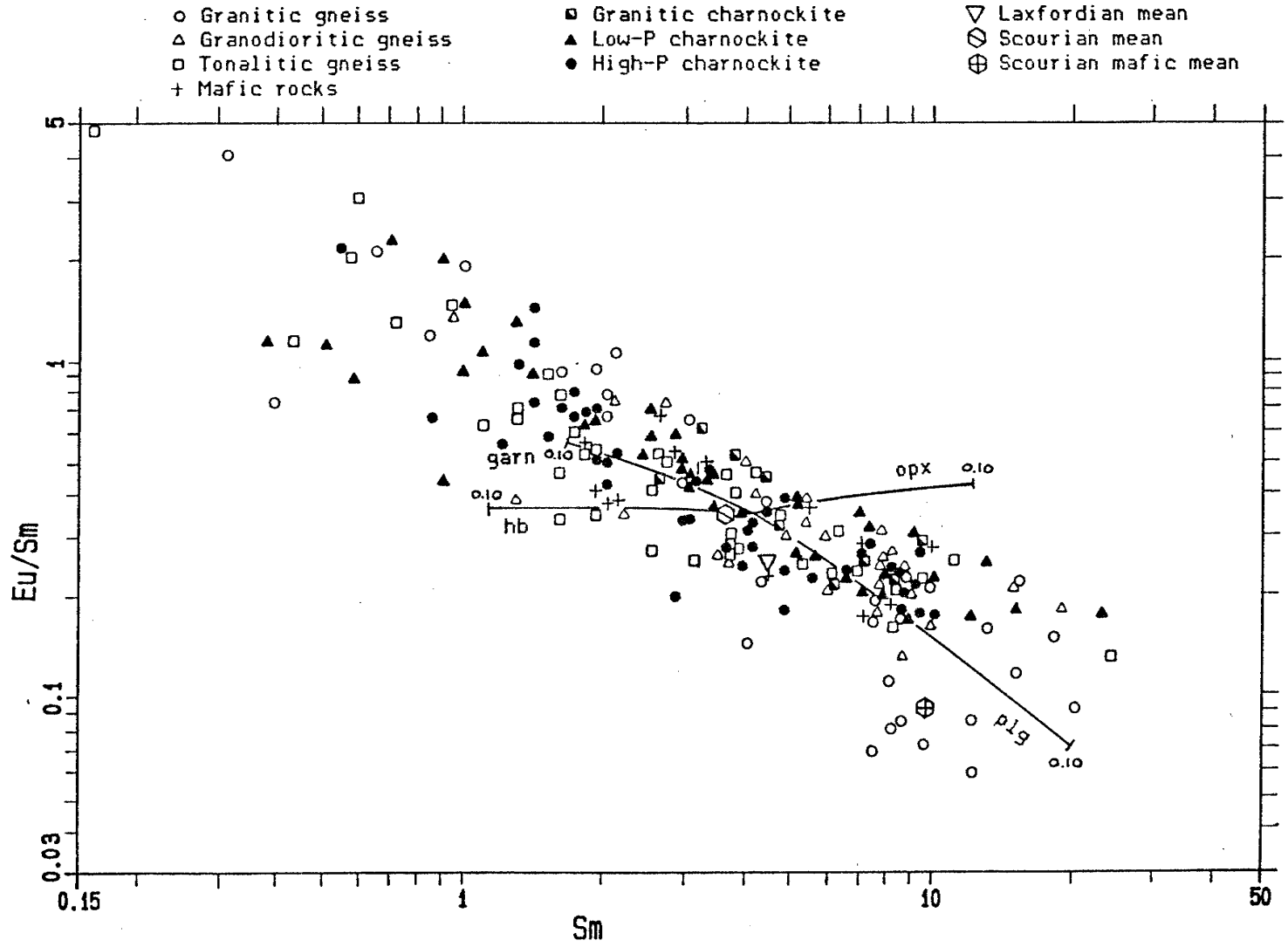

Fig. VI-4. Eu/Sm vs Sm plot. Data from Appendix C. Partial melting vectors to F=0.10 for garnet, hornblende, orthopyroxene, and plagioclase are shown.

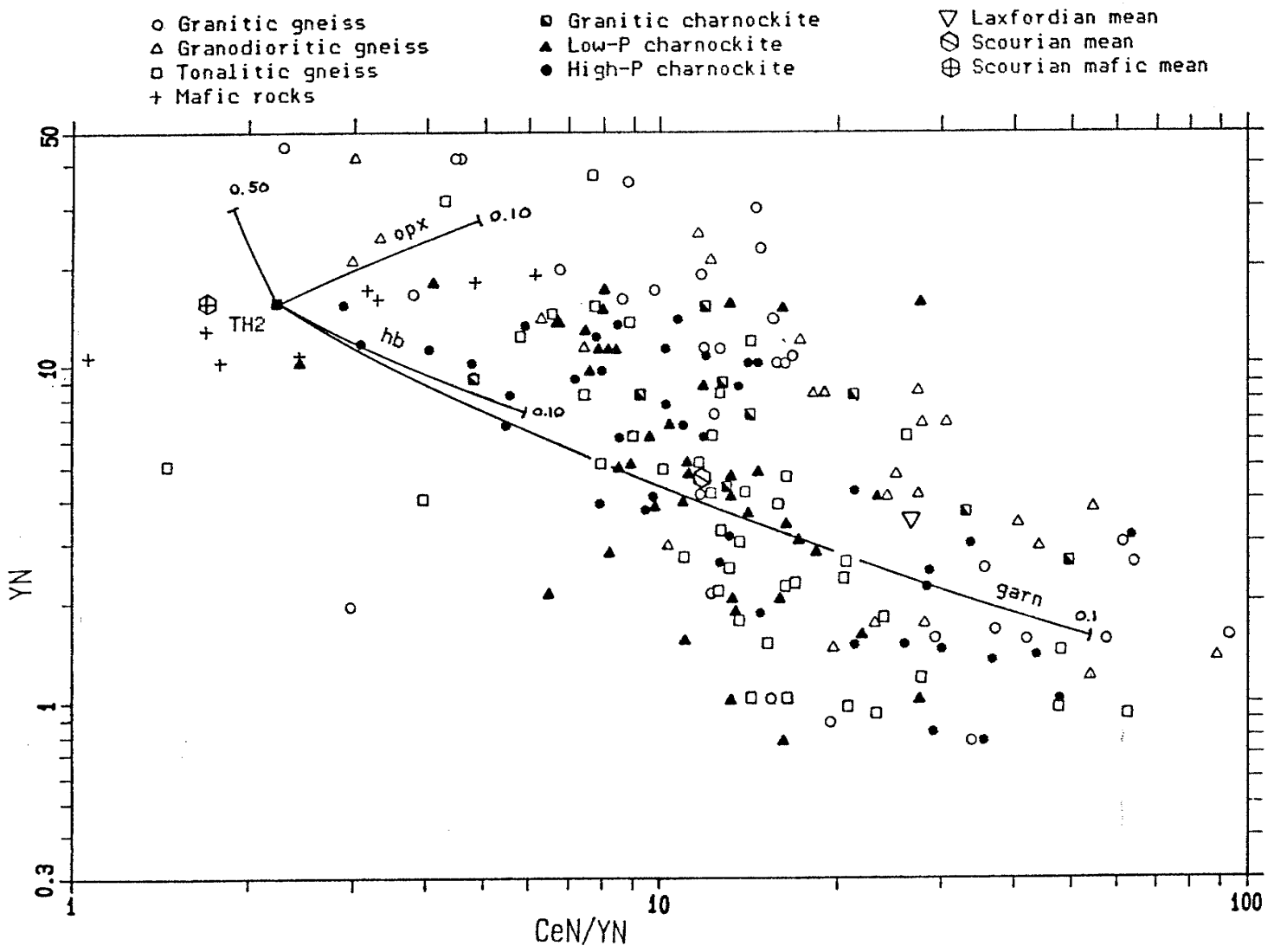

Fig. VI-5. YN vs CeN/YN plot. Data from Appendix C. Partial melting vectors to F=0.10 for garnet, hornblende, orthopyroxene, and plagioclase are shown.

The relationship between fractionation of lREE and hREE is shown on a CeN/TbN - TbN/YbN plot (Fig. VI-6). The pattern is largely scattered, however, there is a rough positive correlation between the fractionation of the lREE (CeN/TbN) and the hREE (TbN/YbN). Partial melting trajectories for garnet are shown at three different distribution coefficients, indicating the sensitivity of garnet fractionation to changes that effect distribution coefficients. It is apparent from the plot that a combination of hornblende and garnet in the residue is required to produce the levels of lREE fractionation, relative to hREE fractionation, that are observed in the south India samples (Fig. VI-6). Similar trends can be seen in the Scourian (Weaver and Tarney, 1980).

It is evident from the plots discussed above that a partial melting process with a combination of garnet, hornblende, pyroxene, and plagioclase in the residue can produce most of the tonalitic gneisses and charnockites. Of these mineral phases, garnet appears to play a greater role than hornblende in providing a range of values similar to the south India tonalites, for example, YN vs CeN/YN, CeN/TbN vs TbN/YbN, and Sc vs Y.

VI.3 Origin of granite - granitic gneiss

The origin of the Gneiss Terrane granitic gneisses, and to a lesser extent the granodioritic and tonalitic gneisses, poses a problem that requires additional study. These granitic gneisses have high total REE, depleted hREE, and significant -Eu anomalies, and higher Rb, Cs, Th, U, Pb, Sc, Y, Nb, and Ta than the granitic gneisses

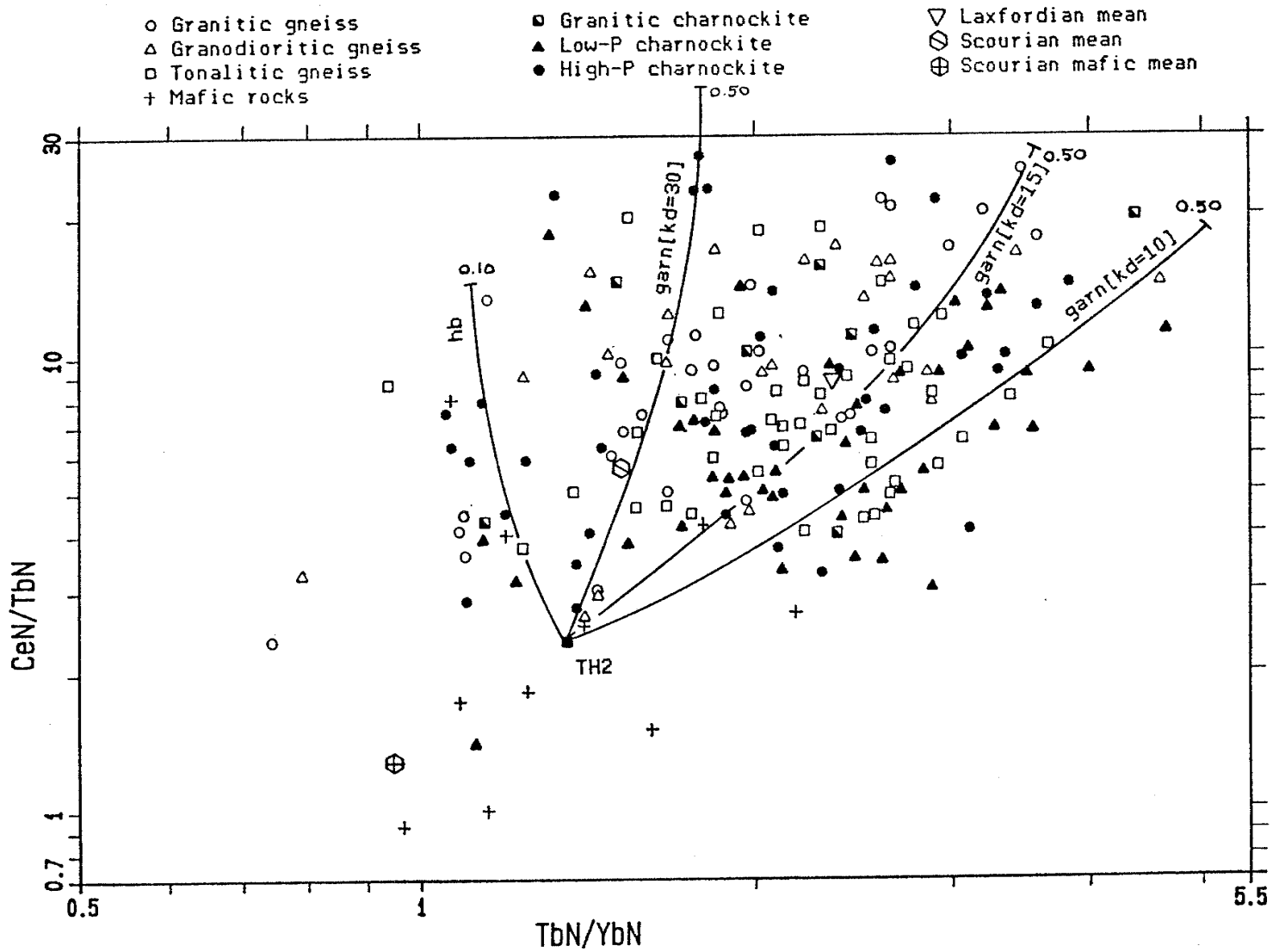

Fig. VI-6. CeN/TbN vs TbN/YbN plot. Data from Appendix C. The partial melting vector to F=0.10 is shown for hornblende. Three vectors, at different Kd values for Tb, are shown for garnet.

to the south, which have generally lower total REE, similarly depleted hREE, but +Eu anomalies and higher Ba and Sr. Though detailed mapping was carried out in the area where this change in chemistry apparently takes place, insufficient samples of gneiss from the mapped area were analysed to make a correlation with mapped lithologies possible. The different patterns and trends are particularly apparent on the K2O - Ba plot (Fig. V-30), where the gneisses have K/Ba ratios >40; the Eu/Eu* vs SiO2 plot (Fig. V-50); the total REE vs SiO2 plot (Fig. V-55); and the Sc vs Y and Nb vs TiO2 plots (Figs. VI-1, VI-2).

Two potential origins for the Gneiss Terrane granitic gneisses are 1) partial melting or fractional crystallization in partnership with gneisses from the Transition Zone, or 2) derivation from a source below the current level of exposed high-pressure granulite terrane. The region in which the majority of the Gneiss Terrane granitic gneiss samples were taken is the extensive area north and east of Bangalore towards Kolar, which covers about 1800 sq km. Additional granodioritic samples, with somewhat similar REE patterns, were taken west of Bangalore. If the tonalitic gneisses of the Transition Zone are involved in the genesis of the Gneiss Terrane granitic gneisses, they can represent either the source (CO), or the residue (Cs) following a partial melting event. (For simplicity, batch partial melting will be considered the operative process, fractional crystallization models give similar results.) For the first case, partial melting of an average Transition Zone tonalite could produce an evolved liquid with higher total REE and a -Eu anomaly, accompanied by a residual solid with lower total REE and a +Eu anomaly. Such an

evolved liquid would also be enriched in Rb, Cs, U, Th, Nb, and Ta, and the solid, assuming residual plagioclase, would be enriched in Ba and Sr. However, the volume of relatively depleted residue required to produce the Gneiss Terran gneiss is not observed in the field. In fact, the relative similarity in compostion of comparable gneiss groups throughout south India, with the exception of specific fluid-phase depletions discussed below, is striking.

The second case was briefly modeled using a straight forward partial melting (batch) model in which the original source (CO) and daughter liquid (CL) were calculated using the average value of the Transition Zone tonalitic gneiss as residue (Cs). The results (Figs. VI-7, VI-8) show that compared to the Gneiss Terrane granite, the model granite (CL) has higher lREE and lower hREE. For some trace elements (Th, Rb, Sm, Y, Tb, Nb, Ba, Sc, and Sr) the fit between the granite and the model are reasonably close. However, U and Ta are sharply lower in the Gneiss Terrane granitic gneisses. However, U has high variability in the Transition Zone and the estimated average value could be biased. Also, the modeled Ta concentration may be high because the assumed modal value of magnetite in the eutectic is high, and the distribution coefficient used for biotite may be too low. In general, there is variable uncertainty in the value of distribution coefficients; also the calculated components in partial melting models are sensitive to the presence or small changes in the trace abundances of allanite and zircon. In any case, a possible problem with considering tonalite as source to the Gneiss Terrane granite is the great volume of tonalite with similar major and trace element

Cs = residue after batch melting, equivalent to average Transition Zone tonalitic gneiss

C0 = calculated hypothetical source rock

CL = calculated evolved liquid for comparison with Gneiss Terrane granite

$$C0 = \frac{Cs(1-F)(D-PF+F)}{D-PF} \qquad CL = \frac{C0}{D+F(1-P)}$$

Dacite Kds

	plg	Kspar	biot	amph	mgt	apat	zir
Rb	.05	.35	3.3	.01	0	0	0
Ba	.4	5.0	10	.04	0	-	-
Sr	3.0	4.0	.12	.02	0	-	-
Th	.05	.01	.3	.01	.4	2	100
U	.06	.005	.02	.4	.14	-	-
Sc	.1	.02	10	10	8	0	60
Y	.06	.1	2.5	.03	.5	20	60
Nb	.03	.05	5.0	1.3	1.0	.1	50
Ta	.08	.05	1.0	1.5	5	0	50
La	.08	.05	.03	0.23	0	20	2.0
Sm	.1	.02	.06	4.0	0	63	3.1
Eu	.8	1.1	.15	3.5	0	30	3.5
Tb	.085	.006	.16	6.0	.1	20	100
Yb	.08	.01	.18	5.0	.1	25	200

	Mode	Eutectic
Qtz	.22	.30
Plg	.60	.30
Kspar	.05	.35
Biot	.07	.03
Amph	.027	.01
Mgt	.01	.008
Apat	.002	.001
Zir	.001	.001

Fig. VI-7. Model granite (CL). Terms, equations, and values used in the batch melting calculation of C0 and CL.

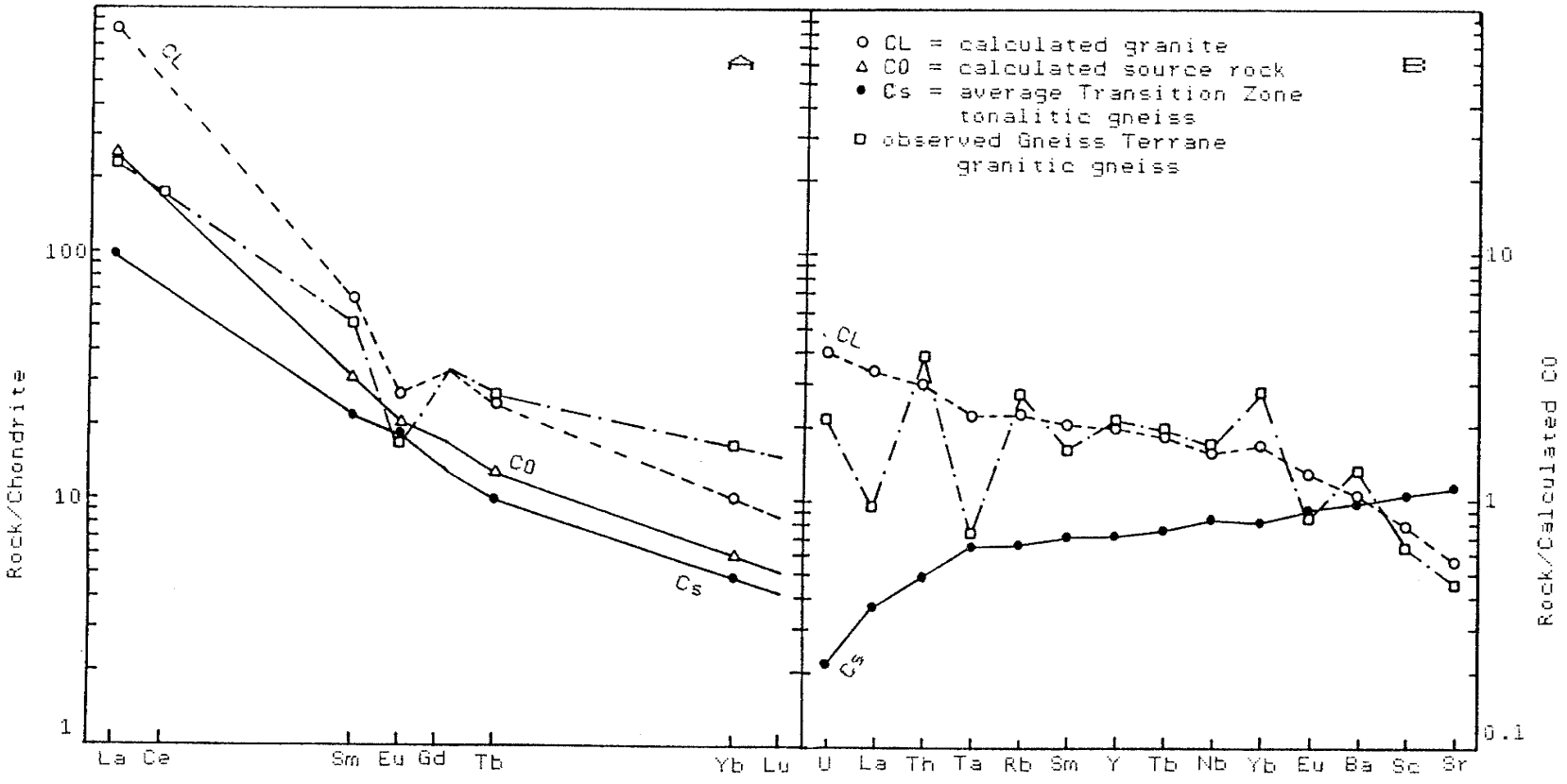

Fig. VI-8a. REE plot of model granite (CL) and observed GneissTerrane granitic gneiss.

Fig. VI-8b. Plot of model granite (CL) and Gneiss Terrane granitic gneiss normalized to calculated parent (CO).

chemistry. If any of the tonalite is residue, then all of the tonalite must be residue given the overall similarty of composition, for example the relatively narrow range of REE patterns. That demands a large volume of granitic gneiss in the Gneiss Terrane, a constraint that argues against mid-crustal derivation of these granitic gneisses. Also, examination of element-area diagrams shows a sharp change in the Gneiss Terrane mean values (and in many of the component rock groups) relative to the higher pressure terranes in south India. This suggests that the Gneiss Terrane granitic gneisses are derived from an outside source. Detailed modeling of these gneisses can sharpen the constraints on origin.

VI.4 Metamorphism and element depletion

Field evidence from the Gneiss Terrane and prograde Transition Zone indicate continuity of features and gradual change as metamorphic grade increases from amphibolite to granulite facies. Orthopyroxene replaces biotite across the orthopyroxene (charnockite margin) isograd, although later minor retrogression obscures the evidence. Consistent increases in temperature and pressure in the Transition Zone (Hansen et al., 1984) and in areas north and south of the transition also support the conclusion that the granulite-facies terrane represents exposure of increasingly lower levels of the crust. The high-pressure, higher grade terranes lie along or south of the Moyar-Bhavani shear zone, and the gradational change that is characteristic of the transition Zone terminates at the shear zone.

Partial melting of the lower crust, or fractional crystallization of a dacitic magma, have been suggested as possible mechanisms to produce a granodioritic upper crust and a refractory granulite in the lower crust (Drury, 1978; Field et al., 1980; Pride and Muecke, 1980). However, the similarity of REE distributions, most incompatible elements, and Ba/Sr ratios between amphibolite and granulite-facies gneisses argues against such an intracrustal melting process for south India. To account for the widespread observed differences in the chemistry between the low and high-grade Archaean crust, studies in south India and elsewhere have addressed the role of volatile-rich (especially CO2-rich) fluids as a depletion mechanism (Collerson and Fryer, 1978; Janardhan et al., 1979; Weaver and Tarney, 1981; this study, Section V.10.3). In south India, analyses of paired samples from across the actual gneiss-charnockite prograde metamorphic transition, which marks the passage of the CO2-rich fluid phase, do not reveal significant and consistent element movement. However, a comparison of amphibolite-facies gneisses and low-pressure charnockites from the Transition Zone with the deeper seated, medium and high-pressure charnockites indicates significant changes in the abundances of Rb, Cs, Th, U, Pb, and K.

These changes are similar to depletions observed in other Archaean terranes: the Canadian Shield (New Quebec) granulite facies is lower in U, Th, and K relative to the adjacent amphibolite facies (Fahrig et al., 1967; Eade and Fahrig, 1971); West Greenland granulite-facies gneisses are lower in U, Th, Rb, with higher K/Rb relative to adjacent amphibolite-facies gneisses (Kalsbeek, 1976;

Wells, 1979); N.W. Scotland (Scourian) granulite facies is lower in U, Th, Rb, Cs, and K, with higher K/Rb and undisturbed REE distribution relative to (Laxfordian) amphibolite facies (Sheraton, 1970; Holland and Lambert, 1975; Rollinson and Windley, 1980a; Weaver and Tarney, 1981); North Norway (Lofoten-Vesteralen) granulite facies is lower in U, Th, Rb, with higher K/Rb and undisturbed REE distribution relative to amphibolite facies (Green et al., 1969; Green et al., 1972; Jacobsen and Wasserburg, 1978; Heier, 1976); and the Western and Central Australia granulite facies is lower in U, Th, Rb, Cs, K, and higher K/Rb relative to the amphibolite facies (Lambert and Heier, 1968a; 1968b; Wilson, 1977).

However, there are Archaean-early Proterozoic high-grade areas that depart from this pattern: Brazil (Jequie Complex) granulite facies gneisses have high U, Rb, Cs, Y, and total REE (Sighinolfi et al., 1981); the North Finland (Fennoscandia) granulite facies are not depleted in Th, K, Ba, Sr, and have an uneven loss of Rb and U (Barbey and Cuney, 1982); South Norway (Svecofennian) granulite facies gneisses are lower in Rb, Ba, K with higher K/Rb relative to amphibolite facies gneisses, however, the amphibolite facies have significantly higher total REE, higher Ce/Yb, and negative Eu anomalies (Field et al., 1980); the Australia (Musgrave Block) granulite facies is low in U, but not in Th, Rb, K, Sr, and K/Rb is normal (Gray, 1977); and the Australia (Arunta Block) granulite facies is low in K, but K/Rb not high (Allen, 1979). These departures, from what has been considered characteristic element distributions in Archaean terranes, have been attributed to differences in the

lithologies of the protolith, effects of partial melting, variation in the CO2/H2O ratio of the fluid phase, different temperature-pressure regimes in the granulite-facies terranes from which samples are taken, and late stage retrogression.

In south India the depletion of Cs, Th, U, and especially Rb, apparently take a quantum jump in the high-P charnockites relative to amphibolite-grade gneisses (Figs. V-25, V-26, V-28, V-29, V-32, V-33, V-34, VI-9). An examination of the magnitude of these depletions in rocks of similar composition (tonalitic amphibolite-grade gneiss and tonalitic high-P charnockite) gives interesting results. In the comparison, tabulated values of K from two metamorphic terranes (Appendix C) are used, and average concentrations for Rb, Cs, Th, U, and Pb are estimated from their patterns on plots (Figs. V-25 to V-34). The results of this rough calculation show a ~24% loss of K2O (1.60% to 1.21%), a ~90% loss of Rb (~70ppm to ~6ppm), Cs (~0.8ppm to ~0.08ppm), and Th (~4ppm to ~0.4ppm), and a ~<85% loss of U (~0.9ppm to ~0.15ppm). Pb is difficult to estimate because so many results are below the detection limit, however, the loss is in the range of 25% to 50%. The depletion of K in the high-grade terrane of south India agrees well with the 29% loss of K2O (1.75% to 1.25%) observed between analogous terranes in the Lewisian (Rollinson and Windley, 1980a).

It was noted earlier (Section V.4.2) that the significant depletion of K ascribed to high grade terranes was largely the result of the predominance of tonalitic rocks, with characteristically low K, in that terrane. The magnitude of K depletion, when compared to Rb, Cs, Th, and U, supports the suggestion that K was not mobilized to the

same degree as these other elements. The behavior of Pb tends to mirror that of K. In the lithologies under consideration here, Rb and Cs predominantly substitute for K in biotite (Heier and Billings, 1970a; 1970b), and the breakdown of biotite in a CO2-rich fluid phase to produce orthopyroxene, K feldspar, and water (Winkler, 1979; Ravindra Kumar et al., 1985) would facilitate the mobilization of Rb and Cs. In addition, Rb is depleted relative to K in both K feldspar and the remaining biotite (R.C. Newton personal communication; Heier and Billings, 1970a). Cs is also lower in granulite-grade biotite relative to amphibolite grade biotite (Heier and Billings, 1970b). If the mineral-fluid distribution coefficients of Rb and Cs are similar to mineral-melt distribution coefficients for K feldspar and orthopyroxene (ie., <1) (Cf. Beswick, 1973; Shaw, 1978), then Rb and Cs will prefer to remain in the fluid phase.

The minerals present in the tonalitic gneisses and charnockites from south India most likely to host U and Th are biotite, hornblende, apatite, garnet, and zircon (Rogers and Adams, 1969a; 1969b). Allanite and sphene, both significant hosts for U and Th, are absent or present in very small trace amounts and probably do not contribute in a major way to the U and Th content of the rocks. The rate of depletion of U and Th in these minerals when exposed to a fluid phase is unknown; however, the mineral-melt distribution coefficients are <<1 and U and Th probably behave similarly to Rb: after the breakdown of biotite, U and Th will remain in the fluid phase and be flushed from the system. A rough calculation indicates that the breakdown of biotite can provide most of the observed

depletion of these two elements in south India high-P charnockites. The calculation assumes an approximate decrease in biotite from ~7% to ~2%, a 10ppm concentration of U in biotite (Rogers and Adams, 1969a; 1969b), and a Th/U ratio of 5 (Fig. V-34), which in turn places ~50ppm of Th in biotite. Though the Th/U ratio for biotite (Th/U=5) is taken from the average Th/U ratio of the whole rocks, this assumption is probably justified. Of the common minerals in tonalite, biotite and hornblende have very high and similar Th/U ratios (Rogers and Adams, 1969a), and the whole rock Th/U ratio either equals or is less than that of biotite and hornblende, since the other important U and Th host minerals have lower Th/U ratios. The result is a calculated decrease in U of ~0.7ppm to ~0.2ppm (observed values are ~0.9ppm to ~0.15ppm), and a depletion of Th from ~3.5ppm to ~1ppm (observed values are ~4ppm to ~0.4ppm). The actual loss of Th is greater than the calculated value, and Th depletion is thus greater than that of U. This is also observed on the U - Th plot (Fig. V-34) where there is an apparent decrease in the Th/U ratio in the high-P charnockites. Also, after initial depletion of Rb as seen on the Rb - Th plot (Fig. V-32), Rb concentration is generally invariant compared with Th. The behavior of Th relative to both U and Rb thus suggests that in addition to the destruction of biotite, and the major loss of Rb and U from the system, Th is still being depleted relative to Rb and U in the remaining biotite and other minerals.

Similar calculations can be made for K and Pb. If an average value of 7.5% K20 is assumed for biotite (Deer et al., 1966), an approximate decrease in biotite from 7% to 2% in the high-P charnockite will result in a K20 loss of ~0.37%, which compares favorably with the observed loss of ~0.39%. As a result, most of the depletion of Rb, Cs, Th, U, K, and Pb in the south India high-P charnockite can be produced by the destruction of biotite, entry of these elements into the fluid phase, and their removal from the system. The small loss of K, increasing K/Rb ratio, decreasing K/Ba ratio, and the relatively constant Sr and REE values and Ba/Sr ratios all suggest that K feldspar and plagioclase are not significantly effected by the fluid phase.

In south India, the REE do not appear to be significantly effected by increases in metamorphic grade (Section V.8.5, Fig. V-49). Observing similarly immobile REE together with highly mobile Rb in the Lewisian, Rollinson and Windley (1980a) used a modified zone-refining equation of Harris (1974) to study the depletion mechanisms for Rb relative to Ce. On a Rb - Rb/Ce plot they constructed a trajectory of Rb and Rb/Ce values relative to fluid volumes, using the relationship of $Cs=Co(1-(1-D)\exp(-nD)$ (where Cs=the residual concentration after the fluid phase has passed, Co= the original concentration, D=the bulk distribution coefficient of either Rb or Ce, and n=the ratio of rock volume/fluid volume). Similar trajectories are shown for the south India samples (Fig. VI-9) for two Rb mineral-fluid distribution coefficients. Beswick (1973) and Shaw (1978) report that mineral-fluid and mineral-melt distribution coefficients

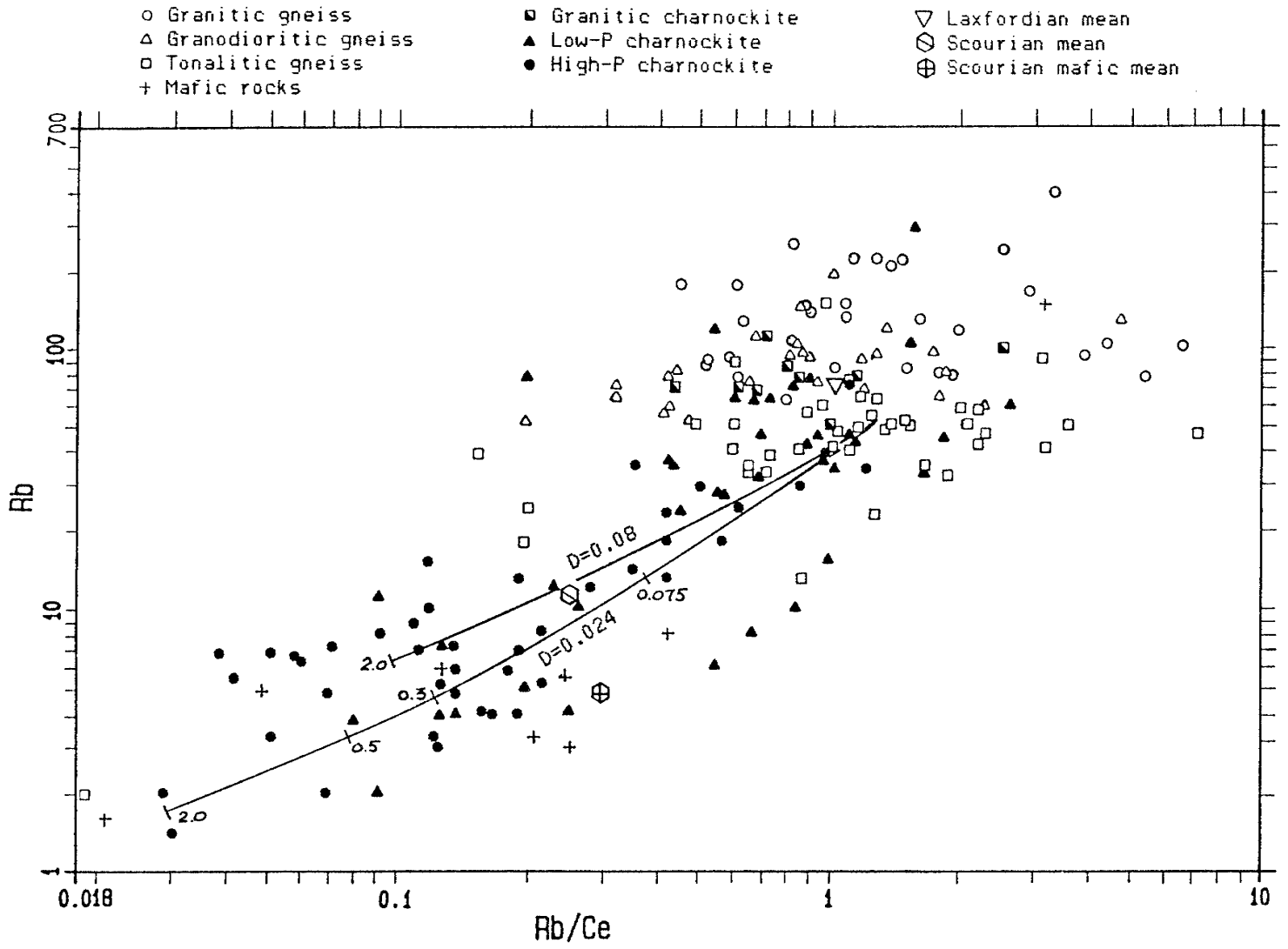

Fib. VI-9. Rb vs Rb/Ce plot. Data from Appendix C. Two trajectories of residual rock (Cs), after passage of indicated volumes of fluid phase, are shown for bulk distribution coefficients of D=0.08 and D=0.024.

for Rb are similar. Rollinson and Windley (1980a) use a bulk distribution coefficient for Rb of 0.024, which probably represents a mode without biotite. A bulk distribution coefficient of 0.08, which includes 2% biotite and 3% K feldspar in the mode, appears representative of average high-P charnockite from south India. The difference in the trajectories using these two bulk distribution coefficients is small; however, to achieve the very low levels of Rb in some of the south India charnockites, the distribution coefficient must be low.

Cullers et al. (1973) report a plagioclase mineral-fluid distribution coefficient for Ce of 25, two orders of magnitude greater than for the plagioclase mineral-melt coefficient of 0.27 (Arth, 1976; K.C. Condie, compiled data). Shaw (1978) felt the distribution coefficient of 25 was high and reduced it to 2.7, but for the zone-refining equation the difference in results is negligable. Though Rollinson and Windley (1980a) use a Ce bulk distribution coefficient of 14.25, a value of 1.7 is used here. Though the lREE have a high concentration in biotite (Herrmann, 1970) and would be released to the fluid phase with the breakdown of biotite, Ce and the other lREE, with mineral-fuid distribution coefficients >1 for plagioclase, preferentially move out of solution and into mineral phases. An average value of Rb=50 ppm and Rb/Ce=1.2 is used to represent undepleted south India tonalitic gneiss. The fluid trajectories on the Rb - Rb/Ce plot (Fig. VI-9) show that most of the depletion in Rb can be accounted for with 0.5 to 2 rock volumes of fluid, similar to the results reported for the Scourian (Rollinson and Windley, 1980a).

However, this approach to the depletion of Rb, Cs, Th, and U in high-grade rocks raises some interesting questions. First, there is no significant depletion along the orthopyroxene isograd, where the replacement of biotite by orthopyroxene, at least in its initial stages, does not result in observable element movement out of the rock. Secondly, the rate of depletion examined with the use of the zone-refining equation is dependent on the diffusion of Rb out of biotite, and other mineral phases, in response to their respective mineral-fluid distribution coefficients. These coefficients are <1 or <<1, except for biotite which has a distribution coefficient of 2-3.5. As a result, biotite with the greatest abundance of Rb (Heier and Billings, 1970) retains its Rb better than K feldspar and plagioclase. However, if biotite is totally destroyed there is no host for Rb to diffuse out of, the biotite distribution coefficient for any element would be zero, and all of the constituent elements would be in solution. As a result, the total breakdown of biotite appears to invalidate the use of the zone-refining equation.

An approach that satisfies these questions is to look at the rate of biotite replacement. At the charnockite margin, orthopyroxene is present but in relatively small amounts, and the abundance of biotite, in comparable samples across the margin, does not change significantly; though the level of biotite is substantially less in the high-pressure terrane (~2%), the averages for the amphibolite-facies gneisses and low-pressure charnockites are virtually the same (6-7%). Elements will be released from biotite as it is destroyed, however, fluid movement will be necessary to carry those elements

still in solution (Rb, Cs, Th, U, and some K and Pb) out of interstitial sites and out of the rock. The relatively good fit of the depletion trajectory on the Rb - Rb/Ce plot suggests that the bulk depletion of Rb out of its principal host mineral phases (biotite, K feldspar, plagioclase,and hornblende) occurs at approximately the same rate as the breakdown of biotite, and that once in solution the same volume of fluids required to leach the mineral-fluid incompatible elements from their host minerals is also required to remove these elements from the charnockite following the breakdown of biotite.

VI.5 South India and the nature of the lower crust

The image that emerges out of the results from south India is a lower to middle crust predominantly of tonalite derived from partial melting of an enriched tholeiite source with garnet, hornblende, pyroxene, and plagioclase in the residue. The deeper portions of the tonalite are emplaced or metamorphosed to a granulite-grade mineral assemblage primarily by a CO2 dominated volatile fluid-phase that essentially dewaters the hydrous phases of the tonalite and removes Rb, Cs, Th, U, and some K and Pb. Waves of H2O-rich and CO2-rich fluids successively promote and then pinch-off localized partial melting that produce small bodies of granites, particularly in the range of temperatures, pressures, and fortuitous H2O/CO2 fluid ratios found in that level of the crust now exposed as the prograde Transition Zone.

A recent estimate of the composition of average continental crust by Weaver and Tarney (1981) is based upon a model that considers the Archaean amphibolite and granulite-facies gneisses to best represent the middle and lower crust, respectively. This model is based upon the following assumptions: 1) 75-85% of the present volume of continental crust was formed by 2.5 by, at the end of the Archaean, and that the current middle and lower crust is predominantly of Archaean middle and lower crust composition, 2) post-Archaean additions to the middle and lower crust approximate Cordilleran-type, continental-margin magmatism, and 3) the upper crust (upper 1/3) has been relatively invariant in composition through the Archaean and post-Archaean. This model is compared with results predicted by the Taylor and McLennan (1981) "andesite" model, which assumes accreting island arcs form an average andesitic crust having a depleted, cumulus lower crust and an enriched, residual-liquid upper crust.

In the Weaver and Tarney (1984) model, the composition of the Lewisian amphibolite and granulite-facies gneisses are used to estimate an average continental crust. The composition of this continental crust is more silicious with higher Rb, Sr, Ba, Pb, Zr, Hf, and lREE, and a more fractionated REE pattern, than the Taylor and McLennan model (Table VI-1). Substituting the results for the south India Transition Zone gneisses (middle crust) and the south India high-P terrane charnockites (lower crust) for the compositions of the Lewisian gneisses in the Weaver and Tarney model gives an estimated average continental crust very similar to that of Weaver and Tarney, which is to be expected given the overall similarity of the Lewisian and south India compositions (Table VI-1). However, the estimate

ref.	T&M Upper Crust 1	Lewis. Middle Crust 2	India Middle Crust 3	Lewis Lower Crust 4	India Lower Crust 5	Post-Arch. Crust 6	W&T Av. Crust 7	India Av. Crust 8	T&M Av. Crust 9
SiO2	66.0	66.7	68.5	61.5	65.6	59.2	63.2	65.0	58.0
TiO2	0.6	0.3	0.4	0.5	0.5	0.9	0.6	0.6	0.8
Al2O3	16.0	16.0	15.5	15.6	15.9	17.2	16.1	16.1	18.0
FeOt	4.5	3.2	3.0	5.3	4.8	6.1	4.9	4.7	7.5
MnO	0.08	0.04	0.04	0.08	0.07	0.12	0.08	0.08	0.14
MgO	2.3	1.4	1.2	3.4	2.4	3.4	2.8	2.4	3.5
CaO	3.5	3.2	3.2	5.6	4.5	5.9	4.7	4.2	7.5
Na2O	3.8	4.9	4.5	4.4	4.2	4.0	4.2	4.1	3.5
K2O	3.3	2.1	2.8	1.0	1.2	2.4	2.1	2.3	1.5
P2O5	0.17	0.14	0.17	0.18	0.17	0.27	0.19	0.19	
Total	100.3	98.0	99.3	97.3	99.3	99.5	98.9	99.7	100.4
Rb	110	74	62	11	13	66	61	60	42
Sr	350	580	602	569	509	601	503	482	400
Ba	700	713	937	757	499	605	707	668	350
Th	10.5	8.4	8.0	0.42	1.4	6.0	5.7	6.0	4.8
U	2.5	2.2	0.6	0.05	0.2	1.25	1.3	1.2	1.25
Pb	15	22	11	13	~3.5	12	15	10	10
Y	22	9	15	7	13	15	14	17	22
Zr	240	193	179	202	134	181	210	183	100
Hf	5.8	3.8	4.9	3.6	3.5	5.8	4.7	4.8	3.0
Nb	25	6	8	5	5.3	10	13	13	11
Cr	35	32	25	88	79	45	56	52	55
Ni	20	20	17	58	41	27	35	29	30
La	30	36	43	22	31	29	28	32	19
Ce	64	69	79	44	60	61	57	64	38
Nd	26	30	27	19	22	23	23	24	16
Sm	4.5	4.4	4.8	3.3	5.1	4.9	4.1	4.8	3.7
Eu	0.88	1.09	1.5	1.18	1.3	1.29	1.09	1.2	1.1
Tb	0.64	0.41	0.54	0.43	0.47	0.65	0.53	0.57	0.64
Yb	2.2	0.76	1.3	1.2	1.1	1.5	1.53	1.56	2.2
Lu	0.32	0.1	0.2	0.18	0.18	0.24	0.23	0.24	0.30
Weight	8	3	3	9	9	4			
K/Rb	249	236	372	755	773	302	286	291	296
Rb/Sr	0.314	0.128	0.103	0.019	0.026	0.110	0.121	0.124	0.105
CeN/YbN	7.4	23	14	9.3	12	10.3	9.5	9.3	4.4

1) Estimate of upper crust from Taylor and McLennan (1981).
2) Composition of Archaean Lewisian amphibolite facies gneisses from Weaver and Tarney (1984).
3) Average south India Transition Zone gneiss, from Appendix C.9.5.
4) Composition of Archaean Lewisian granulite-facies gneisses from Weaver and Tarney (1984).
5) Average south India medium to high-P charnockite, from Table V-1.
6) Estimate of post-Archaean middle and lower crust, from Weaver and Tarney (1984).
7) Estimate of average continental crust using the weighted averages of T&M upper crust, Lewisian middle and lower crust, and post-Archaean crust. Proportion weights from Weaver and Tarney (1984).
8) Estimate of average continental crust using the weighted averages of T&M upper crust, south India middle and lower crust, and post-Archaean crust.
9) Average continental crust from Taylor and Mclennan (1981).

Table VI-1. Compositions of upper, middle, and lower crust, with estimates of average continental crust.

using the Indian results is slightly more silicic (SiO_2=65% vs 63.2%) and slightly less mafic (FeO+MgO=7.1% vs 7.7%) than the Weaver and Tarney estimate. Trace elements, in particular the REE, and element ratios are also very close.

The results from south India thus do not support the andesite model of Taylor and McLennan (1981), with a depleted, cumulus lower crust and an enriched, residual liquid upper crust. With the exception of Rb, Cs, Th, U, K, and Pb, which are lost to a CO_2-rich fluid phase and not the result of melt fractionation, the composition of the tonalitic high-pressure charnockites is in general comparable to the tonalitic component in the amphibolite-facies gneisses.

VII Conclusions

The major conclusions of this study are the following:

1.) The medium to high-pressure charnockite (granulite-facies) terrane has a lower proportion of granitic rock than the amphibolite-facies gneiss and low-pressure charnockite terranes. The mean composition of the higher grade terrane is tonalitic, and similar to tonalitic gneisses and low-pressure charnockites from the Transition Zone.

2.) Tonalitic gneiss and charnockite can be produced by the partial melting of a mafic parent with variable amounts of garnet, hornblende, pyroxene, and plagioclase in the residue. Garnet appears to play a more important role than hornblende in providing the range of REE depletions observed.

3.) The amphibolite-granulite transition is marked by the incipient replacement of biotite and hornblende by orthopyroxene (hypersthene), however, there is in general no significant element movement observed in this transition across the orthopyroxene isograd.

4.) In the medium and high-pressure charnockite terrane, there is significant depletion of Rb, Cs, Th, and U, and to a lesser degree K and Pb, relative to the amphibolite-facies gneiss and low-pressure charnockite terranes. The low K values observed in the high-grade terrane are largely the result of low K in the tonalitic gneiss

protoliths and not from fluid-phase depletion processes.

5.) The depletion of Rb, Cs, Th, and U, and some K and Pb, in the high grade terranes is the result of the breakdown of hydrous biotite in the presence of a CO2-rich fluid phase, which then progressively flushes these elements from the host rock. The lack of significant element movement in the Transition Zone, across the orthopyroxene isograd, is the result of relatively little biotite breakdown and the lack of sufficient fluid volume to flush the system.

6.) There is a significant compositional change in the granitic gneiss between the Transition Zone and the Gneiss Terrane. The former has high Ba and Sr, and low total REE with significant +Eu anomalies. Granitic gneisses from the Gneiss Terrane are enriched in Rb, Cs, Th, U, Nb, and Ta, and have a REE patterns that are characterized by high total REE with significant -Eu anomalies that are similar to other low-grade Archaean granites. This compositional change may correlate with a Bouguer gravity low that lies in the area of the Transition Zone granitic gneisses. Modeling shows that the enriched Gneiss Terrane granitic gneisses could be derived by partial melting of tonalitic gneiss but evidence of large volumes of residue is lacking.

References

Alderton D.H.M., Pearce J.A., Potts P.J. (1980) Rare earth mobility during granite alteration: Evidence from southwest England. Earth Planet. Sci. Lett. 49: 149-165.

Allen A.R. (1979) Metasomatism of a depleted granulite facies terrain in the Arunta Block, central Australia. Contrib. Mineral. Petrol. 71: 85-98.

Anantha Iyer G.V. and Narayanan Kutty (1975) Petrology of garnetiferous cordierite gneisses from the vicinity of the Closepet granite. Indian Jour. Earth Sci. 2: 125-141.

Armstrong R.L. and Hein S.M. (1973) Computer simulation of Pb and Sr isotope evolution of the earth's crust and upper mantle. Geochim. Cosmochim. Acta 37: 1-18.

Arth J.G. and Hanson G.N. (1972) Quartz diorites derived by partial melting of eclogite or amphibolite at mantle depths. Contrib. Mineral. Petrol. 37: 161-174.

Arth J.G. (1976) Behavior of trace elements during magmatic processes - a summary of theoretical models and their applications. Jour. Res. U.S. Geol. Survey 4: 41-47.

Arth J.G. and Barker F. (1976) Rare-earth partitioning between hornblende and dacitic liquid and implications for the genesis of trondhjemitic-tonalitic magmas. Geology 4: 534-536.

Bandurkin G.A. (1961) Behavior of the rare earths in fluorine-bearing media. Geochemistry No. 2: 143-149.

Barbey P. and Cuney M. (1982) K, Rb, Sr, Ba, U, and Th Geochemistry of the Lapland granulites (Fennoscandia). LILE fractionation controlling factors. Contrib. Mineral. Petrol. 81: 304-316.

Barker F. and Arth, J.G. (1976) Generation of trondhjemitic-tonalitic liquids and Archean bimodal trondhjemite-basalt suites. Geol. 4: 596-600.

Barker F. (1979) Trondhjemite: Definition, environment, and hypotheses of origin. In, Trondhjemites, dacites, and related rocks (ed. Barker F.). Elsevier, Amsterdam, 1-12.

Barker F., Arth J.G., Hudson T. (1981) Tonalites in crustal evolution. Phil. Trans. R. Soc. Lon. A301: 293-303.

Barron E.J., Harrison C.G.A., Hay W.W. (1978) A revised reconstruction of the southern continents. EOS Trans. Amer. Geophys. Union 59: 436-449.

Barsukova M.L., Kuznetsov V.A., Dorofeyeva, V.A., Khodakovskiy L.I. (1979) Measurement of the solubility of rutile TiO2 in fluride solutions at elevated temperatures. Geokhimiya 7: 1017-1027.

Barth T.F.W. (1959) Principles of classification and norm calculation of metamorphic rocks. Jour. Geol. 67: 135-152.

Barth T.F.W. (1962) A final proposal for calculating the mesonorm of metamorphic rocks. Jour. Geol. 70: 497-498.

Bavington O.A. and Taylor S.R. (1980) Rare earth element abundances in Archaean metasediments from Kambalda, Western Australia. Geochim. Cosmochim. Acta 44: 639-648.

Beach A. and Tarney J. (1978) Major and trace element patterns established during retrogressive metamorphism of granulite-facies gneisses, NW Scotland. Precamb. Res. 7: 325-348.

Beckinsale R.D., Drury S.A., Holt R.W. (1980) 3,360-Myr old gneisses from the South India Craton. Nature 283: 469-470.

Beckinsale R.D., Reeves-Smith G.J., Gale N.H., Holt R.W. and Thompson B. (1982) Rb-Sr and Pb-Pb whole rock isochron ages and REE data for Archaean gneisses and granites, Karnataka State, south India. In, Indo-US workshop on Precambrians of south India, Abstracts of the papers. National Geophysical Reserch Inst., Hyderabad, India, 35-36.

Beswick A.E. (1973) An experimental study of alkali metal distributions in feldspars and micas. Geochim. Cosmochim. Acta 37: 183-208.

Beus A.A. (1958) The role of complexes in transfers and accumulations of rare elements in endogenic solutions. Geochemistry No. 4: 388-397.

Bhattacharyya G.K., and Johnson R.A. (1977) Statistical concepts and methods. Wiley and Sons, New York, 639 p.

Bridgewater D. and Collerson K.D. (1976) The major petrological and geochemical characters of the 3,600 m.y. Uivak gneisses from Labrador. Contrib. Mineral. Petrol. 54: 43-59.

Buhl D., Grauert B., Raith M. (1983) U-Pb zircon dating of Archean rocks from the south India craton: Results from the amphibolite to granulite facies transition zone at Kabbal Quarry, southern Karnataka. Fortsch. Mineral. 61: 43-45.

Butler J.R. and Thompson A.J. (1965) Zirconium:Hafnium ratio in some igneous rocks. Geochim. Cosmochim. Acta 29: 167.

Chadwick B., Ramakrishnan M., Viswanatha M.N. (1981) Structural and metamorphic relations between Sargur and Dharwar supracrustal rocks and Peninsular Gneiss in central Karnataka. Jour. Geol. Soc. India 22: 557-569.

Collerson K.D. and Fryer B.J. (1978) The role of fluids in the formation and subsequent development of early continental crust. Contrib. Mineral. Petrol. 67: 151-167.

Compton P. (1978) Rare earth evidence for the origin of the Nuk gneisses, Buksefjorden region, southern West Greenland. Contrib. Mineral. Petrol. 66: 283-293.

Condie K.C. (1969) Petrology and geochemistry of the Laramie batholith and related metamorphic rocks of Precambrian age, eastern Wyoming. Bull. Geol. Soc. Am. 80: 57-82.

Condie K.C., Hunter D.R. (1976) Trace element geochemistry of Archaean granitic rocks from the Barberton region, South Africa. Earth Planet. Sci. Lett. 29:389-400.

Condie K.C. (1981a) Archaean greenstone belts. Elsevier, Amsterdam, 434 pp.

Condie K.C. (1981b) Geochemical and isotopic constraints on the origin and source of Archean granites. Spec. Publs. Geol. Soc. Aust. 7: 469-479.

Condie K.C., Allen P., Narayana B.L. (1982) Geochemistry of the low- to high-grade transition zone, southern India. Contr. Miner. Petrol. 81: 157-167.

Condie K.C. and Allen P. (1984) Origin of Archean charnockites from southern India. In, Archaean geochemistry (eds. Kroner A., Goodwin A.M., Hanson G.M.). Springer-Verlag, Berlin, 182-203.

Crawford A.R. (1969) Reconnaissance Rb-Sr dating of the Precambrian rocks of southern Peninsular India. Jour. Geol. Soc. India 10: 117-166.

Crawford A.R. (1974) Indo-Antarctica, Gondwanaland, and the distortion of a granulite belt. Tectonophysics 22: 141-157.

Crawford A.R. (1978) Narmada-Son lineament of India traced into Madegascar. Jour. Geol. Soc. India 19: 144-153.

Cullers R.L., Medaris L.G., Haskin L.A. (1973) Experimental studies of the distribution of rare earths as trace elements among silicate minerals and liquids and water. Geochim. Cosmochim. Acta 37: 1499-1512.

Deer W.A., Howie R.A., Zussman J. (1966) An introduction to the rock-forming minerals. Longman, London, 528 p.

DePaolo D.J., Manton W.I., Grew E.S., Halpern, M. (1982) Sm-Nd, Rb-Sr, and U-Th-Pb systematics of granulite rocks from Fyfe Hills, Endeby Land, Antarctica. Nature 298: 614-618.

Divakara Rao V., Naqvi S.M., Satyanarayana K., Hussain S.M. (1974) Geochemistry and origin of the Peninsular Gneisses of Karnataka, India. Jour. Geol. Soc. India 15: 270-277.

Drury S.A. (1973) The geochemistry of Precambrian granulite-facies rocks from the Lewisian complex ot Tiree, Inner Hebrides, Scotland. Chem. Geol. 11: 167-188.

Drury S.A. (1974) REE distribution in a high-grade Archaean gneiss complex in Scotland: Implications for the genesis of ancient sialic crust. Precamb. Res. 7: 237-257.

Drury S.A. and Holt R.W. (1980) The tectonic framework of the south Indian craton: a reconnaissance involving LANDSAT imagery. Tectonophysics 65: T1-T15.

Drury S.A., Holt R.W., Van Calsteren P.C., Beckinsale R.D. (1983) Sm-Nd and Rb-Sr ages for Archaean rocks in western Karnataka, south India. Jour. Geol. Soc. India 24: 454-459.

Drury S.A., Harris N.B.W., Holt R.W., Reeves-Smith G.J., Wightman R.T. (1984) Precambrian tectonics and crustal evolution in south India. Jour. Geol. 92: 3-20.

Eade K.E. and Fahrig W.F. (1973) Regional, lithological, and temporal variation in the abundances of some trace elements in the Canadian Shield. Geol. Survey Canada Paper 72-46, 46 p.

Erlank A.J., Smith H.S., Marchant J.W., Cardoso M.P., Ahrens L.H. (1978a) Zirconium (sections B-O). In, Handbook of geochemistry. Springer-Verlag, Berlin.

Erlank A.J., Smith H.S., Marchant J.W., Cardoso M.P., Ahrens L.H. (1978b) Hafnium (sections B-O). In, Handbook of geochemistry. Springer-Verlag, Berlin.

Ermonovics I.F. and Davison W.L. (1976) The Pikwitonei granulites in relation to the northwestern Superior Province of the Canadian Shield. In, The early history of the earth (ed. Windley B.F.). Wiley and Sons, London, 331-347.

Flynn R.T. and Burnham C.W. (1978) An experimental determination of rare earth partition coefficients between a chloride containing vapor phase and silicate melts. Geochim. Cosmochim. Acta 42: 685-701.

Friend C.R.L. (1981) Charnockite and granite formation and influx of CO2 at Kabbuldurga. Nature 294: 550-552.

Friend C.R.L. (1983) The link between charnockite formation and granite productin: Evidencefrom Kabbuldurga, Karnataka, southern India. In, Migmatites, melting, and metamorphism (eds. Atherton M.P. and Gribble C.D.). Shiva Pub., Cheshire, U.K., 264-276.

Friend C.R.L. (1984) The origins of the Closepet granites and the implications for the crustal evolution of southern Karnataka. Jour. Geol. Soc. India 25: 73-84.

Gerasimovskiy V.I., Nesmeyanova L.I., Kakhana M.M. and Khazizova V.D. (1972) Trends in the Zr and Hf distributions for lavas of the East African Rift zones. Geochemistry No. 12: 1078-1086.

Gibson I.L. and Jagam P. (1980) Instrumental neutron activation analysis of rocks and minerals. In, Short course in neutron activation analysis in the geosciences (ed. G.K. Muecke). Mineralogical Association of Canada, Halifax, 109-131.

Gladney E.S., Burns C.E., Roelandts (1983) 1982 Compilation of elemental concentrations in eleven United States Geological Survey rock standards. Geostandards Newsletter 7: 3-226.

Glickson A.Y. and Lambert I.B. (1973) Relations in space and time between major Precambrian shield units: An interpretation of western Australian data. Earth Plan. Sci. Lett. 20: 395-403.

Gopalakrishnan K., Sugavaram E.B., Rao V.B. (1975) Are there rocks older than Dharwars? A reference to rocks in Tamil Nadu. Indian Mineral. 16: 26-34.

Gordon G.E., Randle K., Goles G., Corliss J., Beeson M., Oxley S. (1968) Instrumental neutron activation analysis of standard rocks with high resolution gamma-ray detectors. Geochim. Cosmochim. Acta 32: 369-396.

Green T.H., Brunfelt A.O., Heier K.S. (1972) Rare-earth element distribution and K/Rb ratios in granulites, mangerites, and anorthosites, Lofoten-Vesteraalen, Norway. Geochim. Cosmochim. Acta 36: 241-257.

Grew E.S. (1978) Precambrian basement at Molodezhnaya Station, East Antarctica. Geol. Soc. Amer. Bull. 89: 801-813.

Grew E.S. and Manton W.I. (1979) Archean rocks in Antarctica: 2.5-billion-year uranium-lead ages of pegmatites in Enderby Land. Science 206: 443-445.

Grew E.S. (1981) Granulite-facies metamorphism at Molodezhnaya Station, East Antarctica. Jour. Petrol. 22: 297-336.

Grew E.S. (1984) Age of allanite from Kabbaldurga quarry, Karnataka. Jour. Geol. Soc. India 25: 193-195.

Gupta M.L., Singh S.B., Sharma S.R., Saxena V.K., Drolia R.K. (1979) Terrestrial heat flow, hydrothermal activity, and geothermal resources. NGRI Geophys. Res. Bull. 17: 243-258.

Gupta M.L. (1982) Heat flow in the Indian Peninsula - Its geological and geophysical implications. Tectonophysics 83: 71-90.

Harris N.B.W., Holt R.W., Drury S.A. (1982) Geobarometry, geothermometry, and late Archean geotherms from the granulite facies terrain of south India. Jour. Geol. 90: 509-527.

Harris N.B.W. and Jayaram S. (1982) Metamorphism of cordierite gneisses from the Bangalore region of the Indian Archaean. Lithos 15: 89-98.

Harris P.G. (1974) Origin of alkaline magmas as a result of anatexis. In, The alkaline rocks (ed. Sorensen H.). Wiley and Sons, London, 427-436.

Haskin L.A., Haskin M.A., Frey F.A., Wildeman T.R. (1968) Relative and absolute terrestrial abundances of the rare earths. In, Origins and distributions of the elements (ed. Ahrens L.H.). Pergamon, Oxford, 889-912.

Heier K.S. and Adams J.A.S. (1964) The geochemistry of the alkali metals. Phys. Chem. Earth 5: 253-381.

Heier K.S. and Billings G.K. (1970a) Rubidium (sections B-C*, D-E, G, I-N). In, Handbook of geochemistry. Springer-Verlag, Berlin.

Heier K.S. and Billings G.K. (1970b) Cesium (sections B-C*, D-E, G, I-N). In, Handbook of geochemistry. Springer-Verlag, Berlin.

Heier K.S. (1973) Geochemistry of granulite facies rocks and problems of their origin. Phil. Trans. R. Soc. Lon. A273: 429-442.

Heinrichs H., Schulz-Dobrick B., Wedepohl K.H. (1980) Terrestrial geochemistry of Cd, Bi, Tl, Pb, Zn, and Rb. Geochim. Cosmochim. Acta 44: 1519-1533.

Henderson P. (1982) Inorganic geochemistry. Pergamon, New York, 353 p.

Herrmann A.G. (1970) Yttrium and lanthanides (sections B-M, O). In, Handbook of geochemistry. Springer-Verlag, Berlin.

Holland J.G. and Lambert R.St.J. (1975) The chemistry and origin of the Lewisian gneisses of the Scottish mainland: The Scourie and Inver assemblages and sub-crustal accretion. Precamb. Res. 2: 161-188.

Holland T.H. (1893) The petrology of Job Charnock's tombstone. Jour. Asiatic Soc. Bengal 62.

Holland T.H. (1900) The charnockite series, a group of Archaean hypersthene rocks in Peninsular India. Mem. Geol. Soc. India 28: 192-249.

Holt R.W. and Wightman R.T. (1983) The role of fluids in the development of a granulite-facies transition zone in south India. Jour. Geol. Soc. Lon. 140: 651-656.

Huang W.L. and Wyllie P.J. (1975) Melting reactions in the system $NaAlSi_3O_8$-$KAlSi_3O_8$-SiO_2 to 35 kilobars, dry and with excess water. Jour. Geol. 83: 737-748.

Hunter D.R. (1974) Crustal development in the Kaapvaal craton, II. The Proterozoic. Precamb. Res. 1: 295-326.

Hunter D.R., Barker F., Millard Jr. H.T. (1978) The geochemical nature of the Archaean Ancient Gneiss Complex and granodiorite suite, Swaziland: A preliminary study. Precamb. Res. 7: 105-127.

Hynes A. (1980) Carbonatization and mobility of Ti, Y, and Zr in Ascot Formation metabasalts, SE Quebec. Contrib. Mineral. Petro. 75: 79-87.

Janardhan A.S., Newton R.C., Smith J.V. (1979) Ancient crustal metamorhism at low P_{H_2O}: charnockite formation at Kabbuldurga, south India. Nature 278: 511-514.

Janardhan A.S., Newton R.C., Hansen, E.C. (1982) The transformation of amphibolite facies gneiss to charnockite in southern Karnataka and northern Tamil Nadu, India. Contrib. Miner. Petrol. 79: 130-149.

Janardhan A.S. and Vidal Ph. (1982) Rb-Sr dating of the Gundlupet gneiss around Gundlupet, southern Karnataka. Jour. Geol. Soc. India 23: 578-580.

Janardhan A.S. and Gopalakrishna D. (1983) Pressure-temperature estimates of the basic granulites and conditions of metamorphism in Sargur terrain, southern Karnataka and adjoining areas. Jour. Geol. Soc. India 24: 219-228.

Jayaram S., Venakatasubramanium V.S., Radhakrishna B.P. (1976) Rb-Sr ages of cordierite-gneisses of southern Karnataka. Jour. Geol. Soc. India 17: 557-561.

Kaila K.L., Roy Chowdhury K., Reddy P.R., Krishna V.G., Hari Narain, Subbotin V.B., Sollogub V.B., Chekunov A.V. Kharetchko G.E., Lazarenko M.A., Ilchenko T.V. (1979) Crustal structure along Kavali-Udipi profile in the Indian Peninsular Shield from Deep Seismic Sounding. Jour. Geol. Soc. India 20: 307-333.

Kaila K.L., Reddy P.R., Dixit M.M. (1981) Deep crustal structure at Koyna, Maharashtra, indicated by Deep Seismic Soundings. Jour. Geol. Soc. India 22: 1-16.

Kailasam L.N. (1979) Plateau uplift in Peninsular India. Tectonophysics 61: 243-269.

Kalsbeek F. (1976) Metamorphism of Archaean rocks of West Greenland. In, The early history of the earth (ed. Windley B.F.). Wiley and Sons, London, 225-235.

Katz M.B. and Premoli C. (1979) India and Madagascar in Gondwanaland based on matching Precambrian lineaments. Nature 279: 312-315.

Korzhinskiy M.A. (1981) Apatite solid solutions as indicators of the fugacity of HClO and HFO in hydrothermal fluids. Geochemistry International 18: 44-60.

Kosinowski M.H.F. (1982) MSONRM, a Fortran program for the improved version of mesonorm calculation. Computers and Geoscience 8: 11-20.

Kosterin A.V. (1959) The possible modes of transport of the rare earths by hydrothermal solutions. Geochemstry No. 4: 381-387.

Krauskopf K.B. (1957) The heavy metal content of magmatic vapor at 600 degrees C. Econ. Geol. 52: 786-807.

Kroner A. (1977) The Precambrian geotectonic evolution of Africa: Plate accretion versus plate destruction. Precamb. Res. 4: 163-213.

Lambert R.St.J., Chamberlain, V.E., Holland J.G. (1976) The geochemistry of Archaean rocks. In, The early history of the earth (ed., Windley B.F.), Wiley and Sons, London, 377-387.

Lambert R.St.J. and Holland J.G. (1976) Amitsoq gneiss geochemistry: Preliminary observations. In, The early history of the earth (ed., Windley B.F.), Wiley and Sons, London, 191-201.

Lewis J.D. and Spooner C.M. (1973) K/Rb ratios in Precambrian granulite terranes. Geochim. Cosmochim. Acta 37: 1111-1118.

Leyreloup A., Dupuy C., Andriambololona R. (1977) Catazonal xenoliths in French Neogene volcanic rocks: Constitution of the lower crust. Contrib. Mineral. Petrol. 62: 283-300.

Luth W.C., Jahns R.H., Tuttle O.F. (The granite system at pressures of 4 to 10 kilobars. Jour. Geophys. Res. 69: 759-773.

Lyakovich V.V. and Shevaleevskii I.D. (1962) Zr:Hf ratio in accessory zircon of granitoids. Geochemistry No. 5: 508-524.

McCarthy T.S. (1976) Chemical interrelationships in a low-pressure granulite terrain in Namaqualand, South Africa, and their bearing on granite genesis and the composition of the lower crust. Geochim. Cosmochim. Acta 40: 1057-1068.

Mahabaleswar B. and Sodashivaiah M.S. (1976) Charnockite of Sivasamudram area, Karnataka. In, Studies in Precambrians, Bangalore Univ., Bangalore. pp. 74-89.

Mason B. and Moore C.B. (1982) Principles of Geochemistry, 4th ed. Wiley and Sons, New York, 344p.

Michard A., Alberede F., Michard G., Minster J.F., Charlou, J.L. (1983) Rare-earth elements and uranium in high-temperature solutions from East Pacific Rise hydrothermal vent field (13 degree N). Nature 303: 795-797.

Mielke P. and Winkler H.G.F. (1979) Eine bessere berechnung der mesonorm fuer granitische gesteine. Neues Jahrb. Miner. Monatsh. 10: 471-480.

Mineyev D.A. (1963) Geochemical differentiation of the rare earths. Geochemistry No. 12: 1129-1149.

Minor M.M., Hensley W.K., Denton M.M., Garcia S.R. (1982) An automated activation analysis system. Jour. Radioanalytical Chem. 70: 459-471.

Moorbath S., Welke H., Gale N.H. (1969) The significance of lead isotope studies in ancient high grade metamorphic basement complexes as exemplified by the Lewisian rocks of northwest Scotland. Earth Planet. Sci. Lett. 6: 245-256.

Morgan J.W. and Wandless G.A. (1980) Rare earth element distribution in some hydrothermal minerals: Evidence for crystallographic control. Geochim. Cosmochim. Acta 44: 973-980.

NGRI. See, National Geophysical Research Institute.

Nance W.B. and Taylor S.R. (1976) Rare earth element patterns and crustal evolution. I. Australian post-Archaean sedimetary rocks. Geochim. Cosmochim. Acta 40: 1539-1551.

Naqvi S.M., Divakara Rao V., Hari Narain (1978) The primitive crust: evidence from the Indian Shield. Precamb. Res. 6: 323-345.

Naqvi S.M., Narayana B.L., Rama Rao P., Ahmad S.M., Uday Raj B. (1980) Geology and geochemistry of paragneisses from the Javanahalli schist belt, Karnataka, India. Jour. Geol. Soc. India 21: 577-592.

Naqvi S.M. (1981) The oldest supracrustals of the Dharwar Craton, India. Jour. Geol. Soc. India 22: 458-469.

Naqvi S.M., Condie K.C., Allen P (1983) Geochemistry of some unusual early Archaean sediments from the Dharwar Craton, India. Precamb. Res. 22: 125-147.

National Geophysical Research Institute (1978) Gravity map series of India. Nat. Geophys. Res. Inst., Hyderabad, India. Five maps and explanatory brochure.

Naumov G.B. (1959) Transportation of uranium in hydrothermal solutions as a carbonate. Geochemistry No.4: 5-20.

Newton R.C. (1978) Experimental and thermodynamic evidence for the operation of high pressures in Archaean metamorphism. In, Archaean geochemistry (eds. Windley B.F. and Naqvi S.M.). Elsevier, New York, 221-240.

Newton R.C., Smith J.V., Windley B.F. (1980) Carbonic metamorphism, granulites and crustal growth. Nature 288: 45-49.

Norrish K. and Hutton J.T. (1969) An accurate X-ray spectrographic method for the analysis of a wide range of geological samples. Geochim. Cosmochim. Acta 33: 431-453.

Norrish K. and Chappell B.W. (1977) X-ray fluoresence spectrometry. In, Physical methods in determinitive mineralogy (ed. J.Zussman). Academic Press Inc., London, 235-237, 257-262.

Nriagu J.O. (1971) Experimental investigation of a portion of the system PbS-NaCl-HCl-H2O at elevated temperatures. Am. Jour. Sci. 271: 157-169.

O'Connor J.T. (1965) A classification for quartz-rich igneous rocks based on feldspar ratios. U.S. Geol. Surv. Prof. Pap. 525-B: 79-84.

O'Hara M.J. and Yarwood G. (1978) High pressure-temperature point on

an Archaean geotherm, implied magma genesis by crustal anatexis, and consequences for garnet-pyroxene thermometry and barometry. Phil. Tran. R. Soc. Lon. A288: 441-456.

O'Nions R.K. and Pankhurst R.J. (1974) Rare-earth element distribution in Archaean gneisses and anorthosites, Godthab area, West Greenland. Earth Planet. Sci. Lett. 22: 328-338.

O'Nions R.K. and Pankhurst R.J. (1978) Early Archaean rocks and geochemical evolution of the earth's crust. Earth Planet. Sci. Lett. 38:211-236.

Pavlenko A.S., Vainshtein E.E., Shevaleevskii I.D. (1957) On the hafnium-zirconium ratio in zircons of igneous and metamorphic rocks. Geochemistry No. 5: 411-430.

Pearce J.A. and Cann J.R. (1973) Tectonic setting of basic volcanic rocks determined using trace element analyses. Earth Planet. Sci. Lett. 19: 290-300.

Puchelt, H. (1972) Barium (sections B-O). In, Handbook of geochemistry. Springer-Verlag, Berlin.

Pichamuthu C.S. (1953) The charnockite problem. Mysore Geologists Assoc., Bangalore, India, 178 p.

Pichamuthu C.S. (1960) Charnockite in the making. Nature 188: 135-136.

Pichamuthu C.S. (1961) Transformation of Peninsular Gneiss into charnockite in Mysore State, India. Jour. Geol. Soc. India 2: 46-49.

Pichamuthu C.S. (1969) Nomenclature of charnockite. Indian Mineral. 10: 23-35.

Pichamuthu C.S. (1970) Some observations on the Peninsular Gneiss complex. In, West commemoration Volume. Saugar University, 82-97.

Pichamuthu C.S. 1972) Job Charnock and charnockite. Jour. Geol. Soc. India 13: 86-91.

Pichamuthu C.S. 1976) Some problems pertaining to the Peninsular Gneissic Complex. Jour. Geol. Soc. India 17: 1-16.

Pichamuthu C.S. 1982) Schist-gneiss relationship in the Archaean of Dharwar Craton. Current Science 51: 118-124.

Powell C.McA., Johnson B.D. and Veevers J.J. (1980) A revised fit of east and west Gondwanaland. Tectonophysics 63: 13-29.

Pride C. and Muecke G.K. (1980) Rare earth element geochemistry of the Scourian Complex N.W. Scotland - evidence for the granite-granulite link. Contrib. Mineral. Petrol. 73: 403-412.

Pride C. and Muecke G.K. (1982) Geochemistry and origin of granitic rocks, Scourian Complex, NW Scotland. Contrib. Mineral. Petrol. 80: 379-385.

Raith M., Raase P., Ackermand D., Lal R.K. (1982) The Archaean craton of southern India: Metamorphic evolution and P-T conditions. Geol. Rundschau 71: 280-290.

Raith M., Rasse P., Ackermand R.K., Lal R.K. (1983) Regional geothermobarometry in the granulite facies terrain of southern India. Trans. Royal Soc. Edinburgh 73: 221-244

Rajagoplan P.T., Jayaram S., Venkatasubramaniam V.S. (1980) Rb-Sr isochron ags of gneisses in the western region of the Dharwar craton. Jour. Geol. Soc. India. 21: 54-56.

Ramakrishnan M., Viswanatha M.N., Nath J.S. (1976) Basement-cover relationships of Peninsular Gneiss with high grade schists and greenstone belts of southern Karnataka. Jour. Geol. Soc. India 17: 97-111.

Ramakrishnan M., Moorbath S., Taylor P.N., Anatha Iyer G.V., Viswanatha M.N. (1984) Rb-Sr and Pb-Pb whole rock isochron ages of basement gneisses in Karnataka craton. Jour. Geol. Soc. India 25: 20-34.

Ramakrishnan M. and Viswanatha M.N. (1983) Crustal evolution of Karnataka Craton: A review of present data and models. In, Proceedings of the Indo-US workshop on the Precambrians of south India (ed. Naqvi S.M.). National Geophysical Research Inst., Hyderabad.

Rama Rao P., Divakara Rao V., Subrahmanyam C. (1979) Integrated geological, geochemical, and geophysical investigations in the Peninsular Shield - A review. NGRI Geophys. Res. Bull. 17: 361-373.

Ramiengar A.S., Ramakrishnan M., Viswanatha M.N. (1978) Charnockite - gneiss-complex relationship in southern Karnataka. Jour. Geol. Soc. India 19: 411-419.

Rao R.U.M. and Jessop A.M. (1975) A comparison of the thermal characters of shields. Canadian Jour. Earth Sci. 12: 347-360.

Rao R.U.M., Rao G.V., Reddy G.K. (1982) Age dependence of continental heat flow - Fantasy and facts. Earth Planet. Sci. Lett. 59: 288-302.

Ravindra Kumar G.R., Srikantappa C., Hansen E. (1985) Charnockite formation at Ponmudi in southern India. Nature 313: 207-209.

Ray S. (1972) "Charnockites" of Kabbul, Mysore - a brief study. Quart. Jour. Geol. Mineral. Met. Soc. India 44: 163-166.

Rogers J.J.W. and Adams J.A.S. (1969a) Thorium (sections D-O). In, Handbook of geochemistry. Springer-Verlag, Berlin.

Rogers J.J.W. and Adams J.A.S. (1969b) Uranium (sections D-O). In, Handbook of geochemistry. Springer-Verlag, Berlin.

Rogers J.J.W. (1974) Problems concerning the evolution of the Precambrian shield of Peninsular India. Geophys. Res. Bul. 12: 203-218.

Rollinson H.R. and Windley B.F. (1980a) Selective elemental depletion during metamorphism of Archaean granulites, Scourie, NW Scotland. Contrib. Mineral. Petrol. 72: 257-263.

Rollinson H.R. and Windley B.F. (1980b) An Archaean granulite-grade tonalite-trondhjemite-granite suite from Scourie, NW Scotland: geochemistry and origin. Contrib. Mineral. Petrol. 72: 265-281.

Schulien S. (1980) Mg-Fe partitioning between biotite and a supercritical chloride solution. Contrib. Mineral. Petrol. 74: 85-93.

Sengupta S., Bandyopadhyay P.K., Van Den Hul H.J. (1983) Geochemistry of the Chakradharpur granite-gneiss complex - a Precambrian trondhjemite body from West Singhbhum, eastern India. Precamb. Res. 23: 57-78.

Shackleton R.M. (1976) Shallow and deep level exposures of Archaean crust in India and Africa. In, The early history of the earth (ed. Windley B.F.). Wiley and Sons, London, 317-321.

Shaw D.M. (1978) Trace element behaviour during anatexis in the presence of a fluid phase. Geochim. Cosmochim. Acta 42: 933-943.

Sheraton J.W. (1970) The origin of the Lewisian gneisses of northwest Scotland, with particular reference to the Drumbeg area, Sutherland. Earth Planet. Sci. Let. 8: 301-310.

Sheraton J.W., Skinner A.C., Tarney J. (1973) The geochemistry of the Scourian gneisses of the Assynt district. In, The early Precambrian of Scotland and related rocks of Greenland (eds., Park R.G. and Tarney J.). Univ. of Keele, 13-30.

Sheraton J.W. and Black L.P. (1983) Geochemistry of Precambrian gneisses: relevance for the evolution of the East Antarctic Sheild. Lithos 16: 273-296.

Sheraton J.W. and Collerson K.D. (1984) Geochemical evolution of Archaean granulite-facies gneisses in the Vestfold Block and comparisons with other Archaean gneiss complexes in the East Antarctic Shield. Contrib. Mineral. Petrol. 87: 51-64.

Shiraki K. (1978) Chromium (sections B-O). In, Handbook of geochemistry. Springer-Verlag, Berlin.

Smeeth W.F. (1916) Outline of the geological history of Mysore. Dept. Mines and Geol., Mysore State, Bull. 6.

Smith A.G. and Hallam A. (1970) The fit of the southern continents. Nature 225:139-144.

Spooner C.M. and Fairbairn H.W. (1970) Strontium 87/Stontium 86 initial ratios in pyroxene granulite terrains. Jour. Geophys. Res. 75: 6706-6713.

Stroh P.T., Monrad J.R., Fullagar P.D., Naqvi S.M., Hussain S.M., Rogers J.J.W. (1983) Geochemistry and mantle derivation of the 2,977-Myr-old Halekote trondhjemite, Dharwar Craton, southern India. In, Proceedings of the Indo-US workshop on the Precambrians of south India (ed. Naqvi S.M.). National Geophysical Research Inst., Hyderabad.

Subrahmanyam C. and Verma R.k. (1980) The nature of free-air, Bouguer, and isostatic anomalies in southern Peninsular India. Tectonophysics 69: 147-162.

Subramaniam A.P. (1959) Charnockites of the type area near Madras - a reinterpretation. Amer. Jour. Sci. 257: 321-353.

Tarney J. (1976) Geochemistry of Archaean high-grade gneisses, with implications as to the origin and evolution of the Precambrian crust. In, The early history of the earth (ed. Windley B.F.). Wiley and Sons, London, 405-417.

Tarney J. and Windley B.F. (1977) Chemistry, thermal gradients, and evolution of the lower crust. J. Geol. Soc. Lond. 134: 153-172.

Taylor P.N., Chadwick B., Moorbath S., Ramakrishnan M., Viswanatha M.N. (1984) Petrography, chemistry, and isotopic ages of Peninsular Gneiss, Dharwar acid volcanic rocks, and the Chitradurga granite with special reference to the late Archaean evolution of the Karnataka craton, southern India. Precamb. Res. 23: 349-375.

Taylor S.R. 1965) The application of trace element data to problems in petrology. Phys. Chem. Earth 6: 133-214.

Taylor S.R (1967) The origin and growth of continents. Tectonoph. 4: 17-34.

Taylor S.R and McLennan S.M. (1981) The composition and evolution of the continental crust: Rare earth element evidence from sedimentary rocks. Phil. Trans. R. Soc. Lon. A301: 381-399.

Taylor R.P. and Fryer B.J. (1980) Multiple-stage hydrothermal alteration in pophyry copper systems in northern Turkey: the temporal interplay of potassic, propylitic, and phyllic fluids. Can. Jour. Earth Sci. 17: 901-926.

Taylor R.P., Strong D.F., Fryer B.J. (1981) Volatile control of contrasting trace element distributions in peralkaline granitic and volcanic rocks. Contrib. Mineral. Petrol. 77: 267-271.

Touret J. (1971) Les facies granulites en Norvege meridionale: II, Les inclusions fluides. Lithos 4: 423-436.

Turekian K.K. (1978a) Cobalt (sections B-0). In, Handbook of geochemistry. Springer-Verlag, Berlin.

Turekian K.K. (1978b) Nickle (sections B-0). In, Handbook of geochemistry. Springer-Verlag, Berlin.

Valley J.W., McLelland J., Essene E.J., Lamb W. (1983) Metamorphic fluids in the deep crust: evidence from the Adirondacks. Nature 301: 226-228.

Venkatasubramanian V.S. and Narayanaswamy R. (1974) Studies in Rb-Sr geochronologyand trace element geochemistry in granitoids of Mysore craton, India. Jour. Indian Inst. Sci. 56: 19-42.

Viswanatha M.N., Tareen J.A.K. (1970) Petrography of the Nilgiri charnockites. Indian Mineral. 11: 78-86.

Viswanatha M.N., Ramakrishnan, M. (1981) Kolar Belt. In, Early Precambrian supracrustals of southern Karnataka (ed. Swami Nath J. and Ramakrishnan M.). Mem. Geol. Surv. Vol. 112: 221-245.

Viswanatha M.N., Ramakrishnan M., Swami Nath J. (1982) Angular unconformity between Sargur and Dharwar supracrustals in Sigegudda, Karnataka Craton, south India. Jour. Geol. Soc. India 23: 85-89.

Vlasov, K.A. (1966) Geochemistry and mineralogy of rare elements and

genetic types of their deposites. Vol I, Geochemistry of rare elements. Jerusalem, Israel Program of Sci. Translations.

Weaver B.L. (1980) Rare-earth element geochemistry of Madras granulites. Contrib. Mineral. Petrol. 71: 271-279.

Weaver B.L. and Tarney J. (1980) Rare earth geochemistry of Lewisian granulite-facies gneisses, northwest Scotland: implications for the petrogenesis of the Arcaean lower continental crust. Earth Planet. Sci. Lett. 51: 279-296.

Weaver B.L. and Tarney J. (1981) Lewisian gneiss geochemistry and Archaean crustal development models. Earth Planet. Sci. Lett. 55: 171-180.

Weaver B.L, Tarney J., Windley B.F., Leake B.E. (1982) Geochemistry and petrogenesis of Archaean metavolcanic amphibolites from Fiskenaesset, S.W. Greenland. Geochim. Cosmochim. Acta 46: 2203-2215.

Weaver B.L. and Tarney J. (1983) Elemental depletion in Archaean granulite-facies rocks. In, Migmatites, melting, and metamorphism (eds. Atherton M.P. and Gribble C.D.). Shiva Pub. Ltd., Cheshire, U.K., 250-263.

Wedepohl K.H. (1972) Zinc (sections B-O). In, Handbook of geochemistry. Springer-Verlag, Berlin.

Wedepohl K.H. (1974) Lead (sections C-O). In, Handbook of geochemistry. Springer-Verlag, Berlin.

Wedepohl K.H. (1978). Tantalum (sections B-G, I-M, O). In, Handbook of geochemistry. Springer-Verlag, Berlin.

Wells P.R.A. (1979) Chemical and thermal evolution of Archaean sialic crust, southern West Greenland. Jour. Petrol. 20: 187-226.

Whitney P.R. (1969) Variations of the K/Rb ratio in migmatitic paragneisses of the Northwest Adirondacks. Geochim. Cosmochim. Acta 33: 1203-1211.

Windley B.F. and Selvan T.A. (1975) Anorthosites and associated rocks of Tamil Nadu, southern India. Jour. Geol. Soc. India 16: 209-214.

Winkler H.F.G. (1979) Petrogenesis of metamorphic rocks, 5th ed. Springer-Verlag, New York.

Wyllie P.J. (1977) Crustal anatexis: An experimental review. Tectonophysics 43: 41-71.

Ziauddin M. and Yadev P.K. (1975) Acid charnockite (metasomatic)

near Sivasamudram, Karnataka State. Jour. Geol. Soc. India 16: 215-219. O).

A. Analytical Methods

A.1 Sample preparation

Most samples were initially crushed in the field to 2-4 cm. Further reduction to coarse powder was made using a "chipmunk" jaw crusher and a high-speed rotary pulverizer, both employing high-purity alumina plates. An automatic agate mortar and pestle was used to reduce the powder to <= 200 mesh, which was split into three aliquots for XRF major and trace element, and NAA analyses.

A.2 X-ray Fluoresence

Analyses were made using an automated Rigaku 3064 XRF spectrometer with associated PDP-11 computer and in-house software at the XRF-XRD Laboratory at the New Mexico Bureau of Mines and Mineral Resources (N.M. Inst. Mining and Tech.), following methods described by Norrish and Hutton (1969) and Norrish and Chappell (1977). Calibration curves were developed using USGS and international standards. Estimated analytical errors based on analyses of replicate standards are less than 5% for major elements and less than 10% for trace elements (Rb, Sr, Zr, Y, Nb, and Pb). Examples of analytical error associated with repeated sample runs is shown in Appendix A.5 Major elements were analyzed using fused discs made from ~0.5 g powdered sample. Pressed-powder pellets for trace element analysis were made from 5-7 g sample powder (based on major element analysis to ensure infinite thickness) and pressed into pellets with a boric acid backing under a pressure of 10 tons/in2. Several drops of polyvinyl alcohol were used in the powder to assist even distribution of pressure and to help adhesion.

A.3 Neutron Activation Analysis

Trace elements Cs, Ba, Sc, Hf, Ta, Cr, Ni, Co, Zn, U, Th, and 8 REE were analyzed by instrumental neutron activation. Rock powders (~0.5 gm) sealed in polyethylene vials were irradiated in the Annular Core Research Reactor at the Sandia National Laboratory, Albuquerque, N.M. in a thermal neutron flux of 10E12 to 10E13 n/cm2/sec at a total energy of 3000-5000 megajoules. USGS G-2 and BCR-1, and in-house LOSP, BLCR, and HI31, were used as standards. G-2 and BCR-1 concentrations are from Gladney (1983). Counts were made at 6 and 35 days with a coaxial intrinsic Ge detector using a Nuclear Data 6600 multichannel analyzer and LSI-11 computer. Analytical methods are similar to those described by Gordon et al. (1968), Gibson and Jagam (1980) Estimated

analytical errors based on analyses of replicate standards are less than 20% for Ni, Zn, and Nd, and less than 10-15% for all other trace elements. Examples of analytical error associated with repeated sample runs is shown in Appendix A.5. Estimated analytical errors for all samples are expressed as a general range because of changes in analytical equipment and method during the history of these analyses.

A.4 Delayed Neutron Activation Analysis

A selected suite of samples were analyzed for U using the Omega West Reactor (OWR) and associated delayed neutron counter (DNC) facility at the Los Alamos National Laboratory, Los Alamos, New Mexico. Sample powders =>5 g were loaded into high purity ethylene-butylene copolymer vials (diam.=1.2 cm, length=6.0 cm) and irradiated in the graphite thermal column of the OWR in a flux of ~6E12 n/cm2/sec for 20 seconds. After a programmed decay of 10 seconds, the samples were counted for 30 seconds in the DNC. Detection limit for U using the DNC at OWR is U=0.01 ppm. A full description of the automatic system at OWR with reactor, irradiation, and DNC parameters can be found in Minor et al., 1982.

	X R F								N A A				
	BLCR(1)			LOSP(2)			HI31(2)			BLCR(3)			LOSP(4)		estimated
	n	mean	%SD	n	mean	%SD	n	mean	%SD	n	mean	%SD	n	mean	%SD	%SD
SiO2	5	56.2	0.3	2	76.0	0.2	2	59.5	0.01	Cs	3	2.5	6.7	2	2.0	3.1	5-10
TiO2	5	0.88	1.3	2	0.19	3.8	2	0.82	0.9	Ba	3	397	6.2	3	998	0.8	5-10
Al2O3	5	17.0	0.4	2	12.0	0.1	2	17.0	0.3	Th	3	4.1	1.4	3	21	3.6	2-8
Fe2O3t	5	7.51	1.5	2	2.23	2.5	2	7.07	0.4	U	3*	1.5	15.6	3	4.8	1.5	5-10
MnO	5	0.14	2.7	2	0.09	8.3	2	0.11	0.00								
MgO	5	5.35	0.6	2	0.11	0.00	2	2.83	0.8	Sc	3	31	0.1	2	4.1	0.00	2-8
CaO	5	7.93	0.3	2	0.66	1.1	2	6.32	0.5	Hf	3	4.4	2.1	2	11	0.7	2-8
Na2O	5	3.53	1.8	2	3.76	10.4	2	3.12	3.2	Ta	2	0.4	5.7	2	2.1	1.0	2-8
K2O	5	1.43	0.5	2	4.78	3.1	2	2.53	1.1								
P2O5	5	0.16	1.0	2	0.03	28.3	2	0.39	1.8	Cr	3	172	3.7				5-15
										Ni	3	106	8.8				10-20
										Co	3	30	0.5	2	0.6	3.6	5-10
	BLCR(5)			LOSP(5)			HI31(5)			Zn	3	80	1.9	2	157	0.7	5-15
Rb	2	37	0.00	2	184	0.00	2	58	0.2	La	3*	11.0	1.5	3*	74	2.4	2-8
Sr	2	231	0.3	2	41	1.0	2	705	0.1	Ce	3	26.5	1.1	2	164	0.3	2-8
Y	2	31	0.9	2	115	0.00	2	32	0.7	Sm	3	3.7	1.1	3	17	2.4	2-8
Zr	2	173	0.00	2	291	0.2	2	184	0.00	Eu	3	1.28	2.1	2	2.73	0.5	2-8
Nb	2	7.2	2.6	2	26	0.8	2	14	0.5	Tb	3	0.72	4.2	3	3.1	2.9	5-15
Pb	2	6	14.3	2	30	2.8	2	5	12.3	Yb	3	3.3	3.8	3	12	1.4	5-15
										Lu	3*	0.52	2.7	3	1.8	3.7	5-15

(1) Analyzed 31 Mar 83
(2) " 16 Mar 83
(3) " Nov 82, * analyzed Jul 83
(4) " Sept 82
(5) " Feb 83

Appendix A.5. Table showing instrumental error associated with repeated analyses of a single sample (n=number of repetitions) by XRF and NAA. BLCR, LOSP, and HI31 are inhouse standards analyzed. Estimated % standard deviation (last column) is largely derived from an examination of calibration curve uncertainty spanning the period during which the samples were analyzed.

	LOSP	BLCR	HI31
SiO2	76.01	55.65	59.46
TiO2	0.19	0.87	0.81
Al2O3	12.03	16.97	17.02
Fe2O3t	2.20	7.43	7.07
MnO	0.08	0.13	0.11
MgO	0.10	5.86	2.81
CaO	0.65	7.90	6.32
Na2O	3.75	3.72	3.12
K2O	4.77	1.45	2.53
P2O5	0.02	0.16	0.38
LOI	0.38	0.34	0.48
Total	100.18	100.48	100.11
Rb	184	38	58
Cs	2.0	2.3	0.56
Sr	41	231	705
Ba	970	375	795
Pb	29	5.8	4.5
Th	19.7	4.1	6.6
U	4.8	1.5	0.7
Sc	4.0	32.0	17.5
Y	117	30.7	32.0
Zr	290	173	184
Hf	11	4.3	5.6
Nb	26	7.2	14
Ta	2.1	0.42	0.73
Cr	2.5	160	38
Co	0.57	29	15
Ni	12	103	14
Zn	150	90	60
La	72.0	11.1	37.0
Ce	163	26.7	80.3
Nd	78.0	14.4	38.0
Sm	17.2	3.7	7.8
Eu	2.7	1.3	2.04
Tb	3.1	0.78	1.2
Yb	12.5	3.1	3.2
Lu	1.85	0.52	0.49

Appendix A.6. In-house standard concentrations.

Sample: BG1
Locality: Bangalore-Kolar
Rock type: Granitic gneiss
Description: light gray, coarse-grained, homogeneous

Pts counted: 6692 An# 30

	(%)	Description
Qtz	28.6	undulose extinction common
Kspar	40.9	subhed. crystls and intrgran megacrysts; perthite
Plag	25.5	some bent twin lamellae; dusty saussuritization
Biot	2.9	yellow to green laths, some epidote alteration
Amph		
Opx		
Cpx		
Garn		
Opaq	0.3	
Sph	tr	
Rut		
Zircn	0.3	
Apat	0.1	
Allan	tr	
Epid	0.3	
Cumm		
Seric	0.6	
Chlor	tr	
Cc	0.2	

Remarks: infrequent myrmekite, texture is hypidiomorphic granular

Sample: KDA2
Locality: Kollegal-Malavalli-KD
Rock type: charnockite
Description: gray, med-grained, homogeneous

Pts counted: 2867 An# 25

	(%)	Description
Qtz	22.8	undulose extinction
Kspar	1.5	usu as elongate, intergran crystals; twinning; some perth
Plag	66.9	twins usu absent; saussurit. common; some antiperthite
Biot	7.4	yellow to v. dk. brn crinkle-tex laths,& red-brn anhedral stains on hyp margin
Amph		
Opx	0.9	pleochro. pl pink to pl grn; some alter. to biot and chlorite
Cpx		
Garn		
Opaq	0.2	
Sph		
Rut		
Zircn	tr	
Apat	0.1	
Allan		
Epid		
Cumm		
Seric	tr	
Chlor	tr	
Cc	0.2	

Remarks: rare myrmekite, some mortar text.; opx appears after biot w/ later regression to anhed biot on margins; texture is hypidiomorphic granular

Sample: KDA3
Locality: Kollegal-Malavalli-KD
Rock type: mafic granulite
Description: dark gray, fine-grained, homogeneous

Pts counted: 2759 An# 24

	(%)	Description
Qtz	2.4	undulose extinction
Kspar	tr	
Plag	38.7	twin lamellae usu absent or deformed; grains are clear
Biot		
Amph	30.5	olive-green
Opx	25.4	faintly pleochroic pl pink to pl green
Cpx		
Garn		
Opaq	2.8	
Sph		
Rut		
Zircn	tr	
Apat	0.2	
Allan		
Epid		
Cumm		
Seric		
Chlor		
Cc	tr	

Remarks: evidence for both prograde and retrograde hyp-hb reactions; retrogression more easily apparent; texture is hypidiomorphic granular

Sample: 1
Locality: Hosur-Krish-Dharm
Rock type: charnockite
Description: gray, greasy, medium-grained, homogeneous

Pts counted: 2482 An# 28

	(%)	Description
Qtz	31.6	undulose extinction
Kspar	tr	coalesced anti-perthite at margins of plagioclase
Plag	57.0	twin lamellae are deformed; some saussuritization
Biot	5.4	yellow to brn laths, and reddish brn stains along margins of hypersthene
Amph	1.9	olive-green and pale green along margins of hypersthene
Opx	1.6	poorly pleochroic; anhed biot and hb on cleavages and margin
Cpx		
Garn		
Opaq	2.1	
Sph		
Rut		
Zircn	0.1	
Apat	0.2	
Allan		
Epid		
Cumm		
Seric		
Chlor		
Cc	tr	thin veinlets in plg

Remarks: hypersthene shows alteration to hb, anhedral biot, and opaques; calcite as small masses and veinlets; texture is hypidiomorphic granular

Sample: 2
Locality: Hosur-Krish-Dharm
Rock type: charnocite
Description: gray, greasey, medium-grained, foliated

Pts counted: 1332 An# 25

	(%)	Description
Qtz	25.5	undulose extinction; elongate grains
Kspar	7.7	small, intergranular grains; twinning is frequent; no perthite
Plag	60.6	twin lamellae absent or deformed; anti-perthite present
Biot	3.8	yellow to gray-brown laths, and reddish brown anhed stains in hyp cleavages
Amph	tr	pale green and olive green along cleavage and margins of hyp
Opx	1.9	poorly pleochroic, altered margins and cleavages
Cpx		
Garn		
Opaq	0.5	
Sph		
Rut		
Zircn	tr	
Apat	tr	
Allan		
Epid		
Cumm		
Seric		
Chlor	tr	
Cc	tr	

Remarks: some myrmekite present; hypersthene altering at margins and cleavages to hb and anhedral biot; lath-shaped biot appears primary; texture is hypidiomorphic granular

Sample: 3
Locality: Hosur-Krish-Dharm
Rock type: granitic gneiss
Description: pink, medium to coarse-grained, homogeneous

Pts counted: 1743 An# 24

	(%)	Description
Qtz	20.6	undulose extinction
Kspar	29.7	sm subhedral grains, and intergran mega-crysts; sieve tex
Plag	45.1	sm subhed grains and lrg porphyroblasts; twin lamellae absent or bent; saussurit.
Biot	4.5	yellow to greenish brown, crinkle-tex laths
Amph		
Opx		
Cpx		
Garn		
Opaq	0.1	
Sph		
Rut	tr	needles in qtz
Zircn	tr	
Apat	tr	
Allan		
Epid	tr	
Cumm		
Seric		
Chlor		
Cc	tr	

Remarks: trace of monazite; some myrmekite and mortar texture; texture is hypidiomorphic granular

Sample: 4-1
Locality: Hosur-Krish-Dharm
Rock type: charnockite
Description: gray, greasy, medium-grained, and foliated

Pts counted: 1411 An# 30

	(%)	Description
Qtz	12.7	large irregular grains; undulose extinction
Kspar	0.3	coalesced anti-perthite along plag margins; no twinning
Plag	71.6	twin lamellae freq absent in larger grains; antiperthite & local saussuritiz.
Biot	4.7	yellow to brown, crinkle-tex laths, and reddish brown and brown stains
Amph	1.9	olive-green
Opx	2.5	poorly pleochroic; reddish brown anhed biot along margins
Cpx	4.0	pale green
Garn		
Opaq	2.3	assoc. with biot
Sph		
Rut		
Zircn	tr	
Apat	tr	
Allan		
Epid		
Cumm		
Seric		
Chlor		
Cc	tr	

Remarks: hypersthene appears to have developed from hornblende with a late-stage regression producing anhed biot along cleavages and margins; texture is hypidiomorphic granular

Sample: 64-1
Locality: Hosur-Krish-Dharm
Rock type: granodioritic gneiss
Description: pink, medium-grained, and foliated

Pts counted: 4810 An# 26

	(%)	Description
Qtz	18.2	undulose extinction
Kspar	8.4	subhedral grains and intergranular megacrysts
Plag	56.6	twin lamellae usu absent or bent; some antiperthite; minor saussuritiz.
Biot	15.4	yellow to dark brown laths, and reddish brown, anhedral stains
Amph	0.1	green to olive-green; appears to develop from lath biotite
Opx		
Cpx		
Garn		
Opaq	0.6	
Sph		
Rut		
Zircn	0.1	
Apat	0.6	
Allan		
Epid		
Cumm		
Seric		
Chlor		
Cc	tr	

Remarks: some myrmekite and mortar texture present; biotite shows rough foliation; texture is hypidiomorphic granular

Sample: 64-2
Locality: Hosur-Krish-Dharm
Rock type: granitic gneiss
Description: pink, medium-grained, homogeneous

Pts counted: 2751 An# 26

	(%)	Description
Qtz	20.9	undulose extinction
Kspar	65.5	intergranular megacrysts
Plag	9.8	twin lamellae usu absent; no anti-perthite; some saussuritization
Biot	3.9	yellow to dark brown laths, and anhedral reddish brown stains
Amph		
Opx		
Cpx		
Garn		
Opaq	0.6	
Sph		
Rut		
Zircn	0.1	
Apat	tr	
Allan		
Epid		
Cumm		
Seric		
Chlor	tr	
Cc	0.2	

Remarks: abundant myrmekite; texture is hypidiomorphic granular to porphyroblastic

Sample: 65
Locality: Hosur-Krish-Dharm
Rock type: granodioritic gneiss
Description: light, pinkish gry, fine-grained, foliated

Pts counted: 2502 An# 22

	(%)	Description
Qtz	29.7	undulose extinction
Kspar	20.4	intergranular crystals and megacrysts
Plag	45.6	twin lamellae usu absent or faint; some saussurit.
Biot	3.7	yellow to dark brown laths, and anhedral stains; some alter. to chlorite
Amph		
Opx		
Cpx		
Garn		
Opaq	0.5	
Sph		
Rut	tr	in quartz
Zircn	0.1	
Apat	tr	
Allan		
Epid		
Cumm		
Seric	tr	
Chlor	tr	
Cc	tr	

Remarks: myrmekite present; texture is hypidiomorphic granular to porphyroblastic

Sample: 66
Locality: Hosur-Krish-Dharm
Rock type: charnockite
Description: dark gray to brownish gray, greasy, and coarse-grained

Pts counted: 1600 An# 24

	(%)	Description
Qtz	18.6	elongate grains; undulose extinction
Kspar	tr	
Plag	64.2	twin lamellae usu absent or deformed; antiperthite; prominent saussurit.
Biot	7.6	yellow to brown laths and reddish brown, anhedral stains
Amph	0.6	
Opx	6.0	poorly pleochroic; alter. to biot and chlorite on cleavage
Cpx		
Garn		
Opaq	2.2	
Sph	tr	
Rut		
Zircn	tr	
Apat	0.4	
Allan		
Epid		
Cumm		
Seric		
Chlor	0.2	
Cc	0.2	

Remarks: pyroxene develops after lath-shaped biot; late-stage growth of reddish brown biot along pyroxene cleavages and margins; text. is hypidiomorphic granular to granoblastic

Sample: 67
Locality: Hosur-Krish-Dharm
Rock type: granitic gneiss
Description: pink to gray, greasy, medium-grained, foliated

Pts counted: 1458 An# 25

	(%)	Description
Qtz	25.5	undulose extinction; elongate grains common
Kspar	36.0	subhedral grains and intergranular mega-crysts; some perth.
Plag	36.6	twin lamellae usu absent or deformed; antiperthite rare; some saussurit.
Biot	1.2	yellow to brown laths and reddish brown, anhedral stains
Amph		
Opx		
Cpx		
Garn		
Opaq	0.7	
Sph		
Rut		
Zircn	tr	
Apat	tr	
Allan		
Epid		
Cumm		
Seric		
Chlor	tr	
Cc	tr	

Remarks: some, small localized veinlets of carbonate, some myrmekite; texture is hypidiomorphic granular

Sample: 68
Locality: Hosur-Krish-Dharm
Rock type: charnockite
Description: dark gray, greasy, medium-grained, homogeneous

Pts counted: 1508 An# 25

	(%)	Description
Qtz	5.4	undulose extinction
Kspar	0.9	small grains usually with plagioclase
Plag	62.1	twin lamellae usu absent in large grains; variable saussur.; antiperth
Biot	15.8	yellow to dark brown laths and reddish brown, anhedral stains on mafics
Amph	0.8	olive-green
Opx	2.4	poorly pleochroic
Cpx	9.3	pale green
Garn		
Opaq	3.1	
Sph		
Rut		
Zircn	tr	
Apat	0.1	
Allan		
Epid		
Cumm		
Seric		
Chlor		
Cc	0.1	

Remarks: pyx after lath-shaped biot and hornblende; minor late-stage alteration of lath-shaped biot and pyx to reddish brown biotite; texture is hypidiomorphic granular

Sample: 69
Locality: Hosur-Krish-Dharm
Rock type: charnockite
Description: gray, glassy to greasy, medium to coarse-grained, homogeneous

Pts counted: 1320 An# 29

	(%)	Description
Qtz	28.7	undulose extinction; some elongate grains
Kspar	tr	
Plag	68.6	twin lamellae usu absent or bent, esp. in lrge grains; some saussur. & anitperth
Biot	1.1	yellow to dark brown laths and reddish brown, anhedral stains on mafics
Amph	tr	
Opx	1.1	pleochroic in pale pink to pale green
Cpx		
Garn		
Opaq	0.5	
Sph		
Rut	tr	needles in quartz
Zircn	tr	
Apat	tr	
Allan		
Epid		
Cumm		
Seric	tr	
Chlor	tr	
Cc	tr	

Remarks: pyx after lath biot and hornblend; minor late-stage alteration of lath biot and pyx to reddish brown biot; texture is hypidiomorphic granular

Sample: 77-1
Locality: Hosur-Krish-Dharm
Rock type: tonalitic gneiss
Description: gray, fine to medium-grained, somewhat foliated

Pts counted: 1518 An# 24

	(%)	Description
Qtz	23.3	undulose extinction
Kspar	2.1	anhedral, intergan-ular crystals
Plag	63.4	twin lamellae usu absent; some anti-perthite; some saussuritization
Biot	10.7	yellow to brown laths and anhedral reddish brown stains
Amph	0.2	green
Opx		
Cpx		
Garn		
Opaq	0.3	
Sph		
Rut		
Zircn	tr	
Apat	tr	
Allan		
Epid		
Cumm		
Seric		
Chlor	tr	
Cc	tr	

Remarks: texture is granoblasic

Sample: 77-2
Locality: Hosur-Krish-Dharm
Rock type: mafic granulite
Description: dark gray, fine to medium-grained, foliated

Pts counted: 1529 An# 39

	(%)	Description
Qtz	1.3	undulose extinction
Kspar		
Plag	33.5	twin lamellae generally well developed
Biot		
Amph	55.4	olive-green
Opx	3.6	poorly pleochroic
Cpx	6.0	pale green
Garn		
Opaq	0.2	
Sph		
Rut		
Zircn	tr	
Apat	tr	
Allan		
Epid		
Cumm		
Seric		
Chlor		
Cc		

Remarks: pyroxene developes in cleavages of hornblende; texture is granoblastic

Sample: 78
Locality: Hosur-Krish-Dharm
Rock type: charnockite
Description: gray, greasy, medium-grained, homogeneous

Pts counted: 1573 An# 29

	(%)	Description
Qtz	19.9	undulose extinction
Kspar	1.0	twinning rare; anhedral, intergran crystals; no perth
Plag	73.3	twins absent or deformed; some antiperthite; some saussuritization
Biot	4.0	yellow to drk brown laths and anhedral reddish brown stains
Amph	tr	green
Opx	1.3	poorly pleochroic in pale green to pink
Cpx		
Garn		
Opaq	0.5	
Sph		
Rut		
Zircn	tr	
Apat	tr	
Allan		
Epid		
Cumm		
Seric	tr	
Chlor	tr	
Cc	tr	

Remarks: hypersthene after lath-shaped biot; late-stage alter to anhedral biot and hornbl along margins and cleavages; texture is hypidiomorphic granular

Sample: 79
Locality: Hosur-Krish-Dharm
Rock type: tonalitic gneiss
Description: pinkish gray, medium to coarse-grained, homogeneous

Pts counted: 1424 An# 30

	(%)	Description
Qtz	19.3	undulose extinction, some elongate grains
Kspar	0.4	twins poorly developed; intergranular, anhedral crystals
Plag	71.3	twins usu absent, esp. in larger grains, or bent; antiperth; saussur.
Biot	8.8	yellow to very dark brown laths and anhedral stains
Amph		
Opx		
Cpx		
Garn		
Opaq	0.2	
Sph		
Rut		
Zircn	tr	
Apat	tr	
Allan		
Epid		
Cumm		
Seric	tr	
Chlor	tr	
Cc	tr	

Remarks: minor fracturing with thin, cross-cutting veinlets of carbonate; rare myrmekite; plag as both small, subhedral grains and large sub- to anhed grains; hypid gran to porphyobl

Sample: 99-1
Locality: Hosur-Kuppam-Krish
Rock type: granodioritic gneiss
Description: light gray, medium to coarse-grained, foliated

Pts counted: 1440 An# 27

	(%)	Description
Qtz	16.1	some undulose extinction
Kspar	17.1	subhedral crystals and intergranular megacrysts
Plag	53.2	twinning generally absent; antiperthite rare; some saussur.
Biot	6.5	yellowish brown laths show rough foliation; anhedral stains uncommon
Amph	4.8	green to yellow; occas. alters to bi in cleav. & margins
Opx		
Cpx		
Garn		
Opaq	0.8	
Sph		
Rut		
Zircn	tr	
Apat	tr	
Allan		
Epid	1.5	
Cumm		
Seric		
Chlor	tr	
Cc	tr	

Remarks: myrmekite, mortar texture, and mylonite variably present; texture is hypidiomorphic granular to cataclastic

Sample: 99-2
Locality: Hosur-Kuppam-Krish
Rock type: granodioritic gneiss
Description: light gray, medium-grained, homogeneous

Pts counted: 1607 An# 24

	(%)	Description
Qtz	15.8	undulose extinction in large grains; mortar texture
Kspar	22.6	subhedral crystals and intergranular megacrysts
Plag	43.4	twinning generally absent; antiperthite rare; minor saussur.
Biot	17.4	yellow to very dark brown laths and anhedral stains
Amph		
Opx		
Cpx		
Garn		
Opaq	0.8	
Sph		
Rut		
Zircn	tr	
Apat	tr	
Allan	tr	
Epid		
Cumm		
Seric		
Chlor	tr	
Cc	tr	

Remarks: myrmekite, mortar texture, and mylonite variably present; texture is granoblastic to cataclastic

Sample: 99-3
Locality: Hosur-Kuppam-Krish
Rock type: granitic gneiss
Description: pinkish gray, medium to coarse-grained, foliated

Pts counted: 1616 An# 28

	(%)	Description
Qtz	16.7	undulose extinction; mortar texture
Kspar	41.0	subhedral crystals and intergran megacrysts; some perth
Plag	38.1	twins usu absent or deformed; saussurit. locally significant; antiperthite rare
Biot	2.9	yellow to olive-brn laths and rel minor anhedral stains
Amph		
Opx		
Cpx		
Garn		
Opaq	0.8	
Sph		
Rut	tr	
Zircn	tr	
Apat	tr	
Allan		
Epid	0.1	
Cumm		
Seric	0.2	
Chlor	tr	
Cc	0.4	

Remarks: myrmekite, mortar texture, and mylonite variably present; texture is porphyroblastic to cataclastic

Sample: 101-1
Locality: Hosur-Kuppam-Krish
Rock type: granodioritic gneiss
Description: pink to dark gray, medium to coarse-grained, foliated

Pts counted: 1648 An# 26

	(%)	Description
Qtz	19.7	undulose extinction; mortar texture
Kspar	25.8	subhedral crystals and intergranular megacrysts
Plag	43.5	twins usu absent or faint and deformed; infreq antiperthite; sauss. local. signif
Biot	10.7	yellow to very dark brwn laths that show rough foliation, and anhedral stains
Amph		
Opx		
Cpx		
Garn		
Opaq	0.3	
Sph		
Rut		
Zircn	tr	
Apat	tr	
Allan	tr	
Epid	tr	
Cumm		
Seric		
Chlor	tr	
Cc	tr	

Remarks: myrmekite, mortar texture, and mylonite variably present; texture is hypidiomorphic granular to cataclastic

Sample: 103
Locality: Hosur-Kuppam-Krish
Rock type: tonalitic gneiss
Description: gray, medium-grained, homogeneous

Pts counted: 1554 An# 22

	(%)	Description
Qtz	26.7	undulose extinction; some elongate grains
Kspar	5.6	subhedral crystals and anhedral, intergranular crystals
Plag	53.2	twin lamellae usu absent; relatively intense saussurit.
Biot	10.6	pale yellow to olive brown laths, and rel minor prismatic to anhedral stains
Amph	2.3	olive-brown
Opx		
Cpx		
Garn		
Opaq	tr	
Sph		
Rut		
Zircn	tr	
Apat	tr	
Allan		
Epid	1.2	
Cumm		
Seric	tr	
Chlor	0.4	
Cc	tr	

Remarks: myrmekite, mortar texture present; relatively high degree of alteration; texture is hypidiomorphic granular to granoblastic

Sample: 104
Locality: Hosur-Kuppam-Krish
Rock type: tonalitic gneiss
Description: gray, medium to coarse-grained, foliated

Pts counted: 1662 An# 25

	(%)	Description
Qtz	20.8	undulose extinction in larger grains; some mortar texture
Kspar	1.1	small subhedral crystals
Plag	65.5	twins usu absent or deformed; antiperth rare; some saussur.
Biot	10.1	yellow to dark brown laths and shreds, and anhedral stains
Amph	0.4	brownish yellow to green; some replace-by anhedral biot
Opx		
Cpx		
Garn		
Opaq	0.6	
Sph	tr	
Rut		
Zircn	tr	
Apat	0.2	
Allan		
Epid	0.6	
Cumm		
Seric	tr	
Chlor	tr	
Cc	0.7	

Remarks: some mortar texture and mylonite present; monazite halo in biotite; texture is hypidiomorphic granular to granoblastic

Sample: 107-1 Locality: Hosur-Krish-Dharm Rock type: charnockite Description: gray, medium-grained, foliated		
Pts counted: 1625	An# 25	
	(%)	Description
Qtz	28.6	undulose extinction
Kspar	1.1	largely as coalesced antiperthite at plag margins; perth. rare
Plag	57.0	twin lamellae usu absent or deformed; some saussurit.; minor antiperthite
Biot	11.7	yellow to dark brown laths, and anhedral, reddish brown stains
Amph	0.7	green; replaces opx
Opx	0.3	poorly pleochroic
Cpx		
Garn		
Opaq	0.6	
Sph		
Rut		
Zircn	tr	
Apat	tr	
Allan		
Epid	tr	
Cumm		
Seric	tr	
Chlor	tr	
Cc	tr	
Remarks: mortar texture and microcracks present; hypersthene is after lath-shaped biot with late-stage alter. to anhedral biot and hb; texture is cataclastic		

Sample: 108-1 Locality: Hosur-Krish-Dharm Rock type: tonalitic gneiss Description: pink, coarse-grained, foliated		
Pts counted: 1484	An# 25	
	(%)	Description
Qtz	20.3	undulose extinction; mortar text. common
Kspar	0.7	
Plag	73.8	twin lamellae usu absent; antipethite present; infrequent saussuritization
Biot	4.9	yellow to brown laths, and as anhedral stains
Amph	tr	green
Opx		
Cpx		
Garn		
Opaq	0.3	
Sph		
Rut	tr	
Zircn	tr	
Apat	tr	
Allan		
Epid	tr	
Cumm		
Seric	tr	
Chlor	tr	
Cc	tr	
Remarks: myrmekite and mortar texture present; texture is hypidiomorphic granular to cataclastic		

Sample: 108-2 Locality: Hosur-Krish-Dharm Rock type: tonalitic gneiss Description: pink, fine to medium grained, homogeneous		
Pts counted: 1559	An# 26	
	(%)	Description
Qtz	20.9	undulose extinction
Kspar	11.2	anhedral, intergranular crystals; usually twinned
Plag	61.7	twin lamellae infreq present; some antiperthite; dusty
Biot	5.7	yellow to dark olive brown laths, and anhedral brown stains
Amph		
Opx		
Cpx		
Garn		
Opaq	0.5	
Sph		
Rut		
Zircn	tr	
Apat	tr	
Allan		
Epid		
Cumm		
Seric		
Chlor		
Cc		
Remarks: myrmekite present; texture is granoblastic		

Sample: 108-3 Locality: Hosur-Krish-Dharm Rock type: charnockite Description: dark gray, medium-grained, foliated		
Pts counted: 1730	An# 34	
	(%)	Description
Qtz	6.3	undulose extinction
Kspar	1.8	anhedral, intergranular crystals; usually twinned
Plag	45.9	twin lamellae freq absent, or faint and deformed; saussur. rare; some antiperth
Biot	11.2	yellow to dark brown laths with rough foliation; and anhed olive-brown stains
Amph	20.4	green to olive-green
Opx	6.9	poorly pleochroic, pale pink to pale green
Cpx	4.2	pale green
Garn		
Opaq	2.8	
Sph		
Rut		
Zircn	tr	
Apat	0.1	
Allan		
Epid	tr	
Cumm		
Seric	tr	
Chlor	tr	
Cc	tr	
Remarks: infrequent myrmekite; late-stage alteration of pyroxene to anhedral biot and pale green hornblende; texture is hypidiomorphic granular to granoblastic		

Sample: 118-2 Locality: Kollegal-Malavalli-KD Rock type: granitic gneiss Description: pink, medium-grained, homogeneous		
Pts counted: 1612	An# 28	
	(%)	Description
Qtz	16.7	undulose extinction
Kspar	33.7	subhedral crystals and intergranular megacrysts
Plag	47.7	twin lamellae usu absent; variable saussuritization; rare antiperthite
Biot	1.4	brown to olive laths and anhedral stains
Amph		
Opx		
Cpx		
Garn		
Opaq	0.3	
Sph		
Rut		
Zircn	0.1	
Apat	0.1	
Allan		
Epid		
Cumm		
Seric	tr	
Chlor		
Cc	tr	
Remarks: myrmekite present; texture is granoblastic		

Sample: 119-2 Locality: Kollegal-Malavalli-KD Rock type: granitic gneiss Description: pink, fine to medium-grained		
Pts counted: 1627	An# 23	
	(%)	Description
Qtz	27.7	undulose extinction
Kspar	34.0	predominantly intergranular megacrysts
Plag	33.6	twin lamellae usu absent or deformed; antiperthite and saussurit. rare
Biot	3.9	pale brown to brown laths and minor anhedral stains
Amph	tr	
Opx		
Cpx		
Garn		
Opaq	0.5	
Sph	0.1	
Rut		
Zircn	0.1	
Apat	0.1	
Allan	tr	
Epid		
Cumm		
Seric	tr	
Chlor	tr	
Cc		
Remarks: myrmekite and microfractures present; texture is granoblastic		

Sample: 119-3 Locality: Kollegal-Malavalli-KD Rock type: granitic charnockite Description: gray, medium to coarse-grained, homogeneous		
Pts counted: 1618	An# 20	
	(%)	Description
Qtz	29.7	undulose extinction; some large, intergranular megacrysts
Kspar	41.1	predom as intergran megacrysts; subhed grains; twinning
Plag	28.2	twins absent or deformed; antiperthite absent; rare saussuritization
Biot	0.3	brown to very dark brown laths, and minor anhedral stains
Amph	0.1	green
Opx	0.1	pleochroic pink to pale green; margins alter to biot & hb
Cpx		
Garn		
Opaq	0.5	
Sph		
Rut		
Zircn	tr	
Apat	tr	
Allan	tr	
Epid		
Cumm		
Seric		
Chlor	tr	
Cc	tr	
Remarks: some myrmekite present; late-stage alter. of hypersthene to anhed biot and hornblende along cleavages and margins		

Sample: 119-4 Locality: Kollegal-Malavalli-KD Rock type: tonalitic gneiss Description: light gray, fine-grained, homogeneous		
Pts counted: 1665	An# 24	
	(%)	Description
Qtz	12.3	undulose extinction
Kspar	1.7	anhedral, intergranular crystals
Plag	55.9	twins usu absent or bent, some lamellae clear; antiperthite rare; dusty
Biot	0.4	yellow to brown laths and reddish brown stains along cleavages in amph
Amph	24.4	olive-green
Opx		
Cpx		
Garn		
Opaq	5.1	
Sph		
Rut		
Zircn	0.1	
Apat	0.1	
Allan		
Epid		
Cumm		
Seric		
Chlor		
Cc		
Remarks: some myrmekite present; late-stage alteration of hornblende; texture is granoblastic		

Sample: 119-5
Locality: Kollegal-Malavalli-KD
Rock type: charnockite
Description: gray, fine to medium-grained, homogeneous

Pts counted: 2555 An# 30

	(%)	Description
Qtz	10.2	undulose extinction common
Kspar		
Plag	41.4	twin lamellae freq absent or deformed; antiperth rare; plag generally fresh look
Biot	8.1	yellow to very dark reddish brwn, crinkle textured laths and anhedral stains
Amph	37.6	olive-green; fresh appearance
Opx		
Cpx	1.7	pale gray-green; fresh appearance
Garn		
Opaq	0.2	
Sph		
Rut		
Zircn	0.1	
Apat	0.3	
Allan		
Epid		
Cumm		
Seric		
Chlor		
Cc	0.4	

Remarks: Cpx appears to develop from hornblende; texture is hypidiomorphic granular to granoblastic

Sample: 120-1
Locality: Kollegal-Malavalli-KD
Rock type: charnockite
Description: gray, medium-grained, foliated

Pts counted: 1476 An# 27

	(%)	Description
Qtz	25.4	undulose extinction
Kspar	tr	
Plag	61.3	twin lamellae usu absent or deformed; some anitperth; some saussuritization
Biot	6.4	yellow to very dark brown, crinkle-tex laths, and anhedral reddish brown stains
Amph	tr	green
Opx	5.6	faintly pleochroic pale pink to green; sometimes lath habit
Cpx		
Garn		
Opaq	1.2	
Sph		
Rut		
Zircn	tr	
Apat	0.1	
Allan		
Epid		
Cumm		
Seric	tr	
Chlor	tr	
Cc	tr	

Remarks: some hyp with lath-shaped habit after biotite; late-stage alter of hyp to hb and anhed biot; biot and hyp show crude foliation; tex is hypidiomor gran to granoblasic

Sample: 120-2
Locality: Kollegal-Malavalli-KD
Rock type: charnockite
Description: gray, medium-grained, foliated

Pts counted: 1648 An# 31

	(%)	Description
Qtz	29.9	freq undulose extinction; some elongate grains
Kspar	tr	generally on margins of plag; twinning and perthite absent
Plag	62.4	twin lamellae usu absent or deformed; antiperth present; minor saussurit.
Biot	0.9	yellow to very dark brown and red-brown laths and anhedral stains
Amph	tr	green, along margins and cleavages of hyp
Opx	4.8	pleochroic pale pink to pale green
Cpx		
Garn		
Opaq	1.4	
Sph		
Rut		
Zircn	tr	
Apat	0.4	
Allan		
Epid		
Cumm		
Seric		
Chlor	tr	
Cc		

Remarks: some mortar texture; hyp after biot with late-stage regression to anhed biot & hb along cleavages and margins; texture is hypidiomorphic granular to porphyroblastic

Sample: 120-3
Locality: Kollegal-Malavalli-KD
Rock type: mafic granulite
Description: dark gray, medium-grained, foliated

Pts counted: 1575 An# 34

	(%)	Description
Qtz	1.8	undulose extinction
Kspar		
Plag	40.3	twins absent, faint and deform, or clear and deformed; anti-perth abs; some saus
Biot	tr	anhedral, brown margins on hyp and hornblende
Amph	37.7	olive-green; some as pale green along margins of hyp
Opx	20.1	pleochroic pale pink to green; initially after olive-grn hb
Cpx		
Garn		
Opaq	0.1	
Sph		
Rut		
Zircn	tr	
Apat	tr	
Allan		
Epid		
Cumm		
Seric	tr	
Chlor	tr	
Cc	tr	

Remarks: hyp after olive-green hb followed by relativel minor regression to pale green hb along margins; texture is hypidiomorphic granular to granoblastic

Sample: 120-4
Locality: Kollegal-Malavalli-KD
Rock type: charnockite
Description: dark gray, medium-grained, foliated

Pts counted: 1577 An# 31

	(%)	Description
Qtz	5.7	undulose extinction; mortar texture
Kspar	tr	
Plag	58.8	lamellae usu absent on large grains; freq saussur.; antiperth absent
Biot	20.1	yellow to very dark brn laths, & anhed, reddish brown stains
Amph	9.4	olive-green
Opx	0.2	poorly pleochroic
Cpx		
Garn		
Opaq	4.9	
Sph		
Rut		
Zircn	0.1	
Apat	0.8	
Allan		
Epid		
Cumm		
Seric	tr	
Chlor	tr	
Cc	tr	

Remarks: mortar texture; rough foliation of biot on shears; hyp alters to anhed biot; rel high degree of saussurit.; texture is granoblastic to cataclastic

Sample: 122-1
Locality: Kollegal-Malavalli-KD
Rock type: charnockite
Description: dark gray, medium-grained, homogeneous

Pts counted: 1574 An# 31

	(%)	Description
Qtz	18.1	undulose extinction; some elongate grains and mortar texture
Kspar		
Plag	70.9	twin lamellae usu absent or deformed; antiperth present; rare saussurit.
Biot	1.3	yellow to brown laths, and anhedral, reddish brn stains along hyp margins
Amph	tr	
Opx	7.8	pleochroic pink to green; lenticular habit after biot
Cpx		
Garn		
Opaq	2.4	
Sph		
Rut		
Zircn	tr	
Apat	tr	
Allan		
Epid		
Cumm		
Seric		
Chlor		
Cc		

Remarks: mortar texture and mylonite; plag augen in fine-grained qtz and plag matrix; texture is cataclastic

Sample: 122-2
Locality: Kollegal-Malavalli-KD
Rock type: charnockite
Description: light gray, medium-grained, foliated

Pts counted: 1601 An# 26

	(%)	Description
Qtz	37.4	undulose extinction; mortar texture
Kspar		
Plag	59.3	twin lamellae usu absent or deformed; some dusty saussur. and antiperthite
Biot	0.5	yellow to very dark brown laths, and anhed, reddish brown stains on hyp
Amph		
Opx	2.2	pleochroic; some lenticular shreds prob after biot
Cpx		
Garn		
Opaq	0.6	
Sph		
Rut		
Zircn	tr	
Apat	tr	
Allan		
Epid		
Cumm		
Seric	tr	
Chlor	tr	
Cc	tr	

Remarks: mortar texture, some mylonite and microfractures present; hyp after lath biot with late-stage alter to anhed biot; texture is cataclastic to porphyroblastic

Sample: 477
Locality: Nilgiris
Rock type: charnockite
Description: dark gray, greasy, medium to coarse-grained, homogeneous

Pts counted: 1570 An# 30

	(%)	Description
Qtz	14.9	undulose extinction; some mortar texture
Kspar	8.8	twinning rare
Plag	41.1	twinning usu absent or deformed; some saussur.; antiperth infrequent
Biot	0.9	yellow to reddish brown laths, & anhed red-brown stains in cleavages of hyp
Amph		
Opx	7.5	poorly pleochroic; some schiller struct
Cpx		
Garn	25.7	subhed; inclus. of other mineral phases
Opaq	0.9	
Sph		
Rut		
Zircn	tr	
Apat	tr	
Allan		
Epid		
Cumm		
Seric	tr	
Chlor	tr	
Cc	0.2	

Remarks: some mortar texture present; texture is porphyroblastic (garnet) to cataclastic

Sample: 478
Locality: Nilgiris
Rock type: charnockite
Description: gray, medium to coarse-grained, foliated

Pts counted: 1859 An# 38

	(%)	Description
Qtz	42.9	undulose extinction; grains freq elongate; mortar texture
Kspar		
Plag	31.6	twin lamellae freq absent or deformed; some antiperthite; infreq. saussurit.
Biot	2.8	yellow to reddish brown laths & anhed stains along margins and cleavages of hyp
Amph		
Opx	6.5	poorly pleochroic
Cpx		
Garn	14.7	subhed; inclus of other mineral phases
Opaq	0.6	
Sph		
Rut		
Zircn	tr	
Apat	tr	
Allan		
Epid		
Cumm		
Seric	tr	
Chlor	tr	
Cc	tr	

Remarks: hypersthene frequently has biotite habit; texture is cataclastic

Sample: 480
Locality: Nilgiris
Rock type: charnockite
Description: light gray, medium-grained, foliated

Pts counted: 1512 An# 36

	(%)	Description
Qtz	20.6	undulose extinction; some mortar texture
Kspar	11.2	anhedral and intergranular; twinning absent; some perth
Plag	53.1	twinning freq absent or deformed; dusty; antiperthitic
Biot	7.0	yellow to reddish brown laths & shreds & anhed stains along hyp cleav. & margins
Amph		
Opx	5.5	faintly pleochroic
Cpx		
Garn	2.2	subhed; inclus of other mineral phases
Opaq	0.4	
Sph		
Rut	tr	
Zircn	tr	
Apat	tr	
Allan		
Epid		
Cumm		
Seric	tr	
Chlor	tr	
Cc	tr	

Remarks: hypersthene frequently has biotite habit; texture is porphyroblastic (garnet) to cataclastic

Sample: 481
Locality: Nilgiris
Rock type: mafic granulite
Description: dark gray, greasy, medium to coarse-grained

Pts counted: 1596 An# 50

	(%)	Description
Qtz	0.3	
Kspar		
Plag	44.1	twinning usually present but deform; infreq saussurit.; some antiperthite
Biot	0.5	reddish brwn prisms and anhedral stains along cleavages and margins of hyp & hb
Amph	29.1	olive-green
Opx	24.1	pleochroic, pl pink to pale green; develops after hb
Cpx		
Garn	1.1	subhed with inclus
Opaq	0.3	
Sph		
Rut		
Zircn	tr	
Apat	tr	
Allan		
Epid		
Cumm		
Seric		
Chlor	0.5	
Cc	tr	

Remarks: hyp initially develops from olive-green hb with minor late-stage alter to anhed biot and pale green hb on margins and cleavages; texture is granoblastic to porphyroblastic

Sample: 483
Locality: Nilgiris
Rock type: charnockite
Description: dark gray, medium-grained, homogeneous

Pts counted: 1542 An# 49

	(%)	Description
Qtz	8.9	undulose extinction
Kspar	4.6	twinning absent
Plag	65.5	twinning sometimes absent, usu deform; saussurit. absent; antiperthite present
Biot	tr	reddish brown, anhed margins to pyx
Amph	9.2	green to olive-green
Opx	8.3	pleochroic, pl pink to pale green
Cpx	1.7	pale green
Garn		
Opaq	1.5	
Sph		
Rut		
Zircn	tr	
Apat	0.3	
Allan		
Epid		
Cumm		
Seric	tr	
Chlor	tr	
Cc		

Remarks: prismatic to anhedral micas freq form thin alter. rim on pyroxene and hb; texture is hypidiomorphic granular to granoblastic

Sample: 484-1a
Locality: Kollegal-Malavalli-KD
Rock type: granitic charnockite
Description: gray, medium-grained, foliated

Pts counted: 1571 An# 25

	(%)	Description
Qtz	25.3	undulose extinction
Kspar	19.9	predominantly as intergranular megacrysts
Plag	47.8	twin lamellae usu absent or deformed; minor saussurit.; no antiperthite
Biot	4.0	yellow to brown laths and minor anhedral stains
Amph	1.1	olive-green
Opx	0.8	
Cpx		
Garn		
Opaq	1.5	
Sph		
Rut		
Zircn	tr	
Apat	0.5	
Allan	tr	
Epid		
Cumm		
Seric		
Chlor		
Cc		

Remarks: some myrmekite; texture is granoblastic

Sample: 484-1b
Locality: Kollegal-Malavalli-KD
Rock type: granodioritic gneiss
Description: gray, medium-grained, foliated

Pts counted: 1466 An# 29

	(%)	Description
Qtz	20.7	undulose extinction
Kspar	18.5	predominantly as intergranular megacrysts
Plag	49.5	twin lamellae usu absent or deformed; minor saussurit.; rare antiperthite
Biot	6.1	yellow to brown laths; anhedral stains not present
Amph	3.3	olive-green
Opx		
Cpx		
Garn		
Opaq	1.4	
Sph		
Rut		
Zircn	0.1	
Apat	0.4	
Allan		
Epid		
Cumm		
Seric		
Chlor		
Cc		

Remarks: some myrmekite; texture is granoblastic

Sample: 485-1
Locality: Toppur
Rock type: mafic granulite
Description: dark gray, coarse-grained, foliated

Pts counted: 1568 An# 61

	(%)	Description
Qtz	tr	
Kspar		
Plag	39.3	sharp lamellae but usually deformed; fresh-looking; rare dust
Biot		
Amph	8.6	olive-green to olive-brown
Opx	20.8	pleochroic pl pink to pale green; schiller structure
Cpx	18.2	pale green
Garn	11.1	large subhed grains & poikilitic clumps
Opaq	1.6	
Sph		
Rut		
Zircn	tr	
Apat	0.2	
Allan		
Epid		
Cumm		
Seric		
Chlor	tr	
Cc	0.2	

Remarks: pyroxene develops in cleavages of hornblende; texture is porphyroblastic garnet)

Sample: 485-2
Locality: Toppur
Rock type: charnockite
Description: dark gray, medium-grained, homogeneous

Pts counted: 1475 An# 47

	(%)	Description
Qtz	10.2	undulose extinction; anhedral, intergranular
Kspar	3.8	anhedral, coalesced antiperthite along margins of plag
Plag	58.5	twin lamellae usu sharp but deformed; fresh looking; some antiperthite
Biot	0.3	brownish yellow, anhedral stains at margins of pyx
Amph	5.7	green to olive-green
Opx	11.7	usually pleochroic pale pink to pl grn
Cpx	6.6	pale green
Garn		
Opaq	2.9	
Sph		
Rut		
Zircn	tr	
Apat	0.3	
Allan		
Epid		
Cumm		
Seric		
Chlor	tr	
Cc	tr	

Remarks: late-stage retrogres. produces thin chlorite and biotite rim on pyroxene; texture is hypidiomorphic granular to granoblastic

Sample: 486-1
Locality: Toppur
Rock type: charnockite
Description: dark gray, medium-grained, homogeneous

Pts counted: 3119 An# 46

	(%)	Description
Qtz	5.9	undulose extinction; some large, inter-granular grains
Kspar	1.4	usually as coalesced antiperthite at plag margins
Plag	61.1	lamellae freq absent else deformed; some saussuritization; antiperthite present
Biot	0.1	yellow to reddish brown small prisms and anhed stains in pyx cleav & margins
Amph	0.4	olive-green; along pyx cleavages and margins
Opx	14.9	pleochroic pale pink to pale green
Cpx	11.5	pale green
Garn	tr	
Opaq	2.2	
Sph		
Rut		
Zircn	0.2	
Apat	0.6	
Allan		
Epid		
Cumm		
Seric	tr	
Chlor	tr	
Cc	1.7	

Remarks: relatively minor late-stage retrogression of pyx to biot and hb along margins and cleavages; some diffuse cross-cutting veins; texture is granoblastic to porphyroblastic

Sample: 488-4
Locality: Hosur-Krish-Dharm
Rock type: charnockite
Description: dark gray, greasy coarse-grained, homogeneous

Pts counted: 3194 An# 27

	(%)	Description
Qtz	21.5	undulose extinction
Kspar		
Plag	70.8	twin lamellae freq deformed; saussurit. and antiperthite common
Biot	0.1	small, pale yellow to brown laths and patches in pyx
Amph	0.4	pale olive-green
Opx	5.7	pleochroic pale pink to pale green
Cpx		
Garn		
Opaq	0.5	
Sph		
Rut		
Zircn	tr	
Apat	0.5	
Allan		
Epid	tr	
Cumm		
Seric		
Chlor		
Cc	0.5	

Remarks: hypersthene appears to develop from biot and hb, with minor late-stage retrogres.; texture is hypidiomorphic granular

Sample: 510-1
Locality: Hosur-Krish-Dharm
Rock type: charnockite
Description: dark gray, coarse-grained, homogeneous

Pts counted: 1571 An# 30

	(%)	Description
Qtz	12.9	undulose extinction
Kspar	tr	
Plag	71.3	twin lamellae faint in larger grains; some saussurit.; antiperthite present
Biot	7.9	yellow to brown laths and anhedral, reddish brown stains
Amph	tr	green
Opx	6.8	faintly pleochroic
Cpx		
Garn		
Opaq	1.1	
Sph		
Rut		
Zircn	tr	
Apat	tr	
Allan		
Epid		
Cumm		
Seric	tr	
Chlor	tr	
Cc	tr	

Remarks: hypersthene clearly develops from lath-shaped biotite; late-stage alter of hyp along margins and cleavages to anhed biot; texture is hypidio gran to granoblastic

Sample: 510-4
Locality: Hosur-Krish-Dharm
Rock type: granitic gneiss
Description: pink to gray, coarse-grained, homogeneous

Pts counted: 1681 An# 26

	(%)	Description
Qtz	32.3	undulose extinction
Kspar	23.7	intergranular mega-crysts
Plag	40.5	twin lamellae usu absent or faint; some antiperthite and saussuritization
Biot	2.7	pale yellow to brown laths and infrequent anhedral stains
Amph		
Opx		
Cpx		
Garn		
Opaq	0.8	
Sph		
Rut		
Zircn	tr	
Apat	tr	
Allan		
Epid		
Cumm		
Seric	tr	
Chlor	tr	
Cc	tr	

Remarks: some myrmekite present; texture is hypidiomorphic granular to porphyroblastic

Sample: 514-2
Locality: Tiruvannamalai
Rock type: tonalitic gneiss
Description: gray, medium-grained, foliated

Pts counted: 1825 An# 25

	(%)	Description
Qtz	32.4	undulose extinction; elongate grains and mortar texture
Kspar	0.9	small, anhedral, intergran crystals
Plag	64.4	twin lamellae usu absent or deformed; some antiperthite
Biot	1.9	yellow to brown laths, and anhed reddish brown stains
Amph		
Opx		
Cpx		
Garn		
Opaq	0.4	
Sph		
Rut		
Zircn	tr	
Apat	tr	
Allan		
Epid		
Cumm		
Seric	tr	
Chlor	tr	
Cc	tr	

Remarks: myrmekite and mortar texture present; texture is granoblastic to cataclastic

Sample: 514-3
Locality: Tiruvannamalai
Rock type: charnockite
Description: gray, greasy, medium-grained, foliated

Pts counted: 1815 An# 23

	(%)	Description
Qtz	13.6	undulose extinction; some mortar texture
Kspar	1.5	small, anhed, intergranular crystals; few twins; no perth
Plag	81.8	twin lamellae absent or deformed; some antiperthite
Biot	1.9	yellow to brown laths, and red-brn, anhed stains on hyp
Amph	tr	green
Opx	0.6	faintly pleochroic
Cpx		
Garn		
Opaq	0.6	
Sph		
Rut		
Zircn	tr	
Apat	tr	
Allan		
Epid		
Cumm		
Seric	tr	
Chlor	tr	
Cc	tr	

Remarks: rare myrmekite; infreq mortar texture; hyp altering along margins to micas and carbonate; texture is granoblastic

Sample: 526-1
Locality: Shevaroy Hills
Rock type: charnockite
Description: gray, greasy, medium-grained, homogeneous

Pts counted: 1700 An# 36

	(%)	Description
Qtz	25.8	undulose ext; some lrg or elong grains; mortar tex prevalent
Kspar	0.2	
Plag	69.3	twin lamellae freq absent or deformed; some antiperthite and saussur. present
Biot	0.3	yellow to brn laths, and brn and red-brn prisms and stains
Amph	0.4	olive-green
Opx	1.4	pleochroic pale pink to pale green
Cpx	tr	neutral to pale grn
Garn		
Opaq	1.8	
Sph		
Rut	tr	
Zircn	tr	
Apat	0.4	
Allan		
Epid		
Cumm		
Seric	tr	
Chlor	tr	
Cc	tr	

Remarks: mortar texture and some mylonite present; pyx alters to micas in cleavages; texture is cataclastic

Sample: 528
Locality: Shevaroy Hills
Rock type: charnockite
Description: gray, glassy, medium-grained, homogeneous

Pts counted: 1791 An# 38

	(%)	Description
Qtz	19.1	undulose extinction; some elongate grains and mortar texture
Kspar		
Plag	64.0	twin lamellae freq absent or deformed; antiperthite and saussur. common
Biot	1.2	reddish brown, anhed small prims & stains along margins & cleavages of hyp
Amph		
Opx	7.2	pleochroic pale pink to pale green; some schiller structure
Cpx		
Garn	6.9	subhedral grains reach 2-4mm
Opaq	1.3	
Sph		
Rut		
Zircn	tr	
Apat	0.1	
Allan		
Epid		
Cumm		
Seric	tr	
Chlor	tr	
Cc	0.2	veinlets and blebs

Remarks: some mortar texture; garnet contains inclusions of other mineral phases; texture is cataclastic

Sample: 531-1
Locality: Shevaroy Hills
Rock type: charnockite
Description: gray, medium to coarse-grained, homogeneous

Pts counted: 1750 An# 36

	(%)	Description
Qtz	24.4	undulose extinction; mortar texture
Kspar	1.7	as coalescing anti-perthite at plag margins
Plag	64.3	twin lamellae usu absent or deformed; grains to 5mm; some saussur.; antiperth
Biot	0.8	reddish brown usu anhed stains in hyp cleavages & margins
Amph	tr	green; grows along cleavages & margins of hypersthene
Opx	5.9	pleochroic pale pink to pale green; some schiller structure
Cpx		
Garn		
Opaq	0.9	
Sph		
Rut		
Zircn	tr	
Apat	0.1	
Allan		
Epid		
Cumm		
Seric	0.1	
Chlor	tr	
Cc	1.8	veinlets & trains

Remarks: mortar texture; carbonate assoc with hyp and plag; hyp altering to anhed biot and hb along margins and cleavage; texture is porphyroblastic (plag) to cataclastic

Sample: 531-2
Locality: Shevaroy Hills
Rock type: charnockite
Description: gray, medium to coarse-grained, foliated

Pts counted: 1442 An# 38

	(%)	Description
Qtz	3.5	undulose extinction
Kspar	tr	
Plag	66.2	twin lamellae usu absent or deformed; some antiperthite and saussuritization
Biot	0.6	reddish brown usu anhed stains in hyp cleavages & margins
Amph		
Opx	16.4	pleochroic pale pink to pale green; some schiller structure
Cpx		
Garn	8.9	grains 2-5mm usu fractured
Opaq	4.4	
Sph		
Rut		
Zircn	tr	
Apat	tr	
Allan		
Epid		
Cumm		
Seric	tr	
Chlor	tr	
Cc	tr	

Remarks: garnet has inclusions of other mineral phases; carbonate present in cross-cutting veinlets and trains; texture is porphyroblastic (garnet) to cataclastic

Sample: 533
Locality: Shevaroy Hills
Rock type: charnockite
Description: gray, medium to coarse-grained, homogeneous

Pts counted: 1786 An# 34

	(%)	Description
Qtz	34.4	undulose extinction; some large grains ~5mm
Kspar	9.7	twinning usu faint
Plag	47.1	twin lamellae freq absent or deformed; some antiperthite and saussuritization
Biot	tr	yellow to reddish brown anhed stains along hyp margins
Amph	0.2	pale green along hyp margins and cleavage as late-stage alter
Opx	6.6	poorly pleochroic
Cpx		
Garn		
Opaq	1.2	
Sph		
Rut	tr	needles is quartz
Zircn	tr	
Apat	0.1	
Allan		
Epid		
Cumm		
Seric	tr	
Chlor	tr	
Cc	0.8	

Remarks: hypersthene varies from relatively fresh to highly altered; texture is porphyroblastic (quartz)

Sample: 535-2
Locality: Shevaroy Hills
Rock type: charnockite
Description: gray, medium-grained, foliated

Pts counted: 1688 An# 38

	(%)	Description
Qtz	26.8	undulose extinction; some mortar texture
Kspar		
Plag	64.0	twin lamellae freq absent or deformed; some antiperthite; minor saussurit.
Biot	0.8	reddish brown, anhed stains along hyp cleavages and margin
Amph	0.1	pale green along hyp margins
Opx	1.0	pleochroic pale pink to pale green; alter in cleavages & marg
Cpx		
Garn	4.6	subhed to anhed with inclusions of qtz
Opaq	2.7	
Sph		
Rut	tr	needles in qtz
Zircn	tr	
Apat	tr	
Allan		
Epid		
Cumm		
Seric	tr	
Chlor	tr	
Cc	tr	

Remarks: cross-cutting carbonate-rich vein; some mortar texture; texture is granoblastic

Sample: 536-1
Locality: Salem
Rock type: charnockite
Description: gray, greasy, medium to coarse-grained, foliated

Pts counted: 1627 An# 38

	(%)	Description
Qtz	18.5	undulose extinction
Kspar		
Plag	64.4	twin lamellae usu absent or deformed; antiperthitic
Biot	1.5	yellow to brn laths, and anhedral stains along hyp cleavages
Amph		
Opx	12.4	poorly pleochroic; prismatic to fibrous corona of micas
Cpx		
Garn		
Opaq	2.5	
Sph		
Rut		
Zircn	tr	
Apat	0.3	
Allan		
Epid		
Cumm	tr	
Seric	0.2	
Chlor	0.2	
Cc	tr	

Remarks: minor mortar texture; hypersthene relative highly altered wears corona of micas and cummingtonite; texture is granoblastic

Sample: 536-2
Locality: Salem
Rock type: retrograde gneiss
Description: gray, medium-grained, foliated

Pts counted: 1634 An# 36

	(%)	Description
Qtz	14.5	undulose extinction
Kspar		
Plag	62.0	twin lamellae usu absent or deformed; some saussurit.; infreq antiperthite
Biot	3.1	yellow to olive-brn laths, & anhed stain along cleavages and margins in hb
Amph	19.1	pl grn to olive-brn; prism. to fibrous corona of micas
Opx		
Cpx		
Garn		
Opaq	0.6	
Sph		
Rut		
Zircn	tr	
Apat	0.4	
Allan		
Epid		
Cumm	tr	
Seric	0.3	
Chlor	tr	
Cc	tr	

Remarks: some mortar texture; hornblende has corona of micas and cummingtonite; texture is granoblastic

Sample: 536-3
Locality: Salem
Rock type: charnockite
Description: gray, greasy, medium to coarse-grained, foliated

Pts counted: 1831 An# 35

	(%)	Description
Qtz	12.3	undulose extinction; some elongate grains
Kspar		
Plag	67.3	twin lamellae usu absent or deformed; some antiperthite and saussuritization
Biot	0.8	yellow to brn laths & anhed stains along hyp cleav & margins
Amph	12.7	pale grn to olive
Opx	4.5	faintly pleochroic; corona of micas
Cpx		
Garn		
Opaq	1.8	
Sph		
Rut		
Zircn	0.1	
Apat	0.5	
Allan		
Epid		
Cumm	tr	
Seric	tr	
Chlor	tr	
Cc	tr	

Remarks: alteration corona around hypersthene; texture is granoblastic

Sample: 537-1
Locality: Salem
Rock type: charnockite
Description: gray, greasy, medium to coars-grained, foliated

Pts counted: 1614 An# 35

	(%)	Description
Qtz	21.1	undulose extinction; some elongate grains
Kspar		
Plag	71.8	twin lamellae usu absent or deformed; rare antiperthite and saussuritization
Biot	0.6	yellow to brn laths, & prism. & anhedral stains on hyp and lath-shaped biot
Amph		
Opx	5.1	faintly pleochroic; freq has alter rim
Cpx		
Garn		
Opaq	1.2	
Sph		
Rut		
Zircn	tr	
Apat	tr	
Allan		
Epid		
Cumm	tr	
Seric	0.1	
Chlor	0.1	
Cc	tr	

Remarks: some mortar texture; hyp, lath-shaped biot, and opaques freq have a prismatic to fibrous reaction corona of micas and cummingtonite; texture is granoblastic

Sample: 537-2
Locality: Salem
Rock type: retrograde gneiss
Description: gray, medium-grained, folitated

Pts counted: 1839 An# 30

	(%)	Description
Qtz	22.1	undulose extinction; some large grains; minor mortar texture
Kspar		
Plag	71.9	twin lamellae usu absent or deformed; saussur. locally intense; antiperth rare
Biot	1.1	small, secondary, olive-green prisms and anhedral stains
Amph		
Opx		
Cpx		
Garn		
Opaq	0.7	
Sph		
Rut		
Zircn	tr	
Apat	tr	
Allan		
Epid	0.8	zoisite,clinozoisite
Cumm	0.8	
Seric	2.0	
Chlor	0.6	
Cc	tr	

Remarks: minor mortar texture; intense alteration: original biot, amph, or pyx replaced by cummingtonite, micas, and epidote group; texture is granoblastic

Sample: 541-3
Locality: Salem
Rock type: charnockite
Description: dark gray, greasy, medium-grained, foliated

Pts counted: 1594 An# 36

	(%)	Description
Qtz	12.1	undulose extinction; some elongate grains and mortar texture
Kspar		
Plag	79.1	twin lamellae usu absent or deformed; some antiperthite and saussuritization
Biot	tr	yellow to brn laths, and anhedral stains in cleavag & margins of hyp & lath biot
Amph	0.4	olive-green; usu has reaction rim but weaker than for hyp
Opx	6.2	poorly pleochroic; fibrous to prismatic rim of micas
Cpx		
Garn		
Opaq	1.9	
Sph	tr	
Rut		
Zircn	tr	
Apat	tr	
Allan		
Epid		
Cumm		
Seric	0.1	
Chlor	0.2	
Cc	tr	

Remarks: minor mortar texture; opaques, apatite, lath-biot, hb, and hyp have reaction rims when grain borders plag, but not with quartz; texture is granoblastic

Sample: 544-1
Locality: Salem
Rock type: charnockite
Description: gray, greasy, medium-grained, foliated

Pts counted: 1589 An# 36

	(%)	Description
Qtz	19.6	undulose extinction; some mortar texture
Kspar		
Plag	65.0	twin lamellae usu absent or deformed; some antiperthite and saussuritization
Biot	0.8	yellow to brn laths, and anhedral stains in hb and hyp cleavages and margins
Amph	9.2	green to olive-grn; freq has thin reac rim when borders plg
Opx	2.8	faintly pleochroic; fibrous reaction rim when borders plag
Cpx		
Garn		
Opaq	2.2	freq with rim of bi
Sph		
Rut		
Zircn	tr	
Apat	0.1	freq with reac rim
Allan		
Epid		
Cumm		
Seric	tr	
Chlor	0.1	
Cc	0.2	

Remarks: saussuritization and and carbonate-chlorite veinlets locally intense; reaction rims or coronas on mafic minerals; texture is granoblastic to cataclastic

Sample: 544-2
Locality: Salem
Rock type: retrograde gneiss
Description: gray, medium-grained, foliated

Pts counted: 1539 An# 36

	(%)	Description
Qtz	15.3	undulose extinction; some large intergran grains; minor mortar
Kspar		
Plag	62.2	twin lamellae usu absent or deformed; saussur. present; infreq antiperthite
Biot	10.9	pl yellow to olive-brn laths, & brn, anhed stains on hb & lath-biot
Amph	5.2	olive to brown; margins have primatic to anhed biot
Opx		
Cpx		
Garn		
Opaq	1.2	
Sph		
Rut		
Zircn	tr	
Apat	0.5	
Allan		
Epid	1.2	zoisite,clinozoisite
Cumm	0.5	
Seric	0.3	
Chlor	1.5	
Cc	1.2	

Remarks: probable pseudomorph after hyp has thick corona of micas and an interior of micas, epidote group, cummingtonite, carbonate, & quartz; texture is granoblastic

Sample: 552-1a
Locality: Bhavanisagar
Rock type: charnockite
Description: gray, greasy, fine to medium-grained, foliated

Pts counted: 1595 An# 39

	(%)	Description
Qtz	1.4	relatively fine-grained, intergranular mortar texture
Kspar		
Plag	69.6	twin lamellae freq absent or deformed; some antiperthite
Biot	0.3	brown, small prisms and anhedral stains along cleavages and margins of hyp
Amph	1.4	olive-green; largely along margins of hyp
Opx	12.7	pleochroic pale pink to pale green; schiller structure
Cpx	11.7	pale green
Garn		
Opaq	2.9	
Sph		
Rut		
Zircn	tr	
Apat	tr	
Allan		
Epid		
Cumm		
Seric	tr	
Chlor	tr	
Cc	tr	

Remarks: pyroxene has reaction rim of micas; texture is granoblastic to cataclastic

Sample: 552-1e
Locality: Bhavanisagar
Rock type: charnockite
Description: gray, greasy, fine to medium-grained, foliated

Pts counted: 1483 An# 37

	(%)	Description
Qtz	25.3	fine and medium-grained intergranular mortar texture
Kspar	0.6	
Plag	65.1	twin lamellae usu absent or deformed; antiperthite rare
Biot	3.1	pl yellow to dark-brn laths, and brn small prisms and anhedral stains
Amph	0.4	pl green to olive-green; along margins of hyp
Opx	1.7	pleochroic pale pink to pale green
Cpx	0.5	pale green
Garn	2.8	subhed; vermicular inclusions of quartz
Opaq	0.5	
Sph		
Rut		
Zircn	tr	
Apat	tr	
Allan		
Epid	tr	
Cumm		
Seric	tr	
Chlor	tr	
Cc	tr	

Remarks: locallized, relatively intense alteration; pyx has reaction corona of micas; texture is granoblastic to cataclastic

Sample: 552-2a
Locality: Bhavanisagar
Rock type: retrograde gneiss
Description: gray, medium-grained, foliated

Pts counted: 1600 An# 38

	(%)	Description
Qtz	19.2	ubiquitous mortar texture
Kspar		
Plag	67.2	twin lamellae usu absent or deformed; rare antiperthite; some saussurit.
Biot	9.4	yellow to brn laths and shreds show strong foliation along microshears
Amph		
Opx		
Cpx		
Garn	3.5	large & small grains
Opaq	tr	
Sph		
Rut		
Zircn	tr	
Apat	tr	
Allan		
Epid		
Cumm		
Seric	tr	
Chlor	tr	
Cc	0.8	usu assoc with biot

Remarks: severe cataclastic deformation: mortar texture, mylonite, biot foliation along shears, rotated plag augen in mortar matrix; texture is cataclastic

Sample: 553
Locality: Biligirirangan Hills
Rock type: charnockite
Description: gray, greasy, medium-grained, foliated

Pts counted: 1498 An# 27

	(%)	Description
Qtz	20.8	undulose extinction; many elongate grains
Kspar	0.4	present as coalesced antiperthite along margins of plag
Plag	74.1	twin lamellae usu absent or deformed; antiperthite and saussurit. present
Biot	3.2	lt brn to very drk brn laths & shreds, freq bent, & prism. to anhed stains
Amph	0.2	
Opx	0.4	almost entirely replaced by micas; pleochr when present
Cpx		
Garn		
Opaq	0.3	
Sph		
Rut		
Zircn	tr	
Apat	0.1	
Allan		
Epid	tr	
Cumm		
Seric	0.5	
Chlor	tr	
Cc	tr	

Remarks: mortar texture, mylonite, and alignment of biot shreds along microshears; fair degree of overall alteration; texture is cataclastic

Sample: 554
Locality: Biligirirangan Hills
Rock type: charnockite
Description: gray, greasy, medium-grained, foliated

Pts counted: 1706 An# 30

	(%)	Description
Qtz	21.6	undulose extinction; freq elongate grain; mortar texture
Kspar	0.5	coalesced antiperth at margins of plag
Plag	70.3	twin lamellae usu absent or defomed; antiperthite; some saussuritization
Biot	1.1	brown laths, and anhed stains along hyp cleavages and margins
Amph	0.4	pale green to green; along hyp cleavages and margins
Opx	4.9	poorly pleochroic
Cpx		
Garn		
Opaq	1.1	
Sph		
Rut		
Zircn	tr	
Apat	0.1	
Allan		
Epid		
Cumm		
Seric	tr	
Chlor	tr	
Cc	tr	

Remarks: mortar texture common; mylonite; late-stage retrogression of hyp to anhed biot and hb; texture is cataclastic

Sample: 555
Locality: Biligirirangan Hills
Rock type: charnockite
Description: gray, greasy, medium-grained, foliated

Pts counted: 1708 An# 31

	(%)	Description
Qtz	18.1	undulose extinction; mortar texture
Kspar	0.7	coalesced antiperth at margins of plag
Plag	75.5	twin lamellae usu absent or deformed; antiperthite; dusty saussuritization
Biot	0.4	yellow to brn laths; & brn, anhed stains along hyp cleavages and margins
Amph	0.2	green; along hyp margins
Opx	3.9	poorly pleochroic
Cpx	0.1	pale green
Garn		
Opaq	0.9	
Sph		
Rut		
Zircn	tr	
Apat	0.2	
Allan		
Epid		
Cumm		
Seric	tr	
Chlor	tr	
Cc	tr	

Remarks: mortar texture common; mylonite; biot laths show rough foliation; hyp retrogresses to anhed biot and hb; texture is cataclastic

Sample: 556
Locality: Biligirirangan Hills
Rock type: charnockite
Description: gray, greasy, medium-grained, foliated

Pts counted: 1595 An# 33

	(%)	Description
Qtz	20.7	undulose extinction; elongate grains; mortar texture
Kspar	1.1	coalesced antiperth at plag margins; twinning rare
Plag	74.5	twin lamellae usu absent or deformed; elongate grains; antiperth & saussur.
Biot	0.5	yellow to brn laths, & brn to reddish brn anhed stains in hyp
Amph	tr	green; along hyp margins
Opx	1.6	poorly pleochroic; some schiller struct
Cpx		
Garn		
Opaq	1.6	some elongte strands
Sph		
Rut		
Zircn	tr	
Apat	tr	
Allan		
Epid		
Cumm		
Seric	tr	
Chlor	tr	
Cc	tr	

Remarks: mortar texture; mylonite; hyp appears to have initially developed from lath-shaped biot and later retrogressed to anhed biot; texture is cataclastic

Sample: 557
Locality: Biligirirangan Hills
Rock type: charnockite
Description: gray, greasy, medium-grained, foliated

Pts counted: 1547 An# 31

	(%)	Description
Qtz	7.7	undulose extinction; some elongate grain; mortar texture
Kspar	0.5	coalesced antiperth at plag margins; twinning rare
Plag	83.1	twin lamellae usu absent or deformed; antiperthite and some saussurit.
Biot	0.2	yellow to brn laths, and anhed stains in hyp
Amph	0.1	
Opx	7.6	poorly pleochroic; some schiller struct
Cpx	tr	
Garn		
Opaq	0.6	
Sph		
Rut		
Zircn	tr	
Apat	tr	
Allan		
Epid		
Cumm		
Seric	tr	
Chlor	tr	
Cc	tr	

Remarks: cataclastic deformation not as severe as for sample 556; some hyp with biot habit appears to be after lath-shaped biot; texture is cataclastic

Sample: 558
Locality: Biligirirangan Hills
Rock type: charnockite
Description: gray, greasy, medium to coarse-grained, foliated

Pts counted: 1503 An# 31

	(%)	Description
Qtz	12.4	undulose extinction; some large grains (~4mm); mortar tex
Kspar	tr	coalesced antiperth at plag margins; twinning rare
Plag	60.7	twin lamellae usu absent or deformed; infreq saussurit.; localized antiperth
Biot	7.5	yellow to brn & red-brn laths, and anhed stains along margins of hyp
Amph	2.4	pale green; along hyp margins
Opx	12.5	pleochroic pale-pink to pale-green; some schiller structure
Cpx	0.1	
Garn		
Opaq	2.3	
Sph		
Rut	tr	needles in quartz
Zircn	tr	
Apat	tr	
Allan		
Epid		
Cumm		
Seric	0.5	
Chlor	0.3	
Cc	0.3	

Remarks: mortar texture common; localized occurances of carbonate grains, veinlets, and trains; hyp with biot habit after biot; texture is porphyroblastic to cataclastic

Sample: 559
Locality: Biligirirangan Hills
Rock type: charnockite
Description: gray, medium-grained, foliated

Pts counted: 1414 An# 30

	(%)	Description
Qtz	18.1	undulose extinction; many elongate grain; mortar texture
Kspar		
Plag	69.6	twin lamellae usu absent or deformed; antiperthitic; saussuritization
Biot	5.5	pale brn to olive-brown laths and shreds, anhed stains
Amph		
Opx	tr	poorly pleochroic; largely altered to micas, cumm, calcite
Cpx		
Garn		
Opaq	0.4	
Sph	tr	
Rut	tr	
Zircn	tr	
Apat	tr	
Allan		
Epid		
Cumm	2.3	
Seric	3.1	
Chlor	tr	
Cc	0.5	

Remarks: mylonite; microfractures; sheared with high degree of alteration; cross-cutting veinlets; hyp (originaly ~5%) largely replaced; texture is cataclastic

Sample: 561-1
Locality: Biligirirangan Hills
Rock type: charnockite
Description: gray, greasy, medium-grained, foliated

Pts counted: 1615 An# 33

	(%)	Description
Qtz	18.1	undulose extinction; mortar texture
Kspar		
Plag	75.3	twin lamellae usu absent or deformed; some saussurit.; antiperthite
Biot	1.9	pale brn to brn laths, and prism. to anhed stains in hyp cleavages & margins
Amph	tr	olive-green; along hyp margins
Opx	2.9	poorly pleochroic
Cpx		
Garn		
Opaq	1.3	
Sph		
Rut		
Zircn	tr	
Apat	tr	
Allan		
Epid		
Cumm		
Seric	tr	
Chlor	tr	
Cc	0.2	

Remarks: hypersthene retrogresses along cleavages and margins to anhed biot and hb; texture is granoblastic to cataclastic

Sample: 561-2
Locality: Biligirirangan Hills
Rock type: retrograde gneiss
Description: gray, medium-grained, foliated

Pts counted: 1448 An# 33

	(%)	Description
Qtz	23.1	undulose extinction; some elongate grains and mortar texture
Kspar		
Plag	67.6	twinning usu absent or deformed; some saussuritization; antiperthite
Biot	8.9	yellow to brn laths and shreds, and rel minor anhed stains
Amph	tr	
Opx		
Cpx		
Garn		
Opaq	0.4	
Sph		
Rut		
Zircn	tr	
Apat	tr	
Allan		
Epid		
Cumm		
Seric	tr	
Chlor	tr	
Cc	tr	

Remarks: biotite shows rough foliation; mortar texture and mylonite; texture is cataclastic

Sample: 562-1
Locality: Kollegal-Malavalli-KD
Rock type: charnockite
Description: dark gray, medium-grained, foliated

Pts counted: 1852 An# 28

	(%)	Description
Qtz	29.6	undulose extinction; mortar texture
Kspar		
Plag	61.3	twin lamellae usu deformed; antiperth; rare sausurrit.
Biot	4.2	predominantly as yellow to dark brown laths
Amph	0.4	green
Opx	3.8	pleochroic pale pink to pale green
Cpx		
Garn		
Opaq	0.3	
Sph		
Rut		
Zircn	0.3	
Apat	0.1	
Allan		
Epid		
Cumm		
Seric	tr	
Chlor	tr	
Cc	tr	

Remarks: mortar texture and mylonite; biot laths oriented along microshears; texture is granoblastic to cataclastic

Sample: 565-1
Locality: Karetur
Rock type: granitic charnockite
Description: dark gray, greasy, medium-grained, foliated

Pts counted: 714 An# 31

	(%)	Description
Qtz	12.2	generally straight extinction; some lrge,elongate grains
Kspar	28.9	twinning absent; some megacrysts; rare pethite
Plag	55.7	twin lamellae freq absent; no antiperth
Biot	0.3	pale yellow to brown laths, and anhed stains along hyp cleavages & margins
Amph		
Opx	1.0	poorly pleochroic
Cpx		
Garn		
Opaq	1.5	
Sph		
Rut		
Zircn	tr	
Apat	0.4	
Allan		
Epid		
Cumm		
Seric		
Chlor		
Cc	tr	

Remarks: some myrmekite at plag microcline joins; mortar texture; some retrogession of hyp to anhed biot and hb; texture is hypidiomorphic granular to granoblastic

Sample: 565-2
Locality: Karetur
Rock type: granitic charnockite
Description: dark gray, greasy, medium-grained, foliated

Pts counted: 1437 An# 31

	(%)	Description
Qtz	15.0	generally straight extinction; some large grains
Kspar	27.3	twinning absent; some megacrysts; infrequent perthite
Plag	52.2	twinning freq absent or faint; straight extinction; rare saussur.; antiperth
Biot	1.1	pale yellow to brown laths, and anhedral stains
Amph		
Opx	0.1	
Cpx	1.4	pale-green
Garn		
Opaq	2.3	
Sph		
Rut		
Zircn	tr	
Apat	0.3	
Allan		
Epid		
Cumm		
Seric	0.3	
Chlor	tr	
Cc	tr	

Remarks: mortar texture; myrmekite; shredded biotite along microshears; texture is granoblastic to cataclastic

Sample: 565-5
Locality: Karetur
Rock type: granitic gneiss
Description: pinkish gray, medium to coarse-grained, homogeneous

Pts counted: 1203 An# 27

	(%)	Description
Qtz	24.1	generally straight extinction; some large grains
Kspar	26.9	twinning usu absent; megacrysts; some perthite
Plag	41.1	twin lamellae usu present & straight; some saussur.; rare antiperthite
Biot	2.8	pale yellow to brown laths, and anhed stains in hb cleav.
Amph	2.3	green to olive-green with anhed bi along cleavages
Opx		
Cpx		
Garn		
Opaq	1.6	
Sph		
Rut		
Zircn	0.1	some large grains
Apat	0.2	sometimes clumped
Allan		
Epid		
Cumm		
Seric	tr	
Chlor	tr	
Cc	0.9	

Remarks: minor retrogression of hornblende to biotite in cleavages; texture is granoblastic to cataclastic

Sample: 567
Locality: Nilgiris
Rock type: charnockite
Description: dark gray, greasy, medium-grained, foliated

Pts counted: 1656 An# 36

	(%)	Description
Qtz	0.5	
Kspar	9.6	some intergranular megacrysts; perthite
Plag	47.4	twin lamellae freq. absent or deformed; antiperthite; saussuritization
Biot	15.3	yellow to reddish brn laths usu bent, and anhedral stains
Amph		
Opx	1.4	faintly pleochroic
Cpx		
Garn	23.9	subhed; inclusions of quartz
Opaq	1.8	
Sph		
Rut		
Zircn	tr	
Apat	0.1	
Allan		
Epid		
Cumm		
Seric	tr	
Chlor	tr	
Cc	tr	locally intense

Remarks: some myrmekite; locally intense saussuritization; texture is granoblastic to to cataclastic

Sample: 569
Locality: Nilgiris
Rock type: charnockite
Description: dark gray, greasy, medium-grained, foliated

Pts counted: 1642 An# 38

	(%)	Description
Qtz	34.5	undulose extinction; elongate grains common
Kspar	7.7	twinning absent; perthite
Plag	39.3	twin lamellae freq absent or deformed; antiperthite; saussuritization
Biot	0.8	yellow to brn laths, and prismatic to anhed stains in hyp cleavages & margins
Amph		
Opx	8.2	poorly pleochroic
Cpx		
Garn	8.2	subhed; inclusions of quartz
Opaq	0.6	
Sph		
Rut		
Zircn	tr	
Apat	tr	
Allan		
Epid		
Cumm	tr	
Seric	0.3	
Chlor	tr	
Cc	0.4	locally intense

Remarks: mortar texture; mylonite; intense saussuritization; late-stage retrogression of hyp to anhedral biot; texture is cataclastic

C.0 Description of tables C.1 to C.9

1.) The total of seven REE is calculated using La, Ce, Sm, Eu*, Tb, Yb, and Lu. When Lu is below the detection limit, only six REE are counted as the Lu contribution is insignificant in any case. Eu* is counted rather than Eu to remove effects of large positive or negative Eu anomalies.

2.) "N.D." indicates element element not detected. " - " indicates element not determined.

3.) The U concentration for the following samples was determined by delayed neutron activation: KDA-2, 1, 4-1, 10-1, 12-1, 22, 35, 65, 66, 68, 69, 70, 77-1, 78, 101-1, 103, 104, 107-1, 108-1, 526-1, 528, 531-1, 531-2, 535-2, 553, 554, 555, 556, 557, 558, 567, 569.

4.) Fe203t = total Fe as Fe203.

5.) Fe203/F = Fe203/FeO ratio used in CIPW norm calculation.

6.) Mesonorms are Barth mesonorms (Barth, 1959; 1962).

Appendix C.0. Cross-reference of sample number to rock type and sample area.

Sample	Rock Type	Location
BG1	granitic gneiss	Bangalore-Kolar
KDA2	lo-P charnockite	Kollegal-Malav-KD
KDA3	lo-P mgranulite	Kollegal-Malav-KD
1	lo-P charnockite	Hosur-Krish-Dharm
2	lo-P charnockite	Hosur-Krish-Dharm
3	granitic gneiss	Hosur-Krish-Dharm
4-1	lo-P charnockite	Hosur-Krish-Dharm
5-1	tonalitic gneiss	Hosur-Krish-Dharm
6	granodior gneiss	Hosur-Krish-Dharm
7-1	granodior gneiss	Hosur-Krish-Dharm
7-2	granodior gneiss	Hosur-Krish-Dharm
8	lo-P charnockite	Hosur-Krish-Dharm
9-1	lo-P charnockite	Hosur-Krish-Dharm
10-1	lo-P hi-K charn	Hosur-Krish-Dharm
10-2	lo-P charnockite	Hosur-Krish-Dharm
11-1	tonalitic gneiss	Hosur-Krish-Dharm
11-2	lo-P hi-K charn	Hosur-Krish-Dharm
12-1	granodior gneiss	Hosur-Krish-Dharm
12-2	amphibolite	Hosur-Krish-Dharm
16-1	tonalitic gneiss	Hosur-Krish-Dharm
22	lo-P charnockite	Hosur-Krish-Dharm
23	granodior gneiss	Hosur-Krish-Dharm
24	tonalitic gneiss	Hosur-Krish-Dharm
25	granodior gneiss	Hosur-Krish-Dharm
26-1	granodior gneiss	Hosur-Krish-Dharm
26-2	granodior gneiss	Hosur-Krish-Dharm
27	tonalitic gneiss	Hosur-Krish-Dharm
28	tonalitic gneiss	Hosur-Krish-Dharm
29	tonalitic gneiss	Hosur-Krish-Dharm
33-1	tonalitic gneiss	Hosur-Krish-Dharm
33-2	tonalitic gneiss	Hosur-Krish-Dharm
35	lo-P charnockite	Hosur-Krish-Dharm
36	tonalitic gneiss	Hosur-Krish-Dharm
37-1	lo-P charnockite	Hosur-Krish-Dharm
37-2	lo-P charnockite	Hosur-Krish-Dharm
38	lo-P charnockite	Hosur-Krish-Dharm
39-1	lo-P charnockite	Hosur-Krish-Dharm
39-2	lo-P hi-K charn	Hosur-Krish-Dharm
40-1	granitic gneiss	Hosur-Krish-Dharm
40-2	lo-P charnockite	Hosur-Krish-Dharm
41	lo-P hi-K charn	Hosur-Krish-Dharm
42	amphibolite	Hosur-Krish-Dharm
43	lo-P charnockite	Hosur-Krish-Dharm
44-1	lo-P charnockite	Hosur-Krish-Dharm
44-2	amphibolite	Hosur-Krish-Dharm
45	lo-P charnockite	Hosur-Krish-Dharm
46	lo-P charnockite	Hosur-Krish-Dharm
47	tonalitic gneiss	Hosur-Krish-Dharm
48	tonalitic gneiss	Hosur-Krish-Dharm
49-1	tonalitic gneiss	Hosur-Krish-Dharm
49-2	amphibolite	Hosur-Krish-Dharm
50-1	tonalitic gneiss	Hosur-Krish-Dharm
51	granodior gneiss	Hosur-Krish-Dharm
52	granitic gneiss	Hosur-Krish-Dharm
55-1	tonalitic gneiss	Hosur-Krish-Dharm
55-2	granitic gneiss	Hosur-Krish-Dharm
56-1	granodior gneiss	Hosur-Krish-Dharm
56-2	granitic gneiss	Hosur-Krish-Dharm
59-1	tonalitic gneiss	Hosur-Krish-Dharm
62	lo-P charnockite	Hosur-Krish-Dharm
64-1	granodior gneiss	Hosur-Krish-Dharm
64-2	granitic gneiss	Hosur-Krish-Dharm
65	granodior gneiss	Hosur-Krish-Dharm
66	lo-P charnockite	Hosur-Krish-Dharm
67	granitic gneiss	Hosur-Krish-Dharm
68	lo-P charnockite	Hosur-Krish-Dharm
69	lo-P charnockite	Hosur-Krish-Dharm
70	lo-P charnockite	Hosur-Krish-Dharm
71	lo-P charnockite	Hosur-Krish-Dharm
77-1	tonalitic gneiss	Hosur-Krish-Dharm
77-2	lo-P mgranulite	Hosur-Krish-Dharm
78	lo-P charnockite	Hosur-Krish-Dharm
79	tonalitic gneiss	Hosur-Krish-Dharm
87-1	granodior gneiss	Hosur-Krish-Dharm
87-2	tonalitic gneiss	Hosur-Krish-Dharm
88-1	granitic gneiss	Hosur-Krish-Dharm
88-2	granodior gneiss	Hosur-Krish-Dharm
88-3	granitic gneiss	Hosur-Krish-Dharm
88-4	tonalitic gneiss	Hosur-Krish-Dharm
89-1	tonalitic gneiss	Hosur-Krish-Dharm
89-2	granitic gneiss	Hosur-Krish-Dharm
89-3	amphibolite	Hosur-Krish-Dharm
99-1	granodior gneiss	Hosur-Kuppam-Krish
99-2	granodior gneiss	Hosur-Kuppam-Krish
99-3	granitic gneiss	Hosur-Kuppam-Krish
101-1	granodior gneiss	Hosur-Kuppam-Krish
103	tonalitic gneiss	Hosur-Kuppam-Krish
104	tonalitic gneiss	Hosur-Kuppam-Krish
107-1	lo-P charnockite	Hosur-Krish-Dharm
108-1	tonalitic gneiss	Hosur-Krish-Dharm
108-2	tonalitic gneiss	Hosur-Krish-Dharm
108-3	lo-P charnockite	Hosur-Krish-Dharm
110-1	tonalitic gneiss	Hosur-Krish-Dharm
110-2	tonalitic gneiss	Hosur-Krish-Dharm
111-1	tonalitic gneiss	Hosur-Krish-Dharm
111-2	tonalitic gneiss	Hosur-Krish-Dharm
111-3	tonalitic gneiss	Hosur-Krish-Dharm
118-2	granitic gneiss	Kollegal-Malav-KD
119-1	granodior gneiss	Kollegal-Malav-KD
119-2	granitic gneiss	Kollegal-Malav-KD
119-3	lo-P hi-K charn	Kollegal-Malav-KD
119-4	tonalitic gneiss	Kollegal-Malav-KD
119-5	lo-P charnockite	Kollegal-Malav-KD
119-6	lo-P charnockite	Kollegal-Malav-KD
120-1	lo-P charnockite	Kollegal-Malav-KD
120-2	lo-P charnockite	Kollegal-Malav-KD
120-3	lo-P mgranulite	Kollegal-Malav-KD
120-4	lo-P charnockite	Kollegal-Malav-KD
121-1	tonalitic gneiss	Kollegal-Malav-KD
122-1	lo-P charnockite	Kollegal-Malav-KD
122-2	lo-P charnockite	Kollegal-Malav-KD
356		Hosur-Kuppam-Krish
378		Hosur-Kuppam-Krish
418-1	tonalitic gneiss	Hosur-Kuppam-Krish
430-1	granitic gneiss	Hosur-Kuppam-Krish
430-2	tonalitic gneiss	Hosur-Kuppam-Krish
435a	amphibolite	Hosur-Kuppam-Krish
455	tonalitic gneiss	Hosur-Kuppam-Krish
462-1	tonalitic gneiss	Hosur-Kuppam-Krish
462-2	granitic gneiss	Hosur-Kuppam-Krish
471	tonalitic gneiss	Hosur-Kuppam-Krish
472	tonalitic gneiss	Hosur-Kuppam-Krish
474	hi-P charnockite	Mettur-Sankaridrug
475	hi-P charnockite	Mettur-Sankaridrug

Sample	Rock Type	Location
477	hi-P charnockite	Nilgiri Massif
478	hi-P charnockite	Nilgiri Massif
480	hi-P charnockite	Nilgiri Massif
481	hi-P mgranulite	Nilgiri Massif
483	hi-P charnockite	Nilgiri Massif
484-1a	lo-P hi-K charn	Kollegal-Malav-KD
484-1b	granodior gneiss	Kollegal-Malav-KD
484-1c	granodior gneiss	Kollegal-Malav-KD
485-1	hi-P mgranulite	Shevaroy-Toppur
485-2	hi-P charnockite	Shevaroy-Toppur
486-1	hi-P charnockite	Shevaroy-Toppur
487-1	hi-P mgranulite	Shevaroy-Toppur
488-1	tonalitic gneiss	Hosur-Krish-Dharm
488-2	lo-P mgranulite	Hosur-Krish-Dharm
488-3	tonalitic gneiss	Hosur-Krish-Dharm
488-4	lo-P charnockite	Hosur-Krish-Dharm
489-1	lo-P hi-K charn	Hosur-Krish-Dharm
489-2	granitic gneiss	Hosur-Krish-Dharm
491-1	granitic gneiss	Bangalore-Kolar
491-2	granitic gneiss	Bangalore-Kolar
493-1	granodior gneiss	Bangalore-Kolar
493-2	granitic gneiss	Bangalore-Kolar
494-1a	granodior gneiss	Bangalore-Kunigal
498	granodior gneiss	Bangalore-Kunigal
500-1	tonalitic gneiss	Bangalore-Kolar
500-2	granitic gneiss	Bangalore-Kolar
500-3	granitic gneiss	Bangalore-Kolar
500-4	granitic gneiss	Bangalore-Kolar
501	granitic gneiss	Bangalore-Kolar
502-1	granodior gneiss	Bangalore-Kolar
502-2	granodior gneiss	Bangalore-Kolar
503-1	tonalitic gneiss	Bangalore-Kolar
503-3	granodior gneiss	Bangalore-Kolar
503-4	granodior gneiss	Bangalore-Kolar
504	granitic gneiss	Bangalore-Kolar
506-1	granitic gneiss	Bangalore-Kunigal
506-2	granitic gneiss	Bangalore-Kunigal
509-2a	granitic gneiss	Hosur-Kuppam-Krish
509-3c	granitic gneiss	Hosur-Kuppam-Krish
509-4a	granodior gneiss	Hosur-Kuppam-Krish
509-5	granodior gneiss	Hosur-Kuppam-Krish
510-1	lo-P charnockite	Hosur-Krish-Dharm
510-2	lo-P charnockite	Hosur-Krish-Dharm
510-4	granitic gneiss	Hosur-Krish-Dharm
511-2	lo-P charnockite	Hosur-Krish-Dharm
513	lo-P charnockite	Tiruvannamalai
514-2	tonalitic gneiss	Tiruvannamalai
514-3	lo-P charnockite	Tiruvannamalai
514-4	lo-P charnockite	Tiruvannamalai
523	lo-P charnockite	Tiruvannamalai
524	hi-P charnockite	Shevaroy-Toppur
525	hi-P charnockite	Shevaroy-Toppur
526-1	hi-P charnockite	Shevaroy-Toppur
527	hi-P charnockite	Shevaroy-Toppur
528	hi-P charnockite	Shevaroy-Toppur
529	hi-P charnockite	Shevaroy-Toppur
530-1	hi-P charnockite	Shevaroy-Toppur
531-1	hi-P charnockite	Shevaroy-Toppur
531-2	hi-P charnockite	Shevaroy-Toppur
532	hi-P charnockite	Shevaroy-Toppur
533	hi-P charnockite	Shevaroy-Toppur
534-1	hi-P charnockite	Shevaroy-Toppur
535-1	hi-P mgranulite	Shevaroy-Toppur
535-2	hi-P charnockite	Shevaroy-Toppur
536-1	hi-P charnockite	Salem
536-2	retrogr gneiss	Salem
536-3	hi-P charnockite	Salem
537-1	hi-P charnockite	Salem
537-2	retrogr gneiss	Salem
540-1	hi-P charnockite	Salem
540-2	retrogr gneiss	Salem
540-3	hi-P charnockite	Salem
541-3	hi-P charnockite	Salem
542-1	hi-P charnockite	Salem
542-2	retrogr gneiss	Salem
544-1	hi-P charnockite	Salem
544-2	retrogr gneiss	Salem
552-1a	hi-P charnockite	Bhavanisagar
552-1c	hi-P charnockite	Bhavanisagar
552-1e	hi-P charnockite	Bhavanisagar
552-1h	hi-P charnockite	Bhavanisagar
552-2a	retrogr gneiss	Bhavanisagar
553	hi-P charnockite	BR Hills
554	hi-P charnockite	BR Hills
555	hi-P charnockite	BR Hills
556	hi-P charnockite	BR Hills
557	hi-P charnockite	BR Hills
558	hi-P charnockite	BR Hills
559	hi-P charnockite	BR Hills
560	hi-P charnockite	BR Hills
561-1	hi-P charnockite	BR Hills
561-2	retrogr gneiss	BR Hills
562-1	lo-P charnockite	Kollegal-Malav-KD
562-2	lo-P mgranulite	Kollegal-Malav-KD
563	granitic gneiss	Bangalore-Kunigal
564-1a	tonalitic gneiss	Bangalore-Kunigal
564-1b	tonalitic gneiss	Bangalore-Kunigal
564-2	tonalitic gneiss	Bangalore-Kunigal
565-1	lo-P hi-K charn	Karetur
565-2	lo-P hi-K charn	Karetur
565-4	granitic gneiss	Karetur
565-5	granitic gneiss	Karetur
566-1	hi-P charnockite	Nilgiri Massif
567	hi-P charnockite	Nilgiri Massif
568	hi-P charnockite	Nilgiri Massif
569	hi-P charnockite	Nilgiri Massif

FILE: I2GTON.DAT

TONALITIC GNEISS

MAJOR AND TRACE ELEMENTS

	5-1	11-1	16-1	24	27	28	29	33-1	33-2	36	47
SiO2	67.42	68.98	71.51	67.13	67.92	71.70	70.64	69.08	59.34	63.13	67.48
TiO2	0.45	0.40	0.17	0.47	0.47	0.21	0.27	0.38	1.53	0.59	0.48
Al2O3	16.88	15.50	15.92	16.49	16.27	16.05	15.72	16.22	17.88	15.29	15.57
Fe2O3T	3.34	3.37	1.47	3.81	3.50	1.34	2.13	3.43	6.11	6.17	4.39
MnO	0.03	0.03	0.01	0.03	0.03	0.01	0.02	0.03	0.04	0.11	0.05
MgO	1.40	1.23	0.49	1.42	1.23	0.69	0.88	1.49	2.03	3.46	1.44
CaO	4.18	3.37	2.58	3.91	3.43	2.99	2.92	3.50	4.44	5.14	3.81
Na2O	4.65	4.57	5.28	4.84	5.06	5.52	5.55	4.58	4.86	4.23	4.43
K2O	1.51	1.53	2.14	1.55	1.54	1.32	1.44	1.52	2.22	1.76	1.32
P2O5	0.11	0.14	0.07	0.16	0.14	0.09	0.09	0.10	0.58	0.19	0.15
LOI	0.17	0.44	0.33	0.33	0.35	0.41	0.63	0.40	1.01	0.23	0.37
TOTAL	100.14	99.56	99.97	100.14	99.94	100.33	100.29	100.73	100.04	100.29	99.49
Rb	40	58	33	40	59	32	42	46	86	50	63
Cs	0.50	0.10	0.30	0.20	0.50	0.30	2.2	0.10	0.20	1.6	1.9
Sr	578	4008	690	648	595	576	477	582	798	352	604
Ba	349	477	908	570	396	328	341	357	951	199	670
Sc	4.5	1.7	1.3	4.3	2.2	0.80	1.4	2.8	4.7	19	5.1
Y	9.0	4.9	1.8	5.0	2.8	< 1.5	1.8	2.9	12	28	12
Zr	132	162	83	103	295	87	134	87	726	154	114
Hf	3.9	4.4	2.6	2.5	7.1	1.7	3.3	2.4	14	4.8	3.0
Th	6.0	0.70	4.2	0.90	5.0	0.50	2.8	0.20	8.0	9.5	8.8
U	0.23	< 0.2	< 0.3	< 0.3	0.30	0.20	0.48	< 0.3	0.20	0.59	1.2
Nb	5.7	6.8	2.0	4.7	4.7	2.6	4.3	4.8	16	13	9.2
Ta	-	-	-	-	-	-	-	-	-	-	-
Cr	16	16	9.0	16	5.0	22	17	12	25	130	34
Ni	51	22	3.0	24	27	3.0	4.0	28	< 30	30	9.0
Co	-	-	-	21	-	-	-	-	-	-	-
Zn	< 30	-	-	-	-	-	-	-	-	-	-
Pb	< 2.0	< 2.0	9.0	8.0	8.5	5.9	8.0	< 2.0	< 2.0	13	10
La	37	13	34	23	38	11	9.1	16	82	41	20
Ce	67	29	51	47	61	17	19	20	143	83	49
Nd	-	-	-	-	-	-	-	-	-	-	-
Sm	3.6	1.3	1.6	2.7	2.5	0.71	1.1	0.94	6.3	8.2	3.7
Eu	1.6	0.90	1.2	1.3	1.0	0.88	0.68	1.3	1.9	1.3	0.97
Eu*	0.93	0.44	0.47	0.76	0.71	0.24	0.33	0.29	1.5	2.5	1.2
Tb	0.29	0.23	0.19	0.28	0.27	0.13	0.14	0.13	0.41	1.1	0.53
Yb	0.66	0.62	0.31	0.49	0.39	0.25	0.32	0.24	0.86	2.1	0.85
Lu	0.080	0.090	0.050	0.080	0.053	0.030	0.050	< .07	< 0.2	0.21	0.12
Eu/Eu*	1.7	2.1	2.6	1.7	1.4	3.7	2.1	4.5	1.3	0.52	0.84
7 REE	110	45	88	74	103	29	30	38	234	138	75
K/Rb	313	219	538	322	217	342	285	274	214	292	174
K/Ba	36	27	20	23	32	33	35	35	19	73	16
Rb/Sr	0.069	0.014	0.048	0.062	0.099	0.056	0.088	0.079	0.11	0.11	0.10
Ba/Sr	0.60	0.12	1.3	0.88	0.67	0.57	0.71	0.61	1.2	0.57	1.1

FILE: I2GTON.DAT

TONALITIC GNEISS

MAJOR AND TRACE ELEMENTS

	48	49-1	50-1	55-1	59-1	77-1	79	87-2	88-4	89-1	103
SiO2	67.54	69.78	67.70	65.31	68.46	71.72	71.57	63.31	53.34	69.45	72.47
TiO2	0.41	0.37	0.48	0.47	0.27	0.30	0.31	0.49	1.13	0.33	0.24
Al2O3	16.22	15.98	15.61	15.85	15.88	15.05	15.44	17.18	17.63	15.84	15.05
Fe2O3T	3.44	2.94	4.17	4.03	2.76	2.35	2.21	4.76	9.24	2.93	1.81
MnO	0.05	0.02	0.04	0.06	0.03	0.03	0.02	0.07	0.20	0.02	0.02
MgO	1.31	1.06	2.22	1.96	1.13	0.67	0.75	2.01	3.30	1.05	0.50
CaO	3.85	3.44	3.25	3.86	4.42	2.68	3.29	4.54	5.99	3.17	2.45
Na2O	5.08	5.21	4.11	4.52	4.92	5.21	4.29	5.23	5.53	4.69	4.69
K2O	1.67	1.03	1.92	1.66	0.84	1.63	1.32	1.53	1.44	1.99	2.14
P2O5	0.14	0.10	0.07	0.18	0.12	0.08	0.08	0.17	0.65	0.07	0.07
LOI	0.35	0.30	0.43	1.50	0.65	0.58	0.40	0.45	1.09	0.21	0.49
TOTAL	100.06	100.23	100.00	99.40	99.48	100.30	99.68	99.74	99.54	99.80	99.93
Rb	40	33	90	74	1.0	48	35	50	39	19	49
Cs	3.7	0.40	1.7	0.40	0.30	< .10	0.63	< .10	0.10	0.30	0.50
Sr	635	785	453	469	664	291	312	662	393	435	371
Ba	494	509	434	394	691	464	337	294	187	563	643
Sc	7.1	2.5	6.8	8.4	6.1	3.8	3.6	10	20	1.6	2.6
Y	10	< 2.0	2.3	12	10	5.8	3.4	29	73	3.4	4.3
Zr	125	103	161	134	172	131	129	160	243	139	118
Hf	2.2	3.2	4.6	4.6	3.1	5.0	4.2	5.2	7.1	3.0	3.9
Th	2.5	5.5	24	6.2	0.50	4.5	0.80	4.4	12	3.2	5.1
U	1.1	0.80	2.4	0.40	< .10	0.42	0.20	0.60	1.2	0.30	0.34
Nb	5.9	2.2	9.9	11	5.0	6.6	5.4	14	38	4.4	5.1
Ta	-	-	-	0.50	-	1.6	3.1	0.30	2.8	0.20	< .10
Cr	25	18	184	57	21	26	-	53	20	10	4.0
Ni	8.0	9.0	53	29	44	-	-	24	22	2.0	-
Co	-	-	-	12	-	19	25	12	23	6.8	5.0
Zn	-	-	-	-	-	43	105	-	-	-	31
Pb	6.7	4.5	13	< 2.0	< 2.0	5.6	11	7.4	13	9.9	2.5
La	16	27	18	34	28	25	14	50	102	25	17
Ce	36	46	29	67	53	36	21	102	254	37	32
Nd	-	-	-	22	-	-	-	44	-	16	-
Sm	3.8	1.9	1.6	4.7	3.7	1.9	1.3	8.4	24	1.8	1.5
Eu	1.0	0.95	0.72	1.6	1.1	1.3	1.2	1.7	3.1	0.91	1.3
Eu*	1.1	0.46	0.53	1.3	1.1	0.60	0.43	2.5	6.6	0.51	0.49
Tb	0.44	0.13	0.27	0.43	0.42	0.28	0.22	1.0	2.3	0.19	0.24
Yb	0.73	0.24	0.45	0.87	0.76	0.56	0.35	2.1	5.3	0.22	0.49
Lu	0.11	0.030	0.060	0.12	0.11	0.090	0.044	0.35	0.82	< .05	0.061
Eu/Eu*	0.90	2.0	1.4	1.3	1.0	2.2	2.8	0.69	0.47	1.8	2.7
Σ REE	58	76	50	108	87	64	37	166	395	65	52
K/Rb	347	259	177	186	6973	282	313	254	306	337	363
K/Ba	28	17	37	35	10	29	33	43	64	29	28
Rb/Sr	0.063	0.042	0.20	0.16	0.002	0.16	0.11	0.076	0.099	0.11	0.13
Ba/Sr	0.78	0.65	0.96	0.84	1.0	1.6	1.1	0.44	0.48	1.3	1.7

FILE: I2GTON.DAT

TONALITIC GNEISS

MAJOR AND TRACE ELEMENTS

	104	108-1	108-2	110-1	110-2	111-1	111-2	111-3	119-4	121-1	418-1
SiO2	70.64	73.51	72.29	67.64	65.55	64.97	69.99	66.18	60.79	69.20	68.61
TiO2	0.35	0.14	0.15	0.35	0.48	0.42	0.19	0.29	1.59	0.30	0.40
Al2O3	15.36	15.28	15.87	15.79	16.53	17.22	16.14	17.59	13.03	15.90	15.77
Fe2O3T	2.81	1.10	1.20	2.91	4.22	3.99	1.86	2.53	10.17	2.99	3.25
MnO	0.02	0.01	0.01	0.05	0.05	0.05	0.02	0.02	0.14	0.01	0.04
MgO	0.81	0.37	0.52	1.25	1.95	1.83	0.70	1.04	2.31	1.01	1.11
CaO	3.01	2.88	2.67	3.45	4.31	4.44	2.45	3.24	5.09	3.14	3.61
Na2O	5.03	5.29	5.12	4.85	5.57	5.92	5.03	6.16	4.09	4.80	5.30
K2O	1.61	1.18	2.38	1.65	1.60	1.56	1.92	2.34	1.47	1.63	1.33
P2O5	0.10	0.04	0.06	0.10	< 0.1	0.17	0.07	0.11	0.53	0.13	0.14
LOI	0.45	0.26	0.08	1.84	0.65	0.10	0.98	1.17	0.04	0.39	0.23
TOTAL	100.19	100.06	100.35	99.88	100.91	100.67	99.35	100.67	99.25	99.72	99.79
Rb	51	23	41	38	46	47	41	49	24	64	35
Cs	0.50	< .10	-	0.80	0.30	1.3	0.30	0.60	0.070	1.4	0.75
Sr	342	512	558	588	804	820	770	820	246	350	564
Ba	501	260	1044	633	2321	398	1719	1365	365	318	386
Sc	1.7	0.60	0.80	5.3	0.30	9.5	0.90	1.3	21	4.9	5.3
Y	4.4	1.9	2.0	8.2	9.9	8.1	1.9	4.5	61	7.5	16
Zr	127	84	75	115	147	140	106	138	360	119	136
Hf	5.1	2.6	2.9	2.8	1.2	3.6	2.8	3.2	11	4.2	3.9
Th	4.2	1.4	0.30	3.0	0.20	2.2	3.5	4.4	8.8	6.8	4.5
U	0.32	0.21	< 0.3	0.90	0.30	0.80	0.70	0.80	1.4	1.1	2.1
Nb	5.4	3.4	1.1	4.8	4.1	4.3	1.6	2.6	19	5.9	8.5
Ta	2.5	6.7	0.70	0.50	0.20	0.40	0.20	0.10	1.2	0.35	1.2
Cr	5.0	4.0	-	26	3.0	52	10	6.0	28	11	12
Ni	-	5.0	-	12	1.0	7.0	2.0	9.0	26	13	5.2
Co	21	33	24	7.6	1.5	9.9	4.6	4.0	22	7.1	6.7
Zn	41	18	26	-	-	-	-	-	129	56	57
Pb	< 2.0	< 2.0	< 2.0	7.7	4.9	9.3	8.5	8.0	14	< 2.0	< 2.0
La	22	15	9.3	25	3.7	22	20	25	58	31	23
Ce	34	18	13	52	6.5	45	41	42	119	54	54
Nd	12	-	-	19	-	18	14	15	-	19	27
Sm	1.4	0.57	0.59	4.2	0.16	3.8	1.7	2.6	11	3.1	6.1
Eu	1.0	1.1	1.7	1.9	0.74	1.5	1.0	1.3	2.7	0.77	1.4
Eu*	0.49	0.20	0.22	1.2	0.060	1.0	0.49	0.74	3.5	0.86	1.7
Tb	0.29	0.11	0.14	0.49	0.040	0.37	0.19	0.28	1.7	0.31	0.63
Yb	0.58	0.21	0.43	0.71	0.18	0.51	0.29	0.66	5.8	0.48	1.6
Lu	0.085	0.030	0.070	0.090	0.040	0.070	0.041	0.092	1.1	0.070	0.25
Eu/Eu*	2.0	5.6	7.8	1.5	12	1.4	2.0	1.8	0.77	0.90	0.82
Σ REE	59	34	24	84	11	73	64	71	200	90	87
K/Rb	262	426	482	360	289	276	389	396	508	211	315
K/Ba	27	38	19	22	5.7	33	9.3	14	33	43	29
Rb/Sr	0.15	0.045	0.073	0.065	0.057	0.057	0.053	0.060	0.098	0.18	0.062
Ba/Sr	1.5	0.51	1.9	1.1	2.9	0.49	2.2	1.7	1.5	0.91	0.68

FILE: I2GTON.DAT

TONALITIC GNEISS

MAJOR AND TRACE ELEMENTS

	430-2	455	462-1	471	472	488-1	488-3	500-1	503-1	514-2	564-1a
SiO2	72.04	68.90	69.67	63.32	-	60.88	63.51	63.69	64.59	76.35	71.60
TiO2	0.15	0.47	0.41	0.58	-	0.33	0.82	0.54	0.65	0.19	0.22
Al2O3	16.07	15.86	15.29	16.97	-	17.62	15.72	16.03	16.19	13.71	15.71
Fe2O3T	1.90	3.24	3.16	4.63	-	5.56	6.10	5.70	5.27	0.76	1.83
MnO	0.02	0.05	0.04	0.07	-	0.10	0.09	0.08	0.09	0.01	0.03
MgO	0.65	1.25	1.10	1.85	-	3.54	2.79	2.88	2.28	0.43	0.55
CaO	2.40	3.50	3.28	4.08	-	6.43	4.36	5.87	3.87	2.18	2.61
Na2O	4.99	4.81	4.60	7.47	-	4.30	3.90	4.41	5.04	4.72	6.50
K2O	1.86	2.01	2.04	0.78	-	1.11	1.97	0.99	1.74	1.16	1.40
P2O5	0.04	0.13	0.13	0.18	-	0.37	0.42	0.14	0.24	0.01	0.09
LOI	0.53	0.39	0.19	0.30	-	0.59	0.30	0.30	0.55	0.22	0.28
TOTAL	100.65	100.61	99.91	100.23	0.00	100.83	99.98	100.63	100.51	99.73	100.82
Rb	50	50	55	2.0	3.0	2.0	18	56	145	13	50
Cs	0.90	-	1.8	-	-	0.20	0.040	1.7	8.2	0.030	1.7
Sr	455	578	558	532	913	717	652	334	624	462	544
Ba	641	-	665	-	-	351	1120	407	464	300	142
Sc	2.6	-	4.4	-	-	14	8.3	14	10	0.70	2.0
Y	7.8	11	9.6	13	13	26	16	24	23	2.0	6.2
Zr	88	118	119	142	137	80	348	160	270	63	95
Hf	3.1	-	3.0	-	-	2.6	14	4.4	6.0	2.1	2.3
Th	5.0	< 1.0	4.2	< 2.0	< 2.0	< 0.2	0.40	8.5	16	0.80	4.0
U	1.0	< 2.0	0.80	< 2.0	< 2.0	< 0.2	< 0.2	1.5	9.6	0.20	0.53
Nb	5.0	6.4	6.4	9.9	9.1	4.6	9.0	10	15	< 1.5	5.6
Ta	1.0	-	0.41	-	-	0.10	0.80	0.64	1.1	< .03	0.60
Cr	9.0	-	11	-	-	68	95	26	49	0.70	4.1
Ni	2.0	-	8.0	-	-	32	26	28	28	< 3.0	7.0
Co	5.1	-	6.6	-	-	17	20	20	15	1.0	3.1
Zn	-	-	52	-	-	-	-	73	84	9.5	39
Pb	9.0	< 2.0	< 2.0	< 2.0	< 2.0	< 2.0	< 2.0	< 2.0	3.3	< 2.0	< 2.0
La	9.1	-	21	-	-	51	52	32	79	9.7	19
Ce	14	-	44	-	-	105	92	63	149	15	36
Nd	-	-	22	-	-	-	34	27	57	3.5	13
Sm	1.3	-	3.7	-	-	10	6.9	5.3	9.3	0.43	2.5
Eu	0.84	-	1.0	-	-	1.7	1.6	1.3	2.0	0.47	0.66
Eu*	0.39	-	1.0	-	-	3.0	2.2	1.6	2.5	0.19	0.64
Tb	0.17	-	0.36	-	-	1.3	1.0	0.74	0.81	0.040	0.20
Yb	0.41	-	0.60	-	-	2.2	1.6	2.0	2.1	0.11	0.32
Lu	0.060	-	0.090	-	-	0.31	0.23	0.33	0.33	0.016	0.040
Eu/Eu*	2.1	-	0.98	-	-	0.56	0.74	0.79	0.81	4.0	1.0
Σ REE	25	-	71	-	-	173	156	105	243	25	59
K/Rb	309	334	308	3237	-	4607	908	147	100	711	232
K/Ba	24	-	25	-	-	26	15	20	31	25	82
Rb/Sr	0.11	0.087	0.099	0.004	0.003	0.003	0.028	0.17	0.23	0.029	0.092
Ba/Sr	1.4	-	1.2	-	-	0.49	1.7	1.2	0.74	0.84	0.26

FILE: I2GTON.DAT

TONALITIC GNEISS

MAJOR AND TRACE ELEMENTS

	564-1b	564-2	N	MEAN	SD %
SiO2	72.87	74.16	45	67.91	6.5
TiO2	0.20	0.13	45	0.43	71.2
Al2O3	15.40	15.37	45	15.96	5.7
Fe2O3T	1.58	0.97	45	3.50	56.5
MnO	0.04	0.02	45	0.05	82.5
MgO	0.49	0.25	45	1.39	60.9
CaO	2.34	2.22	45	3.61	27.8
Na2O	5.36	5.38	45	5.02	13.0
K2O	1.70	2.01	45	1.61	23.5
P2O5	0.06	0.09	44	0.16	88.8
LOI	0.39	0.28	45	0.48	75.0
TOTAL	100.45	100.88			
Rb	57	50	46	45	54.7
Cs	1.8	1.0	39	1.0	141.1
Sr	502	597	46	635	83.8
Ba	154	165	43	567	74.5
Sc	2.5	1.1	43	5.4	98.7
Y	5.2	4.2	44	12	120.6
Zr	82	80	46	153	70.6
Hf	2.1	2.2	43	4.2	66.3
Th	2.0	2.3	42	4.7	97.6
U	1.2	0.40	35	0.99	160.1
Nb	8.4	4.6	45	7.5	81.6
Ta	1.0	0.30	26	1.1	127.9
Cr	3.2	1.2	41	28	130.0
Ni	3.0	5.0	36	17	84.5
Co	2.9	1.3	29	12	72.0
Zn	38	25	16	52	62.5
Pb	3.0	2.0	26	7.9	42.2
La	15	14	43	29	72.2
Ce	26	24	43	55	83.8
Nd	-	8.4	17	22	60.6
Sm	1.9	1.6	43	3.8	108.7
Eu	0.64	0.53	43	1.3	42.8
Eu*	0.51	0.44	43	1.1	106.1
Tb	0.17	0.16	43	0.44	103.1
Yb	0.25	0.20	43	0.94	126.9
Lu	0.034	0.020	40	0.15	141.7
Eu/Eu*	1.3	1.2	43	2.1	102.4
Σ REE	44	40	43	90	80.8
K/Rb	248	334	45	631	196.5
K/Ba	92	101	43	33	62.5
Rb/Sr	0.11	0.084	46	0.087	61.3
Ba/Sr	0.31	0.28	43	1.00	57.0

FILE: I2GTON.DAT

TONALITIC GNEISS

CIPW NORMS

	5-1	11-1	16-1	24	27	28	29	33-1	33-2	36	47
Fe2O3/F	0.44	0.44	0.44	0.44	0.44	0.44	0.44	0.44	0.44	0.44	0.44
Qtz	22.92	28.16	26.21	21.88	22.80	27.12	24.99	26.15	10.34	15.41	25.37
Corund	0.26	0.62	0.36	0.11	0.38	0.32	0.00	0.92	0.77	0.00	0.27
Zircon	0.03	0.03	0.02	0.02	0.06	0.02	0.03	0.02	0.15	0.03	0.02
Or	8.92	9.04	12.65	9.16	9.10	7.80	8.51	8.98	13.12	10.49	7.80
Ab	38.92	35.71	44.17	40.48	42.38	46.28	46.61	38.32	40.53	35.53	37.04
An	20.24	17.13	12.72	18.64	16.33	14.47	13.92	16.93	18.62	17.67	18.20
diop	0.00	0.00	0.00	0.00	0.00	0.00	0.14	0.00	0.00	5.45	0.00
Hyp	5.97	5.66	2.35	6.43	5.67	2.66	3.73	6.40	8.41	11.04	7.05
Olivine	0.00	0.00	0.00	0.00	0.00	0.00	0.00	0.00	0.00	0.00	0.00
Mgt	1.37	1.38	0.60	1.56	1.44	0.55	0.87	1.41	2.51	2.53	1.80
Chrmite	0.01	0.01	0.00	0.01	0.00	0.01	0.01	0.01	0.01	0.05	0.02
Ilmen	0.86	0.76	0.32	0.89	0.89	0.40	0.51	0.72	2.91	1.13	0.91
Apat	0.26	0.32	0.16	0.37	0.32	0.21	0.21	0.23	1.34	0.41	0.35

BARTH MESONORM

Qtz	24.38	28.19	25.36	23.67	24.17	26.31	25.02	27.50	0.00	18.32	27.58
Corund	0.91	1.16	0.67	0.79	1.07	0.64	0.31	1.53	0.00	0.00	1.00
Or	3.43	3.97	10.51	3.32	3.91	5.28	5.03	3.22	0.00	2.09	1.51
Ab	41.82	41.61	47.38	43.60	45.63	49.33	49.77	41.13	0.00	38.11	40.45
An	18.49	14.61	11.75	16.77	14.53	13.45	12.94	15.39	0.00	17.69	16.53
Biot	8.80	8.31	3.39	9.40	8.37	3.98	5.55	9.22	0.00	13.31	10.27
Actin	0.00	0.00	0.00	0.00	0.00	0.00	0.00	0.00	0.00	7.08	0.00
Edenite	0.00	0.00	0.00	0.00	0.00	0.00	0.00	0.00	0.00	0.00	0.00
Hyp	0.00	0.00	0.00	0.00	0.00	0.00	0.00	0.00	0.00	0.00	0.00
Mgt	0.99	1.01	0.43	1.13	1.04	0.39	0.63	1.02	0.00	1.83	1.32
Sphene	0.94	0.85	0.36	0.99	0.99	0.44	0.56	0.79	0.00	1.23	1.02
Apat	0.23	0.30	0.15	0.34	0.29	0.19	0.19	0.21	0.00	0.40	0.32

FILE: I2GTON.DAT

TONALITIC GNEISS

CIPW NORMS

	48	49-1	50-1	55-1	59-1	77-1	79	87-2	88-4	89-1	103
Fe2O3/F	0.44	0.44	0.44	0.44	0.44	0.44	0.44	0.44	0.44	0.44	0.44
Qtz	21.13	26.11	25.06	20.70	25.50	27.92	32.97	13.81	0.00	25.45	30.67
Corund	0.00	0.27	1.03	0.03	0.00	0.02	1.16	0.00	0.00	0.36	0.71
Zircon	0.03	0.02	0.03	0.03	0.04	0.03	0.03	0.03	0.05	0.03	0.02
Or	9.87	6.09	11.35	9.81	4.96	9.63	7.80	9.04	8.51	11.76	12.65
Ab	42.52	43.51	34.44	37.90	41.14	43.87	36.07	43.77	46.50	39.36	39.41
An	16.77	16.74	15.83	18.15	19.03	12.92	15.94	19.14	19.18	15.49	11.91
Diop	1.39	0.00	0.00	0.00	2.03	0.00	0.00	2.05	5.29	0.00	0.00
Hyp	5.26	4.86	8.73	8.03	4.05	3.46	3.49	7.83	5.13	4.91	2.61
Olivine	0.00	0.00	0.00	0.00	0.00	0.00	0.00	0.00	5.70	0.00	0.00
Mgt	1.41	1.21	1.71	1.65	1.13	0.96	0.91	1.95	3.79	1.29	0.74
Chrmite	0.01	0.01	0.08	0.03	0.01	0.01	0.00	0.02	0.01	0.00	0.00
Ilmen	0.78	0.70	0.91	0.89	0.51	0.57	0.59	0.93	2.15	0.63	0.46
Apat	0.32	0.23	0.16	0.42	0.28	0.19	0.19	0.39	1.51	0.16	0.16

BARTH MESONORM

Qtz	22.22	26.62	28.10	23.93	25.39	27.77	32.87	16.53	2.06	26.29	30.02
Corund	0.00	0.82	1.81	0.70	0.00	0.46	1.73	0.00	0.00	0.87	1.14
Or	4.69	1.66	3.43	2.58	1.70	6.50	4.64	1.83	0.00	7.37	10.35
Ab	45.70	46.82	37.27	41.53	44.74	46.94	39.09	47.09	50.32	42.39	42.49
An	16.56	15.14	14.14	16.72	19.01	11.77	14.94	18.94	19.29	14.21	10.96
Biot	8.31	7.09	12.85	11.92	5.32	5.06	5.24	11.57	13.79	7.11	3.85
Actin	0.35	0.00	0.00	0.00	2.19	0.00	0.00	1.24	3.81	0.00	0.00
Edenite	0.00	0.00	0.00	0.00	0.00	0.00	0.00	0.00	0.00	0.00	0.00
Hyp	0.00	0.00	0.00	0.00	0.00	0.00	0.00	0.00	4.18	0.00	0.00
Mgt	1.02	0.87	1.25	1.22	0.83	0.70	0.66	1.41	2.77	0.89	0.54
Sphene	0.86	0.77	1.01	1.00	0.57	0.63	0.66	1.03	2.39	0.69	0.51
Apat	0.29	0.21	0.15	0.39	0.25	0.17	0.17	0.36	1.38	0.15	0.15

FILE: I2GTON.DAT

TONALITIC GNEISS

CIPW NORMS

	104	108-1	108-2	110-1	110-2	111-1	111-2	111-3	119-4	121-1	418-1
Fe2O3/F	0.44	0.44	0.44	0.44	0.44	0.44	0.44	0.44	0.44	0.44	0.44
Qtz	26.97	31.40	26.78	23.29	14.86	12.73	26.75	12.96	17.17	26.21	23.10
Corund	0.10	0.16	0.11	0.00	0.00	0.00	1.40	0.00	0.00	0.91	0.00
Zircon	0.03	0.02	0.02	0.02	0.03	0.03	0.02	0.03	0.10	0.03	0.03
Or	9.51	6.97	14.06	9.75	9.46	9.22	11.35	13.83	8.69	9.63	7.86
Ab	42.31	44.38	42.91	40.61	46.54	49.49	41.99	51.52	34.43	40.36	44.43
An	14.45	14.23	13.21	16.67	15.69	16.13	12.26	13.76	12.95	14.86	15.53
Diop	0.00	0.00	0.00	0.06	5.22	4.17	0.00	1.72	7.49	0.00	1.40
Hyp	4.15	1.75	2.21	5.36	5.62	5.70	3.23	3.71	9.31	4.87	4.58
Olivine	0.00	0.00	0.00	0.00	0.00	0.00	0.00	0.00	0.00	0.00	0.00
Mgt	1.15	0.45	0.49	1.19	1.73	1.64	0.76	1.04	4.17	1.22	1.33
Chrmite	0.00	0.00	0.00	0.01	0.00	0.02	0.00	0.00	0.01	0.01	0.01
Ilmen	0.67	0.27	0.29	0.67	0.91	0.80	0.36	0.55	3.02	0.72	0.76
Apat	0.23	0.09	0.14	0.23	0.00	0.39	0.16	0.26	1.23	0.30	0.32

BARTH MESONORM

Qtz	27.28	29.91	25.73	24.80	14.94	13.00	26.73	13.37	20.32	27.06	23.72
Corund	0.61	0.37	0.38	0.49	0.00	0.00	1.93	0.00	0.00	1.57	0.00
Or	5.77	5.38	11.97	4.96	5.64	5.23	8.58	10.36	0.00	5.21	3.33
Ab	45.38	47.53	45.68	44.40	49.55	52.31	45.79	54.74	38.03	43.49	47.76
An	13.12	13.55	12.25	15.54	15.24	15.56	11.19	13.30	13.31	13.53	15.37
Biot	6.06	2.56	3.20	7.97	5.96	6.15	4.67	5.31	14.39	7.16	7.29
Actin	0.00	0.00	0.00	0.00	6.44	5.38	0.00	1.35	5.28	0.00	0.44
Edenite	0.00	0.00	0.00	0.00	0.00	0.00	0.00	0.00	0.00	0.00	0.00
Hyp	0.00	0.00	0.00	0.00	0.00	0.00	0.00	0.00	0.97	0.00	0.00
Mgt	0.84	0.33	0.35	0.88	1.24	1.16	0.56	0.74	3.12	0.80	0.97
Sphene	0.73	0.29	0.31	0.75	0.99	0.86	0.40	0.60	3.44	0.80	0.84
Apat	0.21	0.08	0.12	0.21	0.00	0.35	0.15	0.23	1.15	0.27	0.29

FILE: I2GTON.DAT

TONALITIC GNEISS

CIPW NORMS

	430-2	455	462-1	471	472	488-1	488-3	500-1	503-1	514-2	564-1a
Fe2O3/F	0.44	0.44	0.44	0.44	-	0.44	0.44	0.44	0.44	0.41	0.44
Qtz	29.30	23.51	25.96	6.30	-	12.47	19.01	17.30	16.21	38.97	22.42
Corund	1.56	0.00	0.06	0.00	-	0.00	0.19	0.00	0.00	0.77	0.00
Zircon	0.02	0.02	0.02	0.03	-	0.02	0.07	0.03	0.05	0.01	0.02
Or	10.99	11.88	12.06	4.61	-	6.56	11.64	5.85	10.28	6.86	8.27
Ab	41.89	40.27	38.51	62.82	-	35.86	32.52	37.07	42.19	39.60	54.60
An	11.88	15.98	15.27	10.68	-	25.78	19.31	21.15	16.66	10.97	9.77
Diop	0.00	0.56	0.35	7.02	-	3.25	0.00	5.88	0.95	0.00	2.29
Hyp	3.21	5.23	4.96	4.74	-	12.15	11.54	8.97	9.30	1.77	1.67
Olivine	0.00	0.00	0.00	0.00	-	0.00	0.00	0.00	0.00	0.00	0.00
Mgt	0.78	1.33	1.30	1.90	-	2.28	2.50	2.34	2.16	0.31	0.75
Chromite	0.00	0.00	0.01	0.00	-	0.03	0.04	0.01	0.02	0.00	0.00
Ilmen	0.29	0.89	0.78	1.10	-	0.63	1.56	1.03	1.23	0.12	0.42
Apat	0.09	0.30	0.30	0.42	-	0.86	0.97	0.32	0.56	0.09	0.21

BARTH MESONORM

Qtz	28.64	24.48	26.82	5.67	-	14.70	24.15	18.54	19.90	37.36	20.39
Corund	1.93	0.35	0.42	0.00	-	0.00	1.43	0.00	0.42	0.96	0.00
Or	8.18	6.76	7.41	2.59	-	0.00	1.04	0.00	1.39	5.28	7.32
Ab	44.73	43.16	41.60	65.80	-	38.46	35.47	39.64	45.27	42.81	57.41
An	11.11	14.87	14.16	10.27	-	25.35	16.24	21.05	15.37	10.51	9.40
Biot	4.46	8.17	7.57	3.08	-	10.45	17.21	9.37	14.22	2.69	1.30
Actin	0.00	0.00	0.00	9.68	-	4.32	0.00	7.97	0.00	0.00	3.01
Edenite	0.00	0.00	0.00	0.00	-	0.00	0.00	0.00	0.00	0.00	0.00
Hyp	0.00	0.00	0.00	0.00	-	3.63	0.00	0.33	0.00	0.00	0.00
Mgt	0.56	0.96	0.94	1.34	-	1.64	1.83	1.69	1.56	0.23	0.53
Sphene	0.31	0.98	0.86	1.19	-	0.69	1.74	1.13	1.36	0.21	0.45
Apat	0.08	0.27	0.27	0.37	-	0.77	0.89	0.29	0.50	0.09	0.19

FILE: I2GTON.DAT

TONALITIC GNEISS

CIPW NORMS

	564-1b	564-2	N	MEAN	SD %
Fe2O3/F	0.44	0.44	45	0.44	0.0
Qtz	29.29	30.18	44	23.0	28.9
Corund	0.70	0.54	26	0.54	79.3
Zircon	0.02	0.02	45	0.032	72.9
Or	10.05	11.88	45	9.5	23.5
Ab	44.98	45.08	45	42.0	13.2
An	11.24	10.61	45	15.7	20.5
Diop	0.00	0.00	19	3.0	81.1
Hyp	2.47	1.37	45	5.4	50.6
Olivine	0.00	0.00	1	5.7	0.0
Mgt	0.65	0.40	45	1.4	56.6
Chrmite	0.00	0.00	40	0.013	120.8
Ilmen	0.38	0.25	45	0.83	71.2
Apat	0.19	0.21	44	0.36	89.0

BARTH MESONORM

Qtz	28.21	28.24	44	23.6	28.2
Corund	1.02	0.75	30	0.94	53.0
Or	7.79	10.53	40	5.3	54.7
Ab	48.00	47.88	44	45.2	12.3
An	10.36	9.89	44	14.6	21.8
Biot	3.57	1.98	44	7.4	50.9
Actin	0.00	0.00	14	4.2	70.1
Edenite	0.00	0.00	0	0.0	0.0
Hyp	0.00	0.00	4	2.3	83.9
Mgt	0.47	0.28	44	1.0	57.8
Sphene	0.42	0.27	44	0.86	65.7
Apat	0.17	0.19	43	0.31	85.9

FILE: I2GN.DAT

GRANODIORITIC GNEISS

MAJOR AND TRACE ELEMENTS

	6	7-1	7-2	12-1	23	25	26-1	26-2	51	56-1	64-1
SiO2	69.18	69.70	69.35	72.52	59.61	62.34	60.74	67.11	69.91	59.70	65.82
TiO2	0.32	0.31	0.26	0.20	1.30	0.62	0.72	0.60	0.34	1.49	0.49
Al2O3	15.33	15.96	16.39	15.21	16.46	15.96	16.44	16.45	15.62	14.86	16.80
Fe2O3T	2.77	2.06	2.39	1.74	7.21	5.06	6.41	3.31	2.97	8.76	3.27
MnO	0.02	< 0.0	< 0.0	0.01	0.08	0.07	0.08	0.01	0.03	0.19	0.03
MgO	1.08	0.84	0.54	0.53	2.04	2.98	3.01	1.14	0.85	1.81	1.33
CaO	2.86	2.64	3.11	2.49	5.27	4.87	5.20	3.05	3.02	4.41	3.32
Na2O	3.63	4.28	4.44	4.51	4.31	4.24	4.33	4.23	4.17	4.01	4.41
K2O	3.76	3.59	2.72	2.88	2.83	2.54	3.37	3.61	2.21	3.51	3.54
P2O5	0.13	< 0.1	0.14	0.07	0.47	0.30	0.34	< 0.1	0.12	0.85	0.18
LOI	0.14	0.48	0.30	0.16	0.48	0.34	-	0.41	0.58	0.29	0.28
TOTAL	99.22	99.86	99.64	100.32	100.06	99.32	100.64	99.92	99.82	99.81	99.53
Rb	72	67	50	57	70	55	< 72	75	63	50	91
Cs	0.20	0.30	0.10	0.20	< 0.6	0.20	< 0.7	0.30	0.50	0.20	-
Sr	775	1094	1091	590	640	809	529	655	396	754	629
Ba	2131	1939	1404	1018	1220	1042	646	1604	527	1500	903
Sc	2.1	1.3	1.0	1.0	12	9.2	24	2.1	1.9	13	4.3
Y	5.6	2.3	2.6	2.8	40	16	27	7.2	3.3	48	9.2
Zr	142	89	53	94	574	148	197	300	125	672	262
Hf	4.8	2.6	1.7	2.4	13	3.9	4.7	7.5	3.4	13	6.3
Th	15	0.20	14	2.0	7.0	9.0	2.0	24	7.2	1.0	12
U	0.20	0.50	0.10	0.27	1.0	0.10	< 0.4	< 0.4	0.60	0.30	< 0.4
Nb	3.4	1.3	1.8	2.2	29	6.1	11	5.5	5.2	34	7.2
Ta	-	-	-	-	-	-	-	-	-	-	-
Cr	10	12	7.0	5.0	13	61	105	11	9.0	12	11
Ni	< 30	< 50	< 13	21	35	76	72	39	9.0	6.0	12
Co	-	-	-	-	-	-	-	-	-	15	18
Zn	< 30	< 30	< 30	-	-	-	-	-	-	-	46
Pb	< 2.0	< 2.0	< 2.0	< 2.0	4.0	< 2.0	< 2.0	< 2.0	14	7.0	2.6
La	65	27	68	14	104	77	34	124	27	121	64
Ce	111	56	105	25	220	133	77	178	35	251	105
Nd	-	-	-	-	-	-	-	-	-	-	-
Sm	4.0	2.7	4.9	0.95	15	8.2	8.7	5.9	2.2	19	4.2
Eu	1.9	1.9	1.4	1.2	3.0	2.1	2.0	1.7	0.73	3.3	1.6
Eu*	1.2	0.78	1.2	0.31	4.0	2.3	2.5	1.3	0.64	5.1	1.1
Tb	0.45	0.31	0.34	0.15	1.3	0.82	0.99	0.32	0.25	1.7	0.37
Yb	0.76	0.79	0.42	0.51	2.7	1.3	2.2	0.24	0.46	2.5	1.1
Lu	-	0.090	0.060	0.080	0.37	0.16	0.29	0.040	0.070	0.40	0.11
Eu/Eu*	1.6	2.4	1.2	3.9	0.76	0.92	0.79	1.3	1.1	0.65	1.4
Σ REE	182	86	180	41	347	223	126	310	66	401	176
K/Rb	433	445	452	419	336	383	389	400	291	583	323
K/Ba	15	15	16	23	19	20	43	19	35	19	33
Rb/Sr	0.093	0.061	0.046	0.097	0.11	0.068	0.14	0.11	0.16	0.065	0.14
Ba/Sr	2.7	1.8	1.3	1.7	1.9	1.3	1.2	2.4	1.3	2.0	1.4

FILE: I2GN.DAT

GRANODIORITIC GNEISS

MAJOR AND TRACE ELEMENTS

	65	87-1	88-2	99-1	99-2	101-1	119-1	484-1b	484-1c	493-1	494-1A
SiO2	73.21	66.26	67.20	69.52	68.38	68.57	69.36	73.29	71.62	-	68.38
TiO2	0.21	0.47	0.35	0.21	0.56	0.41	0.69	0.44	0.59	-	0.45
Al2O3	14.97	15.95	16.50	15.06	16.30	15.26	13.72	13.08	13.38	-	15.88
Fe2O3T	1.61	3.82	2.87	2.85	2.99	3.37	4.77	3.25	4.19	-	2.99
MnO	0.01	0.04	0.05	0.05	0.03	0.04	0.08	0.04	0.05	-	0.05
MgO	0.42	1.46	0.90	1.06	1.02	1.03	0.93	0.68	0.86	-	0.84
CaO	2.06	3.17	2.62	2.87	2.56	2.63	2.76	2.16	2.48	-	2.33
Na2O	4.11	4.38	4.66	3.74	4.26	3.83	4.14	3.64	3.99	-	4.51
K2O	3.35	4.07	3.64	4.22	3.81	3.98	2.70	3.22	2.73	-	3.62
P2O5	0.07	0.20	0.11	0.15	0.18	0.24	0.20	0.15	0.19	-	0.14
LOI	0.51	0.22	0.48	0.48	0.26	0.64	0.07	0.08	0.19	-	0.68
TOTAL	100.53	100.04	99.38	100.21	100.35	100.00	99.41	100.03	100.27	0.00	99.87
Rb	78	79	63	88	109	< 100	91	93	91	124	184
Cs	0.50	0.10	0.10	0.50	0.40	< 0.5	0.56	0.53	0.71	-	3.9
Sr	487	582	423	612	642	683	134	128	129	311	236
Ba	1100	1738	820	1170	1307	1345	438	472	385	-	595
Sc	1.4	8.4	4.3	1.4	3.4	2.0	9.7	6.3	6.4	-	5.3
Y	3.3	13	16	2.2	3.6	6.5	82	40	47	16	23
Zr	129	245	215	78	347	121	268	116	149	215	322
Hf	4.0	7.1	6.4	4.8	8.5	4.2	8.0	4.5	5.0	-	8.6
Th	5.8	11	16	13	23	18	23	1.1	3.6	34	25
U	0.51	0.40	0.40	< 0.3	0.80	0.19	1.8	0.40	0.50	2.0	2.0
Nb	3.8	5.2	6.1	8.2	6.7	6.6	26	10	15	13	25
Ta	3.9	0.30	0.30	-	-	3.7	2.6	0.50	0.60	-	1.0
Cr	< 2.0	30	17	13	12	13	2.4	6.2	6.6	-	20
Ni	-	6.0	3.0	-	-	-	4.0	8.0	12	-	24
Co	28	7.8	5.6	16	16	22	7.4	5.9	7.8	-	6.6
Zn	25	-	-	59	60	75	73	49	60	-	61
Pb	7.0	14	18	8.8	5.4	9.0	20	17	18	10	14
La	28	93	97	43	103	89	58	30	35	-	99
Ce	42	180	198	74	163	119	112	54	71	-	180
Nd	13	89	47	-	-	47	-	23	35	-	57
Sm	2.1	7.8	7.7	8.1	5.4	5.4	9.9	6.0	7.6	-	8.6
Eu	1.5	2.3	1.8	1.9	1.7	2.0	1.5	1.2	1.3	-	1.1
Eu*	0.61	1.9	2.0	2.3	1.6	1.4	3.4	2.0	2.5	-	2.3
Tb	0.24	0.56	0.67	0.89	0.61	0.40	1.8	1.1	1.3	-	0.79
Yb	0.49	1.0	1.1	1.9	0.56	0.64	9.9	3.3	3.8	-	2.0
Lu	0.070	0.13	0.13	0.23	0.080	0.075	1.7	0.53	0.58	-	0.34
Eu/Eu*	2.5	1.2	0.88	0.82	1.1	1.5	0.46	0.59	0.52	-	0.47
Σ REE	74	284	307	130	274	216	197	97	122	-	293
K/Rb	357	428	480	398	290	330	246	287	249	-	163
K/Ba	25	19	37	30	24	25	51	57	59	-	51
Rb/Sr	0.16	0.14	0.15	0.14	0.17	0.15	0.68	0.73	0.71	0.40	0.78
Ba/Sr	2.3	3.0	1.9	1.9	2.0	2.0	3.3	3.7	3.0	-	2.5

FILE: I2GN.DAT

GRANODIORITIC GNEISS

MAJOR AND TRACE ELEMENTS

	498	502-1	502-2	503-3	503-4	509-4A	509-5	N	MEAN	SD %
SiO2	-	69.90	71.75	71.06	67.60	68.73	-	26	68.11	5.6
TiO2	-	0.45	0.30	0.28	0.42	0.60	-	26	0.50	60.0
Al2O3	-	15.13	15.10	14.81	16.00	15.04	-	26	15.45	6.3
Fe2O3T	-	3.35	2.35	2.04	3.16	3.67	-	26	3.59	46.8
MnO	-	0.04	0.03	0.03	0.05	0.06	-	24	0.04	52.8
MgO	-	0.82	0.90	0.49	0.83	1.29	-	26	1.14	58.0
CaO	-	2.85	2.54	2.03	2.48	2.95	-	26	3.03	29.8
Na2O	-	4.38	4.36	4.12	4.26	4.17	-	26	4.20	6.3
K2O	-	2.27	2.71	3.44	3.81	3.49	-	26	3.29	17.0
P2O5	-	0.14	0.06	0.08	0.18	0.17	-	24	0.20	81.5
LOI	-	0.88	0.80	0.85	0.41	0.19	-	25	0.41	57.5
TOTAL	0.00	100.21	100.93	99.23	99.20	100.36	0.00			
Rb	-	58	88	116	140	123	0.0	27	87	35.3
Cs	-	0.75	2.5	3.5	3.6	1.4	0.0	22	0.96	127.9
Sr	-	536	393	448	701	201	0.0	27	541	47.4
Ba	-	1089	810	851	1289	303	0.0	26	1063	45.5
Sc	-	2.9	3.1	2.1	3.0	0.30	0.0	26	5.6	98.0
Y	-	16	8.0	7.8	13	5.6	0.0	27	18	104.3
Zr	-	310	149	159	276	57	0.0	27	215	67.5
Hf	-	7.3	4.4	3.9	6.8	1.7	0.0	26	5.7	51.2
Th	-	13	12	20	26	16	0.0	27	13	68.5
U	-	0.90	3.5	3.3	4.6	1.8	0.0	23	1.1	108.1
Nb	-	7.6	4.6	7.7	10	2.5	0.0	27	9.8	88.7
Ta	-	0.62	0.34	0.68	1.2	0.26	0.0	14	1.2	100.8
Cr	-	0.0	22	3.9	6.3	0.60	0.0	24	17	130.8
Ni	-	10	10	5.0	8.0	< 3.0	0.0	18	20	110.8
Co	-	5.5	6.1	3.6	4.9	0.70	0.0	17	10	71.4
Zn	-	59	42	41	61	11	0.0	14	52	34.2
Pb	-	15	15	20	23	12	0.0	20	13	45.6
La	-	70	49	49	89	14	0.0	26	64	51.6
Ce	-	136	99	86	164	26	0.0	26	115	53.6
Nd	-	47	29	25	64	10	0.0	12	41	56.2
Sm	-	7.7	3.7	3.5	8.9	1.3	0.0	26	6.5	62.2
Eu	-	1.6	0.91	0.88	1.8	0.48	0.0	26	1.6	38.3
Eu*	-	2.2	0.96	0.89	2.2	0.37	-	26	1.8	62.0
Tb	-	0.81	0.33	0.27	0.60	0.14	0.0	26	0.67	68.8
Yb	-	1.2	0.63	0.62	0.96	0.40	0.0	26	1.6	121.5
Lu	-	0.16	0.090	0.090	0.13	0.060	0.0	25	0.24	139.3
Eu/Eu*	-	0.74	0.92	0.99	0.83	1.3	-	26	1.2	63.5
Σ REE	-	218	154	140	266	42	-	26	190	51.5
K/Rb	-	325	256	246	226	236	-	26	345	27.9
K/Ba	-	17	28	34	25	96	-	26	32	57.1
Rb/Sr	-	0.11	0.22	0.26	0.20	0.61	-	27	0.25	93.6
Ba/Sr	-	2.0	2.1	1.9	1.8	1.5	-	26	2.1	30.7

FILE: I2GN.DAT

GRANODIORITIC GNEISS

CIPW NORMS

	6	7-1	7-2	12-1	23	25	26-1	26-2	51	56-1	64-1
Fe2O3/F	0.44	0.44	0.44	0.44	0.44	0.44	0.44	0.44	0.44	0.41	0.44
Qtz	25.45	23.75	25.50	28.87	9.91	13.51	7.61	19.60	28.86	11.43	17.13
Corund	0.28	0.14	0.76	0.27	0.00	0.00	0.00	0.00	1.15	0.00	0.14
Zircon	0.03	0.02	0.01	0.02	0.12	0.03	0.04	0.06	0.03	0.11	0.05
Or	22.22	21.21	16.07	17.02	16.72	15.01	19.91	21.33	13.06	20.71	20.92
Ab	30.14	35.41	36.76	37.73	36.00	35.28	36.25	35.31	34.99	33.37	36.85
An	13.96	13.79	15.11	12.25	17.46	17.33	15.68	15.49	14.39	12.49	15.61
Diop	0.00	0.00	0.00	0.00	4.97	4.29	6.65	0.10	0.00	3.71	0.00
Hyp	4.83	3.54	3.19	2.66	7.48	9.24	9.27	4.96	4.43	8.80	5.67
Olivine	0.00	0.00	0.00	0.00	0.00	0.00	0.00	0.00	0.00	0.00	0.00
Mgt	1.14	0.85	0.98	0.71	2.96	2.08	2.63	1.36	1.22	3.59	1.34
Chrmite	0.00	0.01	0.00	0.00	0.01	0.03	0.05	0.01	0.00	0.01	0.01
Ilmen	0.61	0.59	0.49	0.38	2.47	1.18	1.37	1.14	0.65	2.81	0.93
Apat	0.30	0.00	0.32	0.16	1.09	0.70	0.79	0.00	0.28	1.99	0.42

BARTH MESONORM

Qtz	26.51	23.90	25.27	28.07	13.27	16.40	9.75	21.08	29.45	16.09	18.99
Corund	0.90	0.69	1.27	0.62	0.00	0.00	0.00	0.88	1.77	0.39	0.87
Or	18.15	18.02	13.35	14.64	8.33	7.27	13.19	16.59	9.21	10.77	15.73
Ab	33.13	38.69	40.23	40.54	39.22	38.47	38.66	38.25	38.02	36.86	39.84
An	12.43	12.10	13.74	11.21	17.44	17.20	15.38	13.14	13.22	11.52	13.68
Biot	7.10	5.33	4.59	3.84	13.79	12.63	10.58	7.81	6.47	16.74	8.51
Actin	0.00	0.00	0.00	0.00	2.04	4.59	8.35	0.00	0.00	0.00	0.00
Edenite	0.00	0.00	0.00	0.00	0.00	0.00	0.00	0.00	0.00	0.00	0.00
Hyp	0.00	0.00	0.00	0.00	0.00	0.00	0.00	0.00	0.00	0.00	0.00
Mgt	0.83	0.61	0.71	0.51	2.16	1.51	1.89	0.99	0.89	2.65	0.97
Sphene	0.68	0.65	0.55	0.42	2.75	1.31	1.50	1.26	0.72	3.17	1.03
Apat	0.28	0.00	0.30	0.15	1.00	0.63	0.71	0.00	0.25	1.84	0.38

FILE: I2GN.DAT

GRANODIORITIC GNEISS

CIPW NORMS

	65	87-1	88-2	99-1	99-2	101-1	119-1	484-1b	484-1c	493-1	494-1A
Fe2O3/F	0.44	0.44	0.44	0.44	0.44	0.44	0.44	0.44	0.44	-	0.44
Qtz	31.19	16.16	18.59	23.67	21.76	23.54	26.95	33.49	30.64	-	21.52
Corund	0.96	0.00	0.36	0.00	0.89	0.39	0.00	0.03	0.00	-	0.65
Zircon	0.03	0.05	0.04	0.02	0.07	0.02	0.05	0.02	0.03	-	0.07
Or	19.80	24.05	21.51	24.94	22.51	23.52	15.96	19.03	16.13	-	21.39
Ab	34.42	36.63	39.12	31.19	35.57	31.90	34.93	30.71	33.67	-	37.99
An	10.08	12.07	12.53	12.08	11.91	11.90	10.93	9.80	10.59	-	10.71
Diop	0.00	2.33	0.00	1.27	0.00	0.00	1.28	0.00	0.44	-	0.00
Hyp	2.25	5.42	4.48	4.46	4.51	5.16	5.21	4.13	5.02	-	4.28
Olivine	0.00	0.00	0.00	0.00	0.00	0.00	0.00	0.00	0.00	-	0.00
Mgt	0.66	1.57	1.18	1.17	1.23	1.38	1.96	1.33	1.72	-	1.23
Chrmite	0.00	0.01	0.01	0.01	0.01	0.01	0.00	0.00	0.00	-	0.01
Ilmen	0.40	0.89	0.67	0.40	1.06	0.78	1.31	0.84	1.12	-	0.86
Apat	0.16	0.46	0.26	0.35	0.42	0.56	0.46	0.35	0.44	-	0.32

BARTH MESONORM

Qtz	30.20	17.56	19.73	24.06	22.68	24.80	28.49	33.84	31.62	-	22.47
Corund	1.40	0.00	0.93	0.00	1.81	1.07	0.37	0.69	0.62	-	1.34
Or	17.84	18.90	17.60	21.28	18.15	19.10	10.75	15.49	11.46	-	17.55
Ab	37.11	39.41	42.21	33.88	38.30	34.87	37.98	33.24	36.37	-	40.88
An	9.08	11.87	11.16	11.95	9.59	10.19	10.20	8.34	9.15	-	9.17
Biot	3.31	8.31	6.54	6.20	7.03	7.58	8.87	6.17	7.87	-	6.46
Actin	0.00	1.42	0.00	1.04	0.00	0.00	0.00	0.00	0.00	-	0.00
Edenite	0.00	0.00	0.00	0.00	0.00	0.00	0.00	0.00	0.00	-	0.00
Hyp	0.00	0.00	0.00	0.00	0.00	0.00	0.00	0.00	0.00	-	0.00
Mgt	0.48	1.13	0.86	0.85	0.89	1.01	1.44	0.98	1.26	-	0.89
Sphene	0.44	0.98	0.74	0.44	1.17	0.87	1.47	0.93	1.25	-	0.95
Apat	0.15	0.42	0.23	0.32	0.38	0.51	0.43	0.32	0.40	-	0.30

FILE: I2GN.DAT

GRANODIORITIC GNEISS

CIPW NORMS

	498	502-1	502-2	503-3	503-4	509-4A	509-5	N	MEAN	SD %
Fe2O3/F	-	0.44	0.44	0.44	0.44	0.44	-	26	0.44	0.0
Qtz	-	27.76	28.77	28.50	21.28	22.57	-	26	22.6	30.2
Corund	-	0.57	0.57	0.79	0.75	0.00	-	16	0.54	60.3
Zircon	-	0.06	0.03	0.03	0.06	0.01	-	26	0.044	70.4
Or	-	13.41	16.01	20.33	22.51	20.62	-	26	19.5	17.0
Ab	-	36.67	36.60	34.53	35.53	35.14	-	26	35.1	6.3
An	-	13.57	12.24	9.78	11.51	12.09	-	26	12.9	17.0
Diop	-	0.00	0.00	0.00	0.00	1.21	-	10	2.6	82.8
Hyp	-	4.56	4.03	2.75	4.47	5.23	-	26	5.0	36.8
Olivine	-	0.00	0.00	0.00	0.00	0.00	-	0	0.0	0.0
Mgt	-	1.38	0.96	0.84	1.30	1.51	-	26	1.5	46.7
Cnrmite	-	0.00	0.01	0.00	0.00	0.00	-	23	0.010	108.4
Ilmen	-	0.86	0.57	0.53	0.80	1.14	-	26	0.96	59.9
Apat	-	0.32	0.21	0.19	0.42	0.39	-	24	0.47	81.4

BARTH MESONORM

Qtz	-	28.53	28.85	28.41	22.33	23.93	-	26	23.7	24.9
Corund	-	1.32	1.07	1.30	1.47	0.23	-	21	1.0	44.3
Or	-	9.37	12.37	18.19	18.70	15.19	-	26	14.9	26.2
Ab	-	39.91	39.28	37.81	38.83	37.61	-	26	38.1	6.0
An	-	11.83	11.01	8.76	9.81	11.49	-	26	11.7	20.4
Biot	-	6.78	5.91	4.14	6.64	8.84	-	26	7.6	40.0
Actin	-	0.00	0.00	0.00	0.00	0.00	-	5	3.5	87.4
Edenite	-	0.00	0.00	0.00	0.00	0.00	-	0	0.0	0.0
Hyp	-	0.00	0.00	0.00	0.00	0.00	-	0	0.0	0.0
Mgt	-	1.01	0.70	0.62	0.95	1.09	-	26	1.1	47.1
Sphene	-	0.95	0.63	0.60	0.89	1.26	-	26	1.1	60.6
Apat	-	0.30	0.19	0.17	0.38	0.36	-	24	0.43	82.0

FILE: I2GGRN.DAT

GRANITIC GNEISS

MAJOR AND TRACE ELEMENTS

	BG-1	3	40-1	52	55-2	56-2	64-2	67	88-1	88-3	89-2
SiO2	72.71	72.56	75.58	68.72	71.68	74.02	72.92	74.24	67.11	71.25	70.42
TiO2	0.19	0.14	0.03	0.35	0.08	0.17	0.27	0.11	0.39	0.11	0.24
Al2O3	13.87	14.90	13.63	15.11	15.18	13.43	14.05	13.95	15.80	15.03	15.21
Fe2O3T	1.69	1.42	0.32	3.29	0.94	1.27	0.98	1.07	3.34	1.02	2.25
MnO	0.04	0.01	< 0.1	0.04	< 0.0	0.02	0.01	0.01	0.06	0.01	0.02
MgO	0.39	0.30	0.08	1.23	0.46	0.39	0.35	0.22	1.17	0.55	0.93
CaO	0.95	1.99	1.56	2.16	2.15	1.71	1.04	1.56	2.64	1.59	1.99
Na2O	3.80	3.81	4.25	4.70	4.39	3.22	3.40	3.34	5.13	4.36	3.69
K2O	5.28	4.01	5.03	4.81	4.54	4.29	7.02	4.63	4.31	5.01	4.79
P2O5	0.04	0.05	0.02	0.17	0.04	0.03	0.07	0.03	0.19	0.09	0.10
LOI	0.53	0.43	0.45	0.31	0.45	1.39	0.40	0.44	0.19	0.09	0.15
TOTAL	99.46	99.62	100.95	100.89	99.91	99.94	100.51	99.60	100.33	99.19	99.79
Rb	219	84	101	129	103	63	146	92	76	83	89
Cs	1.4	< 0.3	0.30	0.40	0.50	0.10	-	0.48	0.20	0.10	0.10
Sr	201	623	550	624	485	644	623	478	394	355	461
Ba	508	1189	1334	1150	1527	2004	2151	1195	736	1007	1828
Sc	3.7	1.6	0.10	3.7	1.0	0.70	1.1	0.50	6.3	0.70	1.2
Y	27	5.8	1.7	14	4.1	3.0	3.1	1.5	31	3.2	5.1
Zr	165	145	23	120	118	94	269	71	207	103	298
Hf	5.0	4.3	1.3	3.1	3.9	2.5	7.3	2.2	5.3	2.7	8.1
Th	47	52	1.0	11	2.9	6.8	32	6.9	17	5.3	15
U	15	0.70	0.20	0.55	0.70	0.30	0.60	0.30	< 0.5	0.60	0.90
Nb	14	3.7	2.5	6.5	4.4	4.3	5.4	< 1.0	16	2.0	2.9
Ta	-	-	0.60	-	0.10	0.20	-	-	1.5	0.20	0.20
Cr	9.0	-	< 15	28	4.0	7.0	7.0	3.0	23	4.0	18
Ni	6.0	6.0	4.0	12	10	5.0	11	9.0	2.0	2.0	6.0
Co	-	30	1.0	-	3.6	3.2	10	24	6.6	2.3	5.6
Zn	< 25	23	5.0	-	16	25	12	-	-	-	-
Pb	32	19	11	16	18	16	18	16	19	18	17
La	106	112	12	37	11	56	98	19	51	27	78
Ce	190	161	15	78	23	78	131	23	121	54	148
Nd	-	-	-	-	-	19	-	8.6	-	13	24
Sm	12	7.5	0.31	4.3	1.0	1.9	3.0	0.65	9.7	2.0	4.4
Eu	1.0	1.4	1.2	0.91	1.8	1.7	1.9	1.3	2.0	1.5	1.6
Eu*	3.1	1.8	0.11	1.2	0.33	0.53	0.87	0.23	2.6	0.51	1.1
Tb	1.0	0.50	0.060	0.43	0.17	0.19	0.34	0.13	0.90	0.16	0.31
Yb	2.1	0.71	0.22	1.2	0.39	0.31	0.45	0.30	1.6	0.19	0.38
Lu	0.31	0.080	0.040	0.19	0.060	0.050	0.053	0.040	0.23	< .04	0.060
Eu/Eu*	0.32	0.77	11	0.76	5.4	3.2	2.2	5.7	0.76	2.9	1.5
7 REE	315	284	28	122	36	137	234	43	187	84	232
K/Rb	200	396	413	310	366	565	399	418	471	501	447
K/Ba	86	28	31	35	25	18	27	32	49	41	22
Rb/Sr	1.1	0.13	0.18	0.21	0.21	0.098	0.23	0.19	0.19	0.23	0.19
Ba/Sr	2.5	1.9	2.4	1.8	3.1	3.1	3.5	2.5	1.9	2.8	4.0

FILE: I2GGRN.DAT

GRANITIC GNEISS

MAJOR AND TRACE ELEMENTS

	99-3	118-2	119-2	430-1	462-2	489-2	491-1	491-2	493-2	500-2	500-3
SiO2	71.84	-	74.55	75.70	76.18	72.30	74.49	74.90	72.74	60.07	73.95
TiO2	0.11	-	0.26	0.07	0.05	0.13	0.10	0.13	0.19	0.73	0.15
Al2O3	15.47	-	12.54	13.65	13.97	14.90	14.20	13.64	14.00	16.33	14.51
Fe2O3T	1.29	-	2.03	1.06	0.44	1.26	1.22	1.47	2.07	8.29	1.35
MnO	0.01	-	0.02	0.04	0.01	< 0.0	0.04	0.04	0.02	0.21	0.03
MgO	0.26	-	0.30	0.20	0.15	0.29	0.24	0.21	0.38	2.85	0.22
CaO	1.79	-	1.10	1.14	1.49	1.68	1.44	0.98	1.33	2.22	1.50
Na2O	3.63	-	3.07	3.70	3.60	3.91	4.22	3.59	3.33	4.56	4.76
K2O	5.29	-	5.05	4.44	4.67	5.16	3.86	4.75	5.25	3.30	3.24
P2O5	0.06	-	0.05	0.02	0.01	0.05	0.04	0.04	0.07	0.27	0.04
LOI	0.28	-	0.07	0.38	0.07	0.31	0.36	0.36	0.45	0.41	0.31
TOTAL	100.03	0.00	99.04	100.40	100.64	99.99	100.21	100.11	99.83	99.29	100.06
Rb	116	-	135	77	76	78	163	206	215	391	131
Cs	0.56	-	0.54	1.1	0.75	0.20	1.5	2.1	3.1	10	1.5
Sr	658	-	107	450	489	763	172	84	205	202	227
Ba	1551	-	557	2274	1664	2963	485	592	845	250	433
Sc	0.60	-	2.0	0.90	0.20	0.50	3.2	3.5	3.0	15	3.8
Y	3.0	-	20	2.0	3.8	3.0	32	33	20	38	22
Zr	90	-	197	78	50	146	89	140	198	239	96
Hf	2.7	-	6.6	2.4	1.8	4.0	3.4	4.8	5.1	5.3	3.4
Th	24	-	34	6.0	1.3	6.0	19	61	50	14	27
U	0.20	-	1.5	0.60	0.50	0.20	3.5	9.0	3.6	2.5	11
Nb	5.3	-	4.8	1.8	1.7	1.1	13	19	8.6	27	11
Ta	-	-	0.14	0.10	0.46	0.20	1.0	0.80	0.40	0.91	1.1
Cr	-	-	2.6	4.2	< 1.0	11	1.9	2.7	2.3	16	1.6
Ni	-	-	3.0	4.0	< 5.0	4.0	< 8.0	5.0	4.0	14	< 8.0
Co	21	-	2.4	2.0	0.60	3.0	1.7	1.3	2.6	18	1.3
Zn	138	-	30	9.0	6.9	15	38	42	36	239	41
Pb	10	-	26	24	14	13	32	45	21	-	25
La	33	-	79	6.7	3.0	25	29	77	82	60	59
Ce	57	-	146	14	5.1	40	55	146	144	116	118
Nd	-	-	48	-	2.0	-	20	52	48	41	46
Sm	2.0	-	7.4	0.84	0.39	1.6	4.0	9.5	8.0	8.5	8.1
Eu	1.3	-	1.2	0.95	0.28	1.4	0.56	0.67	0.87	0.79	0.64
Eu*	0.63	-	2.0	0.28	0.14	0.43	1.3	2.9	2.1	2.7	2.3
Tb	0.30	-	0.71	0.15	0.092	0.15	0.72	1.3	0.71	1.3	0.86
Yb	0.48	-	1.7	0.38	0.27	0.32	2.8	3.7	1.8	2.8	1.5
Lu	0.070	-	0.26	0.064	0.040	0.040	0.42	0.55	0.30	0.39	0.24
Eu/Eu*	2.0	-	0.59	3.4	1.9	3.2	0.41	0.23	0.41	0.25	0.28
Σ REE	93	-	237	22	9.0	68	93	241	239	192	190
K/Rb	379	-	311	479	510	549	197	191	203	70	205
K/Ba	28	-	75	16	23	14	66	67	52	110	62
Rb/Sr	0.18	-	1.3	0.17	0.16	0.10	0.95	2.5	1.0	1.9	0.58
Ba/Sr	2.4	-	5.2	5.1	3.4	3.9	2.8	7.0	4.1	1.2	1.9

FILE: I2GGRN.DAT

GRANITIC GNEISS

MAJOR AND TRACE ELEMENTS

	500-4	501	504	506-1	506-2	509-2a	509-3c	510-4	563	565-1	565-5
SiO2	74.31	75.36	72.94	66.86	71.89	75.98	72.86	75.61	70.68	67.19	75.67
TiO2	0.15	0.10	0.44	0.44	0.35	0.07	0.28	0.18	0.34	1.09	0.24
Al2O3	13.44	13.56	13.14	16.69	13.54	13.59	14.11	12.96	15.09	13.99	12.72
Fe2O3T	1.45	1.17	2.76	2.70	2.29	0.65	2.36	1.67	2.57	5.30	1.46
MnO	0.03	0.04	0.05	0.03	0.03	0.01	0.02	0.02	0.04	0.09	0.02
MgO	0.18	0.20	0.50	0.51	0.35	0.10	0.39	0.35	0.78	0.93	0.26
CaO	0.82	0.93	1.37	1.97	1.06	1.24	1.64	1.66	2.07	2.73	1.08
Na2O	3.74	3.63	3.16	4.25	2.83	3.73	3.40	3.07	4.84	3.27	2.73
K2O	5.24	4.72	5.29	6.24	6.57	4.29	4.85	4.53	2.94	4.89	5.31
P2O5	0.04	0.02	0.13	0.10	0.07	0.02	0.08	0.08	0.16	0.31	0.05
LOI	0.45	0.84	0.16	0.48	0.63	0.15	0.33	0.56	0.35	0.07	0.24
TOTAL	99.85	100.57	99.94	99.97	99.61	99.83	100.32	100.69	99.86	99.81	99.78
Rb	217	236	247	173	175	126	142	< 83	105	89	79
Cs	1.6	1.5	3.1	3.3	1.4	2.0	1.3	< .05	2.5	0.10	0.030
Sr	179	70	205	285	231	294	363	358	468	271	275
Ba	749	560	718	945	1038	870	1197	962	381	1531	1694
Sc	3.3	3.8	2.3	2.2	1.8	9.0	1.4	0.70	3.4	20	2.3
Y	82	89	14	70	58	37	21	4.9	22	92	8.1
Zr	145	105	276	305	323	270	267	115	231	416	187
Hf	4.6	4.2	9.5	11	10	9.8	6.8	4.4	5.6	16	7.6
Th	49	27	64	46	77	26	18	14	22	8.1	5.0
U	21	12	9.0	9.4	4.6	4.1	2.7	0.50	1.9	0.40	0.30
Nb	12	18	33	26	17	19	11	1.8	15	32	4.3
Ta	1.0	0.90	3.6	3.6	1.8	2.1	1.2	< .05	1.0	1.7	0.20
Cr	3.6	3.2	9.1	6.6	4.8	20	2.5	4.7	17	4.1	1.6
Ni	< 8.0	< 8.0	2.0	8.0	5.0	20	< 7.0	< 7.0	8.0	6.0	5.0
Co	1.2	0.90	3.8	2.7	2.8	9.3	4.2	2.7	5.2	6.6	1.5
Zn	42	41	53	42	38	73	30	17	58	76	22
Pb	35	43	35	38	33	10	11	11	10	32	33
La	81	46	147	136	194	90	79	46	70	82	28
Ce	165	92	295	279	381	196	159	79	126	168	43
Nd	66	39	98	107	134	75	56	23	48	65	14
Sm	12	7.4	15	16	20	13	8.4	2.9	8.7	15	2.1
Eu	0.70	0.50	1.7	2.6	1.8	2.0	1.4	1.2	1.9	3.1	2.1
Eu^*	3.9	2.9	4.3	5.3	5.8	3.7	2.3	0.71	2.3	4.9	0.66
Tb	2.0	2.1	1.7	2.2	2.3	1.4	0.84	0.20	0.79	2.5	0.31
Yb	7.7	12	4.1	6.1	4.4	3.2	1.4	0.32	1.7	9.6	0.83
Lu	1.2	1.9	0.59	0.85	0.56	0.45	0.17	0.040	0.23	1.5	0.13
Eu/Eu^*	0.18	0.17	0.39	0.49	0.31	0.54	0.60	1.7	0.81	0.63	3.2
Σ REE	273	164	468	447	608	308	251	129	210	294	75
K/Rb	200	166	178	299	312	283	284	453	232	450	558
K/Ba	58	70	61	55	53	41	34	39	64	26	26
Rb/Sr	1.2	3.4	1.2	0.61	0.76	0.43	0.39	0.23	0.22	0.33	0.29
Ba/Sr	4.2	8.0	3.5	3.3	4.5	3.0	3.3	2.7	0.81	5.6	6.2

FILE: I2GGRN.DAT

GRANITIC GNEISS

MAJOR AND TRACE ELEMENTS

	N	MEAN	SD %
SiO2	32	72.41	4.8
TiO2	32	0.24	89.8
Al2O3	32	14.26	7.1
Fe2O3T	32	1.95	78.2
MnO	29	0.03	108.1
MgO	32	0.49	105.7
CaO	32	1.57	31.1
Na2O	32	3.78	16.1
K2O	32	4.80	17.8
P2O5	32	0.08	93.1
LOI	32	0.38	67.2
TOTAL			
Rb	32	139	51.2
Cs	29	1.4	133.0
Sr	32	369	51.1
Ba	32	1153	54.8
Sc	32	3.2	130.8
Y	32	25	105.1
Zr	32	174	53.4
Hf	32	5.5	58.3
Th	32	25	83.3
U	31	3.8	136.5
Nb	31	11	83.2
Ta	25	1.0	96.9
Cr	28	7.9	91.2
Ni	24	6.7	63.6
Co	30	6.0	123.1
Zn	26	45	107.5
Pb	31	23	46.1
La	32	64	67.9
Ce	32	120	71.7
Nd	22	48	70.8
Sm	32	6.9	79.1
Eu	32	1.4	46.2
Eu*	32	2.0	80.8
Tb	32	0.84	88.3
Yb	32	2.3	123.0
Lu	31	0.36	125.7
Eu/Eu*	32	1.8	129.2
Σ REE	32	197	69.9
K/Rb	32	344	39.1
K/Ba	32	45	50.4
Rb/Sr	32	0.65	115.7
Ba/Sr	32	3.5	46.4

FILE: I2GGRN.DAT

GRANITIC GNEISS

CIPW NORMS

	BG-1	3	40-1	52	55-2	56-2	64-2	67	88-1	88-3	89-2
Fe2O3/F	0.44	0.44	0.44	0.44	0.44	0.44	0.44	0.44	0.44	0.44	0.44
Qtz	27.38	29.86	29.18	16.78	29.81	34.35	24.14	33.22	13.79	22.63	24.47
Corund	0.30	0.75	0.00	0.00	0.00	0.34	0.00	0.63	0.00	0.00	0.48
Zircon	0.03	0.03	0.01	0.02	0.02	0.02	0.05	0.01	0.04	0.02	0.06
Or	31.20	23.70	29.72	28.42	26.83	25.35	41.48	27.36	25.47	29.61	28.31
Ab	32.01	31.78	35.56	39.31	36.79	26.77	28.31	27.91	43.12	36.63	30.88
An	4.46	9.92	3.47	6.17	8.50	8.85	2.59	7.87	7.51	6.78	9.67
Diop	0.00	0.00	0.91	3.10	1.88	0.00	2.15	0.00	3.76	0.64	0.00
Hyp	2.31	2.42	0.00	4.15	0.99	1.93	0.33	1.40	3.69	1.82	4.09
Olivine	0.00	0.00	0.00	0.00	0.00	0.00	0.00	0.00	0.00	0.00	0.00
Mgt	0.68	0.58	0.13	1.35	0.39	0.52	0.40	0.44	1.37	0.42	0.92
Chrmite	0.00	0.00	0.00	0.01	0.00	0.00	0.00	0.00	0.01	0.00	0.01
Ilmen	0.36	0.27	0.06	0.67	0.15	0.32	0.51	0.21	0.74	0.27	0.46
Apat	0.09	0.12	0.05	0.39	0.09	0.07	0.16	0.07	0.44	0.19	0.23

BARTH MESONORM

Qtz	26.94	29.09	24.46	16.56	25.99	33.70	22.13	32.00	13.41	21.98	25.04
Corund	0.57	1.07	0.00	0.00	0.00	0.75	0.00	0.91	0.00	0.00	0.97
Or	29.61	21.92	32.74	25.18	25.32	24.22	41.30	26.61	22.91	27.97	24.83
Ab	34.68	34.63	38.02	41.86	37.44	29.70	30.61	30.55	45.73	39.40	33.40
An	3.85	9.17	3.25	5.88	7.89	7.91	2.35	7.30	7.30	6.69	8.45
Biot	3.35	3.29	0.00	4.81	0.26	2.91	0.47	2.01	3.79	2.91	5.92
Actin	0.00	0.00	6.35	3.66	2.59	0.00	2.14	0.00	4.68	0.28	0.00
Edenite	0.00	0.00	0.00	0.00	0.00	0.00	0.00	0.00	0.00	0.00	0.00
Hyp	0.00	0.00	0.00	0.00	0.00	0.00	0.00	0.00	0.00	0.00	0.00
Mgt	0.50	0.43	0.09	0.97	0.26	0.39	0.29	0.32	0.98	0.30	0.67
Sphene	0.40	0.30	0.06	0.73	0.16	0.36	0.57	0.23	0.81	0.29	0.51
Apat	0.09	0.11	0.04	0.35	0.08	0.06	0.15	0.06	0.39	0.17	0.21

FILE: I2GGRN.DAT

GRANITIC GNEISS

CIPW NORMS

	99-3	118-2	119-2	430-1	462-2	489-2	491-1	491-2	493-2	500-2	500-3
Fe2O3/F	0.44	-	0.44	0.44	0.44	0.44	0.44	0.44	0.44	0.44	0.44
Qtz	26.08	-	34.01	34.05	33.88	26.57	31.42	33.00	29.35	9.71	30.02
Corund	0.60	-	0.14	0.60	0.22	0.00	0.57	0.92	0.59	2.00	0.55
Zircon	0.02	-	0.04	0.02	0.01	0.03	0.02	0.03	0.04	0.05	0.02
Or	31.26	-	29.84	26.24	27.60	30.49	22.81	28.07	31.02	19.50	19.15
Ab	30.23	-	25.90	30.98	30.10	32.52	35.58	30.32	28.03	38.44	40.11
An	8.93	-	5.18	6.07	7.76	8.17	6.92	4.60	6.22	8.98	7.24
Diop	0.00	-	0.00	0.00	0.00	0.53	0.00	0.00	0.00	0.00	0.00
Hyp	1.71	-	2.28	1.46	0.73	1.44	1.67	1.78	2.64	14.06	1.64
Olivine	0.00	-	0.00	0.00	0.00	0.00	0.00	0.00	0.00	0.00	0.00
Mgt	0.53	-	0.83	0.44	0.18	0.52	0.50	0.60	0.85	3.40	0.55
Chrmite	0.00	-	0.00	0.00	0.00	0.01	0.00	0.00	0.00	0.01	0.00
Ilmen	0.21	-	0.49	0.13	0.10	0.25	0.19	0.25	0.36	1.50	0.29
Apat	0.14	-	0.12	0.05	0.02	0.12	0.09	0.09	0.16	0.63	0.09

BARTH MESONORM

Qtz	25.07	-	33.61	32.55	31.76	25.27	30.08	31.84	28.98	16.53	28.71
Corund	0.88	-	0.53	0.91	0.41	0.12	0.75	1.19	0.92	3.23	0.80
Or	29.97	-	28.51	25.23	26.98	28.90	21.52	26.88	29.22	7.24	17.76
Ab	32.80	-	28.31	33.51	32.38	35.01	38.13	32.64	30.41	41.62	42.91
An	8.16	-	4.34	5.33	7.17	7.54	6.58	4.20	5.57	6.51	6.69
Biot	2.37	-	3.41	1.97	1.05	2.41	2.29	2.46	3.72	20.13	2.33
Actin	0.00	-	0.00	0.00	0.00	0.00	0.00	0.00	0.00	0.00	0.00
Edenite	0.00	-	0.00	0.00	0.00	0.00	0.00	0.00	0.00	0.00	0.00
Hyp	0.00	-	0.00	0.00	0.00	0.00	0.00	0.00	0.00	0.00	0.00
Mgt	0.38	-	0.62	0.32	0.13	0.37	0.36	0.44	0.62	2.49	0.40
Sphene	0.23	-	0.56	0.15	0.10	0.27	0.21	0.28	0.40	1.68	0.31
Apat	0.13	-	0.11	0.04	0.02	0.10	0.08	0.08	0.15	0.57	0.08

FILE: I2GGRN.DAT

GRANITIC GNEISS

CIPW NORMS

	500-4	501	504	506-1	506-2	509-2a	509-3c	510-4	563	565-4	565-5
Fe2O3/F	0.44	0.44	0.44	0.44	0.44	0.44	0.44	0.44	0.44	0.40	0.44
Qtz	30.11	33.53	30.17	13.40	26.97	34.94	29.88	36.03	25.40	28.60	36.41
Corund	0.23	0.86	0.06	0.13	0.00	0.58	0.44	0.14	0.58	0.80	0.54
Zircon	0.03	0.02	0.06	0.06	0.07	0.05	0.05	0.02	0.05	0.00	0.04
Or	30.97	27.89	31.26	36.87	38.82	25.35	28.66	26.77	17.37	9.10	31.38
Ab	31.52	30.66	26.59	35.75	23.78	31.35	28.50	25.71	40.61	40.70	22.90
An	3.86	4.45	5.98	7.79	4.93	6.20	7.87	7.96	9.37	15.30	5.40
Diop	0.00	0.00	0.00	0.00	0.02	0.00	0.00	0.00	0.00	0.00	0.00
Hyp	1.63	1.52	3.23	3.16	2.51	0.77	2.79	2.20	3.89	3.50	1.68
Olivine	0.00	0.00	0.00	0.00	0.00	0.00	0.00	0.00	0.00	0.00	0.00
Mgt	0.60	0.48	1.13	1.11	0.94	0.27	0.97	0.69	1.06	0.90	0.60
Chrmite	0.00	0.00	0.00	0.00	0.00	0.01	0.00	0.00	0.01	0.00	0.00
Ilmen	0.29	0.19	0.84	0.84	0.67	0.13	0.53	0.34	0.65	0.70	0.45
Apat	0.09	0.05	0.30	0.23	0.16	0.05	0.19	0.19	0.37	0.20	0.12

BARTH MESONORM

Qtz	29.08	32.16	30.24	14.19	27.00	33.08	29.47	34.96	25.66	28.40	35.51
Corund	0.46	1.07	0.66	0.78	0.51	0.77	0.92	0.50	1.10	1.40	1.03
Or	29.94	26.91	28.70	33.92	37.31	24.95	26.47	25.17	13.88	5.70	30.44
Ab	34.05	32.98	28.88	38.24	26.02	33.88	30.90	27.96	43.71	43.80	25.08
An	3.33	4.18	4.49	6.11	3.67	5.84	6.72	7.19	8.09	13.70	4.29
Biot	2.31	2.10	4.98	4.84	3.89	1.10	4.05	3.17	5.74	5.50	2.62
Actin	0.00	0.00	0.00	0.00	0.00	0.00	0.00	0.00	0.00	0.00	0.00
Edenite	0.00	0.00	0.00	0.00	0.00	0.00	0.00	0.00	0.00	0.00	0.00
Hyp	0.00	0.00	0.00	0.00	0.00	0.00	0.00	0.00	0.00	0.00	0.00
Mgt	0.43	0.35	0.83	0.80	0.69	0.19	0.71	0.50	0.76	0.60	0.44
Sphene	0.32	0.21	0.94	0.92	0.75	0.15	0.59	0.38	0.71	0.80	0.51
Apat	0.08	0.04	0.28	0.21	0.15	0.04	0.17	0.17	0.34	0.20	0.11

FILE: I2GGRN.DAT

GRANITIC GNEISS

CIPW NORMS

	N	MEAN	SD %
Fe2O3/F	32	0.44	1.5
Qtz	32	28.1	23.9
Corund	24	0.54	72.1
Zircon	31	0.033	49.4
Or	32	27.7	21.9
Ab	32	32.2	16.5
An	32	7.0	34.6
Diop	8	1.6	81.7
Hyp	31	2.6	92.0
Olivine	0	0.0	0.0
Mgt	32	0.76	75.4
Chrmite	25	0.004	93.3
Ilmen	32	0.42	70.8
Apat	32	0.17	79.4

BARTH MESONORM

Qtz	32	27.4	21.4
Corund	26	0.89	61.9
Or	32	25.9	27.8
Ab	32	34.7	15.7
An	32	6.2	35.7
Biot	31	3.6	93.7
Actin	6	3.3	64.3
Edenite	0	0.0	0.0
Hyp	0	0.0	0.0
Mgt	32	0.55	76.2
Sphene	32	0.47	71.4
Apat	32	0.15	79.8

FILE: I2CTRN.DAT

LOW-P CHARNOCKITE

MAJOR AND TRACE ELEMENTS

	KDA2	1	2	4-1	8	9-1	10-2	22	35	37-1	37-2
SiO2	70.20	68.68	73.59	66.44	57.64	67.21	54.54	70.59	70.42	70.87	64.11
TiO2	0.29	0.36	0.28	0.44	0.71	0.44	1.15	0.35	0.26	0.40	0.53
Al2O3	16.25	16.55	14.80	16.85	16.02	15.93	17.85	14.81	16.57	15.40	16.21
Fe2O3T	2.25	2.93	2.26	3.86	7.51	5.10	8.47	2.92	2.58	2.93	5.53
MnO	0.02	0.04	0.02	0.04	0.10	0.06	0.10	0.03	0.02	0.03	0.08
MgO	0.76	1.07	0.66	1.54	4.37	1.66	3.96	0.99	0.79	1.09	2.31
CaO	2.71	4.51	2.75	4.41	7.02	4.65	7.11	3.41	4.40	4.57	4.48
Na2O	5.70	5.06	3.75	4.54	4.95	4.19	4.89	3.73	4.47	3.39	4.06
K2O	1.65	0.52	1.85	1.34	1.83	0.93	1.58	2.33	0.68	1.31	1.45
P2O5	0.09	0.05	0.08	0.10	0.27	0.13	0.41	0.13	0.06	0.10	0.20
LOI	0.28	0.41	0.45	0.20	0.37	0.09	0.23	0.59	0.45	0.67	0.47
TOTAL	100.20	100.18	100.49	99.76	100.79	100.39	100.29	99.88	100.70	100.69	99.43
Rb	34	4.0	32	37	62	7.1	11	27	2.0	41	45
Cs	0.80	0.56	< 0.4	< 0.4	0.40	0.10	0.10	0.20	0.10	< 0.3	0.10
Sr	489	418	219	490	657	469	973	629	556	398	497
Ba	480	353	541	502	669	208	478	1143	311	266	192
Sc	3.7	3.8	3.3	7.8	22	8.0	19	3.1	3.1	4.7	8.0
Y	7.5	< 2.0	7.2	9.8	29	9.2	33	6.6	3.6	6.3	10
Zr	143	136	166	95	162	149	228	120	33	146	63
Hf	6.2	4.0	4.6	3.4	3.6	3.7	6.1	3.2	0.70	4.0	1.6
Th	3.0	0.30	5.0	4.1	1.0	0.40	0.50	0.30	0.20	1.2	1.0
U	0.21	0.13	< 0.3	0.20	0.10	0.20	0.20	0.10	0.080	0.20	< 0.3
Nb	5.3	2.3	8.9	6.3	8.4	5.5	14	5.2	2.7	8.9	9.5
Ta	4.9	3.8	1.1	1.6	-	-	-	-	-	-	-
Cr	5.0	4.0	7.0	12	128	24	61	12	78	21	40
Ni	-	-	-	-	116	30	81	< 50	15	20	14
Co	34	32	43	25	-	-	-	-	-	-	-
Zn	104	54	38	< 30	< 30	< 30	-	-	-	-	-
Pb	2.0	5.0	< 2.0	< 2.0	< 2.0	< 2.0	< 2.0	< 2.0	< 2.0	< 2.0	< 2.0
La	23	13	30	21	50	32	53	28	14	22	21
Ce	33	16	46	38	103	55	120	49	22	37	40
Nd	-	-	-	16	-	-	-	-	-	-	-
Sm	2.5	0.70	2.8	2.9	9.9	3.4	12	2.5	1.1	1.8	3.3
Eu	1.4	1.5	1.6	1.4	2.1	1.5	2.0	1.7	1.1	1.1	1.4
Eu*	0.87	0.26	0.97	0.91	2.8	0.92	3.4	0.73	0.35	0.53	0.89
Tb	0.50	0.16	0.55	0.42	1.0	0.32	1.3	0.29	0.17	0.21	0.30
Yb	0.86	0.37	0.89	0.86	1.5	0.34	2.7	0.35	0.42	0.39	0.72
Lu	0.12	0.050	0.14	0.11	0.19	0.38	0.39	0.040	0.050	0.050	0.10
Eu/Eu*	1.6	5.9	1.6	1.5	0.76	1.6	0.59	2.3	3.1	2.1	1.6
Σ REE	81	31	81	64	168	92	193	81	38	62	66
K/Rb	403	1079	480	301	245	1087	1192	716	2822	265	267
K/Ba	29	12	28	22	23	37	27	17	18	41	63
Rb/Sr	0.070	0.010	0.15	0.076	0.094	0.015	0.011	0.043	0.004	0.10	0.091
Ba/Sr	0.98	0.84	2.5	1.0	1.0	0.44	0.49	1.8	0.56	0.67	0.39

FILE: I2CTRN.DAT

LOW-P CHARNOCKITE

MAJOR AND TRACE ELEMENTS

	38	39-1	40-2	43	44-1	45	46	62	66	68	69
SiO2	62.72	62.82	61.32	64.82	70.26	70.12	63.69	66.87	64.78	57.99	72.25
TiO2	0.66	0.61	0.58	0.74	0.38	0.39	0.64	0.49	0.54	0.82	0.25
Al2O3	15.32	16.23	15.91	15.35	15.63	14.64	16.49	16.24	16.30	17.02	15.77
Fe2O3T	5.52	5.60	5.98	5.40	2.69	3.28	4.99	3.74	4.62	7.15	1.80
MnO	0.09	0.05	0.09	0.07	0.03	0.05	0.05	0.03	0.07	0.10	0.02
MgO	3.17	2.38	3.37	2.81	1.00	1.66	2.18	1.24	2.67	3.26	0.59
CaO	5.11	4.90	5.29	4.74	4.20	3.56	4.64	3.93	4.71	6.13	3.94
Na2O	4.05	4.93	4.38	4.22	4.47	4.20	4.69	4.57	4.20	4.90	4.57
K2O	2.09	1.74	2.03	1.22	1.01	2.35	1.77	1.44	1.20	1.51	0.64
P2O5	0.24	0.28	0.25	0.15	0.12	0.14	0.26	0.16	0.22	0.33	0.07
LOI	0.62	0.67	0.65	0.62	0.62	0.40	0.34	0.88	0.41	0.61	0.33
TOTAL	99.59	100.21	99.85	100.14	100.41	100.79	99.74	99.59	99.72	99.80	100.23
Rb	73	61	58	62	3.7	71	58	26	12	36	5.0
Cs	0.30	0.10	3.2	0.60	< 0.3	0.50	0.70	0.10	0.60	1.0	< 0.3
Sr	618	705	614	517	484	405	563	506	572	728	584
Ba	398	409	496	764	147	675	321	695	873	388	510
Sc	15	9.6	34	18	2.8	4.9	8.0	2.7	13	19	1.5
Y	22	17	20	8.0	5.5	9.5	13	5.9	12	24	2.0
Zr	200	188	136	141	164	121	199	239	156	174	79
Hf	4.8	4.8	2.9	5.0	3.9	3.2	4.2	5.0	6.0	5.3	2.3
Th	4.9	6.2	4.2	7.0	0.60	5.8	4.1	1.0	0.50	2.2	0.30
U	< 0.5	0.40	0.80	0.40	0.30	0.30	0.10	0.30	0.14	0.63	0.070
Nb	9.5	7.1	8.6	9.2	4.9	6.6	8.3	7.1	5.9	13	2.0
Ta	-	-	-	-	-	-	-	-	2.5	1.9	2.4
Cr	115	26	129	27	21	31	35	20	38	29	< 4.0
Ni	23	23	126	25	2.0	48	63	5.0	13	21	-
Co	-	-	-	-	-	-	-	-	24	25	18
Zn	-	-	-	-	-	-	-	-	60	180	45
Pb	< 2.0	< 2.0	< 2.0	< 2.0	< 2.0	11	2.0	< 2.0	< 2.0	2.0	< 2.0
La	49	53	90	48	33	34	41	26	35	50	21
Ce	81	91	22	85	46	63	61	46	52	95	25
Nd	34	-	-	-	12	-	-	-	21	39	9.5
Sm	7.3	6.5	3.9	7.8	1.9	3.4	5.1	2.4	5.1	9.0	0.90
Eu	2.2	1.4	1.3	1.8	1.2	1.2	1.3	1.2	1.8	2.6	1.7
Eu*	2.1	1.9	1.4	2.5	0.52	0.97	1.4	0.65	1.6	3.0	0.33
Tb	0.79	0.72	0.85	1.2	0.18	0.37	0.48	0.22	0.80	1.5	0.20
Yb	1.6	0.86	3.2	3.3	0.23	0.58	0.62	0.20	1.3	2.2	0.46
Lu	-	0.13	0.49	0.52	0.30	0.070	0.080	0.030	0.15	0.31	0.070
Eu/Eu*	1.1	0.75	0.93	0.72	2.3	1.2	0.94	1.9	1.1	0.89	5.2
Σ REE	142	154	141	148	82	102	110	75	96	151	48
K/Rb	238	237	291	163	2266	275	253	460	830	355	1063
K/Ba	44	35	34	13	57	29	46	17	11	33	10
Rb/Sr	0.12	0.087	0.094	0.12	0.008	0.18	0.10	0.051	0.021	0.047	0.009
Ba/Sr	0.64	0.58	0.81	1.5	0.30	1.7	0.58	1.4	1.5	0.53	0.87

FILE: I2CTRN.DAT

LOW-P CHARNOCKITE

MAJOR AND TRACE ELEMENTS

	70	71	78	107-1	108-3	119-5	119-6	120-1	120-2	120-4	122-1
SiO2	61.27	66.58	70.28	69.61	53.37	61.23	50.57	68.61	67.33	51.46	63.44
TiO2	0.55	0.46	0.32	0.52	1.40	1.62	1.05	0.44	0.49	1.30	0.73
Al2O3	17.69	15.43	15.36	15.59	14.94	13.10	12.85	16.33	16.76	19.37	17.42
Fe2O3T	5.88	4.13	3.54	2.36	10.80	10.25	10.35	3.40	3.71	9.69	5.72
MnO	0.06	0.05	0.05	0.02	0.16	0.15	0.18	0.03	0.05	0.06	0.08
MgO	2.33	1.52	1.03	1.10	5.21	2.13	8.07	1.34	1.53	2.76	1.65
CaO	5.72	3.78	3.55	3.52	7.69	5.11	7.49	3.88	4.04	6.10	4.83
Na2O	4.97	4.33	3.84	5.23	3.95	4.15	3.21	4.64	5.09	5.02	5.07
K2O	1.21	2.31	1.22	1.32	1.39	1.49	4.26	1.23	1.11	2.23	0.87
P2O5	< 0.1	0.17	0.08	0.11	0.26	0.53	0.70	0.16	0.20	0.69	0.26
LOI	0.53	1.03	0.21	0.44	0.44	0.24	0.35	0.48	0.46	1.19	0.04
TOTAL	100.21	99.79	99.48	99.82	99.61	100.00	99.08	100.54	100.77	99.85	100.11
Rb	10	45	33	44	35	100	280	23	10	2.0	41
Cs	0.30	0.10	< 0.3	< 0.5	-	1.9	7.1	0.50	0.30	1.4	0.40
Sr	840	601	298	419	460	211	1170	449	529	882	487
Ba	530	670	360	439	274	205	872	654	444	908	199
Sc	9.9	5.5	5.2	3.4	25	23	18	6.5	5.6	12	10
Y	22	8.0	5.4	4.0	27	35	30	10	7.7	29	9.3
Zr	152	149	74	98	176	217	200	158	154	364	161
Hf	3.5	2.7	3.5	2.7	4.5	5.8	4.8	3.4	3.0	7.9	6.9
Th	0.60	3.2	1.2	1.5	2.4	4.0	6.0	1.0	0.30	11	3.1
U	0.13	0.20	0.14	0.24	0.10	2.4	1.0	< 0.3	0.15	< 0.3	2.2
Nb	7.7	7.0	5.4	6.6	18	21	20	4.6	5.0	13	6.4
Ta	-	-	3.3	3.2	-	2.1	1.0	-	-	-	-
Cr	26	24	8.0	24	58	138	320	37	27	14	31
Ni	221	31	-	-	57	155	205	14	5.0	9.0	< 40
Co	-	-	23	32	40	36	36	-	-	-	-
Zn	-	-	95	36	109	116	120	-	-	-	-
Pb	< 2.0	< 2.0	< 2.0	< 2.0	7.1	18	9.5	< 2.0	< 2.0	< 2.0	< 2.0
La	38	33	15	19	42	31	93	29	24	122	24
Ce	83	48	20	24	81	65	178	51	38	211	47
Nd	-	-	-	10	-	23	80	19	17	83	22
Sm	7.8	2.9	1.3	1.4	6.9	5.6	13	3.0	3.0	15	5.2
Eu	1.8	1.3	1.6	1.2	2.3	1.4	3.1	1.3	1.2	2.6	1.9
Eu*	2.3	0.71	0.45	0.48	2.4	1.9	3.4	0.88	0.85	3.8	1.6
Tb	0.89	0.20	0.26	0.26	1.3	1.1	1.0	0.36	0.32	1.1	0.65
Yb	1.4	0.28	0.64	0.44	2.6	3.8	1.5	0.62	0.56	1.5	2.4
Lu	0.20	0.040	0.070	0.056	0.37	0.71	0.23	0.10	0.070	0.20	0.36
Eu/Eu*	0.80	1.8	3.5	2.5	0.97	0.72	0.92	1.5	1.4	0.69	1.2
Σ REE	134	85	38	46	137	109	280	85	67	355	81
K/Rb	1004	426	307	249	330	124	126	444	921	<256	176
K/Ba	19	29	28	25	42	60	41	16	21	20	36
Rb/Sr	0.012	0.075	0.11	0.11	0.076	0.47	0.24	0.051	0.019	0.002	0.084
Ba/Sr	0.63	1.1	1.2	1.0	0.60	0.97	0.75	1.5	0.84	1.0	0.41

FILE: I2CTRN.DAT

LOW-P CHARNOCKITE

MAJOR AND TRACE ELEMENTS

	122-2	488-4	510-1	510-2	511-2	513	514-3	514-4	523	562-1
SiO2	77.27	60.33	61.59	57.94	58.50	71.74	73.39	75.89	73.30	72.90
TiO2	0.25	0.59	0.63	1.16	0.73	0.46	0.17	0.07	0.21	0.36
Al2O3	13.01	16.31	15.66	18.07	15.70	14.86	15.05	13.68	14.74	15.10
Fe2O3T	1.33	6.69	6.16	7.27	7.75	2.39	1.33	1.11	1.58	1.91
MnO	0.01	0.10	0.12	0.08	0.13	0.03	0.02	0.02	0.02	0.03
MgO	0.29	3.87	3.52	1.73	4.54	1.02	0.39	0.34	0.89	0.73
CaO	2.67	6.38	5.55	4.54	5.81	2.96	2.55	2.09	3.31	3.33
Na2O	4.11	4.36	4.57	4.97	4.16	4.42	5.20	4.86	4.58	4.66
K2O	0.90	1.01	1.55	2.79	1.89	1.51	1.15	1.09	0.92	1.05
P2O5	0.01	0.29	0.21	0.62	0.29	0.03	0.05	0.01	0.05	0.03
LOI	0.53	0.50	0.27	0.37	0.58	0.42	0.54	0.18	-	0.17
TOTAL	100.38	100.43	99.83	99.54	100.08	99.84	99.84	99.34	99.60	100.30
Rb	4.0	< 2.0	45	75	69	15	10	8.0	6.0	3.9
Cs	< 0.5	0.40	0.040	0.030	0.090	-	< .08	< .03	0.030	-
Sr	204	750	470	716	613	383	439	445	532	394
Ba	309	281	389	906	581	352	400	381	190	263
Sc	2.2	17	22	6.6	19	3.7	1.9	1.4	1.5	3.2
Y	4.0	22	19	30	25	3.0	4.1	2.0	1.5	3.1
Zr	219	100	122	583	122	105	83	68	79	174
Hf	6.3	3.5	4.1	13	3.4	3.0	2.7	2.2	1.9	4.3
Th	2.0	0.20	1.6	30	1.9	0.10	0.20	0.70	0.10	1.0
U	0.10	< 0.2	0.10	2.3	0.10	0.20	0.30	0.30	0.17	0.10
Nb	4.8	7.1	9.2	24	8.8	5.6	2.8	3.5	2.5	4.5
Ta	-	0.20	0.20	1.3	0.11	0.34	0.23	< .03	0.060	0.16
Cr	82	80	115	20	174	2.8	2.4	1.0	11	7.6
Ni	< 40	47	55	14	43	< 7.0	< 8.0	3.0	14	17
Co	-	22	18	14	23	4.9	2.2	1.3	4.2	4.9
Zn	-	-	114	105	117	37	27	22	22	31
Pb	< 2.0	< 2.0	< 2.0	32	4.5	< 2.0	< 2.0	2.0	< 2.0	< 2.0
La	21	41	29	186	36	9.1	6.4	7.9	6.9	19
Ce	29	78	65	375	84	15	12	12	11	31
Nd	-	-	32	153	38	2.9	4.0	3.0	-	8.1
Sm	1.0	7.8	7.1	23	8.5	0.51	0.90	0.38	0.58	0.99
Eu	1.4	1.5	1.4	3.9	1.4	0.54	0.38	0.41	0.49	0.89
Eu*	0.29	2.3	2.0	5.7	2.4	0.17	0.27	0.12	0.20	0.27
Tb	0.11	0.96	0.73	1.6	0.85	0.090	0.12	0.050	0.12	0.090
Yb	0.24	1.7	1.5	2.1	1.9	0.25	0.26	0.15	0.27	0.29
Lu	< .05	0.22	0.21	0.24	0.25	0.040	0.030	0.023	0.043	0.050
Eu/Eu*	4.9	0.65	0.70	0.69	0.59	3.2	1.4	3.6	2.4	3.3
7 REE	52	132	106	594	134	25	20	21	19	52
K/Rb	1868	-	286	309	227	836	955	1131	1273	2235
K/Ba	24	30	33	26	27	36	24	24	40	33
Rb/Sr	0.020	-	0.096	0.10	0.11	0.039	0.023	0.018	0.011	0.010
Ba/Sr	1.5	0.37	0.83	1.3	0.95	0.92	0.91	0.86	0.36	0.68

FILE: I2CTRN.DAT

LOW-P CHARNOCKITE

MAJOR AND TRACE ELEMENTS

	N	MEAN	SD %
SiO2	43	65.55	10.0
TiO2	43	0.58	58.6
Al2O3	43	15.79	8.3
Fe2O3T	43	4.76	55.4
MnO	43	0.06	68.1
MgO	43	2.08	74.8
CaO	43	4.56	29.7
Na2O	43	4.49	11.5
K2O	43	1.51	43.9
P2O5	42	0.20	83.9
LOI	42	0.46	49.7
TOTAL			
Rb	42	39	118.1
Cs	30	0.73	187.1
Sr	43	543	35.2
Ba	43	475	48.8
Sc	43	9.7	82.1
Y	42	13	75.0
Zr	43	158	55.9
Hf	43	4.2	47.6
Th	43	2.9	165.6
U	37	0.41	147.9
Nb	43	8.1	61.8
Ta	19	1.6	90.4
Cr	42	49	123.5
Ni	31	49	117.8
Co	21	22	58.7
Zn	19	75	60.2
Pb	11	8.6	106.6
La	43	36	88.3
Ce	43	65	98.2
Nd	20	31	115.8
Sm	43	4.9	93.1
Eu	43	1.5	43.1
Eu*	43	1.4	84.4
Tb	43	0.58	75.3
Yb	43	1.1	85.7
Lu	41	0.18	89.3
Eu/Eu*	43	1.8	72.3
7 REE	43	108	93.0
K/Rb	41	695	92.4
K/Ba	43	30	41.6
Rb/Sr	42	0.076	108.3
Ba/Sr	43	0.93	48.6

FILE: I2CTRN.DAT

LOW-P CHARNOCKITE

CIPW NORMS

	KDA2	1	2	4-1	8	9-1	10-2	22	35	37-1	37-2
Fe2O3/F	0.44	0.44	0.44	0.44	0.44	0.44	0.44	0.44	0.44	0.44	0.44
Qtz	23.41	25.33	37.30	22.21	2.13	25.50	0.00	30.67	30.63	34.55	20.59
Corund	0.36	0.00	1.79	0.14	0.00	0.00	0.00	0.20	0.62	0.45	0.31
Zircon	0.03	0.03	0.03	0.02	0.03	0.03	0.05	0.02	0.01	0.03	0.01
Or	9.75	3.07	10.93	7.92	10.81	5.50	9.34	13.77	4.02	7.71	8.57
Ab	47.87	42.81	31.57	38.05	41.40	35.11	40.66	31.10	37.41	27.80	33.99
An	13.08	20.91	13.28	21.46	16.35	22.10	22.47	16.48	21.68	22.17	21.08
DiopP	0.00	0.99	0.00	0.00	13.82	0.26	8.58	0.00	0.00	0.00	0.00
Hyp	3.59	4.44	3.37	6.85	10.29	8.24	11.15	4.72	4.01	4.89	10.27
Olivine	0.00	0.00	0.00	0.00	0.00	0.00	0.62	0.00	0.00	0.00	0.00
Mgt	0.92	1.20	0.93	1.58	3.08	2.09	3.48	1.20	1.06	1.20	2.27
Chrmite	0.00	0.00	0.00	0.01	0.06	0.01	0.03	0.01	0.03	0.01	0.02
Ilmen	0.55	0.68	0.53	0.84	1.35	0.84	2.18	0.67	0.49	0.76	1.01
Apat	0.21	0.12	0.19	0.23	0.63	0.30	0.95	0.30	0.14	0.23	0.46

BARTH MESONORM

Qtz	23.39	25.17	36.81	24.32	1.68	26.93	3.63	31.42	30.44	35.13	24.48
Corund	0.81	0.05	2.41	0.79	0.00	0.49	0.00	0.79	1.05	1.07	1.08
Or	6.44	0.00	7.98	1.75	7.62	0.00	0.00	9.68	0.45	3.29	0.00
Ab	50.91	45.57	34.11	41.06	44.03	37.93	43.79	34.12	40.28	30.29	37.14
An	11.79	20.86	12.30	19.84	15.94	20.86	22.03	15.13	20.61	20.95	19.44
Biot	5.22	4.93	4.95	9.96	4.95	8.86	14.89	6.96	5.73	7.33	13.96
Actin	0.00	0.00	0.00	0.00	21.55	0.00	9.72	0.00	0.00	0.00	0.00
Edenite	0.00	0.00	0.00	0.00	0.00	0.00	0.00	0.00	0.00	0.00	0.00
Hyp	0.00	1.69	0.00	0.00	0.00	2.19	0.18	0.00	0.00	0.00	0.67
Mgt	0.66	0.87	0.68	1.15	2.20	1.52	2.50	0.88	0.77	0.82	1.67
Sphene	0.60	0.75	0.58	0.93	1.47	0.93	2.40	0.75	0.55	0.85	1.13
Apat	0.19	0.10	0.17	0.21	0.56	0.27	0.85	0.28	0.13	0.21	0.43

FILE: I2CTRN.DAT

LOW-P CHARNOCKITE

CIPW NORMS

	38	39-1	40-2	43	44-1	45	46	62	66	68	69
Fe203/F	0.44	0.44	0.44	0.44	0.44	0.44	0.44	0.44	0.44	0.41	0.44
Qtz	15.78	13.63	11.88	20.69	29.59	26.50	16.20	23.80	20.79	6.00	33.65
Corund	0.00	0.00	0.00	0.00	0.00	0.00	0.00	0.37	0.01	0.00	0.54
Zircon	0.04	0.04	0.03	0.03	0.03	0.02	0.04	0.05	0.03	0.01	0.02
Or	12.35	10.28	12.00	7.21	5.97	13.89	10.46	8.51	7.09	9.10	3.78
Ab	33.81	41.20	36.61	35.33	37.47	35.24	39.28	38.30	35.12	40.92	38.24
An	17.69	17.29	18.00	19.54	19.79	14.31	18.93	18.73	22.28	20.18	19.37
Diop	5.13	4.47	5.58	2.66	0.36	2.16	2.12	0.00	0.00	6.83	0.00
Hyp	9.70	8.14	10.54	9.74	4.29	5.64	8.17	5.89	10.27	10.41	2.81
Olivine	0.00	0.00	0.00	0.00	0.00	0.00	0.00	0.00	0.00	0.00	0.00
Mgt	2.26	2.30	2.45	2.22	1.10	1.35	2.05	1.54	1.90	2.91	0.74
Chrmite	0.05	0.01	0.06	0.01	0.01	0.01	0.02	0.01	0.02	0.01	0.00
Ilmen	1.25	1.16	1.18	1.41	0.72	0.74	1.22	0.93	1.03	1.56	0.48
Apat	0.56	0.65	0.58	0.35	0.28	0.32	0.60	0.37	0.51	0.77	0.16

BARTH MESONORM

Qtz	18.46	15.58	14.75	23.03	29.90	27.12	19.35	25.61	23.63	8.96	32.79
Corund	0.00	0.00	0.00	0.00	0.35	0.00	0.00	1.14	0.82	0.00	0.97
Or	4.67	3.86	4.19	0.00	1.84	8.85	2.37	3.17	0.00	1.27	1.20
Ab	36.89	44.50	39.66	38.33	40.48	37.80	42.42	41.75	38.12	44.27	41.32
An	17.71	17.03	17.91	19.57	18.89	14.19	18.85	17.04	20.27	20.03	18.35
Biot	12.56	10.35	12.65	11.67	6.68	8.10	13.06	8.78	11.00	12.61	4.17
Actin	6.14	5.16	7.31	0.94	0.00	1.86	0.57	0.00	0.00	8.30	0.00
Edenite	0.00	0.00	0.00	0.00	0.00	0.00	0.00	0.00	0.00	0.00	0.00
Hyp	0.00	0.00	0.00	2.97	0.00	0.00	0.00	0.00	2.71	0.00	0.00
Mgt	1.66	1.66	1.78	1.62	0.80	0.97	1.49	1.13	1.38	2.13	0.54
Sphene	1.40	1.28	1.22	1.56	0.80	0.82	1.35	1.04	1.14	1.72	0.53
Apat	0.51	0.59	0.53	0.32	0.25	0.29	0.55	0.34	0.46	0.60	0.15

FILE: I2CTRN.DAT

LOW-P CHARNOCKITE

CIPW NORMS

	70	71	78	107-1	108-3	119-5	119-6	120-1	120-2	120-4	122-1
Fe2O3/F	0.44	0.44	0.44	0.44	0.44	0.44	0.44	0.44	0.44	0.44	0.44
Qtz	11.38	21.76	33.11	25.09	1.74	17.48	0.00	26.00	21.98	0.00	16.73
Corund	0.00	0.00	1.45	0.00	0.00	0.00	0.00	0.66	0.30	0.00	0.00
Zircon	0.03	0.03	0.02	0.02	0.04	0.04	0.04	0.03	0.03	0.07	0.03
Or	7.15	13.65	7.21	7.80	8.21	8.81	25.17	7.27	6.56	13.19	5.14
Ab	41.43	36.20	32.27	43.95	33.08	34.96	19.03	38.93	42.68	40.51	42.54
An	22.72	16.08	17.23	15.33	19.11	12.80	8.53	18.46	18.99	24.09	22.40
Diop	4.50	1.53	0.00	1.30	14.28	7.63	19.66	0.00	0.00	1.70	0.03
Hyp	8.15	6.29	5.49	3.53	14.25	8.80	0.00	5.89	6.62	0.00	8.47
Olivine	0.00	0.00	0.00	0.00	0.00	0.00	13.71	0.00	0.00	9.73	0.00
Mgt	2.41	1.70	1.45	0.97	4.43	4.21	4.25	1.40	1.52	3.97	2.35
Chrmite	0.01	0.01	0.00	0.01	0.03	0.06	0.14	0.02	0.01	0.01	0.01
Ilmen	1.05	0.87	0.61	0.99	2.66	3.08	1.99	0.84	0.93	2.47	1.39
Apat	0.00	0.39	0.19	0.26	0.60	1.23	1.62	0.37	0.46	1.60	0.60

BARTH MESONORM

Qtz	13.10	23.75	34.17	25.43	4.23	20.49	0.00	27.30	23.73	3.36	18.46
Corund	0.00	0.00	2.08	0.13	0.00	0.00	0.00	1.34	1.07	1.09	1.00
Or	1.18	7.62	2.46	3.68	0.00	0.00	17.02	1.88	0.49	0.29	0.00
Ab	44.70	39.58	35.21	47.18	36.14	38.41	21.30	41.82	45.54	45.73	45.64
An	22.43	16.13	16.31	14.91	19.29	13.11	8.17	16.74	16.97	21.54	19.78
Biot	9.58	10.03	7.84	6.65	13.39	14.52	13.50	8.66	9.66	20.91	8.25
Actin	6.12	0.30	0.00	0.00	19.33	5.46	8.10	0.00	0.00	0.00	0.00
Edenite	0.00	0.00	0.00	0.00	0.00	0.00	25.11	0.00	0.00	0.00	0.00
Hyp	0.00	0.00	0.00	0.00	0.81	0.25	0.00	0.00	0.00	0.00	3.11
Mgt	1.74	1.24	1.07	0.70	3.26	3.13	3.10	1.01	1.09	2.91	1.70
Sphene	1.15	0.98	0.68	1.09	2.98	3.49	2.22	0.92	1.02	2.76	1.53
Apat	0.00	0.36	0.17	0.23	0.55	1.14	1.48	0.34	0.42	1.46	0.55

FILE: I2CTRN.DAT

LOW-P CHARNOCKITE

CIPW NORMS

	122-2	488-4	510-1	510-2	511-2	513	514-3	514-4	523	562-1
Fe2O3/F	0.44	0.44	0.44	0.44	0.44	0.44	0.44	0.44	0.44	0.44
Qtz	43.44	11.89	12.24	5.63	7.77	31.87	32.50	38.18	34.50	33.15
Corund	0.43	0.00	0.00	0.08	0.00	0.63	0.72	0.72	0.31	0.31
Zircon	0.04	0.02	0.03	0.12	0.03	0.02	0.02	0.01	0.02	0.01
Or	5.32	5.97	9.16	16.49	11.17	8.92	6.80	6.44	5.44	6.21
Ab	34.63	36.34	38.32	41.53	34.75	37.12	43.68	40.80	38.36	39.15
An	13.31	22.24	17.82	18.83	18.82	14.67	12.54	10.52	16.30	16.50
Diop	0.00	6.35	6.94	0.00	6.80	0.00	0.00	0.00	0.00	0.00
Hyp	1.57	12.10	10.40	9.45	14.36	4.11	1.99	1.82	3.41	3.12
Olivine	0.00	0.00	0.00	0.00	0.00	0.00	0.00	0.00	0.00	0.00
Mgt	0.55	2.75	2.53	2.98	3.18	0.98	0.55	0.46	0.65	0.80
Chrmite	0.04	0.03	0.05	0.01	0.08	0.00	0.00	0.00	0.01	0.00
Ilmen	0.48	1.12	1.20	2.20	1.39	0.87	0.32	0.13	0.40	0.69
Apat	0.02	0.67	0.49	1.44	0.67	0.07	0.12	0.02	0.12	0.07

BARTH MESONORM

Qtz	41.81	13.37	14.43	10.53	12.76	32.20	31.28	36.67	33.96	32.55
Corund	0.85	0.00	0.00	1.75	0.00	1.36	1.10	0.93	0.64	0.85
Or	3.81	0.00	2.07	7.62	0.00	5.00	5.01	4.95	2.33	3.29
Ab	37.51	39.26	41.23	45.11	37.62	40.18	47.00	44.23	41.50	42.09
An	12.52	21.99	17.72	14.59	18.72	13.05	11.81	10.20	15.50	15.11
Biot	2.55	9.57	11.41	14.47	17.99	6.46	2.92	2.53	5.05	4.85
Actin	0.00	8.69	9.54	0.00	8.40	0.00	0.00	0.00	0.00	0.00
Edenite	0.00	0.00	0.00	0.00	0.00	0.00	0.00	0.00	0.00	0.00
Hyp	0.00	3.29	0.00	0.00	0.00	0.00	0.00	0.00	0.00	0.00
Mgt	0.40	1.98	1.83	2.17	2.31	0.72	0.40	0.33	0.47	0.53
Sphene	0.53	1.24	1.32	2.45	1.54	0.97	0.36	0.15	0.44	0.76
Apat	0.02	0.61	0.44	1.31	0.61	0.06	0.11	0.02	0.11	0.06

FILE: I2CTRN.DAT

LOW-P CHARNOCKITE

CIPW NORMS

	N	MEAN	SD %
Fe2O3/F	43	0.44	0.0
Qtz	40	22.4	46.7
Corund	20	0.52	83.0
Zircon	43	0.032	55.2
Or	43	8.9	43.9
Ab	43	37.4	13.1
An	43	18.0	20.0
Diop	23	5.4	93.0
Hyp	41	7.0	48.5
Olivine	3	8.0	83.7
Mgt	43	2.0	55.4
Chrmite	41	0.023	120.2
Ilmen	43	1.1	58.6
Apat	42	0.47	83.9

BARTH MESONORM

Qtz	42	22.8	44.4
Corund	26	1.00	51.8
Or	32	4.3	61.3
Ab	43	40.5	12.6
An	43	17.1	20.3
Biot	43	9.3	44.9
Actin	17	7.5	77.3
Edenite	1	25.1	0.0
Hyp	10	1.8	68.7
Mgt	43	1.4	55.7
Sphene	43	1.2	59.1
Apat	42	0.43	84.1

FILE: I2CGRN.DAT

LOW-P HIGH-K CHARNOCKITE

MAJOR AND TRACE ELEMENTS

	10-1	11-2	39-2	41	119-3	484-1a	489-1	565-1	565-2	N	MEAN	SD	%
SiO2	66.77	70.03	69.17	60.46	75.32	73.87	64.95	70.21	69.48	9	68.92	6.5	
TiO2	0.51	0.23	0.26	0.69	0.31	0.29	0.62	0.81	0.75	9	0.50	46.1	
Al2O3	15.82	15.07	15.48	16.17	12.66	12.94	15.06	13.76	13.16	9	14.46	9.2	
Fe2O3T	3.87	2.56	2.27	6.12	2.01	2.87	4.76	4.03	5.74	9	3.80	39.5	
MnO	0.04	0.03	0.02	0.08	0.05	0.05	0.07	0.04	0.07	9	0.05	40.0	
MgO	1.24	0.85	0.70	2.86	0.35	0.43	2.56	0.54	0.62	9	1.13	83.1	
CaO	2.95	2.83	2.57	5.22	1.37	1.73	3.96	2.40	2.39	9	2.82	41.1	
Na2O	4.08	4.15	3.85	3.85	3.16	3.46	3.87	4.36	3.57	9	3.82	9.7	
K2O	3.54	3.66	4.16	3.32	4.44	3.89	3.30	3.66	4.25	9	3.80	10.6	
P2O5	0.07	0.11	0.16	0.32	0.06	0.09	0.21	0.20	0.24	9	0.16	54.1	
LOI	0.59	0.61	0.64	0.64	0.09	0.44	0.38	0.17	0.16	9	0.41	54.3	
TOTAL	99.48	100.13	99.28	99.73	99.82	100.06	99.74	100.18	100.43				
Rb	71	76	85	65	109	98	75	50	70	9	78	22.7	
Cs	0.10	0.50	0.20	0.40	0.33	0.36	0.60	< .10	< .10	7	0.36	47.7	
Sr	648	435	706	890	141	132	706	641	281	9	509	53.6	
Ba	880	1439	1739	932	665	523	257	2109	1393	9	1104	54.9	
Sc	3.8	7.3	0.90	14	2.5	3.0	16	4.9	11	9	7.0	76.7	
Y	5.1	14	7.2	17	16	18	16	8.5	30	9	15	50.7	
Zr	226	122	107	326	194	150	114	322	459	9	224	54.1	
Hf	6.3	2.6	2.5	4.0	7.9	4.9	3.3	12	15	9	6.5	67.7	
Th	20	6.0	19	2.0	23	17	< 0.3	0.50	15	8	13	68.0	
U	0.37	0.40	0.46	0.20	1.4	0.70	< 0.2	0.20	0.30	8	0.50	80.1	
Nb	6.2	6.3	2.9	9.9	11	8.2	7.3	12	11	9	8.3	35.4	
Ta	-	-	-	-	1.1	0.60	0.50	0.70	0.70	5	0.72	31.7	
Cr	17	17	7.1	65	2.6	4.9	61	4.0	3.7	8	20	122.7	
Ni	29	< 50	10	27	4.3	7.0	20	7.0	5.0	8	14	74.1	
Co	-	-	-	-	2.6	4.0	20	3.9	4.7	5	7.0	103.5	
Zn	-	-	23	-	30	44	-	37	78	5	42	50.4	
Pb	9.4	3.5	13	< 2.0	22	22	< 2.0	27	28	7	18	52.3	
La	73	55	72	53	89	24	37	31	90	9	58	41.9	
Ce	114	90	108	98	154	39	67	50	161	9	98	43.2	
Nd	-	-	-	41	41	14	-	18	54	5	34	50.5	
Sm	3.8	4.4	4.7	7.0	6.1	2.6	7.9	3.2	9.4	9	5.5	42.0	
Eu	1.9	1.9	1.5	1.7	1.3	1.1	1.8	1.9	2.5	9	1.7	23.4	
Eu*	1.1	1.2	1.1	1.8	1.7	0.89	2.3	0.96	2.7	9	1.5	42.5	
Tb	0.39	0.44	0.29	0.52	0.57	0.49	0.90	0.41	1.1	9	0.57	46.3	
Yb	0.72	0.76	0.28	1.1	1.6	1.8	1.6	0.76	2.7	9	1.3	58.8	
Lu	-	0.10	0.030	0.14	0.25	0.29	0.24	0.11	2.5	8	0.46	181.4	
Eu/Eu*	1.8	1.6	1.4	0.97	0.79	1.2	0.79	2.0	0.91	9	1.3	34.8	
Σ REE	193	152	186	162	253	69	117	86	269	9	165	41.6	
K/Rb	414	400	406	424	338	329	365	608	504	9	421	20.7	
K/Ba	33	21	20	30	55	62	107	14	25	9	41	72.1	
Rb/Sr	0.11	0.17	0.12	0.073	0.77	0.74	0.11	0.078	0.25	9	0.27	104.6	
Ba/Sr	1.4	3.3	2.5	1.0	4.7	4.0	0.36	3.3	5.0	9	2.8	57.8	

FILE: I2CGRN.DAT

LOW-P HIGH-K CHARNOCKITE

CIPW NORMS

	10-1	11-2	39-2	41	119-3	484-1a	489-1	565-1	565-2	N	MEAN	SD	%
Fe2O3/F	0.44	0.44	0.44	0.44	0.44	0.44	0.44	0.44	0.44	9	0.44	0.0	0
Qtz	20.37	24.35	24.09	10.35	36.00	33.72	17.63	25.15	25.76	9	24.2	32.2	
Corund	0.05	0.00	0.27	0.00	0.29	0.10	0.00	0.00	0.00	4	0.18	67.8	
Zircon	0.05	0.03	0.02	0.07	0.04	0.03	0.02	0.07	0.09	9	0.047	53.8	
Or	20.92	21.63	24.58	19.62	26.24	22.99	19.50	21.63	25.12	9	22.5	10.8	
Ab	34.05	34.80	32.06	31.92	26.64	29.18	32.23	36.42	30.00	9	31.9	9.4	
An	14.51	11.85	12.22	17.38	6.50	8.07	14.25	7.42	7.44	9	11.1	35.0	
Diop	0.00	1.52	0.00	5.59	0.00	0.00	3.45	3.19	2.71	5	3.3	45.0	
Hyp	6.00	3.47	3.49	9.20	2.36	3.41	8.32	2.30	4.50	9	4.8	52.7	
Olivine	0.00	0.00	0.00	0.00	0.00	0.00	0.00	0.00	0.00	0	0.0	0.0	
Mgt	1.59	1.05	0.93	2.51	0.83	1.18	1.95	1.65	2.36	9	1.6	39.5	
Chrmite	0.01	0.01	0.03	0.03	0.00	0.00	0.03	0.00	0.00	9	0.013	101.5	
Ilmen	0.97	0.44	0.49	1.31	0.59	0.55	1.18	1.54	1.42	9	0.94	46.1	
Apat	0.16	0.26	0.37	0.74	0.14	0.21	0.49	0.46	0.56	9	0.38	53.9	

BARTH MESONORM

Qtz	22.35	24.24	24.53	12.86	35.35	33.71	20.17	24.92	26.86	9	25.0	27.0	
Corund	0.81	0.00	0.78	0.00	0.78	0.49	0.00	0.00	0.00	4	0.72	21.1	
Or	15.67	18.78	21.81	12.65	24.54	20.43	12.15	18.35	20.32	9	18.3	22.6	
Ab	37.23	37.59	35.18	35.03	28.95	31.72	35.11	39.59	32.64	9	34.8	9.4	
An	12.61	11.79	10.96	17.27	5.43	7.13	14.23	7.25	7.58	9	10.5	37.3	
Biot	8.93	4.86	5.13	11.57	3.56	4.86	12.08	5.63	8.40	9	7.2	43.3	
Actin	0.00	1.27	0.00	6.64	0.00	0.00	3.08	0.93	0.36	5	2.5	103.9	
Edenite	0.00	0.00	0.00	0.00	0.00	0.00	0.00	0.00	0.00	0	0.0	0.0	
Hyp	0.00	0.00	0.00	0.00	0.00	0.00	0.00	0.00	0.00	0	0.0	0.0	
Mgt	1.16	0.76	0.68	1.84	0.61	0.86	1.43	1.21	1.72	9	1.1	39.6	
Sphene	1.08	0.48	0.55	1.46	0.66	0.62	1.31	1.71	1.60	9	1.1	46.2	
Apat	0.15	0.23	0.34	0.68	0.13	0.19	0.44	0.42	0.51	9	0.34	54.1	

FILE: I2CHIP.DAT

MEDIUM TO HIGH-P CHARNOCKITE

MAJOR AND TRACE ELEMENTS

	474	475	477	478	480	483	485-2	486-1	524	525	526-1
SiO2	70.96	55.99	56.26	71.86	67.76	60.41	60.71	56.47	65.53	60.37	70.77
TiO2	0.30	1.00	0.75	0.38	0.54	0.78	0.72	0.88	0.57	0.99	0.29
Al2O3	15.05	17.27	17.36	11.71	14.72	17.03	15.77	15.89	16.58	16.95	15.37
Fe2O3T	2.31	8.45	14.26	6.96	5.11	6.92	6.71	8.51	4.40	7.19	2.75
MnO	0.03	0.12	0.14	0.09	0.05	0.09	0.09	0.12	0.05	0.10	0.03
MgO	0.83	3.95	4.66	2.28	2.74	3.31	3.80	5.00	2.11	2.86	0.81
CaO	3.00	7.05	3.58	3.43	2.94	6.05	6.15	7.45	4.56	5.59	3.64
Na2O	4.35	4.60	1.89	2.35	3.64	3.97	4.07	4.37	5.29	4.89	4.73
K2O	2.28	1.33	1.51	0.49	2.30	1.65	1.52	0.82	1.32	1.39	1.20
P2O5	0.10	0.28	0.13	0.08	0.15	0.34	0.31	0.28	0.24	0.31	0.10
LOI	0.32	0.46	0.18	0.79	0.51	0.03	0.45	0.67	0.12	0.25	0.31
TOTAL	99.53	100.50	100.66	100.42	100.46	100.58	100.31	100.46	100.77	100.49	100.00
Rb	29	35	49	7.2	71	7.2	10	2.0	8.8	6.3	8.2
Cs	0.10	0.50	0.10	0.20	0.10	0.10	0.30	0.20	0.060	-	0.11
Sr	410	751	211	162	363	1097	812	784	942	850	555
Ba	739	398	586	36	792	798	909	418	519	719	547
Sc	2.4	18	29	12	8.0	18	18	20	0.0	12	1.9
Y	2.9	26	28	16	13	22	24	26	8.3	17	2.8
Zr	110	191	109	92	82	132	124	193	155	151	154
Hf	2.6	5.9	2.8	2.1	2.6	3.8	3.8	5.3	3.8	4.3	3.4
Th	0.20	0.60	0.50	1.1	3.9	< 0.3	< 0.3	0.20	0.40	0.59	0.10
U	0.50	0.20	0.20	0.20	0.20	< 0.2	0.10	0.30	0.18	0.19	0.12
Nb	4.1	10	10	6.2	6.6	6.3	6.3	8.7	6.3	8.0	3.2
Ta	0.10	1.0	0.40	0.40	0.30	0.30	0.10	0.30	0.20	0.25	0.060
Cr	7.0	87	217	108	65	48	105	133	61	29	9.0
Ni	7.0	35	97	19	25	13	29	61	38	26	9.0
Co	5.0	28	40	17	16	24	21	30	13	20	7.3
Zn	-	-	-	-	-	-	-	-	54	90	30
Pb	< 2.0	< 2.0	< 2.0	11	13	< 2.0	< 2.0	< 2.0	< 2.0	< 2.0	< 2.0
La	24	36	14	19	37	44	40	36	45	53	25
Ce	34	99	-	-	64	101	84	69	80	104	38
Nd	-	-	-	-	-	-	-	-	28	38	13
Sm	1.3	9.3	4.8	2.8	4.1	9.3	9.1	8.4	4.8	7.3	1.7
Eu	1.2	1.6	0.84	0.54	1.3	2.4	1.9	1.9	1.8	2.0	1.3
Eu*	0.46	2.8	1.6	0.95	1.3	2.7	2.7	2.5	1.2	2.0	0.46
Tb	0.27	1.2	0.87	0.51	0.55	1.1	1.1	0.99	0.38	0.71	0.16
Yb	0.46	2.7	2.5	1.7	1.6	2.2	1.5	2.0	0.63	1.2	0.19
Lu	0.050	0.39	0.40	0.25	0.24	0.31	0.20	0.28	0.090	0.16	0.023
Eu/Eu*	2.6	0.57	0.52	0.57	1.0	0.88	0.71	0.77	1.5	0.99	2.8
7 REE	61	151	-	-	109	161	139	119	132	168	66
K/Rb	653	315	256	565	269	1902	1262	3403	1245	1739	1215
K/Ba	26	28	21	113	24	17	14	16	21	15	18
Rb/Sr	0.071	0.047	0.23	0.044	0.20	0.007	0.012	0.003	0.009	0.007	0.015
Ba/Sr	1.8	0.53	2.8	0.22	2.2	0.73	1.1	0.53	0.55	0.85	0.99

FILE: I2CHIP.DAT

MEDIUM TO HIGH-P CHARNOCKITE

MAJOR AND TRACE ELEMENTS

	527	528	529	530-1	531-1	531-2	532	533	534-1	535-2	536-1
SiO2	59.91	63.73	63.76	67.74	59.12	55.89	68.24	67.60	74.45	66.53	64.41
TiO2	0.54	0.67	0.62	0.44	0.61	0.93	0.23	0.50	0.19	0.60	0.66
Al2O3	16.09	16.28	15.88	16.19	16.00	17.50	16.32	15.68	14.40	17.30	16.16
Fe2O3T	7.03	6.78	6.83	3.28	7.34	10.69	2.62	3.53	1.57	3.85	5.67
MnO	0.11	0.09	0.09	0.04	0.12	0.13	0.04	0.05	0.02	0.05	0.06
MgO	3.94	3.10	2.72	1.64	4.08	4.17	1.58	1.49	0.99	1.41	2.48
CaO	5.89	4.02	4.45	4.28	5.98	4.69	3.78	3.90	4.16	4.45	4.81
Na2O	4.49	4.05	3.95	4.60	4.32	3.91	4.18	4.30	3.34	3.93	4.63
K2O	1.50	1.35	1.23	1.16	1.07	1.38	2.58	1.83	0.96	1.27	0.80
P2O5	0.28	0.16	0.15	0.13	0.18	0.04	0.13	0.15	0.01	0.19	0.26
LOI	0.39	0.29	0.53	0.70	0.65	0.31	0.18	0.72	0.23	0.29	0.16
TOTAL	100.17	100.52	100.18	100.20	99.47	99.64	99.88	99.75	100.32	99.87	100.10
Rb	13	29	14	5.2	5.8	13	34	12	4.0	8.1	3.3
Cs	-	0.050	0.040	0.070	0.10	0.040	-	< 0.5	-	< .03	0.030
Sr	728	537	416	610	570	542	1017	697	393	879	612
Ba	750	381	283	556	428	552	1501	681	371	600	359
Sc	17	16	17	3.9	17	22	4.2	4.8	3.5	5.3	11
Y	19	18	16	3.6	13	7.3	2.9	2.6	1.6	5.8	12
Zr	122	124	98	130	74	117	55	83	130	188	189
Hf	3.6	3.0	2.5	2.8	1.9	2.8	1.5	2.2	3.7	4.5	5.0
Th	0.10	0.30	0.10	0.10	0.10	0.20	0.050	< .10	0.10	4.7	0.80
U	0.10	0.16	0.13	0.050	0.060	0.16	< .10	0.040	0.20	0.13	0.20
Nb	6.1	7.8	7.6	4.0	6.9	10	1.5	2.7	1.7	4.4	5.9
Ta	0.10	0.20	0.20	0.050	0.10	0.20	< .04	0.10	0.040	0.040	0.20
Cr	102	127	145	24	270	220	62	28	11	19	48
Ni	35	54	76	18	152	176	25	13	19	39	28
Co	22	24	26	10	29	41	9.3	9.0	5.2	11	13
Zn	104	82	84	38	82	142	36	44	19	54	70
Pb	< 2.0	< 2.0	< 2.0	< 2.0	< 2.0	< 2.0	< 2.0	5.8	< 2.0	< 2.0	2.7
La	31	32	23	15	16	20	18	25	14	49	33
Ce	68	58	40	24	32	31	28	43	21	88	64
Nd	32	18	-	7.2	-	7.8	11	-	5.7	29	23
Sm	7.0	4.4	3.1	1.6	4.0	1.4	1.8	2.1	0.54	51	4.8
Eu	1.8	1.5	1.3	1.1	1.2	1.9	1.2	1.1	1.1	1.7	1.1
Eu*	2.0	1.3	0.99	0.42	1.2	0.44	0.47	0.58	0.15	5.8	1.4
Tb	0.73	0.53	0.48	0.14	0.52	0.21	0.15	0.21	0.050	0.35	0.51
Yb	1.3	1.8	1.7	0.18	0.96	0.78	0.19	0.44	0.16	0.46	1.1
Lu	0.21	0.30	0.26	0.030	0.14	0.14	0.030	0.070	0.030	0.069	0.14
Eu/Eu*	0.91	1.2	1.3	2.6	0.99	4.3	2.6	1.8	7.5	0.29	0.81
Σ REE	110	98	70	41	55	54	49	71	36	195	105
K/Rb	958	386	729	1852	1531	881	630	1266	1992	1302	2012
K/Ba	17	29	36	17	21	21	14	22	21	18	18
Rb/Sr	0.018	0.054	0.034	0.009	0.010	0.024	0.033	0.017	0.010	0.009	0.005
Ba/Sr	1.0	0.71	0.68	0.91	0.75	1.0	1.5	0.98	0.94	0.69	0.59

FILE: I2CHIP.DAT

MEDIUM TO HIGH-P CHARNOCKITE

MAJOR AND TRACE ELEMENTS

	536-3	537-1	540-1	540-3	541-3	542-1	544-1	552-1a	552-1c	552-1e	552-1h
SiO2	63.50	73.05	61.72	62.82	-	61.64	64.27	58.97	70.62	69.81	69.87
TiO2	0.64	0.25	0.71	0.73	-	0.72	0.49	0.54	0.38	0.40	0.41
Al2O3	16.99	15.08	17.17	16.45	-	16.79	16.59	16.83	15.63	15.55	15.54
Fe2O3T	5.36	1.97	5.69	5.78	-	6.16	5.43	6.49	3.48	3.76	3.33
MnO	0.06	0.01	0.05	0.05	-	0.07	0.06	0.10	0.05	0.05	0.04
MgO	2.55	0.56	2.83	2.91	-	2.97	2.37	4.38	1.30	1.40	1.57
CaO	5.27	3.33	5.63	5.85	-	5.40	5.50	8.50	4.14	4.41	4.10
Na2O	4.77	4.80	4.78	4.53	-	4.49	4.43	3.99	4.00	4.12	4.09
K2O	0.87	0.73	0.89	0.88	-	1.32	1.01	0.62	1.02	1.01	1.12
P2O5	0.26	0.06	0.32	0.29	-	0.33	0.22	0.12	0.12	0.13	0.13
LOI	0.09	0.30	0.14	0.18	-	0.26	0.23	0.30	0.01	0.11	0.17
TOTAL	100.36	100.14	99.93	100.47	0.00	100.15	100.60	100.84	100.75	100.81	100.37
Rb	4.8	4.1	6.6	5.5	-	15	6.8	1.4	3.3	4.8	2.0
Cs	< .03	< .03	0.030	< .03	-	< .04	< .05	< .03	< .03	< .03	< .03
Sr	634	545	690	573	-	567	520	436	371	357	497
Ba	441	360	587	609	-	1243	617	182	457	382	554
Sc	11	1.1	17	18	-	13	18	19	5.2	7.7	4.0
Y	15	< 1.5	21	27	-	20	20	12	7.6	8.0	5.1
Zr	172	71	205	178	-	231	195	79	73	91	100
Hf	4.6	1.9	5.8	5.2	-	6.3	5.6	2.4	2.3	2.7	2.7
Th	0.60	0.10	2.2	1.9	-	1.4	1.2	1.1	< .10	0.060	< .10
U	0.10	0.10	0.30	0.20	-	0.20	0.10	0.10	< .10	< 0.2	< .10
Nb	5.2	1.2	5.1	5.3	-	6.1	3.6	3.8	3.3	2.3	3.3
Ta	0.20	0.10	0.20	0.10	-	0.070	0.050	0.10	0.060	0.040	0.080
Cr	44	3.3	48	52	-	74	41	142	21	28	36
Ni	28	3.0	41	46	-	46	17	112	11	17	14
Co	13	3.1	15	16	-	19	14	23	8.6	9.2	9.4
Zn	65	20	74	70	-	85	78	65	40	41	53
Pb	3.1	2.3	2.8	3.3	-	< 2.0	2.9	2.8	< 2.0	4.5	< 2.0
La	34	17	55	60	-	63	65	22	15	20	16
Ce	89	26	113	130	-	127	132	46	27	35	29
Nd	29	6.4	44	55	-	43	49	18	-	13	-
Sm	5.5	0.85	8.5	10	-	8.1	8.6	3.0	1.5	2.0	1.7
Eu	1.2	0.55	1.5	1.7	-	1.9	1.7	0.97	0.85	0.82	1.1
Eu*	1.6	0.21	2.4	2.8	-	2.2	2.4	0.93	0.48	0.60	0.47
Tb	0.59	0.060	0.89	0.98	-	0.73	0.89	0.42	0.23	0.25	0.17
Yb	1.2	0.14	1.9	2.3	-	1.3	1.5	1.6	0.91	1.0	0.50
Lu	0.15	< .03	0.26	0.31	-	0.21	0.20	0.30	0.16	0.20	0.080
Eu/Eu*	0.77	2.6	0.63	0.62	-	0.88	0.70	1.0	1.8	1.4	2.3
7 REE	112	44	182	206	-	203	211	74	45	59	48
K/Rb	1505	1478	1119	1328	-	730	1233	3676	2566	1799	4649
K/Ba	16	17	13	12	-	8.8	14	28	19	23	17
Rb/Sr	0.008	0.008	0.010	0.010	-	0.026	0.013	0.003	0.009	0.013	0.004
Ba/Sr	0.70	0.66	0.85	1.1	-	2.2	1.2	0.42	1.2	1.1	1.1

FILE: I2CHIP.DAT

MEDIUM TO HIGH-P CHARNOCKITE

MAJOR AND TRACE ELEMENTS

	553	554	555	556	557	558	559	560	561-1	56[illegible]-1	567
SiO2	69.43	69.51	69.64	69.85	68.71	65.57	69.02	71.00	70.39	66.69	59.39
TiO2	0.31	0.41	0.41	0.40	0.12	0.63	0.40	0.31	0.33	0.56	0.68
Al203	15.89	15.98	15.63	16.16	16.43	15.60	16.10	16.06	16.18	14.93	16.84
Fe203T	2.85	2.88	3.19	2.20	1.89	4.46	2.64	2.55	2.15	7.67	10.70
MnO	0.03	0.03	0.03	0.02	0.03	0.05	0.04	0.03	0.02	0.10	0.13
MgO	0.91	1.00	1.19	0.89	1.26	2.21	1.46	0.91	0.96	3.15	4.01
CaO	3.00	3.51	3.41	3.60	3.78	3.73	3.86	3.82	3.32	3.09	3.80
Na2O	5.12	5.04	5.01	5.03	5.16	5.69	4.96	4.83	5.58	3.06	2.62
K2O	1.35	1.12	1.18	1.14	1.08	1.09	1.01	0.94	1.14	1.23	1.02
P2O5	0.11	0.11	0.18	0.10	0.13	0.23	0.16	0.10	0.09	0.16	0.14
LOI	0.66	0.22	0.23	0.33	0.54	0.30	0.37	0.14	0.25	0.26	0.27
TOTAL	99.66	99.81	100.10	99.72	99.13	99.56	100.02	100.69	100.41	100.80	99.60
Rb	23	7.2	6.8	5.2	5.9	7.0	6.9	3.0	4.0	39	24
Cs	0.040	< .03	0.030	< .03	0.040	0.050	-	0.030	< .04	0.20	0.10
Sr	590	661	640	981	983	916	555	359	784	161	227
Ba	323	315	319	437	390	311	345	211	453	247	276
Sc	2.9	2.8	4.4	2.7	2.3	4.7	2.5	4.9	2.4	18	25
Y	4.3	2.7	6.1	< 1.5	2.0	4.8	6.1	1.5	< 1.5	22	30
Zr	138	161	188	134	118	147	265	143	133	129	68
Hf	3.1	3.7	4.4	3.5	2.8	3.6	7.1	3.3	3.8	2.7	1.9
Th	3.8	2.5	15	0.20	0.40	0.60	0.70	0.10	0.20	2.0	1.0
U	0.13	0.090	0.26	0.12	0.070	0.17	0.40	0.20	0.20	0.39	0.46
Nb	3.0	3.3	4.2	3.0	2.1	6.1	3.4	1.9	< 1.0	8.3	7.9
Ta	0.050	0.060	0.060	0.050	0.030	0.10	< .03	0.060	0.040	0.40	0.30
Cr	9.0	10	19	8.2	47	93	35	5.0	6.3	252	268
Ni	3.0	17	14	15	32	49	15	6.0	5.0	43	136
Co	5.9	6.3	7.3	5.7	7.0	17	8.9	5.3	5.3	20	36
Zn	47	41	46	27	31	51	30	36	38	71	93
Pb	< 2.0	< 2.0	< 2.0	< 2.0	< 2.0	< 2.0	< 2.0	7.4	6.8	< 2.0	< 2.0
La	32	31	96	26	26	33	20	14	13	22	22
Ce	55	53	174	41	43	62	36	24	24	40	39
Nd	15	15	42	9.6	12	20	11	-	10	17	18
Sm	3.0	1.9	6.5	1.4	1.9	3.3	2.0	1.2	1.4	3.9	4.1
Eu	0.97	0.92	1.5	1.5	1.3	1.5	0.95	0.65	1.0	0.92	1.1
Eu*	0.74	0.46	1.5	0.32	0.43	0.82	0.58	0.34	0.34	1.3	1.4
Tb	0.21	0.13	0.35	0.080	0.10	0.24	0.23	0.13	0.090	0.62	0.73
Yb	0.32	0.19	0.56	0.19	0.24	0.49	0.53	0.18	0.10	1.9	2.8
Lu	0.040	0.020	0.090	0.020	0.044	0.090	0.084	< .03	< .02	0.33	0.40
Eu/Eu*	1.3	2.0	1.0	4.7	3.1	1.8	1.6	1.9	3.0	0.73	0.80
Σ REE	91	87	279	69	72	100	59	40	39	70	70
K/Rb	487	1291	1440	1820	1520	1293	1215	2601	2366	262	353
K/Ba	35	30	31	22	23	29	24	37	21	41	31
Rb/Sr	0.039	0.011	0.011	0.005	0.006	0.008	0.012	0.008	0.005	0.24	0.11
Ba/Sr	0.55	0.48	0.50	0.45	0.40	0.34	0.62	0.59	0.58	1.5	1.2

FILE: I2CHIP.DAT

MEDIUM TO HIGH-P CHARNOCKITE

MAJOR AND TRACE ELEMENTS

	568	569	N	MEAN	SD %
SiO2	65.42	70.24	45	65.55	7.7
TiO2	0.56	0.49	45	0.53	38.5
Al2O3	14.20	12.03	45	15.91	7.4
Fe2O3T	8.77	7.64	45	5.33	51.9
MnO	0.12	0.10	45	0.07	54.8
MgO	3.02	3.14	45	2.37	51.5
CaO	4.30	2.67	45	4.48	28.6
Na2O	2.13	1.97	45	4.22	21.4
K2O	0.61	0.97	45	1.21	34.8
P2O5	0.11	0.09	45	0.17	49.7
LOI	0.24	0.23	45	0.32	59.5
TOTAL	99.48	99.57			
Rb	18	18	45	13	106.4
Cs	0.19	0.20	26	0.11	93.8
Sr	173	227	45	586	41.7
Ba	158	295	45	499	53.8
Sc	18	15	44	11	69.0
Y	20	23	42	13	67.9
Zr	103	127	45	134	34.7
Hf	2.8	3.0	45	3.5	36.8
Th	5.2	2.3	40	1.4	181.7
U	1.3	0.43	40	0.22	95.3
Nb	9.0	6.8	44	5.3	46.7
Ta	0.40	0.30	43	0.17	99.6
Cr	200	207	45	79	98.1
Ni	69	111	45	41	99.4
Co	23	21	45	16	60.4
Zn	71	61	37	58	44.9
Pb	< 2.0	< 2.0	13	5.3	65.4
La	24	18	45	31	55.3
Ce	43	32	43	60	60.4
Nd	16	11	30	22	63.4
Sm	3.6	2.9	45	5.1	146.2
Eu	0.96	0.93	45	1.3	32.7
Eu*	1.2	1.0	45	1.3	81.9
Tb	0.57	0.62	45	0.47	69.4
Yb	1.7	1.9	45	1.1	72.2
Lu	0.30	0.28	42	0.18	66.5
Eu/Eu*	0.82	0.90	45	1.6	81.9
Σ REE	74	57	43	100	58.3
K/Rb	281	447	45	1374	68.4
K/Ba	32	27	45	24	63.0
Rb/Sr	0.10	0.079	45	0.036	159.1
Ba/Sr	0.91	1.3	45	0.93	55.9

FILE: I2CHIP.DAT

MEDIUM TO HIGH-P CHARNOCKITE

CIPW NORMS

	474	475	477	478	480	483	485-2	486-1	524	525	526-1
Fe203/F	0.44	0.44	0.44	0.44	0.44	0.44	0.44	0.44	0.44	0.44	0.44
Qtz	28.84	3.47	19.66	43.05	26.07	12.80	12.83	5.41	17.01	10.87	29.16
Corund	0.18	0.00	6.39	1.27	1.23	0.00	0.00	0.00	0.00	0.00	0.00
Zircon	0.02	0.04	0.02	0.02	0.02	0.03	0.03	0.04	0.03	0.03	0.03
Or	13.47	7.86	8.92	2.90	13.59	9.75	8.98	4.85	7.80	7.80	7.09
Ab	36.51	38.37	15.84	19.77	30.53	32.78	33.84	36.40	44.07	40.16	39.61
An	14.49	22.84	17.06	16.55	13.83	24.20	20.59	21.63	17.97	21.05	17.38
Diop	0.00	8.66	0.00	0.00	0.00	3.34	6.79	11.23	2.84	3.79	0.25
Hyp	3.82	12.19	23.98	11.81	10.87	12.06	11.50	13.83	7.19	10.71	4.08
Olivine	0.00	0.00	0.00	0.00	0.00	0.00	0.00	0.00	0.00	0.00	0.00
Mgt	0.95	3.47	5.85	2.86	2.10	2.84	2.75	3.49	1.81	2.91	1.13
Chrmite	0.00	0.04	0.09	0.05	0.03	0.02	0.05	0.06	0.03	0.01	0.00
Ilmen	0.57	1.90	1.42	0.72	1.03	1.48	1.37	1.67	1.08	1.71	0.55
Apat	0.23	0.65	0.30	0.19	0.35	0.79	0.72	0.65	0.56	0.72	0.23

BARTH MESONORM

Qtz	29.10	6.29	24.27	43.31	30.27	16.72	15.81	6.00	18.71	13.71	29.28
Corund	0.66	0.00	8.32	2.00	2.15	0.00	0.00	0.00	0.00	0.00	0.31
Or	10.11	0.00	0.00	0.00	3.84	0.00	0.41	0.00	1.15	0.00	3.38
Ab	39.57	41.35	17.53	21.99	33.06	35.68	36.77	39.39	47.04	43.31	42.82
An	13.36	22.58	14.77	15.82	11.86	23.80	20.40	21.41	17.43	20.73	16.53
Biot	5.66	12.59	14.74	4.83	15.84	15.61	13.80	7.78	10.51	12.49	6.04
Actin	0.00	10.69	0.00	0.00	0.00	1.95	8.65	16.18	2.19	2.12	0.00
Edenite	0.00	0.00	0.00	0.00	0.00	0.00	0.00	0.00	0.00	0.00	0.00
Hyp	0.00	1.33	14.10	8.91	0.00	1.83	0.00	4.28	0.00	2.93	0.00
Mgt	0.69	2.50	4.36	2.15	1.53	2.05	2.00	2.53	1.29	2.10	0.82
Sphene	0.64	2.09	1.62	0.83	1.14	1.63	1.51	1.85	1.18	1.83	0.61
Apat	0.21	0.59	0.28	0.17	0.32	0.71	0.65	0.59	0.50	0.65	0.21

FILE: 12CHIP.DAT

MEDIUM TO HIGH-P CHARNOCKITE

CIPW NORMS

	527	528	529	530-1	531-1	531-2	532	533	534-1	535-?	536-1
Fe2O3/F	0.44	0.44	0.44	0.44	0.44	0.44	0.44	0.44	0.44	0.44	0.44
Qtz	9.59	19.90	20.66	24.42	10.49	7.85	23.23	24.52	40.54	26.71	19.60
Corund	0.00	1.22	0.36	0.00	0.00	1.12	0.02	0.00	0.31	1.81	0.00
Zircon	0.03	0.03	0.02	0.03	0.02	0.02	0.01	0.02	0.03	0.04	0.04
Or	8.86	7.98	7.27	6.86	6.32	8.16	15.25	10.81	5.67	7.51	4.73
Ab	37.46	33.87	32.86	38.47	36.13	32.69	34.62	35.87	27.97	32.61	38.73
An	19.60	19.13	21.28	20.34	21.33	23.28	18.51	18.35	20.77	21.23	21.19
DioP	6.65	0.00	0.00	0.28	6.05	0.00	0.00	0.30	0.00	0.00	1.02
Hyp	12.55	13.20	12.37	6.41	13.34	19.20	6.11	6.18	3.68	6.29	10.08
Olivine	0.00	0.00	0.00	0.00	0.00	0.00	0.00	0.00	0.00	0.00	0.00
Mgt	2.89	2.78	2.80	1.35	3.01	4.39	1.08	1.45	0.64	1.59	2.33
Chrmite	0.04	0.06	0.06	0.01	0.12	0.10	0.03	0.01	0.01	0.01	0.02
Ilmen	1.03	1.27	1.18	0.84	1.16	1.77	0.44	0.95	0.36	1.11	1.25
Apat	0.65	0.37	0.35	0.30	0.42	0.09	0.30	0.35	0.02	0.41	0.60

BARTH MESONORM

Qtz	12.95	23.20	23.73	26.18	12.54	12.22	24.63	26.35	40.04	28.39	20.67
Corund	0.00	2.29	1.29	0.50	0.00	2.59	0.42	0.59	0.63	2.85	0.44
Or	0.11	0.00	0.00	0.84	0.00	0.00	9.84	5.03	2.35	1.63	0.00
Ab	40.42	36.61	35.76	41.60	39.35	35.77	37.67	39.20	30.43	35.75	41.82
An	19.37	19.68	19.24	18.99	21.41	20.14	17.17	16.88	20.21	18.99	19.99
Biot	14.03	12.85	11.81	9.70	10.26	13.29	8.74	9.51	5.45	9.56	7.61
Actin	9.31	0.00	0.00	0.00	8.00	0.00	0.00	0.00	0.00	0.00	0.00
Edenite	0.00	0.00	0.00	0.00	0.00	0.00	0.00	0.00	0.00	0.00	0.00
Hyp	0.00	4.60	4.48	0.00	4.56	10.71	0.00	0.00	0.00	0.00	5.86
Mgt	2.08	2.02	2.05	0.98	2.20	3.22	0.78	1.06	0.47	1.15	1.68
Sphene	1.13	1.41	1.32	0.93	1.29	1.98	0.48	1.06	0.40	1.27	1.39
Apat	0.59	0.34	0.32	0.27	0.38	0.09	0.27	0.32	0.02	0.40	0.55

FILE: I2CHIP.DAT

MEDIUM TO HIGH-P CHARNOCKITE

CIPW NORMS

	536-3	537-1	540-1	540-3	541-3	542-1	544-1	552-1a	552-1c	552-1e	552-1n
Fe2O3/F	0.44	0.44	0.44	0.44	-	0.44	0.44	0.44	0.44	0.44	0.44
Qtz	16.82	34.03	14.04	16.34	-	13.98	18.80	9.94	31.81	29.47	30.00
Corund	0.00	0.47	0.00	0.00	-	0.00	0.00	0.00	0.68	0.00	0.43
Zircon	0.04	0.01	0.04	0.04	-	0.05	0.04	0.02	0.02	0.02	0.02
Or	5.14	4.31	5.26	5.20	-	7.80	5.97	3.66	6.03	6.15	6.62
Ab	39.89	40.21	39.94	37.91	-	37.57	37.10	33.44	33.57	34.60	34.24
An	22.63	16.37	23.04	22.18	-	21.98	22.60	26.35	19.96	21.00	19.76
Diop	1.72	0.00	2.56	4.28	-	2.51	2.89	12.31	0.00	0.19	0.00
Hyp	9.65	2.87	10.12	9.54	-	10.95	8.94	10.38	6.01	6.49	6.46
Olivine	0.00	0.00	0.00	0.00	-	0.00	0.00	0.00	0.00	0.00	0.00
Mgt	2.20	0.81	2.34	2.37	-	2.53	2.23	2.66	1.43	1.51	1.37
Chrmite	0.02	0.00	0.02	0.02	-	0.03	0.02	0.06	0.01	0.01	0.02
Ilmen	1.22	0.48	1.35	1.39	-	1.37	0.93	1.03	0.72	0.76	0.78
Apat	0.60	0.14	0.74	0.67	-	0.77	0.51	0.28	0.28	0.30	0.30

BARTH MESONORM

Qtz	18.03	33.19	15.43	17.33	-	17.02	20.37	9.36	32.74	30.73	31.44
Corund	0.06	0.90	0.00	0.00	-	0.00	0.00	0.00	1.27	0.55	1.03
Or	0.00	1.71	0.00	0.00	-	0.00	0.00	0.28	0.65	0.31	0.73
Ab	42.77	43.38	43.01	40.70	-	40.48	39.83	35.67	36.09	37.12	36.98
An	22.19	15.36	22.82	21.97	-	21.85	22.44	25.99	18.52	19.71	18.19
Biot	8.21	4.21	8.43	8.32	-	12.53	9.56	5.38	8.65	9.33	9.50
Actin	0.00	0.00	0.90	3.95	-	0.55	2.62	20.02	0.00	0.00	0.00
Edenite	0.00	0.00	0.00	0.00	-	0.00	0.00	0.00	0.00	0.00	0.00
Hyp	5.26	0.00	5.56	3.88	-	3.54	2.09	0.00	0.00	0.00	0.00
Mgt	1.59	0.59	1.69	1.72	-	1.83	1.61	1.92	1.03	1.11	0.99
Sphene	1.34	0.53	1.49	1.53	-	1.51	1.03	1.12	0.80	0.81	0.86
Apat	0.54	0.13	0.67	0.61	-	0.69	0.46	0.25	0.25	0.27	0.27

FILE: I2CHIP.DAT

MEDIUM TO HIGH-P CHARNOCKITE

CIPW NORMS

	553	554	555	556	557	558	559	560	561-1	56[illegible]-1	567
Fe2O3/F	0.44	0.44	0.44	0.44	0.44	0.44	0.44	0.44	0.44	0.41	0.44
Qtz	26.17	26.45	26.51	27.12	24.53	17.17	25.60	29.26	24.86	30.59	22.38
Corund	0.81	0.36	0.34	0.34	0.21	0.00	0.20	0.39	0.00	3.49	4.84
Zircon	0.03	0.03	0.04	0.03	0.02	0.03	0.05	0.03	0.03	0.03	0.01
Or	7.98	6.62	6.97	6.74	6.38	6.44	5.97	5.56	6.74	7.27	6.03
Ab	42.89	42.16	41.92	41.84	42.94	47.47	41.56	40.61	46.64	25.77	22.00
An	14.40	16.96	16.00	17.60	18.29	14.17	18.35	18.45	16.04	13.91	18.05
Diop	0.00	0.00	0.00	0.00	0.00	2.59	0.00	0.00	0.15	0.00	0.00
Hyp	4.52	4.61	5.37	3.68	4.78	7.51	5.55	4.23	3.85	14.33	19.21
Olivine	0.00	0.00	0.00	0.00	0.00	0.00	0.00	0.00	0.00	0.00	0.00
Mgt	1.17	1.18	1.31	0.90	0.78	1.83	1.08	1.05	0.88	3.15	4.39
Chrmite	0.00	0.00	0.01	0.00	0.02	0.04	0.02	0.00	0.00	0.11	0.12
Ilmen	0.59	0.78	0.78	0.76	0.23	1.20	0.76	0.59	0.63	1.06	1.29
Apat	0.26	0.26	0.42	0.23	0.30	0.53	0.37	0.23	0.21	0.37	0.32

BARTH MESONORM

Qtz	26.75	27.01	27.41	27.10	25.15	18.97	26.73	29.24	24.80	33.20	25.07
Corund	1.34	0.97	0.95	0.94	0.40	0.00	0.79	0.86	0.42	4.67	6.45
Or	3.98	2.36	2.07	3.21	2.20	0.00	0.79	1.71	3.04	0.00	0.00
Ab	46.44	45.50	45.14	45.43	46.74	51.20	44.66	43.28	49.76	27.96	24.32
An	13.22	15.35	14.37	15.91	17.64	13.84	16.76	17.18	14.63	12.10	16.10
Biot	6.53	6.86	7.88	5.70	6.78	10.33	8.31	6.13	5.84	11.83	9.97
Actin	0.00	0.00	0.00	0.00	0.00	1.51	0.00	0.00	0.00	0.00	0.00
Edenite	0.00	0.00	0.00	0.00	0.00	0.00	0.00	0.00	0.00	0.00	0.00
Hyp	0.00	0.00	0.00	0.00	0.00	1.03	0.00	0.00	0.00	6.40	13.05
Mgt	0.85	0.86	0.95	0.66	0.56	1.32	0.78	0.75	0.63	2.31	3.27
Sphene	0.65	0.86	0.86	0.84	0.25	1.32	0.84	0.65	0.68	1.19	1.47
Apat	0.23	0.23	0.38	0.21	0.27	0.48	0.34	0.21	0.19	0.31	0.30

FILE: I2CHIP.DAT

MEDIUM TO HIGH-P CHARNOCKITE

CIPW NORMS

	568	569	N	MEAN	SD %
Fe2O3/F	0.44	0.44	45	0.44	0.1
Qtz	33.89	41.98	45	22.4	41.9
Corund	2.48	3.09	24	1.3	121.9
Zircon	0.02	0.03	45	0.028	34.3
Or	3.61	5.73	45	7.1	34.8
Ab	17.90	16.50	45	35.3	21.3
An	20.69	12.78	45	19.2	16.2
Diop	0.00	0.00	21	3.8	93.4
Hyp	15.11	14.41	45	9.3	50.8
Olivine	0.00	0.00	0	0.0	0.0
Mgt	3.60	3.14	45	2.2	51.9
Chrmite	0.09	0.09	45	0.035	97.3
Ilmen	1.06	0.93	45	1.0	38.4
Apat	0.26	0.21	45	0.40	49.7

BARTH MESONORM

Qtz	34.96	44.15	45	24.0	36.9
Corund	3.64	4.25	31	1.8	109.0
Or	0.00	0.00	24	2.6	102.4
Ab	19.97	18.49	45	38.2	20.7
An	19.49	11.45	45	18.1	18.9
Biot	6.02	9.58	45	9.3	32.8
Actin	0.00	0.00	14	6.3	96.0
Edenite	0.00	0.00	0	0.0	0.0
Hyp	11.74	8.45	21	5.9	64.6
Mgt	2.71	2.36	45	1.6	52.9
Sphene	1.22	1.07	45	1.1	38.4
Apat	0.24	0.20	45	0.36	49.3

FILE: I2RETG.DAT

RETROGRESSED GNEISS

MAJOR AND TRACE ELEMENTS

	536-2	537-2	540-2	542-2	544-2	552-2a	561-2	N	MEAN	SD %
SiO2	60.58	69.49	64.31	64.71	63.77	70.44	70.97	7	66.32	6.0
TiO2	0.79	0.38	0.60	0.54	0.61	0.32	0.38	7	0.52	32.3
Al2O3	16.80	16.24	16.26	16.47	16.52	15.59	16.00	7	16.27	2.4
Fe2O3T	6.19	2.81	4.84	4.50	5.04	3.05	2.06	7	4.07	36.0
MnO	0.06	0.02	0.05	0.05	0.06	0.04	0.01	7	0.04	47.1
MgO	3.12	0.88	2.32	2.08	2.41	0.87	0.88	7	1.79	51.0
CaO	6.25	3.55	5.12	5.01	5.13	4.02	3.13	7	4.60	23.5
Na2O	4.41	5.53	4.54	4.75	4.57	4.43	4.87	7	4.73	8.3
K2O	0.91	0.75	0.81	1.00	1.03	1.04	1.54	7	1.01	25.5
P2O5	0.31	0.12	0.27	0.21	0.24	0.12	0.08	7	0.19	45.2
LOI	0.67	0.36	0.88	0.77	1.02	0.84	0.27	7	0.69	40.3
TOTAL	100.09	100.13	100.00	100.09	100.40	100.76	100.19			
Rb	7.4	8.3	5.7	8.8	11	4.2	28	7	10	76.6
Cs	< .03	< .03	< .03	0.080	0.19	< .03	0.13	3	0.13	41.3
Sr	588	579	677	560	534	348	738	7	575	21.4
Ba	405	363	569	855	653	435	499	7	540	31.6
Sc	26	2.1	12	8.8	16	4.6	2.2	7	10	84.6
Y	35	1.9	16	13	12	3.8	< 1.5	6	14	86.9
Zr	169	127	179	147	139	121	137	7	148	17.4
Hf	6.0	3.7	6.1	5.0	5.8	4.1	3.6	7	4.9	22.4
Th	1.0	9.5	3.5	0.70	2.2	0.10	2.8	7	2.8	112.4
U	0.10	0.10	0.10	0.10	0.20	0.10	< 0.2	6	0.12	35.0
Nb	7.3	2.0	3.4	5.2	4.5	1.6	1.8	7	3.7	57.4
Ta	0.10	0.10	0.10	0.070	0.080	< .03	0.050	6	0.083	24.8
Cr	62	7.8	42	55	57	11	6.9	7	35	72.6
Ni	39	6.0	39	30	39	6.0	7.0	7	24	69.9
Co	18	5.9	13	13	17	5.5	5.5	7	11	47.6
Zn	87	32	63	65	95	38	39	7	60	41.5
Pb	4.9	4.8	4.0	< 2.0	6.2	5.3	8.1	6	5.6	26.0
La	50	36	57	54	62	14	12	7	41	50.6
Ce	121	58	111	98	115	24	25	7	79	53.9
Nd	57	18	40	35	45	-	12	6	35	48.9
Sm	12	2.2	7.0	5.1	7.9	1.6	1.4	7	5.3	74.1
Eu	1.9	0.62	1.3	1.7	1.8	0.68	1.1	7	1.3	40.4
Eu*	3.4	0.54	2.0	1.4	2.2	0.47	0.35	7	1.5	76.6
Tb	1.3	0.15	0.80	0.49	0.79	0.19	0.10	7	0.55	81.2
Yb	2.9	0.30	1.3	0.94	1.4	0.62	0.90	7	1.2	70.4
Lu	0.37	0.040	0.21	0.14	0.18	0.090	< .02	6	0.17	66.9
Eu/Eu*	0.56	1.2	0.64	1.2	0.82	1.4	3.2	7	1.3	69.2
7 REE	191	97	179	160	189	41	40	7	128	53.0
K/Rb	1021	750	1180	943	777	2055	457	7	1026	49.6
K/Ba	19	17	12	9.7	13	20	26	7	17	33.0
Rb/Sr	0.013	0.014	0.008	0.016	0.021	0.012	0.038	7	0.017	56.4
Ba/Sr	0.69	0.63	0.84	1.5	1.2	1.3	0.68	7	0.98	36.3

FILE: I2RETG.DAT

RETROGRESSED GNEISS

CIPW NORMS

	536-2	537-2	540-2	542-2	544-2	552-2a	561-2	N	MEAN	SD %
Fe2O3/F	0.00	0.40	0.40	0.40	0.40	0.40	0.40	6	0.40	0.0
Qtz	0.00	13.50	25.10	20.10	19.20	18.20	30.10	6	21.0	27.5
Corund	0.00	0.00	0.20	0.00	0.00	0.00	0.10	2	0.15	47.1
Zircon	0.00	0.00	0.00	0.00	0.00	0.00	0.00	0	0.0	0.0
Or	0.00	5.40	4.40	4.80	5.90	6.10	6.10	6	5.4	13.2
Ab	0.00	36.90	46.40	37.90	39.80	38.30	37.20	6	39.4	9.1
An	0.00	23.60	17.10	21.90	20.90	21.70	19.40	6	20.8	10.9
Diop	0.00	4.60	0.00	1.70	2.40	2.00	0.00	4	2.7	49.2
Hyp	0.00	10.20	4.30	8.60	7.50	8.90	4.60	6	7.4	32.8
Olivine	0.00	0.00	0.00	0.00	0.00	0.00	0.00	0	0.0	0.0
Mgt	0.00	2.50	1.20	2.00	1.80	2.10	1.30	6	1.8	27.3
Chrmite	0.00	0.00	0.00	0.00	0.00	0.00	0.00	0	0.0	0.0
Ilmen	0.00	1.50	0.70	1.10	1.00	1.20	0.60	6	1.0	32.6
Apat	0.00	0.70	0.30	0.60	0.50	0.60	0.30	6	0.50	33.5

BARTH MESONORM

Qtz	0.00	14.90	25.50	21.10	20.90	20.10	30.50	6	22.2	23.9
Corund	0.00	0.00	0.70	0.00	0.00	0.00	0.60	2	0.65	10.9
Or	0.00	0.00	0.50	0.00	0.00	0.00	2.10	2	1.3	87.0
Ab	0.00	39.90	49.70	41.30	43.00	41.40	40.20	6	42.6	8.6
An	0.00	23.50	15.50	21.80	20.80	21.70	18.20	6	20.3	14.3
Biot	0.00	8.70	6.30	7.80	9.50	9.80	6.60	6	8.1	18.1
Actin	0.00	4.40	0.00	0.00	1.40	0.40	0.00	3	2.1	100.7
Edenite	0.00	0.00	0.00	0.00	0.00	0.00	0.00	0	0.0	0.0
Hyp	0.00	4.40	0.00	4.70	1.40	3.30	0.00	4	3.4	43.3
Mgt	0.00	1.80	0.80	1.50	1.30	1.50	0.90	6	1.3	29.6
Sphene	0.00	1.70	0.80	1.30	1.10	1.30	0.70	6	1.2	32.0
Apat	0.00	0.60	0.30	0.60	0.40	0.50	0.30	6	0.45	30.6

FILE: I2MAF.DAT

MAFIC ROCKS

MAJOR AND TRACE ELEMENTS

	KDA3	12-2	42	44-2	49-2	77-2	89-3	120-3	435a	481	485-1
SiO2	50.45	42.07	48.43	50.53	49.02	48.79	49.33	51.57	53.56	50.09	48.48
TiO2	1.36	1.86	0.87	0.84	0.81	1.07	0.81	0.46	0.87	0.89	0.78
Al2O3	14.21	11.89	15.16	13.69	14.22	14.58	13.92	14.36	13.32	17.63	15.28
Fe2O3T	14.39	19.34	12.91	12.11	12.70	13.49	13.30	10.43	7.59	10.44	12.41
MnO	0.22	0.23	0.20	0.18	0.18	0.20	0.25	0.18	0.13	0.15	0.19
MgO	6.37	10.45	8.04	7.32	8.53	6.97	6.91	7.74	9.27	8.09	8.54
CaO	10.22	8.00	11.53	11.35	10.66	10.81	10.50	11.35	10.63	9.04	11.44
Na2O	3.57	1.59	2.75	3.41	3.14	3.20	3.83	3.48	3.28	2.69	2.74
K2O	0.38	3.04	0.45	0.93	0.65	0.42	0.91	0.69	0.51	0.51	0.31
P2O5	0.11	0.04	0.07	0.07	0.06	0.09	0.07	0.07	0.35	0.11	0.06
LOI	0.79	0.79	0.14	0.50	0.32	0.34	0.22	0.46	0.36	0.19	0.21
TOTAL	102.07	99.30	100.55	100.93	100.29	99.96	100.05	100.79	99.87	99.85	100.44
Rb	3.0	144	1.0	1.6	3.3	8.0	6.0	5.6	1.0	6.0	3.0
Cs	< 0.3	1.7	0.10	0.60	0.20	< 0.5	0.10	0.50	-	0.30	0.30
Sr	113	135	118	229	103	111	204	91	1242	317	158
Ba	107	284	<120	182	77	< 50	93	60	-	117	< 80
Sc	45	58	40	36	42	44	46	48	-	27	37
Y	33	31	21	35	20	25	33	21	19	19	21
Zr	92	57	50	61	54	68	53	60	115	85	47
Hf	2.8	1.7	1.0	1.4	2.8	1.8	1.4	0.90	-	1.5	1.6
Th	0.80	1.5	0.40	0.30	0.30	0.80	0.30	0.70	5.0	0.30	0.10
U	0.10	0.10	0.20	< 0.5	0.10	< 0.5	0.10	< 0.3	< 2.0	< 0.2	< 0.2
Nb	11	12	7.5	9.5	6.0	7.5	9.3	7.5	9.0	11	8.0
Ta	0.74	-	-	-	-	1.1	0.40	-	-	0.50	0.60
Cr	43	27	331	240	281	85	202	373	-	198	244
Ni	52	< 50	144	280	145	52	155	42	-	146	145
Co	48	-	-	-	-	48	51	-	-	44	47
Zn	159	-	-	-	-	-	-	-	-	-	-
Pb	< 2.0	< 2.0	< 2.0	< 2.0	2.4	3.8	7.3	< 2.0	< 2.0	7.0	< 2.0
La	4.9	18	3.9	33	6.6	7.3	20	9.7	-	14	6.5
Ce	12	46	10	76	16	19	47	23	-	-	-
Nd	-	-	-	-	-	-	-	-	-	-	-
Sm	3.2	8.1	2.0	7.1	2.1	2.6	5.3	1.8	-	4.4	2.8
Eu	1.4	1.5	0.72	1.2	0.78	1.7	1.9	0.93	-	0.95	1.4
Eu*	1.1	2.3	0.67	2.2	0.76	0.95	1.8	0.60	-	-	1.0
Tb	0.65	0.92	0.36	0.97	0.47	0.59	0.96	0.31	-	0.0	0.65
Yb	2.4	1.8	0.95	2.3	1.6	2.3	2.9	1.1	-	2.8	2.6
Lu	0.32	0.24	0.17	0.32	0.22	0.35	0.47	0.21	-	0.42	0.40
Eu/Eu*	1.2	0.64	1.1	0.55	1.0	1.8	1.1	1.6	-	0.0	1.4
Σ REE	25	77	18	122	28	33	78	37	-	-	-
K/Rb	1051	175	3735	4825	1635	436	1259	1023	4234	747	858
K/Ba	29	89	-	42	70	-	81	95	-	38	-
Rb/Sr	0.027	1.1	0.008	0.007	0.032	0.072	0.029	0.062	0.0	0.019	0.019
Ba/Sr	0.95	2.1	-	0.79	0.75	-	0.46	0.66	-	0.37	-

FILE: I2MAF.DAT

MAFIC ROCKS

MAJOR AND TRACE ELEMENTS

	487-1	488-2	535-1	562-2	N	MEAN	SD %
SiO2	49.92	49.06	51.57	48.95	15	49.45	5.0
TiO2	0.88	0.92	1.09	0.83	15	0.96	32.9
Al2O3	10.70	14.91	18.06	14.54	15	14.43	12.8
Fe2O3T	13.30	12.55	11.87	12.53	15	12.62	19.6
MnO	0.20	0.18	0.19	0.20	15	0.19	15.3
MgO	11.25	8.31	5.24	8.71	15	8.11	18.7
CaO	11.58	9.74	8.62	12.25	15	10.52	11.4
Na2O	1.80	3.08	2.49	1.95	15	2.87	23.4
K2O	0.55	1.21	0.49	0.12	15	0.75	92.4
P2O5	0.17	0.06	0.32	0.06	15	0.12	82.2
LOI	0.09	0.29	0.58	0.26	15	0.37	58.6
TOTAL	100.44	100.31	100.52	100.40			
Rb	4.0	2.0	5.0	1.0	15	13	280.0
Cs	0.30	0.10	< .03	-	10	0.42	114.4
Sr	420	227	934	106	15	301	112.3
Ba	65	173	423	156	11	158	69.4
Sc	38	37	25	45	14	41	20.8
Y	22	25	37	21	15	26	25.1
Zr	113	60	116	44	15	72	35.9
Hf	2.2	1.2	3.5	1.2	14	1.8	43.0
Th	7.9	0.50	5.0	0.050	15	1.6	148.8
U	0.20	< 0.2	0.54	< 0.2	7	0.19	84.0
Nb	7.9	8.1	10	7.3	15	8.8	19.1
Ta	0.10	0.10	0.50	0.20	9	0.47	68.8
Cr	379	186	37	402	14	216	60.5
Ni	456	104	36	122	13	145	79.1
Co	67	47	40	54	9	50	15.4
Zn	-	-	108	126	3	131	10.7
Pb	< 2.0	< 2.0	< 2.0	< 2.0	4	5.1	47.0
La	15	14	52	2.1	14	15	90.9
Ce	-	-	102	7.0	10	36	89.0
Nd	24	-	43	-	2	34	40.1
Sm	7.2	3.2	9.8	1.9	14	4.4	60.4
Eu	1.9	1.5	2.6	0.75	14	1.4	39.2
Eu*	2.1	1.1	2.4	0.68	13	1.4	50.9
Tb	0.88	0.58	0.68	0.41	13	0.65	35.2
Yb	1.7	2.5	2.7	1.8	14	2.1	29.4
Lu	0.22	0.32	0.42	0.33	14	0.32	29.3
Eu/Eu*	0.89	1.4	1.1	1.1	14	1.1	42.5
Σ REE	-	-	170	14	10	60	85.7
K/Rb	1141	5022	813	996	15	1863	89.8
K/Ba	70	58	9.6	6.4	11	54	57.2
Rb/Sr	0.010	0.009	0.005	0.009	15	0.092	295.0
Ba/Sr	0.15	0.76	0.45	1.5	11	0.81	68.0

FILE: I2MAF.DAT

MAFIC ROCKS

CIPW NORMS

	KDA3	12-2	42	44-2	49-2	77-2	89-3	120-3	435a	481	485-1
Fe2O3/F	0.44	0.44	0.44	0.43	0.44	0.44	0.44	0.44	0.44	0.44	0.44
Qtz	0.00	0.00	0.00	0.00	0.00	0.00	0.00	0.00	1.16	0.00	0.00
Corund	0.00	0.00	0.00	0.00	0.00	0.00	0.00	0.00	0.00	0.00	0.00
Zircon	0.02	0.01	0.01	0.01	0.01	0.01	0.01	0.01	0.02	0.02	0.01
Or	2.25	17.96	2.66	5.50	3.84	2.48	5.38	4.08	3.01	3.19	1.83
Ab	30.13	3.19	23.18	26.95	26.43	27.00	26.01	29.38	26.84	22.41	23.07
An	21.67	16.38	2.74	19.39	22.83	24.22	18.18	21.56	20.60	34.60	28.54
DioP	23.25	18.76	23.58	29.72	24.08	23.55	27.40	27.77	24.11	7.79	22.58
Hyp	8.52	0.00	3.12	0.00	0.00	3.77	0.00	1.41	17.63	23.61	4.55
Olivine	5.69	23.74	12.04	10.31	14.92	9.84	11.34	10.01	0.00	0.92	12.02
Mgt	5.91	7.94	5.30	4.97	5.21	5.54	5.46	4.28	3.11	4.23	5.09
Cnrmite	0.02	0.01	0.14	0.10	0.12	0.04	0.09	0.16	0.00	0.09	0.11
Ilmen	2.58	3.53	1.65	1.60	1.54	2.03	1.54	0.87	1.65	1.60	1.48
Apat	0.26	0.09	0.16	0.16	0.14	0.21	0.16	0.16	0.81	0.32	0.14

BARTH MESONORM

Qtz	0.00	0.00	0.00	0.00	0.00	0.00	0.00	0.00	0.00	0.10	0.00
Corund	0.00	0.00	0.00	0.00	0.00	0.00	0.00	0.00	0.00	0.00	0.00
Or	0.00	0.00	0.00	8.38	0.00	0.00	5.92	6.32	0.00	0.00	0.00
Ab	27.34	8.67	17.46	18.10	20.49	22.66	21.44	20.51	28.30	24.23	16.87
An	21.79	17.06	27.91	19.39	22.95	24.66	18.31	21.48	20.07	34.73	28.66
Biot	3.62	30.01	4.29	0.00	6.19	4.05	0.00	0.00	4.81	5.11	2.95
Actin	20.83	7.31	17.08	12.70	16.91	18.55	6.58	17.00	37.64	9.90	14.34
Edenite	15.86	19.99	23.75	40.50	25.29	21.23	42.68	34.11	3.43	0.00	25.22
Hyp	3.18	6.85	3.69	0.00	2.55	2.31	0.00	0.00	0.97	20.52	6.51
Mgt	4.29	5.98	3.85	3.60	3.78	4.07	3.98	3.08	2.24	3.11	3.69
Sphene	2.86	4.06	1.83	1.76	1.70	2.28	1.71	0.96	1.81	1.87	1.64
Apat	0.23	0.09	0.15	0.15	0.13	0.19	0.15	0.15	0.73	0.21	0.13

FILE: I2MAF.DAT

MAFIC ROCKS

CIPW NORMS

	487-1	488-2	535-1	562-2	N	MEAN	Sd %
Fe2O3/F	0.44	0.44	0.44	0.44	15	0.44	0.5
Qtz	0.00	0.00	6.53	0.00	2	3.8	98.8
Corund	0.00	0.00	0.00	0.00	0	0.0	0.0
Zircon	0.02	0.01	0.02	0.01	15	0.013	35.3
Or	3.25	7.15	2.90	0.71	15	4.4	92.4
Ab	14.92	25.70	20.38	16.42	15	22.8	30.4
An	19.66	23.37	37.02	30.61	15	22.8	35.8
Diop	29.66	19.99	3.31	24.16	15	22.0	33.7
Hyp	22.03	0.00	21.26	19.45	10	12.5	71.9
Olivine	2.29	15.74	0.00	0.98	13	10.0	64.5
Mgt	5.46	5.15	4.87	5.14	15	5.2	19.7
Chrmite	0.16	0.08	0.02	0.18	14	0.094	59.7
Ilmen	1.67	1.75	2.07	1.58	15	1.8	32.9
Apat	0.39	0.14	0.74	0.14	15	0.27	82.3

BARTH MESONORM

Qtz	0.00	0.00	6.87	0.00	2	3.5	133.8
Corund	0.00	0.00	0.00	0.00	0	0.0	0.0
Or	0.00	0.00	0.00	0.00	3	6.9	19.2
Ab	12.49	22.55	22.87	13.63	15	19.8	27.3
An	19.69	23.43	37.51	31.02	15	24.6	25.0
Biot	5.25	11.51	4.74	1.15	12	7.0	109.8
Actin	39.69	16.53	0.34	28.56	15	17.6	61.6
Edenite	12.27	16.88	0.00	13.25	13	22.7	49.7
Hyp	4.41	3.30	21.07	6.74	12	6.8	99.0
Mgt	3.98	3.74	3.59	3.76	15	3.8	20.8
Sphene	1.86	1.93	2.33	1.76	15	2.0	34.3
Apat	0.36	0.13	0.68	0.13	15	0.25	81.0

	GNEISS: GRANITIC			GNEISS: GRANODIORITIC			GNEISS: TONALITIC COMPOSITE			TERRANE GNEISS: TONALITIC SILICIC			TERRANE GNEISS: INTERMEDIATE		
	n	Mean	%SD	n	Mean	%SD	n	Mean	%SD	n	Mean	%SD	n	Mean	%SD
SiO2	17	72.56	5.4	9	69.32	2.0	12	69.38	5.3	9	71.22	2.7	3	63.87	1.0
TiO2	17	0.23	82.5	9	0.41	31.3	12	0.36	48.4	9	0.29	43.4	3	0.59	9.4
Al2O3	17	14.28	7.2	9	15.40	3.4	12	15.76	3.3	9	15.54	2.1	3	16.40	3.1
Fe2O3t	17	2.05	85.7	9	2.97	17.2	12	3.01	50.4	9	2.28	36.9	3	5.20	10.4
MnO	17	0.04	112	9	0.04	25.9	12	0.04	56.8	9	0.03	37.5	3	0.08	12.5
MgO	17	0.47	137	9	0.92	24.0	12	1.14	70.6	9	0.75	45.9	3	2.34	22.1
CaO	17	1.39	28.7	9	2.58	11.2	12	3.27	31.7	9	2.82	18.9	3	4.61	23.9
Na2O	17	3.81	14.5	9	4.18	6.1	12	5.30	16.4	9	5.18	11.0	3	5.64	28.7
K2O	17	4.72	21.0	9	3.48	17.8	12	1.63	26.5	9	1.79	16.4	3	1.17	43.1
P2O5	17	0.07	91.9	9	0.15	32.0	12	0.12	45.0	9	0.10	33.5	3	0.19	27.0
LOI	17	0.36	47.5	9	0.58	44.1	12	0.36	32.8	9	0.36	33.3	3	0.38	37.7
Rb	17	177	43.5	10	113	30.2	13	50	67.7	10	45	35.2	3	68	107
Cs	17	2.3	94.2	8	2.1	71.6	10	1.9	121	8	1.1	50.4	2	4.9	92.9
Sr	17	281	55.6	10	476	39.0	13	532	28.2	10	542	28.9	3	497	29.8
Ba	17	886	59.9	9	4.0	99.1	10	4.6	90.7	8	412	56.4	2	436	9.3
Th	17	34	63.3	10	20	35.3	10	5.6	72.9	8	3.9	29.6	2	12	43.3
U	17	6.5	89.4	9	2.1	67.8	10	1.8	158	8	0.84	72.2	2	5.6	103
Pb	16	26	48.4	10	13	40.6	6	<3.5	79.0	10	<2.5	87.8	3	<2.5	30.8
Sc	17	3.6	98.2	9	4.0	99.1	10	4.6	90.7	8	2.8	50.4	2	12	23.6
Y	17	36	73.5	10	12	56.8	13	11	62.1	10	8.2	50.4	3	20	30.4
Zr	17	180	49.3	10	203	51.9	13	129	38.2	10	110	19.9	3	191	36.3
Hf	17	5.6	50.8	9	5.6	42.0	10	3.6	36.3	8	3.2	32.7	2	5.2	21.8
Nb	17	15	57.5	10	9.2	67.8	13	7.6	38.4	10	6.4	25.4	3	12	25.1
Ta	15	1.3	78.3	7	~1	106	9	<9	67.3	7	1.0	73.9	2	0.87	37.4
Cr	14	7.2	87.0	8	11	65.8	10	12	118	8	6.2	63.8	2	38	43.4
Ni	10	7.6	71.9	5	11	64.3	8	11	100	6	5	45.3	2	28	
Co	16	4.9	124	9	9.0	79.0	10	8.7	80.7	8	6.5	95.4	2	18	20.2
Zn	15	61	92.9	9	52	35.6	9	49	40.0	7	40	27.5	2	79	9.9
La	17	76	65.0	9	67	45.0	10	25	79.3	8	18	26.8	2	56	59.9
Ce	17	149	66.6	9	116	43.1	10	48	80.7	8	33	37.4	2	106	57.4
Nd	14	59	58.5	7	40	48.1	7	24	69.1	5	16	46.9	2	42	50.5
Sm	17	9.2	60.5	9	5.8	45.5	10	3.5	77.1	8	2.5	66.3	2	7.3	38.8
Eu	17	1.2	56.5	9	1.4	39.4	10	1.1	41.8	8	0.92	34.1	2	1.7	30.0
Tb	17	1.2	60.9	9	0.54	49.3	10	0.38	67.0	8	0.28	57.1	2	0.77	6.4
Yb	17	3.3	90.4	9	0.99	59.9	10	0.85	86.9	8	0.56	80.2	2	2.1	3.4
Lu	17	0.49	95.8	9	0.14	66.0	10	0.13	94.9						
Eu/Eu*	17	0.75	116	9	0.96	31.3	10	1.4	48.4	8	1.5	44.3	2	0.80	1.8
ΣREE		242			192			78.8			55.1			175	
K/Rb	17	258	43.8	9	274	25.3	12	516	167	9	300	14.6	3	1161	155
K/Ba	17	56	41.5	9	36	66.0	10	46	69.8	8	51	67.0	2	26	30.1
Rb/Sr	17	0.99	89.6	10	0.30	74.0	13	0.10	60.5	10	0.093	43.2	3	0.13	87.6
Ba/Sr	17	3.6	51.6	9	2.0	13.4	10	0.93	58.6	8	0.92	65.9	2	0.98	34.2

Appendix C.9.1. Gneiss Terrane gneisses.

	TRANSITION ZONE GNEISS											
	GRANODIORITIC GNEISS						TONALITIC GNEISS					
	SILICIC			INTERMEDIATE			SILICIC			INTERMEDIATE		
	n	Mean	%SD	n	Mean	%SD	n	Mean	%SD	n	Mean	%SD
SiO2	13	69.58	3.6	4	60.60	2.1	26	69.19	3.9	7	60.61	5.9
TiO2	13	0.41	38.4	4	1.03	41.2	26	0.34	35.6	7	0.92	54.5
Al2O3	13	15.34	8.1	4	15.93	4.7	26	15.95	4.5	7	16.34	10.8
Fe2O3t	13	3.00	30.9	4	6.86	22.5	26	2.82	37.5	7	6.87	29.3
MnO	11	0.03	61.9	4	0.08	15.3	26	0.03	51.0	7	0.11	48.1
MgO	13	0.89	34.7	4	2.47	24.9	26	1.14	43.4	7	2.78	24.1
CaO	13	2.75	14.1	4	4.94	7.7	26	3.36	18.2	7	5.14	15.6
Na2O	13	4.20	7.4	4	4.22	3.8	26	5.00	9.8	7	4.59	13.5
K2O	13	3.23	16.7	4	3.06	14.9	26	1.59	23.1	7	1.64	22.5
P2O5	11	0.14	33.5	4	0.49	51.9	25	0.10	40.2	7	0.42	44.8
LOI	13	0.30	58.1	3	0.37	28.0	26	0.52	80.6	7	0.53	74.6
Rb	13	75	19.0	4	62	17.7	26	44	40.9	7	38	71.1
Cs	12	0.34	61.6	2	0.20		23	0.79	111	6	0.37	165
Sr	13	547	58.5	4	683	18.2	26	711	96.9	7	546	38.8
Ba	13	1114	53.8	4	1102	32.5	26	643	75.1	7	495	76.4
Th	13	10	76.2	4	4.8	81.3	26	3.8	125	6	7.2	57.6
U	11	~0.5	87.3	3	0.47	101	20	~0.6	81.8	5	~0.7	64.4
Pb	13	<9	81.5	4	3.5	75.6	26	<6	59.0	7	<7.5	74.7
Sc	13	3.9	77.1	4	15	44.7	26	3.4	77.2	7	14	46.1
Y	13	18	134	4	33	43.1	24	5.5	63.7	7	35	65.7
Zr	13	168	47.4	4	398	66.4	26	127	35.1	7	296	73.0
Hf	13	4.9	41.8	4	8.6	58.2	26	3.3	36.7	7	8.4	55.1
Nb	13	7.1	94.9	4	20	67.7	25	4.9	50.1	7	16	65.8
Ta	6	<1.4	111	1	<1.3		12	<1.2	159	5	~1	103
Cr	12	11	67.9	4	48	93.2	24	25	146	7	60	68.5
Ni	9	13	88.8	4	47	70.1	22	17	97.0	6	27	14.0
Co	7	11	73.5	1	15		14	13	79.4	5	19	23.6
Zn	5	51	35.2	0			6	43	81.1	1	129	
La	13	56	59.3	4	84	45.2	26	21	44.0	7	62	34.8
Ce	13	98	59.4	4	170	46.8	26	37	46.4	7	128	45.8
Nd	5	41	71.3	0			8	16	35.4	2	39	18.1
Sm	13	5.1	53.2	4	13	40.9	26	2.2	61.3	7	11	57.0
Eu	13	1.5	25.8	4	2.6	24.9	26	1.1	30.9	7	2.0	32.5
Tb	13	0.61	82.9	4	1.2	32.2	26	0.25	53.0	7	1.3	47.7
Yb	13	1.8	145	4	2.2	28.4	26	0.46	48.2	7	2.9	66.8
Lu	12	0.30	159	4	0.30	35.2	24	0.068	44.7	6	0.51	71.5
Eu/Eu*	13	1.5	66.0	4	0.78	14.5	26	2.7	92.0	7	0.71	36.9
?REE	13	163	56.8	4	274	45.2	26	61.6	44.8	7	209	42.0
K/Rb	13	370	22.1	4	423	25.9	26	582	225	7	1013	158
K/Ba	13	31	50.9	4	26	46.3	26	26	37.8	7	39	57.1
Rb/Sr	13	0.25	104	4	0.095	35.7	26	0.081	61.7	7	0.079	61.2
Ba/Sr	13	2.3	34.4	4	1.6	25.1	26	1.1	57.1	7	0.91	59.6

Appendix C.9.2. Transition Zone gneisses.

	TRANSITION ZONE GNEISSES								
	GRANITIC			GRANODIORITIC			TONALITIC		
	n	Mean	%SD	n	Mean	%SD	n	Mean	%SD
SiO2	15	72.32	4.0	17	67.47	6.7	33	67.37	6.8
TiO2	15	0.52	98.6	17	0.55	64.4	33	0.46	74.6
Al2O3	15	14.23	7.2	17	15.48	7.4	33	16.03	6.3
Fe2O3t	15	1.84	69.1	17	3.91	50.8	33	3.68	57.5
MnO	12	0.03	83.6	15	0.05	62.7	33	0.05	89.8
MgO	15	0.52	69.7	17	1.26	62.4	33	1.49	57.8
CaO	15	1.78	28.9	17	3.27	31.5	33	3.74	26.2
Na2O	15	3.76	18.3	17	4.20	6.5	33	4.91	10.9
K2O	15	4.89	14.1	17	3.19	16.1	33	1.60	22.7
P2O5	15	0.09	94.2	15	0.24	86.4	32	0.17	92.7
LOI	15	0.37	87.3	16	0.31	52.0	33	0.52	78.2
Rb	15	95	24.9	17	72	20.0	33	43	46.6
Cs	12	0.25	71.9	14	0.32	62.3	29	0.71	119
Sr	15	467	37.7	17	579	49.9	33	676	91.7
Ba	15	1455	42.2	17	1111	48.8	33	612	75.4
Th	15	14	98.3	17	9.1	82.5	32	4.4	108
U	10	<0.6	63.9	14	<0.5	86.4	25	<0.65	76.7
Pb	15	15	63.8	10	<10	52.8	22	<8.5	37.3
Sc	15	2.8	177	17	6.4	94.6	33	5.6	101
Y	15	13	164	17	21	105	31	12	135
Zr	15	167	59.8	17	222	75.2	33	163	75.6
Hf	15	5.2	70.5	17	5.8	56.3	33	4.4	70.5
Nb	14	6.6	125	17	10	98.6	32	7.4	95.0
Ta	9	<0.5	128	7	<1.4	102	17	<1.2	145
Cr	12	9.2	96.9	16	20	134	31	33	121
Ni	11	4.9	65.4	13	23	108	28	19	79.4
Co	13	8.7	112	8	12	66.4	19	14	64.6
Zn	6	68	98.0	5	51	35.2	7	55	82.3
La	15	51	63.6	17	63	56.4	33	30	70.9
Ce	15	87	62.2	17	115	59.8	33	57	84.8
Nd	8	27	72.9	5	41	71.3	10	20	54.8
Sm	15	4.3	95.4	17	6.9	67.8	33	4.0	115
Eu	15	1.6	32.7	17	1.8	35.8	33	1.3	42.4
Tb	15	0.47	129	17	0.75	71.5	33	0.47	109
Yb	15	1.2	192	17	1.9	121	33	0.97	135
Lu	14	0.20	193	16	0.30	137	30	0.16	151
Eu/Eu*	15	2.9	96.8	17	1.3	68.3	33	2.3	103
ΣREE	15	145		17	190		33	93.8	
K/Rb	15	440	18.3	17	382	23.1	33	673	202
K/Ba	15	33	45.5	17	30	49.8	33	29	48.7
Rb/Sr	15	0.27	103	17	0.21	110	33	0.080	60.7
Ba/Sr	15	3.4	40.5	17	2.1	36.0	33	1.0	57.1

Appendix C.9.3. Transition Zone gneisses.

	TRANSITION ZONE CHARNOCKITE: TONALITIC SILICIC			CHARNOCKITE INTERMEDIATE			GRANITIC CHARNOCKITE			CHARNOCKITE COMPOSITE		
	n	Mean	%SD	n	Mean	%SD	n	Mean	%SD	n	Mean	%SD
SiO2	24	70.35	4.4	19	59.47	7.3	7	68.65	7.5	52	66.13	9.6
TiO2	24	0.36	32.9	19	0.85	38.1	7	0.42	45.2	52	0.56	57.1
Al2O3	24	15.48	6.1	19	16.19	9.8	7	14.74	9.4	52	15.56	9.0
Fe2O3t	24	2.86	39.8	19	7.15	27.0	7	3.49	43.1	52	4.59	54.3
MnO	24	0.03	49.0	19	0.10	38.2	7	0.05	43.6	52	0.06	65.7
MgO	24	1.06	45.2	19	3.37	44.5	7	1.28	79.4	52	1.92	78.6
CaO	24	3.63	20.0	19	5.73	17.6	7	2.95	44.5	52	4.26	34.5
Na2O	24	4.48	12.2	19	4.51	11.0	7	3.77	9.3	52	4.38	12.7
K2O	24	1.30	38.6	19	1.77	42.7	7	3.76	11.4	52	1.91	56.3
P2O5	24	0.10	57.9	18	0.35	48.8	7	0.15	64.0	51	0.20	81.3
LOI	23	0.45	49.6	19	0.48	50.9	7	0.48	41.6	51	0.45	50.1
Rb	24	22	83.1	18	67	90.1	7	83	19.0	51	48	94.5
Cs	12	<0.28	87.4	18	1.0	165	7	0.36	47.0	37	<0.62	199
Sr	24	434	32.3	19	660	32.2	7	523	56.5	52	529	41.0
Ba	24	437	50.5	19	523	46.3	7	919	56.3	52	584	68.4
Th	24	1.4	112	19	4.8	139	6	15	58.3	51	4.5	147
U	21	0.19	41.2	16	0.69	122	6	0.58	75.0	45	0.42	134
Pb	4	<5	84.9	8	<15	102	5	12	79.2	51	<6.5	150
Sc	24	4.1	49.6	19	17	40.6	7	6.8	87.8	52	9.3	82.3
Y	23	5.9	46.7	19	22	35.3	7	13	38.2	51	14	70.4
Zr	24	126	39.8	19	199	54.7	7	177	44.7	52	170	57.1
Hf	24	3.4	38.6	19	5.3	43.1	7	4.5	44.7	52	4.6	57.8
Nb	24	5.3	39.2	19	12	47.1	7	7.4	36.1	52	8.1	57.6
Ta	11	<1.9	88.6	8	<1.2	80.9	3	0.73	43.8	24	<1.4	94.2
Cr	23	22	98.5	19	82	91.9	7	35	89.8	51	45	125
Ni	13	17	78.4	18	72	91.7	6	19	57.0	39	42	126
Co	12	19	79.0	9	26	33.6	3	8.9	109	26	19	69.8
Zn	11	46	60.2	8	115	28.3	2	37	26.8	23	70	61.3
La	24	21	40.5	19	54	74.1	7	58	38.9	52	39	79.3
Ce	24	34	44.9	19	104	76.1	7	96	38.1	52	70	87.1
Nd	10	10	57.7	10	53	79.6	3	32	48.7	25	32	103
Sm	24	1.9	54.9	19	8.8	51.1	7	5.2	35.8	52	5.0	85.0
Eu	24	1.2	32.8	19	2.0	34.5	7	1.6	19.4	52	1.6	39.9
Tb	24	0.24	53.4	19	0.99	29.4	7	0.51	37.6	52	0.57	70.8
Yb	24	0.44	50.1	19	2.0	42.4	7	1.1	50.4	52	1.1	80.5
Lu	23	0.088	97.3	18	0.29	54.2	6	0.18	57.7	49	0.22	163
Eu/Eu*	24	2.6	50.3	19	0.83	21.5	7	1.2	31.9	52	1.7	71.0
7REE	24	58	42.7	19	172	71.9		163		52	118	82.8
K/Rb	24	922	78.3	18	364	85.3	7	382	9.9	51	637	92.6
K/Ba	24	28	44.9	19	32	38.0	7	47	66.0	52	32	52.8
Rb/Sr	24	0.088	189	18	0.11	92.3	7	0.30	105	51	0.13	142
Ba/Sr	24	4.0	366	19	0.81	41.5	7	2.5	65.7	52	2.7	380

Appendix C.9.4. Transition Zone charnockite.

	TONALITIC GNEISS						GNEISSES					
	SILICIC			INTERMEDIATE			GNEISS TERRANE			TRANSITION ZONE		
	N	MEAN	SD %	N	MEAN	SD %	N	MEAN	SD %	N	MEAN	SD %
SiO2	34	69.85	3.7	11	61.90	5.4	38	70.79	5.3	65	68.54	6.8
TiO2	34	0.32	38.0	11	0.79	55.6	38	0.32	59.0	65	0.44	78.0
Al2O3	34	15.80	4.0	11	16.43	8.6	38	15.01	6.9	65	15.47	8.2
Fe2O3T	34	2.64	38.3	11	6.15	30.8	38	2.57	59.0	65	3.31	62.2
MnO	34	0.03	47.3	11	0.09	47.2	38	0.04	79.1	60	0.04	84.8
MgO	34	1.01	46.7	11	2.57	25.3	38	0.79	87.4	65	1.20	69.6
CaO	34	3.19	18.9	11	4.93	17.1	38	2.27	46.5	65	3.16	37.8
Na2O	34	5.02	9.8	11	5.00	20.8	38	4.37	20.5	65	4.46	15.9
K2O	34	1.64	22.0	11	1.51	28.2	38	3.45	44.6	65	2.78	51.4
P2O5	33	0.10	37.8	11	0.33	56.7	38	0.11	62.5	62	0.17	97.5
LOI	34	0.49	75.7	11	0.45	75.5	38	0.42	47.3	64	0.43	80.8
Rb	35	44	39.5	11	47	86.6	40	120	65.3	65	62	46.6
Cs	30	0.86	95.4	9	1.5	175.2	35	2.1	94.7	55	0.51	128.1
Sr	35	660	91.0	11	557	35.6	40	412	47.5	65	602	79.0
Ba	33	595	75.8	10	474	65.8	36	777	60.6	65	937	66.5
Sc	33	3.1	70.2	10	13	42.1	36	4.0	94.0	65	5.2	109.9
Y	33	6.3	62.2	11	28	71.8	40	22	97.9	63	15	131.3
Zr	35	122	33.3	11	253	71.4	40	169	51.0	65	179	73.6
Hf	33	3.3	36.0	10	7.3	58.0	36	5.0	49.5	65	4.9	66.4
Th	33	3.9	109.1	9	7.8	62.3	37	23	84.9	64	8.0	116.4
U	27	0.70	79.8	8	2.0	157.7	36	4.1	117.8	49	0.61	76.6
Nb	34	5.4	44.0	11	14	66.3	40	11	65.3	63	8.0	102.6
Ta	18	1.2	136.4	8	0.92	92.7	31	1.2	81.8	33	1.0	138.4
Cr	31	19	169.4	10	55	64.4	32	9.9	100.2	59	25	135.7
Ni	27	14	106.1	9	25	29.5	23	9.5	82.7	52	17	104.2
Co	21	10	90.3	8	17	27.3	35	7.0	96.6	40	12	77.2
Zn	13	42	57.3	3	95	31.1	33	55	72.9	18	58	79.9
Pb	22	6.7	49.1	6	10	41.5	32	18	72.3	47	11	61.3
La	33	20	42.7	10	57	42.8	36	60	73.4	65	43	72.0
Ce	33	36	45.5	10	116	50.6	36	113	76.0	65	79	75.9
Nd	12	16	40.4	5	36	42.0	28	46	67.7	23	27	73.3
Sm	33	2.2	63.1	10	9.3	60.1	36	6.8	72.0	65	4.8	95.7
Eu	33	1.1	32.2	10	1.9	31.4	36	1.2	48.2	65	1.5	40.0
Eu*	33	0.53	59.7	10	2.7	57.3	36	2.0	73.0	65	1.4	95.6
Tb	33	0.25	54.3	10	1.1	54.5	36	0.79	79.6	65	0.54	100.6
Yb	33	0.48	60.2	10	2.5	70.5	36	2.1	117.6	65	1.3	148.3
Lu	31	0.071	62.5	9	0.42	77.4	36	0.30	123.3	60	0.20	159.2
Eu/Eu*	33	2.5	92.9	10	0.80	38.7	36	0.97	76.2	65	2.2	103.5
K/Rb	34	516	222.0	11	986	152.0	38	343	143.0	65	543	179.2
K/Ba	33	32	66.1	10	36	53.9	36	48	55.1	65	30	47.7
Rb/Sr	35	0.085	56.0	11	0.092	76.4	40	0.53	133.5	65	0.16	124.1
Ba/Sr	33	1.0	57.6	10	0.88	54.2	36	2.4	70.9	65	1.9	69.2

Appendix C.9.5. Gneiss Terrane and Transition Zone.

	TON & GRANODIOR GNEISSES						LOW-PRESSURE CHARNOCKITE					
	MALAV-KD			KRISH-DHARM			MALAV-KD			KRISH-DHARM		
	N	MEAN	SD %	N	MEAN	SD %	N	MEAN	SD %	N	MEAN	SD %
SiO2	5	68.85	7.0	44	67.04	6.4	10	64.33	13.5	27	64.39	8.3
TiO2	5	0.74	66.6	44	0.47	68.1	10	0.71	65.2	27	0.60	46.0
Al2O3	5	13.84	8.9	44	16.12	4.6	10	15.65	13.6	27	16.04	5.5
Fe2O3T	5	5.07	57.9	44	3.67	51.5	10	5.53	64.1	27	5.10	42.0
MnO	5	0.07	61.1	42	0.04	83.0	10	0.07	80.4	27	0.07	55.2
MgO	5	1.16	56.2	44	1.46	58.3	10	2.31	98.6	27	2.30	55.2
CaO	5	3.13	37.0	44	3.66	26.8	10	4.65	34.9	27	4.87	23.2
Na2O	5	4.13	10.2	44	4.73	11.9	10	4.60	15.0	27	4.42	10.1
K2O	5	2.35	32.4	44	2.14	41.1	10	1.58	65.1	27	1.56	33.4
P2O5	5	0.24	68.6	41	0.19	92.9	10	0.30	87.0	26	0.21	59.1
LOI	5	0.15	93.3	43	0.49	73.6	10	0.42	73.3	27	0.49	43.5
Rb	5	73	40.9	44	51	40.1	9	68	131.5	27	39	60.1
Cs	5	0.65	73.5	37	0.59	128.4	8	1.4	165.8	20	0.43	162.5
Sr	5	197	50.1	44	698	77.4	10	556	54.2	27	569	25.1
Ba	5	396	15.3	44	834	66.6	10	462	57.6	27	503	47.2
Sc	5	9.7	68.1	44	5.6	100.1	10	10	71.0	27	11	75.4
Y	5	48	57.9	42	12	119.8	10	16	76.1	27	14	65.1
Zr	5	208	49.3	44	183	79.6	10	189	37.7	27	158	61.9
Hf	5	6.5	44.5	44	4.7	67.6	10	5.2	31.8	27	4.1	52.5
Th	5	8.7	98.6	43	5.9	101.4	10	3.2	104.4	27	3.3	175.3
U	5	1.0	57.1	33	0.57	80.9	7	0.88	116.1	25	0.31	143.5
Nb	5	15	51.5	44	7.6	104.9	10	9.2	70.7	27	8.5	53.1
Ta	5	1.0	88.1	19	1.3	136.7	5	1.7	117.8	9	1.8	63.1
Cr	5	11	92.9	41	31	120.5	10	74	129.4	26	50	89.9
Ni	5	13	65.8	36	21	91.3	7	65	125.9	22	48	107.2
Co	5	10	67.4	21	15	58.6	5	27	50.6	10	24	30.7
Zn	5	73	44.0	6	44	72.8	4	93	45.0	9	96	46.1
Pb	4	17	14.5	28	8.5	44.5	4	18	97.1	6	9.8	116.9
La	5	42	33.9	44	42	77.5	10	42	81.3	27	38	86.2
Ce	5	82	38.4	44	77	83.7	10	76	85.1	27	71	93.8
Nd	3	26	32.4	11	30	76.3	7	36	87.4	11	35	114.4
Sm	5	7.5	41.9	44	4.8	102.0	10	5.7	85.3	27	5.5	83.9
Eu	5	1.5	48.3	44	1.5	40.8	9	1.6	40.6	27	1.7	35.8
Eu*	5	2.5	44.1	44	1.3	99.3	10	1.8	76.0	27	1.6	76.0
Tb	5	1.3	46.3	44	0.49	94.3	10	0.62	64.9	27	0.64	69.0
Yb	5	4.6	74.8	44	0.93	101.9	10	1.3	82.1	27	1.2	78.5
Lu	5	0.79	78.1	40	0.14	107.7	9	0.23	89.4	26	0.19	78.3
Eu/Eu*	5	0.64	28.3	44	2.1	102.0	9	1.8	77.9	27	1.6	69.0
K/Rb	5	301	39.7	44	602	196.1	9	718	111.7	27	610	105.1
K/Ba	5	49	21.7	44	27	48.3	10	31	41.6	27	30	43.6
Rb/Sr	5	0.48	64.9	44	0.088	52.3	9	0.12	123.3	27	0.073	61.6
Ba/Sr	5	2.5	48.8	44	1.3	55.3	10	0.90	42.3	27	0.90	45.8

Appendix C.9.6. Transition Zone gneiss and charnockite.

	NILGIRIS			BR HILLS			BHAVANISAGAR			SALEM			SHEVAROY HILLS		
	N	MEAN	SD %	N	MEAN	SD %	N	MEAN	SD %	N	MEAN	SD %	N	MEAN	SD %
SiO2	10	64.50	9.4	9	69.24	2.2	4	67.32	8.3	7	64.49	6.1	15	64.05	8.3
TiO2	10	0.60	33.9	9	0.37	36.4	4	0.43	16.8	7	0.60	29.1	15	0.58	39.5
Al2O3	10	15.11	13.7	9	16.00	1.7	4	15.89	4.0	7	16.46	4.2	15	16.15	4.8
Fe2O3T	10	7.88	40.2	9	2.76	27.5	4	4.26	35.0	7	5.15	27.7	15	5.53	46.6
MnO	10	0.10	35.7	9	0.03	29.8	4	0.06	45.1	7	0.05	37.9	15	0.08	47.9
MgO	10	3.10	33.7	9	1.20	35.6	4	2.16	68.6	7	2.38	35.1	15	2.65	50.1
CaO	10	3.98	36.5	9	3.56	7.9	4	5.29	40.6	7	5.11	16.6	15	4.86	22.5
Na2O	10	3.06	33.3	9	5.16	5.6	4	4.05	1.6	7	4.63	3.3	15	4.29	10.9
K2O	10	1.34	46.2	9	1.12	10.2	4	0.95	23.6	7	0.93	20.8	15	1.37	30.2
P2O5	10	0.16	54.0	9	0.13	34.7	4	0.13	4.6	7	0.25	36.8	15	0.18	52.1
LOI	10	0.33	64.1	9	0.34	49.1	4	0.15	76.8	7	0.19	37.6	15	0.41	49.5
Rb	10	30	66.4	9	7.7	77.4	4	2.9	52.5	7	6.6	59.5	15	12	76.7
Cs	10	0.17	73.6	5	0.038	22.0	0	0.0	0.0	2	0.030	0.0	9	0.11	81.5
Sr	10	378	82.1	9	719	29.7	4	415	15.5	7	592	9.8	15	689	27.6
Ba	10	433	64.1	9	345	21.3	4	394	40.1	7	602	50.5	15	614	48.1
Sc	10	16	47.0	9	3.3	32.2	4	9.0	76.4	7	13	47.0	14	12	62.6
Y	10	20	39.3	7	3.9	48.1	4	8.2	34.9	6	19	27.1	15	11	74.2
Zr	10	114	29.8	9	159	28.1	4	86	14.1	7	177	28.6	15	127	30.7
Hf	10	3.0	37.5	9	3.9	32.5	4	2.5	8.2	7	4.9	29.3	15	3.3	31.4
Th	9	1.9	90.9	9	2.6	184.4	2	0.58	126.8	7	1.2	62.9	13	0.53	235.5
U	9	0.43	79.7	9	0.18	55.5	1	0.10	0.0	7	0.17	44.1	14	0.13	52.1
Nb	10	7.5	24.9	8	3.4	39.1	4	3.2	19.8	7	4.6	37.0	15	5.7	46.2
Ta	10	0.39	59.8	8	0.056	36.7	4	0.070	36.9	7	0.13	50.6	14	0.14	61.0
Cr	10	146	63.9	9	26	112.4	4	57	100.7	7	44	47.5	15	90	88.1
Ni	10	56	81.6	9	17	84.7	4	39	127.4	7	30	53.6	15	51	96.8
Co	10	23	43.6	9	7.6	48.4	4	13	55.6	7	13	37.3	15	19	55.7
Zn	4	74	18.3	9	39	21.7	4	50	23.6	7	66	32.3	13	66	52.8
Pb	2	12	11.8	2	7.1	6.0	2	3.7	32.9	6	2.8	12.1	1	5.8	0.0
La	10	26	37.2	9	32	77.3	4	18	18.1	7	47	39.8	15	29	43.2
Ce	8	57	50.6	9	57	80.6	4	34	24.9	7	94	44.0	15	54	49.4
Nd	3	17	5.9	8	17	63.8	2	16	22.8	7	36	47.7	10	19	62.2
Sm	10	4.6	57.5	9	2.5	66.0	4	2.1	32.5	7	6.6	47.3	15	7.2	172.1
Eu	10	1.2	43.7	9	1.1	27.4	4	0.94	13.9	7	1.4	33.6	13	1.5	23.1
Eu*	10	1.5	51.2	9	0.61	60.2	4	0.62	34.7	7	1.8	47.4	15	1.5	96.9
Tb	10	0.70	40.0	9	0.17	52.0	4	0.27	40.1	7	0.66	47.6	15	0.45	71.6
Yb	10	1.9	34.8	9	0.31	55.4	4	1.0	45.3	7	1.3	50.5	15	0.90	71.8
Lu	10	0.30	35.3	7	0.055	57.5	4	0.19	49.4	6	0.21	30.7	15	0.13	72.0
Eu/Eu*	10	0.94	64.5	9	2.3	49.7	4	1.6	34.1	7	1.0	71.7	15	2.0	92.0
K/Rb	10	530	94.5	9	1559	40.8	4	3172	39.4	7	1344	29.3	15	1359	53.2
K/Ba	10	36	77.2	9	28	20.7	4	22	23.7	7	14	23.7	15	20	29.5
Rb/Sr	10	0.11	73.2	9	0.012	90.2	4	0.007	64.3	7	0.011	62.7	15	0.018	76.8
Ba/Sr	10	1.3	59.2	9	0.50	18.8	4	0.96	38.3	7	1.0	53.8	15	0.88	27.7

Appendix C.9.7. Medium and high-P charnockite.

	AMPHIBOLITE			MAFIC GRANULITES					
				LOW-PRESSURE			HIGH-PRESSURUE		
	N	MEAN	SD %	N	MEAN	SD %	N	MEAN	SD %
SiO2	7	48.86	7.1	4	49.94	2.6	4	50.01	2.5
TiO2	7	1.00	38.3	4	0.93	41.0	4	0.91	14.3
Al2O3	7	13.87	7.9	4	14.42	1.2	4	15.42	21.9
Fe2O3T	7	12.93	26.5	4	12.71	13.4	4	12.00	10.0
MnO	7	0.19	20.2	4	0.20	8.2	4	0.18	12.1
MgO	7	8.40	14.2	4	7.45	13.6	4	8.26	29.8
CaO	7	10.34	11.5	4	11.16	7.7	4	10.18	15.2
Na2O	7	3.01	23.5	4	3.05	24.6	4	2.43	17.8
K2O	7	1.10	81.4	4	0.40	58.0	4	0.47	23.6
P2O5	7	0.10	106.5	4	0.08	26.9	4	0.17	63.0
LOI	7	0.37	57.5	4	0.46	50.4	4	0.27	80.3
Rb	7	23	236.3	4	4.4	69.3	4	4.5	28.7
Cs	6	0.47	136.0	1	0.50	0.0	4	0.23	60.9
Sr	7	323	126.7	4	105	9.5	4	457	73.4
Ba	5	162	51.1	3	108	44.6	3	202	95.9
Sc	6	43	18.8	4	46	3.8	4	32	21.1
Y	7	26	25.3	4	25	22.6	4	25	33.4
Zr	7	64	35.3	4	66	30.3	4	90	35.5
Hf	6	1.6	40.4	4	1.7	50.0	4	2.2	41.8
Th	7	1.2	146.4	4	0.59	61.5	4	3.3	114.2
U	4	0.13	40.0	1	0.10	0.0	2	0.30	47.1
Nb	7	8.8	21.3	4	8.3	21.5	4	9.2	16.6
Ta	2	0.25	84.9	3	0.68	66.6	4	0.43	52.2
Cr	6	211	49.5	4	226	83.3	4	212	66.8
Ni	5	166	40.4	4	67	55.2	4	196	92.5
Co	2	49	5.8	3	50	6.9	4	50	24.3
Zn	0	0.0	0.0	2	143	16.4	1	108	0.0
Pb	2	4.9	71.4	1	3.8	0.0	1	7.0	0.0
La	6	16	65.8	4	6.0	54.3	4	22	93.4
Ce	5	39	68.5	4	15	46.8	1	102	0.0
Nd	0	0.0	0.0	0	0.0	0.0	2	34	40.1
Sm	6	4.6	56.2	4	2.4	27.6	4	6.1	51.1
Eu	6	1.3	36.2	4	1.2	36.3	4	1.7	41.1
Eu*	6	1.5	49.5	4	0.84	28.9	3	1.9	39.3
Tb	6	0.71	38.4	4	0.49	32.1	3	0.74	17.0
Yb	6	2.0	34.9	4	1.9	31.3	4	2.4	20.7
Lu	6	0.29	36.5	4	0.30	20.8	4	0.36	26.6
Eu/Eu*	6	0.95	32.4	4	1.4	21.8	4	0.83	70.6
K/Rb	7	3243	68.6	4	877	33.6	4	890	19.5
K/Ba	5	68	27.1	3	44	105.6	3	39	77.0
Rb/Sr	7	0.16	241.6	4	0.042	69.2	4	0.013	52.0
Ba/Sr	5	0.97	66.5	3	1.0	40.2	3	0.33	47.2

Appendix C.9.8. Mafic rocks.

	Laxfordian					ARCHAEAN AVERAGE ABUNDANCES LEWISIAN											
										Scourian							
	Tonal(S)	%SD	Tonal(I)	%SD	Mean	Granit	%SD	Granod(S)	%SD	Tonal(S)	%SD	Tonal(I)	%SD	Mafic	%SD	Mean	%SD
SiO2	69.3	3.4	60.1	8.4	68.8	75.4	1.0	73.1	0.1	68.8	5.9	60.2	4.7	48.6	4.4	61.2	11.3
TiO2	0.18	82.8	0.57	32.2	0.34	0.10	59.2	0.15	43.9	0.37	56.9	0.70	27.6	0.98	46.1	0.54	50.0
Al2O3	15.9	3.1	17.1	5.4	15.9	14.0	6.6	15.5	3.2	15.6	9.6	16.8	7.4	16.2	9.9	15.6	10.5
Fe2O3t	2.25	49.2	6.05	44.8	3.41	0.69	40.1	1.21	5.3	3.14	43.2	6.23	26.2	12.8	31.3	5.93	72.2
MnO	0.03	54.5	0.07	45.2	0.06	0.02	79.1	0.02		0.04	47.0	0.09	33.7	0.22	27.6	0.08	62.5
MgO	0.88	53.0	2.2	45.6	1.48	0.27	40.5	0.55	5.1	1.38	52.1	3.22	29.1	6.59	27.1	3.36	67.6
CaO	2.54	22.7	4.2	25.9	3.20	1.09	33.3	1.56	5.0	4.31	29.0	6.67	18.3	11.6	14.6	5.57	46.7
Na2O	5.03	6.6	4.7	8.2	4.28	4.03	8.4	4.54	1.2	4.51	13.6	4.36	9.2	2.40	29.6	4.42	24.0
K2O	2.26	27.3	2.5	39.5	2.29	4.40	10.9	3.62	1.8	0.91	33.2	0.92	71.6	0.52	102	1.03	61.2
P2O5	0.13	74.0	0.31	46.8	0.13	0.02	47.1	0.03	47.1	0.09	47.0	0.21	73.6	0.07	62.3	0.18	94.4
Total	98.5		97.8		99.9	100.1		100.2		99.2		99.4		100.0		99.8	
Rb	83	4.1	81	38.6	75	53	34.9	39	18.1	5	74.7	6	151	5	122	11	100
Cs																	
Sr	606	12.9	672	3.9	542	268	34.8	302	24.4	454	24.6	441	44.7	183	24.2	569	42.7
Ba	818	24.8	907	50.9	759	597	40.6	962	37.3	1151	120	549	74.6	261	56.4	757	66.6
Th	6.8	114	14.3	101	10	1.7	109	1	141	0.93	176	~0.8	95	~0.3	110	0.42	250
U										0.08	66.1	0.05		0.01	10.9		
Pb					20	18	24.2	14	5.2	7	24.3	9	44.7	5	51.9	13	38.5
Sc						1.1	64.0			12	19.9	16	22.1	49	10.1		
Y	~2.5	64	13	68.0	7	<4	151	0.90	31.4	~2	107	14	44.8	21	61.9	9	88.9
Zr	190	48.1	277	53.2	189	46	44.9	133	17.0	150	58.3	172	49.6	51	61.8	202	92.1
Hf	2.4	50.0	5.0	41.5	3.8	1.4	57.8			3.2	59.4	4.6	49.7	1.7	40.9	3.6	
Nb	5.5	23.5	7.5	44.2	6	~1	65.5	2	70.7	~3	63	7	62.1	4	76.1	5	
Ta	0.52	23.0	0.38	18.9	0.45					0.69	26.4	0.70	48.8	0.38	66.3	0.56	
Cr	18	62.5	20	84.7	31	2.3	24.7	3.5	101	42	93.1	87	87.1	317	44.0	88	116
Ni	12	82.0	13	28.1	19	1	34.6	1		18	104	54	87.4	114	58.0	58	107
Co										14	20.0	17	27.8	54	17.6		
Zn						4.7	44.6	20	39.9	27	72.9	83	48.1	104	28.3		
La	24	102	71	104	36	10	35.7	13	65.3	16	46.4	24	80.6	6.2	69.2	22	
Ce	44	95.5	123	88.5	69	14	31.5	28	12.9	28	35.7	50	79.1	16	60.5	44	
Nd	14	90.0	49	62.2	30					8.5	40.0	30	81.0			19	
Sm	2.0	99.2	6.5	26.1	4.4	0.41	45.5			1.7	54.9	4.3	46.0	9.5	94.7	3.3	
Eu	0.63	28.5	1.4	11.9	1.1	0.73	35.1			0.97	19.6	1.2	34.8	0.88	44.2	1.2	
Tb	0.15	76.5	0.58	38.5	0.41	0.11	46.6			0.19	44.6	0.51	49.1	0.64	47.0	0.43	
Yb	0.29	63.3	1.01	65.4	0.76	0.47	99.9			0.39	47.8	1.1	41.0	2.9	67.3	1.2	
Lu			0.23			0.09	90.9			0.09	46.3	0.18	28.1	0.38	42.1		
Eu/Eu*	1.96	74.9	0.81	10.9	0.91	5.44	61.0			2.8	65.8	1.0	21.3	0.87	12.0	1.2	
7REE	71	97.4	204	90.3	112	28.2	27.1			51.2	30.4	87.0	81.3	29.5	53.0	71.9	
K/Rb	227	30.8	261	30.9	236	766	33.0	782	16.4	1890	43.7	~2100	52	1067	41.7	777	
K/Ba	22.8	5.7	24.1	18.2	24.4	77.4	64.2	33.5	35.7	9.74	39.2	15.2	19.4	29.2	45.8	11.0	
Rb/Sr	0.14	13.0	0.12	38.5	0.13	0.21	70.4	0.13	6.5	0.012	72.9	0.019	146	0.061	113	0.019	
Ba/Sr	1.35	29.9	1.38	51.9	1.23	2.19	8.1	3.14	13.8	2.38	94.5	1.27	70.1	1.61	85.6	1.33	
n	4		4		329/39	10		2		14		12		13		254	
Source	1		2		3	4		5		6		7		8		9	

Appendix C.10.1. For sources from which data taken, see Appendix C.11.

ARCHAEAN AVERAGE ABUNDANCES

	W Fiskenaesset Mafics	%SD	E S T Granod(S)	%SD	G R E E N L A N D Tonal(S)	%SD	Tonal(I)	%SD	AmphFac	%SD	GranFac	%SD
SiO2	47.8		70.1	3.0	67.6	3.2	57.6	5.5	67.2	5.7	63.3	9.7
TiO2	0.99		0.35	35.4	0.40	17.8	0.81	15.6	0.44	35.9	0.65	57.0
Al2O3	14.8		14.8	3.0	15.7	2.5	16.9	13.1	15.8	8.6	15.8	8.0
Fe2O3t	12.3		2.37	27.8	3.34	18.2	7.73	9.5	3.26	51.6	5.12	64.0
MnO	0.21								0.06	52.7	0.09	48.4
MgO	7.60		0.67	80.1	1.22	21.2	3.92	59.5	1.46	73.6	2.08	78.6
CaO	12.3		2.92	16.7	4.57	23.3	7.05	14.3	3.92	29.8	5.17	40.0
Na2O	1.82		4.02	7.7	4.55	12.4	4.63	21.0	4.76	11.3	4.02	10.3
K2O	0.34		3.30	28.4	1.39	70.5	1.13	42.2	2.16	41.0	2.07	55.8
P2O5	0.07											
Total	98.2		98.5		98.7		99.8		98.99		98.26	
Rb	6	83.0	109	73.8	28	73.1	20	153	55	58.1	45	111
Cs												
Sr	79	31.2	216	33.4	343	19.4	456	8.7	341	27.5	275	37.8
Ba	35	127	2101	21.9	708	49.0	620	17.7	787	42.6	949	32.7
Th	0.31	43.7	22.0	52.5	0.23	55.9	0.40	90.1				
U												
Pb												
Sc												
Y	23	66.4										
Zr	64	60.3	316		44	144	<140		142	46.5	137	50.4
Hf	1.75	64.6	5.53	38.7	3.57	19.1	3.40	51.0				
Nb	3	74.5							2	158	4	153
Ta	0.22	64.7	0.81	52.3	0.81	17.7	0.53	39.0				
Cr	198	57.8							29	103	35	151
Ni	147	70.9							24	112	42	117
Co												
Zn	96	37.3										
La	3.0	61.8	58	54.5	12	39.8	22	19.5	46	115	36	52.7
Ce	9.5	75.6	107	65.9	21	39.7	43.2	9.4	66	35.0	67	47.8
Nd	8.4	66.4	31	72.4	7.1	32.0	23	13.6				
Sm	2.6	65.3	4.4	65.1	1.2	32.2	4.5	11.8				
Eu	0.92	57.0	0.93	40.6	0.80	18.0	1.3	3.2				
Tb	0.64	63.7	0.36	57.9	0.11	30.3	0.49	18.2				
Yb	2.6	62.1	0.40	60.4	0.28	28.1	1.2	20.8				
Lu	0.42	64.0	0.054	67.3	0.059	56.1	0.18	27.9				
Eu/Eu*	0.98	7.2	0.94	26.0	2.3	28.4	0.97	16.1				
ΣREE	19.8		172	61.2	34.9	38.3	72.8	12.2				
K/Rb	492	50.7	304	33.2	992	124	2214	78.7	401	83.4	776	49.1
K/Ba	540	148	13.4	28.3	16.1	35.0	14.8	24.6	24.8	37.2	19.6	45.4
Rb/Sr	0.10	103	0.37	50.3	0.087	76.9	0.041	152	0.19	83.2	0.18	109
Ba/Sr	0.64	146	8.85	17.2	2.22	60.6	1.36	12.8	2.57	65.2	3.13	68.9
n	68/7		7		4		3		40		19	
Source	10		11		12		13		14		15	

Appendix C.10.2. For sources from which data taken, see Appendix C.11.

	WEST ARCHAEAN GREENLAND						AVERAGE ARCHAEAN		LABRADOR			SWAZILAND		COMPOSITE LOW-GRADE GRANITE				
	Granit	%SD	Amitsoq Granod(S)	%SD	Tonal(S)	%SD	Tonal(I)	%SD	Migmatit granit	Gneiss Granod(I)	UivakI Ton(S)	Ancnt Ton(S)	Gn Com %SD	Larami Granit	Lochiel Granit	Salisb Granit	Matpos Granit	Chilmz Granit
SiO2	72.7	4.3	66.4	1.8	70.6	7.4	61.4	4.4	71.3	62.5	68.6	70.1	3.6	72.9	71.3	73.6	72.0	75.1
TiO2	0.34	45.3	0.89	8.3	0.43	30.9	1.51	40.9	0.25	0.84	0.40	0.30	40.2	0.30	0.32	0.21	0.32	0.19
Al2O3	13.8	8.6	14.5	5.3	14.5	14.6	13.3	9.5	15.1	16.7	15.9	15.2	4.6	14.2	14.4	13.9	14.5	14.0
Fe2O3t	2.41	55.7	6.23	6.6	3.46	38.7	10.6	25.9	1.70	5.56	2.53	2.84	35.6	2.35	2.51	1.17	1.66	1.09
MnO	0.04	50.5	0.08	10.2	0.05	57.8	0.14	20.2	0.03	0.06	0.03	0.04	73.6					
MgO	0.47	50.7	1.15	12.0	1.23	60.3	1.63	20.0	0.48	2.05	0.94	1.18	53.2	0.49	0.57	0.50	0.40	0.12
CaO	1.71	19.2	3.55	9.3	4.25	9.9	5.14	29.7	1.89	3.64	2.60	3.17	20.1	1.19	1.33	1.07	1.72	1.09
Na2O	3.36	5.3	3.71	12.7	4.28	13.1	3.12	4.3	4.33	4.53	5.28	4.95	10.1	3.45	3.92	3.78	3.98	3.62
K2O	5.00	26.4	3.26	24.9	1.03	33.0	2.55	57.0	4.24	3.06	2.47	1.71	35.6	4.60	4.59	4.80	4.42	4.31
P2O5	0.11	62.0	0.30	5.0	0.14	47.6	0.56	47.1	0.09	0.20	0.13	0.11	42.3					
Total	99.99		100.07		99.99		99.95		99.81	100.04	98.88	100.43		99.48	98.94	99.03	99.00	99.52
Rb	124	19.8	70	26.7	35	28.2	50	52.9	123	136	111	61	40.2	184	196	328	193	276
Cs	0.83		1.0															
Sr	184	30.6	233	22.7	338	20.8	262	14.9	312	471	725	433	29.4	112	122	135	462	114
Ba	825	48.9	728	13.2	264	74.4	640	36.2	1083	1223	263	894	93.3	632	500	571	1130	657
Th	~1.8		0.80	24.7	0.28		0.39											
U	~1		0.47	19.8	0.14		0.16											
Pb	12		12															
Sc																		
Y	10	68.8	35	38.2	7.8	78.4	49	33.5										
Zr	212	55.8	355	13.8	153	64.2	415	30.9	151	319	137			130	100	122	187	99
Hf	5.1		8.2															
Nb	7.6	54.7	13	30.4	4	35.4	14	10.1										
Ta																		
Cr									15	128	17			4	10	8	8	6
Ni	~2		6	40.8	10	112	5	84.9	23	59	23			7	7	5	6	5
Co														2	6	3	5	2
Zn	35	58.0	91	9.0	47	55.3	143	21.3	43	84	48							
La	16		48									28	31.1	54	70	59	77	37
Ce	42		120									47	30.3	120	131	131	149	86
Nd	22		58									18	31.7					
Sm	4.2		11									2.9	37.5	7.5	9.1	7.8	7.0	4.5
Eu	1.9		1.8									0.94	9.9	0.76	1.5	0.50	1.1	0.35
Tb	0.57		1.4									0.26	37.8	0.78	1.3	0.51	0.46	0.58
Yb	2.1		3.5									1.05	80.1	2.4	2.5	1.5	1.5	2.2
Lu												0.18	81.9	0.41	0.36	0.26	0.22	0.39
Eu/Eu*	1.47		0.54									1.39	47.4	0.37	0.52	0.27	0.59	0.26
ΣREE	66.2		187											186	216	201	237	131
K/Rb	331	12.3	397	21.7	261	44.7	421	4.8	286	186	184	341	93.0	208	194	121	190	130
K/Ba	55.0	28.3	37.5	25.0	38.7	44.9	31.7	23.1	33	21	78	28.7	57.1	60.4	76.2	69.8	32.5	54.4
Rb/Sr	0.695	14.5	0.324	44.7	0.111	45.2	0.201	66.0	0.394	0.289	0.153	0.151	51.4	1.6	1.6	2.4	0.42	2.4
Ba/Sr	4.32	19.0	3.20	15.1	0.812	68.9	2.54	49.8	3.47	2.60	0.363	1.70	100	5.6	4.1	4.2	2.4	5.8
n	5		4		5		2		11	3	10	7		15	8	6	4	7
Source	16		17		18		19		20	21	22	23		24	25	26	26	26

Appendix C.10.3. For sources from which data taken, see Appendix C.11.

	ARCHAEAN AVERAGE ABUNDANCES															
	EAST ANTARCTIC SHIELD GRANULITES									MADRAS						
	Enderbyland					Mossel	Fyfe Hills		Tryne	Charnockite				Mafic Granulites			
	Granit	Granod(S)	Tonal(S)	Tonal(S)	%SD	Tonal(S)	Mafic	%SD	Mafic	Granit	%SD	Tonal(I)	%SD	Group I	%SD	Group II	%SD
SiO2	74.7	69.8	68.5	72.0	3.9	69.8	49.3	3.0	49.1	72.6	4.4	59.0	2.6	50.1	3.7	49.4	1.6
TiO2	0.19	0.32	0.47	0.54	43.6	0.43	0.60	94.4	1.21	0.37	48.6	1.59	18.9	1.80	11.1	0.93	30.1
Al2O3	13.2	14.9	14.9	13.2	3.9	14.5	17.4	24.7	15.0	13.5	9.6	13.7	5.5	13.2	5.9	13.1	0.53
Fe2O3t	1.76	3.32	4.49	4.61	33.6	3.86	11.5	49.7	12.0	3.62	30.7	12.6	12.7	18.5	4.8	12.7	11.8
MnO	0.03	0.05	0.05	0.01	40.4	0.04	0.21	50.5	0.21	0.05	40.0	0.20	26.1	0.23	17.8	0.18	11.0
MgO	0.52	1.39	1.87	1.92	32.1	1.30	8.42	39.5	6.73	1.16	43.1	2.62	14.5	5.13	21.8	8.36	13.2
CaO	1.71	2.98	4.11	4.76	24.7	3.99	10.1	15.5	11.5	1.67	61.7	5.96	15.9	7.36	26.6	11.8	14.8
Na2O	3.23	4.09	4.22	2.16	20.3	4.43	1.85	42.8	3.06	2.88	16.3	3.20	16.9	2.85	14.7	2.00	21.0
K2O	4.59	2.78	1.10	0.38		0.77	0.36	24.5	0.53	4.08	40.7	0.75	17.3	0.87	40.2	0.41	105
P2O5	0.02	0.07	0.12	0.11	87.5	0.12	~0.1	~68	0.13	0.07	57.1	0.40	51.5	0.29	49.1	0.09	30.8
Total	99.95	99.70	99.83	99.75		99.28	99.84		99.39	100.02		99.99		100.43		98.99	
Rb	117	50	14	2	7.3	7	5	107	6	100	45.0	5	20.0	17	129	4	100
Cs																	
Sr	166	330	360	113	3.8	318	100	38.3	140	166	74.7	180	19.4	150	15.3	113	25.7
Ba	1373	1163	692			383			86	879	41.9	308	60.4	319	73.7	67	53.7
Th	18	7	4	2.55	83.7	2.6	1.68	65.6	<1	19	15.8	7	71.4	<3	100	<3	33.3
U	~0.8	~0.7	~0.4	1.27	131	~0.6	0.10	66.8	~0.5								
Pb	29	20	10	6	0.01	6	6	37.1	3	19	36.8	9	33.3	7	57.1	5	40.0
Sc						8			40	4.0	57.4			38.5	5.2	34.1	29.9
Y	4	7	10			8			27	23	113	30	30.0	41	26.8	20	25.0
Zr	106	126	152	264	121	217	63	113	72	277	48.0	158	13.9	112	22.3	56	32.1
Hf										8.5	21.9			3.0	9.2	1.25	63.0
Nb	3	4	4			5			3	9	77.8	13	7.7	13	53.8	4	25.0
Ta																	
Cr	16	41	40	55	12.9	19	197	51.8	263	16	125	20	70.0	38	78.9	351	35.9
Ni	10	21	22	62	16.0	10	133	31.1	114	3	167	4	125	33	124	152	16.4
Co																	
Zn	22	40	50			45			94	43	46.5	124	13.7	136	24.3	83	15.7
La	68	30	29			24			5	45	47.1	39	15.4				
Ce	84	44	44			40			14	79	59.2	71	16.9				
Nd				13	90.5		8.5	83.2		30	72.5						
Sm										5.9	96.5						
Eu										1.8	40.1						
Tb										0.50	102						
Yb										3.5	150						
Lu																	
Eu/Eu*										2.4	105						
ΣREE										136	59.9						
K/Rb	326	461	650	1478	7.3	313	1285	98.0	733	373		1187		832		730	
K/Ba	27.8	19.8	13.2			16.7			51.2	38.5		20.2					
Rb/Sr	0.70	0.15	0.039	0.02	9.4	0.022	0.09	154	0.042	0.89		0.03		0.11		0.04	
Ba/Sr	8.27	3.52	1.92			1.2			0.61	7.08		1.62		2.14		0.65	
n	7	12	21	2		29	4		9	28		4		7		10	
Source	27	28	29	30		31	32		33	34		35		36		37	

Appendix C.10.4. For sources from which data taken, see Appendix C.11.

C.11 Data Sources for Archaean Terranes

1.) Laxfordian tonalitic (silicic) gneiss: samples 5319, 5322, 5127, 5228 (Weaver and Tarney, 1981).

2.) Laxfordian tonalitic (intermediate) gneiss: samples 5424, 5422, 5420, 5326 (Weaver and Tarney, 1981).

3.) Laxfordian gneisses: mean of 329 samples from sources cited (columns A, B, C) in Tarney (1976). For trace elements, mean of 61 samples from sources cited (columns B and C) cited in Tarney (1976). For Hf, Ta, and REE, mean of 39 samples from Sheraton and coworkers (column 4) cited in Weaver and Tarney, 1981.

4.) Scourian granitic charnockite: samples 8, 11, 88 (Rollinson and Windley, 1980b); samples 67-117, 56-190, 65-198, M19, CRE474, 5, 79 (Pride and Muecke, 1982).

5.) Scourian granodioritic (silicic) charnockite: samples 19, 3 (Rollinson and Windley, 1980b).

6.) Scourian tonalitic (silicic) charnockite: samples 20F, 18Z, 16Y, 1Z, 18V, 18L (Weaver and Tarney, 1980); samples 189, 176, 216 (Rollinson and Windley, 1980b); samples 66-25, 67-34, 67-119, 65-181, 67-41 (Pride and Muecke, 1980). Calculated trace element abundances may not include all samples.

7.) Scourian tonalitic (intermediate) charnockite: samples 15Z, 2H, 19D, 20I, 20C (Weaver and Tarney, 1980); samples 84A, 190, 266 (Rollinson and Windley, 1980b); samples 65-18, 67-66, 67-52, 65-191 (Pride and Muecke, 1980). Calculated trace element abundances may not include all samples.

8.) Scourian mafic granulites: samples 15H, 7D, 8H, 14C, 20N (Weaver and Tarney, 1980); samples 65-39, 65-38, 64-41, 66-11, 65-33, 64-12, 65-165, 67-30 (Pride and Muecke, 1980). Calculated trace element abundances may not include all samples.

9.) Scourian granulites: mean of 254 samples (Sheraton, 1970); REE data from Weaver and Tarney (1980); Hf and Ta data reported in Weaver and Tarney (1981).

10.) Fiskenaesset mafic rocks: for major elements, mean of 68 samples (groups 1 and 2) (Weaver et al., 1982); for trace elements, samples 119664A, 84430, 121679, 121659, 121642, 121660, 121675 (Weaver et al., 1982).

11.) Nuk granodioritic (silicic) gneiss: samples 175766, 174816,

205854, 205759, 205008, 204967, 204995, (Compton, 1978).

12.) Nuk tonalitic (silicic) gneiss: samples 205755, 205761, 205832, 775736 (Compton, 1978).

13.) Nuk tonalitic (intermediate) gneiss: samples 205787, 205845, 205788 (Compton, 1978).

14.) Nuk gneisses: mean of 40 amphibolite facies samples from Buksefjorden (Wells, 1979).

15.) Nuk granulites: mean of 19 medium-pressure granulite facies samples from Buksefjorden (Wells, 1979).

16.) Amitsoq granitic gneiss; samples 155818, 110986, 110987, 110866, 110869 (Lambert and Holland, 1976).

17.) Amitsoq granodioritic (silicic) gneiss: samples 110858, 110857, 155819, 155817 (Lambert and Holland, 1976).

18.) Amitsoq tonalitic (silicic) gneiss: samples 110988X, 110999, 110802, 110865, 110988Y (Lambert and Holland, 1976).

19.) Amitsoq tonalitic (intermediate) gneiss: samples 155820, 110860 (Lambert and Holland, 1976).

20.) Labrador "migmatitic gneiss" ("Nuk equivalent") granitic gneiss: mean of 11 samples (groups 6, 7) (Collerson et al., 1976).

21.) Labrador "migmatitic gneiss" ("Nuk equivalent") granodioritic (intermediate) gneiss: mean of 3 samples (Collerson et al., 1976).

22.) Labrador Uivak I ("Amitsoq equivalent") tonalitic (silicic) gneiss: mean of 10 samples (Collerson et al., 1976).

23.) Swaziland Ancient Gneiss Complex tonalitic (silicic) gneiss: samples SWZ-6, SWZ-7, SWZ-9, H1138, H1147, H1241, H430 (Hunter et al., 1978).

24.) Archaean low-grade granite: Laramie (Condie, 1969; 1981a; 1981b).

25.) Archaean low-grade granite: Lochiel (Hunter, 1974; Condie and Hunter, 1976; Condie, 1981b).

26.) Archaean low-grade granite: Salisbury, Matopos, and Chilimanzi (Condie, 1981b).

27.) East Antarctic Shield, Enderbyland, granitic gneisses: mean of 7 "undepleted" samples (Sheraton and Black, 1983).

28.) East Antarctic Shield, Enderbyland, granodioritic gneisses: mean of 12 "undepleted" samples (Sheraton and Black, 1983).

29.) East Antarctic Shield, Enderbyland, tonalitic gneisses: mean of 21 "undepleted" samples (Sheraton and Black, 1983).

30.) East Antarctic Shield, Enderbyland, Fyfe Hills tonalitic (silicic) charnockite: samples 28-VIII, 28-VI (DePaulo et al., 1982).

31.) East Antarctic Shield, Vestfold Block, Mossel tonalitic (silicic) charnockite: mean of 29 samples (Sheraton and Collerson, 1984).

32.) East Antarctic Shield. Enderbyland, Fyfe Hills mafic granulite: samples28-I, 28-II, 28-III, 28-IV (DePaulo et al., 1982).

33.) East Antarctic Shield, Vestfold Block, Tryne mafic granulite: mean of 9 samples (Sheraton and Collerson, 1984).

34.) Madras, India, granitic charnockite: mean of 28 samples labeled "charnockite", REE calculated from samples MP45, MP50, MP24, MP14, MP36, MP17 (Weaver et al., 1978; Weaver, 1980).

35.) Madras, India, tonalitic (intermediate) charnockite: mean of 4 samples (Weaver et al., 1978; Weaver, 1980).

36.) Madras, India, mafic granulite I: mean of 7 samples labeled "basic granulites I" (Weaver et al., 1978).

37.) Madras, India, mafic granulite II: mean of 10 samples labeled "basic granulites II" (Weaver et al., 1978).

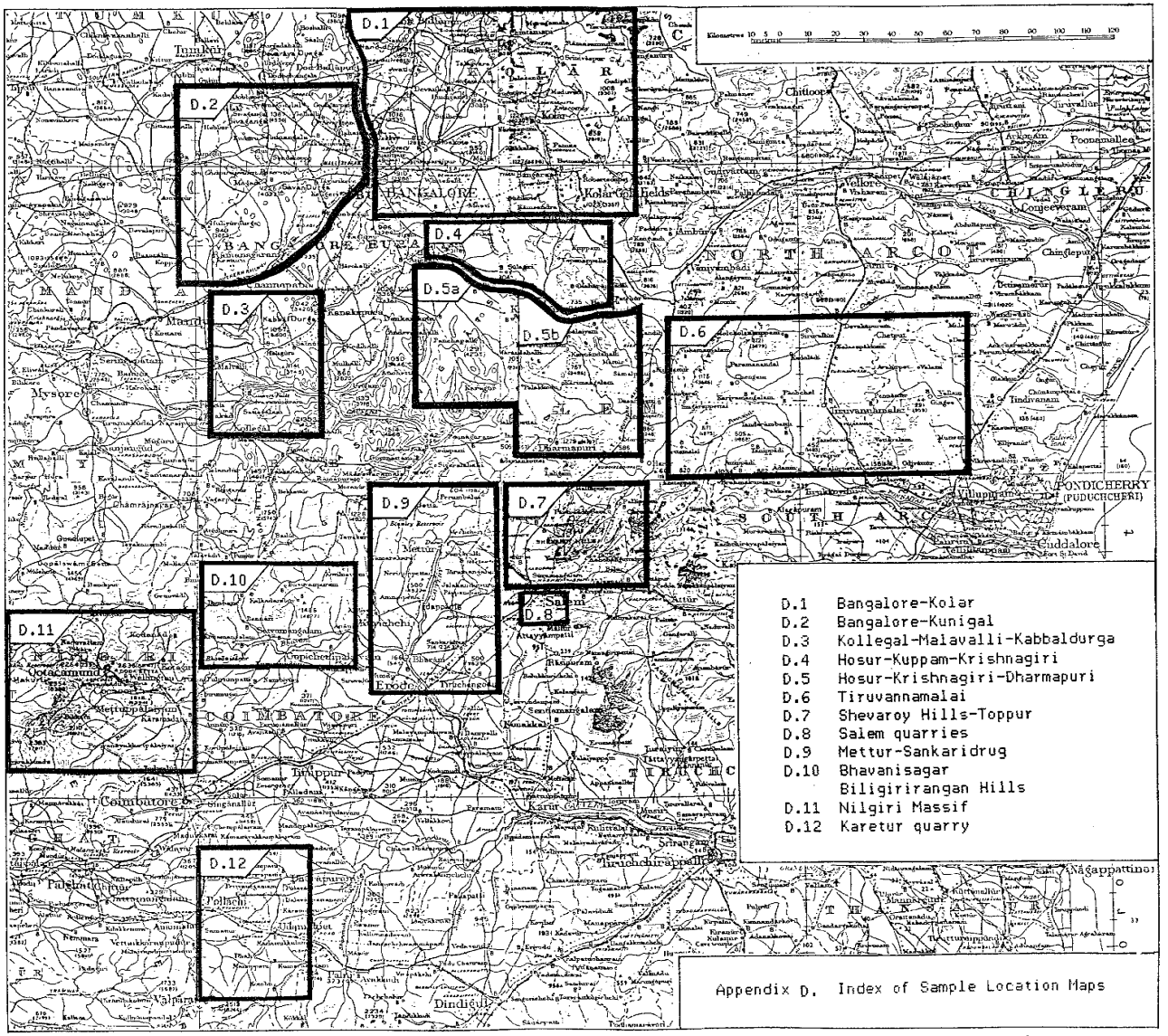

Appendix D. Index of Sample Location Maps

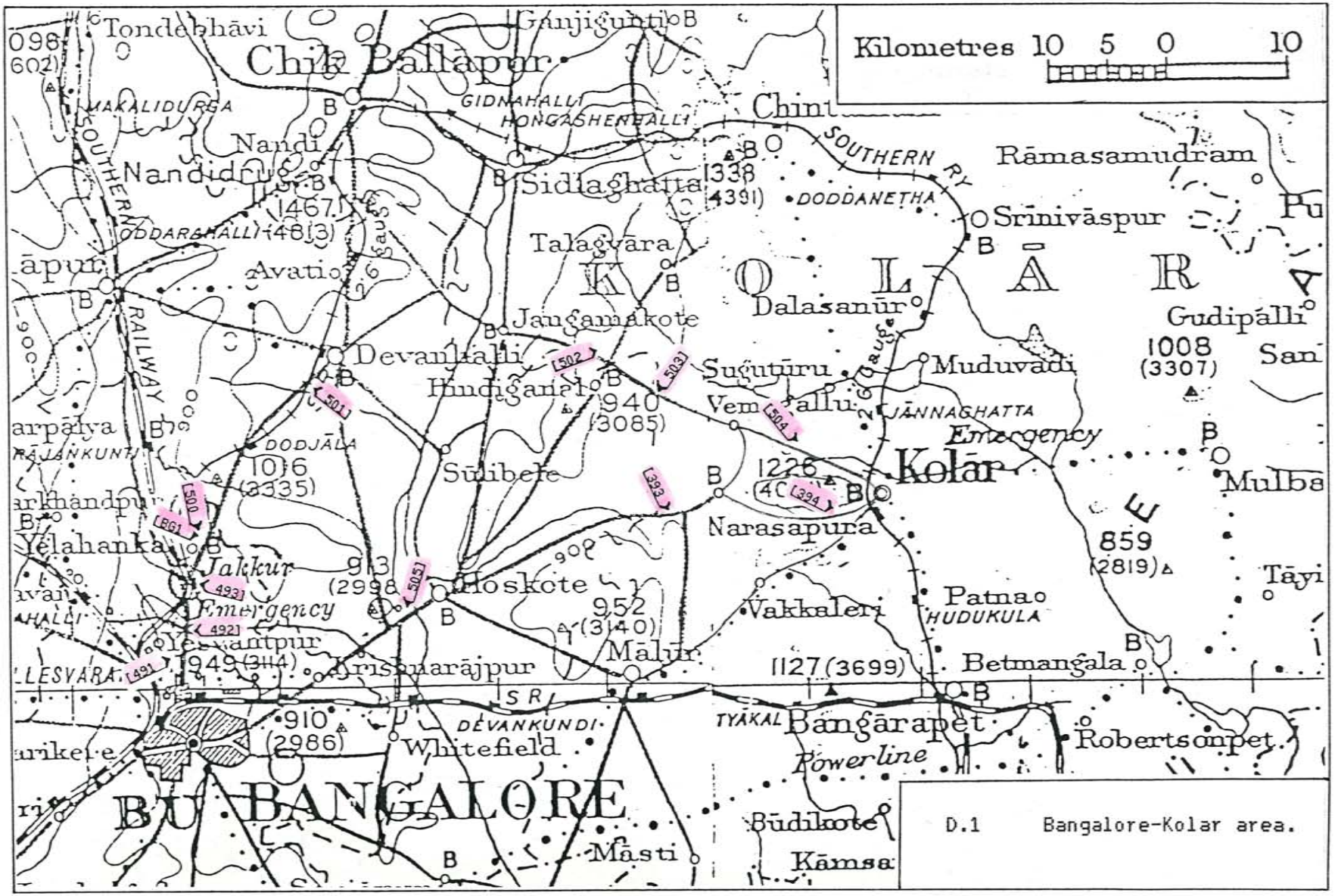

D.1 Bangalore-Kolar area.

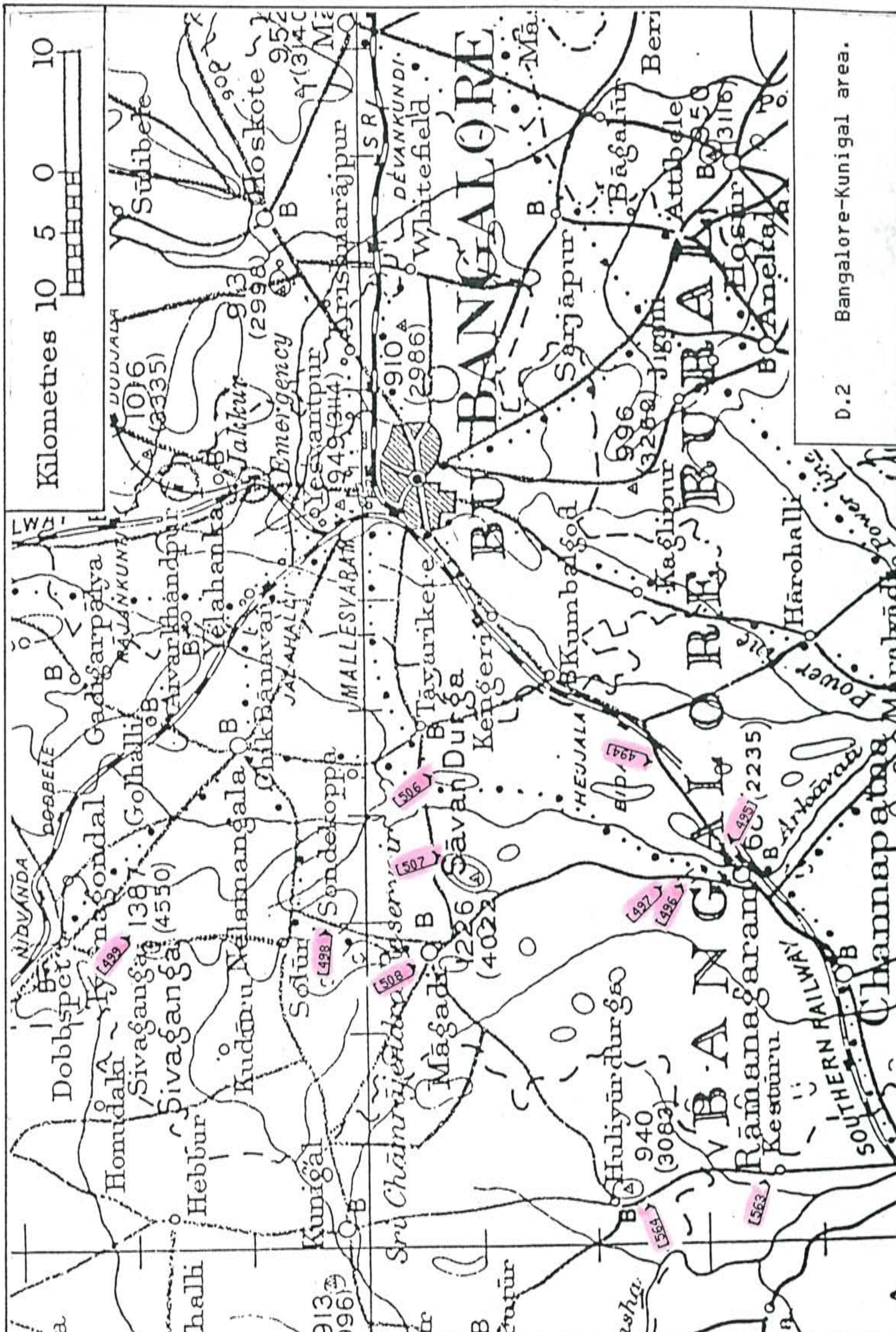

D.2 Bangalore-Kunigal area.

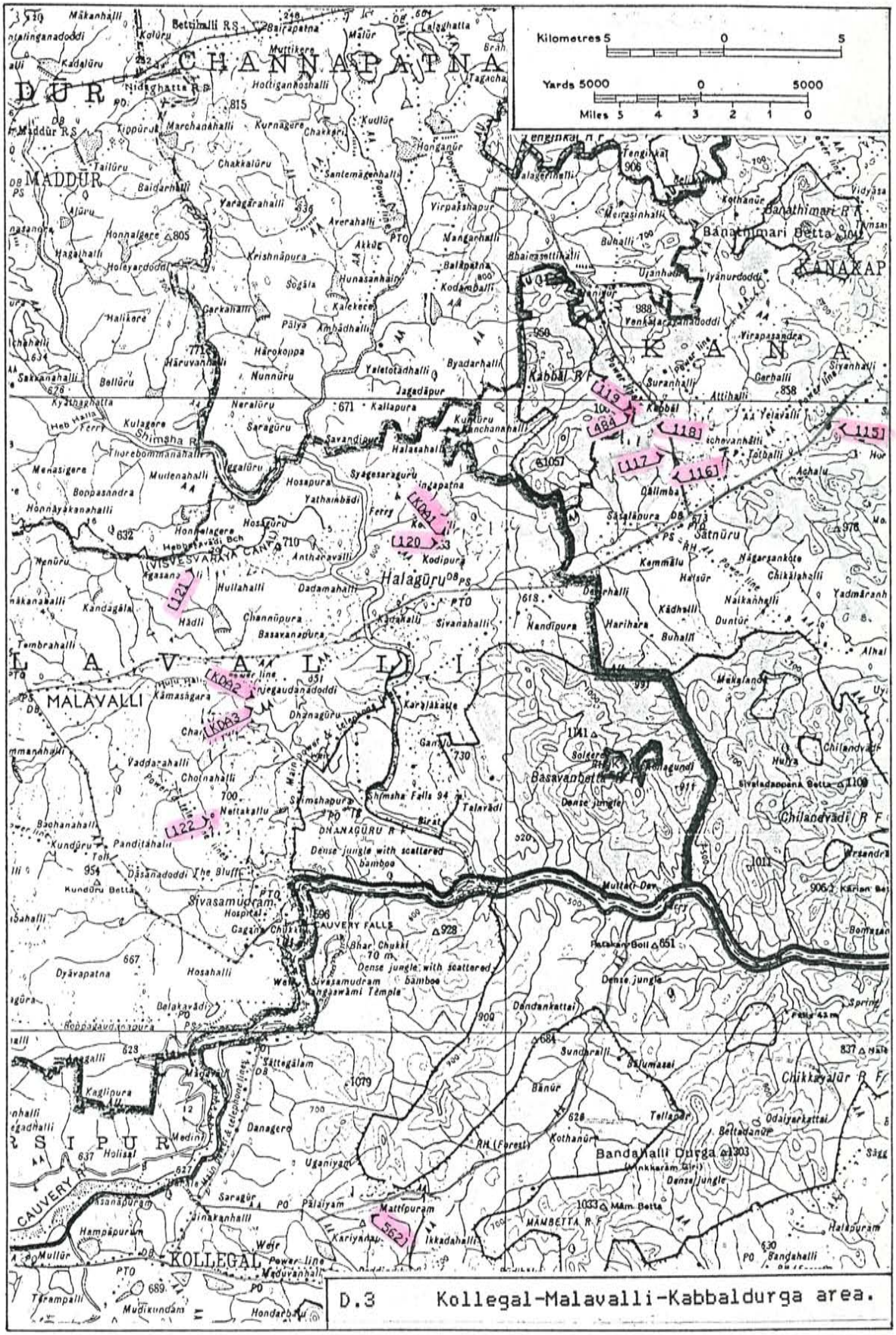

D.3 Kollegal-Malavalli-Kabbaldurga area.

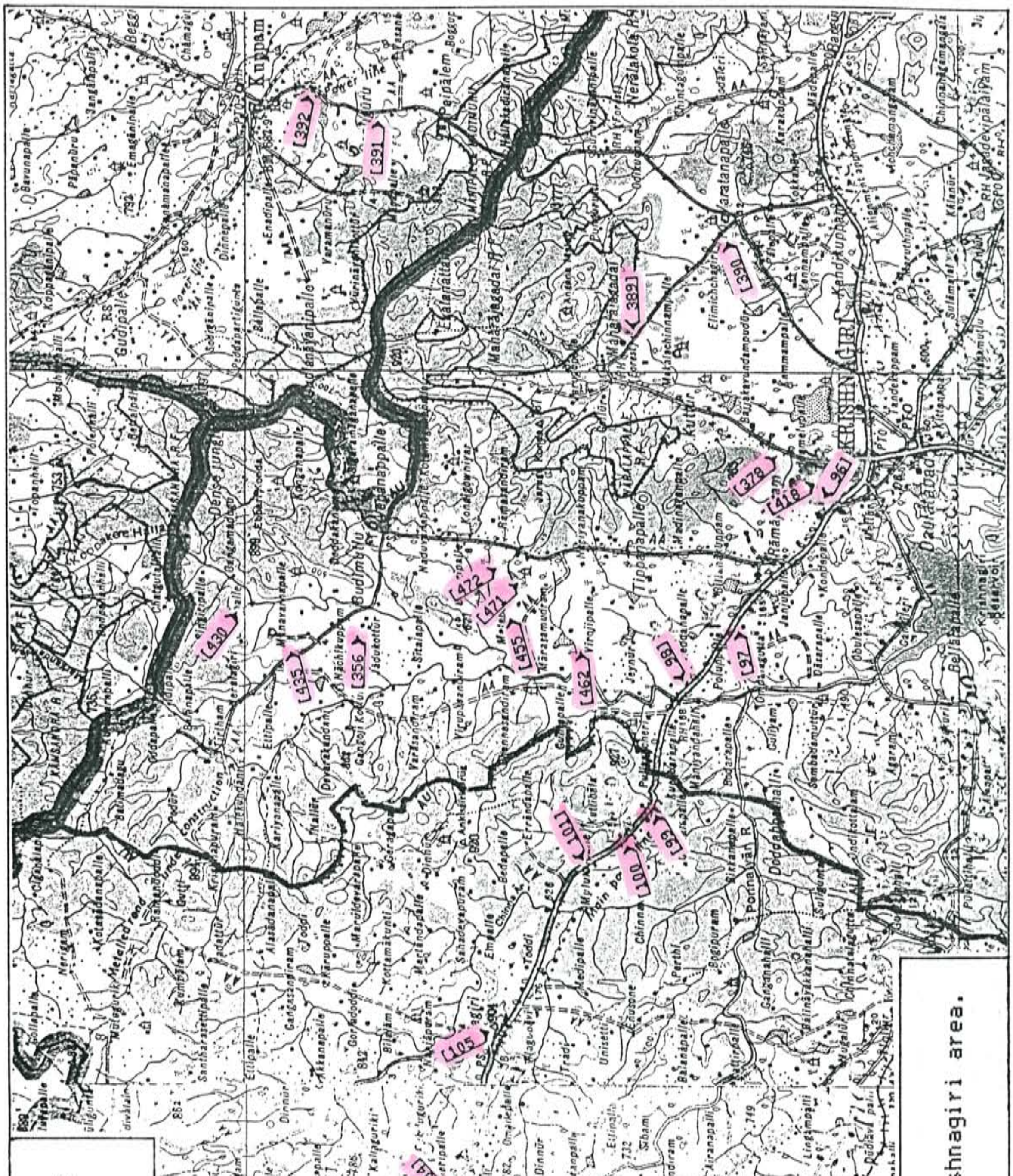

D.4 Hosur-Kuppam-Krishnagiri area.

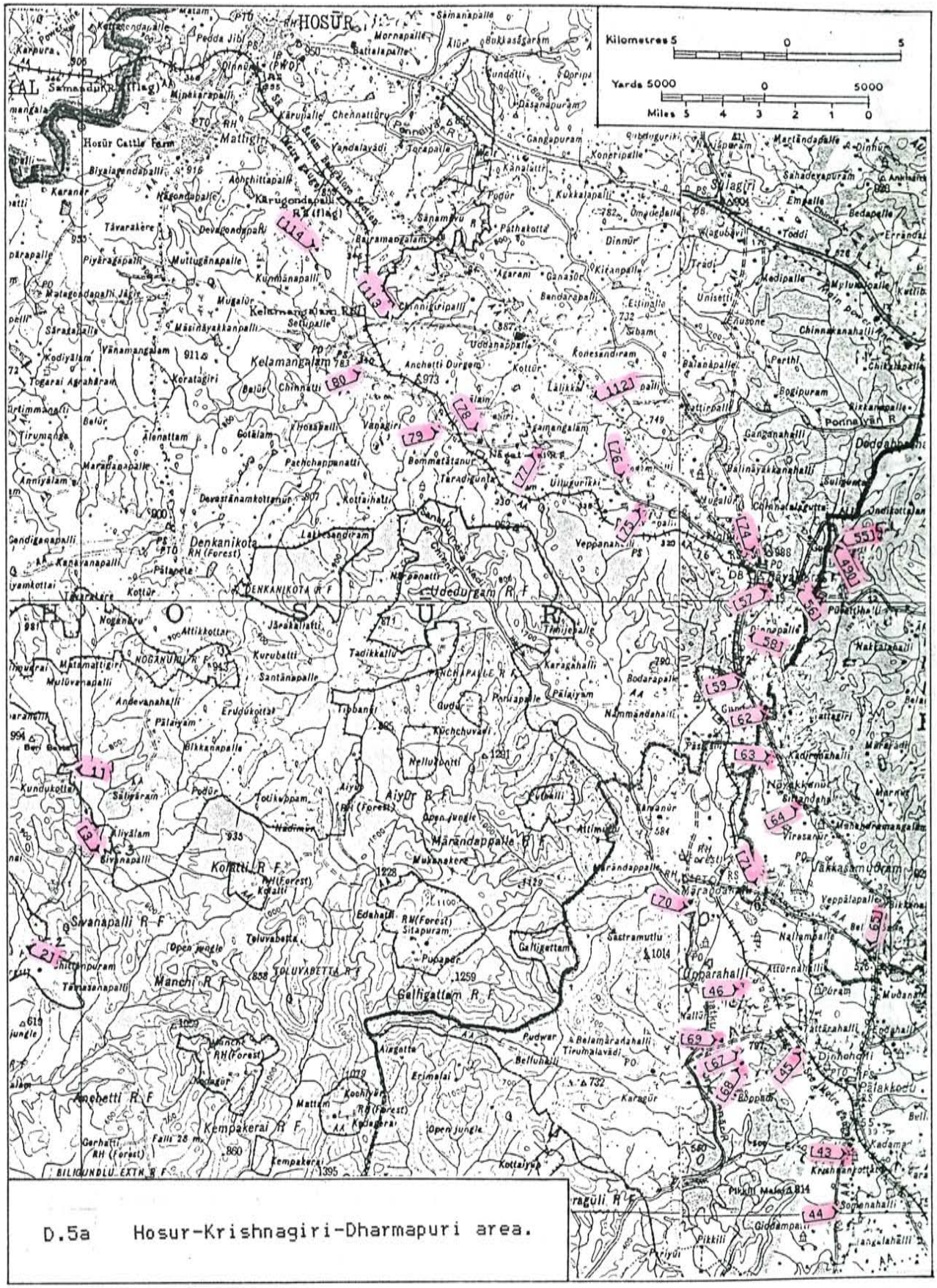

D.5a Hosur-Krishnagiri-Dharmapuri area.

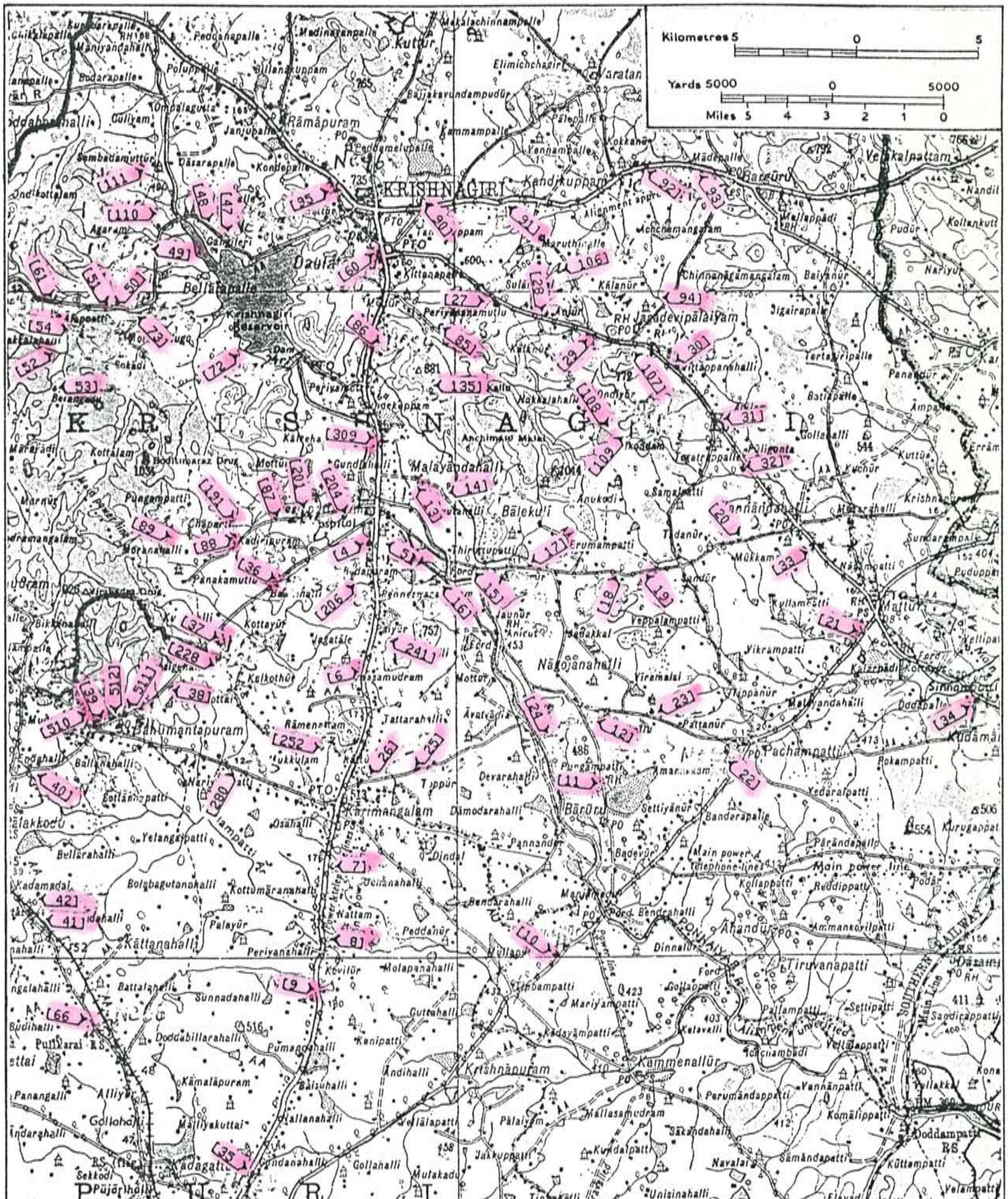

D.5b Hosur-Krishnagiri-Dharmapuri area.

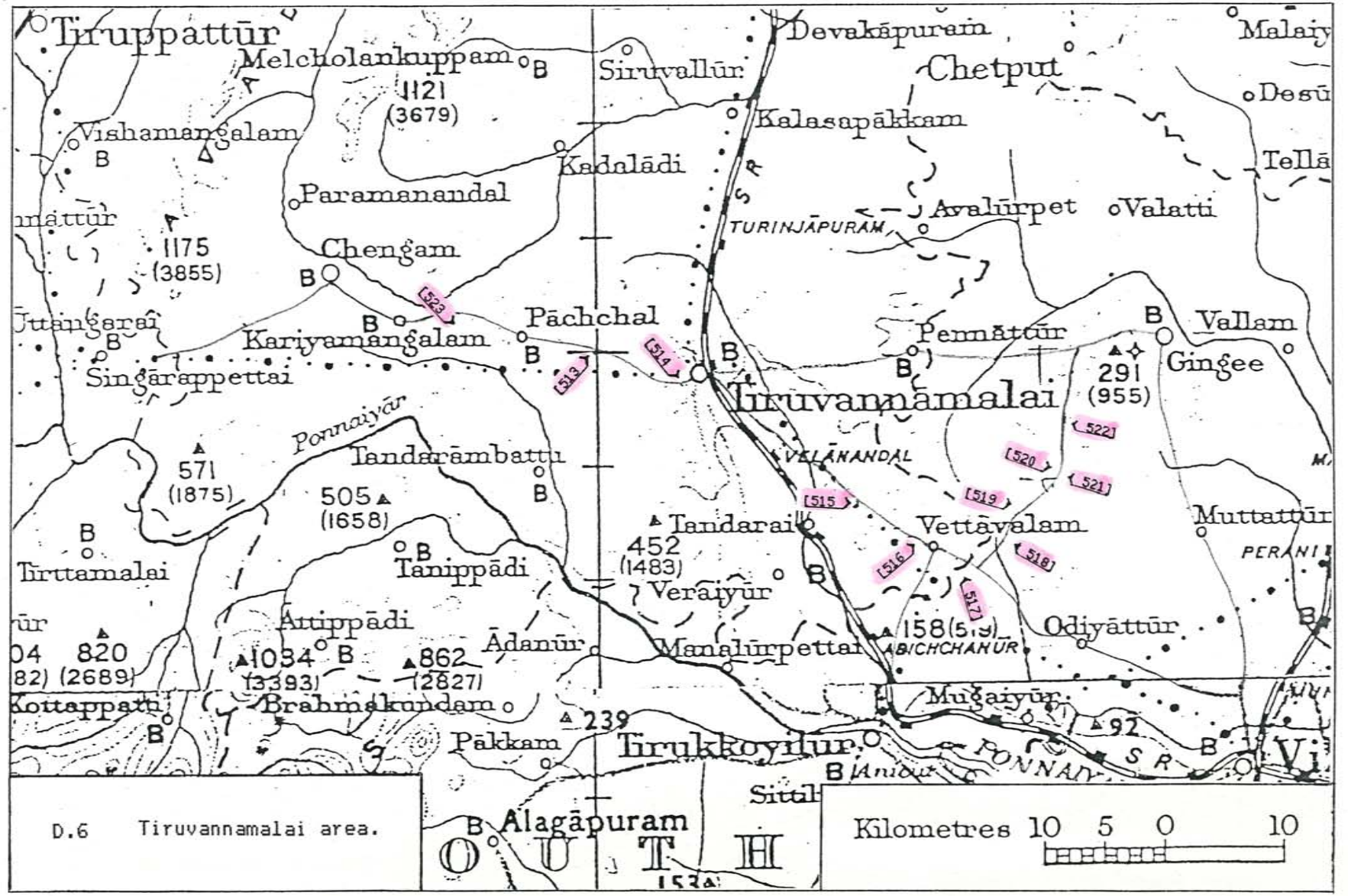

D.6 Tiruvannamalai area.

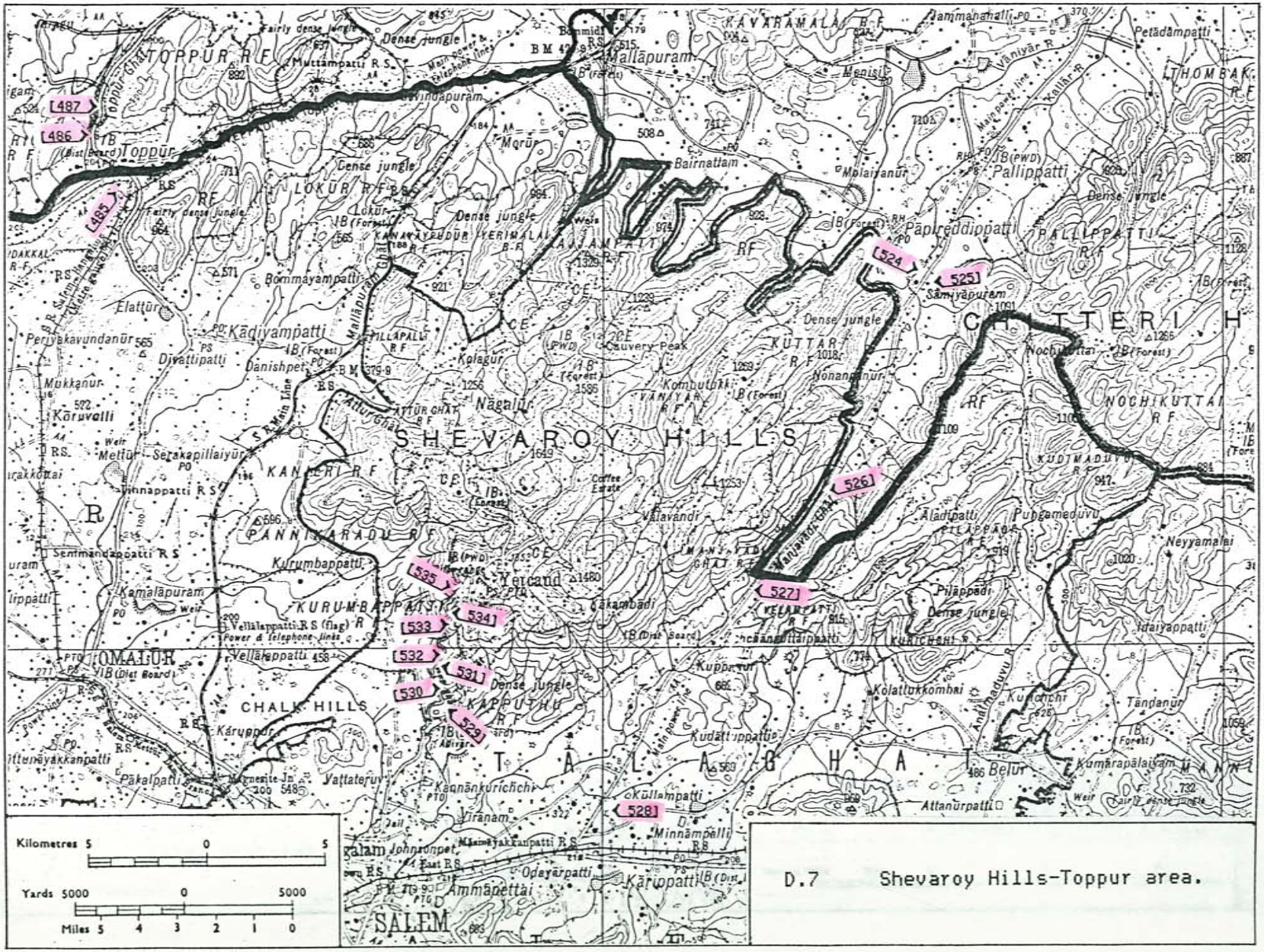

D.7 Shevaroy Hills-Toppur area.

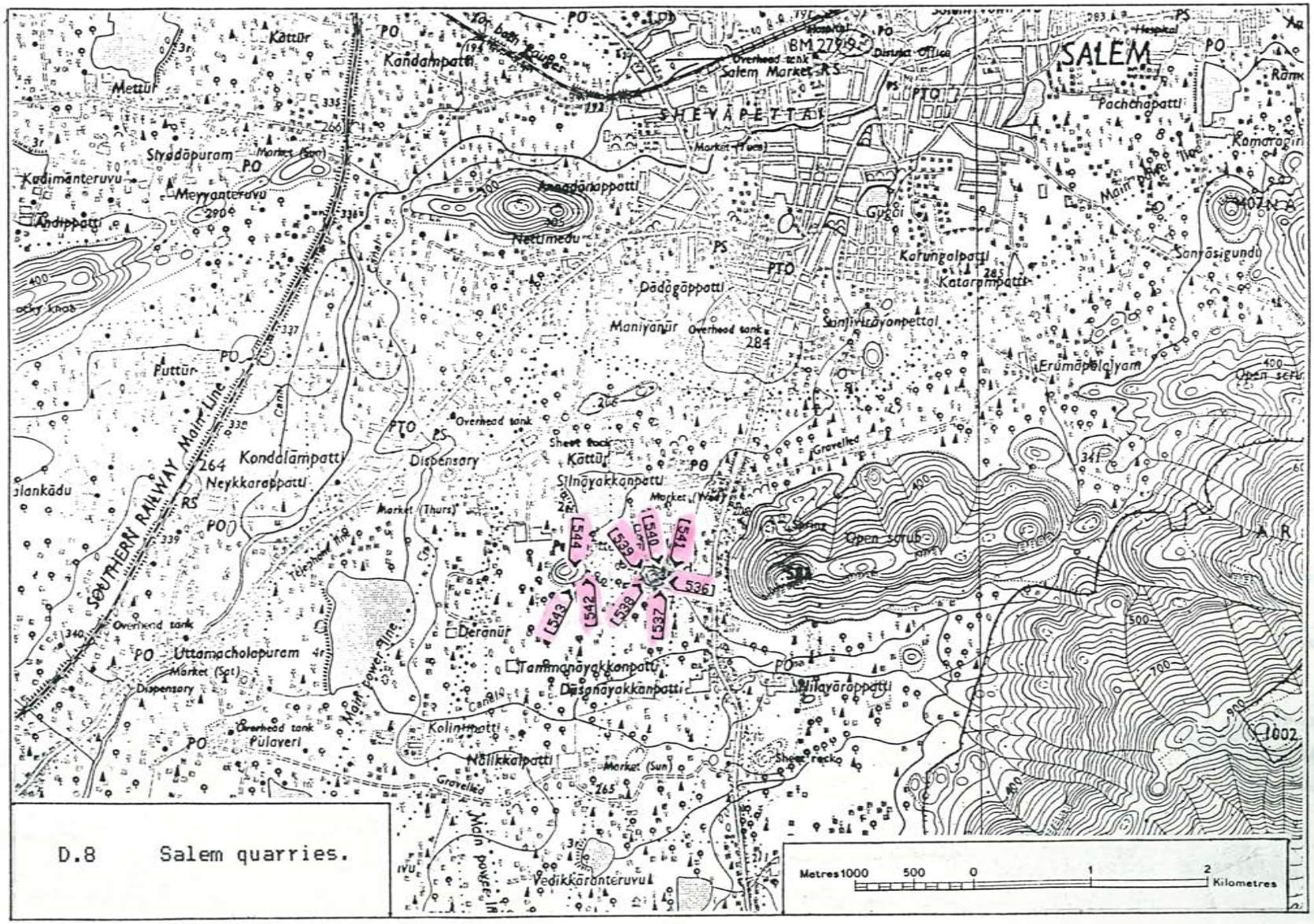

D.8 Salem quarries.

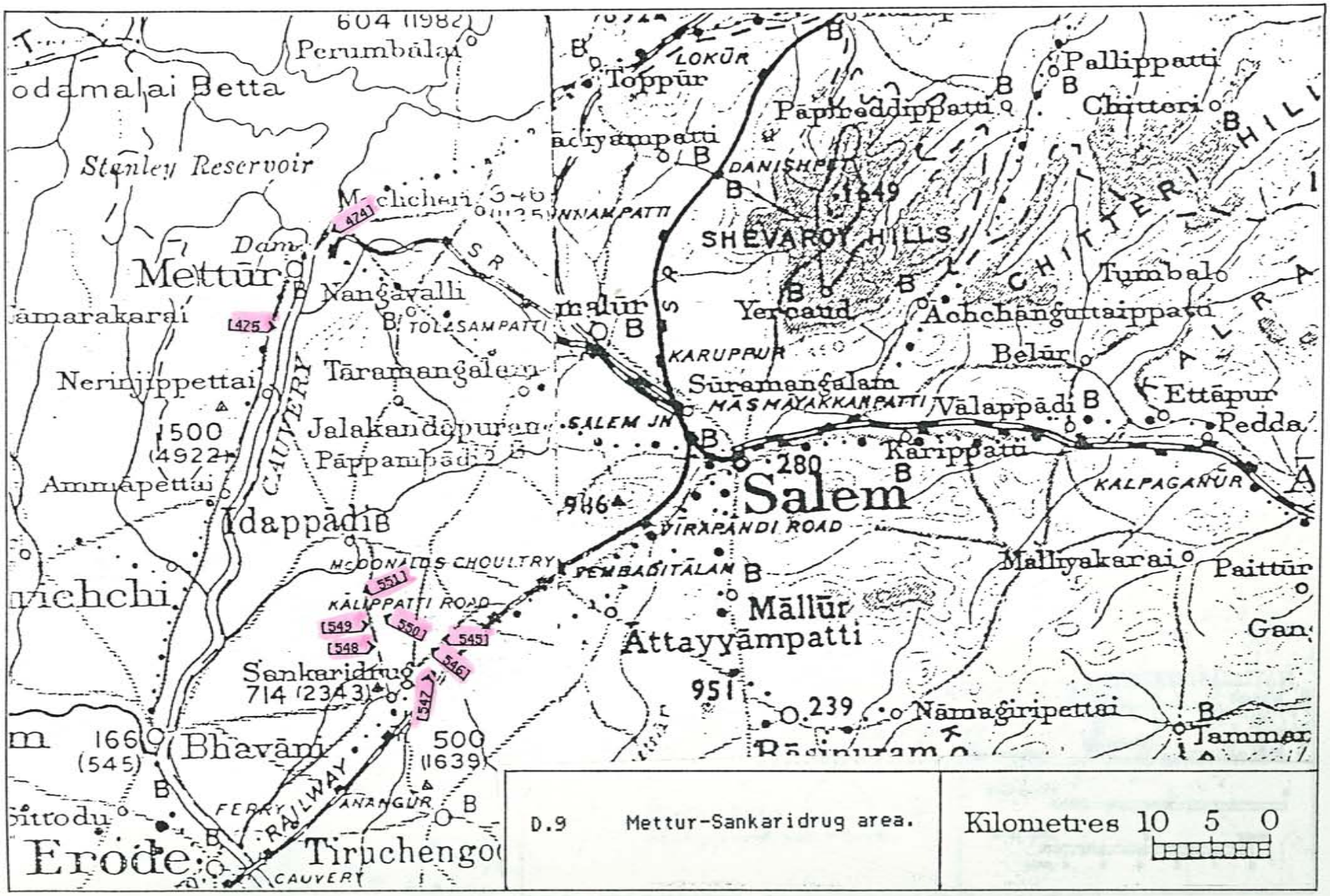
Perumbālai
odamalai Betta
Stanley Reservoir
Dam
Mettūr
Nangavalli
TOLASAMPATTI
Nerinjippettai
Tāramangalam
Jalakandāpuram
Pāppambādi
Ammāpettai
Idappādi
MCDONALDS CHOULTRY
KALIPPATTI ROAD
Sankaridrug
714 (2343)
Bhavāni
Erode
Tiruchengo
CAUVERY
RAILWAY
FERRY
ANANGUR
Toppūr
LOKUR
Pallippatti
Chitteri
Pāpireddippatti
DANISHPET
1649
SHEVAROY HILLS
Yercaud
Āchchāngunaippatti
Tumbalo
Belūr
Ettāpur
Pedda
Sūramangalam
MĀSMAYAKKANPATTI
Vālappādi
Karippatti
Salem
KALPAGANUR
VIRAPANDI ROAD
PEMBAGITĀLAN
Mallīyakarai
Paittūr
Māllūr
Attayyāmpatti
951
239
Nāmagiripettai
Tammar
SALEM JN
KARUPPUR
986
280
500
(4922)
500
(1639)
166
(545)
604 (1982)
(474)
(425)
(551)
(549)
(550)
(548)
(545)
(546)
(547)
D.9 Mettur-Sankaridrug area.
Kilometres 10 5 0

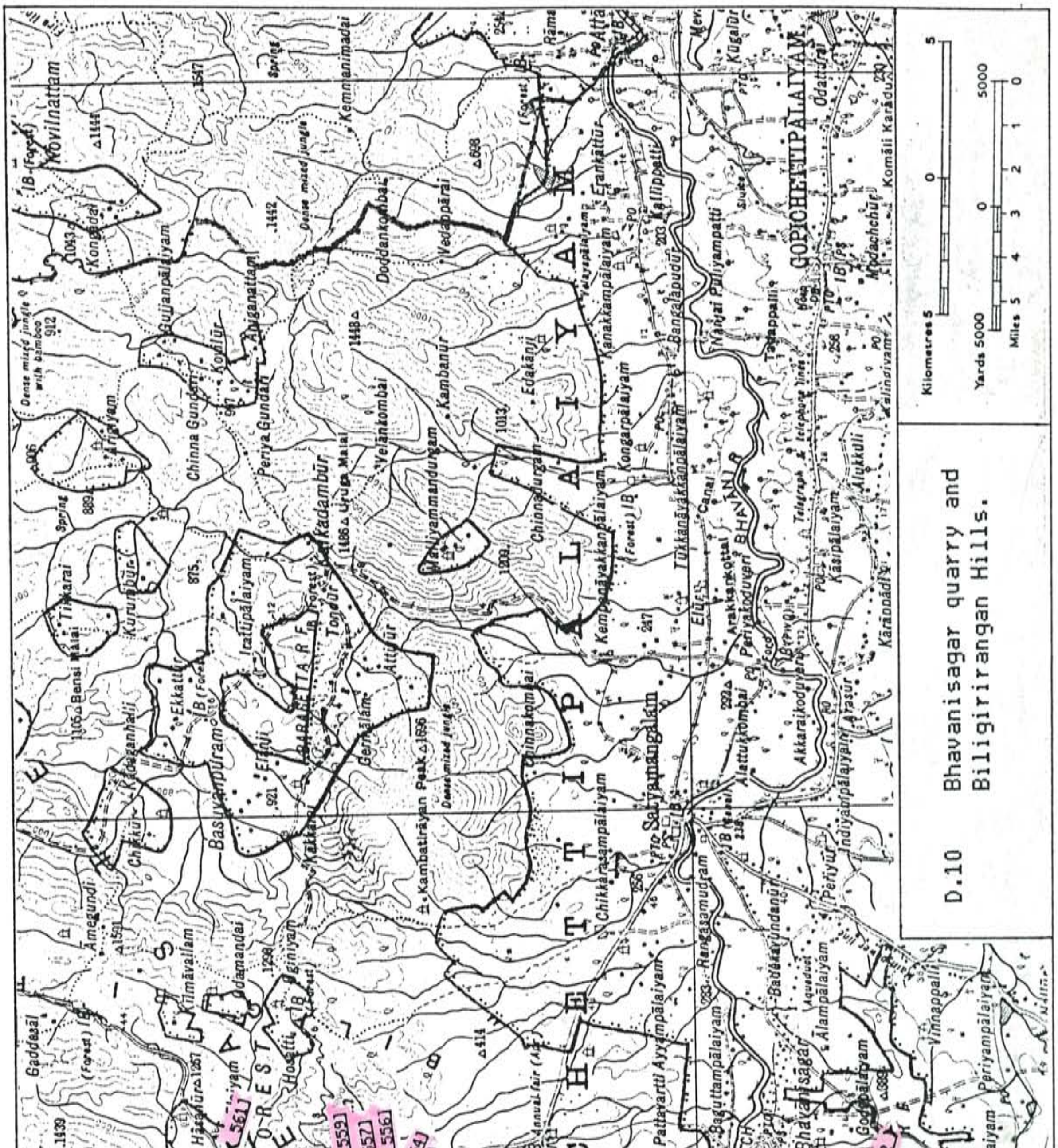

D.10 Bhavanisagar quarry and Biligirirangan Hills.

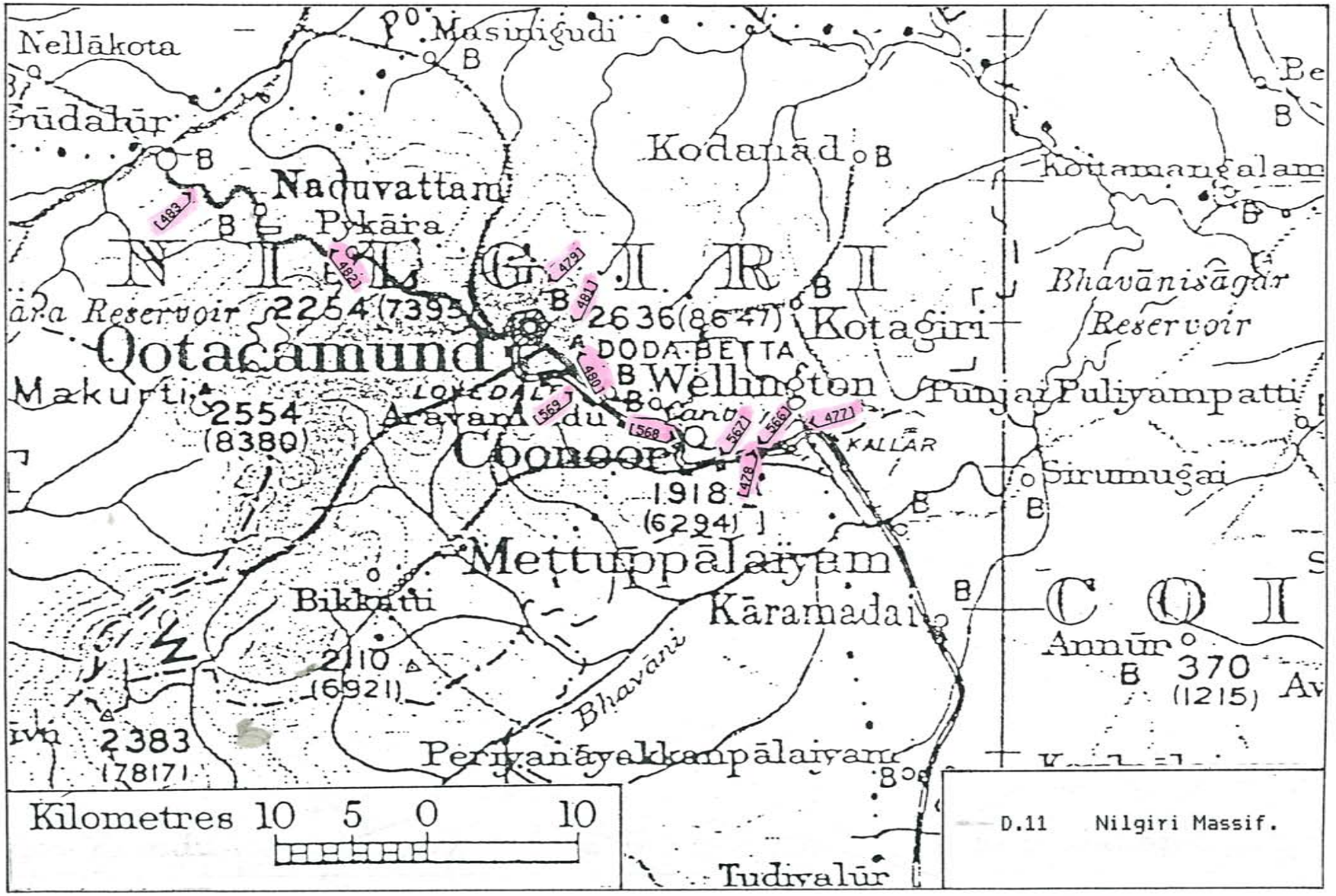

D.11 Nilgiri Massif.

D.12 Karetur quarry.

This dissertation is accepted on behalf of the faculty of the Institute by the following committee:

Adviser

9 May 1985
Date